



Fire Design of Steel Structures

2nd Edition

Eurocode 1: Actions on Structures
Part 1-2: Actions on structures exposed to fire
Eurocode 3: Design of Steel Structures
Part 1-2: Structural fire design

Jean-Marc Franssen
Paulo Vila Real



ECCS
CECM
EKS

WILEY

Ernst & Sohn
A Wiley Brand

ECCS Eurocode Design Manuals

FIRE DESIGN OF STEEL STRUCTURES

2ND EDITION

ECCS EUROCODE DESIGN MANUALS

ECCS EDITORIAL BOARD

Luís Simões da Silva (ECCS)

António Lamas (Portugal)

Jean-Pierre Jaspart (Belgium)

Reidar Bjorhovde (USA)

Ulrike Kuhlmann (Germany)

DESIGN OF STEEL STRUCTURES – 1ST EDITION REVISED SECOND IMPRESSION

Luís Simões da Silva, Rui Simões and Helena Gervásio

FIRE DESIGN OF STEEL STRUCTURES – 2ND EDITION

Jean-Marc Franssen and Paulo Vila Real

DESIGN OF PLATED STRUCTURES

Darko Beg, Ulrike Kuhlmann, Laurence Davaine and Benjamin Braun

FATIGUE DESIGN OF STEEL AND COMPOSITE STRUCTURES

Alain Nussbaumer, Luís Borges and Laurence Davaine

DESIGN OF COLD-FORMED STEEL STRUCTURES

Dan Dubina, Viorel Ungureanu and Raffaele Landolfo

AVAILABLE SOON

DESIGN OF JOINTS IN STEEL AND COMPOSITE STRUCTURES

Jean-Pierre Jaspart, Klaus Weynand

DESIGN OF COMPOSITE STRUCTURES

Markus Feldman and Benno Hoffmeister

DESIGN OF STEEL STRUCTURES FOR BUILDINGS IN SEISMIC AREAS

Raffaele Landolfo, Federico Mazzolani, Dan Dubina and Luís Simões da Silva

ECCS – SCI EUROCODE DESIGN MANUALS

DESIGN OF STEEL STRUCTURES, U. K. EDITION

Luís Simões da Silva, Rui Simões, Helena Gervásio and Graham Couchman

INFORMATION AND ORDERING DETAILS

For price, availability, and ordering visit our website www.steelconstruct.com.

For more information about books and journals visit www.ernst-und-sohn.de.

FIRE DESIGN OF STEEL STRUCTURES

2ND EDITION

Eurocode 1: Actions on structures

**Part 1-2 – General actions – Actions on
structures exposed to fire**

Eurocode 3: Design of steel structures

Part 1-2 – General rules – Structural fire design

Jean-Marc Franssen

Paulo Vila Real



Design of Steel Structures

2nd Edition, 2015

Published by:

ECCS – European Convention for Constructional Steelwork

publications@steelconstruct.com

www.steelconstruct.com

Sales:

Wilhelm Ernst & Sohn Verlag für Architektur und technische Wissenschaften
GmbH & Co. KG, Berlin

All rights reserved. No parts of this publication may be reproduced, stored in a retrieval system, or transmitted in any form or by any means, electronic, mechanical, photocopying, recording or otherwise, without the prior permission of the copyright owner.

ECCS assumes no liability with respect to the use for any application of the material and information contained in this publication.

Copyright © 2015 ECCS – European Convention for Constructional Steelwork

ISBN (ECCS): 978-92-9147-128-7

ISBN (Ernst & Sohn): 978-3-433-03143-8

Printed in Multicomp Lda, Mem Martins, Portugal

Photo cover credits: Michael Meadows

TABLE OF CONTENTS

FOREWORD	xiii
PREFACE	xv
NOTATIONS	xix
Chapter 1	
<u>INTRODUCTION</u>	<u>1</u>
1.1. Relations between different Eurocodes	1
1.2. Scope of EN 1993-1-2	3
1.3. Layout of the book	3
Chapter 2	
<u>MECHANICAL LOADING</u>	<u>7</u>
2.1. General	7
2.1.1. General rule	7
2.1.2. Simplification 1	10
2.1.3. Simplification 2	10
2.1.4. Simplification 3	12
2.2. Examples	13
2.3. Indirect actions	14
Chapter 3	
<u>THERMAL ACTION</u>	<u>17</u>
3.1. General	17
3.2. Nominal temperature-time curves	18
3.3. Parametric temperature-time curves	21
3.4. Zone models	29
3.5. CFD models	31
3.6. Localised fires	32
3.7. External members	39

TABLE OF CONTENTS

Chapter 4

TEMPERATURE IN STEEL SECTIONS **45**

4.1. Introduction	45
4.2. The heat conduction equation and its boundary conditions	45
4.3. Advanced calculation model. Finite element solution of the heat conduction equation	47
4.3.1. Temperature field using the finite element method	48
4.4. Section factor	51
4.5. Temperature of unprotected steelwork exposed to fire	54
4.6. Temperature of protected steelwork exposed to fire	61
4.7. Internal steelwork in a void protected by heat screens	76
4.8. External steelwork	78
4.8.1. General principles	78
4.8.2. Example	80
4.9. View factors in the concave part of a steel profile	88
4.10. Temperature in steel members subjected to localised fires	92
4.10.1. Unprotected steel members	92
4.10.2. Protected steel members	93
4.10.3. Thermal response of steel members in case of multiple localised fires	95
4.10.3.1. <i>Multiple localised fires due to simultaneously burning cars: an example of a car park</i>	95
4.10.3.1.1. <i>Characterization of the fire and definition of the fire scenarios</i>	95
4.10.3.1.2. <i>Temperature of the main beam</i>	98
4.11. Temperature in stainless steel members	101
4.11.1. Example	104

Chapter 5

MECHANICAL ANALYSIS **105**

5.1. Basic principles	105
5.2. Mechanical properties of carbon steel	110
5.3. Classification of cross sections	115

5.3.1. Cross section under combined bending and axial-compression at normal temperature	120
5.3.1.1. <i>First methodology for Class 1 and Class 2 cross sections</i>	123
5.3.1.2. <i>Second methodology for the case of Class 1 and Class 2 cross sections</i>	125
5.3.1.3. <i>First methodology for Class 3 cross sections</i>	127
5.3.1.4. <i>Second methodology for Class 3 cross sections</i>	128
5.3.1.5. <i>Advantages and disadvantages of the two presented methodologies</i>	130
5.3.2. Cross section under combined bending and tension at normal temperature	132
5.3.3. Classification under fire conditions	132
5.4. Effective cross section	134
5.5. Fire resistance of structural members	136
5.5.1. General	136
5.5.2. Members with Class 4 cross sections	138
5.5.3. Tension members	139
5.5.4. Compression members	140
5.5.5. Shear resistance	143
5.5.6. Laterally restrained beams	145
5.5.6.1. <i>Uniform temperature distribution</i>	145
5.5.6.2. <i>Non-uniform temperature distribution</i>	147
5.5.6.3. <i>Bending and shear</i>	150
5.5.7. Laterally unrestrained beams	152
5.5.7.1. <i>The elastic critical moment for lateral-torsional buckling</i>	152
5.5.7.2. <i>Resistance to lateral-torsional buckling</i>	156
5.5.8. Members subjected to combined bending and axial compression	159
5.5.9. Some verifications of the fire resistance not covered by EN 1993-1-2	163
5.5.9.1. <i>Shear buckling resistance for web without intermediate stiffeners</i>	163
5.5.9.2. <i>Cross section verification of a member subjected to combined bending and axial force (compression or tension)</i>	164

TABLE OF CONTENTS

5.5.9.2.1. Class 1 and 2 rectangular solid sections	165
5.5.9.2.2. Class 1 and 2 doubly symmetric I- and H-sections	166
5.5.9.2.3. Class 3 doubly symmetric I- and H-sections	168
5.5.9.2.4. Class 4 cross sections	169
5.5.9.3. Bending, shear and axial force	169
5.6. Design in the temperature domain. Critical temperature	170
5.7. Design of continuous beams	180
5.7.1. General	180
5.7.2. Continuous beams at room temperature	181
5.7.3. Continuous beams under fire conditions	184
5.8. Fire resistance of structural stainless steel members	186
5.9. Design examples	193

Chapter 6**ADVANCED CALCULATION MODELS**

273

6.1. General	273
6.2. Thermal response model	275
6.3. Mechanical response model	282
6.4. Some comparisons between the simple and the advanced calculation models	288
6.4.1. Shadow factor	289
6.4.2. Buckling curves	293
6.4.3. Factor κ_2	295
6.4.4. Factor κ_1	296

viii

Chapter 7**JOINTS**

299

7.1. General	299
7.2. Strength of bolts and welds at elevated temperature	300
7.3. Temperature of joints in fire	301
7.4. Bolted connections	302
7.4.1. Design fire resistance of bolts in shear	303

7.4.1.1. <i>Category A: Bearing type</i>	303
7.4.1.2. <i>Category B (slip resistance at serviceability) and Category C (slip resistance at ultimate state)</i>	303
7.4.2. Design fire resistance of bolts in tension	303
7.4.2.1. <i>Category D and E: Non-preloaded and preloaded bolts</i>	303
7.5. Design fire resistance of welds	304
7.5.1. Butt welds	304
7.5.2. Fillet welds	304
7.6. Design examples	304
Chapter 8	
<u>THE COMPUTER PROGRAM “ELEFIR-EN”</u>	315
8.1. General	315
8.2. Brief description of the program	316
8.2.1. Available thermal calculations	316
8.2.2. Available mechanical calculations	322
8.3. Default constants used in the program	329
8.4. Design example	329
Chapter 9	
<u>CASE STUDY</u>	343
9.1. Description of the case study	343
9.2. Fire resistance under standard fire	344
9.2.1. Thermal calculations	344
9.2.2. Structural calculation	345
9.2.2.1. <i>Loading</i>	345
9.2.2.2. <i>Fire resistance by the simple calculation model</i>	349
9.2.2.3. <i>Fire resistance by the general calculation model</i>	351
9.3. Fire resistance under natural fire	353
9.3.1. Temperature development in the compartment	353
<u>REFERENCES</u>	359

TABLE OF CONTENTS

Annex A

THERMAL DATA FOR CARBON STEEL AND STAINLESS

STEEL SECTIONS **369**

A.1. Thermal properties of carbon steel	369
A.1.1. Specific heat	369
A.1.2. Thermal conductivity	370
A.1.3. Thermal elongation	371
A.2. Section factor A_m/V [m^{-1}] for unprotected steel members	372
A.3. Section factor A_p/V [m^{-1}] for protected steel members	374
A.4. Tables and nomograms for evaluating the temperature in unprotected steel members subjected to the standard fire curve ISO 834	375
A.5. Tables and nomograms for evaluating the temperature in protected steel members subjected to the standard fire curve ISO 834	380
A.6. Thermal properties of some fire protection materials	384
A.7. Thermal properties of stainless steel	385
A.7.1. Specific heat	385
A.7.2. Thermal conductivity	385
A.7.3. Thermal elongation	386
A.8. Tables and nomograms for evaluating the temperature in unprotected stainless steel members subjected to the standard fire curve ISO 834	387
A.9. Thermal properties of some fire compartment lining materials	394

x

Annex B

INPUT DATA FOR NATURAL FIRE MODELS **395**

B.1. Introduction	395
B.2. Fire load density	395
B.3. Rate of heat release density	398
B.4. Ventilation control	403
B.5. Flash-over	406

Annex C	
MECHANICAL PROPERTIES OF CARBON STEEL AND STAINLESS STEEL	407
C.1 Mechanical properties of carbon steel	407
C.1.1. Mechanical properties of carbon steel at room temperature (20°C)	407
C.1.2. Stress-strain relationship for carbon steel at elevated temperatures (without strain-hardening)	410
C.1.3. Stress-strain relationship for carbon steel at elevated temperatures (with strain-hardening)	418
C.1.4. Mechanical properties to be used with Class 4 cross sections and simple calculation models	419
C.2. Mechanical properties of stainless steel	421
Annex D	
TABLES FOR SECTION CLASSIFICATION AND EFFECTIVE WIDTH EVALUATION	429
Annex E	
SECTION FACTORS OF EUROPEAN HOT ROLLED IPE AND HE PROFILES	435
Annex F	
CROSS SECTIONAL CLASSIFICATION OF THE EUROPEAN HOT ROLLED IPE AND HE PROFILES	443
F.1. Cross sectional classification for pure compression and pure bending	443
F.2. Cross sectional classification for combined compression and bending moment	450

FOREWORD

Designing for fire is an important and essential requirement in the design process of buildings and civil engineering structures. Within Europe the fire resistance requirements for buildings are specified in the national Building Regulations. All buildings must meet certain functional requirements and these are usually linked to the purpose and height of the building. For the purpose of this publication, the most important requirement is for the building to retain its stability for a reasonable period. This requirement has traditionally been linked to the required time of survival in the standard fire test. The most common method of designing a steel structure for the fire condition is to design the building for the ambient temperature loading condition and then to cover the steel members with proprietary fire protection materials to ensure that a specific temperature is not exceeded. Although this remains the simplest approach for the majority of regular steel framed buildings, one of the drawbacks with this approach is that it is often incorrectly assumed that there is a one to one correspondence between the survival time in the standard fire test and the survival time in a real fire. This is not the case and real fire can be more or less severe than the standard fire test depending on the characteristics of the fire enclosure.

xiii

The fire parts of the Eurocodes set out a new way of approaching structural fire design. To those more familiar with the very simple prescriptive approach to the design of structures for fire, the new philosophy may appear unduly complex. However, the fire design methodology in the Eurocodes affords the designer much greater flexibility in his approach to the subject. The options available range from a simple consideration of isolated member behaviour subject to a standard fire to a consideration of the physical parameters influencing fire development coupled with an analysis of the entire building.

The Eurocode process can be simplified into three components consisting of the characterisation of the fire model, a consideration of the temperature distribution within the structure and an assessment of the structural response

to the fire. Information on thermal actions for temperature analysis is given in EN 1991-1-2 and the method used to calculate the temperature rise of structural steelwork (either protected or unprotected) is found in EN 1993-1-2. The design procedures to establish structural resistance are set out in EN 1993 but the actions (or loads) to be used for the assessment are taken from the relevant parts of EN 1991.

This publication follows this sequence of steps. Chapter 2 explains how to calculate the mechanical actions (loads) in the fire situation based on the information given in EN 1990 and EN 1991. Chapter 3 presents the models that may be used to represent the thermal actions. Chapter 4 describes the procedures that may be used to calculate the temperature of the steelwork from the temperature of the compartment and Chapter 5 shows how the information given in EN 1993-1-2 may be used to determine the load bearing capacity of the steel structures. The methods used to evaluate the fire resistance of bolted and welded connections are described in Chapter 7. In all of these chapters the information given in the Eurocodes is presented in a practical and usable manner. Each chapter also contains a set of easy to follow worked examples.

Chapter 8 describes a computer program called 'Elefir-EN' which is based on the simple calculation model given in the Eurocode and allows designers to quickly and accurately calculate the performance of steel components in the fire situation. Chapter 9 looks at the issues that a designer may be faced with when assessing the fire resistance of a complete building. This is done via a case study and addresses most of the concepts presented in the earlier chapters. Finally the annexes give basic information on the thermal and mechanical properties for both carbon steel and stainless steel.

The concepts and fire engineering procedures given in the Eurocodes may seem complex to those more familiar with the prescriptive approach. This publication sets out the design process in a logical manner giving practical and helpful advice and easy to follow worked examples that will allow designers to exploit the benefits of this new approach to fire design.

David Moore

BCSA Director of Engineering

PREFACE TO THE 2ND EDITION

The first edition of *Fire Design of Steel Structures* was published by ECCS as paperback in 2010. Since 2012, this publication is also available in electronic format as an e-book. Nevertheless, the interest for this publication was so high that it appeared rapidly that the paper copies would be sold out within a short time and a second edition would have to be printed.

The authors took the opportunity of this second edition to review their own manuscript. The standards that are described and commented in this book, namely EN 1991-1-2 and 1993-1-2, are still in application in the same versions as those that prevailed at the time of writing the first edition. It was nevertheless considered that an added value would be given by, first, rephrasing some sentences or sections that had generated questions by some readers but, above all, adding some new material for the benefit of completeness.

The new material namely comprises:

- A section dealing with the thermal response of steel members under several separate simultaneous localised fires, including one worked example with multiple fire scenarios in a car park (Chapter 4);
- An important section on classification of cross sections. The case of combined bending and axial force, including one worked example comparing different methodologies to obtain the position of the neutral axis, has been added (Chapter 5);
- A worked example of a beam-column with Class 4 cross section (Chapter 5);
- A new section with comparisons between the simple and the advanced calculation models in Chapter 6 (shadow factor – including one example, buckling curves and adaptation factors κ_1 and κ_2);
- New references have been included.

Jean-Marc Franssen

Paulo Vila Real

June 2015

PREFACE 1ST EDITION

When a fire breaks out in a building, except in very few cases, the structure has to perform in a satisfactory manner in order to meet various objectives such as, e.g., to limit the extension of the fire, to ensure evacuation of the occupant or to allow safe operations by the fire brigade. Steel structures are no exception to this requirement.

Eurocode 3 proposes design methods that allow verifying whether the stability and resistance of a steel structure is ensured. A specific Part 1-2 of Eurocode 3 is dedicated to the calculation of structures subjected to fire. Indeed, the fact that the stress-strain relationship becomes highly non-linear at elevated temperatures, plus the fact that heating leads to thermal expansion with possible restraint forces, make the rules derived for ambient temperature inaccurate in the fire situation.

After a long evolution and maturation, the Eurocodes have received the status of European standards. The fire part of Eurocode 3 is EN 1993-1-2. This makes the application of these rules mandatory in member states of the European Community. In many other parts of the world, these standards are considered as valuable pieces of information and their application may be rendered mandatory, either by law or by contractual imposition.

Nevertheless, standards are not written with pedagogic objectives. Yet, for a designer who has not been involved in the research projects that are at the base of the document, some questions may arise when the rules have to be applied to practical cases.

The objective of this book is to explain the rules, to give some information about the fundamental physics that is at the base of these rules and to show by examples how they have to be applied in practice. It is expected that a designer who reads this book will reduce the probability of doing a non appropriate application of the rules and, on the contrary, will be in a better position to make a design in a situation that has not been explicitly foreseen in the code.

PREFACE

A design in the fire situation is based on load combinations that are different from those considered at room temperatures. Actions on structures from fire exposure are classified as accidental actions and the load combinations for the fire situation are given in the Eurocode, EN 1990. The thermal environment created by the fire must also be defined in order to calculate the temperature elevation in the steel sections and different models are given in part 1.2 of Eurocode 1 for representing the fire. In order to encompass in one single document all aspects that are relevant to the fire design of steel structures, this book deals with the fire part of Eurocode 1 as well as that of Eurocode 3.

The requirements, i.e., for example, the duration of stability or resistance that has to be ensured to the structure, is not treated in the Eurocodes. This aspect is indeed very often imposed by the legal environment, especially when using a prescriptive approach, or has to be treated separately by, for example, a risk analysis based on evacuation time. In line with the Eurocodes, this book does not deal with the requirement.

A computer program, Elefir-EN, which has been developed for the fire design of structural members in accordance with the simple calculation models given in the Eurocodes, is supplied with this book. The software is an essential tool for structural engineers in the design office, enabling quick and accurate calculations to be produced, reducing design time and the probability of errors in the application of the equations. It can also be used by academics and students.

xviii

The program has been carefully checked for reliability and do not contain any known errors, but the authors and the publisher assume no responsibility for any damage resulting from the use of this program. No warranty of any type is given or implied concerning the correctness or accuracy of any results obtained from the program. It is the responsibility of the program user to independently verify any analysis results. Please contact the authors if any errors are discovered. The program is licensed to the purchasers of this book who are strongly encouraged to register in its web site so that any updated version can be delivered.

Jean-Marc Franssen
Paulo Vila Real
March 2010

NOTATIONS

Latin lower case letters

b	material parameter in the walls, width of a steel section, width of a plate
c	specific heat, width of a plate in an open steel section
c_a	specific heat of steel
c_p	specific heat of protection material
d	diameter of a circular hollow section
d_{eq}	characteristic size of a structural member
d_f	flame thickness
d_p	thickness of a fire protection material
f	factor for the effect of non-uniform bending moment distribution on lateral torsional buckling
f_b	stress due to bending moment
f_c	stress due to axial force
$f_{0.2p,\theta}$	0.2% proof strength
$f_{p,\theta}$	limit of proportionality of steel at temperature θ
f_u	ultimate strength at 20 °C
$f_{u,\theta}$	ultimate strength of steel at temperature θ
f_y	yield strength at 20 °C
$f_{y,\theta}$	effective yield strength of steel at temperature θ
h	height of an opening, height of a radiating surface, height of a steel section, height of a component being considered above the bottom of the beam
\dot{h}	impinging heat flux
\dot{h}_{net}	heat flux at the surface of a steel element
h_{eq}	averaged height of the vertical openings
h_w	depth of the web
i	radius of gyration of a cross section
k	multiplication factor in the parametric fire model

NOTATIONS

$k_{2\%,\theta}$	correction factor for the determination of the yield strength of stainless steel at elevated temperature
$k_{b,\theta}$	reduction factor for bolts
$k_{p0.2\theta}$	reduction factor for the 0.2% proof strength
$k_{E,\theta}$	reduction factor for the Young's modulus
$k_{E,\theta,com}$	reduction factor for the Young's modulus at the maximum steel temperature in the compression flange
$k_{p,\theta}$	reduction factor for the limit of proportionality
k_{sh}	correction factor for the shadow effect
$k_{u,\theta}$	reduction factor for tensile strength of stainless steel at elevated temperature
k_w	effective length factor referring to end warping
$k_{w,\theta}$	reduction factor for welds
$k_{y,\theta}$	reduction factor for the effective yield strength
$k_{y,\theta,com}$	reduction factor for the yield strength of steel at the maximum temperature in the compression flange
$k_{y,\theta,web}$	reduction factor for the yield strength at the web temperature θ_{web}
k_z	effective length factor referring to end rotation on plan
k_θ	reduction factor for a strength or deformation property
k_σ	plate buckling factor
l	length of a member
l_{fi}	buckling length in fire situation
p	moisture content of a protection material
q_c	heat flux by convection
q_{cr}	combine heat flux by convection and radiation
q_{Ed}	design value of a distributed load in the normal situation
$q_{f,d}$	design value of the fire load density related to the floor area
$q_{fi,Ed}$	design value of a distributed load in the fire situation
q_r	heat flux by radiation
$q_{t,d}$	design value of the fire load density related to the total area of enclosure
r	horizontal distance from the fire plume, distance between an emitting and a receiving surface, root fillet
t	time, thickness of the walls in a hollow section, plate thickness in general
t^*	expanded time in the parametric fire model
t_f	flange thickness

$t_{fi,d}$	design value of the fire resistance
$t_{fi,req}$	required fire resistance time
t_{lim}	limit time in the parametric fire model
t_{max}	duration of the heating phase in the parametric fire model
t_v	length of the horizontal plateau in a heating curve
t_w	thickness of the web
w	width of a radiating surface
w_t	sum of the window widths
x	cartesian coordinate
y	parameter in a localised fire model, cartesian coordinate
z	vertical elevation in a fire plume
z'	vertical position of the virtual heat source
z_g	level of the application of the load
z_i	distance from the plastic neutral axis to the centroid of an elemental area
z_0	vertical position of the virtual origin of the fire source

Latin upper case letters

A	area of a wall, cross section area of a steel member, surface area of a member exposed to the heat flux
A_c	gross cross sectional area of a plate
$A_{c,eff}$	effective area of the compression zone of a plate
A_d	indirect fire actions
A_m	surface area of a member exposed to the heat flux
A_m/V	section factor of unprotected sections
A_p/V	section factor of protected sections
$[A_m/V]_b$	box value of the section factor
A_f	floor area
A_{fire}	area of a fire source
A_p	appropriate area of fire protection material per unit length of a member
A_t	total area of an enclosure, including the openings
A_v	area of a vertical opening, shear area
C	matrix of capacity, compression force
C'	compression force
D	the diameter of a fire, depth of a beam

NOTATIONS

D/W	ratio for the external members
E	Young's modulus of steel
$E_{a,\theta}$	Young's modulus of steel at temperature θ
E_d	effects of actions in the normal situation
$E_{fi,d}$	design effect of actions for the fire situation
$E_{fi,d,t}$	design effect of actions for the fire situation at time t
EI_z	flexural stiffness of a section
EI_w	warping stiffness of a section
F	thermal load vector
$F_{b,Rd}$	design bearing resistance of bolts at normal temperature
$F_{b,t,Rd}$	design bearing resistance of bolts in the fire situation
$F_{t,Rd}$	design tension resistance of bolts at normal temperature
$F_{ten,t,Rd}$	design tension resistance of bolts in the fire situation
$F_{v,Rd}$	design shear resistance of a bolt per shear plane in the normal situation
$F_{v,t,Rd}$	fire design resistance of a bolt loaded in shear
$F_{w,Rd}$	design weld resistance per unit length at normal temperature
$F_{w,t,Rd}$	design weld resistance per unit length in the fire situation
G	shear modulus
G_k	characteristic value of a permanent action
GI_t	torsional stiffness of a section
H	altitude above mean sea level, vertical distance from the fire source to the ceiling
I	second moment of area
I_f	radiative heat flux from an opening
I_t	torsion constant
I_w	warping constant
I_z	second moment of area about the minor axis, radiative heat flux from a flame
K	matrix of conductivity
L	column length, unrestrained length of the beam
L_f	vertical length of a flame
L_h	horizontal flame length
L_L	vertical extension of a flame above the top of the window
L_X	distance from the window
M	bending moment
$M_{b,fi,t,Rd}$	design lateral-torsional buckling resistance moment at time t

M_{cr}	elastic critical moment for lateral-torsional buckling
M_{el}	elastic moment
M_{Ed}	design value of a bending moment in the normal situation
$M_{fi,Ed}$	design value of a bending moment in the fire situation
$M_{fi,t,Rd}$	design value of bending moment resistance in the fire situation
$M_{fi,\theta,Rd}$	design moment resistance of a cross section with a uniform temperature θ_a
$M_{N,fi,Rd}$	design plastic moment resistance reduced due to the axial force
M_{pl}	plastic moment
M_Q	maximum moment due to lateral load only
M_{Rd}	design resistance for bending for normal temperature design
$M_{y,V,fi,Rd}$	design plastic resistance moment in fire situation, allowing for the shear force effect
N	axial force
$N_{b,fi,Ed}$	design value of the compression force in fire situation
$N_{b,fi,t,Rd}$	design buckling resistance at time t of a compression member
$N_{b,fi,\theta,Rd}$	design resistance of a compression member, with a uniform steel temperature θ_a
$N_{fi,Ed}$	design value of axial force in the fire situation
$N_{fi,t,Rd}$	design value of axial resistance force in the fire situation
$N_{fi,\theta,Rd}$	design resistance of a tension member with a uniform temperature θ_a
N_{Rd}	design resistance of the cross section for normal temperature
O	opening factor of an opening
P	perimeter of a section exposed to the fire, prestressing load
Q	rate of heat release of a fire
\dot{Q}	internal heat source
Q_c	convective part of the rate of heat release
Q_D^*	non-dimensional rate of heat release, related to D
Q_H^*	non-dimensional rate of heat release, related to H
Q_k	characteristic value of a variable action
$Q_{k,1}$	characteristic value of the leading variable action
R	fire resistance criterion for load bearing capacity
$R_{fi,d,t}$	design value of the resistance in the fire situation at time t
RHR_f	maximum rate of heat release per square meter
T	tension force
T_f	temperature in the fire compartment

NOTATIONS

T_W	flame temperature at the window
T_Z	temperature of the flame along the axis, flame temperature
V	volume of the member per unit length
$V_{fi,Ed}$	design value of a shear force in fire situation
$V_{fi,t,Rd}$	design shear resistance at time t
$V_{pl,Rd}$	design plastic shear resistance of a gross cross section for normal temperature design
V_{Rd}	design shear resistance of a gross cross section for normal temperature design
$W_{el,y}$	elastic section modulus
$W_{pl,y}$	plastic section modulus
W_2	size of the fire compartment perpendicular to wall 1
$X_{d,fi}$	design values of mechanical material properties in fire situation
X_k	characteristic value of a strength or deformation property

Greek lower case letters

α	parameter for time integration, convective heat transfer coefficient, imperfection factor for buckling curves or for lateral torsional buckling
α_c	coefficient of convection
α_{cr}	combined convection and radiation coefficient
α_f	absorptivity of a flame
α_r	coefficient of heat transfer by radiation
$\beta_{M,y}$	equivalent uniform moment factor about the y-y axis
$\beta_{M,z}$	equivalent uniform moment factor about the z-z axis
$\beta_{M,LT}$	equivalent uniform moment factor for lateral torsional buckling
γ_G	partial safety factor for the permanent action
$\gamma_{M,fi}$	partial safety factor for the relevant material property, for the fire situation
γ_{M0}	partial safety factor for the resistance of cross sections
$\gamma_{Q,1}$	partial safety factor for the leading variable action
ε	emissivity, parameter for section classification
ε_f	emissivity of a fire, emissivity of a flame
ε_m	surface emissivity of a member
$\varepsilon_{p,\theta}$	strain at the proportional limit at elevated temperature
$\varepsilon_{y,\theta}$	yield strain at elevated temperature

$\varepsilon_{t,\theta}$	limiting strain for yield strength at elevated temperature
$\varepsilon_{u,\theta}$	ultimate strain at elevated temperature
η_{fi}	reduction factor for the loads in the fire situation
θ	temperature
$\theta_{a,com}$	maximum temperature in the compression flange
$\theta_{a,cr}$	critical temperature of steel
$\theta_{a,max}$	maximum steel temperature in a section
$\theta_{cr,d}$	design value of the critical temperature
θ_d	design value of steel temperature
θ_g	gas temperature
θ_h	temperature at height h of the steel beam
θ_m	surface temperature of a steel member
θ_{max}	gas temperature at the end of the heating phase
θ_r	radiation temperature of the fire environment
$\theta_{(z)}$	temperature in a fire plume
θ_{web}	average temperature of a web
θ_0	bottom flange temperature of a steel beam remote from the connection
θ_∞	surrounding ambient temperature
k_1	adaptation factor for non-uniform temperature across the cross section
k_2	adaptation factor for non-uniform temperature along the beam
λ	thermal conductivity, member slenderness
λ_f	effective thermal conductivity of a fire protection material
λ_1	eulerian slenderness
λ_a	thermal conductivity of steel
λ_p	thermal conductivity of protection material
$\bar{\lambda}$	non-dimensional slenderness at room temperature
$\bar{\lambda}_{LT}$	non-dimensional slenderness for lateral torsional buckling
$\bar{\lambda}_p$	normalised plate slenderness
$\bar{\lambda}_\theta$	non-dimensional slenderness for the temperature θ_a
μ_0	degree of utilization
ν	Poisson's ratio
ρ	specific density, reduction factor for plate buckling
ρ_a	specific density of steel
σ	Stephan Boltzmann constant, equal to $5.67 \times 10^{-8} \text{ W/m}^2\text{K}^4$

NOTATIONS

σ_c	compression stress
σ_{cr}	elastic critical buckling stress
σ_t	tension stress
τ_F	free burning duration time
χ_{fi}	reduction factor for flexural buckling in the fire design situation
$\chi_{LT,fi}$	reduction factor for lateral-torsional buckling in the fire design situation
ψ	ratio between tension and compression stress, ratio between bending moments at both ends of a member
ψ_1	coefficient for the frequent value of an action
ψ_2	coefficient for the quasi-permanent value of an action
ψ_{fi}	coefficient for the variable loads in the fire situation, equal to ψ_1 or ψ_2

Greek upper case letters

Γ	expansion coefficient in the parametric fire model
D	prefix for increment
ϕ	amount of heat stored in the protection
ϕ_f	overall configuration factor of a member from an opening
ϕ_{pl}	rotation needed to form a fully plastic stress distribution
Φ	geometrical configuration factor

Chapter 1

INTRODUCTION

1.1. RELATIONS BETWEEN DIFFERENT EUROCODES

The structural Eurocodes are a set of reference documents recognised by the Member States of the European Community and of the European Free Trade Association as a suitable means for demonstrating the compliance of building structures with the essential requirements listed in the Council Directive 89/106/CEE on construction products, in particular essential requirement No. 1, mechanical resistance and stability, and essential requirement No. 2, safety in case of fire.

EN 1990 forms the basic document of all Eurocodes because it gives the basis of design, i.e., the principles and the requirements for safety, serviceability and durability of structures. It is thus the first document to read when the fire resistance of a structure has to be evaluated.

The Eurocode philosophy is based on the concept of limit states, either ultimate limit states or serviceability limit states. The occurrence of limit states is verified according to a semi-probabilistic approach. This means that deterministic verifications are being carried out on the base of design values of applied loads and material strength. The design values are obtained from characteristic values, corresponding to 5% or 95% probability of occurrence, multiplied or divided by partial safety factors. The partial safety factors have been calibrated by the code writers to ensure that the probability of occurrence of the limit states is lower than a defined accepted probability, but the real probability of occurrence in a particular design is not known to the designer.

The fire resistance of a structure can be assessed using the Eurocodes provided the structure has been designed according to the rules given in the

1. INTRODUCTION

Eurocodes for the ambient temperature situation. The design at room temperature is based on EN 1991, where the actions on structures are defined independently of the material of the structure. The mechanical behaviour of steel structures in buildings at room temperature is assessed on the basis of EN 1993-1-1.

In the fire situation, the combinations of actions are different from those at room temperature. EN 1991-1-2 gives the combinations for mechanical actions that have to be applied to the structure in the fire situation, as well as the fire actions, i.e., the thermal environment created by the fire. This Eurocode is independent of the material of the structure. Characteristic values of the loads are required to determine the mechanical load combinations applied to the structure; the characteristic values are given in EN 1991-1-1, 1991-1-3 and 1991-1-4.

For steel structures, EN 1993-1-2 gives the rules for calculating the temperature development in the structure together with the rules for calculating the mechanical behaviour of the structure at elevated temperatures.

For composite steel-concrete structures, EN 1994-1-1 should be used for assessing the mechanical behaviour at ambient temperature and EN 1994-1-2 should be used to determine the behaviour, thermal and mechanical, in the fire situation.

Fig. 1.1 shows the relationships between the different Eurocodes in a schematic way.

2

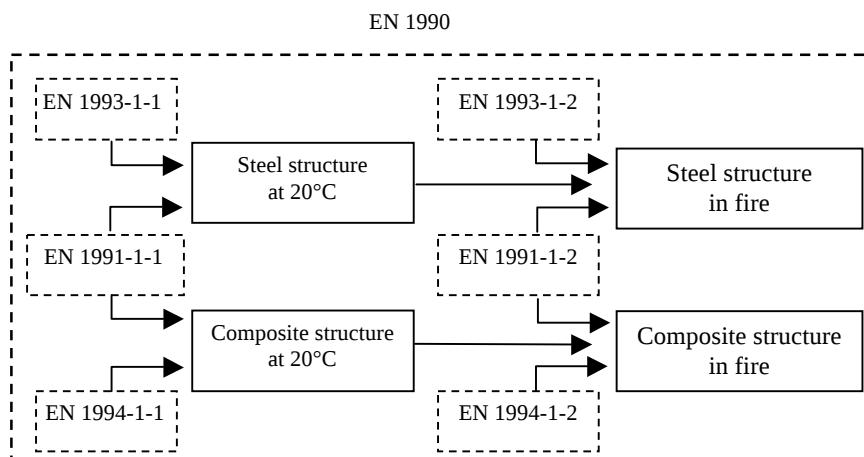


Figure 1.1 – Relationships between different Eurocodes

This book is about steel structures subjected to fire. The concepts and rules presented in EN 1993-1-2 are thus widely discussed.

Some basic concepts contained in EN 1990 and most of the rules and models contained in EN 1991-1-2 are also presented. The information given in this publication can thus also be used as a starting point for the verification of the fire resistance of other types of structure such as composite steel-concrete structures.

The rules and concepts given here for steel structures are supported by practical worked examples which demonstrate the procedures used for verifying the fire resistance.

1.2. SCOPE OF EN 1993-1-2

EN 1993-1-2, the fire part of Eurocode 3 for steel structures, deals with passive fire protection. Active protection measures such as automatic extinguishing systems, detection and alarm, are not treated here. It has yet to be noted that the presence of these active measures can be accounted for in a semi-probabilistic way when determining the design value of the fire load, see Annex B.

EN 1993-1-2 deals with the load bearing function of the structure. The separating function, quantified by the criteria of integrity and insulation, is not treated in this document.

3

The methods given in EN 1993-1-2 can be used for the following ranges of steel:

- structural steel grades S235, S275, S355, S420 and S460 of EN 10025 and all grades of EN 10210 and EN 10219;
- cold-formed steel members and sheeting within the scope of EN 1993-1-3;
- stainless steel members and sheeting within the scope of EN 1993-1-4;
- any steel grade for which material properties at elevated temperatures are available, based on harmonized European standards.

1.3. LAYOUT OF THE BOOK

The layout of this book follows the sequence of steps normally used in a structural fire design.

1. INTRODUCTION

Chapter 2 explains how the mechanical actions in the fire situation are evaluated. They are either explicitly calculated for this accidental situation or, alternatively, calculated from the actions that have been considered for the design at room temperature. In the latter case, it is likely that determining the mechanical actions in the fire situation will be the first step of the structural fire design, directly following the design of the structure at room temperature.

In Chapter 3 are presented and discussed the models that can be used to represent the fire action, either be it in form of gas temperatures in a compartment/or directly in the form of heat fluxes transmitted from the fire to the structural elements. Localised fires as well as fully developed fires are considered.

Once the fire actions have been determined, the temperatures induced in the steel structure by the fire can be calculated. Chapter 4 focuses on the rules for calculating the temperatures in thermally protected and unprotected steel members. Most rules are given for members located in the fire compartment. Some specific rules are given for members protected by membranes and for external members.

Chapter 5 is dedicated to the evaluation of the load bearing capacity, or the fire resistance time, of steel structures. General principles are discussed, followed by a detailed explanation of the simple calculation method applied to simple elements.

4

Chapter 6 is a discussion about the advanced calculation models. These models are implemented in non-linear numerical tools that allow analysing complete structures, subjected to any fire curve, taking into account the effects of large displacements and of indirect effects of action, i.e., the variations of the effects of actions due to restrained thermal expansion.

Because a steel structure is made of several members linked together, the fire resistance of the joints has to be evaluated. This is covered in Chapter 7.

Chapter 8 is dedicated to the presentation of the computer software, Elefir-EN that has been developed by the authors to allow fast, user-friendly and reliable application of the simple calculation models given in the Eurocodes and discussed in Chapter 5. A copy of this software is included with each copy of this book.

Chapter 9 presents a complete worked example. Although the structure is an academic case study, it addresses most of the rules described in earlier chapters and presents, in an integrated manner, the complete sequence of tasks that have to be performed to determine the fire resistance of a steel structure.

Some annexes contain additional information that may be important but has been detached from the main text for clarity reasons.

Annex A gives the thermal properties of carbon steel and stainless steel to be used for calculating the temperatures in steel members. For the standard fire, tables and graphs are presented that give the value of the uniform temperature at different times in sections with defined section factors, as a function of the thermal insulation if present. Some information on the thermal properties of different insulating products is also given.

Annex B explains how the different inputs that have to be introduced in natural fire models can be determined. This annex also explains how to determine the Rate of Heat Release curve.

Annex C presents the mechanical properties of carbon steel and stainless steel.

Annex D is dedicated to the width-thickness ratio for evaluating the class of steel sections in the fire situation.

Annex E gives tables with values of the section factors for unprotected and protected I and H European hot rolled steel profiles.

Finally, Annex F presents tables with the cross sectional classification of European hot rolled IPE and HE profiles subjected to pure compression, pure bending and combined compression and bending about major and minor axis.

This book is the second volume of the ECCS Eurocode Design Manuals that aim to cover all aspects of design of steel and composite structures. It has the ambition to serve as a design guide. This means that, although the necessary background is mentioned as well as the theory and main hypotheses that are at the base of the design equations, the main objective is not to discuss these hypotheses in detail but to provide guidance to the reader for understanding how the design equations proposed in the Eurocodes have to be used in different situations. The reader should be able to transfer the knowledge gained from this book directly into practice.

Those who wish to see more information on the background to these rules, or more information on the way that steel structures are designed in

1. INTRODUCTION

other parts of the world (namely in North America) should refer to, for example, Franssen *et al* (2009).

Those who wish to see more information about structural design in the fire situation in general, for various materials, should refer to, for example, Buchanan (2001), Purkiss (2007) or Wang (2002).

Chapter 2

MECHANICAL LOADING

2.1. GENERAL

At room temperature, different load combinations must be considered for different situations. For example, the load combinations are different for verifying serviceability and ultimate limit states. The occurrence of a fire creates a situation that is different to those at ambient temperature and consequently specific and different load combinations must be considered for the fire limit state. Specific design values of actions have to be taken into account for the fire situation. These values are usually lower than the values considered for ambient temperature design. This is because the fire is a rare event and a higher probability of failure is accepted in the fire situation than in normal conditions. For example, society will probably accept that one in every one hundred buildings suffers from a fire collapse whereas such a probability of failure would certainly not be accepted in normal conditions.

7

2.1.1. General rule

The fire situation is classified as an accidental situation in EN 1990 "Basis of structural design". The design effect of actions for the fire situation, $E_{fi,d,t}$, can be obtained using the combination of actions for accidental situation given by Eq. (2.1a) or Eq. (2.1b).

$$\sum_{j \geq 1} G_{k,j} + P + A_d + \psi_{1,1} Q_{k,1} + \sum_{i \geq 2} \psi_{2,i} Q_{k,i} \quad (2.1a)$$

$$\sum_{j \geq 1} G_{k,j} + P + A_d + \sum_{i \geq 1} \psi_{2,i} Q_{k,i} \quad (2.1b)$$

2. MECHANICAL LOADING

In these equations, the symbol + means that the different loads have to be combined. They are not added in a mathematical sense because they are of different nature, as explained below.

All permanent actions must be taken into account with their characteristic value, $G_{k,j}$. As will be explained below, in the fire situation, significantly lower values of variable loads are considered than at ambient temperature. This makes even low permanent loads relatively more important in the fire situation than under normal conditions. It may be essential, for example, to evaluate as precisely as possible the dead weight of the air conditioning ducts, false ceilings, etc., especially in light weight structures that are designed at room temperature for high variable loads (e.g. snow load).

The characteristic values of variable actions are denoted by $Q_{k,i}$ in Eq. (2.1a) and Eq. (2.1b).

The prestressing load P must also be considered if present. However, methods of analysis for which the theory says that the prestressing load has no influence can still be used, for example when determining the ultimate bending resistance of a prestressed section using a plastic model.

The term A_d represents the indirect fire actions. These are the variations of effects of actions induced by restrained thermal expansion. They are of a different nature to the other actions. Whereas G and Q represent "external" loads applied on the structure, A_d represents "internal" effects of actions, such as axial forces, shear forces and bending moments, that appear in the elements because of the temperature increase. In fact, they have more to do with the structural analysis than with the applied loads. These indirect effects of actions will be discussed in more details in Section 2.3.

The difference between Eq. (2.1a) and Eq. (2.1b) lies in the coefficient that is applied to the leading variable action, $Q_{k,1}$. The coefficient for the frequent value ψ_1 is considered in Eq. (2.1a), whereas the coefficient for the quasi-permanent value ψ_2 is considered in Eq. (2.1b). Table 2.1 gives the recommended values for the coefficients ψ_1 and ψ_2 . The choice to use one or the other option is left to each Member State and the decision must be given in the relevant National Annex. Some countries have adopted Eq. (2.1a) that was present in the ENV version of Eurocode 1 Part 1-2, while other countries have adopted Eq. (2.1b) because this is consistent with the accidental design for the seismic situation. Other countries have decided to take Eq. (2.1b) except when the leading action is wind, in which case

Eq. (2.1a) should be used. This is because the quasi-permanent value of the wind is equal to 0.0, which is not a problem in a seismic design where horizontal actions are induced by the earthquake, but will lead to the situation where no horizontal action is considered in the fire situation if Eq. (2.1b) is applied.

Table 2.1 – Recommended values of the coefficients ψ for buildings

Action	ψ_1	ψ_2
Live loads in buildings;		
category A: domestic, residential	0.5	0.3
category B: offices	0.5	0.3
category C: congregation areas	0.7	0.6
category D: shopping	0.7	0.6
category E: storage	0.9	0.8
category F: traffic, vehicles ≤ 30 kN	0.7	0.6
category G: traffic, vehicles ≤ 160 kN	0.5	0.3
category H: roofs	0.0	0.0
Snow loads		
Finland, Iceland, Norway, Sweden	0.5	0.2
Other countries, altitude $H > 1\ 000$ m	0.5	0.2
Other countries, altitude $H \leq 1\ 000$ m	0.2	0.0
Wind loads	0.2	0.0

Decrease of applied load due to combustion should not be taken into account. Such a reduction would have limited consequences for steel elements because, in most situations, combustion takes place underneath the structural elements that are subjected to the effects of the fire and these elements would thus not be affected by the load reduction.

Reduction of the snow load because of melting from the action of the fire should be assessed separately. This provision has to be distinguished from the fact that, in most regions, the quasi-permanent value of the snow load is equal to 0. If the snow load applied in the fire situation is equal to 0, there is no question about melting. But, if snow load is present, it must not be considered that it will melt from the fire, except if this is assessed explicitly.

Actions resulting from industrial operations need not be considered, as industrial operations are normally interrupted during a fire. There may yet be some special cases where it is impossible to interrupt an industrial process immediately. A turbine for production of electricity, for example, may

2. MECHANICAL LOADING

require a significant amount of time before the rotation of the rotor comes to a rest. This should be assessed on a case per case basis.

Impact resulting from the collapse of other structural elements or machinery may need to be considered. Fire walls may be required to resist a horizontal load according to EN 1363-2.

Simultaneous occurrence with other independent accidental actions need not be considered. It is very unlikely that, for example, an earthquake will happen during the relatively short duration of a fire in a building. However, the contrary is not true; fires are very likely to develop after an earthquake has hit an urban zone. It may thus be necessary to consider the scenario of a fire after an earthquake but nothing is mentioned in the Eurocode about this scenario. This field is still a topic of ongoing research.

2.1.2. Simplification 1

In cases where indirect fire actions are non existent, such as, for example, in statically determinate structures, or need not be considered (which may be the case for the analysis of elements or substructures, see Section 2.3), the mechanical loads determined from Eq. (2.1) are constant during the fire. The value of the loads determined in the fire at time $t = 0$ does not change during the fire and the effects of actions determined at time $t = 0$ may be considered as constant throughout fire exposure¹.

If a global structure is being analysed, the external loads $G_{k,j}$ and $Q_{k,i}$ are usually considered as constant. The indirect effects of action A_d and, if present, the prestressing loads P may vary during the fire.

2.1.3. Simplification 2

This further simplification can only be used in those cases where indirect fire actions need not be considered.

Very often, the design of the structure has been performed at ambient temperature before the fire situation is considered. The effects of actions in the normal situation E_d have thus been determined in the structure for the various load combinations that must be considered at room temperature. If the determination of the effects of actions is a long and painful process², it

¹ Except if 2nd order effects from large displacements are considered explicitly.

² This is less and less often the case, with the generalisation of software for the elastic structural analysis of structures.

may be worth capitalising on these results. Eurocode 1 allows considering that the effects of action in the fire situation $E_{fi,d}$ are obtained, for each load combination, from the multiplication of the effects determined at room temperature E_d by a scalar reduction factor η_{fi} , see Eq. (2.2).

$$E_{fi,d,t} (= E_{fi,d,t=0} \text{ also noted } E_{fi,d}) = \eta_{fi} E_d \quad (2.2)$$

According to Eurocode 3, the reduction factor can be determined from Eq. (2.3).

$$\eta_{fi} = \frac{G_k + \psi_{fi} Q_{k,1}}{\gamma_G G_k + \gamma_{Q,1} Q_{k,1}} \quad (2.3)$$

In this equation, G_k is called in Clause 2.4.2 (3) of Eurocode 3 *the characteristic value of a permanent action*. It must probably be understood as *the sum of all permanent actions* in agreement with Eq. (2.1). There is indeed no reason why *one* permanent action would be considered and not all permanent actions. The partial safety factors γ_G and $\gamma_{Q,1}$ are the partial safety factors used for the permanent action and for the leading variable action at room temperature. The coefficient ψ_{fi} is taken as ψ_1 or ψ_2 depending on the choice made in the National Annex between Eq. (2.1a) and (2.1b), see Section 2.1.1.

If the National Annex states that the design load at room temperature should be calculated in accordance with Eqs. (6.10a) and (6.10b) rather than Eq. (6.10) from EN 1990, then a slightly different expression to Eq. (2.3) should be used. This alternative expression is given in Eurocode 3.

Application of Eqs. (2.2) and (2.3) yields the same distribution of the effects of actions in the structure as application of Eq. (2.1) only if there is one single variable load and if the permanent load and the variable load have the same distribution and direction. This is the case, for example, if both loads are either a vertical force on a column, or a uniformly distributed load on a beam. In other cases, application of Eqs. (2.2) and (2.3) yields approximate results. In some cases, it is not possible to apply the simplification described in this section directly, for example when the permanent action and the variable action have different units, kN and kN/m for example. It is nevertheless possible to apply the simplification if all actions present in Eq. (2.3) are replaced by the total value of the force generated by each action. Concentrated loads should for example be summed and distributed loads should be integrated on the length of application, thus

2. MECHANICAL LOADING

leading also to forces. In fact, the sign + present in Eq. (2.3) should probably be written as ‘+’, as in Eq (2.1)¹.

If the reduction factor η_{fi} is given in tabulated data as a reference load level, this load level is the ratio between the actions in the fire situation $E_{fi,d}$ and the design value of the resistance of the member at room temperature R_d , see Eq. (2.4).

$$\eta_{fi} = \frac{E_{fi,d}}{R_d} \quad (2.4)$$

Eq. (2.4) can be used in a verification process, when the size of the member is known and it is possible to calculate R_d . In a design process, when the size of the section has to be determined, it is not possible to calculate R_d and the load level has to be determined as the ratio between loads applied in the fire situation and loads applied at room temperature, either exactly, on the base of Eqs. (2.1) and (2.2), or in an approximate manner, from Eq. (2.3). Tabulated data are given in Eurocode 4 for composite steel-concrete members, not in Eurocode 3. Tabulated data may nevertheless be present in National Annexes as additional not contradictory information to the Eurocode.

2.1.4. Simplification 3

12

The maximum value of the load level η_{fi} given by Eq. (2.3) is obtained when the structure is subjected to permanent loads only. Assuming a value of 1.35 for γ_G yields a maximum value of η_{fi} equal to $1/1.35 = 0.74$. The load level in the fire situation is reduced by variable loads, particularly when the ratio $Q_{k,1}/G_k$ is high and ψ_{fi} is low. Except for very high values of ψ_{fi} , the value of the load level is usually not higher than 0.65.

This is why, as a further simplification, Eurocode 3 allows the value of $\eta_{fi} = 0.65$ to be used for most situations. There is no need to apply Eq. (2.3).

For load category E according to EN 1991-1-1 (i.e., areas susceptible of accumulation of goods, including access areas), the recommended value of η_{fi} is 0.7.

¹ If some actions are concentrated moments, in kNm for example, Eq. (2.3) can definitively not be applied.

2.2. EXAMPLES

For all the examples given in this section, the values of the loads are characteristic values. Furthermore, it has been considered that $\gamma_G = 1.35$ and $\gamma_Q = 1.5$.

Example 2.1: Simply supported beam with uniformly distributed loads.

A simply supported beam in a residential building, with a span of 6 meters, is subjected to a permanent load of 12 kN/m and a live load of 8 kN/m. Find the maximum bending moment in the fire situation taking $\psi_{fi} = \psi_2$.

According to Section 2.1.1

$$q_{fi,Ed} = 12 + 0.3 \times 8 = 14.40 \text{ kN/m, see Eq. (2.1b) and Table (2.1)}$$

$$M_{fi,Ed} = 14.40 \times 6^2 / 8 = 64.80 \text{ kNm}$$

According to Section 2.1.3,

at room temperature:

$$q_{Ed} = 1.35 \times 12 + 1.5 \times 8 = 28.20 \text{ kN/m}$$

$$M_{Ed} = 28.20 \times 6^2 / 8 = 126.90 \text{ kNm}$$

Note: *this value is normally available from the design at room temperature.*

$$\begin{aligned} \eta_{fi} &= (12 + 0.3 \times 8) / (1.35 \times 12 + 1.5 \times 8) \\ &= 14.40 / 28.20 = 0.511, \text{ see Eq. (2.3)} \end{aligned}$$

$$M_{fi,Ed} = 0.511 \times 126.90 = 64.80 \text{ kNm}$$

According to Section 2.1.4

$$M_{fi,Ed} = 0.65 \times 126.90 = 82.49 \text{ kNm (overestimation of 27 \%)}$$

Example 2.2: Simply supported beam with concentrated load.

A simply supported beam in a residential building, with a span of 6 meters, is subjected to a permanent load of 12 kN/m and a concentrated load of 48 kN at mid span. Find the maximum bending moment in the fire situation taking $\psi_{fi} = \psi_2$.

2. MECHANICAL LOADING

According to Section 2.1.1

$$q_{fi,Ed} = 12 \text{ kN/m, see Eq. (2.1b)}$$

$$P_{fi,Ed} = 0.3 \times 48 = 14.40 \text{ kN, see Eq. (2.1b) and Table (2.1)}$$

$$M_{fi,Ed} = 12 \times 6^2 / 8 + 14.40 \times 6 / 4 = 75.60 \text{ kNm}$$

According to Section 2.1.3

at room temperature:

$$q_{Ed} = 1.35 \times 12 = 16.20 \text{ kN/m}$$

$$P_{Ed} = 1.5 \times 48 = 72 \text{ kN}$$

$$M_{Ed} = 16.20 \times 6^2 / 8 + 72 \times 6 / 4 = 180.90 \text{ kNm}$$

Note: *this value is normally available from the design at room temperature.*

$$\begin{aligned} \eta_{fi} &= (12 \times 6 + 0.3 \times 48) / (1.35 \times 12 \times 6 + 1.5 \times 48) \\ &= 86.4 / 169.2 = 0.511, \text{ see Eq. (2.3)} \end{aligned}$$

Note: *the distributed load has been multiplied by the span in order to obtain the same unit as the concentrate load.*

$$M_{fi,Ed} = 0.511 \times 180.90 = 92.37 \text{ kNm (overestimation of 22\%)}$$

According to Section 2.1.4

$$M_{fi,Ed} = 0.65 \times 126.90 = 82.49 \text{ kNm (overestimation of 9\%)}$$

2.3. INDIRECT ACTIONS

Indirect fire actions are effects of actions induced in the elements by restrained thermal expansion. These indirect actions are mentioned in different clauses of Eurocode 1 and Eurocode 3.

According to clause 4.1 (1)P of Eurocode 1, indirect fire actions have to be considered except if one of the two following conditions is met:

- 1) They may be recognised a priori to be either negligible or favourable. Indirect actions cannot develop in statically determinate structures but no specific guidance is given in the Eurocodes on how to judge whether or not the indirect fire actions are negligible or favourable in a statically
-

undeterminate structure. A designer will therefore have to substantiate his case if he wants to use this clause to ignore indirect fire actions.

- 2) They are accounted for by conservatively chosen support models and boundary conditions, and/or implicitly considered by conservatively specified fire safety requirements. The recommendations given in various clauses related to boundary conditions for elements, substructures or global structure show how the part of this clause related to support models and boundary conditions must be applied in practice. No guidance is given in this clause about conservatively specified fire safety requirements.

The following are examples of restrained expansion leading to indirect fire actions that may be considered:

- a) Constrained thermal expansion of members subjected to the fire, e.g. columns in multi-storey frame structures with stiff walls. Such effects can also appear in members subjected to localised fires.
- b) Differing thermal expansion between the upper part and the lower part of a section within statically indeterminate members, e.g. continuous floor slabs or beams.
- c) Non-linear thermal gradients within cross sections giving internal stresses.
- d) Thermal expansion of adjacent members, such as the expansion of slabs that result in displacements of columns head.
- e) Thermal expansion of members affecting other members outside the fire compartment.

Indirect actions from adjacent members (see cases d) and e)) need not be considered when fire safety requirements refer to *members* under *standard fire* conditions. Although it is not pointed out in the Eurocode, it seems as if a standard fire constitutes what is called in exception 2) *conservatively specified fire safety requirements*. It seems surprising that it is allowed to neglect a fire action that, in some cases, is not negligible or favourable. However, it has to be considered that the mechanical analysis of an element under standard fire condition does not represent the true behaviour of the element in the real structure. The aim of such element analysis is simply to represent, in the mechanical model, what would occur if this isolated element was tested in a furnace under this fire curve. In such a test, indirect effects from adjacent members are obviously not considered. If the fire and the mechanical model (an isolated element) are arbitrary and do not represent the real situation, why should there be an attempt to create a more accurate model by introducing the indirect effects of actions. As mentioned by Professor A. Buchanan from

2. MECHANICAL LOADING

Canterbury University in his talks, there must be a *consistent level of crudeness*.

When analysing an element in conditions other than the standard fire exposure, indirect fire actions are not to be considered except those resulting from thermal gradients through the section.

In the Eurocode nomenclature, the expression *effect of actions* refers to internal forces such as axial forces or bending moments. Thermal expansion has another consequence than a variation in effects of action; it may induce a variation in displacements, especially in statically determinate structures. One case that is particularly sensitive to thermal gradients is that of an axially loaded column or wall. Especially in cantilevered columns, thermal gradients lead to large displacements that can be very detrimental for overall stability. It has been shown (Anderberg & Oredsson, 1995) that, for slender simply supported columns, a linear thermal gradient through the thickness of the section can lead to a fire resistance lower than that of a uniform temperature equal to the maximum value of the temperature with the thermal gradient.

When analysing part of a structure, also called a *substructure*, appropriate support and boundary conditions should be applied at the boundary between the substructure and the remaining structure. At the boundary, a choice must be made for each displacement and rotational degree of freedom. Either the displacement is fixed, or the force linked to this degree of freedom is fixed. If the force is fixed, its value is equal to the effect of actions that comes from an analysis of the entire structure in the fire situation at time $t = 0$. This means that indirect fire actions are not taken into account at this stage¹. It is the responsibility of the designer to define the substructure in such a way that the approximation of constant boundary conditions is realistic, see Clause 2.4.3 (3) in Eurocode 3. When the support and boundary conditions have been fixed, the analysis of the substructure in the fire situation is performed and any indirect fire actions that may develop in the substructure must be considered. A detailed procedure for a substructure analysis is described by Franssen *et al* (2009). An example of this procedure is presented in Chapter 9.

In a global analysis, i.e., the analysis of the entire structure, indirect fire actions must be considered throughout the structure. Because global analyses can only be performed with a general calculation model, this implies that such a model must take into account all indirect fire actions.

¹ It is also accepted, as an alternative, to determine the effects of action for normal temperature, see Section 2.1.3.

Chapter 3

THERMAL ACTION

3.1. GENERAL

The thermal action represents the action of the fire on the structure and Eurocode 1 gives different possibilities for the thermal action to be considered.

One possibility consists of time-temperature relationships. These are relationships that give the evolution as a function of time of a temperature that represents the environment¹ surrounding the structure. This temperature, together with the appropriate boundary conditions, can be used to determine the heat flux transmitted from the environment to the structure.

Another possibility consists of relationships that give directly the heat flux impinging on the structure. This impinging heat flux is then combined with the flux reemitted by the structure to determine the evolution of the temperatures in the structure.

In Eurocode 1, the distinction is made between *nominal temperature-time curves* comprising the standard temperature-time curve, the hydrocarbon curve and the external fire curve, on one hand, and *natural fire models* on the other hand.

The thermal action to be used is normally a legal requirement defined by the country or region where the building is located and depending on its size, use and occupancy.

Some countries give prescriptive requirements that define both the time-temperature curve and the time (called *the fire resistance*) the structure must survive when exposed to this curve. For example, a hotel located in the country A must have a resistance to the standard curve of 60 minutes,

¹ i.e., the fire, the hot gases and the walls of the compartment.

3. THERMAL ACTION

whereas a railway station located in the country B must have a resistance to the hydrocarbon curve of 30 minutes. In such cases, the designer must ensure that the structure complies with the requirement and he must use the prescribed time-temperature curve.

In other countries or regions, the legal environment may be more flexible and allow the designer to make a performance based design. In such a case, it is the responsibility of the designer to use an appropriate representation of the fire, although the Eurocode gives some guidance in the form of limits of application to some of the proposed natural fire models. Ideally, such natural fire models should be used with performance based requirements linked, for example, to the time required for evacuation or intervention. It is recommended to have approval of the authority having jurisdiction on the design fire and design scenario before starting any performance-based design.

3.2. NOMINAL TEMPERATURE-TIME CURVES

Temperature-time curves are analytical functions of time that give a temperature. The term *curve* comes from the fact that these functions are continuous and can be used to draw a curve in a time-temperature plane.

They are called *nominal* because they are not supposed to represent a real fire. They have to be considered as conventional, or arbitrary, functions. This is why the term *fire curve* is rather inappropriate because it seems to imply that the temperature is the temperature of a fire. In fact, the temperature is of the same order of magnitude as temperatures observed in fires. Because they are conventional, such relationships are thus to be used in a prescriptive regulatory environment. Any requirement that is expressed in terms of a nominal curve is thus also prescriptive and, in a sense, arbitrary. The resistance of a structure to a nominal fire should not be compared to the duration required for evacuation or intervention.

Eurocode 1 proposes three different nominal temperature-time curves.

The *standard temperature-time curve* is the one that has been historically used, and it is still used today, in standard fire tests to rate structural and separating elements. It is used to represent a fully developed fire in a compartment. It is often referred to as *the ISO curve* because the expression was taken from the ISO 834 standard. This standard curve is given by Eq. (3.1).

$$\theta_g = 20 + 345 \log_{10}(8t + 1) \quad (3.1)$$

where θ_g is the gas temperature in °C and t is the time in minutes.

When a requirement is expressed in a legal document as Rxx, with xx equal to 30 or 60 minutes for example, this implicitly means that the standard fire curve has to be used to evaluate the duration fire resistance of the structural elements.

The *external time-temperature curve* is used for the outside surface of separating external walls of a building which are exposed to a fire that develops outside the building or to the flames coming through the windows of a compartment situated below or adjacent to the external wall.

Note: *this curve should not be used for calculating the effects of a fire on an external load bearing structure, for example steel beams and columns, located outside the envelope of the building. The thermal attack on external structural steel elements is described in Annex B of Eurocode 1.*

The external curve is given by Eq. (3.2).

$$\theta_g = 20 + 660 \left(1 - 0.687e^{-0.32t} - 0.313e^{-3.8t} \right) \quad (3.2)$$

The *hydrocarbon time-temperature curve* is used for representing the effects of a hydrocarbon type fire. It is given by Eq. (3.3).

$$\theta_g = 20 + 1080 \left(1 - 0.325e^{-0.167t} - 0.675e^{-2.5t} \right) \quad (3.3)$$

19

The standard and the hydrocarbon curves are compared in Fig. 3.1. It shows that the hydrocarbon curve increases very quickly and reaches a constant value of 1100 °C after half an hour, whereas the standard curve increases more progressively but keeps on increasing with time.

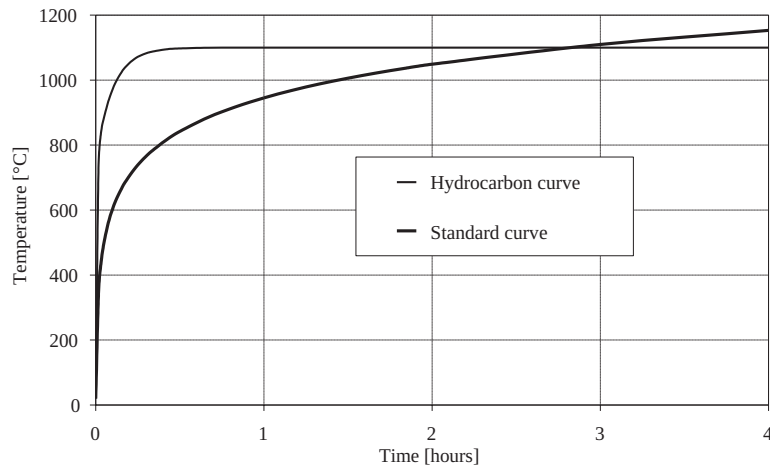
When the environment is represented by a gas temperature, as is the case for nominal curves, Eq. (3.4) should be used to model the heat flux at the surface of a steel element.

$$\dot{h}_{net} = \alpha_c (\theta_g - \theta_m) + \Phi \varepsilon_m \varepsilon_f \sigma \left[(\theta_r + 273)^4 - (\theta_m + 273)^4 \right] \quad (3.4)$$

where α_c is the coefficient of convection which is taken as 25 W/m²K for the standard or the external fire curve and 50 W/m²K for the hydrocarbon curve, θ_g is the gas temperature in the vicinity of the surface either calculated from Eqs. (3.1), (3.2) or (3.3) or taken as 20 °C, θ_m is the surface temperature of the

3. THERMAL ACTION

steel member (the evolution of which has to be calculated, see Chapter 4), Φ is a configuration factor that is usually taken equal to 1.0 but can also be calculated using Annex G of Eurocode 1 when so-called position or shadow effects have to be taken into account, ε_m is the surface emissivity of the member taken as 0.7 for carbon steel, 0.4 for stainless steel and 0.8 for other materials, ε_f is the emissivity of the fire, in general taken as 1.0, σ is the Stephan Boltzmann constant equal to $5.67 \times 10^{-8} \text{ W/m}^2\text{K}^4$ and θ_r is the radiation temperature of the fire environment taken as equal to θ_g in the case of fully engulfed members.



20

Figure 3.1 – Comparison between two nominal temperature-time curves

Example 3.1: How long will it take before the standard curve reaches a temperature of 1000 °C?

The answer can be determined by solving Eq. (3.1), in which θ_g is set to 1000 °C. This yields the following equation:

$$t = \frac{10^{\frac{1000-20}{345}} - 1}{8} = 86.5 \text{ min}$$

Example 3.2: Using the international system of units, write a procedure that returns the value of the hydrocarbon time-temperature curve for a given time.

```

Procedure hydrocarbon(time,temperature)
c  input          time          time in seconds
c  intermediate   time_m        time in minutes
c                   temp_c       temperature in degrees Celsius
c  output         temperature    temperature in degrees Kelvin
Implicit none
Real: time, time_m, temp_c, temperature
time_m = time/60.
temp_c=20.+1080.*(1-0.325*exp(-0.167*time_m)-0.675*exp(-2.5*time_m))
temperature = temp_c +275.15
end procedure

```

3.3. PARAMETRIC TEMPERATURE-TIME CURVES

Parametric temperature-time curves are analytical functions that give the evolution of the gas temperature in a compartment as a function of time, based on parameters that represent the most important physical phenomena that influence the development of a compartment fire. Such a parametric curve is described in Annex A of Eurocode 1. It is valid for fire compartments up to 500 m² of floor area, without openings in the roof and for a maximum compartment height of 4 meters.

The three parameters that describe the curve are:

1) A parameter b which accounts for the thermal properties of the enclosure. It is related to the faculty of the boundaries of the compartment (walls, floor and ceiling) to absorb part of the energy released by the fire. It is calculated using Eq. (3.5) when the walls are made of a single material:

$$b = \sqrt{c\rho\lambda} \quad (3.5)$$

where c is the specific heat of the material forming the boundaries in J/kgK, ρ is the density of the material, in kg/m³, and λ is the thermal conductivity of the material, in W/mK. Table of the Annex A.9 gives the values of these properties for some enclosure surface materials.

3. THERMAL ACTION

As a simplification, these three properties may be taken at room temperature.

When different parts of the walls, the floor or the ceiling are made from different materials, a global value is calculated for the parameter b of the compartment by factoring the value of each part with respect to its area (openings not included), see Eq. (3.6).

$$b = \frac{\sum b_i A_i}{\sum A_i} \quad (3.6)$$

where b_i is the value of the factor for part i and A_i is the area of part i , openings not included.

When a surface is made of different layers of material, only the value b of the material of the innermost layer is considered, provided this value is lower than the value of the second layer of material. If the b value of the inner layer is higher than the b value of the second layer, then the b value of the inner layer may be used if this layer is thick; if this layer is thin, the influence of the second layer is also taken into account following the procedure given by Eq. (A.4) in the Eurocode.

The parameter b should have a value between 100 and 2200 J/m²s^{1/2}K.

The parameter b is based on the theory of heat penetration by conduction in a semi-infinite medium. In a wall made of two layers of gypsum board separated by a cavity filled with air, for example, applying the equations of the Eurocode with the values of c , ρ and λ of the air would not be correct because heat travels by radiation and not by conduction in the air cavity. Similarly, it would not be correct to apply this model for a wall made of a thin steel sheet, in an industrial building for example. This model would be valid for steel only if the steel wall has infinite thickness, which is not practical (furthermore b for steel is around 13400, which is in excess of the admissible value of 2200).

2) A parameter O that accounts for the openings in the vertical walls. Higher values of this parameter mean more ventilation for the compartment. The value of this parameter has to be in the range 0.02 to 0.20 for the model of the Eurocode to be applicable. If a single rectangular opening is present in the compartment, the opening factor is calculated using Eq. (3.7). This equation has been derived from the integration of the Bernoulli equation for a pressure differential between the outside and the inside of the compartment that varies linearly as a function of the vertical position.

$$O = A_v \sqrt{h} / A_t \quad (3.7)$$

where A_v is the area of the opening, h is the height of the opening and A_t is the total area of the enclosure (walls, ceiling and floor), including the openings.

Eq. (3.7) shows that, for a given area, a vertically oriented opening is more efficient in venting the compartment than a horizontally oriented opening. When several rectangular openings are present in the compartment, the opening factor is calculated from Eq. (3.8).

$$O = A_v \sqrt{h_{eq}} / A_t \quad (3.8)$$

where A_v is the total area of the vertical openings, h_{eq} is the averaged height of the window openings, calculated from Eq. (3.9).

$$h_{eq} = \sum_i A_{vi} h_i / A_v \quad (3.9)$$

3) The last parameter is the design fire load density related to the total area of the enclosure $q_{t,d}$: floor, ceiling and walls, openings included. Annex E of Eurocode 1 allows determining the design value related to the floor area $q_{f,d}$ on the basis of the type of occupation of the compartment and the presence of active fire protection measures. Both values are related by Eq. (3.10).

$$q_{t,d} = q_{f,d} A_f / A_t \quad (3.10)$$

where A_f is the floor area and A_t is the total area of the enclosure.

23

The model is valid for values of $q_{t,d}$ between 50 and 1000 MJ/m².

Application of the model starts by calculating an expansion coefficient Γ from Eq. (3.11).

$$\Gamma = \left(\frac{O/0.04}{b/1160} \right)^2 \quad (3.11)$$

The evolution of temperature during the heating phase is given by Eq. (3.12) as a function of an expanded time t^* given by Eq. (3.13).

$$\theta_g = 20 + 1325 \left(1 - 0.324e^{-0.2t^*} - 0.204e^{-1.7t^*} - 0.472e^{-19t^*} \right) \quad (3.12)$$

$$t^* = \Gamma t \quad (3.13)$$

where t is the time in hours.

3. THERMAL ACTION

The curve that can be plot from Eq. (3.12) as a function of t^* is very close to the standard temperature-time curve. Eq. (3.13) shows that, when Γ is greater than 1¹, the temperature increase as a function of the real time t is faster than for lower values of Γ .

The duration of the heating phase t_{\max} is given, in hours, by Eq. (3.14).

$$t_{\max} = 0.0002q_{t,d}/O \quad (3.14)$$

This value has to be compared with a limit value t_{lim} that depends on the growth rate associated to the occupancy of the compartment, see Table (3.1).

Table 3.1 – Values of t_{lim} as a function of the growth rate

Growth rate	t_{lim} in minutes	t_{lim} in hours
<i>Slow</i> (transport (public space))	25	0.417
<i>Medium</i> (dwelling, hospital room, hotel room, office, classroom of a school)	20	0.333
<i>Fast</i> (library, shopping centre, theatre/cinema)	15	0.250

The comparison between the value calculated for t_{\max} and the value of t_{lim} can lead to two different situations:

- Either $t_{lim} \leq t_{\max}$ and the fire is ventilation controlled. The procedure for this situation is explained below.

The value of the gas temperature at the end of the heating phase, θ_{\max} , is calculated by substituting the value of t_{\max} for t in Eq. (3.13) and (3.12).

The expanded time that corresponds to the maximum time is calculated from Eq. (3.15).

$$t_{\max}^* = \Gamma t_{\max} \quad (3.15)$$

The time-temperature in the cooling phase is given by:

$$\theta_g = \theta_{\max} - 625(t^* - t_{\max}^*) \quad \text{for } t_{\max}^* \leq 0.5 \quad (3.16a)$$

$$\theta_g = \theta_{\max} - 250(3 - t_{\max}^*)(t^* - t_{\max}^*) \quad \text{for } 0.5 < t_{\max}^* < 2.0 \quad (3.16b)$$

$$\theta_g = \theta_{\max} - 250(t^* - t_{\max}^*) \quad \text{for } 2.0 \leq t_{\max}^* \quad (3.16c)$$

¹ Highly ventilated compartments or compartments with lightweight walls

- Or $t_{\max} < t_{lim}$ and the fire is fuel controlled. The procedure for this situation is explained below:

Eq. (3.17) is used instead of Eq. (3.13) to compute the evolution of the temperature during the heating phase.

$$t^* = \Gamma_{lim} t \quad (3.17)$$

with

$$\Gamma_{lim} = \left(\frac{O_{lim}/0.04}{b/1160} \right)^2 \quad (3.18)$$

and

$$O_{lim} = 0.0001 q_{t,d} / t_{lim} \quad (3.19)$$

If $O > 0.04$ and $q_{t,d} < 75$ and $b < 1160$, then Γ_{lim} in Eq. (3.18) has to be multiplied for the factor k given by Eq. (3.20).

$$k = 1 + \left(\frac{O - 0.04}{0.04} \right) \left(\frac{q_{t,d} - 75}{75} \right) \left(\frac{1160 - b}{1160} \right) \quad (3.20)$$

The expanded time that corresponds to the time of maximum temperature is calculated from Eq. (3.21).

$$t_{\max}^* = \Gamma_{lim} t_{lim} \quad (3.21)$$

The value of the gas temperature at the end of the heating phase, θ_{\max} , is calculated by substituting the value of t_{\max}^* for t^* in Eq. (3.12).

25

The time-temperature in the cooling phase is given by:

$$\theta_g = \theta_{\max} - 625(t^* - \Gamma t_{lim}) \quad \text{for } t_{\max}^* \leq 0.5 \quad (3.22a)$$

$$\theta_g = \theta_{\max} - 250(3 - t_{\max}^*)(t^* - \Gamma t_{lim}) \quad \text{for } 0.5 < t_{\max}^* < 2.0 \quad (3.22b)$$

$$\theta_g = \theta_{\max} - 250(t^* - \Gamma t_{lim}) \quad \text{for } 2.0 \leq t_{\max}^* \quad (3.22c)$$

When applying Eq. (3.22), t^* and t_{\max}^* are calculated from Eqs. (3.13) and (3.15), and not from Eqs. (3.17) and (3.21).

It has to be noted that there is a discontinuity in the model at the transition from a fuel controlled fire to a ventilation controlled fire, because of the different factors being present in Eq. (3.14) and Eq. (3.19). An infinitely

3. THERMAL ACTION

small variation of a parameter can produce two time-temperature curves that are not close to each other. In other words, when t_{\max} is exactly equal to t_{lim} , the equations for a ventilation controlled fire lead to a fire curve that is different from the one obtained by the equations of a fuel controlled fire.

When a parametric fire model is used, the heat flux at the surface of a steel member is calculated from Eq. (3.4) with a coefficient of convection α_c equal to 35 W/m²K.

Example 3.3: Calculate and plot the parametric time-temperature curve for the room described below.

The room is a bedroom in a hotel. The plan view is rectangular with dimensions of 3.20 m by 6.40 m. The floor to ceiling height is 2.60 m. The floor and the ceiling are made of normal weight concrete and the walls are made of normal weight concrete covered by a 12.6 mm thick layer of gypsum. The only opening is a door of size 1.10 m by 2.20 m.

b for the floor and ceiling, see Eq. (3.5):

$$b = (1000 \times 2300 \times 1.6)^{0.5} = 1918 \text{ J/m}^2\text{s}^{0.5}\text{K}$$

$$\text{Area} = 2 \times 3.2 \times 6.4 = 40.96 \text{ m}^2$$

26

b for the walls:

$$b = (1000 \times 1150 \times 0.488)^{0.5} = 749 \text{ J/m}^2\text{s}^{0.5}\text{K}$$

Note: because the factor b of the gypsum cover is lower than the factor of the concrete wall, only the factor of the layer exposed to the fire is considered for the walls.

$$\text{Area} = 2 \times (3.2 + 6.4) \times 2.6 - 1.1 \times 2.2 = 47.50 \text{ m}^2$$

b for the compartment, see Eq. (3.6):

$$b = (1918 \times 40.96 + 749 \times 47.50) / (40.96 + 47.50) = 1290 \text{ J/m}^2\text{s}^{0.5}\text{K}$$

Opening factor, see Eq. (3.7):

$$O = 1.10 \times 2.20 \times 2.20^{0.5} / 90.88 = 0.0395 \text{ m}^{0.5}$$

Expansion coefficient, see Eq. (3.11):

$$\Gamma = \left(\frac{0.0395/0.04}{1290/1160} \right)^2 = 0.788$$

Note: a value of Γ lower than 1.0 means that the fire curve will increase more slowly than the standard time-temperature curve.

Design fire load, see Eq. (3.10): table E.4 of Eurocode 1 gives for hotels a value of $q_{f,k}$ equal to 377 MJ/m². Assuming that the influence of active measures is not taken into account, this leads to $q_{f,d} = q_{f,k} = 377$ MJ/m². A combustion factor could be taken as $m = 0.8$ if the fire load is known to be cellulosic. A value of the factor $m = 1.0$ was nevertheless considered here.

$$q_{t,d} = 377 \times (3.2 \times 6.4) / 90.88 = 84.96 \text{ MJ/m}^2$$

Duration of the heating phase, see Eq. (3.14):

$$t_{\max} = 0.0002 \times 84.96 / 0.0395 = 0.43 \text{ hour (26 min.)}$$

Limit value of time, see table 3.1:

$$t_{lim} = 0.333 \text{ hour}$$

Because $t_{lim} < t_{\max}$, the fire is ventilation controlled.

Temperature at the end of the heating phase, see Eqs. (3.15) and (3.12):

$$t_{\max}^* = 0.7885 \times 0.43 = 0.339 \text{ hour}$$

$$\theta_{\max} = 20 + 1325 \left(1 - 0.324e^{-0.2 \times 0.339} - 0.204e^{-1.7 \times 0.339} - 0.472e^{-19 \times 0.339} \right)$$

$$\theta_{\max} = 791 \text{ }^\circ\text{C}.$$

Time at the end of the cooling phase, see Eq. (3.16a):

$$t_{20}^* = (791 - 20) / 625 + 0.339 = 1.573 \text{ hours}$$

$$t_{20} = 1.573 / 0.7885 = 1.995 \text{ hours (120 min.)}$$

The complete time-temperature curve is shown as a continuous line in Fig. 3.2.

3. THERMAL ACTION

Example 3.4: Calculate and plot the parametric time-temperature for the room of example 3.3 if, in addition to the door, a window (2 m wide and 1 m high) is also open.

$$b = (1918 \times 40.96 + 749 \times 45.50) / (40.96 + 45.50) = 1303 \text{ J/m}^2 \text{ s}^{0.5} \text{ K},$$

see example 3.3 with a reduction of 2 m² for the area of the walls.

$$q_{t,d} = 84.96 \text{ MJ/m}^2, \text{ see example 3.3.}$$

Opening factor, see Eq. (3.8) and (3.9):

$$h_{eq} = (1.1 \times 2.2 \times 2.2 + 1.0 \times 2.0 \times 1.0) / (1.1 \times 2.2 + 1.0 \times 2.0) = 1.657 \text{ m}$$

$$O = (1.1 \times 2.2 + 1.0 \times 2.0) \times 1.657^{0.5} / 90.88 = 0.0626 \text{ m}^{1/2}$$

Expansion coefficient, see Eq. (3.11):

$$\Gamma = ((0.0626/0.04) / (1303/1160))^2 = 1.94$$

Duration of the heating phase, see Eq. (3.14):

$$t_{\max} = 0.0002 \times 84.96 / 0.0626 = 0.27 \text{ hour (16 min.)}$$

$$t_{lim} = 0.333 \text{ hour}$$

Because $t_{\max} < t_{lim}$, the fire is fuel controlled.

$$O_{lim} = 0.0001 \times 84.96 / 0.333 = 0.0255 \text{ m}^{1/2}, \text{ see Eq. 3.19.}$$

$$\Gamma_{lim} = ((0.0255/0.04) / (1303/1160))^2 = 0.322$$

Temperature at the end of the heating phase, see Eq. (3.21) and (3.12):

$$t_{\max}^* = 0.322 \times 0.333 = 0.107 \text{ hour.}$$

Note: this value is used to calculate the maximum temperature, at the end of the heating phase.

$$\theta_{\max} = 20 + 1325 \left(1 - 0.324e^{-0.2 \times 0.107} - 0.204e^{-1.7 \times 0.107} - 0.472e^{-19 \times 0.107} \right)$$

$$\theta_{\max} = 618^\circ \text{C}$$

Time at the end of the cooling phase:

$$t_{\max}^* = 1.94 \times 0.27 = 0.54 \text{ hour, see Eq. (3.15)}$$

Note: this value is used to calculate the slope during the cooling down phase.

Slope of the cooling down phase: $250 (3 - 0.54) = 615 \text{ }^\circ\text{C}/\text{hour}$, see Eq.(3.22b)

$$t_{20}^* = (618 - 20) / 615 + 0.333 \times 1.94 = 1.618 \text{ hours}$$

$$t_{20} = 1.618 / 1.94 = 0.834 \text{ hours (50 min.)}$$

The complete time-temperature curve is show as a dotted line in Fig. 3.2.

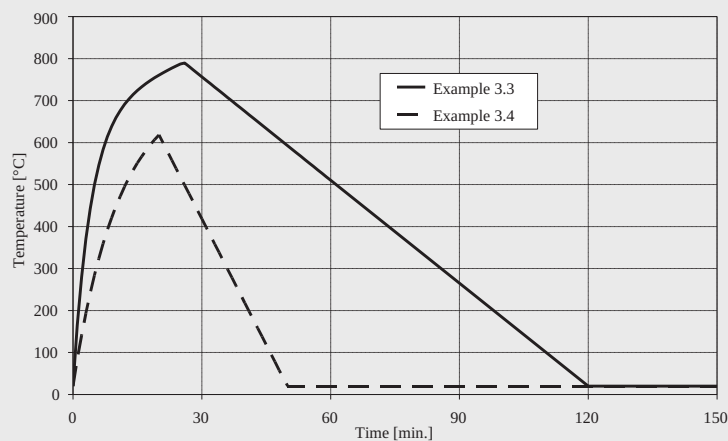


Figure 3.2 – Examples of parametric time-temperature curves

3.4. ZONE MODELS

Zone models are models that can be used to compute the development of the temperature in the fire compartment¹ on the basis of differential equations expressing mass balance and energy balance equilibrium.

The main parameters that influence the development of the temperature are the same as those used for parametric fire models.

The openings in the boundaries play a crucial role because they provide the air that feeds the fire and because they can vent the compartment. But, whereas all the openings are represented by a single lumped parameter O in parametric models, each individual opening can be

¹ And, for multiroom models, also in the adjacent compartments.

3. THERMAL ACTION

represented in a zone model with its own dimensions and position. Openings in the walls as well as in the ceiling can be taken into account. Some may be closed at the beginning of the fire and opened at a given time (human intervention) or at a given temperature criteria (braking of the windows). Forced ventilation can also be considered if needed.

The energy absorbed by the walls is also important but, whereas in parametric models all the boundaries of the compartment are represented by a lumped parameter b and the heat penetration theory in semi-infinite media is used, each wall can be represented individually in a zone model, each with all the different layers that may be present. The energy absorbed by the boundaries can be calculated precisely on the basis of the heat absorbed and transmitted to the exterior of the compartment by conduction and radiation in cavities when relevant.

The amount of fuel q present in the compartment is of course of primary importance. For a zone model, not only the total quantity present in the compartment must be given as a data but also the rate at which it will be released (Rate of Heat Release, RHR) as well as the associated mass loss rate (pyrolysis rate). The user can find some guidance on these rates in Annex E.4 of Eurocode 1. If the pyrolysis rate and/or the RHR introduced by the user are at any time higher than those that the air flow entering through the openings can accommodate, a zone model can detect this situation and modify the data accordingly, either by a modification of the pyrolysis rate (and the duration of the fire is extended) or by a modification of the RHR (corresponding to some part of the combustion taking place outside of the compartment). Zone models don't have any prescribed shape embedded for the time-temperature curve, as is the case for parametric models. The shape of the time-temperature curve is different for each case, although it is strongly linked to the shape of the RHR curve that has been introduced.

Such models are called "zone models" because the compartment is divided into several zones in which the situation is assumed to be uniform. The most commonly used models are *one zone models* where the whole compartment consist of one single zone and *two zone models* in which a lower zone comprises cold and clean air and an upper zone contains hot combustion products. One zone models represent a post-flash-over situation whereas two zone models represent a pre-flash-over situation. Some models may start in a two zone situation and shift automatically to a one zone situation when some predefined criteria are met. More refined models can

distinguish zones at a more detailed level such as, for example, the plume or the ceiling jet, but such models are not envisaged in Eurocode 1.

Eurocode 1 gives very few recommendations on zone models except that gas properties, mass exchanges and energy exchanges should be considered and that an iterative procedure is involved. This means that the differential equations have to be integrated with time to yield the time-temperature curve. This cannot be done by hand and computer software is required. Several computer programs are available and two zone models produced by research institutions can be downloaded for free, namely CFAST from NIST in the U.S.A. (http://www.nist.gov/el/fire_research/cfast.cfm) and OZone from the University of Liege in Belgium (<http://sections.arcelormittal.com/download-center/design-software/fire-calculations.html>).

When a steel member is located in the hot zone of a two zone model, or when it is located in a compartment modelled by a one zone model, the heat flux at the surface is calculated from Eq. (3.4) with a coefficient of convection α_c equal to 35 W/m²K.

When a steel member is located in the lower and cold zone of a two zone model, heat transfer is by convection with the air of the cold zone, but radiation from different surfaces should theoretically also be considered, for example, from the separation plane with the upper zone, from the floor and parts of the walls that are in the cold zone and from the fire plume. The evaluation of the temperature of steel members located in the cold zone is usually not performed because the temperatures are not normally significant for structural steel elements located in that zone. An exception to this is when the steel members are close enough to the fire source that the effect of heat transfer from the source is significant. Localised fire models allow this effect to be considered, see Section 3.6.

3.5. CFD MODELS

CFD models have become more and more popular in fire safety engineering in the last decade. CFD stands for *Computational Fluid Dynamics*. Such models rely on a division of the compartment into a very high number of cells in which the Navier-Stokes equations are written and solved in space and time. Such models produce a large number of results at a very detailed level, for example, pressure, temperature, velocity, chemical components and optical obstruction in every cell and at every chosen time

3. THERMAL ACTION

step. Application of such models requires specific software, powerful computers and well educated and highly experienced users. They are mentioned in Eurocode 1 without any recommendation. A detailed description of such models is beyond the scope of this design guide.

3.6. LOCALISED FIRES

Except in very exceptional circumstances, every fire in a building starts as a small *localised* fire. The fire ceases to be localised when flash-over occurs. Even a localised fire may have a significant impact on a structure, depending on the type of structure and relative position of the fire with respect to the structural elements.

Eurocode 1 states that thermal actions of a localised fire should be taken into account “*where flash-over is unlikely to occur*”. Apart from the fact that the term *unlikely* is vague and cannot be transformed into an operational recommendation, this sentence is misleading. For example, a localised fire near a main column in an airport hall may lead to the collapse of the column and, perhaps, of the whole buildings. Although flash-over is unlikely to occur in such a big hall, does this mean that this action can be ignored? Probably not. More correctly the wording of the sentence should say “*when the flash-over has not yet occurred*”. This means that localised fires can be ignored if the fire model is a post-flash-over model such as for nominal time-temperature fire curves and one zone models. Effects of a localised fire are automatically taken into account in a CFD model, at least during the first stage of the fire. In a two zone model, effects of the localised fire should be considered, at least as long as the flash-over has not occurred. In that case, Eurocode 1 explicitly recommends that the maximum between the effect of the localised fire and the effect of the hot zone be considered.

Two models are presented in Annex C of Eurocode 1 for the effects of a localised fire. Which one has to be used depends on the vertical length of the flame that would develop in the absence of any ceiling. This length L_f is evaluated from Eq. (3.23)

$$L_f = 0.0148Q^{0.4} - 1.02D \quad (3.23)$$

where D is the diameter of the fire and Q is the rate of heat release of the fire according to Annex E.4.

Example 3.5: What is the flame length of a localised fire in a shopping centre 5 minutes after the start of the fire?

Table E.5 recommends a *fast* fire for a shopping centre, with a time constant t_α of 150 seconds. Eq. (E.5) of Eurocode 1 yields:

$$Q = 10^6 (5 \times 60 / 150)^2 = 4 \text{ MW.}$$

The same table recommends a heat release rate density of 250 kW/m². The fire surface required to release a power of 4 MW is thus given by:

$$A_{\text{fire}} = 4 / 0.25 = 16 \text{ m}^2.$$

Assuming a circular shape of the fire yields a diameter:

$$D = (4 \times 16 / \pi)^{0.5} = 4.514 \text{ m}$$

The length of the flame is thus calculated from Eq. (3.23)

$$L_f = 0.0148 \times (4 \times 10^6)^{0.4} - 1.02 \times 4.514 = 1.869 \text{ m}$$

Fig. 3.3, taken from Annex C of Eurocode 1, shows the length of the flame L_f when the fire source is on the floor and the flame does not impact the ceiling. Depending on the particular situation, the vertical location of the fire source might be at a higher level than the floor level. The Eurocode says that the flame does not impact the ceiling when $L_f < H$, but this condition must be modified when the fire source is not located on the floor. In that case, H has to be understood as the vertical distance from the fire source to the ceiling.

33

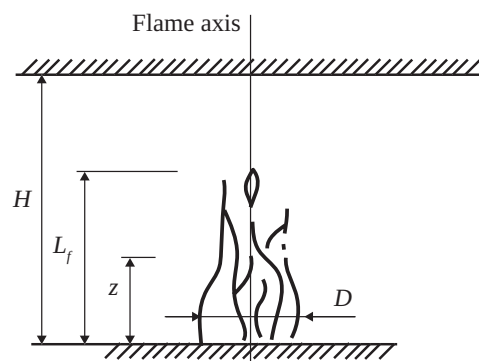


Figure 3.3 – Flame on the floor and not impacting the ceiling

3. THERMAL ACTION

When the flame is not impacting the ceiling or if the fire is in the open air, the temperature $\theta_{(z)}$ in the plume along the symmetrical vertical flame axis is given by Eq. (3.24).

$$\theta_{(z)} = 20 + 0.25 Q_c^{2/3} (z - z_0)^{-5/3} \leq 900 \quad (3.24)$$

where Q_c is the convective part of the rate of heat release [W], taken as 0.8 Q by default, z is the height along the flame axis from the position of the source [m] and z_0 is the virtual origin of the fire source, calculated from Eq. (3.25).

$$z_0 = 0.00524 Q^{0.4} - 1.02 D \quad (3.25)$$

It has to be noted that this model is a steady state model except if a variation of Q , and hence of D , is considered.

The net heat flux \dot{h}_{net} received by the surface of a structural member from the fire source should be calculated from Eq. (3.26), see Section 3.1 in Eurocode 1.

$$\dot{h}_{net} = \alpha_c (\theta_g - \theta_m) + \phi \varepsilon_m \varepsilon_f \sigma \left[(\theta_r + 273)^4 - (\theta_m + 273)^4 \right] \quad (3.26)$$

where α_c is the coefficient of convection taken here as 35 W/m²K, θ_g is the gas temperature in the vicinity of the surface either calculated from Eq. (3.24) if the surface is in the fire plume or taken as 20 °C if the surface is in air at ambient temperature¹, θ_m is the surface temperature of the member or of the thermal protection material, Φ is a configuration factor to be calculated using Annex G of Eurocode 1, ε_m is the surface emissivity of the member taken as 0.7 for carbon steel, 0.4 for stainless steel and 0.8 for other materials, ε_f is the emissivity of the fire, in general taken as 1.0², σ is the Stephan Boltzmann constant equal to 5.67×10^{-8} W/m²K⁴ and θ_r is the radiation temperature of the fire environment.

To apply Eq. (3.26), the second term of the right-hand part, taking radiation into account, should be split in a spatial integration on the hemisphere normal to the surface, with different view factors considered for

¹ That means, out of the plume and out of the eventual hot zone when the model is combined with a zone model.

² Eq. (B.16) of Annex B of Eurocode 1 could be used and yield an emissivity lower than 1.0 if the flame is thin (when D is small).

parts of the solid angle that don't comprise the fire plume (and where θ_r should be taken as 20 °C) and for parts of the solid angle that comprise the fire plume (where θ_r should be calculated from Eq. (3.24)). A hypothesis has thus to be made on the shape of the fire plume, for example, cylindrical or conical. The solid angle that encompasses the plume should itself be divided into several vertical slices, because the temperature of the flame varies with elevation. The section of the steel member itself must be divided into several surfaces, each with a different orientation, some facing the fire, some not seeing the fire, and some seeing it only partially. Practical application of the model can quickly become complex.

Example 3.6: What is the temperature of the flame at a distance of 1.5 meter above the fire source and 5 minutes after the start of the fire for the case developed in example 3.5?

Virtual origin of the fire source, see Eq. (3.25):

$$z_0 = 0.00524 \times (4 \times 10^6)^{0.4} - 1.02 \times 4.51 = -2.312 \text{ m}$$

Temperature on the flame axis, see Eq. (3.24):

$$\theta_{(z)} = 20 + 0.25(0.8 \times 4 \times 10^6)^{2/3} (1.5 + 2.312)^{-5/3} = 604^\circ\text{C}$$

When the flame is impacting the ceiling, a different model has to be used. The parameters in this model are shown in Fig. 3.4, which is taken from Annex C of Eurocode 1. This Figure must also be modified if the fire source is not located on the floor. The field of application of this model is, according to the Eurocode, limited to situations where the diameter of the fire source D is not larger than 10 meters and the rate of heat release of the fire source Q is not higher than 50 MW. With the rate of heat release density that does not exceed 500 kW/m² according to Table E.5 of Eurocode 1, the first limit is always reached first and the fire source is limited in power to 39 MW for a library and a theater and to 20 MW for other occupancies. Because libraries and theaters both lead to fast fires, the model is not valid beyond 15.6 minutes.

In this model, two non-dimensional rates of heat release are calculated from Eqs. (3.27) and (3.28).

3. THERMAL ACTION

$$Q_H^* = Q / (1.11 \times 10^6 H^{2.5}) \quad (3.27)$$

$$Q_D^* = Q / (1.11 \times 10^6 D^{2.5}) \quad (3.28)$$

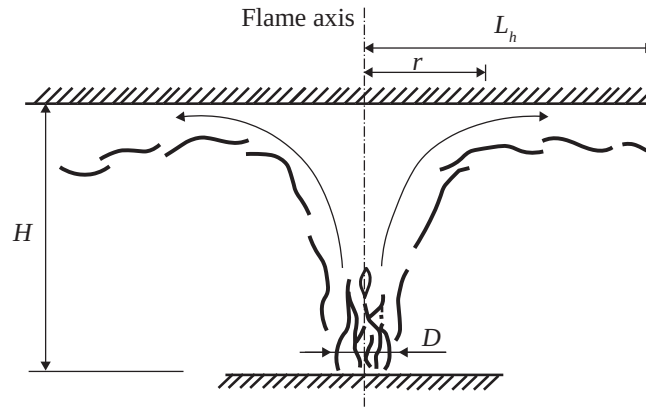


Figure 3.4 – Flame on the floor and impacting the ceiling

The horizontal flame length L_h is calculated from Eq. (3.29).

$$L_h = \left(2.9H(Q_H^*)^{0.33} \right) - H \quad (3.29)$$

36

The vertical position of the virtual heat source z' is calculated from Eq. (3.30).

$$z' = 2.4D(Q_D^{*2/5} - Q_D^{*2/3}) \quad \text{when } Q_D^* < 1.0 \quad (3.30)$$

$$z' = 2.4D(1.0 - Q_D^{*2/5}) \quad \text{when } Q_D^* \geq 1.0$$

If r is the horizontal distance from the flame axis to the point under the ceiling where the flux is evaluated, the non-dimensional parameter y is the relative distance from the virtual fire source to the point under consideration with respect to the total length of the flame, from virtual origin to tip. The point under consideration is in the flame when y is smaller than 1.0. The parameter y is calculated from Eq. (3.31).

$$y = \frac{r + H + z'}{L_h + H + z'} \quad (3.31)$$

Finally, the heat flux received by the ceiling at the point of consideration is calculated from Eq. (3.32).

$$\begin{aligned} \dot{h} &= 100\,000 && \text{if } y \leq 0.30 \\ \dot{h} &= 136\,300 - 121\,000y && \text{if } 0.30 < y < 1.0 \quad [\text{W/m}^2] \\ \dot{h} &= 15\,000y^{-3.7} && \text{if } y \geq 1.0 \end{aligned} \quad (3.32)$$

Because Eq. (3.32) only gives the flux received at the surface, the net heat flux has to be calculated from Eq. (3.33).

$$\dot{h}_{net} = \dot{h} - \alpha_c (\theta_m - 20) - \Phi \varepsilon_m \varepsilon_f \sigma \left[(\theta_m + 273)^4 - 293^4 \right] \quad (3.33)$$

This equation verifies the condition that, when the impinging flux \dot{h} is equal to 0, a temperature of the member θ_m of 20 °C will lead to a situation where the net flux received at the surface \dot{h}_{net} is equal to 0.

It also shows that, when the impinging flux is constant for a long period, the temperature of the member tends toward an equilibrium temperature (corresponding to $\dot{h}_{net} = 0$) that is directly linked to the value of the impinging flux. With a coefficient of convection α_c equal to 35 W/m²K and an emissivity of steel equal to 0.7 (emissivity of the flame and configuration factor equal to 1.0) the temperature of a steel member cannot exceed 880 °C for an impinging flux that cannot exceed 100 kW/m², see Eq. (3.32).

In the experimental tests that are at the basis of this model, the flux meters were located at ceiling level. This is the location for which Eq. (3.32) gives the received flux. For a steel element, say a steel beam, located under the ceiling, not all surfaces are located at the level of the ceiling. The level that should be considered when applying the model is not given in the Eurocode. For a section located just above the fire source, considering each surface with its own level or assuming that all surfaces have the same level as the lower flange are probably on the safe side. For a section located far away from the fire source, the model is theoretically only applicable for surfaces located at the level of the ceiling. Considering the flux received at that level for all surfaces of the section is probably on the safe side in this case, because the flame is normally constrained under the ceiling. If the depth of the beam is relatively small compared to the fire source to ceiling distance, then it may be reasonable to consider the level of the axis of the beam for all surfaces in all sections. Engineering judgement is required here.

3. THERMAL ACTION

Example 3.7: What is the maximum flux received at the level of the ceiling in a library 15 minutes after the start of the fire if the vertical distance from the fire source to the ceiling is 3 meters?

Table E.5 recommends a *fast* fire for a library, with a time constant t_α of 150 seconds. Eq. (E.5) of Eurocode 1 yields:

$$Q = 10^6 (15 \times 60 / 150)^2 = 36 \text{ MW.}$$

The same table recommends a rate of heat release rate density of 500 kW/m². The fire surface required to release a power of 36 MW is thus given by:

$$A_{\text{fire}} = 36 / 0.50 = 72 \text{ m}^2.$$

Assuming a circular shape of the fire yields a diameter:

$$D = (4 \times 72 / \pi)^{0.5} = 9.58 \text{ m}$$

The length of the flame is thus calculated from Eq. (3.23)

$$L_f = 0.0148 \times (36 \times 10^6)^{0.4} - 1.02 \times 9.58 = 5.816 \text{ m}$$

Because this length is higher than the source to ceiling distance, the second model has to be used.

$$Q_H^* = 36 \times 10^6 / (1.11 \times 10^6 \times 3^{2.5}) = 2.081$$

$$Q_D^* = 36 \times 10^6 / (1.11 \times 10^6 \times 9.58^{2.5}) = 0.114$$

Horizontal flame length, see Eq. (3.29).

$$L_h = 2.9 \times 3 \times 2.081^{0.33} - 3 = 8.080 \text{ m}$$

Virtual position of the fire source, see Eq. (3.30)

$$z' = 2.4 \times 9.58 (0.114^{2/5} - 0.114^{2/3}) = 4.240 \text{ m.}$$

The maximum flux occurs just above the fire source, where $r = 0$. At this location, the parameter y is calculated from Eq. (3.31).

$$y = (3 + 4.24) / (8.080 + 3 + 4.24) = 0.473$$

The heat flux received is given by Eq. (3.32)

$$\dot{h} = 136.3 - 121 \times 0.473 = 79.1 \text{ kW/m}^2$$

Example 3.8: What is the maximum temperature that can be reached in an unprotected steel section subjected to the flux obtained in example 3.7?

To answer this question, Eq. (3.33) has to be solved with \dot{h}_{net} set equal to 0 (this situation prevails when a steady state situation is established) and \dot{h} is equal to 79.1 kW/m². A fourth order polynomial equation is not so easily solved, but different techniques can be used. Here, the curve that gives the reemitted flux as a function of the steel temperature has been drawn. It is given by the last two terms of Eq. (3.33) with a coefficient of convection α_c equal to 35 W/m²K and an emissivity of steel equal to 0.7 (emissivity of the flame and configuration factor equal to 1.0). The result is given on Fig. 3.5.

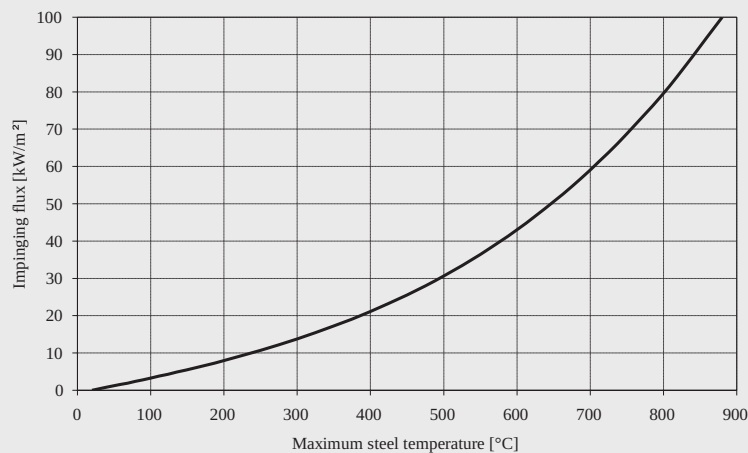


Figure 3.5 – Relationship between the impinging flux and the steel temperature in a steady state situation

From Fig. 3.5, a flux of 79.1 kW/m² leads to a maximum steel temperature of 797 °C.

3.7. EXTERNAL MEMBERS

Some buildings are designed in such a way that part of the load bearing structure is located outside the envelope of the building. When a fire develops in one or several compartments of the buildings, the fire can

3. THERMAL ACTION

anyway influence the external part of the structure through the openings in the envelope (mainly the windows).

Annex B of Eurocode 1 gives a method for determining the radiation and convection parameters that can be used in a thermal analysis for calculating the temperature in the external elements. To calculate the radiation and convection parameters, the maximum temperature of the compartment fire as well as the size and temperature of the flames from the openings are first calculated.

The model assumes a steady state situation of a fully developed fire in the compartment; the pre-flash-over phase and the cooling down phase of the fire are neglected.

The method is valid only for fire loads $q_{f,d}$ higher than 200 MJ per square meter of floor area and the size of the compartment should not exceed 70 m in length, 18 m in width and 5 m in height.

Application of the method starts by evaluating the ratio D/W which depends on the number of walls that contain windows, the number of windows in the relevant wall and the presence of a core in the compartment. Reference is made in the Eurocode to *wall 1* as the wall assumed to contain the greatest window area. It is likely that, if a compartment has openings in several walls, the method should be applied successively for each wall with *wall 1* being, in each case, the wall that is relevant for the external structural element under consideration.

If there are windows only in wall 1 and there is no core in the fire compartment, the ratio D/W is calculated from Eq. (3.34).

40

$$D/W = \frac{W_2}{w_1} \quad (3.34)$$

where W_2 is the width of the wall perpendicular to wall 1 in the fire compartment (i.e., the size of the fire compartment perpendicular to wall 1), and w_1 is the width of wall 1.

Other equations are proposed if windows are present in several walls or if there is a core in the fire compartment. All parts of an external wall that don't have the fire resistance (REI) required for the stability of the building have to be considered as windows. If the total window area in a wall exceeds 50% of the area of the wall, two subsequent calculations have to be made, first with the total window area and then with only half of the total window area being active (window panes broken). The location of the active part of the windows must be chosen as the most severe for the structural elements.

The wind has two effects on the model. First, the flames can leave the fire compartment through the windows either perpendicular to the façade or at a horizontal angle of 45° to the façade. A strict interpretation of this recommendation means that three different directions should be considered for the flames from the opening: -45°, 0° and +45°. Second, if there are openings on opposite sides of the fire compartment, the calculation shall be made in forced draught conditions. This is also the case if additional air is being fed in the compartment from another source (other than the windows), but this situation is not common.

If there is no forced draught, the rate of heat release in the compartment is given by Eq. (3.35).

$$Q = \min \left[\frac{A_f q_{f,d}}{\tau_F}; 3.15(1 - e^{-0.036/O}) A_v \sqrt{\frac{h_{eq}}{D/W}} \right] \quad (3.35)$$

where τ_F is the free burning duration assumed to be equal to 1200 seconds¹.

The first term in the parenthesis of Eq. (3.35) represents a fuel controlled situation whereas the second term represents a ventilation controlled situation.

The steady state temperature of the fire compartment is given by Eq. (3.36).

$$T_f = 6000(1 - e^{-0.1/O}) \sqrt{O} (1 - e^{-0.00286\Omega}) + T_0 \quad (3.36)$$

41

where

$$\Omega = \frac{A_f q_{f,d}}{\sqrt{A_v} A_t} \quad (3.37)$$

and the opening factor O is given by Eq. (3.8).

The flame exits through the upper 2/3 of the window height whereas fresh air flows into the compartment through the lower 1/3. From the window, the width of the flame is not modified; it remains equal to the window width.

On exiting the window, the flame is deflected upward and, from the top of the window, the thickness of the flame perpendicular to the wall is equal to 2/3 of the window height whereas the flame height (i.e., the vertical extension of the flame above the top of the window), is given by Eq. (3.38).

¹ Note the similarity with t_{lim} used in the parametric fire model.

3. THERMAL ACTION

$$L_L = 1.9 \left(\frac{Q}{w_t} \right)^{2/3} - h_{eq} \quad (3.38)$$

Other expressions are used to calculate L_H , the horizontal distance from the wall to the centerline of the flame at the top of the flame. The geometrical shape of the flame is thus fully defined. The flame trajectory may be deflected by the presence of balconies and awnings and Eurocode 1 gives modified equations for these cases.

The flame temperature at the window is given by Eq. (3.39).

$$T_w = 520 / \left(1 - 0.4725 (L_f w_t / Q) \right) + T_0 \quad (3.39)$$

with $L_f w_t / Q < 1$.

The emissivity of the flames at the window may be taken as $\varepsilon_f = 1.0$.

The temperature of the flame along the axis at a distance L_x from the window is given by Eq. (3.40).

$$T_z = (T_w - T_0) \left(1 - 0.4725 (L_x w_t / Q) \right) + T_0 \quad (3.40)$$

with $L_x w_t / Q < 1$.

The emissivity of the flame may be calculated from Eq. (3.41).

$$\varepsilon_f = 1 - e^{-0.3d_f} \quad (3.41)$$

42

where d_f is the flame thickness.

The convective heat transfer coefficient is given by Eq. (3.42).

$$\alpha_c = 4.67 d_{eq}^{-0.4} \left(Q / A_v \right)^{0.6} \quad (3.42)$$

where d_{eq} is the characteristic size of the structural member, for example, its diameter or width.

Some equations are given for the configuration factors between an opening or a flame (assumed to be rectangular in shape) and the side of a member.

Annex G gives the equations for calculating the configuration factor from a radiating surface to a receiving surface. The configuration factor is calculated at the center P of each surface of the structural member.

When the radiating surface and the receiving surface are parallel, a perpendicular line is drawn from point P to the radiating surface that it intersects at point X, see Fig. 3.6 taken from Eurocode 1. The radiating surface is then divided into 4 rectangular surfaces, each one having its own height h and width w . Equation G.2 given in the Eurocode is in fact valid for a radiating surface that has the intersection point X at one of its corners. This equation has thus to be applied 4 times, once for each rectangle, and the sum of the 4 contributions yields the configuration factor between the radiating surface and the receiving surface.

When the radiating surface and the receiving surface are perpendicular, a perpendicular line is drawn from point P to the radiating surface which it intersects at point X, see Fig. 3.7 which is taken from Eurocode 1. If part of the radiating surface cannot "see" the receiving surface, this part does not contribute to the radiating factor. The contributing part of the radiating surface is then divided into two rectangular surfaces, each one having its own height h and width w . Equation G.3 given in the Eurocode is valid for a radiating surface that has the intersection point X at one of its corners. This equation has to be applied twice, once for each rectangle, and the sum of the two contributions yields the configuration factor between the radiating surface and the receiving surface.

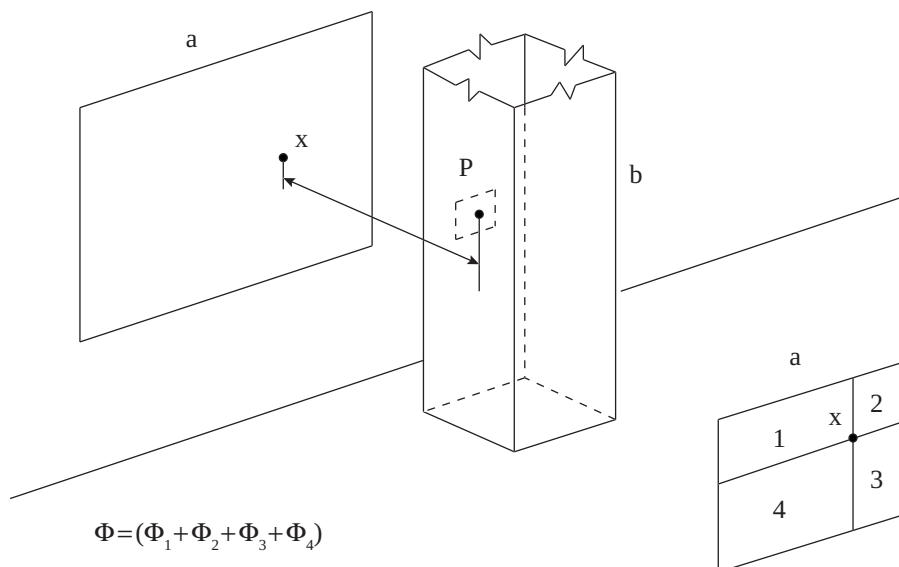


Figure 3.6 – Configuration factor for two parallel surfaces

3. THERMAL ACTION

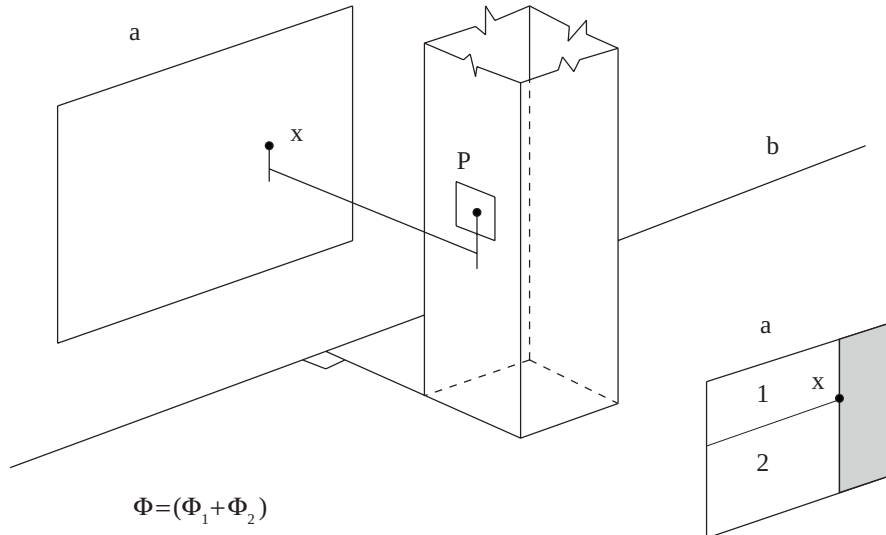


Figure 3.7 – Configuration factor for two perpendicular surfaces

If the intersection point X is outside the radiating surface, the radiating surface must be extended to the Point X and some negative contributions must be taken into account, see Fig. 3.8.

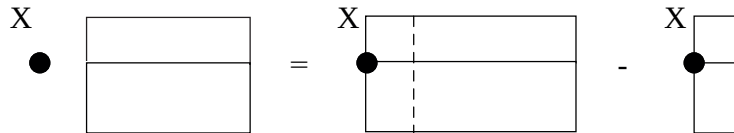


Figure 3.8 – Configuration factor when point P is outside the radiating surface

When the configuration factor has been calculated for the four faces of a structural member, the overall configuration factor can be calculated from Eq. (3.43). This equation can be applied whether the radiating surface is a window or a flame.

$$\Phi = \frac{\sum_{i=1}^4 C_i \Phi_i d_i}{\sum_{i=1}^4 C_i d_i} \quad (3.43)$$

where C_i is equal to 0 for a thermally protected face and equal to 1 otherwise, Φ_i is the configuration factor of face i and d_i is the cross sectional dimension of face i .

Chapter 4

TEMPERATURE IN STEEL SECTIONS

4.1. INTRODUCTION

The increase in steel temperature depends on the temperature of the fire compartment, the area of steel exposed to the fire and the amount of the applied fire protection. This chapter will focus on the transfer of the heat from the fire compartment to the structural elements. Several fire protection systems can be used to improve the performance of steel profiles in a fire and these are described later in this chapter.

The heat transfer from the hot gases into the surface of the structural elements by a combination of convection and radiation is normally treated as a boundary condition. The heat transfer within the structural member is by conduction and is governed by the well known Fourier equation of heat transfer. The chapter starts by presenting the complex governing equation for heat conduction and goes on to show how simplified and more practical methods can be developed for steel elements.

45

4.2. THE HEAT CONDUCTION EQUATION AND ITS BOUNDARY CONDITIONS

The governing equation for the two-dimensional non-linear, transient heat conduction within the cross section of a structural element, takes the following form:

$$\frac{\partial}{\partial x} \left(\lambda_a \frac{\partial \theta}{\partial x} \right) + \frac{\partial}{\partial y} \left(\lambda_a \frac{\partial \theta}{\partial y} \right) + \dot{Q} = \rho_a c_a \frac{\partial \theta}{\partial t} \quad (4.1)$$

4. TEMPERATURE IN STEEL SECTIONS

where λ_a is the thermal conductivity, \dot{Q} the internal heat source that is equal to zero in the case of non-combustible members, ρ_a the unit mass of steel, c_a the specific heat of steel, θ the temperature and t the time.

The temperature field which satisfies Eq. (4.1) within the structural element must satisfy the following boundary conditions:

- i) prescribed temperatures $\bar{\theta}$ on a part Γ_θ of the boundary;
- ii) specified heat flux \bar{q} on a part Γ_q of the boundary;
- iii) heat transfer by convection between the part Γ_c of the boundary at temperature θ and the surrounding ambient temperature θ_∞

$$q_c = \alpha_c (\theta - \theta_\infty) \quad \text{on } \Gamma_c \quad (4.2)$$

where α_c is the coefficient of heat transfer by convection [W/m²K] and q_c is the heat flux by convection per unit area.

- iv) heat transfer by radiation between the part Γ_r of the boundary at an absolute temperature θ and the fire environment at an absolute temperature θ_r

$$q_r = \sigma \varepsilon (\theta^4 - \theta_r^4) \quad \text{on } \Gamma_r \quad (4.3)$$

where σ is the Stephan Boltzmann constant (5.67×10^8 W/m²K⁴), ε the emissivity and q_r is the heat flux by radiation per unit area. This equation can become linear as follows:

46

$$q_r = \sigma \varepsilon (\theta^4 - \theta_r^4) = \underbrace{\sigma \varepsilon (\theta^2 + \theta_r^2)}_{\alpha_r} (\theta + \theta_r) (\theta - \theta_r) = \alpha_r (\theta - \theta_r) \quad \text{on } \Gamma_r \quad (4.4)$$

where α_r can be considered as the coefficient of heat transfer by radiation.

In the case of combined convection and radiation and if, as usually happens, $\theta_r = \theta_\infty$, the combined heat flux is given by:

$$q_{cr} = q_c + q_r = \alpha_c (\theta - \theta_\infty) + \alpha_r (\theta - \theta_r) = \alpha_{cr} (\theta - \theta_\infty) \quad (4.5)$$

where

$$\alpha_{cr} = \alpha_c + \alpha_r \quad (4.6)$$

is the combined convection and radiation coefficient which is temperature dependent.

The first type of boundary condition, i. e., prescribed temperatures on the surface of the structural elements is not common in fire situation.

It should be noted that both the governing Eq. (4.1) and boundary condition Eq. (4.5) are non-linear. The former is due to the thermal conductivity and specific heat that are temperature dependent (see Annex A), and the latter is due to the radiative boundary condition which involves a non-linear term of the temperature, as shown in Eq. (4.4). Therefore a closed-form solution to the governing Eq. (4.1) and its boundary condition Eq. (4.5) is not possible, even for the cases with the simplest geometry. Numerical methods such as the finite element method are usually required to solve this kind of heat transfer problems and such a method is presented in the next section. EN 1993-1-2 gives simplified methods for unprotected and protected steelwork exposed to the fire, and these methods are presented in Sections 4.5 and 4.6, respectively.

4.3. ADVANCED CALCULATION MODEL. FINITE ELEMENT SOLUTION OF THE HEAT CONDUCTION EQUATION

Using finite elements Ω^e to discretize the domain Ω , together with a weak formulation and using the Galerkin method for choosing the weighting functions, the following system of differential equations is obtained:

$$\mathbf{K}\boldsymbol{\theta} + \mathbf{C}\dot{\boldsymbol{\theta}} = \mathbf{F} \quad (4.7)$$

47

where

$$K_{lm} = \sum_{e=1}^E \int_{\Omega^e} \left(\frac{\partial N_l}{\partial x} \lambda_a \frac{\partial N_m}{\partial x} + \frac{\partial N_l}{\partial y} \lambda_a \frac{\partial N_m}{\partial y} \right) d\Omega^e + \sum_{e=1}^H \int_{\Gamma_c^e} \alpha_{cr} N_l N_m d\Gamma_c^e \quad (4.8)$$

$$C_{lm} = \sum_{e=1}^E \int_{\Omega^e} \rho_a c_a N_l N_m d\Omega^e \quad (4.9)$$

$$F_l = \sum_{e=1}^E \int_{\Omega^e} N_l \dot{Q} d\Omega^e - \sum_{e=1}^Q \int_{\Gamma_q^e} N_l \bar{q} d\Gamma_q^e + \sum_{e=1}^H \int_{\Gamma_c^e} N_l \alpha_{cr} \theta_{\infty} d\Gamma_c^e \quad (4.10)$$

and E is the total number of elements, Q is the number of elements with boundary type Γ_q , H is the number of elements with boundary type Γ_c and (or) Γ_r , and N_l and N_m are shape functions.

4. TEMPERATURE IN STEEL SECTIONS

Adopting a finite difference discretisation in time, the system of ordinary differential equations (4.7) can be rewritten for the time $t_{n+\alpha}$:

$$\hat{\mathbf{K}}_{n+\alpha} \boldsymbol{\theta}_{n+\alpha} = \hat{\mathbf{F}}_{n+\alpha} ; 0 < \alpha \leq 1 \quad n \in (0, 1, 2, \dots, N-1) \quad (4.11)$$

where

$$\hat{\mathbf{K}}_{n+\alpha} = \mathbf{K}_{n+\alpha} + \frac{1}{\alpha \Delta t} \mathbf{C}_{n+\alpha} ; 0 < \alpha \leq 1 \quad (4.12)$$

and

$$\hat{\mathbf{F}}_{n+\alpha} = \mathbf{F}_{n+\alpha} + \frac{1}{\alpha \Delta t} \mathbf{C}_{n+\alpha} \boldsymbol{\theta}_n ; 0 < \alpha \leq 1 \quad (4.13)$$

Solving the system of equations (4.11), for $\boldsymbol{\theta}_{n+\alpha}$, at time $t_{n+\alpha}$, the value of $\boldsymbol{\theta}$ at the end of the time interval Δt , (i. e., at time t_{n+1}) is given by:

$$\boldsymbol{\theta}_{n+1} = \frac{1}{\alpha} \boldsymbol{\theta}_{n+\alpha} + \left(1 - \frac{1}{\alpha} \right) \boldsymbol{\theta}_n \quad (4.14)$$

These are the initial conditions for the next time interval. Varying the α parameter, several time integration schemes are obtained. If $\alpha \neq 0$ the methods are called implicit. The most popular schemes are those for which:

- $\alpha = 1/2$ (*Crank-Nicolson*);
- $\alpha = 2/3$ (*Galerkin*);
- $\alpha = 1$ (*Euler Backward*).

The algorithm from equations (4.11) to (4.14) has the same stability criteria for both linear and non-linear problems and is unconditionally stable for $\alpha \geq 1/2$, in the sense that the process will always converge, although some oscillation can occur if the time interval is too big.

4.3.1. Temperature field using the finite element method

Numerical simulation of the thermal response of a steel HE 400 B profile subjected to the standard fire curve ISO 834 acting on all four sides as shown in Fig. 4.1 is presented in this section.

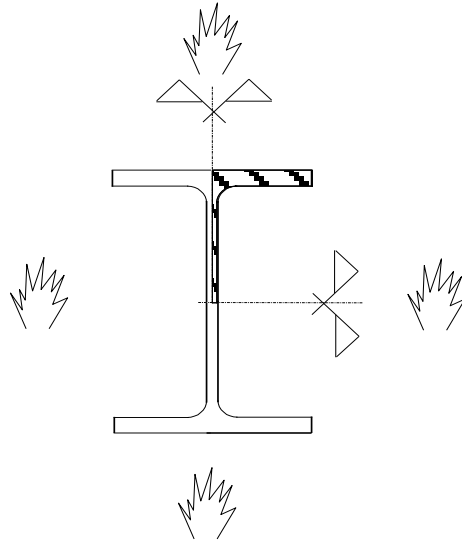


Figure 4.1 – Steel profile exposed to fire on all four sides

Due to the symmetry, only one quarter of the cross section is analysed. Fig. 4.2 shows the finite element mesh adopted.

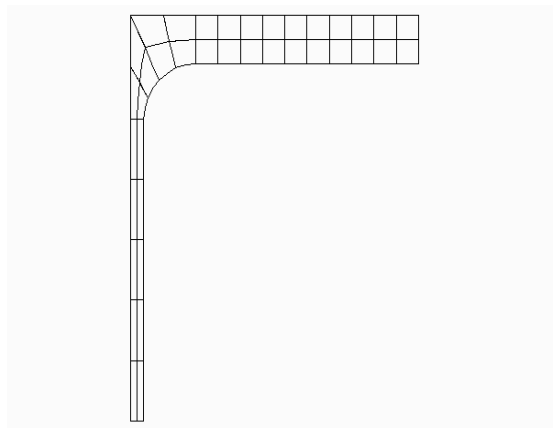


Figure 4.2 – Finite element mesh used

The temperature field after a standard fire duration of 15, 30, 60 and 90 minutes is shown in Fig. 4.3. The emissivity in Eq. (4.3) was taken as $\varepsilon = 0.5$. The coefficient of heat transfer by convection, α_c , in Eq. (4.2) was taken as $25 \text{ W/m}^2\text{K}$.

4. TEMPERATURE IN STEEL SECTIONS

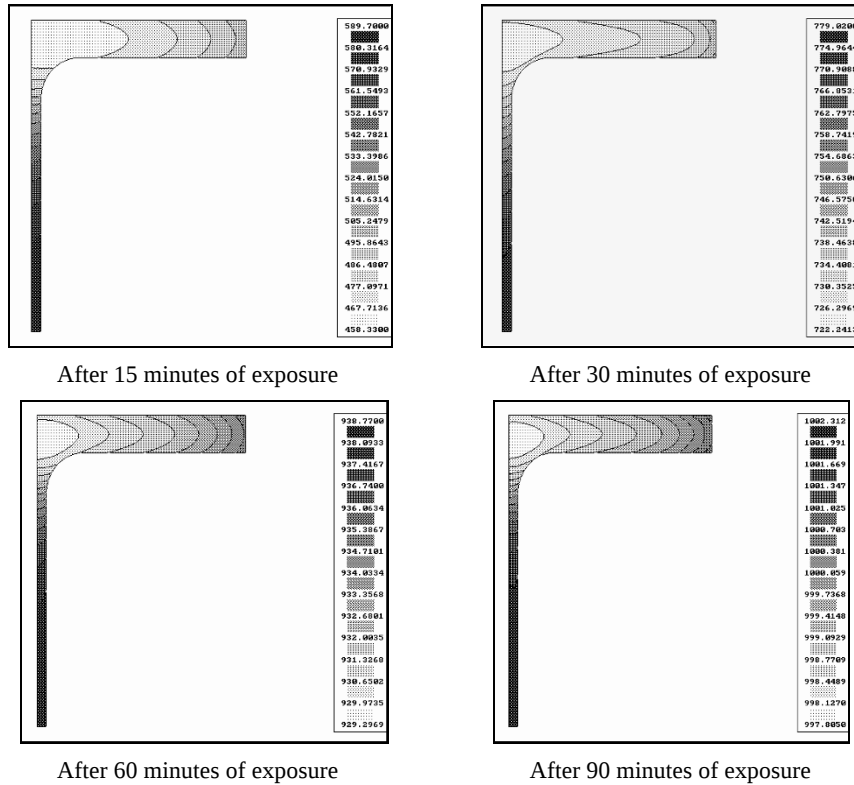


Figure 4.3 – Temperature field of an HE 400 B heated on all four sides

50

The temperature field on the steel profile HE 400 B after 30 minutes depicted in Fig. 4.3, shows an almost uniform temperature field where the difference between the maximum and minimum temperature is only 57 °C. This result is normally attributed to the high value of the thermal conductivity of the steel that leads to a quick propagation of heat producing an almost uniformly distributed field of temperature in the cross section. It can be shown that this difference is due to the relative thickness of the sections and not to the high value of the thermal conductivity of steel. In fact, the notion of relative thickness is translated physically through the notion of section factor, see Section 4.4.

Assuming a uniform temperature distribution makes Eq. (4.1) much simpler to apply as it will be shown in Section 4.5

Simple models, such as the “lumped capacitance model” (Incropera and De Witt, 1990), for the calculation of the steel temperature are based on the assumption of a uniform temperature distribution throughout the cross section as given in EN 1993-1-2 and presented in Eq. (4.16). The lumped

capacitance model is a common approximation in transient conduction heat transfer, which may be used whenever the resistance to heat transfer by conduction within the body is much less than the resistance to the heat transfer across the boundary of the body (Incropera and De Witt, 1990).

4.4. SECTION FACTOR

Before presenting the simple methods for the evaluation of the thermal response of a steel member, the concept of a parameter that governs the rate of temperature rise is presented.

The rate of temperature rise depends on the mass and the surface area of the member exposed to the fire. Light members such as purlins or lattice girders heat up much faster than heavy sections such as columns. The rate of heating of a given member is described by its “*Section Factor*” or “*Massivity Factor*”, A/V , which is the ratio of the surface area exposed to the heat flux and the volume of the member per unit length.

For unprotected members Eurocode 3 defines the section factor as A_m/V [m^{-1}].

For prismatic members with boundary conditions that are constant along the length, the temperature distribution is two-dimensional and the massivity factor is the ratio of the perimeter of the section exposed to the fire, in meters, and the cross sectional area of the member, in m^2 as follows

$$\frac{A_m}{V} = \frac{P \times l}{A \times l} = \frac{P}{A} \left[\text{m}^{-1} \right] \quad (4.15)$$

where l the length of the member¹.

Table 4.1 and Table 4.2 show the basic principle for evaluating the “*Section Factor*” or “*Massivity Factor*” for unprotected and protected steel members, respectively.

The cross sectional area A is always the area of the steel section. The heated perimeter A_m of an unprotected member will depend on the number of sides exposed to the fire. The perimeter A_p of protected members also depends on the number of heated sides and on the type of insulation used. For box

¹ This factor is in fact the specific surface of the member, in m^2/m^3

4. TEMPERATURE IN STEEL SECTIONS

protection, generally the box perimeter that corresponds to the smallest box surrounding the section is considered and for sprayed insulation or intumescent paint, the perimeter of the steel cross section is used. More detailed cases are shown in Annex A.

The rate at which a steel member will increase in temperature is proportional to the surface, A , of steel exposed to the fire and inversely proportional to the mass or volume, V , of the member. In a fire, a member with a low section factor will heat up more slowly than one with a high section factor. This is illustrated in Fig. 4.4.

Table 4.1 – Definition of section factors for unprotected steel members

Sketch	Description	Section factor (A_m/V)
	4 sides exposed	$\frac{\text{steel perimeter exposed to fire}}{A}$
	3 sides exposed	$\frac{\text{steel perimeter exposed to fire}}{A}$
	4 sides exposed	$\frac{2(b + h)}{A}$

Note: A is the steel cross section area.

52

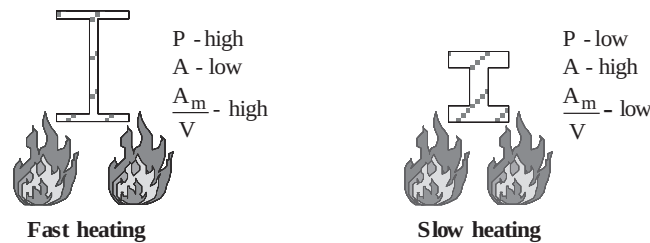


Figure 4.4 – The section factor

Table 4.2 – Definition of section factors for protected steel members

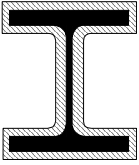
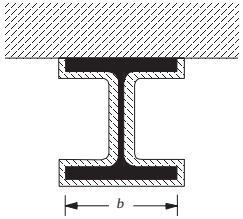
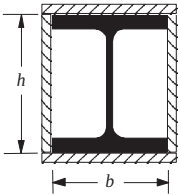
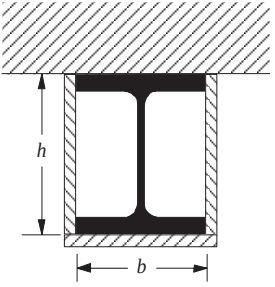
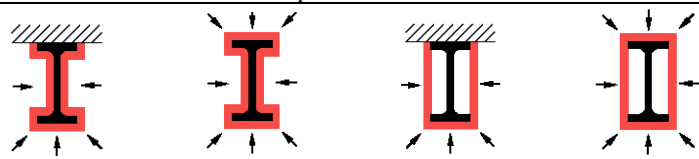
Sketch	Description	Section factor (A_p/V)
	Contour encasement of uniform thickness exposed to fire on four sides	$\frac{\text{steel perimeter}}{A}$
	Contour encasement of uniform thickness, exposed to fire on three sides	$\frac{\text{steel perimeter} - b}{A}$
	Hollow encasement of uniform thickness exposed to fire on four sides	$\frac{2(b + h)}{A}$
	Hollow encasement of uniform thickness, exposed to fire on three sides	$\frac{b + 2h}{A}$
Note: A is the steel cross section area.		

Table 4.3 shows some examples of section factors for protected sections. The section factor for a profile with contour encasement is the same as that for the unprotected profile.

4. TEMPERATURE IN STEEL SECTIONS

Table 4.3 – Some examples of section factors

Profile				
	contour 3 sides	contour 4 sides	box 3 sides	box 4 sides
IPE 100	334	388	247	300
HE 100 A	217	264	137	185
IPE 400	152	174	116	137
HE 400 A	101	120	68	87
IPE 600	115	129	91	105
HE 600 A	87	100	65	78

4.5. TEMPERATURE OF UNPROTECTED STEELWORK EXPOSED TO FIRE

EN 1993-1-2 provides a simple equation for calculating the thermal response of unprotected steel members. Assuming an equivalent uniform temperature distribution throughout the cross section, the increase in temperature $\Delta\theta_{a,t}$ in an unprotected steel member during a time interval Δt is given by:

$$\Delta\theta_{a,t} = k_{sh} \frac{A_m / V}{c_a \rho_a} \dot{h}_{net,d} \Delta t \quad [^{\circ}\text{C}] \quad (4.16)$$

where

- k_{sh} is the correction factor for the shadow effect, from Eq. (4.17);
- A_m / V is the section factor for unprotected steel members, (≥ 10) [m^{-1}];
- A_m is the surface area of the member per unit length, [m^2/m];
- V is the volume of the member per unit length, [m^3/m];
- c_a is the specific heat of steel, [J/kgK];
- $\dot{h}_{net,d}$ is the design value of the net heat flux per unit area according to Eq. (3.4) from Chapter 3, representing the

thermal actions and reproduced here. This flux is the sum of a convective part $\dot{h}_{net,c}$ and a radiative part $\dot{h}_{net,r}$:

$$\dot{h}_{net,d} = \dot{h}_{net,c} + \dot{h}_{net,r} \quad [\text{W/m}^2];$$

where

$$\dot{h}_{net,c} = \alpha_c (\theta_g - \theta_m) \quad [\text{W/m}^2];$$

α_c is the coefficient of heat transfer by convection given in Eq.(3.4) and reproduced in table 4.4;

θ_g is the gas temperature of the fire compartment defined in Chapter 3, [°C];

θ_m is the surface temperature of the steel member;

$$\dot{h}_{net,r} = \Phi \cdot \varepsilon_f \cdot \varepsilon_m \cdot 5.67 \times 10^{-8} \cdot \left[(\theta_r + 273)^4 - (\theta_m + 273)^4 \right] [\text{W/m}^2];$$

Φ is the view factor or configuration factor that is usually taken equal to 1.0 (see Chapter 3 or Table 4.4);

ε_m is the surface emissivity of the member (see Eq.(3.4)), taken as 0.7 for carbon steel, 0.4 for stainless steel and 0.8 for other materials unless given in the material related fire design parts of the Eurocodes;

ε_f is the emissivity of the fire (usually $\varepsilon_f = 1.0$);

θ_r is the radiation temperature of the fire environment normally taken $\theta_r = \theta_g$;

ρ_a is the unit mass of steel, 7850 [kg/m³];

Δt is the time interval [s] (≤ 5 [s]).

Table 4.4 – Coefficient of heat transfer by convection and view factor

	α_c [W/m ² K]	Φ
Unexposed side of separating elements		
Radiation considered separately	4	≠ 0
Radiation implicitly considered in the convection	9	= 0
Surface exposed to the fire		
Standard fire curve ISO 834	25	≠ 0
Hydrocarbon curve	50	≠ 0
Parametric fire, zone fire models or external members	35	≠ 0

4. TEMPERATURE IN STEEL SECTIONS

In equation (4.16) the value of the section factor A_m / V should not be taken less than 10 m^{-1} (because such a massive section would not have a uniform temperature)¹ and Δt should not be taken as more than 5 seconds.

Eq. (4.16) can only be solved if the initial conditions and the boundary conditions (convection and radiation) are known. A common assumption regarding the initial conditions is that prior to the occurrence of fire the temperature of the whole section is $20 \text{ }^\circ\text{C}$.

The values for the coefficients of both radiative and convective heat transfer proposed in Eurocode 3 were chosen such that a reasonable agreement with test results was obtained. However, empirical coefficients taking into account the so-called “shadow effect” (see Fig. 4.5) had to be introduced in Eq. (4.16) so that realistic values of the surface emissivity of steel ($\varepsilon_m = 0.7$, a high but physically realistic value) and the fire emissivity ($\varepsilon_f = 1.0$, a direct consequence of using the plate thermometer for furnace control in fire tests) can be used (Twilt *et al*, 2001).

The view factor is always taken as 1.0 if the radiative flux given by the above equation is used in Eq. (4.16) written for a fully engulfed element. This factor can be calculated with a value lower than 1.0 when the fire source is localised and only part of the flux radiated by the fire source reaches the element (see Fig. 4.5) or when the concave shape of the profile is taken in to account, as will be shown in Section 4.9.



Figure 4.5 – Influence of shape on the shadow effect

For cross sections with a convex shape (e.g. rectangular or circular hollow sections) fully embedded in fire, the shadow effect does not play a role and consequently the correction factor k_{sh} equals unity.

¹ This condition is verified for all commercial sections.

For I-sections under nominal fire actions, the correction factor for the shadow effect may be determined from:

$$k_{sh} = 0.9[A_m/V]_b/[A_m/V] \quad (4.17a)$$

where

$[A_m/V]_b$ is the box value of the section factor. The box value of the section factor of a steel section is defined as the ratio between the exposed surface area of a notional bounding box to the section and the volume of steel, as shown in Table 4.5, $[m^{-1}]$.

In all other cases, the value of k_{sh} shall be taken as:

$$k_{sh} = [A_m/V]_b/[A_m/V] \quad (4.17b)$$

Ignoring the shadow effect (i.e., $k_{sh} = 1$) leads to conservative solutions.

Instead of using the modified section factor, $k_{sh}[A_m/V]$, in Eq. (4.16), one can use

$$k_{sh}[A_m/V] = 0.9[A_m/V]_b \quad (4.18a)$$

if the correction factor for the shadow effect is given by Eq. (4.17a) or

$$k_{sh}[A_m/V] = [A_m/V]_b \quad (4.18b)$$

if the correction factor for the shadow effect is given by Eq. (4.17b).

In both cases only the box value of the section factor, $[A_m/V]_b$, is needed.

Annex E presents tables (Vila Real *et al*, 2009a) with values of the section factor for unprotected (A_m/V) and protected (A_p/V) I and H European hot rolled steel profiles as well as values of the modified section factor ($k_{sh}A_m/V$) including the correction factor for the shadow effect (k_{sh}) in accordance with EN 1993-1-2.

An iterative procedure must be used to solve the simplified heat conduction equation (4.16) because the specific heat c_a and the net heat flux $\dot{h}_{net,d}$ are both temperature dependent.

4. TEMPERATURE IN STEEL SECTIONS

Table 4.5 – Box value of the section factor $[A_m/V]_b$

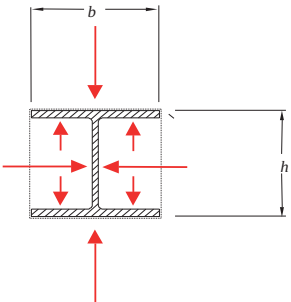
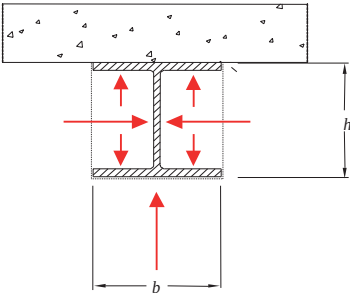
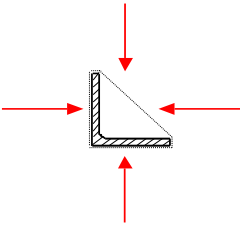
Sketch	Section factor $[A_m/V]_b$
	$\frac{2(b + h)}{\text{Steel cross Section area}}$
	$\frac{2h + b}{\text{Steel cross Section area}}$
	$\frac{\text{box perimeter}^*}{\text{Steel cross Section area}}$
<p>* The dotted line defines the box perimeter that corresponds to the smallest box surrounding the section (Franssen <i>et al</i>, 2009)</p>	

Table 4.6 gives the temperature after 30 minutes and 60 minutes of standard fire ISO 834 exposure, for different values of the modified section factor $k_{sh}[A_m/V]$.

4.5. TEMPERATURE OF UNPROTECTED STEELWORK EXPOSED TO FIRE

Table 4.6 – Temperatures after 30 and 60 min of ISO 834 exposure

$k_{sh} [A_m/V] [m^{-1}]$	θ_a (30 min) [°C]	θ_a (60 min) [°C]
10	257.2	549.3
20	431.3	735.6
30	553.9	834.4
40	636.2	900.5
50	690.3	922.9
60	721.3	930.7
70	734.1	934.0
80	741.0	935.8
90	753.0	937.1
100	767.3	938.0
120	792.5	939.3
140	809.0	940.2
160	818.8	940.9
180	824.6	941.4
200	828.2	941.8
250	832.6	942.5
300	834.7	943.0

Fig. 4.6 shows the development of the temperature for some HEB profiles, obtained using Eq. (4.16), considering $k_{sh} = 1.0$ and the section factors given in Table 4.7.

Table 4.7 – Section factors for HEB profiles

	HE100B	HE200B	HE300B	HE400B	HE500B	HE600B
$A_m/V [m^{-1}]$	218	147	116	98	89	86

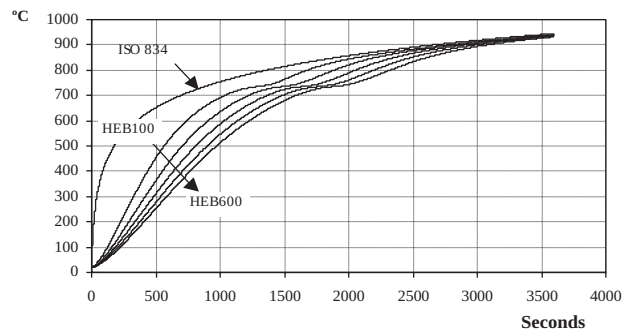


Figure 4.6 – Influence of section factor A_m/V on the temperature rise in HEB profiles

4. TEMPERATURE IN STEEL SECTIONS

The S shape observed in the rise of the steel temperature between 700 °C and 800 °C is due to the latent heat of metallurgical phase change of the steel in this range of temperatures. This effect is taken into account through the rapid increase in the specific heat of steel around 735 °C shown in Fig. A.1 of Annex A.

If a constant specific heat of 600 [J/(kgK)] is used, as suggested for simple calculation methods in the ENV version of the Eurocode 3 (1995), this plateau does not exist, as shown in Fig. 4.7.

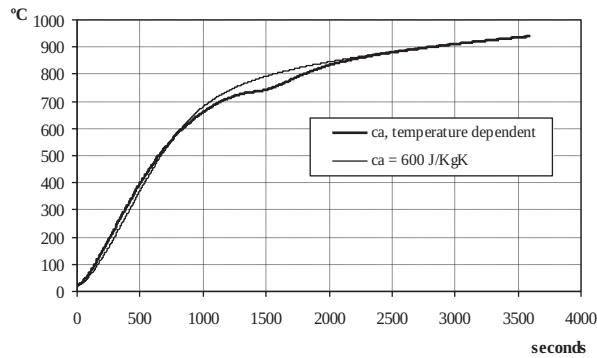


Figure 4.7 – Influence of the use of a constant value of the steel specific heat of 600 J/(KgK)

By programming Eq. (4.16), it is easy to build tables or nomograms like the ones presented in Annex A for unprotected steel profiles subjected to the ISO 834 fire curve. The use of these tables and nomograms avoids the need to solve Eq. (4.16). The nomograms from Annex A are reproduced in Figs. 4.8 and 4.9. Knowing the section factor of the steel profile, $k_{sh} [A_m/V]$ the temperature at a given time can be evaluated using these nomograms.

60

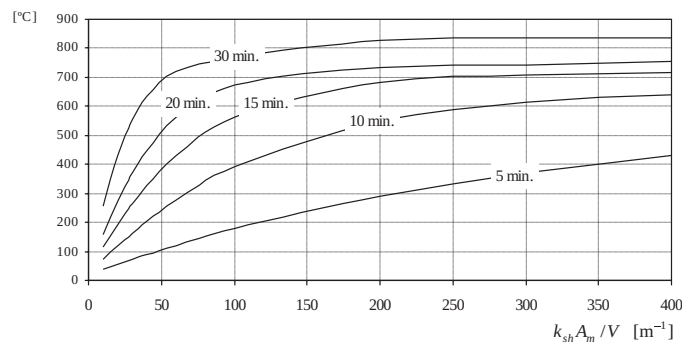


Figure 4.8 – Temperature as a function of the massivity factor for various times for unprotected sections subjected to the ISO 834 fire

4.6. TEMPERATURE OF PROTECTED STEELWORK EXPOSED TO FIRE

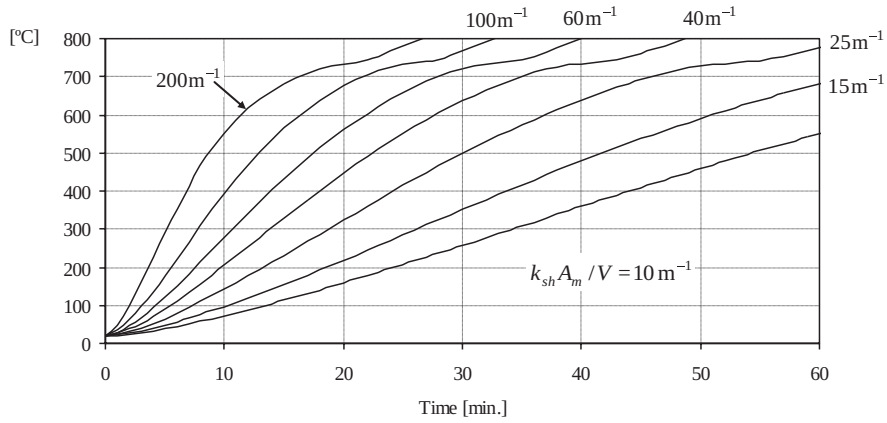


Figure 4.9 – Temperature as a function of time for various massivity factors for unprotected sections subjected to the ISO 834 fire

For a parametric fire as defined in Chapter 3, it is not easy to build such nomograms or tables and numerical calculation must be used. Fig. 4.10 shows the temperature development of a HE 220 B profile heated on all four sides by a parametric fire. These results were obtained with the program Elefir-EN, which is presented in Chapter 8.

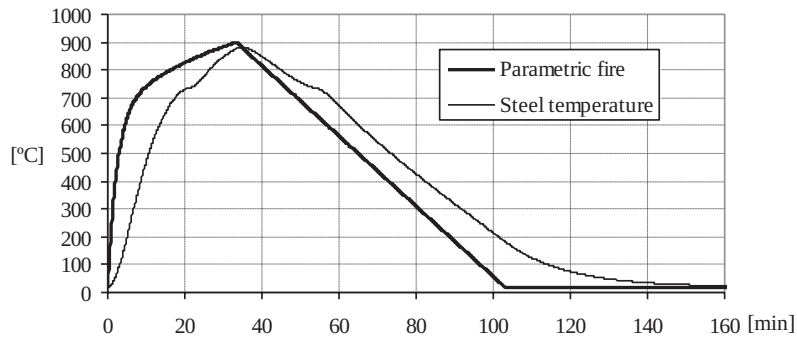


Figure 4.10 – Temperature development in a compartment with a parametric fire and the corresponding temperature of an unprotected HE 220 B

4.6. TEMPERATURE OF PROTECTED STEELWORK EXPOSED TO FIRE

It is common practice to use thermal insulation to protect the steel where fire resistance higher than 30 minutes is required. There are many

4. TEMPERATURE IN STEEL SECTIONS

forms of passive fire protection systems available to control the rate of temperature rise in steel members exposed to fire. It was shown in Table 4.2 that the insulation materials can be applied as contour encasement or hollow encasement. Basically there are three types of insulating materials:

- Sprays;
- Boards;
- Intumescent paint.

EN 1993-1-2 provides a simple design method to evaluate the temperature development of steel members insulated with fire protection materials. Assuming uniform temperature distribution, the temperature increase $\Delta\theta_{a,t}$ of an insulated steel member during a time interval Δt , is given by

$$\Delta\theta_{a,t} = \frac{\lambda_p A_p / V}{d_p c_a \rho_a} \frac{(\theta_{g,t} - \theta_{a,t})}{(1 + \phi / 3)} \Delta t - (e^{\phi/10} - 1) \Delta\theta_{g,t} \quad [^\circ\text{C}] \quad (4.19)$$

and

$$\Delta\theta_{a,t} \geq 0 \text{ if } \Delta\theta_{g,t} > 0$$

where the amount of heat stored in the protection is

$$\phi = \frac{c_p d_p \rho_p}{c_a \rho_a} \cdot \frac{A_p}{V} \quad (4.20)$$

and

62

- A_p / V is the section factor for steel members insulated by fire protection material, [m^{-1}]. Annex A.3 gives the section factor for a range of practical cases;
- A_p is the appropriate area of fire protection material per unit length of the member [m^2/m];
- V is the volume of the member per unit length, [m^3/m];
- λ_p is the thermal conductivity of the fire protection material, [W/mK]. Annex A.6 gives the thermal conductivity for a range of practical fire protection materials;
- d_p is the thickness of the fire protection material, [m];
- c_p is the specific heat of the fire protection material, [J/kgK]. Annex A.6 gives the specified heat for a range of fire protection materials;

- ρ_p is the unit mass of the protection. Annex A.6 gives the unit mass for a range of fire protection materials [kg/m^3];
- c_a is the temperature dependent specific heat of steel, from Annex A.1 [J/kgK];
- $\theta_{a,t}$ is the steel temperature at time t [$^{\circ}\text{C}$];
- $\theta_{g,t}$ is the ambient gas temperature at time t [$^{\circ}\text{C}$];
- $\Delta\theta_{g,t}$ is the increase of the ambient gas temperature during the time interval Δt [K];
- ρ_a is the unit mass of steel, 7850 [kg/m^3];
- Δt the time interval [seconds] (≤ 30 [s]).

Equation (4.19) is an approximation and only valid for small values of the factor ϕ . According to Wang (2004) this factor should normally not be higher than 1.5, but this limitation is not given in the Eurocode.

The design value of the net heat flux reflecting the heat transfer by convection and radiation does not appear in Eq. (4.19). In fact the temperature drop over the insulation is relatively large and, consequently, the surface temperature of the insulation is close to the gas temperature. The thermal resistance between the gas and the surface of the insulation is neglected ($\theta_g \approx \theta_m$) and the temperature rise in the steel section is governed by the difference in temperature between the surface of the insulation (i. e., the gas temperature) and the steel profile, with only the insulation material

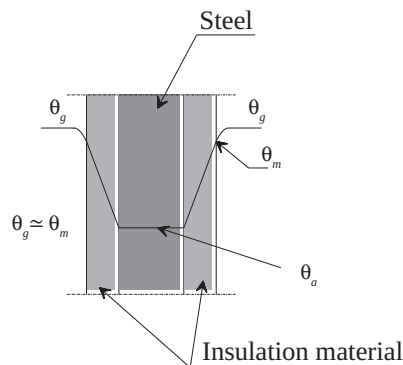


Figure 4.11 – Temperature in protected steelwork

4. TEMPERATURE IN STEEL SECTIONS

The thermal properties of the insulation material that appear in Eq. (4.19) must be determined experimentally in accordance with prEN 13381-4 (2008). According to this European standard, tests on loaded and unloaded beams as well as tests on unloaded short columns, with various massivity factors and various protection thicknesses, subjected to the standard fire should be made. The thermal conductivity of the insulation material is calculated from the recorded steel temperature using the inverse of Eq. (4.19). The unit mass and the constant specific heat must be provided by the manufacturer of the product. If the specific heat is unknown, a value of 1000 J/kgK should be assumed, Franssen *et al* (2009).

The thermal conductivity of most commonly used passive fire protection materials increases with increasing temperature. Therefore the values of the thermal properties given for room temperature applications should not be used as this will lead to unsafe results in the fire situation.

Eq. (4.19) has to be integrated with respect to time to obtain the development of the temperature in the steel section as a function of time. EN 1993-1-2 recommends that the time step interval Δt should not be taken as more than 30 seconds, a value that will ensure convergence even with an explicit integration scheme.

Any negative increment of the temperature $\Delta\theta_{a,t}$, given by Eq. (4.19), corresponding to an increase of the gas temperature, $\Delta\theta_{g,t} > 0$, must be considered as zero.

64

In the absence of specific data, the generic data given in table of the Annex A.6 may be used, (ECCS, 1995).

The tabulated values for the thermal conductivity, λ_p , are normally for dry materials. For moist fire protection materials, the steel temperature increase, $\Delta\theta_{a,t}$, may be modified to allow for a time delay t_v in the rise of the steel temperature when it reaches 100 °C, due to the latent heat of vaporization of the moisture, as shown in Fig. 4.12. The length of the horizontal plateau at 100 °C can be evaluated from the following expression, ECCS (1983):

$$t_v = \frac{p\rho_p d_p^2}{5\lambda_p} \quad [\text{min.}] \quad (p \text{ in } \%) \quad (4.21)$$

where, p is the moisture content of the protection material. No delay is allowed if the moisture is included in the value of the thermal conductivity, ECCS (1983).

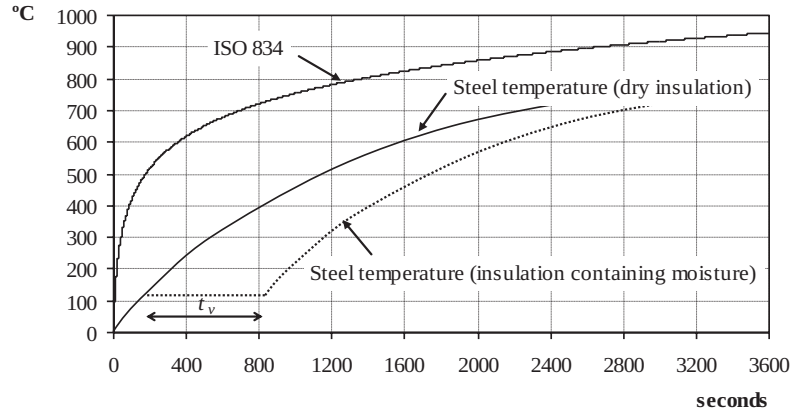


Figure 4.12 – Time delay due to the moisture content

For light weight insulation materials Eq. (4.19) can be simplified by taking $\phi = 0$. The method given in ECCS (1983) suggests that the heat capacity of the protection material can be ignored if it is less than half that of steel section, such that

$$d_p A_p c_p \rho_p < \frac{c_a \rho_a V}{2} \quad (4.22a)$$

In this expression, $\rho_a = 7850 \text{ [kg/m}^3\text{]}$ and a value $c_a = 600 \text{ [J/kgK]}$, for the specific heat of the steel can be used to check if the material is a light weight material or not.

Equation (4.22a) can be rewritten as

$$\phi = \frac{c_p d_p \rho_p}{c_a \rho_a} \cdot \frac{A_p}{V} < 0.5 \quad (4.22b)$$

If the specific heat of the protection material, c_p , is neglected, the amount of heat stored at the protection can be taken as $\phi = 0$ and Eq. (4.19) becomes

$$\Delta\theta_{a,t} = \frac{\lambda_p A_p}{d_p V c_a \rho_a} (\theta_{g,t} - \theta_{a,t}) \Delta t \quad (4.23)$$

The advantage of using this equation is that it is possible to build tables of two entries or nomograms like the ones presented in Annex A. One of the entries is the time and the other is the modified massivity factor

4. TEMPERATURE IN STEEL SECTIONS

$$\frac{A_p}{V} \cdot \frac{\lambda_p}{d_p} \quad (4.24)$$

The table and the nomograms presented in Annex A.5 have been developed for the standard fire curve ISO 834 using Eq. (4.23) with a time step of 10 seconds. This table and the nomograms provide conservative results, because the amount of heat stored in the protection together with any moisture it may contain have been neglected.

The use of the table and the nomograms from Annex A.5 avoid the need for solving the Eq. (4.19). The nomograms from Annex A have been reproduced schematically in Fig. 4.13 and 4.14. In both nomograms the temperature is given as a function of the modified massivity factor, given in Eq. (4.24).

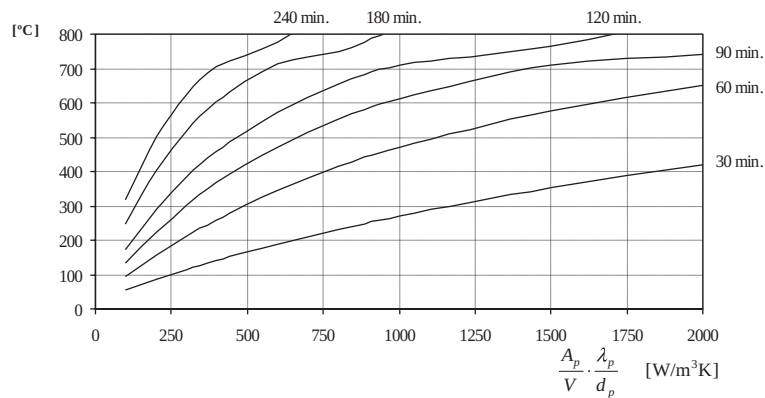


Figure 4.13 – Temperature as a function of the modified massivity factor for various times, for protected profiles subjected to the ISO 834 curve

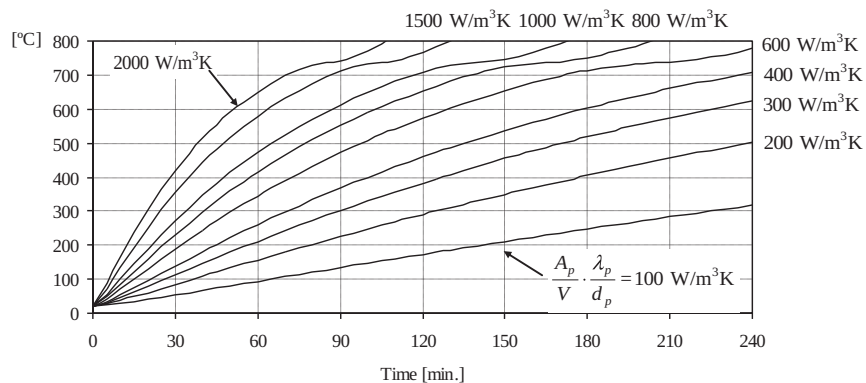


Figure 4.14 – Temperature as a function of time for various modified massivity factors, for protected profiles subjected to the ISO 834 curve

The table and the nomograms given in Annex A.5 were created assuming $\phi = 0$, and are therefore only valid for light weight insulation material.

The table and nomograms can be used for heavy materials provided the modified massivity factor is corrected, using the following expression, according to ECCS (1985):

$$\frac{A_p}{V} \cdot \frac{\lambda_p}{d_p} \cdot \left(\frac{1}{1 + \phi/2} \right) \quad (4.25)$$

This procedure gives good results for temperatures in the range of 350 °C to 700 °C, which is representative of the critical temperatures that normally occur in structural steel members. This is helpful in the pre-design phase when estimating the thickness of fire protection. The estimated thickness together with Eq. (4.19) can be used to obtain a more accurate result.

The importance of correcting the modified massivity factor (4.24) according to the expression (4.25) is demonstrated in the following example.

Consider a steel member protected with gypsum boards, which is a heavy fire insulation material with the following characteristics:

$$\frac{A_p}{V} = 110 \text{ m}^{-1}$$

$$\lambda_p = 0.2 \text{ W/(mK)}$$

$$c_p = 1700 \text{ J/(kgK)}$$

$$d_p = 0.023 \text{ m}$$

$$\rho_p = 800 \text{ kg/m}^3$$

These values lead to a ratio of heat stored in the protection:

$$\phi = \frac{c_p d_p \rho_p}{c_a \rho_a} \cdot \frac{A_p}{V} = \frac{1700 \cdot 0 \cdot 0.023 \cdot 800}{600 \cdot 7850} \cdot 110 = 0.731$$

The table given below shows the temperatures obtained with the Eq. (4.19) using the program Elefir-EN and with the nomograms from Annex A.5 considering the modified massivity factor given by Eq. (4.24) and the same factor corrected as in Eq. (4.25).

4. TEMPERATURE IN STEEL SECTIONS

Time (minutes)	Eq. (4.19) (°C)	Nomogram with $\frac{A_p \cdot \lambda_p}{V \cdot d_p}$	Nomogram with $\frac{A_p \cdot \lambda_p}{V \cdot d_p} \cdot \left(\frac{1}{1 + \phi/2} \right)$
15	84	140 (+67.2%)	112 (+31.0%)
30	186	263 (+41.3%)	210 (+13.1%)
60	370	460 (+24.4%)	381 (+2.9%)
120	627	699 (+11.5%)	616 (-1.7%)

() error comparing with the solution from Eq. (4.19).

From this table it can be concluded that the nomogram built for light weight insulation materials gives good approximation to the results from Eq. (4.19) if the corrected massivity factor Eq. (4.25) is used.

Fig. 4.15 shows the influence of the parameter ϕ for this example.

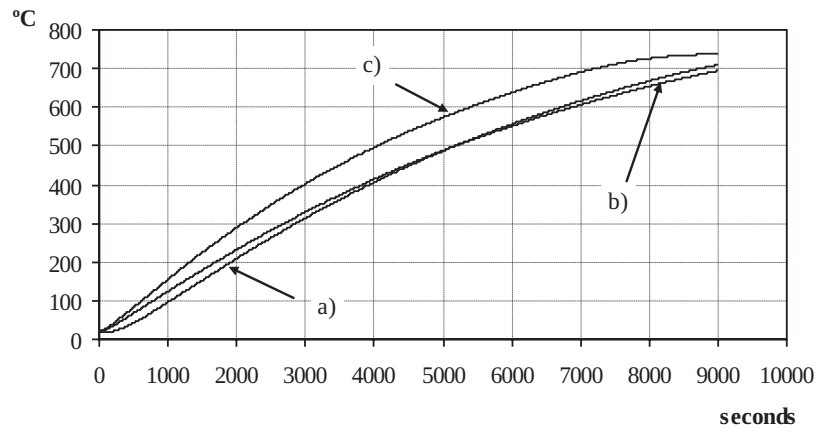


Figure 4.15 – Influence of the parameter ϕ , in a heavy fire insulation material
a) Eq. (4.19); b) Eq. 4.23 with Eq. (4.25); c) Eq. 4.19 with $\phi = 0$ or Eq. (4.23)

Consider now a steel profile protected with a light weight fire insulation material, such as mineral wool, the characteristics of which are listed below:

$$\frac{A_p}{V} = 225 \text{ m}^{-1}$$

$$\lambda_p = 0.2 \text{ W/(mK)}$$

$$c_p = 1200 \text{ J/(kgK)}$$

$$d_p = 0.02 \text{ m}$$

$$\rho_p = 150 \text{ kg/m}^3$$

The ratio of heat stored in the protection now takes the value $\phi = 0.17$.

Fig. 4.16 shows that the influence of the amount of heat stored in the protection, ϕ , is not relevant, in this case and so Eq. (4.19) can be used with $\phi = 0.0$, for light weight fire insulation material, i. e., tables or nomograms, like the ones presented in Annex A, can be used without any correction.

Light weight protection material

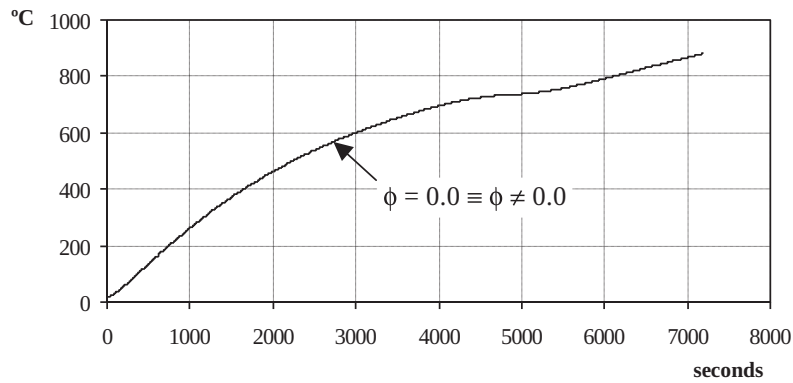


Figure 4.16 – Influence of the parameter, ϕ , in light weight fire insulation material

Fig. 4.17 shows the temperature development of an unprotected HE 220 A profile heated on four sides by the fire defined in example 3.3.

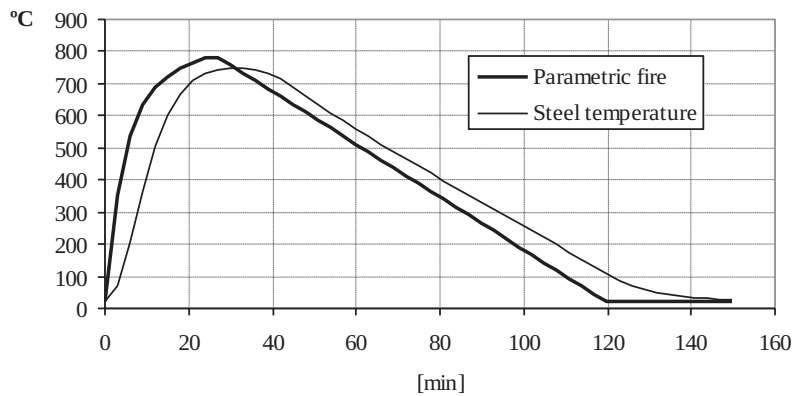


Figure 4.17 – Temperature of an unprotected HE 220 A heated by the parametric fire from example 3.3

4. TEMPERATURE IN STEEL SECTIONS

If the same profile is fire protected with gypsum board encasement with a thickness of $d_p = 15 \text{ mm}$, the temperature development is shown in Fig. 4.18.

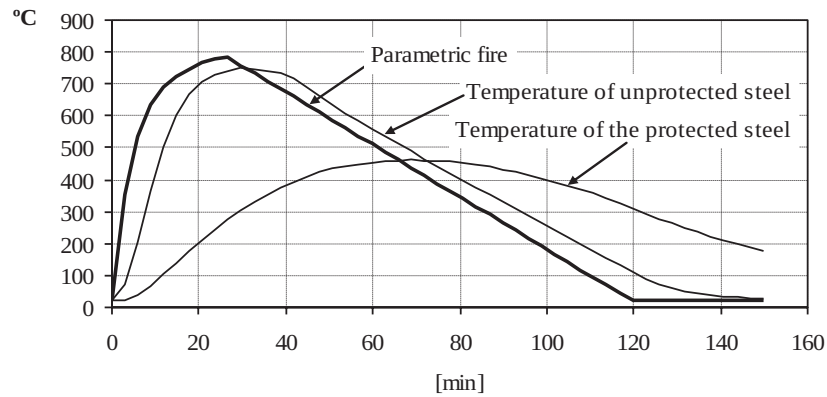


Figure 4.18 – Temperature of a HE 220 A heated by the parametric fire of example 3.3

Example 4.1: What is the temperature of an unprotected rectangular bar with a cross section of $200 \times 50 \text{ mm}^2$ after 30 minutes of standard fire exposure on four sides?

70

The section factor of this convex section takes the value:

$$A_m/V = \frac{2 \times (b+t)}{b \times t} = \frac{2 \times (0.2+0.05)}{0.2 \times 0.05} = 50 \text{ m}^{-1}$$

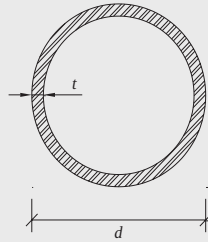
As the section is convex, $k_{sh} = 1$, and the modified section factor is

$$k_{sh} [A_m/V] = 1.0 \cdot 50 = 50 \text{ m}^{-1}$$

With this section factor and by interpolation in table of the Annex A.4, a temperature of 678.5 °C is obtained.

If Eq. (4.16) is used with the program Elefir-EN, a value of the temperature of 690 °C is obtained.

Example 4.2: What is the temperature of an unprotected circular hollow section with a diameter of $d = 220$ mm and a thickness of $t = 5$ mm after 60 minutes of standard fire exposure?



The external perimeter is

$$P = \pi \cdot d = 691.15 \text{ mm}$$

The area of the cross section is

$$A = \frac{\pi}{4} \left[d^2 - (d - 2t)^2 \right] = 3377.21 \text{ mm}^2$$

The section factor is

$$\frac{A_m}{V} = \frac{P}{A} = 0.2047 \text{ mm}^{-1} = 204.7 \text{ m}^{-1}$$

According to Annex A.2, the section factor is given by:

$$\frac{A_m}{V} = \frac{P}{A} = \frac{d}{(d-t)t} \approx \frac{1}{t} = 200 \text{ m}^{-1}$$

As the section is convex, $k_{sh} = 1$, and the modified section factor, using the later value of the section factor, is

$$k_{sh} [A_m / V] = 200 \text{ m}^{-1}$$

Table of the Annex A.4 gives the temperature of 942 °C.

Example 4.3: What is the temperature of an unprotected HE 200 A profile after 30 minutes of standard fire exposure on four sides?

4. TEMPERATURE IN STEEL SECTIONS

The section factor for an HE 200 A is:

$$A_m / V = 211 \text{ m}^{-1}$$

The HE 200 A has the following geometric characteristics:

$$b = 200 \text{ mm}$$

$$h = 190 \text{ mm}$$

$$A = 53.83 \text{ cm}^2$$

and the box value of the section factor $[A_m / V]_b$ takes the value

$$[A_m / V]_b = \frac{2 \times (b + h)}{A} = \frac{2 \times (0.2 + 0.19)}{53.83 \times 10^{-4}} = 144.9 \approx 145 \text{ m}^{-1}$$

The shadow factor, k_{sh} is given by:

$$k_{sh} = 0.9 [A_m / V]_b / [A_m / V] = 0.9 \cdot 144.9 / 211 = 0.618$$

Taking into account the shadow effect, the modified section factor has the value

$$k_{sh} [A_m / V] = 0.618 \cdot 211 = 130.5 \text{ m}^{-1}$$

This value should be obtained without evaluating k_{sh} , using Eq. (4.18a):

$$k_{sh} [A_m / V] = 0.9 [A_m / V]_b = 0.9 \cdot 145 = 130.5 \text{ m}^{-1}$$

Interpolating in table of the Annex A.4 yields a temperature of 786 °C.

If Eq. (4.16) is used, a temperature of 802 °C is obtained.

Example 4.4: What is the thickness of fibre-cement board encasement for a IPE 300 heated on three sides to be classified as R90 if the critical temperature is 654 °C?

The following thermal properties of the fibre-cement are defined in Annex A.6:

$$\lambda_p = 0.15 \text{ W}/(\text{m} \cdot \text{K})$$

$$c_p = 1200 \text{ J}/(\text{kgK})$$

$$\rho_p = 800 \text{ kg}/\text{m}^3$$

The massivity factor for the IPE 300 with hollow encasement heated on three sides is:

$$A_p / V = 139.4 \text{ m}^{-1}$$

By interpolation in table of the Annex A.5, for a temperature of 654 °C, at 90 minutes of standard fire exposure, the modified section factor is:

$$\frac{A_p}{V} \cdot \frac{\lambda_p}{d_p} \leq 1210 \text{ W}/(\text{m}^3 \cdot \text{K})$$

and the thickness is

$$d_p \geq \frac{A_p / V}{1210} \lambda_p = \frac{139.4}{1210} \cdot 0.15 = 0.017 \text{ m} = 17 \text{ mm}$$

This thickness can be corrected if the amount of heat stored in the protection, ϕ , is taken into account, according Eq. (4.20) and using Eq. (4.25) to obtain the corrected thickness.

$$\frac{A_p}{V} \cdot \frac{\lambda_p}{d_p} \cdot \frac{1}{1 + \phi/2} \leq 1210 \text{ W}/(\text{m}^3 \cdot \text{K})$$

The following iterative procedure is needed to evaluate the corrected thickness:

d_p	$\phi = \frac{c_p d_p \rho_p}{c_a \rho_a} \cdot \frac{A_p}{V}$	$d_p \geq \frac{A_p}{V} \cdot \frac{\lambda_p}{1210} \cdot \frac{1}{1 + \phi/2}$
0.017	$\frac{1200 \cdot 0.017 \cdot 800}{600 \cdot 7850} \cdot 139$	0.0139
0.0139	$\frac{1200 \cdot 0.0139 \cdot 800}{600 \cdot 7850} \cdot 139$	0.0144
0.0144	$\frac{1200 \cdot 0.0144 \cdot 800}{600 \cdot 7850} \cdot 139$	0.0143
0.0143	$\frac{1200 \cdot 0.0143 \cdot 800}{600 \cdot 7850} \cdot 139$	0.0143

With this procedure a thickness of 14.3 mm is obtained, instead of 17 mm.

Example 4.5: At what time will a HE 220 B column protected with a 20mm thick gypsum board reach a temperature of 559 °C when heated by the standard fire curve on four sides?

The massivity factor for the HE 220 B with hollow encasement heated on four sides is $A_p / V = 96.7 \text{ m}^{-1}$.

Annex A.6 gives the thermal properties of gypsum boards:

$$\begin{aligned}\lambda_p &= 0.2 \text{ W/(m} \cdot \text{K)} \\ c_p &= 1700 \text{ J(kg} \cdot \text{K)} \\ \rho_p &= 800 \text{ kg/m}^3 \\ p &= 20\% \text{ (moisture content)}\end{aligned}$$

As the thickness of the insulation is known, the ratio of heat stored in the protection can be evaluated as

$$\phi = \frac{c_p d_p \rho_p}{c_a \rho_a} \cdot \frac{A_p}{V} = \frac{1700 \cdot 0.02 \cdot 800}{600 \cdot 7850} \cdot 96.7 = 0.558$$

and the corrected modified section factor

$$\frac{A_p}{V} \cdot \frac{\lambda_p}{d_p} \cdot \frac{1}{1 + \phi/2} = 96.7 \cdot \frac{0.2}{0.02} \cdot \frac{1}{1 + 0.558/2} = 756 \text{ W/(m}^3 \cdot \text{K)}$$

Based on this value and for the temperature of 559 °C, a double interpolation in the table of the Annex A.5 gives a time of 97 minutes.

The delay time due to the moisture content is, according to Eq. (4.21):

$$t_v = \frac{p \rho_p d_p^2}{5 \lambda_p} = \frac{20 \cdot 800 \cdot 0.02^2}{5 \cdot 0.2} = 6 \text{ min.}$$

The time to reach the temperature of 559 °C is then:

$$t = 97 + 6 = 103 \text{ min.}$$

If the program Elefir-EN is used the temperature of 559 °C is reached after 98.9 minutes, as shown in Fig. 4.19.

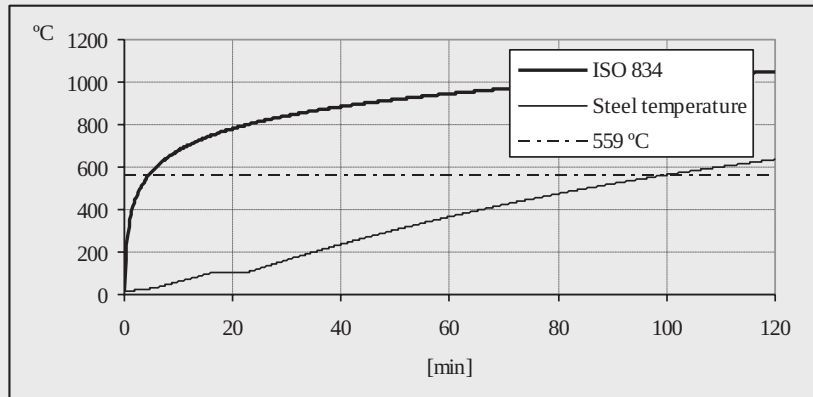


Figure 4.19 – Temperature of a HE 220 B protected with gypsum boards

Example 4.6: Consider a IPE 300 profile protected with 20 mm thick fibre-cement board encasement. Calculate the temperature after 60 minutes of standard fire exposure on four sides taking into account the amount of heat stored in the protection and the time delay due to the moisture content.

The following thermal properties of the fibre-cement board are defined in Annex A.6:

$$\begin{aligned}\lambda_p &= 0.15 \text{ W/(m}\cdot\text{K)} \\ c_p &= 1200 \text{ J/(kgK)} \\ \rho_p &= 800 \text{ kg/m}^3 \\ p &= 5\% \text{ (moisture content)}\end{aligned}$$

From Annex E, the section factor of the IPE 300 is $A_p/V = 167.3 \text{ m}^{-1}$.

The ratio of heat stored in the protection takes the value:

$$\phi = \frac{c_p d_p \rho_p}{c_a \rho_a} \cdot \frac{A_p}{V} = \frac{1200 \cdot 0.02 \cdot 800}{600 \cdot 7850} \cdot 167.3 = 0.682$$

and the corrected section factor:

$$\frac{A_p}{V} \cdot \frac{\lambda_p}{d_p} \cdot \frac{1}{1 + \phi/2} = 937 \text{ W/(m}^3\text{K)}$$

4. TEMPERATURE IN STEEL SECTIONS

Interpolating in table of the Annex A.5 yields a temperature of 453 °C.

If Eq. (4.19) is used, for example with the software Elefir-EN, the temperature of 451 °C is obtained, which is close to the value obtained by interpolation.

The time increase in fire resistance due to the moisture content of the protection can be calculated as follows:

$$t_v = \frac{p\rho_p d_p^2}{5\lambda_p} = \frac{5 \cdot 800 \cdot 0.02^2}{5 \cdot 0.15} = 2.13 \cong 2 \text{ min.}$$

Taking into account this delay, the temperature is calculated after $60 - 2 = 58$ minutes instead of 60 minutes. Eq. (4.19) gives, after 58 minutes, the temperature

$$\theta = 439 \text{ °C}$$

With the software Elefir-EN a temperature of 443 °C is obtained if the moisture content is taken into account.

It should be noted that if the fibre-cement board was considered as light weight insulation material and the corrected section factor was not used, then table of the Annex A.5 would give for

76

$$\frac{A_m}{V} \cdot \frac{\lambda_p}{d_p} = 167.3 \cdot \frac{0.15}{0.02} = 1254.8 \text{ W/(m}^3\text{K)}$$

a temperature of $\theta = 526 \text{ °C}$ instead of the 453 °C previously obtained, with an error of $\approx 16.7\%$, but on the safe side.

4.7. INTERNAL STEELWORK IN A VOID PROTECTED BY HEAT SCREENS

This section deals with two different geometrical situations.

The first situation is when a steel beam is underneath a slab, with a horizontal heat screen present underneath the profile, as shown in Figure 4.20.

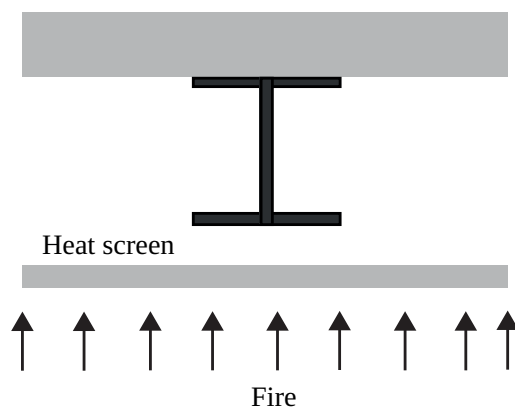


Figure 4.20 – Steel beam with a heat screen underneath (elevation)

The second situation is when a steel column is located between two vertical heat screens. Fig. 4.21 shows a column with heat screens on both sides and the fire on one side only. The fire could also be on each side of the column.

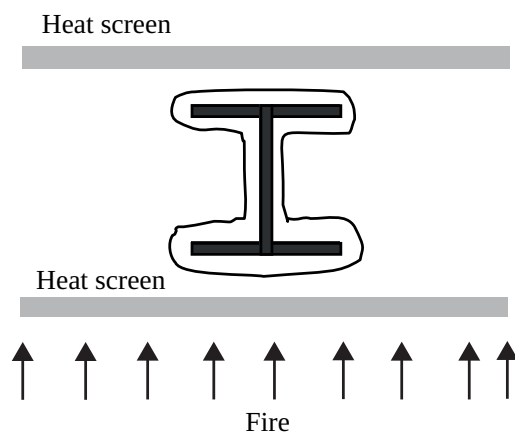


Figure 4.21 – Protected steel column with heat screens on both sides (plan view)

In both cases, there is a gap between the heat screen and the steel section. If the heat screen touches the steel section, the method describes in this section does not apply.

The development of the temperature in the steel section must be calculated by one of the methods described in Sections 4.5 or 4.6, depending on whether or not the steel member is thermally protected. The fire temperature is taken as the gas temperature in the void, and this is

4. TEMPERATURE IN STEEL SECTIONS

determined experimentally according to EN 13381-1 (2006), for horizontal protective membranes, or EN 13381-2 (2008), for vertical protective membranes, as appropriate.

4.8. EXTERNAL STEELWORK

4.8.1. General principles

This section deals with steel members that are located outside the envelope of the building and are heated by flames coming from inside the building. The temperature and the size of the flames are determined using the methods given in Section 3.7.

The temperature distribution in external steelwork is determined in a steady state situation based on the steady state radiative fluxes determined according to Section 3.7. This means that a temperature will be determined in the steel section, but no information will be available about the time required for this temperature to be established. As a consequence, the verification of the stability of the steel member is only possible in the temperature or in the load domain, but not in the time domain. The result will be either a fail or a pass. If the calculation shows that the stability is ensured, any fire requirement expressed in term of fire class will be satisfied. If the calculation shows that the stability is not ensured, it will not be possible to determine the time of collapse and, thus, the fire resistance class of the member. Recent research work has been undertaken to extend the theory to transient situations, but the results of this work have not yet been introduced in the Eurocode.

The temperature in the steel section results from an energy balance between the radiative heat flux received from the fire compartment and the radiative and convective heat flux emanating from the openings, on one hand, and the radiative and convective heat flux lost to the ambient atmosphere, on the other hand.

The influence of heat screens must be considered. If the heat screens are non-combustible and have a fire resistance EI of at least 30 minutes according to EN ISO 13501-2, it is assumed that there is no radiative heat transfer to those sides of the section that are protected by the screens.

Geometrical parameters such as size and location of the steel member

with respect to the compartment and its openings and size of the openings must be considered.

The detailed procedure is described in Annex B of Eurocode 3. Only the general principles are described in this book.

The assumptions are that the fire is confined to one compartment only and that all openings in the façade are rectangular.

A distinction is made between members that are engulfed in flames and members that are not engulfed in flames, depending on their position relative to the openings:

- A member that is not engulfed in flames receives heat from all the openings in the wall that it is facing and from all flames coming out of these openings.
- A member that is engulfed in flames receives heat only from the engulfing flame (convection and radiation) and from the opening from which this flame is emanating (radiation).

The equilibrium temperature in the steel member T_m is calculated from the heat balance given in Eq. (4.26) for a member not engulfed in flames and in Eq. (4.27) for a member engulfed in flames.

$$\sigma T_m^4 + \alpha T_m = \sum I_z + \sum I_f + \alpha 293 \quad (4.26)$$

$$\sigma T_m^4 + \alpha T_m = I_z + I_f + \alpha T_z \quad (4.27)$$

where σ is the Stefan Boltzmann constant equal to 5.67×10^{-8} W/m²K⁴, α is the convective heat transfer coefficient, I_z is the radiative heat flux from a flame, I_f is the radiative heat flux from an opening and T_z is the flame temperature.

The convective heat transfer coefficient α is calculated from the rules given in Annex B of Eurocode 1, see Section 3.7 of this book, using an effective cross section dimension equal to the average of both dimensions in the section.

The radiative heat flux from an opening is calculated from Eq. (4.28).

$$I_f = \phi_f (1 - \alpha_f) \sigma T_f^4 \quad (4.28)$$

where ϕ_f is the overall configuration factor of the member from that opening and α_f is the absorptivity of the flame, to be determined according to the rules given in Annex B of Eurocode 3.

4. TEMPERATURE IN STEEL SECTIONS

It is not possible to repeat in detail in this book all the rules that are given in Eurocode 1 and Eurocode 3. An example is given hereafter that will allow the reader to follow the procedure for a simple case and find his way through all the clauses of the Eurocodes where this procedure is described.

4.8.2. Example

A hotel is constructed from a steel skeleton that supports modular prefabricated rooms. Part of the structure is external, as shown in Figure 4.22.

The floor to floor height is 2.8 m and the grid is 3 m wide. The windows are 1.5 m wide and 1 m high. The external steel structure is 1 m away from the façade. Each room is 2.8 m wide and 6 m deep, with a floor to ceiling height of 2.5 m. The effect of the wind is not considered.

Calculate the temperature in the external 0.2 m × 0.2 m steel square tube columns.

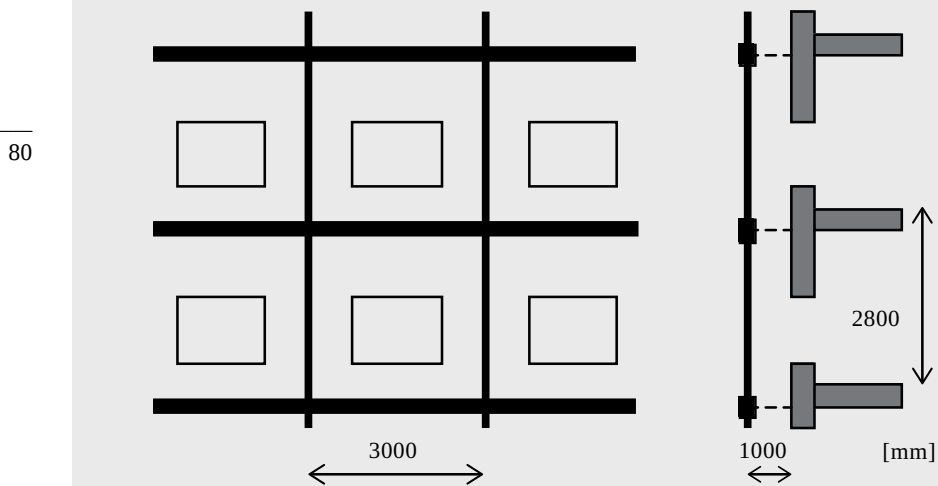


Figure 4.22 – Two elevations of the façade of a hotel

The area of the window (1.5 m^2) is less than 50% of the area of the wall (7 m^2). There is no forced draught and the door of the room is assumed to be closed.

Rate of heat release in the compartment

$$\text{Floor area } A_f = 6 \times 2.8 = 16.8 \text{ m}^2$$

$$\text{Design fire load } q_{f,d} = 377 \text{ MJ/m}^2 \text{ (taken as } q_{f,k})$$

$$Q_{fuel\ control} = 377 \times 16.8 / 1200 = 5.28 \text{ MW, see Eq. (3.35)}$$

$$D/W = 6 / 2.8 = 2.14, \text{ see Eq. (3.34) (B.1 in Eurocode 1)}$$

$$\text{Height of the window } h_{eq} = 1 \text{ m}$$

$$\text{Area of vertical openings } A_v = 1.5 \times 1 = 1.5 \text{ m}^2$$

$$\text{Total area of enclosure } A_t = 2 \times 16.8 + 2 \times 2.5(6 + 2.8) = 77.6 \text{ m}^2$$

$$\text{Opening factor } O = 1.5 \times (1)^{0.5} / 77.6 = 0.019 \text{ m}^{1/2}$$

$$Q_{air\ control} = 3.15(1 - e^{-0.036/0.019}) 1.5 \sqrt{\frac{1}{2.14}} = 2.74 \text{ MW, see Eq. (3.35)}$$

$$\Rightarrow Q = 2.74 \text{ MW}$$

Temperature of the fire compartment

$$\Omega = \frac{16.8 \times 377}{\sqrt{1.5 \times 77.6}} = 587, \text{ see Eq. (3.37)}$$

$$T_f = 6000(1 - e^{-0.1/0.019}) \sqrt{0.019} (1 - e^{-0.00286 \times 587}) + 20 = 689^\circ\text{C}$$

Flame height

$$L_L = 1.9 \left(\frac{2.74}{1.5} \right)^{2/3} - 1 = 1.84 \text{ m, see Eq. (3.38)}$$

Flame temperature at the window

$$L_f = 1.84 + 1/2 = 2.34$$

$$L_f w_t / Q = 2.34 \times 1.5 / 2.74 = 1.401 > 1. \text{ We take } L_f w_t / Q = 1.0$$

$$T_w = 520 / (1 - 0.4725 \times 1.0) + 20 = 1006^\circ\text{C}$$

4. TEMPERATURE IN STEEL SECTIONS

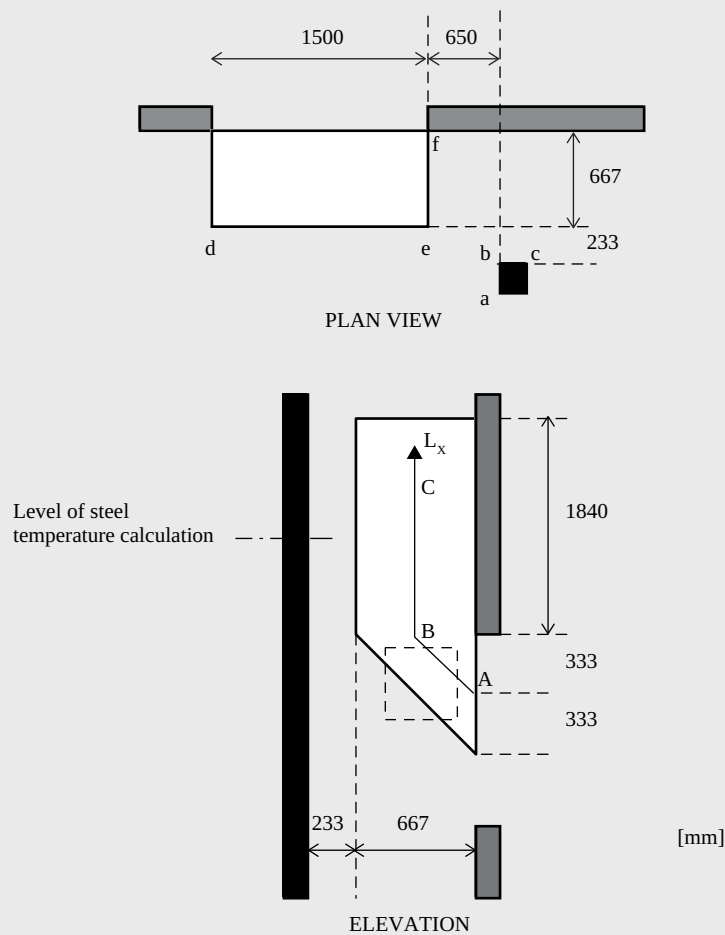


Figure 4.23 – Shape of the flame

Shape of the flame

See Fig. 4.23

Temperature along the flame

$$L_x w_t / Q = L_x \times 1.5 / 2.74 = 0.55 L_x, \text{ must be smaller than 1.}$$

L_x must be lower than 1.83 m.

$$\begin{aligned} T_z &= (1006 - 20)(1 - 0.4725 \times 0.55 L_x) + 20 = 986(1 - 0.26 \times L_x) + 20 \\ &= 1006 - 256 L_x, \text{ see Eq. (3.40)} \end{aligned}$$

The temperature varies linearly along the flame axis. From 1006 °C at the window, see point A on Figure 4.23, the temperature decreases to 885 °C at point B ($L_x = 0.471$ m) and 538 °C at point C, located $1.83 - 0.471 = 1.359$ m above point B.

Above Point C, where $L_x w_t / Q$ is larger than 1, the Eurocode is not clear about the temperature distribution. It is assumed here that the term $L_x w_t / Q$ is replaced by 1 in the equation and the temperature keeps the same value of 538 °C until the tip of the flame.

Clause B.1.4 (4) of Eurocode 3 states that the radiative heat flux from the flames may be based on the dimensions of an equivalent rectangular flame. This approximation would clearly simplify the process but it has nevertheless not been made here. This is because the Eurocode is not very clear about the size and equivalent temperature of this equivalent rectangular flame. For example, Fig. B.3 shows a height z of the equivalent flame, and z is said to be defined in Annex B of Eurocode 1 but z is not used in Eurocode 1. If z is the height of the window, then the equivalent rectangular flame is not linked to the height of the real flame L_L . Also, the temperature of the flame should be taken at a distance l from the opening equal to $h/2$ (Eq. B.11a) and, assuming that h is the height of the window, this point has also no correlation with the flame length.

This is why physical principals and "*using appropriate adaptations of the treatments given in B.2*", see B.1.3 (4), have been used here.

It is not possible to determine directly the vertical position along the column where the level of temperature is the highest. Strictly speaking, the temperature should be evaluated at different positions along the column. The crushing load of the column is then determined by the maximum temperature of all sections. If the failure mode is by buckling, it will be more difficult to evaluate the load bearing capacity of the column using simple models with a temperature that varies along the length.

Because of the longer length of the vertical part of the flame (i.e., the part that extends along the wall above the window), it is assumed that the point of maximum temperature is facing this vertical part. Because of higher temperatures prevailing in the lower part of the flame, it is assumed that the point of maximum temperature is slightly below mid-level of the vertical part. The temperature will be calculated in this example only at a level of 0.6 m above point B.

4. TEMPERATURE IN STEEL SECTIONS

For a precise determination of the steel temperature at this point, the vertical part of the flame should be divided along the height in a number of different zones, each one having its own temperature. For simplicity, the temperature in the vertical part of the flame will be approximated as constant and equal to the value at 0.6 m, i.e., $L_x = 1.071$ m. This temperature is 732 °C.

The lateral triangular part of the flame (the part that contains the line A-B on the elevation of Figure 4.23) is also visible from the section, see the plan view. To allow direct application of the formulae for view factors, it will be approximated as a square surface of equal surface area ($0.222 \text{ m}^2 = 0.47 \text{ m} \times 0.47 \text{ m}$), with a uniform temperature equal to 945 °C (average between T_A and T_B) and located at the centre of gravity of the triangle. This equivalent square surface is represented by a dotted line on the elevation.

View factors

1.a) Between the centre of side b-c on the profile and the vertical plane d-e on the flame, see the plan view on Figure 4.23. The planes are parallel and the configuration corresponds to the one depicted in Fig. 3.6 and Fig. 3.8. Distance (horizontal) between the two planes $s = 0.233$ m.

The vertical part of the flame is divided into 4 zones (2 of them with negative contribution) and the calculations are summarized in the following table.

	h (vertical)	w (horizontal)	ϕ
Zone 1	0.60	2.25	0.233
Zone 2	0.60	0.75	-0.227
Zone 3	1.24	2.25	0.245
Zone 4	1.24	0.75	-0.237
Total	-	-	0.014

1.b) Between the centre of side b-c on the profile and the plane e-f on the flame, see the plan view on Figure 4.23. The planes are perpendicular and the configuration corresponds to the one depicted in Fig. 3.7 and Fig. 3.8.

Distance (horizontal) between points P and x: $s = 0.75$ m.

The vertical part of the flame is divided into 4 zones and the calculations are summarized in the following table.

	h (vertical)	w (horizontal)	ϕ
Zone 1	0.60	0.900	0.059
Zone 2	0.60	0.233	-0.008
Zone 3	1.24	0.900	0.081
Zone 4	1.24	0.233	-0.010
Total	-	-	0.121

The total view factor from the side b-c to the section of the flame at 732 °C is thus equal to $0.014 + 0.121 = 0.135$.

2) Between the centre of side b-c on the profile and the lateral triangular part of the flame. The planes are perpendicular and the configuration corresponds to the one depicted in Fig. 3.7.

Distance (horizontal) between points P and x: $s = 0.75$ m.

The vertical part of the flame is divided into 4 zones and the calculations are summarized in the following table.

	h (vertical)	w (horizontal)	ϕ
Zone 1	1.057	0.913	0.078
Zone 2	1.057	0.443	-0.031
Zone 3	0.587	0.913	-0.059
Zone 4	0.587	0.443	0.024
Total	-	-	0.012

85

3.a) Between the centre of side a-b on the profile and the vertical plane e-f on the flame, see plan view on Figure 4.23. Distance (horizontal) between the two parallel planes $s = 0.65$ m. The calculations are summarized in the following table.

	h (vertical)	w (horizontal)	ϕ
Zone 1	0.60	1.00	0.154
Zone 2	0.60	0.33	-0.089
Zone 3	1.24	1.00	0.195
Zone 4	1.24	0.33	-0.108
Total	-	-	0.151

4. TEMPERATURE IN STEEL SECTIONS

3.b) Between the centre of side a-b on the profile and the plane e-d on the flame, see the plan view on Figure 4.23. The planes are perpendicular.

Distance (horizontal) between points P and x: $s = 0.333$ m.

	h (vertical)	w (horizontal)	ϕ
Zone 1	0.60	2.15	0.163
Zone 2	0.60	0.65	-0.119
Zone 3	1.24	2.15	0.196
Zone 4	1.24	0.65	-0.133
Total	-	-	0.106

The total view factor from the side a-b of the section to the flame at 732 °C is thus equal to $0.151 + 0.106 = 0.257$.

4) Between the centre of side a-b on the profile and the lateral triangular part of the flame. Distance (horizontal) between the two parallel planes $s = 0.65$ m.

	h (vertical)	w (horizontal)	ϕ
Zone 1	1.057	1.013	0.189
Zone 2	1.057	0.543	-0.147
Zone 3	0.587	1.013	-0.152
Zone 4	0.587	0.543	0.121
Total	-	-	0.011

5) Between the centre of side b-c on the profile and the window. Distance (horizontal) between the two parallel planes $s = 0.90$ m.

	h (vertical)	w (horizontal)	ϕ
Zone 1	1.6	2.25	0.209
Zone 2	1.6	0.75	-0.149
Zone 3	0.6	2.25	-0.135
Zone 4	0.6	0.75	0.102
Total	-	-	0.027

6) Between the centre of side a-b on the profile and the window. The planes are perpendicular. Distance (horizontal) between points P and x: $s = 1.0$ m.

	h (vertical)	w (horizontal)	ϕ
Zone 1	1.6	2.15	0.121
Zone 2	1.6	0.65	-0.037
Zone 3	0.6	2.15	-0.069
Zone 4	0.6	0.65	0.024
Total	-	-	0.039

Radiative heat flux from the opening, see Eq. (B.3) in Eurocode 3

Overall configuration factor from the opening, see Eq. (B.4) in Eurocode 3:

$$\phi_f = (0.027 \times 200 + 0.039 \times 200) / (4 \times 200) = 0.017$$

Emissivity of the opening, see B.1.3 (6) in Eurocode 3:

$$\varepsilon_f = 1.0$$

Absorptivity of the flame, see B.2.4 (1) in Eurocode 3:

$$a_z = 0$$

$$I_f = 0.017 \times 1 \times (1 - 0) \times 5.67 \times 10^{-8} \times (689 + 273)^4 = 826 \text{ W/m}^2$$

87

Radiative heat flux from the flame

Radiation from the part of the flame above the window.

Overall configuration factor from the flame, see Eq. (B.5) in Eurocode 3.

$$\phi_z = (0.135 \times 200 + 0.257 \times 200) / (4 \times 200) = 0.098$$

Emissivity of the flame:

Flame thickness = 1.5 m, Eq. (B.10a) in Eurocode 3.

$$\varepsilon_f = 1 - e^{-0.3 \times 1.5} = 0.362, \text{ Eq. (B.26) in Eurocode 1}$$

$$I_{z1} = 0.098 \times 0.362 \times 5.67 \times 10^{-8} \times (732 + 273)^4 = 2052 \text{ W/m}^2$$

Radiation from the triangular part of the flame.

Overall configuration factor from the flame, see Eq. (B.5) in Eurocode 3

$$\phi_z = (0.012 \times 200 + 0.011 \times 200) / (4 \times 200) = 0.006$$

$$I_{z1} = 0.006 \times 0.362 \times 5.67 \times 10^{-8} \times (945 + 273)^4 = 271 \text{ W/m}^2$$

Convective heat transfer coefficient

Effective cross sectional dimension:

$$d_{eq} = 0.2, \text{ see B.1.3 (2) in Eurocode 3}$$

$$\alpha_c = 4.67(1/0.2)^{0.4} (2.74/1.5)^{0.6} = 12.8, \text{ see B.4.1 (12) in Eurocode 1}$$

Equation of equilibrium, Eq. (B.1) in Eurocode 3

$$5.67 \times 10^{-8} T^4 + 12.8 T = 826 + 2052 + 271 + 293 \times 12.8$$

This yields as a solution: $T = 412 \text{ K}$ or 139°C .

This temperature is, in this academic example, rather low. A new calculation should normally be made taking into account the effect of wind. The process is similar to the one described here; only the geometrical quantities are more complicated.

4.9. VIEW FACTORS IN THE CONCAVE PART OF A STEEL PROFILE

A view factor can be introduced to account for “parts” of the structural element that shielded from radiative heat (ECCS TC3, 2001). It is defined as the ratio between radiative heat leaving an emitting surface and the radiative heat arriving at a receiving surface.

The general formula for the view factor is (ECCS TC3, 2001, Drysdale, 1999)

$$\phi = \frac{1}{A_r} \int \int_{A_e, A_r} \frac{\cos \phi_e \cos \phi_r}{\pi r^2} dA_e dA_r \quad (4.29)$$

For two-dimensional cases (see Fig. 4.24) the view factor can be given by (ECCS TC3, 2001):

$$\phi = \frac{AC + BD - AD - BC}{2CD} \text{ but } \phi \leq 1.0 \quad (4.30)$$

By definition, the value of the view factor is between zero and unity. Its value depends on the distance between the two surfaces, the size of the surfaces and their relative orientation (see Fig. 4.24).

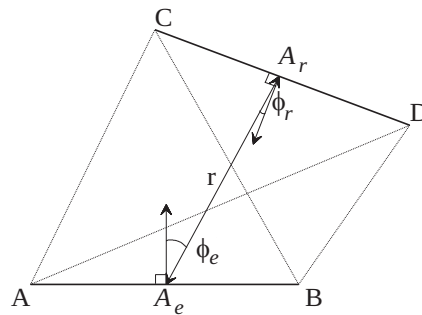


Figure 4.24 – Emitting and receiving surfaces for radiative heat
(A_e - emitting surface; A_r - receiving surface)

As an example, Fig. 4.25 shows the values of the view factors for the internal surfaces of a fully fire engulfed HE 400 B. These are the view factors between the surface of the box contour through which the energy passes and each of the internal surfaces of the section that receive this energy. Each view factor can be calculated according to Eq. (4.30) and using Fig. 4.26 for this particular case.

- i) For the web surface according to Fig. 4.26a

$$\phi = \frac{AC + BD - AD - BC}{2CD} = \frac{2 \cdot 143.25 - 2 \cdot \sqrt{143.25^2 + 352^2}}{2 \cdot 352} = 0.67$$

- ii) For the top flange surface according to Fig. 4.26b

$$\phi = \frac{AC + BD - AD - BC}{2CD} = \frac{\sqrt{143.25^2 + 352^2} + 0 - 352 - 143.25}{2 \cdot 143.25} = 0.40$$

4. TEMPERATURE IN STEEL SECTIONS

iii) For the bottom flange surface according to Fig. 4.26c

$$\phi = \frac{\overline{AC} + \overline{BD} - \overline{AD} - \overline{BC}}{2CD} = \frac{143.25 + 352 - 0 - \sqrt{143.25^2 + 352^2}}{2 \cdot 143.25} = 0.40$$

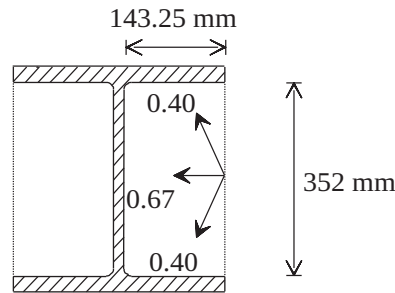


Figure 4.25 – View factors for an HE 400 B

It can be verified that the total amount of energy received by the chamber of the section is proportional to $2 \times 0.40 \times 143.25 + 0.67 \times 352 = 352$, which is exactly equal to the factor proportional to the energy crossing the dotted line on Fig. 4.25, considering $\phi = 1.0$, i.e., $1.0 \times 352 = 352$.

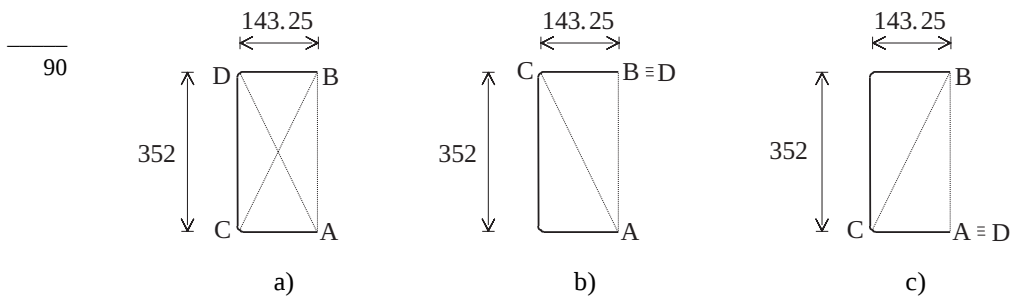


Figure 4.26 – Emitting (AB) and receiving (CD) surfaces for radiative heat.

a) For the web surface; b) For the top flange surface; c) For the bottom flange surface

This concept can be used, for example, when the temperature of the web of a section has to be determined in order to evaluate the shear resistance of the web. This procedure is more detailed and more precise than the utilisation of the shadow factor present in Eq. (4.16) because the shadow

factor is the weighted average value of the view factors calculated on the whole perimeter of the section¹.

For example, for the HE 400 B and neglecting the radius of root fillet between the web and the flanges, the values for the perimeter, A_m , the box value of the perimeter, $A_{m,b}$, the area of the cross section, V , the box value of the section factor, $[A_m/V]_b$ and the section factor, A_m/V , are:

$$A_m = 1973 \text{ mm}$$

$$A_{m,b} = 1400 \text{ mm}$$

$$V = 19152 \text{ mm}^2$$

$$[A_m/V]_b = 1400/19152 = 0.073 \text{ mm}^{-1} = 73 \text{ m}^{-1}$$

$$A_m/V = 1973/19152 = 0.103 \text{ mm}^{-1} = 103 \text{ m}^{-1}$$

The correction factor for the shadow effect given by Eq. (4.17b), takes the value:

$$k_{sh} = [A_m/V]_b / [A_m/V] = 0.073/0.103 = 0.708$$

which is exactly the same as the weighted average value of the view factors, $\bar{\Phi}$, calculated on the whole perimeter of the section

$$\bar{\Phi} = \frac{4 \cdot 0.4 \cdot 143.5 + 2 \cdot 0.67 \cdot 352 + 2 \cdot 1.0 \cdot 300 + 4 \cdot 1.0 \cdot 24}{1973} = 0.708$$

91

For the calculation of the temperature using an advanced calculation model, the view factors can be evaluated and applied individually to each surface, as shown on Fig. 4.25. For all the external surfaces of the profile a view factor $\Phi = 1.0$ can be conservatively adopted or evaluated as in Annex G of Eurocode 1. If a simpler solution is sought and some level of approximation is acceptable, the averaged value of the view factor (equal to the shadow factor) can be applied to the whole cross section.

Using the shadow factor in the simple design equation (4.16) is an approximation because the convective part of the net heat flux, $\dot{h}_{net,c}$, is also affected by the correction factor k_{sh} .

¹ Except for the factor 0.9 for hot rolled H or I sections, that has no physical meaning and is deemed to disappear in the next revision of the Eurocode.

4.10. TEMPERATURE IN STEEL MEMBERS SUBJECTED TO LOCALISED FIRES

EN 1993-1-2 gives two different equations for calculating the temperature of steel members subjected to localised fire depending on whether the members are protected or not. The procedures that are used to evaluate the temperature in the case of localised fires are presented in this section.

4.10.1. Unprotected steel members

For unprotected sections, the heat flux is given by Eq. (4.16) and this is used to evaluate the temperature. This heat flux, $\dot{h}_{net,d} = \dot{h}_{net,c} + \dot{h}_{net,r}$, defined in Eq. (4.16), is easily calculated if the gas temperature, θ_g , is known. For localised fires not impinging the ceiling, the gas temperature is given by Eq. (3.24) (Heskestad Method). In the case where the localised fire impinges on the ceiling, the heat flux is given by Eq. (3.32) (Hasemi Method), and this can be used directly for calculating the temperature in unprotected steel members.

Fig. 4.27 shows the development of the flame length for the localized fire given in Example 3.7, with the same maximum fire area of 72 m², but with a distance from the source to the ceiling of 6 meters, instead of 3 meters. As the maximum length of the flame is 5.8 meters, the flame is not impinging the ceiling and the temperature of the gas is given by Eq. (3.24). For this case, the temperature of an unprotected IPE 300 beam heated on four sides is depicted in Fig. 4.28. The cross section of the beam is on the flame axis and located at the level of the ceiling.

92

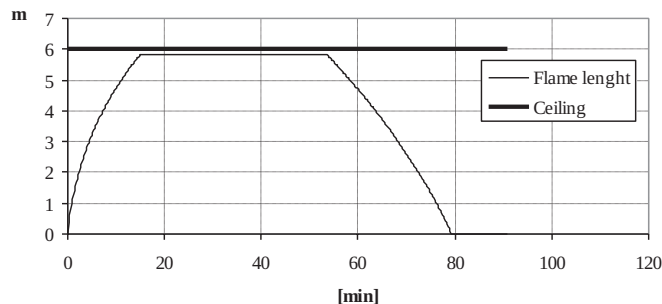


Figure 4.27 – Length of the flame

4.10. TEMPERATURE IN STEEL MEMBERS SUBJECTED TO LOCALISED FIRES

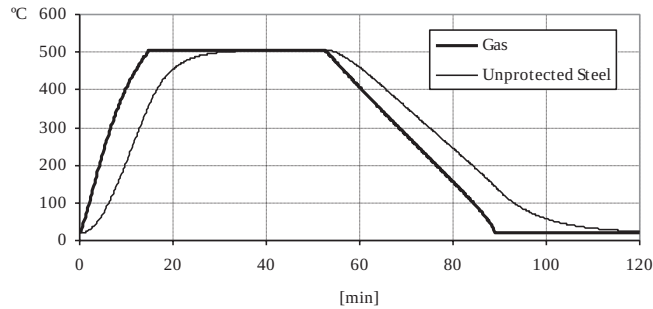


Figure 4.28 – Gas and unprotected IPE 300 temperature development when the flame does not impinge the ceiling

Fig. 4.29 shows the temperature development of an IPE 300 heated on four sides, by the same localised fire but with a distance from the source to the ceiling of 3 meters, i.e., the flame is impinging the ceiling.

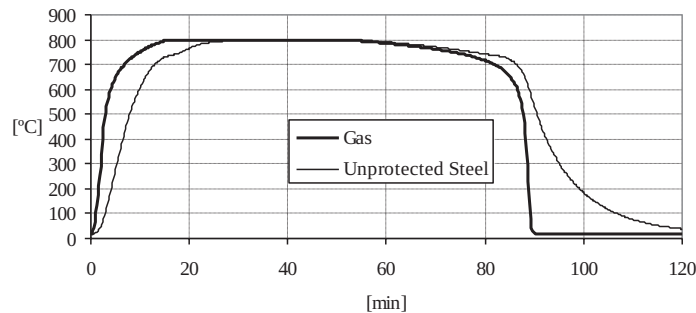


Figure 4.29 – Gas and unprotected IPE 300 temperature development when the flame is impinging the ceiling

4.10.2. Protected steel members

For protected steel members, the equation used for calculating the temperature is only based on the gas temperature, see Eq. (4.19). For localised fires not impinging the ceiling the gas temperature is given by Eq. (3.24) and the development of the steel temperature is calculated from Eq. (4.19). Fig. 4.30 shows the temperature development of a cross section on the axis of the flame of a protected IPE 300 with 10 mm of vermiculite cement in the contour, heated on four sides by the localised fire of example 3.7 with the a maximum fire area of 72 m² and a distance from the source to the ceiling of 6 meters, i.e., not impinging the ceiling.

4. TEMPERATURE IN STEEL SECTIONS

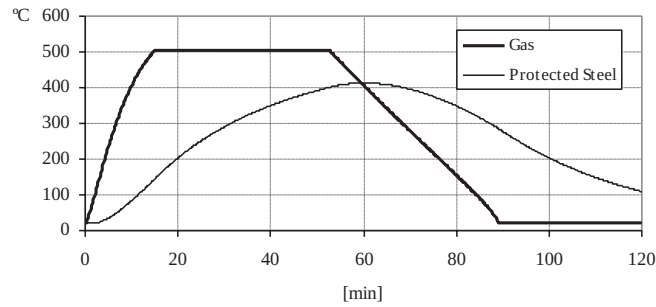


Figure 4.30 – Temperature development of gas and protected IPE 300 when the flame does not impinge the ceiling

Eq. (4.19) can not be applied directly in the case of a fire impinging the ceiling, because the effect of the fire is given as an impinging flux, see Eq. (3.32). A procedure has to be established to transform the impinging heat flux into an equivalent gas temperature. Cadorin *et al* (2003) suggests deducing a fictitious temperature that has the same effect on steel elements as the heat flux calculated with this method. This is the temperature of a steel profile with a very high massivity factor. This steel profile has a temperature which is very close to the gas temperature. This procedure is used in the program Elefir-EN presented in Chapter 8. The program first evaluates the gas temperature as the temperature of an unprotected steel profile with very high section factor ($A_m/V = 10000 \text{ m}^{-1}$ is adopted) using Eq. (4.16) and the net heat flux given by Eq. (3.33). After evaluating the gas temperature, the temperature of the protected steel profile is then calculated using Eq. (4.19).

94

If the distance from the source to the ceiling is 3 meters, as in Example 3.7, the flame impinges the ceiling and the temperature development of a protected IPE 300 just above the fire source is shown in Fig. 4.31.

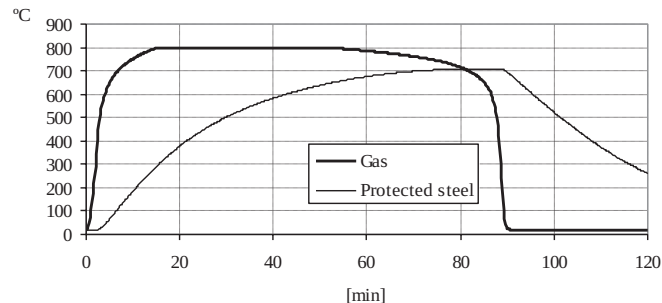


Figure 4.31 – Temperature development of Gas and protected IPE 300 when the flame impinges the ceiling

4.10.3. Thermal response of steel members in case of multiple localised fires

In case of several separate localised fires, Eq. (3.32) from Chapter 3 may be used in order to obtain the different individual heat fluxes \dot{h}_1 , \dot{h}_2 , \dot{h}_3 , etc., received by the fire exposed unit surface area at the level of the ceiling. According to the Annex C of EN 1991-1-2 the total heat flux may be taken as:

$$\dot{h}_{tot} = \dot{h}_1 + \dot{h}_2 + \dot{h}_3 + \dots \leq 100000 \quad [\text{W/m}^2] \quad (4.31)$$

The net heat flux \dot{h}_{net} received by the fire exposed unit surface area at the level of the ceiling is, according to the Eq. (3.33), given by:

$$\dot{h}_{net} = \dot{h}_{tot} - \alpha_c \cdot (\theta_m - 20) - \Phi \cdot \varepsilon_f \cdot \varepsilon_m \cdot \sigma \cdot [(\theta_m + 273)^4 - 293^4] \quad [\text{W/m}^2] \quad (4.32)$$

4.10.3.1. Multiple localised fires due to simultaneously burning cars: an example of a car park

The software Elefir-EN, which will be presented in detail in Chapter 8, will be used to model multiple localised fires due to simultaneously burning cars in a car park (Vial Real *et al*, 2011).

95

4.10.3.1.1. Characterization of the fire and definition of the fire scenarios

According to the European Project “Demonstration of real fire tests in car parks and high buildings” (European Commission, 2001) the classification of cars based on its calorific potential is given in Table 4.8. These results were obtained using the calorimetric hood to collect all smokes, combustion products and pollutants emitted during the combustion of real car burning. From the tests several experimental curves of the Rate of Heat Release (RHR) function of the time were obtained and simplified curves were proposed and validated.

4. TEMPERATURE IN STEEL SECTIONS

Table 4.8 – Classification of cars

Type	Category 1	Category 2	Category 3	Category 4	Category 5
Peugeot	106	306	406	605	806
Renault	Twingo-Clio	Mégane	Laguna	Safrane	Espace
Citroen	Saxo	ZX	Xantia	XM	Evasion
Ford	Fiesta	Escort	Mondeo	Scorpio	Galaxy
Opel	Corsa	Astra	Vectra	Omega	Frontera
Fiat	Punto	Bravo	Tempra	Croma	Ulysse
Wolkswagen	Polo	Golf	Passat	-	Sharan
Energy	6000 MJ	7500 MJ	9500 MJ	1200 MJ	

Fig. 4.32 a) shows the simplified RHR curve for a class 3 car fire. The referred project also suggests curves for the same type of cars that start burning with a delay of 12 and 24 minutes. In Fig. 4.32 b) these curves are shown and a fourth curve of a car that starts to burn with a delay of 36 minutes has been added.

96

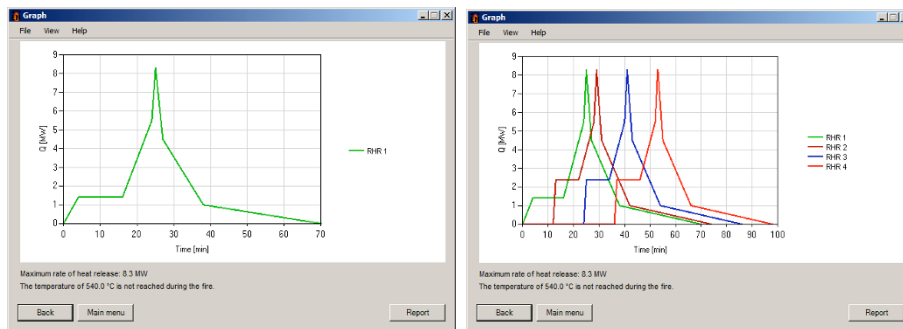


Figure 4.32 – a) Rate of heat release of a single class3 car fire; b) Rate of heat release of a single class 3 car fire with a delay of 12 minutes

Table 4.9 gives the values of the rate of heat release as a function of time of each car with a time delay of 12 minutes.

Table 4.9 – Values of the rate of heat release of four burning class 3-cars

Time (min)	1 st Car	Time (min)	2 nd Car	Time (min)	3 rd Car	Time (min)	4 th Car
0	0	12	0	24	0	36	0
4	1.4	13	2.4	25	2.4	37	2.4
16	1.4	22	2.4	34	2.4	46	2.4
24	5.5	28	5.5	40	5.5	52	5.5
25	8.3	29	8.3	41	8.3	53	8.3
27	4.5	31	4.5	43	4.5	55	4.5
38	1	42	1	54	1	66	1
70	0	74	0	86	0	98	0

Five fire scenarios, as shown in Fig. 4.33, have been considered according to the Rate of Heat Release of a class 3 car (see Table 4.8):

- i) Fire scenario 1: One car burning below the beam at mid-span;
- ii) Fire scenario 2: Three cars in a normal parking bay with an ignition time delay for each car of 12 minutes;
- iii) Fire scenario 3: Four cars in a normal parking bay with an ignition time delay for each car of 12 minutes. It will be shown that the burning of the fourth car does not affect the maximum temperature of the beam, comparing with Scenario 2;
- iv) Fire scenario 4: Three cars in a normal parking bay with an ignition time delay for each car of 12 minutes;
- v) Fire scenario 5: Four cars in a normal parking bay with an ignition time delay for each car of 12 minutes.

Fig.4.33 also shows the sequence of ignition of the cars for the five analysed fire scenarios.

The temperature of the beam was evaluated at the mid-span section with the rate of heat release of Fig.4.32 a) for fire scenario 1 and at the extremity of the beams considering the rate of heat release of Fig. 4.32 b) in the other fire scenarios.

4. TEMPERATURE IN STEEL SECTIONS

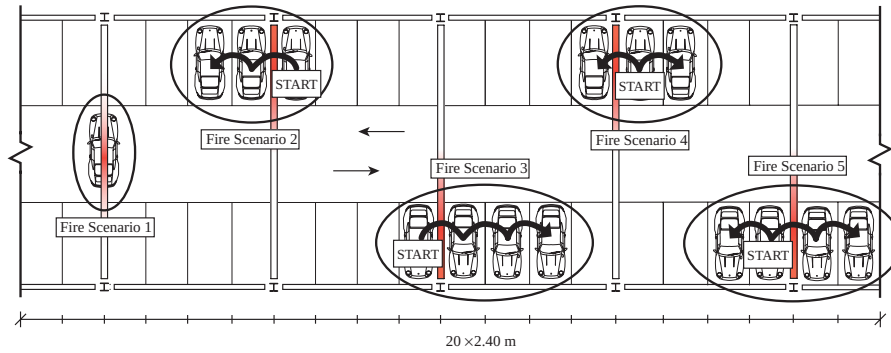


Figure 4.33 – Fire scenarios and sequence of ignition

4.10.3.1.2. Temperature of the main beam

First the length of the flames corresponding to each car should be evaluated to decide which method has to be used (Heskestad or Hasemi). In the case of multiple localised fires only the fires in which the flame impacts the ceiling are considered and the others are ignored. Fig. 4.34 shows the flame length development during the fire of one car burning, considering that the diameter of the car is $D = 3.9$ m. The height of the compartment $H = 2.7$ m is also plotted on the Figure.

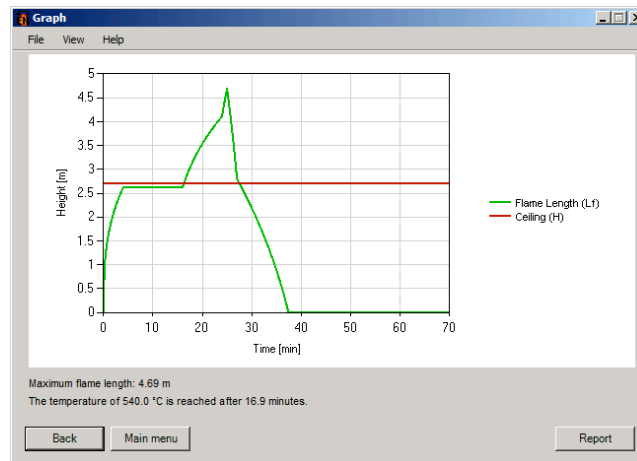


Figure 4.34 – Flame length development for a single burning car

Fig. 4.35 shows, for scenario 2, the distance between the vertical axis of the flame of each car and the position in the beam where the temperature should be evaluated, i. e., the extremity of the beam.

4.10. TEMPERATURE IN STEEL MEMBERS SUBJECTED TO LOCALISED FIRES

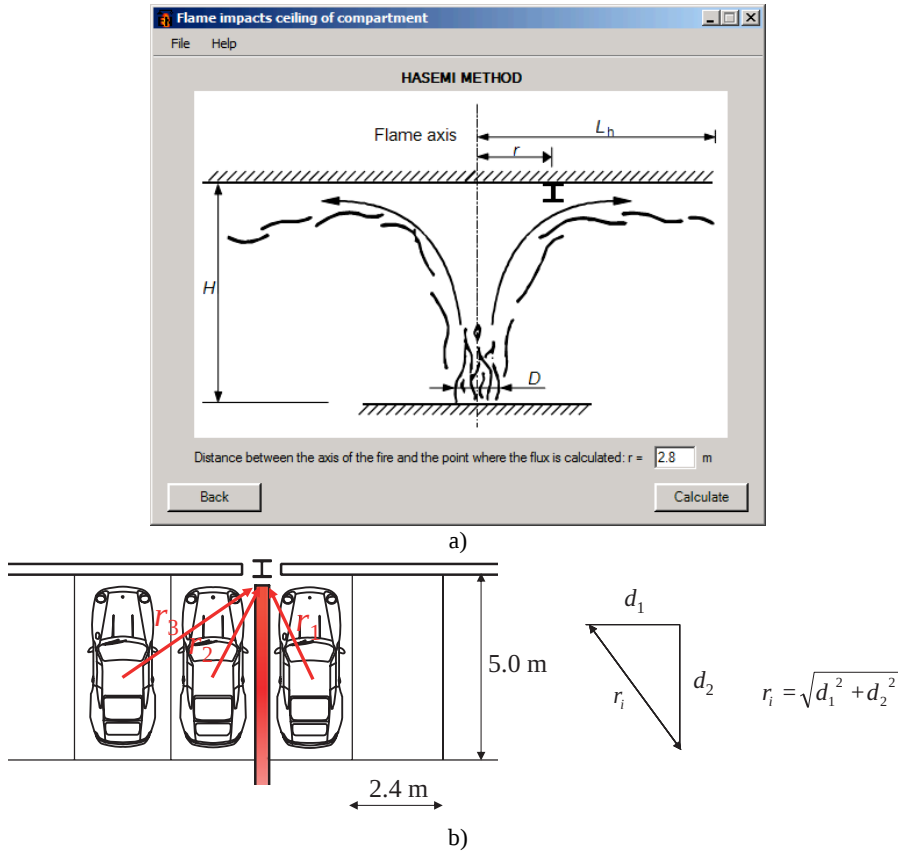


Figure 4.35 – a) Scheme showing the distance r ; b) Distances to be considered for scenario 2

In Table 4.10 the distance r between the vertical axis of the flame and the position of the beam where the temperature is evaluated for the case of Fire scenario 3 (see Fig. 4.33) are given.

Table 4.10 – Distances r between the axis of the flame and the position where the temperature is evaluated

r_1 [m]	r_2 [m]	r_3 [m]	r_4 [m]
2.8	2.8	4.4	6.5

Fig. 4.36 shows the gas temperature and the temperature of the steel beam, supposing that it is made of IPE 500. A limiting temperature of 540 °C, was also drawn.

4. TEMPERATURE IN STEEL SECTIONS

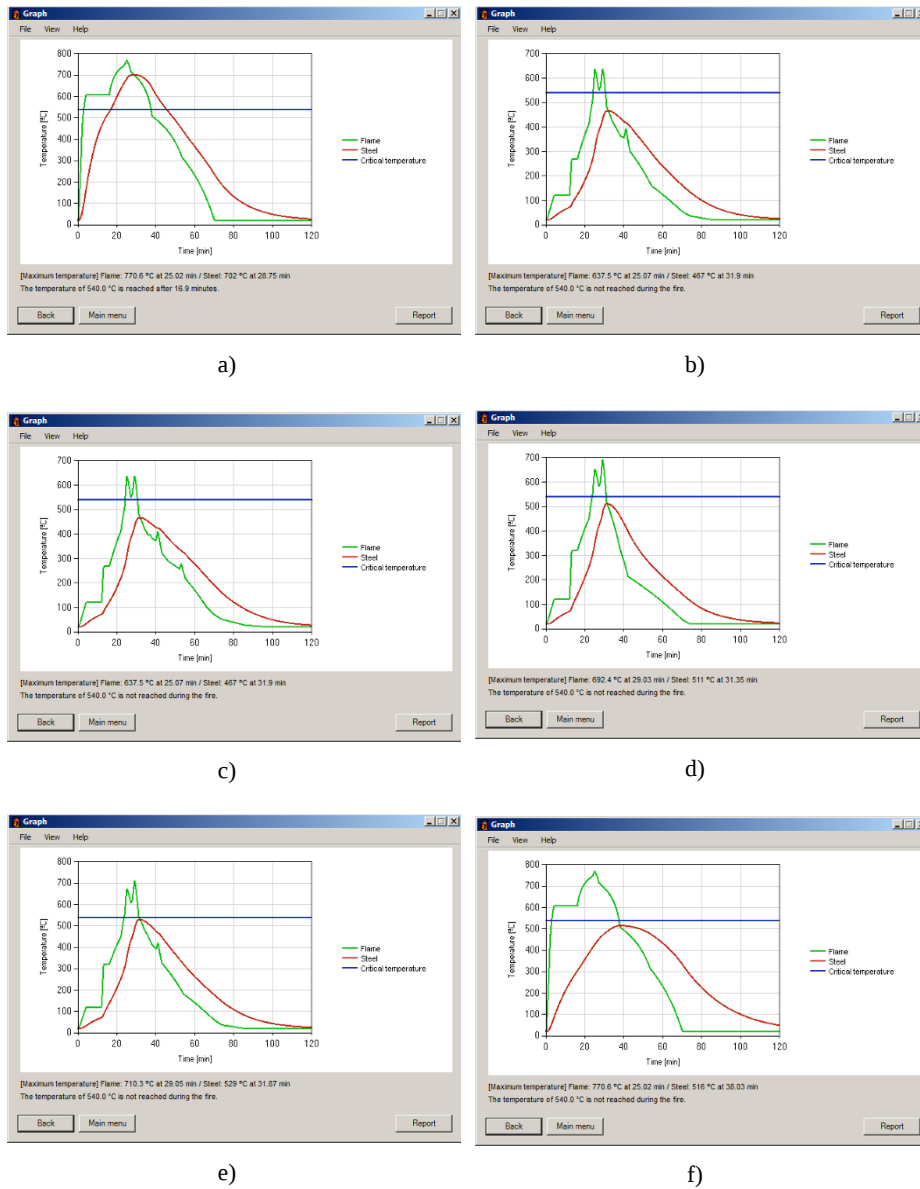


Figure 4.36 –Temperature development. a) Scenario 1; b) Scenario 2; c) Scenario 3
d) Scenario 4; e) Scenario 5; f) Scenario 1 with the beam protected

Table 4.11 shows the maximum temperature obtained for the beam in all fire scenarios. From that table it can be concluded that, due to the scenario 1 the main beams should be protected so that the temperature

doesn't reach the assumed limiting temperature of 540 °C during the complete duration of the fire including the decay phase or during a required period of time. If, for example, the load-bearing function is required during the complete duration of the fire, the program Elefir-EN suggests that 5 mm of sprayed vermiculite cement on the contour of the beam (see Fig. 4.36 f) should be applied.

Table 4.11 – Maximum temperatures of the main beam

	Scenario 1	Scenario 2	Scenario 3	Scenario 4	Scenario 5
$\theta_{\sigma, \max}$ [°C]	701.8	467.2	467.2	511.4	529.5

From Table 4.11 it can be concluded that the burning of the fourth car in the scenario 3, does not affect the maximum temperature of the beam, if compared with scenario 2

4.11. TEMPERATURE IN STAINLESS STEEL MEMBERS

Annex C of EN 1993-1-2 provides guidance on the thermal properties of stainless steels. These properties can also be found in the Annex A of this book.

Compared with carbon steel, the thermal properties of stainless steel are quite different. The main differences are:

- The increase of specific heat with increasing temperature is slightly lower in stainless steel than in carbon steel. Furthermore carbon steel has a larger increase in specific heat at 735 °C due to a metallurgical phase change which is not present in stainless steel. This is shown in Fig. 4.37.
- Compared to carbon steel, at ambient temperature, stainless steel has a much lower thermal conductivity. However, the thermal conductivity of stainless steel increases at elevated temperature and even exceeds the value for carbon steel at temperatures above 1000 °C. This behaviour is shown in Fig. 4.38.

4. TEMPERATURE IN STEEL SECTIONS

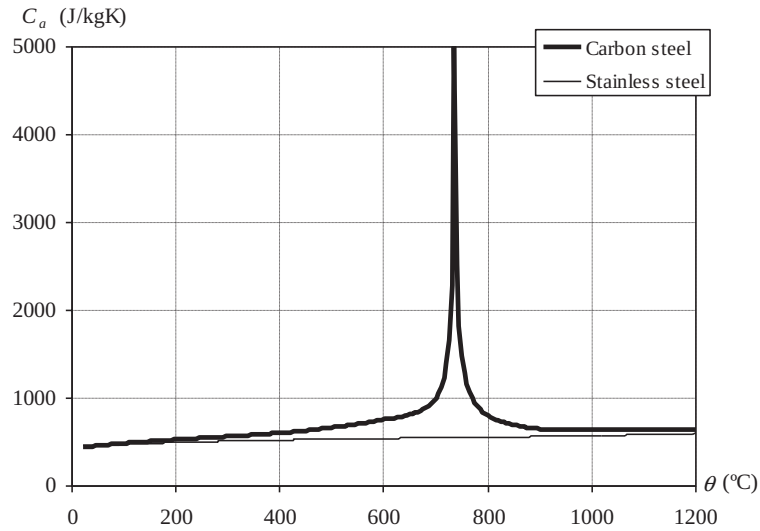


Figure 4.37 – Specific heat of stainless steel and carbon steel as a function of temperature

Another difference lies in the surface emissivity of the member, ϵ_m , which is equal to 0.4 for stainless steel and 0.7 for carbon steel.

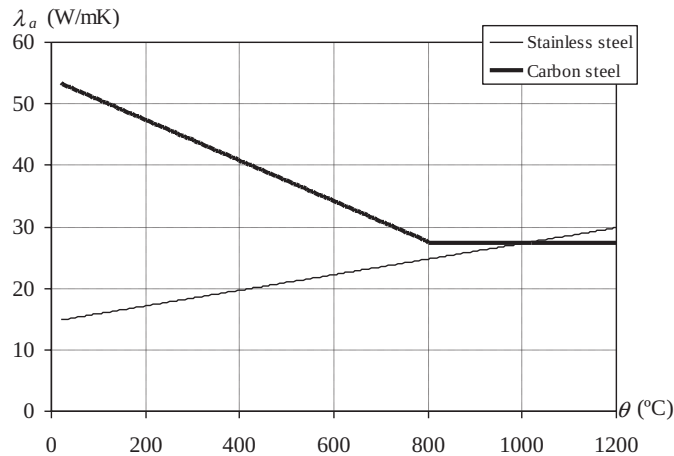


Figure 4.38 – Conductivity of stainless steel and carbon steel as a function of temperature

Fig. 4.39 compares the temperature development of an IPE 450 exposed on four sides to the ISO 834 fire curve.

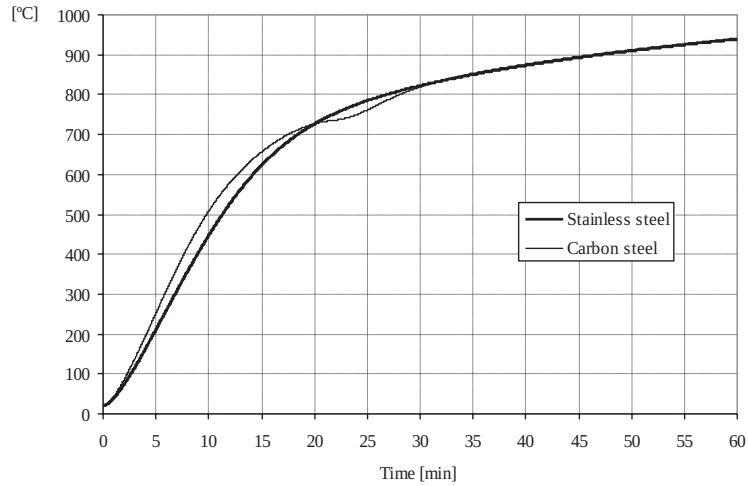


Figure 4.39 – Temperature development of a carbon steel and a stainless steel IPE 450, heated on four sides by the ISO 834 fire curve

This figure shows that the time-temperature curve for stainless steel does not exhibit the S shape of the carbon steel curve in the temperature range between 700 °C and 800 °C; this is due to the absence of the peak value on the heat capacity of stainless steel (see Fig. 4.37). The slower increase in temperature of stainless steel in the early stage of the fire is due to a combination of the lower values of thermal diffusivity $\lambda_a / (\rho_a c_a)$ (see Fig. 4.40) and surface emissivity compared to carbon steel. In the later stage of the fire, both steel temperature curves tend toward the ISO fire curve. In this case, the role played by the surface emissivity is much more important than the role played by the thermal diffusivity.

103

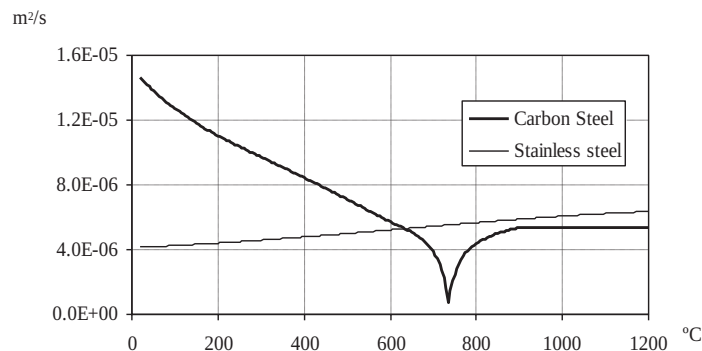


Figure 4.40 – Thermal diffusivity of carbon steel and stainless steel

4. TEMPERATURE IN STEEL SECTIONS

Annex A provides tables and nomograms to evaluate the temperature of unprotected stainless steel profiles exposed to the standard fire curve ISO 834, avoiding the need to perform the time integration of Eq. (4.16), as illustrated in the next example.

4.11.1. Example

What is the temperature of the unprotected circular hollow section of Example 4.2 after 15 minutes of standard fire curve exposure if it is made of stainless steel?

Solution:

According to Annex A.2, the section factor is given by:

$$\frac{A_m}{V} = \frac{P}{A} = \frac{d}{(d-t)t} \approx \frac{1}{t} = 200 \text{ m}^{-1}$$

As the section is convex, $k_{sh} = 1$, and the modified section factor is given by:

$$k_{sh} \left[\frac{A_m}{V} \right] = 200 \text{ m}^{-1}$$

Table of the Annex A.8 gives a temperature of 663°C, which is smaller than a temperature of 682°C for the same cross section in carbon steel.

Chapter 5

MECHANICAL ANALYSIS

5.1. BASIC PRINCIPLES

This chapter deals with the basic principles of fire design of steel structures, as they are defined in Part 1-2 of Eurocode 3. The focus will be on the fire resistance of individual members. Where mechanical resistance to fire is required, steel structures shall be designed and constructed in such a way that they maintain their load bearing function during the relevant fire exposure. According to EN 1991-1-2, the mechanical analysis shall be performed for the same duration as used in the temperature analysis and the verification of fire resistance should be made in one of the following three domains:

1. in the time domain (see 1 in Fig. 5.1):

$$t_{fi,d} \geq t_{fi,requ} \quad (5.1a)$$

2. in the strength domain (see 2 in Fig. 5.1):

$$E_{fi,d,t} \leq R_{fi,d,t}, \text{ at time } t_{fi,requ} \quad (5.1b)$$

3. in the temperature domain (see 3 in Fig. 5.1):

$$\theta_d \leq \theta_{cr,d}, \text{ at time } t_{fi,requ} \quad (5.1c)$$

where

- $t_{fi,d}$ is the design value of the fire resistance, i.e., the failure time;
- $t_{fi,requ}$ is the required fire resistance time;
- $E_{fi,d,t}$ is the design value of the relevant effects of actions in the fire situation at time t , which is normally considered constant during the fire, $E_{fi,d}$;

5. MECHANICAL ANALYSIS

- $R_{fi,d,t}$ is the design value of the resistance of the member in the fire situation at time t ;
- θ_d is the design value of steel temperature;
- $\theta_{cr,d}$ is the design value of the critical temperature, i.e., the collapse temperature of the structural steel member.

In Fig. 5.1 these three possible domains are represented for the case of a steel member subjected to a nominal fire as defined in Chapter 3. This figure shows the temperature of the structural steel element, θ_d , assuming a uniform temperature throughout the cross section, the design value of the effect of actions in the fire situation, $E_{fi,d}$, which is considered as constant, the progressive loss of strength, $R_{fi,d,t}$ and the critical temperature of the member, $\theta_{cr,d}$.

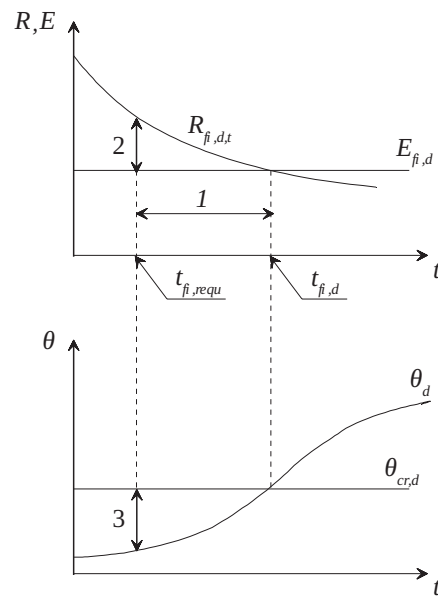


Figure 5.1 – Time (1), load (2), and temperature (3) domains for a nominal fire

According to EN 1993-1-2, for the standard fire exposure, members shall comply with the fire resistance criterion R (load bearing capacity). This criterion is defined in the national regulations for fire safety of buildings as a function of the type of building, the occupancy and its height and should be identified by the letter R followed by a number representing the required fire resistance period. For example, R60 means that this criterion is assumed to

be satisfied where the load bearing function is maintained for 60 minutes of standard fire exposure ($t_{fi,requ} = 60$ minutes in this case).

For parametric fires and for all natural fires with a cooling phase, the load bearing function is ensured when collapse is prevented either during the complete duration of the fire, including the cooling phase (see Fig. 5.2a) or during a specified period of time (see $t_{fi,requ}^1$ in Fig. 5.2b). From Fig. 5.2b) it can be concluded that for fires with a cooling phase verification in either the temperature domain or in the strength domain, must be avoided. This is because if the specified fire resistance time (see $t_{fi,requ}^2$ in Fig. 5.2b) is greater than the time needed for the collapse, $t_{fi,d}$, the load bearing capacity is satisfied at $t = t_{fi,requ}^2$. This can lead to the wrong conclusion because failure has already occurred at time $t_{fi,d}$.

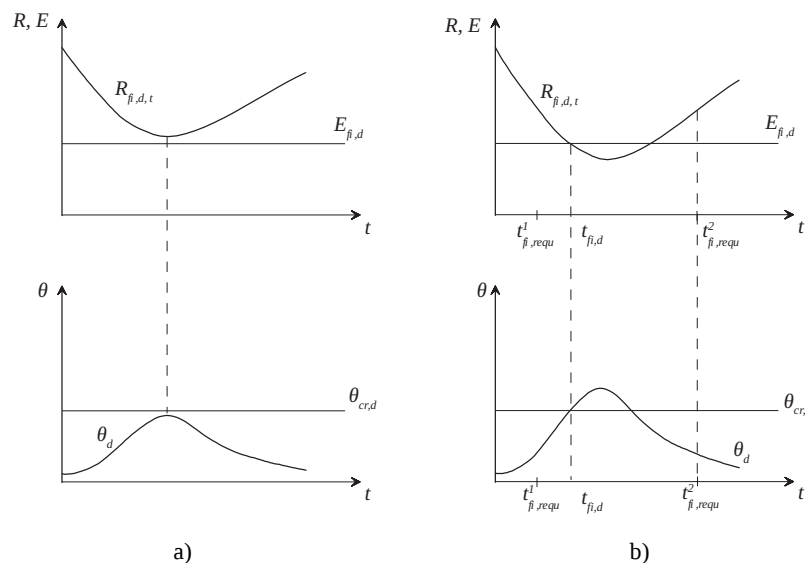


Figure 5.2 – With parametric or natural fires a) $\theta_d \leq \theta_{cr,d}$, b) $t_{fi,d} \geq t_{fi,requ}$

The design effect of actions for the fire design situation, $E_{fi,d}$, can be obtained either by using the accidental load combination as defined in Eq. (2.1) or in a simplified way by using Eq. (2.2).

The design resistance $R_{fi,d,t}$ at time t is determined, by assuming a uniform temperature throughout the cross section or throughout its parts (webs and flanges), and by modifying the design resistance for normal

temperature design to EN 1993-1-1, to take into account the mechanical properties of steel at elevated temperatures, see Section 5.5.

Three different assessment models can be used to determine the fire resistance of a structure or a single element. Each of these models is described below and increase in complexity:

- *Tabulated data* obtained from tests in standard furnaces, empirical methods or numerical calculations. Tabulated data are widely used for concrete and composite steel and concrete structures in Eurocodes 2 and 4, respectively. However, no tabulated data are presented in Eurocode 3, probably because the simple calculation models presented in Eurocode 3 are easy to apply and it is relatively straightforward to build tables or nomograms, Franssen *et al* (2009), for the evaluation of the temperature of protected and unprotected steel profiles. Nomograms for protected and unprotected steel profiles are present in Annex A of this book;
- *Simple calculation models* making use of simple analytical formulae for isolated members. This approach is presented in Section 5.5;
- *Advanced calculation models*, which can be used in the following ways:
 - i) *Global structural analysis* (Fig. 5.3a). When a global structural analysis for the fire situation is carried out, the relevant failure mode, the temperature-dependent material properties and member stiffness, the effects of thermal expansions and deformations (indirect fire actions) shall be taken into account;
 - ii) *Analysis of part of the structure*, for example a portal frame or any other substructure (Fig. 5.3b). The boundary conditions at supports and at the ends of members may be assumed to remain unchanged throughout the fire exposure;
 - iii) *Member analysis*, for example beams or columns (Fig. 5.3c), where only the effects of thermal deformations resulting from thermal gradients across the cross section need to be considered. The effects of axial or in-plane thermal expansions may be neglected. The boundary conditions at supports and at the ends of member may be assumed to remain unchanged throughout the fire exposure.

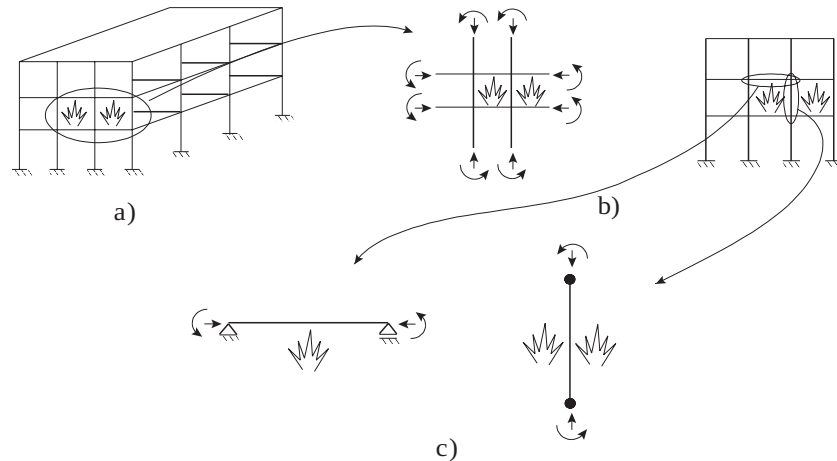


Figure 5.3 – Structural schematisation. a) Global structure, b) Substructures, c) Members

Tabulated data and simple calculation models normally apply only to member analyses.

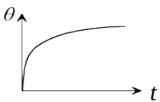
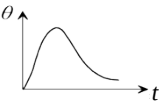
Eurocode 3 states that *for verifying standard fire resistance requirements, a member analysis is sufficient*. However, a member analysis can also be made for some simple structures subject to other types of fires, such as natural fires.

The choice of the type of structural analysis also depends on the fire model that is being used. Table 5.1 clearly shows the different possibilities for the three fire assessment methods under nominal and natural fire conditions.

Regarding this Table, member analysis can be applied to isolated structural elements (extracted from the whole structure, element by element) and can be performed either by using simple calculation models or advanced calculation models. This type of analysis is largely used under nominal fire conditions like the standard fire defined in ISO 834. When analysing part of the structure or carrying out a global analysis, a certain number of structural members should be considered to act together so that the interaction effect between them is directly taken into account (load redistribution from weak heated parts to cold parts outside the fire compartment). Advanced calculation methods, normally based on the Finite Element Method together with a global analysis provide more realistic models of mechanical response of structures in fire than tabulated data or simple models. More information about advanced calculation models is presented in Chapter 6.

5. MECHANICAL ANALYSIS

Table 5.1 – Relation between calculation models, structural schematization and fire model

	Nominal Fires			Natural Fires		
						
Type of Analysis	Tabulated data	Simple Calculation Models	Advanced Calculation Models	Tabulated data	Simple Calculation Models	Advanced Calculation Models
Member analysis	Not available in EC3-1-2	Yes	Yes	No	Yes (if available)	Yes
Analysis of parts of the structure	No	Yes (if available)	Yes	No	No	Yes
Global structural analysis	No	No	Yes	No	No	Yes

5.2. MECHANICAL PROPERTIES OF CARBON STEEL

The strength of steel decreases as the temperature increases beyond 400 °C. For S235 structural steel, Fig. 5.4 shows the strength as a function of temperature as well as the stress-strain relationships at elevated temperature. This figure also shows that the stiffness of steel also decreases with increasing temperature. At elevated temperature, the shape of the stress-strain diagram is modified compared to the shape at room temperature. Instead of a linear-perfectly plastic behaviour as for normal temperature, the model recommended by EN 1993-1-2 at elevated temperature is an elastic-elliptic-perfectly plastic model, followed by a linear descending branch introduced at large strains when the steel is used as material in advanced calculation models to avoid numerical problems. Detailed aspects from this behaviour can be seen in Fig. 5.5. More details on the stress-strain relationship for steel grades S235, S275, S355 and S460 are given in Annex C.

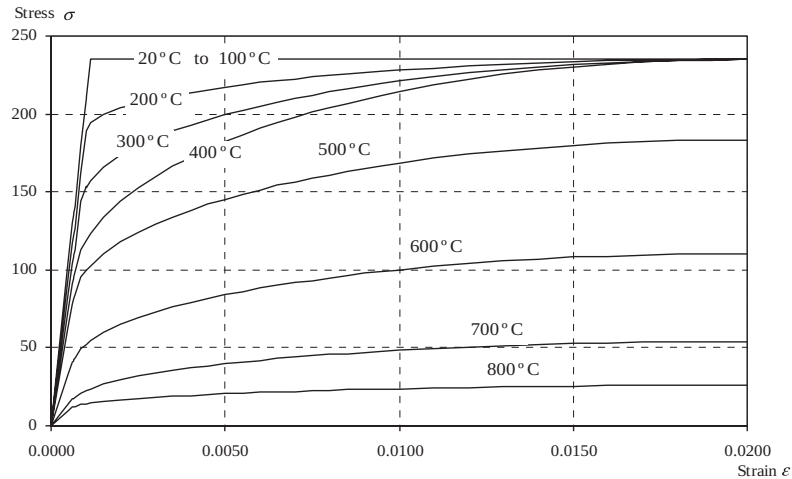


Figure 5.4 – Stress-strain relationship for carbon steel S235 at elevated temperatures

In an accidental limit state such as fire, higher strains are acceptable. For this reason Eurocode 3 recommends a yield strength corresponding to 2% total strain rather than the conventional 0.2% proof strain (see Fig 5.5). However, for members with Class 4 cross sections, EN 1993-1-2 recommends, in its Annex E, a design yield strength based on the 0.2% proof strain.

The stress-strain relationship at elevated temperature shown in Fig 5.5 is characterised by the following three parameters:

- The limit of proportionality, $f_{p,\theta}$
- The effective yield strength, $f_{y,\theta}$
- The Young's modulus, $E_{a,\theta}$

111

The design values for the mechanical (strength and deformation) material properties in the fire situation $X_{d,fi}$ are defined in Eurocode 3, as follows:

$$X_{d,fi} = k_{\theta} X_k / \gamma_{M,fi} \quad (5.2)$$

where

- X_k is the characteristic value of a strength or deformation property (*generally* f_k or E_k) for normal temperature design to EN 1993-1-1;
- k_{θ} is the reduction factor for a strength or deformation property ($X_{k,\theta}/X_k$), dependent on the material temperature;
- $\gamma_{M,fi}$ is the partial safety factor for the relevant material property, for the fire situation, taken as $\gamma_{M,fi} = 1.0$, or other value defined in the National Annex.

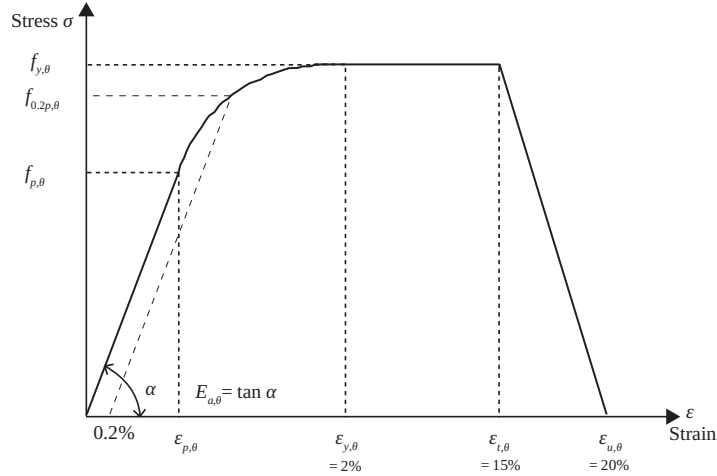


Figure 5.5 – Stress-strain relationship for carbon steel at elevated temperatures

Following Eq. (5.2) the yield strength at temperature θ , i.e., $f_{y,\theta}$, is a function of the yield strength, f_y , at 20 °C, given by:

$$f_{y,\theta} = k_{y,\theta} f_y \quad (5.3)$$

The Young's modulus at temperature θ , i.e., $E_{a,\theta}$, is a function of the Young's modulus, E_a , at 20 °C, given by:

$$E_{a,\theta} = k_{E,\theta} E_a \quad (5.4)$$

112

In the same way the proportional limit at elevated temperature is given by:

$$f_{p,\theta} = k_{p,\theta} f_y \quad (5.5)$$

According to Annex E of EN 1993-1-2 for members with Class 4 cross section under fire conditions, the design yield strength of steel should be taken as the 0.2% proof strain and thus for this class of cross section the yield strength at temperature θ , i.e., $f_{y,\theta}$, is a function of the yield strength, f_y , at 20 °C given by:

$$f_{y,\theta} = f_{0.2p,\theta} = k_{0.2p,\theta} f_y \quad (5.6)$$

Table 5.2 presents the reduction factors for the stress-strain relationship of carbon steel at elevated temperatures and Fig. 5.6 is a graphical representation of these data. In this table the reduction factor (relative to f_y) for the design strength of hot rolled and welded thin-walled sections (Class 4), given in Annex E of EN 1993-1-2, is also presented.

Table 5.2 shows that carbon steel begins to lose strength above 400 °C. For example, at 700 °C it has 23 % of its strength at normal temperature and at 800 °C it retains only 11% of that strength, and its strength reduces to 6% at 900 °C. Concerning the Young’s modulus it begins to decrease earlier at 100 °C.

The reduction of the effective yield strength given by Table 5.2, which was obtained experimentally, can be approximated by the following equation:

$$k_{y,\theta} = \left\{ 0.9674 \left(e^{\frac{\theta_a - 482}{39.19}} + 1 \right) \right\}^{-1/3.833} \leq 1 \quad (5.7)$$

When inverted, this equation yields an equation that gives the temperature of the steel function of the reduction of the effective yield strength, i. e., $\theta_a = f(k_{y,\theta})$, see Eq. (5.109) and Eq. (5.110) in section 5.5. This equation is used by the Eurocode to obtain the critical temperature.

Table 5.2 – Reduction factors for carbon steel for the design at elevated temperatures

Steel Temperature θ_a	Reduction factors at temperature θ_a relative to the value of f_y or E_a at 20 °C			
	Reduction factor (relative to f_y) for effective yield strength $k_{y,\theta} = f_{y,\theta} / f_y$	Reduction factor (relative to f_y) for proportional limit $k_{p,\theta} = f_{p,\theta} / f_y$	Reduction factor (relative to E_a) for the slope of the linear elastic range $k_{E,\theta} = E_{a,\theta} / E_a$	Reduction factor (relative to f_y) for the design strength of hot rolled and welded thin walled sections (Class 4) $k_{0.2p,\theta} = f_{0.2p,\theta} / f_y$
20 °C	1.000	1.000	1.000	1.000
100 °C	1.000	1.000	1.000	1.000
200 °C	1.000	0.807	0.900	0.890
300 °C	1.000	0.613	0.800	0.780
400 °C	1.000	0.420	0.700	0.650
500 °C	0.780	0.360	0.600	0.530
600 °C	0.470	0.180	0.310	0.300
700 °C	0.230	0.075	0.130	0.130
800 °C	0.110	0.050	0.090	0.070
900 °C	0.060	0.0375	0.0675	0.050
1000 °C	0.040	0.0250	0.0450	0.030
1100 °C	0.020	0.0125	0.0225	0.020
1200 °C	0.000	0.0000	0.0000	0.000

NOTE: For intermediate values of the steel temperature, linear interpolation may be used.

5. MECHANICAL ANALYSIS

Fig. 5.7 shows the comparison between the values of the reduction factor for the effective yield strength, $k_{y,\theta}$, given by Table 5.2 and the ones obtained using Eq. (5.7). The two curves are very close.

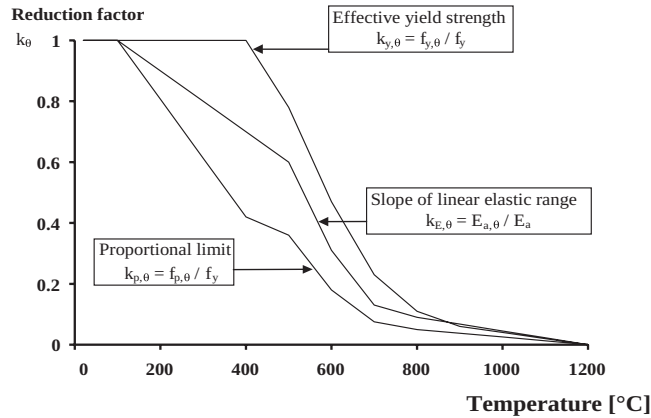


Figure 5.6 – Reduction factors for the stress-strain relationship of carbon steel at elevated temperatures (see Fig. 3.2 from EN 1993-1-2)

It should be mentioned that the reduction factors for the 0.2% proof strength at elevated temperatures, $k_{0.2p,\theta}$ given in the Table E.1 of Part 1.2 of Eurocode 3 present here in Table 5.2 do not correspond to the ones calculated according to the stress-strain relationship of steel at elevated temperatures given in the same norm (see Fig. 5.5), and it is unknown to the authors where the values given in the Part 1.2 of Eurocode 3 come from. The values of $k_{0.2p,\theta}$ calculated according to the stress-strain relationship of carbon steel at elevated temperatures depend on the steel grade. These values are presented in Table 5.3.

114

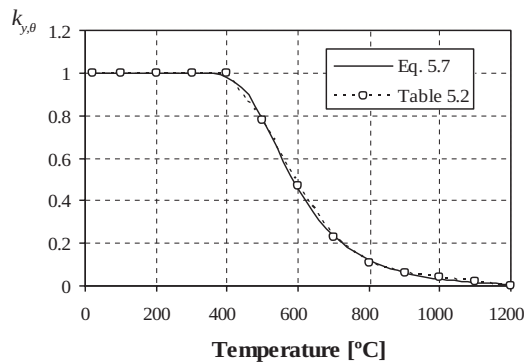


Figure 5.7– Reduction factors for the yield strength, $k_{y,\theta}$, at elevated temperatures

Table 5.3 – Reduction factors $k_{0.2p,\theta}$ for carbon steel

Steel Temperature θ_a (°C)	Reduction factor (relative to f_y) for the design strength of hot rolled and welded thin walled sections $k_{0.2p,\theta} = f_{0.2p,\theta} / f_y$				
	S235	S275	S355	S460	EN 1993-1-2
20	1.000	1.000	1.000	1.000	1.000
100	1.000	1.000	1.000	1.000	1.000
200	0.894	0.895	0.896	0.897	0.890
300	0.789	0.790	0.793	0.797	0.780
400	0.687	0.689	0.695	0.702	0.650
500	0.552	0.554	0.557	0.562	0.530
600	0.314	0.315	0.318	0.322	0.300
700	0.147	0.148	0.150	0.153	0.130
800	0.077	0.078	0.078	0.079	0.070
900	0.048	0.048	0.048	0.048	0.050
1000	0.032	0.032	0.032	0.032	0.030
1100	0.016	0.016	0.016	0.016	0.020
1200	0.000	0.000	0.000	0.000	0.000

5.3. CLASSIFICATION OF CROSS SECTIONS

Rolled or welded structural sections may be considered as an assembly of individual plate elements, some of which are internal elements like the webs of open sections or the flanges of hollow sections, and others are outstand elements like the flanges of open sections. Examples of internal and outstand elements are shown in Fig. 5.8. As the plate elements in structural sections are relatively thin compared with their width, when loaded in compression (as a result of axial loads applied to the whole section and/or from bending) they may buckle locally (see Fig 5.9).

115

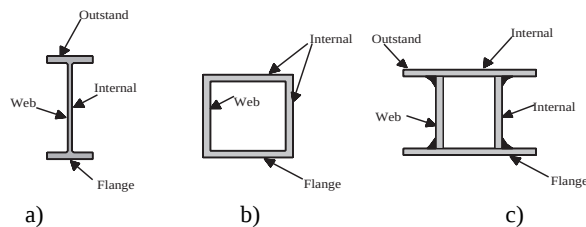


Figure 5.8 – Internal and outstand elements
a) Rolled section; b) Hollow section; c) Welded section

The tendency of a plate element within the cross section to buckle may limit the axial load-carrying capacity, or the bending resistance of the section, because collapse can occur before the section reaches its yield strength. Premature failure as a result of local buckling can be avoided by limiting the width-to-thickness ratio of the individual elements within the cross section. An approach which classifies sections according to their ability to resist local buckling is introduced in Eurocode 3 and this approach is described below.

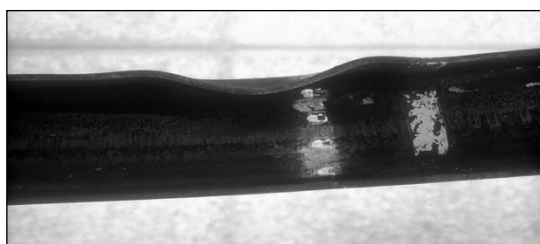


Figure 5.9 – Local buckling of the upper flange of a beam subject to bending (ESDEP, 1995)

Eurocode 3 defines four cross section classes depending on the slenderness of each constitutive plate (defined by a width-to-thickness ratio) and on the compressive stress distribution, i.e., uniform or linear:

- **Class 1** cross sections are those which can form a plastic hinge with the rotation capacity required from plastic analysis without reduction of the resistance.
- **Class 2** cross sections are those which can develop their plastic moment resistance, but have limited rotation capacity because of local buckling.
- **Class 3** cross sections are those in which the stress in the extreme compression fibre of the steel member assuming an elastic distribution of stresses can reach the yield strength, but local buckling is liable to prevent development of the plastic moment resistance.
- **Class 4** cross sections are those in which local buckling will occur before reaching the yield strength in one or more parts of the cross section.

Fig. 5.10 shows the moment-rotation curves for each of the four classes, highlighting the strength and the rotation capacity that can be reached before local buckling occurs. In this figure, ϕ_{pl} is the rotation needed

to form a full plastic stress distribution in the most loaded section of the beam, i.e., the rotation needed to form a plastic hinge in that section, M_{pl} is the plastic moment and M_{el} the elastic moment.

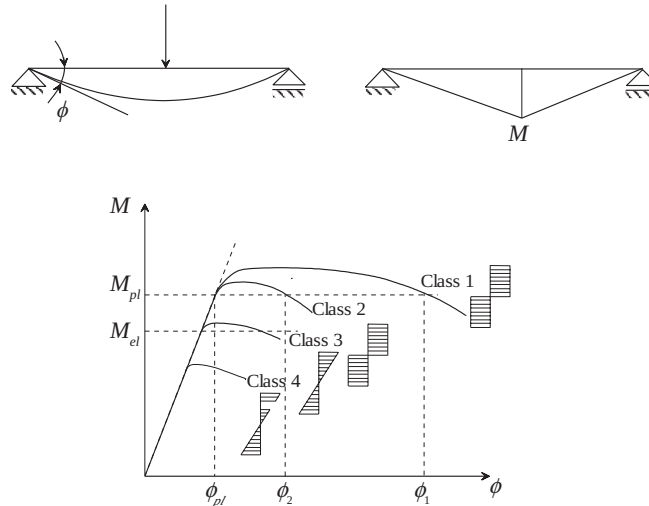


Figure 5.10 – Moment-rotation curves

A key parameter used when analysing plate buckling for I-sections girders and box girders is the normalised plate slenderness, $\bar{\lambda}_p$, given by (EN 1993-1-5):

$$\bar{\lambda}_p = \sqrt{\frac{f_y}{\sigma_{cr}}} \quad (5.8)$$

117

where σ_{cr} is the elastic critical buckling stress, which can be found in any textbook for stability analysis or in Annex A of EN 1993-1-5, given by:

$$\sigma_{cr} = \frac{k_\sigma \pi^2 E}{12(1-\nu^2)} \left(\frac{t}{b}\right)^2 \quad (5.9)$$

where

- k_σ is the plate buckling factor which accounts for edge support conditions and stress distribution;
- ν is Poisson's coefficient;
- E is the Young's modulus;
- t is the plate thickness;
- b is the width of the plate.

Substituting from Eq. (5.9) into Eq. (5.8) and rearranging gives:

$$\begin{aligned}
 \bar{\lambda}_p &= \sqrt{\frac{f_y}{\sigma_{cr}}} = \sqrt{\frac{f_y}{k_\sigma \frac{\pi^2 E t^2}{12(1-\nu^2) b^2}}} = \frac{b/t}{\sqrt{k_\sigma} \sqrt{\frac{\pi^2}{12(1-\nu^2)}}} \frac{1}{\sqrt{\frac{E}{f_y}}} = \\
 &= \frac{b/t}{\sqrt{k_\sigma} \sqrt{\frac{\pi^2}{12(1-\nu^2)}}} \frac{1}{\sqrt{\frac{210000}{235}} \sqrt{\frac{235}{f_y}} \sqrt{\frac{E}{210000}}} = \\
 &= \frac{b/t}{28.4 \sqrt{k_\sigma} \sqrt{\frac{235}{f_y}} \sqrt{\frac{E}{210000}}} = \frac{b/t}{28.4 \sqrt{k_\sigma}} \frac{1}{\varepsilon} = \frac{b/t}{28.4 \varepsilon \sqrt{k_\sigma}} \quad (5.10)
 \end{aligned}$$

where

$$\varepsilon = \sqrt{\frac{235}{f_y}} \sqrt{\frac{E}{210000}} \quad \text{with } f_y \text{ and } E \text{ in MPa} \quad (5.11)$$

Introducing the parameter ε allows the expression for the normalised slenderness $\bar{\lambda}_p$ to be defined independent of the steel grade. Eq. (5.11) is used, for example, in EN 1993-1-4 for stainless steel, which has several Young's modulus values depending on the steel grade. This is not the case for carbon steel where the Young's modulus can be considered as constant at room temperature, $E = 210000$ MPa. Eurocode 3 defines the following parameter for carbon steel:

$$\varepsilon = \sqrt{235/f_y} \quad \text{with } f_y \text{ in MPa} \quad (5.12)$$

Eq. (5.11) and Eq. (5.12) are only applicable for carbon steel at room temperature. The benefit of using Eq. (5.11) also for carbon steel will appear as soon as high temperatures have to be considered or when a different value of the Young's modulus resulting from tests on coupons has to be used.

Table 5.4 summarizes the maximum width-to-thickness ratio (slenderness) limits for the constitutive plates of hot rolled profiles in compression or subject to bending about the strong axis, for Class 1, 2 and 3 cross sections. Complete information on hot rolled and welded section classification can be found in the Annex D or in EN 1993-1-1. For elements with slenderness greater than the Class 3 limits, the cross section should be classified as Class 4. The various compression parts in a cross section (such

as a web or flange) can, in general, be of different classes. A cross section is classified according to the highest class of its compression parts.

Table 5.4 – Maximum slenderness for compression parts of cross section

Element	Class 1	Class 2	Class 3
Flange	$c/t = 9\epsilon$	$c/t = 10\epsilon$	$c/t = 14\epsilon$
Web subject to compression	$c/t = 33\epsilon$	$c/t = 38\epsilon$	$c/t = 42\epsilon$
Web subject to bending	$c/t = 72\epsilon$	$c/t = 83\epsilon$	$c/t = 124\epsilon$

The procedure for evaluating the class of a cross section is relatively simple for the case of pure compression and pure bending as shown in Table 5.4. However, when the section is subjected to combined bending and compression ($M+N$) a more laborious procedure is needed. For simplicity, section classification may initially be conducted under the most severe conditions, for the web, pure axial compression. If the result is a Class 1 web, nothing is to be gained by conducting additional calculations considering the actual pattern of the stresses. However if the result is Class 2, Class 3 or Class 4, then it is normally advisable for economic reasons to repeat the classification calculation more precisely (SCI, 2005), using a parameter α for Class 1 or 2 cross sections or a parameter ψ for a Class 3 cross section that defines the position of the plastic or the elastic neutral axis respectively, see Fig. 5.11 for the case of bending about y-y, as presented in EN 1993-1-1 and in Table D.1 of this book.

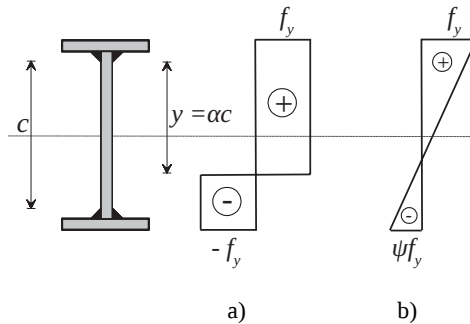


Figure 5.11 – Pattern of normal stresses for: a) Class 1 or Class 2; b) Class 3

According to Eurocode 3 the cross sectional classification must be done considering that the ultimate limit state has been reached. There are two ways that are commonly used for obtaining the position of the plastic and the elastic neutral axis, Vila Real (2014): *i*) keeping the design value of the axial force constant and separately increasing the design value of the bending moment until the full plastic or the full elastic limit state is reached; or *ii*) increasing the axial force and the bending moment proportionally and simultaneously until the ultimate limit state is reached. As it will be shown, for the first methodology the position of the neutral axis depends on the steel grade (the yield strength, f_y), which is not a problem at normal temperature but under fire conditions it means that the classification of a cross section may change with the increasing temperature during the fire development. By using the second methodology the position of the neutral axis does not depend on the steel grade and consequently it does not depend on the temperature.

The procedure is illustrated in the next sections for the case of double symmetric cross sections.

5.3.1. Cross section under combined bending and axial-compression at normal temperature

When a cross section is submitted to bending and axial compression the ultimate limit state is defined by interaction curves as shown in Fig. 5.12. The bi-linear plastic interaction diagram proposed in Eurocode 3, for Class 1 or 2 cross sections, is an approximation of the theoretical curve obtained by the theory of plasticity and shown in Fig. 5.12.

The bi-linear interaction curve of Eurocode 3 for Class 1 and Class 2 doubly symmetric I- and H-sections, is given by (see Eq. (5.97a)):

$$\frac{N_{Ed}}{N_{pl}} + \frac{M_{y,Ed}}{M_{pl}/(1-0.5a)} = 1 \quad \text{but } M_{y,Ed} < M_{pl,y} \quad (5.13)$$

where

$$a = (A - 2bt_f)/A \quad \text{but } a \leq 0.5.$$

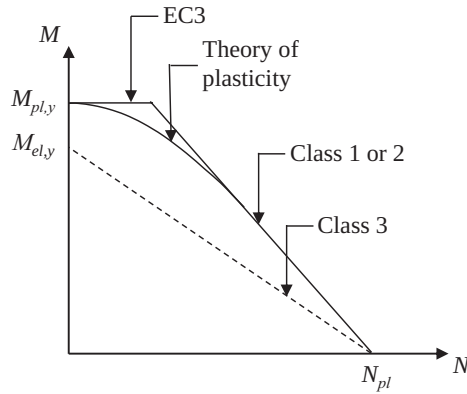


Figure 5.12 – Plastic and elastic M - N interaction curves

The theoretical interaction curve from the theory of plasticity can be easily obtained, at least for welded sections where it is not necessary to consider the radius of the root fillet.

For Class 3 cross sections the interaction curve is linear and defined by:

$$\frac{N_{Ed}}{N_{pl}} + \frac{M_{y,Ed}}{M_{el,y}} = 1 \quad (5.14)$$

Normally the combined design value of the axial compression force, N_{Ed} and the design value of the bending moment, $M_{y,Ed}$, does not correspond to an ultimate limit state (elastic or plastic). Four cases can occur considering the position of the point $(N_{Ed}, M_{y,Ed})$ in the plane N - M , as shown in Fig. 5.13 for point a) to point c).

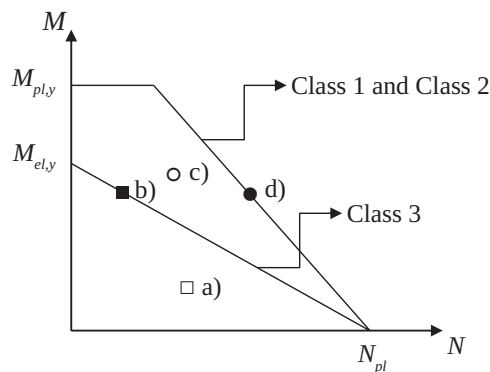


Figure 5.13 – M - N interaction curves

For each pair $(N_{Ed}, M_{y,Ed})$ plotted in Fig. 5.13 corresponds a distribution of the normal stresses depicted in Fig. 5.14: *i*) elastic distribution (see Fig. 5.14 a)); *ii*) elastic distribution corresponding to the ultimate elastic limit state, if the cross section is Class 3 (see Fig. 5.14 b)); *iii*) elastoplastic distribution (see Fig. 5.14 c)) and *iv*) plastic distribution which corresponds to the ultimate plastic limit state for a Class 1 or 2 cross section (see Fig. 5.14 d)).

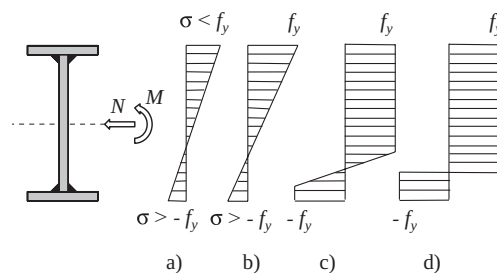


Figure 5.14 – Pattern of normal stresses distribution for combined bending and axial compression. a) and b) Elastic stress distribution; c) elastoplastic stress distribution; d) Plastic stress distribution

As already mentioned, according to Part 1-1 of Eurocode 3, the cross sectional classification must be obtained using the ultimate limit state, i. e. considering case b) or case d) of Fig. 5.13 and Fig. 5.14 if the cross section is Class 3 or if it is Class 1 or 2, respectively. As normally the design value of the axial compression force, N_{Ed} and bending moment, $M_{y,Ed}$, do not fit with the ultimate limit state, an amplification factor must be applied to one or both of these two values in order to reach the ultimate limit state. Fig. 5.15 shows three possible methodologies:

1. Assuming that axial compression N_{Ed} is kept constant and the bending moment $M_{y,Ed}$ is increased separately until the ultimate limit state is reached;
2. Increasing proportionally and simultaneously N_{Ed} and $M_{y,Ed}$ until the ultimate limit state is reached;
3. Assuming that the bending moment $M_{y,Ed}$ is kept constant and the axial compression N_{Ed} is increased separately until the ultimate limit state is reached.

It is worth mentioning, however, that there is, of course, an infinity of possibilities to move the pair $(N_{Ed}, M_{y,Ed})$ until a limit state. However only the two first cases will be addressed in this book.

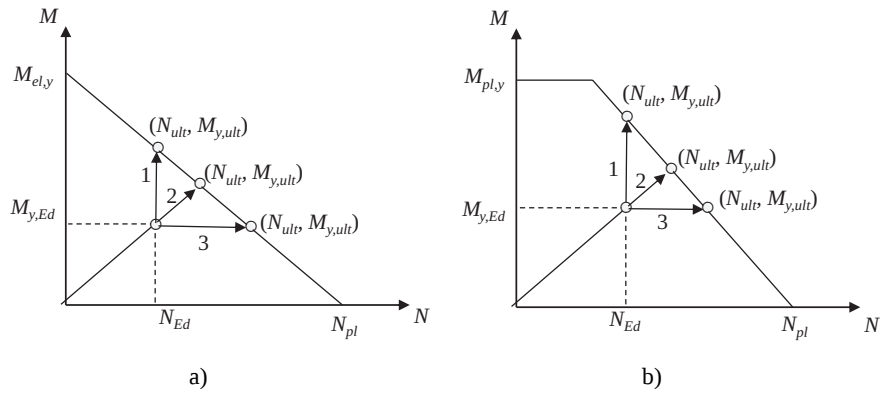


Figure 5.15 – The three possible methodologies to reach the ultimate limit state
 a) Ultimate elastic limit state; b) Ultimate plastic limit state

5.3.1.1. First methodology for Class 1 and Class 2 cross sections

In this methodology it is assumed that N_{Ed} is kept constant and the bending moment $M_{y,Ed}$ is increased separately until the full plastic limit state is reached ($M_{y,Ed} = M_{y,ult}$), as shown in Fig. 5.16.

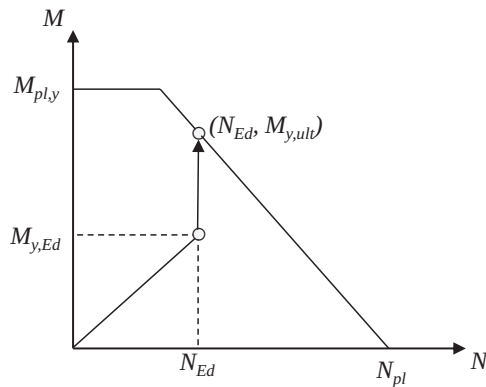


Figure 5.16 – Plastic interaction diagram with the pair $(N_{Ed}; M_{y,ult})$

The full plastic limit state is reached when:

$$\begin{cases} N_{ult} = N_{Ed} \\ M_{y,ult} = \mu_{ult} M_{y,Ed} \end{cases} \quad (5.15)$$

where μ_{ult} , is an amplificatory factor.

This methodology, for the common case of I and H doubly symmetric cross section subjected to compression and major axis bending, has been used by many authors (some examples can be found in Bureau, 2005, SCI, 2005, SCI, 2012, Gardner and Nethercot, 2005, Simões da Silva *et al*, 2010) and corresponds to assume the decomposition of the normal stress diagram as shown in Fig. 5.17.

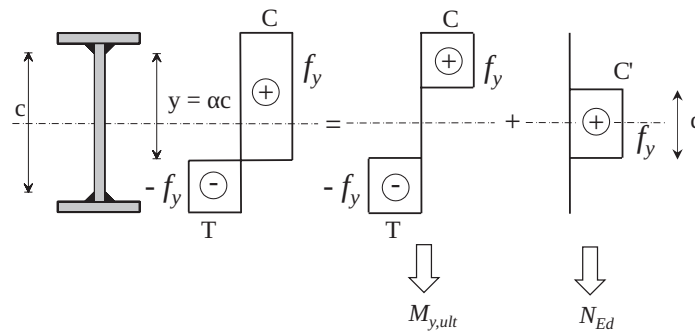


Figure 5.17 – Pattern of normal stresses for Class 1 or 2 I-section.
Positive – Compression (C and C’); Negative – Tension (T)

According to Fig. 5.17, for equilibrium:

$$C = T$$

$$N_{Ed} = C'$$

C and T together resist to bending $M_{y,ult}$

Block C' must be symmetric about the geometrical axis, and therefore:

$$dt_w f_y = 2 \left(y - \frac{c}{2} \right) t_w f_y = N_{Ed} \quad (5.16)$$

and the parameter α defining the position of the plastic neutral axis is given by ($N_{Ed} > 0$ – compression; $N_{Ed} < 0$ – tension)

$$\alpha = \frac{y}{c} = \frac{1}{2} + \frac{N_{Ed}}{2ct_w f_y} \quad (5.17)$$

If $\alpha > 1$, the entire web is under compression.

From Eq. (5.17) it can be concluded that, with this methodology, the position of the plastic neutral axis depends on the steel grade (the yield strength, f_y), which means that it also depends on the temperature (see section 5.3.3).

5.3.1.2. Second methodology for the case of Class 1 and Class 2 cross sections

Increasing simultaneously N_{Ed} and $M_{y,Ed}$ until the full plastic limit state is reached, as shown in Fig. 5.18.

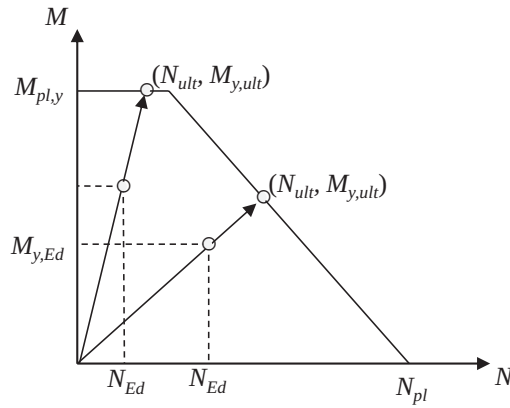


Figure 5.18 – Plastic interaction diagram with the pair $(N_{ult}, M_{y,ult})$

The full plastic limit state is reached when:

$$\begin{cases} N_{ult} = \mu_{ult} N_{Ed} \\ M_{y,ult} = \mu_{ult} M_{y,Ed} \end{cases} \quad (5.18)$$

The amplification factor μ_{ult} is obtained substituting N_{ult} and M_{ult} in Eq. (5.13), which is an approximation to theoretical interaction curve (see Fig. 5.12), coming:

$$\frac{\mu_{ult} N_{Ed}}{N_{pl,Rd}} + \frac{\mu_{ult} M_{y,Ed}}{M_{pl,y,Rd} / (1 - 0.5a)} = 1 \quad \Rightarrow \quad \mu_{ult} \quad (5.19)$$

If $\mu_{ult} M_{y,Ed} > M_{pl,y,Rd}$, then

$$\mu_{ult} = \frac{M_{pl,y,Rd}}{M_{y,Ed}} \quad (5.20)$$

Once the amplification factor is obtained the position of the plastic neutral axis is given using Eq. (5.17), coming:

$$\alpha = \frac{y}{c} = \frac{1}{2} + \frac{N_{ult}}{2ct_w f_y} = \frac{1}{2} + \frac{\mu_{ult} N_{Ed}}{2ct_w f_y} \quad (5.21)$$

This procedure is obviously an approximation because it uses the approximate interaction formula from the Eurocode, Eq. (5.13). The exact position of the plastic neutral axis can be achieved using interaction curve of the theory of plasticity (see Fig. 5.12), which is not difficult to use as it will be shown next.

Considering Fig. 5.17, but now with $N_{ult} = \mu_{ult} N_{Ed}$ instead of the applied axial force N_{Ed} , the two equilibrium equations can be written:

$$\mu_{ult} N_{Ed} = dt_w f_y \quad (5.22)$$

$$\mu_{ult} M_{y,Ed} = M_{pl,y,Rd} - M_{pl,y,w} \quad (5.23)$$

where $d = 2(y - c/2)$ and $M_{pl,y,w}$ is the plastic resistance moment of the part d of the web, that takes the value:

$$M_{pl,y,w} = \frac{t_w d^2}{4} f_y \quad (5.24)$$

From the equilibrium equation Eq. (5.22):

$$d = \frac{\mu_{ult} N_{Ed}}{t_w f_y} \quad (5.25)$$

Substituting Eq. (5.25) into Eq. (5.24) and the result in Eq. (5.23), the following quadratic equation is obtained:

$$\frac{N_{Ed}^2}{4t_w f_y} \mu_{ult}^2 + M_{y,Ed} \mu_{ult} - M_{pl,y,Rd} = 0 \quad (5.26)$$

This equation has two solutions, one of them only being physically meaningful:

$$\mu_{ult} = \frac{2t_w f_y}{N_{Ed}^2} \left[-M_{y,Ed} + \sqrt{M_{y,Ed}^2 + M_{pl,y,Rd} \frac{N_{Ed}^2}{t_w f_y}} \right] \quad (5.27)$$

Knowing the amplification factor the position of the plastic neutral axis is given using Eq. (5.21). Substituting Eq. (5.27) into Eq. (5.21), gives:

$$\alpha = \frac{1}{2} + \frac{-M_{y,Ed} + \sqrt{M_{y,Ed}^2 + W_{pl,y} \frac{N_{Ed}^2}{t_w}}}{cN_{Ed}} \quad (5.28)$$

It is worth mentioning that with the second methodology (increasing simultaneously N_{Ed} and $M_{y,Ed}$ until the full plastic limit state is reached) independently of using Eq. (5.19) or Eq. (5.27), the position of the plastic neutral axis does not depend on the steel grade because $\mu_{ult} = \mu_{ult}(f_y)$ and then α given by Eq. (5.21) does not depend on the yield strength, f_y , as can be confirmed by Eq. (5.28). Thus, using this procedure the classification of the cross section does not depend on the temperature.

Comparing the parameter α given by the first methodology, Eq. (5.17), with its value obtained using the second methodology, Eq. (5.21), it can be concluded that the second methodology is always more conservative because in this case, the value of α is always bigger than the value given by the first methodology (due to the fact that $\mu_{ult} \geq 1$).

5.3.1.3. First methodology for Class 3 cross sections

If the web is not Class 1 or 2 under combined axial force and bending, the classification of the cross section is made using the ratio, $\psi = \sigma_t / \sigma_c$, (which is the ratio of the tensile and compressive stresses at the extreme fibres, as shown in Fig. 5.19).

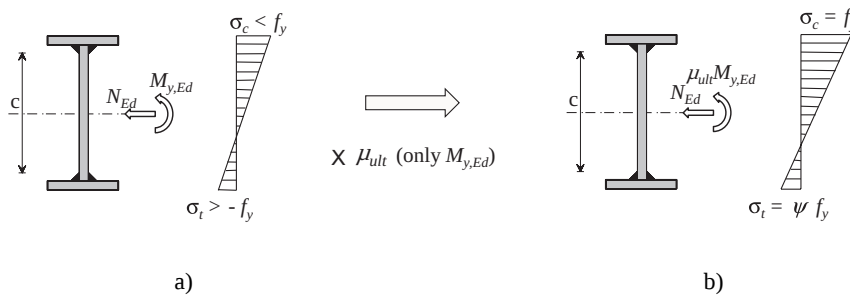


Figure 5.19 – Reaching the ultimate elastic limit state amplifying only $M_{y,Ed}$
 a) Actual direct strength diagram; b) Direct strength diagram at ultimate limit state

At the ultimate limit state represented in Fig. 5.19b) and Fig. 5.20 the compressive and tensile stresses are given by:

$$\begin{cases} \sigma_c = \frac{N_{Ed}}{A} + \frac{M_{y,ult}}{W_{el}} = f_y \\ \sigma_t = \frac{N_{Ed}}{A} - \frac{M_{y,ult}}{W_{el}} = \psi f_y \end{cases} \quad (5.29)$$

adding member by member of this equation, comes

$$\sigma_c + \sigma_t = 2 \frac{N_{Ed}}{A} = (1 + \psi) f_y \Rightarrow \psi = 2 \frac{N_{Ed}}{A f_y} - 1 \quad (5.30)$$

This ratio, that is necessary for the classification of internal parts (webs) under bending and compression, according to the Eurocode 3, varies from $\psi = -1$, for full bending, to $\psi = 1$, for full compression. From Eq. (5.30) it can be concluded that using this methodology to obtain ψ , the classification of the cross section depends on the steel grade, i. e. depends on the temperature.

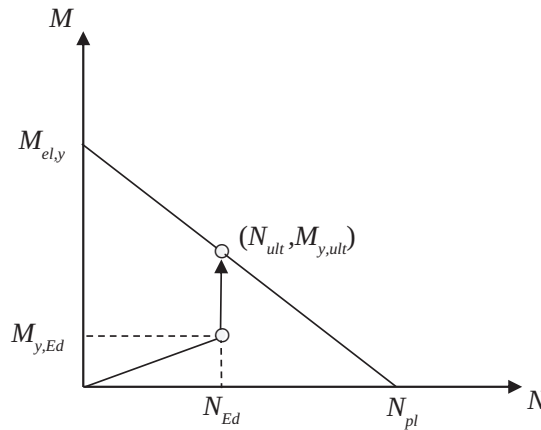


Figure 5.20 – Reaching the ultimate elastic limit state amplifying only $M_{y,Ed}$

5.3.1.4. Second methodology for Class 3 cross sections

With the second methodology the axial compression and the bending moment are both amplified proportionally and simultaneously until the ultimate limit state is reached, as shown in Fig. 5.21.

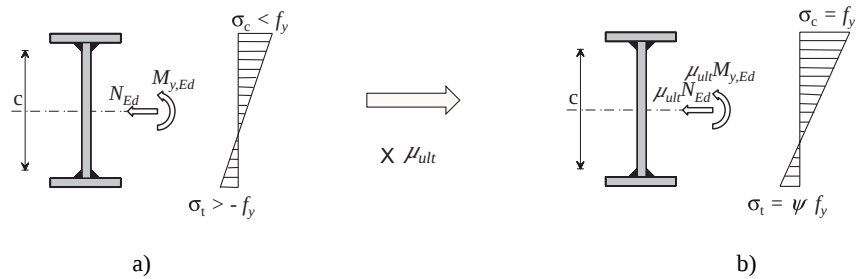


Figure 5.21 – Reaching the ultimate elastic limit state amplifying simultaneously N_{Ed} and $M_{y,Ed}$
 a) Actual direct strength diagram; b) Direct strength diagram at ultimate limit state

The ratio ψ that corresponds to the ultimate elastic limit state depicted in Fig. 5.21b) and Fig. 5.22 can be obtained as follows:

$$\psi = \frac{\sigma_t}{\sigma_c} = \frac{\frac{\mu_{ult} N_{Ed}}{A} - \frac{\mu_{ult} M_{y,Ed}}{W_{el}}}{\frac{\mu_{ult} N_{Ed}}{A} + \frac{\mu_{ult} M_{y,Ed}}{W_{el}}} = \frac{\frac{N_{Ed}}{A} - \frac{M_{y,Ed}}{W_{el}}}{\frac{N_{Ed}}{A} + \frac{M_{y,Ed}}{W_{el}}} \quad (5.31)$$

From this equation it can be concluded that the classification of the cross sections does not depend on the steel grade, i. e., does not depend on the temperature.

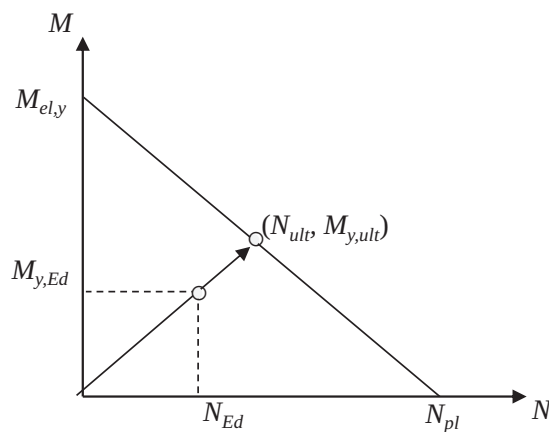


Figure 5.22 – Reaching the ultimate elastic limit state amplifying simultaneously N_{Ed} and $M_{y,Ed}$

5.3.1.5. Advantages and disadvantages of the two presented methodologies

Although the second methodology, i.e. increasing proportionally and simultaneously both axial compression and bending moment, has been suggested in the European project SEMI-COMP+ (2012) there are more adepts for the first methodology than for the second one. In fact, the first method, Eq. (5.17), is the most commonly reported in the literature. Some advantages that can be found supporting the first methodology are: i) the method is easier to apply, giving simple expressions for the evaluation of the position of the neutral axis (parameters α and ψ), ii) the axial force, N_{Ed} , is normally constant along the length of the elements and consequently the class of its cross section doesn't change in the entire element, iii) as the parameters α and ψ are only dependent on the axial force, N_{Ed} it is easy to build tables that give the class of a profile as function only of the axial force, like the ones presented in Annex F of this book, Vila Real *et al* (2009b).

As an example consider a beam-column made of IPE 500 in steel grade S355 with 7000 mm length, submitted to an axial compression force of 100 kN and a moment of 200 kNm about the major axis in one of its extremities and no moment at the other extremity. Use the two presented methodologies to classify the cross section of the profile at normal temperature.

Although in one extremity the moment is zero and the cross section is only submitted to compression being of Class 4, normally designers ignore this fact and classify the beam-column according to the first methodology, assuming that it is submitted to bending and axial force. In this case, considering that the axial compression force is 100 kN, the cross section is classified as Class 1 (Table F.2, that uses Eq. (5.17) and Eq. (5.30) classifies the IPE 500 in S355 as Class 1 until the compression force reaches the value 526 kN, from this value until 803 kN, the cross section is Class 2, from 803 kN until 2984 kN, is Class3 and for an axial load greater than 2984 kN, is class 4).

If the second methodology is used this beam-column has different classes, from Class1 to Class 4, along its length as shown in Fig. 5.23, which has been obtained with the software GeM, Ferreira *et al* (2014). In this figure α_{UltK} is the load amplifier of the design loads to reach the characteristic resistance of the cross sections along the element. In this case the critical cross section, which corresponds to the section where α_{UltK} takes the

minimum value, is the right extremity. According to the aforementioned project SEMI-COMP+, the class that should be considered for checking the buckling resistance of members is the one of the critical cross section. For checking the cross sectional resistance there is no problem of changing the class along the element because the verification is made according to the class of the cross section under consideration.

Annex F, Vila Real *et al* (2009b), gives tables with the cross sectional classification at normal and in fire situation of European hot rolled IPE and HE profiles subjected to pure compression, pure bending about strong axis (M_y), pure bending about weak axis (M_z) and combined compression and bending moment (M_y and M_z), on steel grades S235, S275, S355 and S460, using the first methodology.

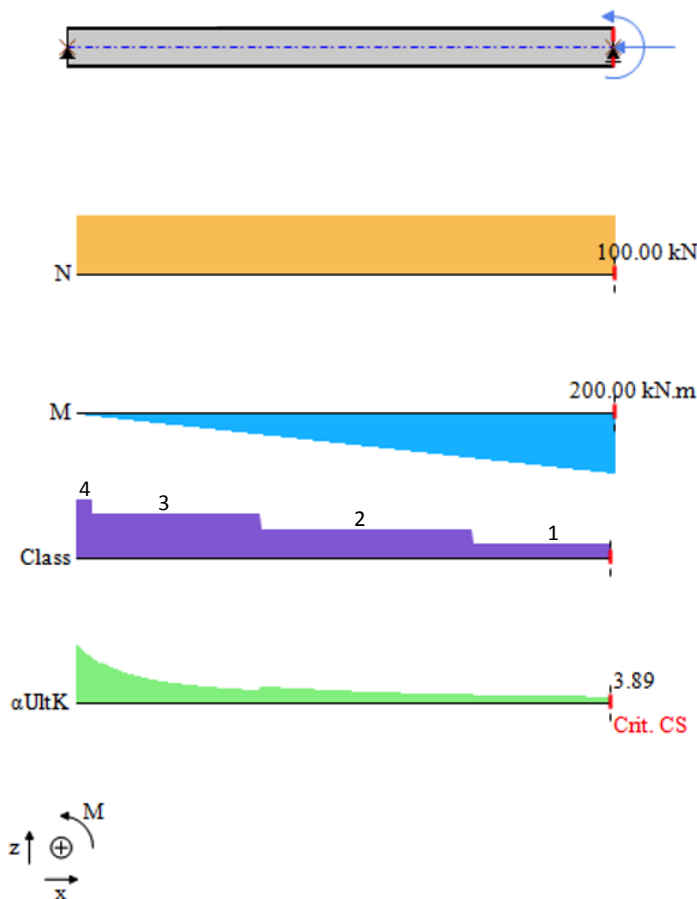


Figure 5.23 – Change of the class in a beam-column using the second methodology

5.3.2. Cross section under combined bending and tension at normal temperature

For the case of combined bending and tension, it is suggested that the compressive ($\sigma_c = N/A + M/W_{el,y}$) and tensile ($\sigma_t = N/A - M/W_{el,y}$) stresses are evaluated first based on the design values N_{Ed} and M_{Ed} and then the ratio $\psi = \sigma_t/\sigma_c$ is calculated. The case $\psi < -1$, is also covered by the Eurocode 3 (see Table D.1).

5.3.3. Classification under fire conditions

At elevated temperature, the Young's modulus and the yield strength are modified as shown in Section 5.2 and Eq. (5.11) must be used instead of Eq. (5.12). For carbon steel ($E = 210000$ MPa) this results in:

$$\begin{aligned}
 \varepsilon_{\theta} &= \sqrt{\frac{235}{f_{y,\theta}}} \sqrt{\frac{E_{\theta}}{210000}} = \\
 &= \sqrt{\frac{235}{k_{y,\theta} f_y}} \sqrt{\frac{k_{E,\theta} E}{210000}} = \\
 &= \sqrt{\frac{k_{E,\theta}}{k_{y,\theta}}} \sqrt{\frac{235}{f_y}} \sqrt{\frac{E}{210000}} = \\
 &= \sqrt{\frac{k_{E,\theta}}{k_{y,\theta}}} \sqrt{\frac{235}{f_y}} \approx 0.85 \sqrt{\frac{235}{f_y}}
 \end{aligned}
 \tag{5.32}$$

with f_y and E in MPa

132

The ratio $\sqrt{k_{E,\theta}/k_{y,\theta}}$ is a function of the temperature and is depicted in Fig. 5.24.

Eurocode 3 recommends that the ratio $\sqrt{k_{E,\theta}/k_{y,\theta}}$ is replaced by a constant value of 0.85. A comparison between this simplification and the ratio $\sqrt{k_{E,\theta}/k_{y,\theta}}$ is shown in Fig. 5.24. Fig. 5.24 shows that this simplification is a good approximation for the range of temperatures between 500 °C and 800 °C, which covers the majority of practical situations.

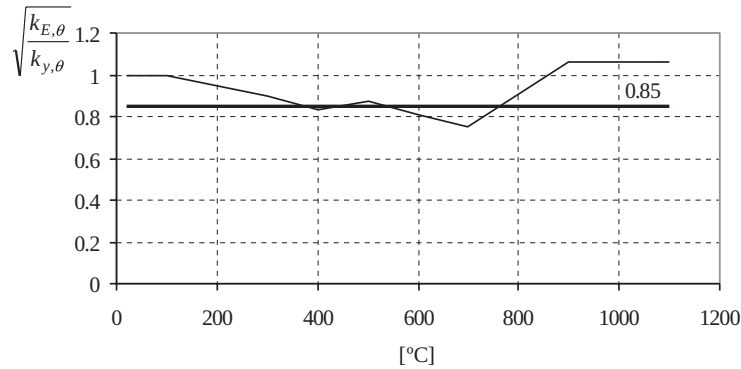


Figure 5.24 – Ratio $\sqrt{k_{E,\theta}/k_{y,\theta}}$ as a function of the temperature

According to Franssen *et al* (2009), the advantage of using this simplification as opposed to the temperature dependent classification model is that it prevents a small temperature increase in the range from 400 to 500 °C or from 700 to 900 °C, improving the classification from Class 3 to Class 2, and consequently increasing the sections load bearing capacity. To avoid changes on the cross sectional classification during the temperature development, EN 1993-1-2 proposes a classification based on the parameter ε given by:

$$\varepsilon = 0.85\sqrt{235/f_y} \quad \text{with } f_y \text{ in MPa} \quad (5.33)$$

which is not temperature dependent. Thus for the purpose of simplified calculation methods, cross sections may be classified as for normal temperature design with a reduced value for ε as given by Eq. (5.33). This is exactly what the Eurocode 3 states and doesn't bring any problem for the case of pure compression and pure bending, but not for the case of combined bending and axial compression, when the first methodology presented in section 5.3.1 is used for cross sectional classification. It was shown that in this case the position of the elastic or plastic neutral axis depends on the temperature and consequently the classification of the cross sections also depends on the temperature. This can be avoided using the second methodology, i. e., obtaining the ultimate limit state for cross sectional classification purpose, increasing proportionally and simultaneously the axial compression force and the bending moment or using the first methodology without updating the classification with the changing temperature, as the Eurocode seems to suggest. This should be the procedure

to be adopted if the first methodology is used, otherwise it can happen that it is impossible to obtain the critical temperature of a profile as it will be shown in the example 5.3 of the present chapter.

Under fire conditions the $M-N$ interaction curves are continuously changing with the increasing temperature until the collapse is reached (see the dashed line in Fig. 5.25, for the case of Class 1 or Class 2 cross sections). This figure shows that under fire conditions the situation is very similar to the second methodology presented in section 5.3.1, where the axial force and the bending moment are increased proportionally and simultaneously until reaching the ultimate limit state. Here, instead of the point $(N_{fi,Ed}, M_{fi,Ed})$ is approaching the yield surface, it is the yield surface that moves towards the point. This seems to suggest that in fire situation the second methodology should be used. The methodology to be used for classifying cross sections under combined bending and axial force is not given in the Eurocode and should be chosen by the designers.

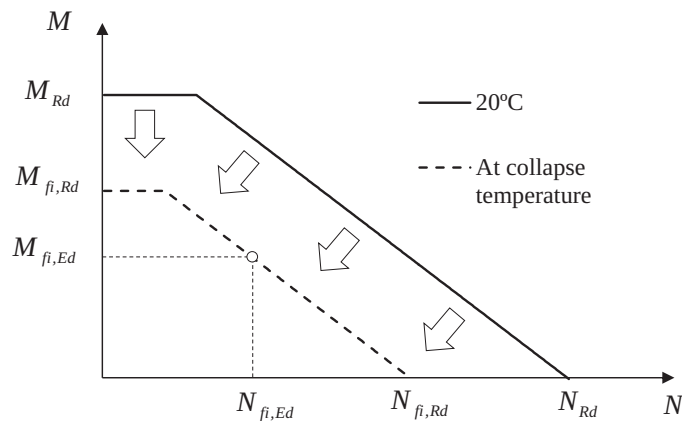


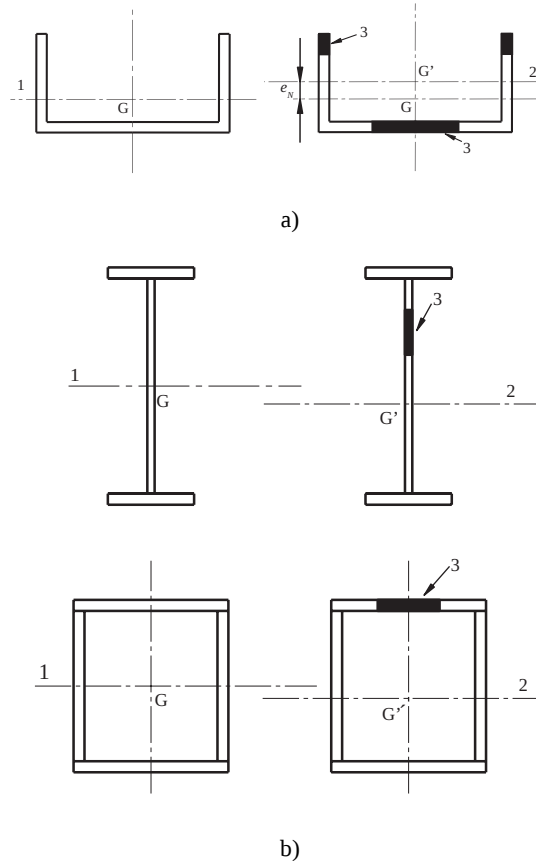
Figure 5.25 – Shrinkage of the $M-N$ interaction curve with the increasing temperature, during a fire

5.4. EFFECTIVE CROSS SECTION

Class 4 cross sections may be replaced by an effective Class 3 cross section. This new section is taken as the gross section minus those parts where local buckling may occur (see non-effective zones in Fig. 5.26). The effective Class 3 section can then be design using elastic cross sectional

resistance limited by yield strength in the extreme fibres. However, under fire conditions, because the original section is Class 4, the yield strength must be taken as the proof strength at 0.2% plastic strain given by Eq. (5.6), rather than the stress at 2% total strain.

The effective area A_{eff} should be determined assuming that the cross section is subject only to stresses due to uniform axial compression (see Fig. 5.26 a)) and the effective section modulus W_{eff} should be determined assuming that the cross section is subject only to bending stresses (see Fig. 5.26 b)). For biaxial bending effective section moduli should be determined about both main axes separately.



G - centroid of the gross cross section; G' - centroid of the effective cross section
 1 - centroidal axis of the gross cross section;
 2 - centroidal axis of the effective cross section;
 3 - non effective zone

Figure 5.26 – Class 4 cross section. a) For axial force; b) For bending moment

The effective areas of flat compression elements should be obtained from Table 4.1 of EN 1993-1-5 for internal elements and Table 4.2 of EN 1993-1-5 for outstand elements. These tables are reproduced in Annex D of this book, as Table D.4 and Table D.5. The effective area of the compression zone of a plate with a gross cross sectional area A_c should be obtained from:

$$A_{c,eff} = \rho A_c \quad (5.34)$$

where ρ is the reduction factor for plate buckling, given by Eq. (5.35) for internal compression elements and by Eq. (5.36) for outstand compression elements. Both equations are dependent on the normalised plate slenderness $\bar{\lambda}_p$, defined in Eq. (5.10). Under fire conditions, the effective cross sectional area should be determined in accordance with EN 1993-1-3 and EN 1993-1-5, based on the material properties at 20 °C.

According to EN 1993-1-5 the reduction factor ρ may be taken as follows:

– internal compression elements:

$$\rho = 1.0 \text{ for } \bar{\lambda}_p \leq 0.5 + \sqrt{0.085 - 0.055\psi}$$

$$\rho = \frac{\bar{\lambda}_p - 0.055(3 + \psi)}{\bar{\lambda}_p^2} \leq 1.0 \text{ for } \bar{\lambda}_p > 0.5 + \sqrt{0.085 - 0.055\psi} \quad (5.35)$$

– outstand compression elements

$$\rho = 1.0 \text{ for } \bar{\lambda}_p \leq 0.748$$

$$\rho = \frac{\bar{\lambda}_p - 0.188}{\bar{\lambda}_p^2} \leq 1.0 \text{ for } \bar{\lambda}_p > 0.748 \quad (5.36)$$

5.5. FIRE RESISTANCE OF STRUCTURAL MEMBERS

5.5.1. General

Structural design at normal temperature requires the structure to support the design ultimate loads (the ultimate limit state) and the deformation and vibrations to be limited under serviceability conditions (the serviceability limit

state). At room temperature most of the design effort of the structure focuses on limiting excessive deformations. Design for the fire situation is mainly concerned with preventing collapse before the specified fire resistance period. Large deformations are accepted during a fire and normally they do not need to be calculated in the fire design, Buchanan, (2001).

The load-bearing function of a steel member is assumed to be lost at time t for a given fire, when:

$$E_{fi,d} = R_{fi,d,t} \quad (5.37)$$

where

- $E_{fi,d}$ is the design value of the relevant effects of actions in the fire situation;
- $R_{fi,d,t}$ is the design value of the resistance of the member in the fire situation at time t .

The design resistance of a member in the fire situation at time t , $R_{fi,d,t}$, can be $M_{fi,t,Rd}$ (design bending moment resistance in the fire situation), $N_{fi,t,Rd}$ (design axial resistance in the fire situation) or any other force (separately or in combination) and the corresponding values of $M_{fi,Ed}$ (design bending moment in the fire situation), $N_{fi,Ed}$ (design axial force in the fire situation), etc. represent $E_{fi,d}$.

The design resistance $R_{fi,d,t}$ at time t shall be determined, (assuming a uniform temperature throughout the cross section) by modifying the design resistance for normal temperature design according EN 1993-1-1, to take account of the mechanical properties of steel at elevated temperatures. The differences in the equations for cold design and fire design are mainly due to the fact that the shape of the stress-strain diagram at room temperature conditions is different from the shape of the diagram at elevated temperature. This is shown schematically in Fig. 5.27. Thus some adaptation to the design equations established for room temperature conditions is needed when they are used at elevated temperature.

If a non-uniform temperature distribution is used, the design resistance for normal temperature design to EN 1993-1-1 should be modified on the basis of this temperature distribution. As an alternative to Eq. (5.37), verification may be carried out in the temperature domain by using a uniform temperature distribution, see Section 5.6.

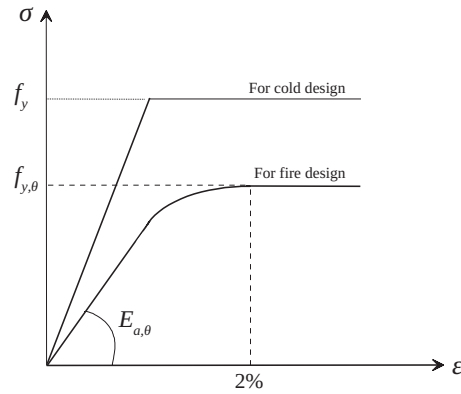


Figure 5.27 – Stress-strain relationship

5.5.2. Members with Class 4 cross sections

For simple calculation models the resistance of members with a Class 4 cross section should be verified using the equations given for compression members, beams and members subject to combined bending and axial compression. In all these equations, the area is replaced by the effective area and the section modulus is replaced by the effective section modulus.

The effective cross sectional area and the effective section modulus should be determined in accordance with EN 1993-1-3 and EN 1993-1-5, i.e., based on the material properties at 20 °C. The cross section classification is more severe in a fire situation than at normal temperature, see section 5.3.3 and Eq. (5.33) (a reduction of 15% in the slenderness limits is considered). For example, a cross section classified as a Class 3 section at normal temperature can be classified as Class 4 in a fire situation, being the effective properties equal to the properties based on the gross cross section without any reduction because the effective properties are based on the properties at room temperature, Franssen *et al* (2009), i.e, they are based on a Class 3 rather than a Class 4 section.

For design under fire conditions the design strength of steel should be taken as the 0.2% proof strength as already mentioned in section 5.2. This design strength may be used to determine the fire resistance of a member (see examples 5.10 and 5.11).

Reduction factors for the design strength of carbon steels relative to the yield strength at 20 °C may be taken from Table 5.2.

When no verification is being conducted, it can be assumed that the fire resistance is maintained as long as the temperature in the section does not exceed a temperature of 350 °C. This value is a nationally determined parameter and a different value may be given in the National Annex.

5.5.3. Tension members

The design value of the tension force in the fire situation, $N_{fi,Ed}$, at each cross section should satisfy the following condition:

$$\frac{N_{fi,Ed}}{N_{fi,\theta,Rd}} \leq 1.0 \quad (5.38)$$

where the design resistance $N_{fi,\theta,Rd}$ of a tension member with a uniform temperature θ_a should be determined from:

$$N_{fi,\theta,Rd} = k_{y,\theta} N_{Rd} \left[\gamma_{M0} / \gamma_{M,fi} \right] \quad (5.39)$$

where

- $k_{y,\theta}$ is the reduction factor for the yield strength of steel at uniform temperature θ_a , reached at time t , see Section 5.2;
- γ_{M0} is the partial safety factor for the resistance of cross sections, whatever the class is;
- $\gamma_{M,fi}$ is the partial safety factor for the fire situation;
- N_{Rd} is the design resistance of the cross section $N_{pl,Rd}$ for normal temperature design, according to EN 1993-1-1, and given by:

$$N_{pl,Rd} = \frac{A f_y}{\gamma_{M0}} \quad (5.40)$$

The recommended value for γ_{M0} and $\gamma_{M,fi}$ is 1.0, but different values may be defined in the National Annex.

Substituting Eq. (5.40) in to Eq. (5.39) leads to

$$N_{fi,\theta,Rd} = A k_{y,\theta} f_y / \gamma_{M,fi} \quad (5.41)$$

According to Annex D of Part 1.2 of Eurocode 3, net-section failure at fastener holes does not need to be considered, provided that there is a fastener in each hole. This is because the steel temperature is lower at joints due to the presence of additional material (e.g. bolts, fittings, etc.).

5. MECHANICAL ANALYSIS

The design resistance $N_{fi,\theta,Rd}$ at time t of a tension member with a non-uniform temperature distribution across the cross section may be determined from:

$$N_{fi,\theta,Rd} = \sum_{i=1}^n A_i k_{y,\theta,i} f_y / \gamma_{M,fi} \quad (5.42)$$

where the subscript i refers to an elemental area of the cross section in which the temperature is considered as uniform.

The design resistance $N_{fi,t,Rd}$ at time t of a tension member with a non-uniform temperature distribution may conservatively be taken as equal to the design resistance $N_{fi,\theta,Rd}$ of a tension member with a uniform steel temperature θ_a equal to the maximum steel temperature $\theta_{a,max}$ reached at time t .

5.5.4. Compression members

The design value of the compression force in the fire situation, $N_{b,fi,Ed}$, at each cross section should satisfy the following condition:

$$\frac{N_{b,fi,Ed}}{N_{b,fi,t,Rd}} \leq 1.0 \quad (5.43)$$

where the design buckling resistance $N_{b,fi,t,Rd}$ at time t of a compression member with a Class 1, Class 2 or Class 3 cross section with a uniform temperature θ_a should be determined from:

$$N_{b,fi,t,Rd} = \chi_{fi} A k_{y,\theta} f_y / \gamma_{M,fi} \quad (5.44a)$$

and for Class 4 cross sections

$$N_{b,fi,t,Rd} = \chi_{fi} A_{eff} k_{0.2p,\theta} f_y / \gamma_{M,fi} \quad (5.44b)$$

where

- $k_{y,\theta}$ is the reduction factor for the yield strength of steel at uniform temperature θ_a , reached at time t , see Section 5.2;
 - $k_{0.2p,\theta}$ is the reduction factor for the 0.2% proof strength of steel at uniform temperature θ_a , reached at time t , see Section 5.2;
 - A_{eff} is the effective area of the cross section when subjected only to uniform compression;
 - χ_{fi} is the reduction factor for flexural buckling in the fire design situation, given by Eq. (5.45).
-

The value of χ_{fi} should be taken as the lower of the values of $\chi_{y,fi}$ and $\chi_{z,fi}$ determined according to:

$$\chi_{fi} = \frac{1}{\phi_{\theta} + \sqrt{\phi_{\theta}^2 - \bar{\lambda}_{\theta}^2}} \quad (5.45)$$

where

$$\phi_{\theta} = \frac{1}{2} [1 + \alpha \bar{\lambda}_{\theta} + \bar{\lambda}_{\theta}^2] \quad (5.46)$$

and the imperfection factor, α , proposed by Franssen *et al* (2005) is given by

$$\alpha = 0.65 \sqrt{235/f_y} \quad (5.47)$$

The non-dimensional slenderness $\bar{\lambda}_{\theta}$ for the temperature θ_a , is given, for Class 1, 2 and 3 by

$$\bar{\lambda}_{\theta} = \bar{\lambda} \sqrt{k_{y,\theta}/k_{E,\theta}} \quad (5.48a)$$

and for Class 4 cross sections

$$\bar{\lambda}_{\theta} = \bar{\lambda} \sqrt{k_{0.2p,\theta}/k_{E,\theta}} \quad (5.48b)$$

where

$\bar{\lambda}$ is the non-dimensional slenderness at room temperature given by Eq. (5.49a) or Eq. (5.49b) using the buckling length in fire situation l_{fi} (see Fig. 5.28).

The non-dimensional slenderness at room temperature, $\bar{\lambda}$, is given by

$$\bar{\lambda} = \sqrt{\frac{Af_y}{N_{cr}}} \quad \text{for Class 1, 2 and 3 cross sections} \quad (5.49a)$$

or

$$\bar{\lambda} = \sqrt{\frac{A_{eff} f_y}{N_{cr}}} \quad \text{for Class 4 cross sections} \quad (5.49b)$$

where

N_{cr} is the elastic critical force for flexural buckling based on the gross cross sectional properties and in the buckling length in fire situation, l_{fi} given by

$$N_{cr} = \frac{\pi^2 EI}{l_{fi}^2} \quad (5.50)$$

where

- E is the Young's modulus at room temperature;
- I is the second moment of area about y-y or x-x axis based on the gross cross sectional properties;
- l_{fi} is the buckling length in fire situation.

The buckling length l_{fi} of a column for the fire design situation should generally be determined as for normal temperature design. In the case of a braced frame, the buckling length l_{fi} of a continuous column may be determined by considering it as fixed to the fire compartments above and below, provided that the fire resistance of the building components that separate these fire compartments is not less than the fire resistance of the column.

For example, in the case of a braced frame in which each storey comprises a separate fire compartment with sufficient fire resistance, in an intermediate storey the buckling length l_{fi} of a continuous column may be taken as $l_{fi} = 0.5L$ and in the top storey the buckling length may be taken as $l_{fi} = 0.7L$, where L is the system length in the relevant storey, see Fig. 5.28.

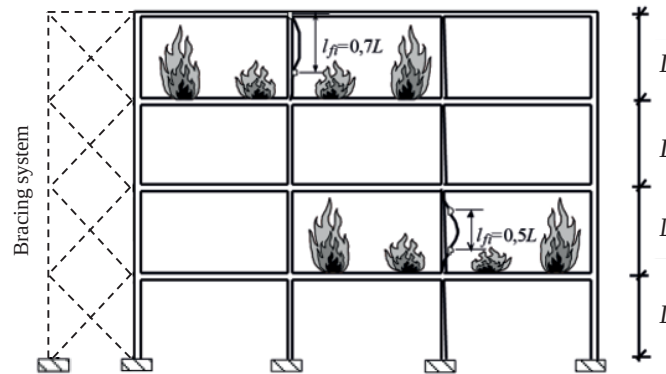


Figure 5.28 – Buckling lengths l_{fi} of columns in braced frames

When designing using nominal fire exposure, the design resistance $N_{b,fi,t,Rd}$ at time t , of a compression member with a non-uniform temperature distribution, may be taken as equal to the design resistance $N_{b,fi,\theta,Rd}$ of a compression member, with a uniform steel temperature θ_a equal to the maximum steel temperature $\theta_{a,max}$ reached at time t .

As the non-dimensional slenderness in the fire situation $\bar{\lambda}_\theta$ depends on the temperature, an iterative procedure is needed if the critical temperature corresponding to a given applied load is to be evaluated, for verification in the time or in the temperature domain (see Eq. 5.1a and Eq. 5.1c). Convergence is usually very fast and one or two iterations are normally sufficient if Eq. (5.48) is approximated, for the first iteration, using the same approximation used in Eq. (5.32), (i.e., $\sqrt{k_{E,\theta}/k_{y,\theta}} \approx 0.85$). This gives the following normalised slenderness at high temperatures, Franssen *et al* (2009).

$$\bar{\lambda}_\theta = \bar{\lambda} \sqrt{k_{y,\theta}/k_{E,\theta}} \approx \bar{\lambda}/0.85 \approx 1.2\bar{\lambda} \quad (5.51)$$

Example 5.4 illustrates this procedure.

5.5.5. Shear resistance

The design value of the shear force in a fire situation, $V_{fi,Ed}$ at each cross section should satisfy

$$\frac{V_{fi,Ed}}{V_{fi,t,Rd}} \leq 1.0 \quad (5.52)$$

where the design shear resistance $V_{fi,t,Rd}$ at time t for a Class 1, Class 2 or Class 3 cross section should be determined from:

$$V_{fi,t,Rd} = k_{y,\theta,web} V_{Rd} \left[\gamma_{M0} / \gamma_{M,fi} \right] \quad (5.53)$$

where

- V_{Rd} is the shear resistance of the gross cross section for normal temperature design, according to EN 1993-1-1, and given in Eq. (5.54);
- θ_{web} is the average temperature of the web;
- $k_{y,\theta,web}$ is the reduction factor for the yield strength of steel at the web temperature θ_{web} .

It should be noted that when a uniform temperature is considered in the design, the average temperature in the web is equal to the uniform temperature in the section. Alternatively, the temperature in the web can be determined using the section factor of the web. For an I-section, the section

5. MECHANICAL ANALYSIS

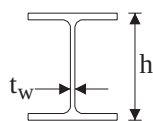
factor can be approximated as $k_{sh}A_m/V = k_{sh}2/t_w$, where the correction factor for the shadow effect is taken for the full section or, in a more accurate way, as the view factor evaluated as shown in Section 4.9.

The shear resistance of the gross cross section for normal temperature design is given (according to EN 1993-1-1) by

$$V_{pl,Rd} = \frac{A_v (f_y / \sqrt{3})}{\gamma_{M0}} \quad (5.54)$$

where A_v is the shear area and may be taken as follows:

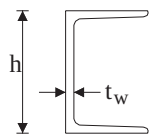
- a) Rolled I- and H- sections, loaded parallel to the web



$$A_v = 1.04ht_w$$

A more accurate value of A_v can be determined from $A_v = A - 2bt_f + (t_w + 2r)t_f$ but not less than $\eta h_w t_w$

- b) Rolled channel sections, loaded parallel to the web

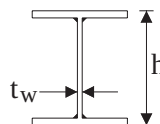


$$A_v = 1.04ht_w$$

A more accurate value of A_v can be determined from $A_v = A - 2bt_f + (t_w + r)t_f$

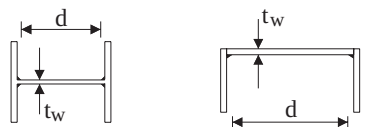
- c) Welded I-, H- and box sections, loaded parallel to the web

144



$$A_v = \eta h_w t_w$$

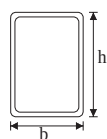
- d) Welded I-, H-, channel and box sections, loaded parallel to the flanges



$$A_v = A - \sum (h_w t_w)$$

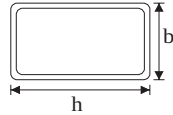
- e) Rolled rectangular hollow sections of uniform thickness:

- load parallel to depth



$$A_v = Ah / (b + h)$$

- load parallel to width



$$A_v = Ab/(b+h)$$

- f) Circular hollow sections and tubes of uniform thickness



$$A_v = 2A/\pi$$

- g) Plates and solid bars



$$A_v = A$$

where

- A is the cross sectional area;
 b is the overall breadth;
 h is the overall depth;
 h_w is the depth of the web;
 r is the root radius;
 t_f is the flange thickness;
 t_w is the web thickness;
 η is a factor given in EN 1993-1-5. May be conservatively taken equal 1.0.

145

Substituting Eq. (5.54) into Eq. (5.53), and considering a uniform temperature distribution, gives the following expression for the design shear resistance

$$V_{fi,t,Rd} = \frac{A_v k_{y,\theta} f_y}{\sqrt{3} \gamma_{M,fi}} \quad (5.55)$$

5.5.6. Laterally restrained beams

5.5.6.1. Uniform temperature distribution

The design value of the bending moment in a fire situation, $M_{fi,Ed}$ at each cross section should satisfy

$$\frac{M_{\bar{f}_i,Ed}}{M_{\bar{f}_i,\theta,Rd}} \leq 1.0 \quad (5.56)$$

where the design moment resistance $M_{\bar{f}_i,\theta,Rd}$ of a Class 1, Class 2 or Class 3 cross section with a uniform temperature θ_a should be determined from:

$$M_{\bar{f}_i,\theta,Rd} = k_{y,\theta} \left[\gamma_{M0} / \gamma_{M,\bar{f}_i} \right] M_{Rd} \quad (5.57a)$$

or for Class 4 cross sections

$$M_{\bar{f}_i,\theta,Rd} = k_{0.2p,\theta} \left[\gamma_{M0} / \gamma_{M,\bar{f}_i} \right] M_{Rd} \quad (5.57b)$$

where

$k_{y,\theta}$ is the reduction factor for the yield strength of steel at uniform temperature θ_a , reached at time t (see Section 5.2);

$k_{0.2p,\theta}$ is the reduction factor for the 0.2% proof strength of steel at uniform temperature θ_a , reached at time t (see Section 5.2);

M_{Rd} is the design resistance for bending about one principal axis of a cross section for normal temperature design, according to EN 1993-1-1, or the reduced moment resistance for normal temperature design, allowing for the effects of shear. EN 1993-1-1 gives the following expressions for calculating M_{Rd} :

146

$$M_{Rd} = M_{pl,Rd} = \frac{W_{pl} f_y}{\gamma_{M0}} \quad \text{for Class 1 or 2 cross sections;}$$

$$M_{Rd} = M_{el,Rd} = \frac{W_{el,min} f_y}{\gamma_{M0}} \quad \text{for Class 3 cross sections;}$$

$$M_{Rd} = \frac{W_{eff,min} f_y}{\gamma_{M0}} \quad \text{for Class 4 cross sections;}$$

where

$W_{el,min}$ and $W_{eff,min}$ corresponds to the fibre with the maximum elastic stress.

Eq. (5.57) thus, becomes:

$$M_{\bar{f}_i,\theta,Rd} = \frac{W_{pl} k_{y,\theta} f_y}{\gamma_{M,\bar{f}_i}} \quad \text{for Class 1 or 2 cross sections} \quad (5.58a)$$

$$M_{fi,\theta,Rd} = \frac{W_{el,min} k_{y,\theta} f_y}{\gamma_{M,fi}} \quad \text{for Class 3 cross sections} \quad (5.58b)$$

$$M_{fi,\theta,Rd} = \frac{W_{eff,min} k_{0.2p,\theta} f_y}{\gamma_{M,fi}} \quad \text{for Class 4 cross sections} \quad (5.58c)$$

It should be noted that Eq. (5.57) and the statement that M_{Rd} has to be reduced for the effects of shear according to EN 1993-1-1 may lead to the wrong conclusion that the ratio at room temperature $V_{Ed}/V_{pl,Rd}$ has to be considered in the reduction at elevated temperature. In fact this ratio must be considered at elevated temperature $V_{fi,Ed}/V_{fi,\theta,Rd}$ as shown in section

5.5.6.2. Non-uniform temperature distribution

A steel beam subject to a non-uniform temperature distribution can be considered as a composite beam, formed of several materials. Normally for an I-shaped beam three different temperatures are considered with simple calculation methods: the temperatures in the upper and lower flanges and the temperature in the web. In this case the beam can be considered as a three-material composite beam, as shown in Fig. 5.29.

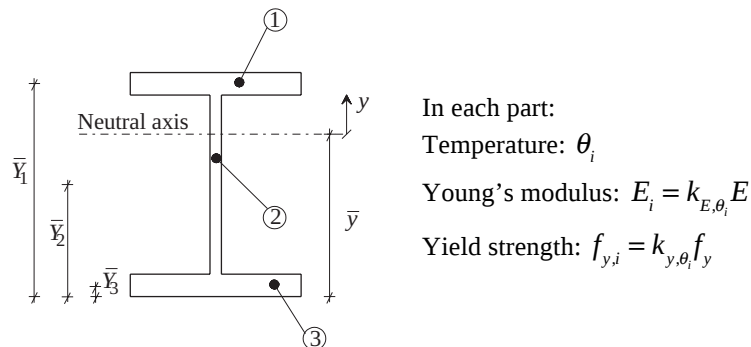


Figure 5.29 – Cross section with non-uniform temperature distribution

The design resistance moment $M_{fi,t,Rd}$ at time t of a Class 1 or Class 2 cross section with a non-uniform temperature distribution across the cross section may be determined from:

$$M_{fi,t,Rd} = \sum_{i=1}^n A_i z_i k_{y,\theta_i} f_{y,i} / \gamma_{M,fi} \quad (5.59)$$

where

- z_i is the distance from the plastic neutral axis to the centroid of the elemental area A_i ;
- $f_{y,i}$ is the nominal yield strength f_y for the elemental area A_i ;
- A_i and $k_{y,\theta,i}$ are as defined in Eq. (5.42).

The plastic neutral axis is evaluated by considering equilibrium of the compressive and tensile normal forces acting on the cross section as follows:

$$\sum_{i=1}^n A_i k_{y,\theta,i} f_{y,i} = 0 \quad (5.60a)$$

or if the yield strength is uniform in the section:

$$\sum_{i=1}^n A_i k_{y,\theta,i} = 0 \quad (5.60b)$$

There are no expressions given in the Eurocode for calculating the design moment of resistance for Class 3 and Class 4 cross sections with a non-uniform temperature distribution across the cross section. However, an expression similar to Eq. (5.60) can be developed using elastic theory and assuming the section is composite. The elastic neutral axis coincides with the centroidal axis of a homogenised cross section in one of the “materials”. The location of the neutral axis is given by

148

$$\bar{y} = \frac{\sum_{i=1}^n A_i E_i \bar{Y}_i}{\sum_{i=1}^n A_i E_i} \quad (5.61)$$

where A_i is the cross section area of material i and \bar{Y}_i is the corresponding centroidal position (see Fig. 5.29). The stress in the material i is given by

$$\sigma_i = \frac{E_i M}{\sum_{i=1}^n E_i I_i} y \quad (5.62)$$

where M is the applied moment, I_i is the second moment of area i about the neutral axis, and y is measured from the neutral axis.

The stress should then be checked against the yield strength in each area according to

$$\sigma_i = \frac{E_i M_{\bar{f}i,Ed}}{\sum_{i=1}^n E_i I_i} y \leq k_{y,\theta_i} \frac{f_y}{\gamma_{M,\bar{f}i}} \quad (5.63)$$

Alternatively, the design moment resistance $M_{\bar{f}i,t,Rd}$ at time t of a member with a non-uniform temperature distribution may be determined from:

$$M_{\bar{f}i,t,Rd} = M_{\bar{f}i,\theta,Rd} / (k_1 k_2) \text{ but } M_{\bar{f}i,t,Rd} \leq M_{Rd} \quad (5.64)$$

where

$M_{\bar{f}i,\theta,Rd}$ is the design moment resistance of the cross section for a uniform temperature θ_a which is equal to the uniform temperature θ_a at time t in a cross section which is not thermally influenced by the supports and given by Eq. (5.58) for Class 1 and Class 2 sections. For Class 3 sections the design resistance moment is given by:

$$M_{\bar{f}i,\theta,Rd} = \frac{W_{el,min} k_{y,\theta,max} f_y}{\gamma_{M,\bar{f}i}} \quad (5.65)$$

where

θ, \max is the maximum steel temperature reached at time t ;

M_{Rd} is the design moment resistance of the cross section at normal temperature;

k_1 is an adaptation factor for non-uniform temperature across the cross section (see Fig. 5.30):

- for a beam exposed on all four sides: $k_1 = 1.0$

- for an unprotected beam exposed on three sides, with a composite or concrete slab on side four: $k_1 = 0.70$

- for a protected beam exposed on three sides, with a composite or concrete slab on side four: $k_1 = 0.85$

k_2 is an adaptation factor for non-uniform temperature along the beam (see Fig. 5.31):

- at the supports of a statically indeterminate beam: $k_2 = 0.85$

- in all other cases: $k_2 = 1.0$

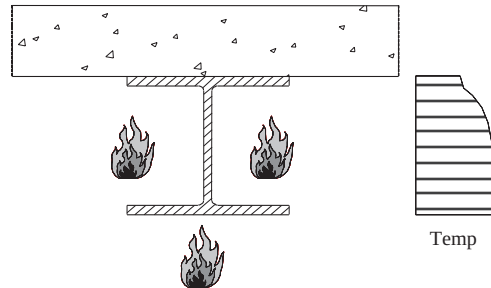


Figure 5.30 – Non-uniform steel temperature distribution across the cross section

Although Eurocode 3 is silent on the protection provided by a composite section with profiled steel sheets, Eurocode 4 states that "for beams connected to slabs with profiled steel sheets a three side fire exposure may be assumed, when at least 85 % of the upper side of the steel profile is directly covered by the steel sheet". A value of $k_1 = 0.70$ should therefore be taken when at least 85% of the upper side of the beam is covered.

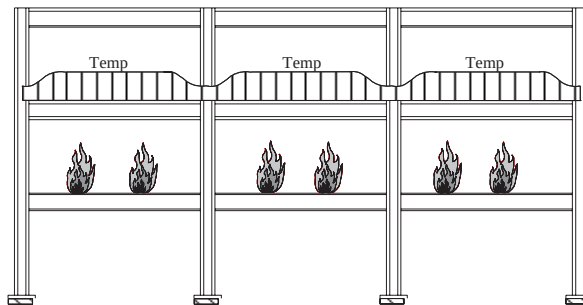


Figure 5.31 – Non-uniform steel temperature distribution along the beam

5.5.6.3. Bending and shear

The effect of the applied shear force on the moment resistance of the section can be neglected when the shear force is less than half the plastic shear resistance of the section.

$$V_{fi,Ed} < 0.5V_{fi,t,Rd} \quad (5.66)$$

Otherwise the reduced moment resistance should be taken as the design resistance of the cross section, calculated using a reduced yield strength

$$(1 - \rho) f_y \tag{5.67}$$

for the shear area (see Fig. 5.32),

where

$$\rho = \left(\frac{2V_{fi,Ed}}{V_{fi,t,Rd}} - 1 \right)^2 \tag{5.68}$$

The design shear resistance $V_{fi,t,Rd}$ at time t for a Class 1, Class 2 or Class 3 cross section should be determined from Eq. (5.55).

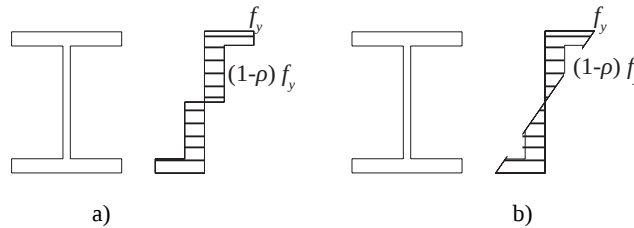


Figure 5.32 – Reduction of the yield strength, in the shear area, due to the shear force
 a) Class 1 or Class 2; b) Class 3

Using the stress diagram from Fig. 5.32a, the design plastic resistance moment in fire situation, allowing for the effect of shear may be obtained for a Class 1 or Class 2 I-cross sections with equal flanges and bending about the major axis, as follows

$$M_{y,V,fi,Rd} = \frac{\left[W_{pl,y} - \frac{\rho A_w^2}{4t_w} \right] k_{y,\theta} f_y}{\gamma_{M,fi}} \tag{5.69}$$

where $A_w = h_w t_w$.

This equation is easily deduced from the stress diagram shown in Fig. 5.33.

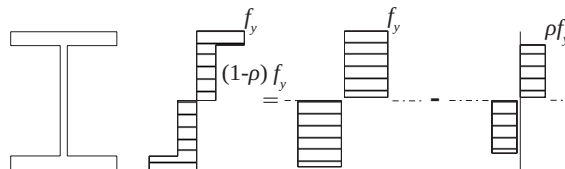


Figure 5.33 – Reduction of the yield strength due to the shear force

For the case of bending about the minor axis, a similar procedure leads to:

$$M_{z,V,fi,Rd} = \frac{\left[W_{pl,z} - \frac{\rho A_f^2}{8t_f} \right] k_{y,\theta} f_y}{\gamma_{M,fi}} \quad (5.70)$$

where $A_f = 2bt_f$.

Eurocode 3 does not give a formula similar to Eq. (5.69) for the case of a Class 3 I-cross sections. However, using a decomposition of the stress diagram of Fig. 5.32b similar to the one depicted in Fig. 5.33 a formula may be obtained. This formula is used in the program Elefir-EN presented in Chapter 8.

5.5.7. Laterally unrestrained beams

5.5.7.1. The elastic critical moment for lateral-torsional buckling

Whenever a slender structural element is loaded in its stiff plane there is a tendency for it to fail by buckling in a more flexible plane. In the case of an I-beam bent about its major axis, failure may occur by a form of buckling which involves both lateral deflection and twisting: lateral-torsional buckling. Fig. 5.34 illustrates the phenomenon with a slender cantilever beam loaded by a vertical end load (SSEDTA, 2001).

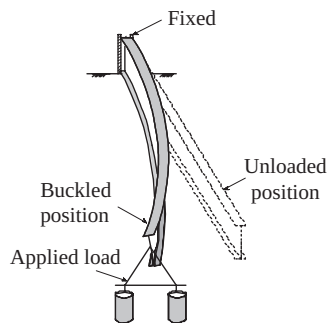


Figure 5.34 – Lateral-torsional buckling of a slender cantilever beam

A design approach for beams that can fail by lateral-torsional buckling must take into account a large number of factors, including i) section shape, ii) the degree of lateral restraint, iii) type of loading, iv) residual stress pattern and v) initial imperfections.

Fig. 5.35 shows the fundamental case of a perfectly elastic, initially straight I-beam loaded by equal and opposite end moments about its major axis. The beam is unrestrained along its length except at each end where the fork supports prevent the section from twisting and moving laterally but allow for rotation both in the plane of the web and on plan.

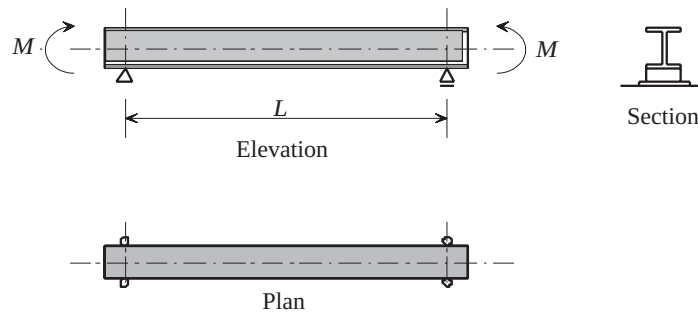


Figure 5.35 – Simple I-beam with fork supports under uniform moment

Considering the differential equation that governs the deformed shape of the beam it is possible to find the elastic critical moment that causes the buckling of the beam under the conditions shown in Fig. 5.35:

$$M_{cr} = \frac{\pi^2 EI_z}{L^2} \sqrt{\frac{I_w}{I_z} + \frac{L^2 GI_t}{\pi^2 EI_z}} \quad (5.71) \quad \text{-----} \quad 153$$

where

- I_t is the torsion constant;
- I_w is the warping constant;
- I_z is the second moment of area about the minor axis;
- L is the unrestrained length of the beam.

The presence of the flexural stiffness (EI_z) and torsional stiffness (GI_t and EI_w) in the equation is a direct consequence of the lateral and torsional components of the buckling deformations. The relative importance of these items will be a reflection of the type of cross section considered. For more details on lateral-torsional behaviour of unrestrained beam the reader is referred to specialised text books on the subject, Allen *et al* (1980), Trahair (1993), Trahair *et al* (1998 and 2001).

5. MECHANICAL ANALYSIS

Uniform moment applied to an unrestrained beam is the most severe case when considering lateral-torsional buckling. An elastic analysis of other load cases results in higher values of elastic critical moments. For example, the elastic critical moment for a uniform moment is given by Eq. (5.71), but for a beam with a central point load it takes the following value

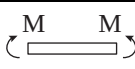


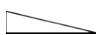
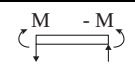
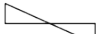
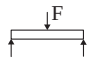
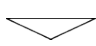
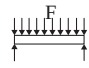

$$M_{cr} = 1.35 \frac{\pi^2 EI_z}{L^2} \sqrt{\frac{I_w}{I_z} + \frac{L^2 GI_t}{\pi^2 EI_z}} \quad (5.72)$$

This is 1.35 times higher than for the fundamental case. The influence of the loading arrangement (shape of the bending moment diagram) is introduced in the formula through the coefficient C_1 , as follows

$$M_{cr} = C_1 \frac{\pi^2 EI_z}{L^2} \sqrt{\frac{I_w}{I_z} + \frac{L^2 GI_t}{\pi^2 EI_z}} \quad (5.73)$$

The value of the coefficient C_1 for a variety of practical loading conditions is given in Table 5.5, valid for the cases where the effective length factors k_z and k_w are both equal to 1.0.

Table 5.5 – Equivalent uniform moment factors C_1

Beam and loads	Bending moment	M_{\max}	C_1
		M	1.00
		M	1.77
		M	2.60
		$\frac{FL}{4}$	1.35
		$\frac{FL^2}{8}$	1.12

Note: The above values correspond to effective length factors k_z and k_w both equal to 1.0

Lateral stability of a beam is dependent not only on the arrangement of loads within the span but also on the level of application of the load relative to the centroid of the cross section. Loads applied to the top flange add a destabilising effect due to the additional twisting moment arising from the action

of the load not passing through the section centroid (see Fig. 5.36). This effect is taken into account by introducing a factor C_2 into the general equation for the elastic critical moment (see Eq. (5.74)). More complete information on the values of the constants C_1 and C_2 , can be found in ECCS (2006) or in Galéa (2002). The program Elefir-EN developed by the authors and presented in Chapter 8 has adopted the values presented in these two sources.

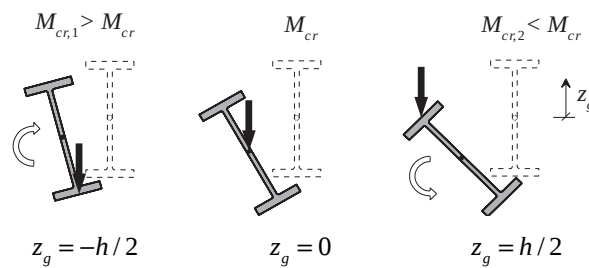


Figure 5.36 – Influence of the level of the application of the load

The influence of end support conditions is also important for the value of the elastic critical moment. A convenient way of including the effect of different support conditions is to redefine the unrestrained length as an effective length, or more precisely with two effective length factors, k_z and k_w . The two factors reflect the two possible types of end fixity, lateral bending restraint and warping restraint. The effective length factors k_z and k_w vary from 0.5 for full restraint to 1.0 for both ends pinned, with 0.7 for one end fixed and one end pinned. The normal conditions of restraint at each end are $k_z = 1.0$, which correspond to restraint against lateral movement and free to rotate on plan; and $k_w = 1.0$ corresponding to restraint against rotation about the longitudinal axis and free to warp. It should be mentioned that the factor k_z that refers to end rotation on plan and is analogous to the ratio L_{cr} / L for a compression member; the factor k_w refers to end warping. Unless special provision for warping restraint is made, k_w should be taken as 1.0. The choice of k_z and k_w is the designer's decision, but conservatively $k_z = k_w = 1.0$ should be adopted.

Eq. (5.72) can thus be written in a more general format as

$$M_{cr} = C_1 \frac{\pi^2 EI_z}{(k_z L)^2} \sqrt{\left(\frac{k_z}{k_w}\right)^2 \frac{I_w}{I_z} + \frac{(k_z L)^2 GI_t}{\pi^2 EI_z}} + (C_2 z_g)^2 - C_2 z_g \quad (5.74)$$

It should be noted that i) where beams have lateral restraints at intervals along the span the segments of the beam between restraints may be

treated as isolated; the design of the beam being based on the most critical segment; ii) lengths of beams between restraints should use an effective length factor k_z of 1.0 and not 0.7, as in the buckled shape the adjacent unrestrained length will buckle in a continuous sinusoidal shape with lateral displacements on opposite sides of the beam for adjacent spans. Beams continuous over a number of spans may be treated as individual spans taking into account the shape of the bending moment diagram within each span.

5.5.7.2. Resistance to lateral-torsional buckling

The design value of the bending moment in a fire situation, $M_{fi,Ed}$ at each cross section should satisfy the following:

$$\frac{M_{fi,Ed}}{M_{b,fi,t,Rd}} \leq 1.0 \quad (5.75)$$

where the design lateral-torsional buckling resistance moment $M_{b,fi,t,Rd}$ at time t for a laterally unrestrained beam with a Class 1, Class 2 or Class 3 cross section is determined from:

$$M_{b,fi,t,Rd} = \chi_{LT,fi} W_y k_{y,\theta,com} f_y / \gamma_{M,fi} \quad (5.76a)$$

and for Class 4 cross sections

$$M_{b,fi,t,Rd} = \chi_{LT,fi} W_{eff,y,min} k_{0.2p,\theta,com} f_y / \gamma_{M,fi} \quad (5.76b)$$

where

- W_y is the plastic section modulus, $W_{pl,y}$ for Class 1 and Class 2 cross sections or the elastic section modulus $W_{el,y}$ for Class 3 cross sections;
- $W_{eff,y,min}$ is the effective section modulus $W_{eff,y}$ for Class 4 cross sections;
- $\chi_{LT,fi}$ is the reduction factor for lateral-torsional buckling in the fire design situation;
- $k_{y,\theta,com}$ is the reduction factor from Section 5.2 for the yield strength of steel at the maximum temperature in the compression flange $\theta_{a,com}$ reached at time t . Conservatively $\theta_{a,com}$ may be assumed to be equal to the uniform temperature θ_a .
- $k_{0.2p,\theta,com}$ is the reduction factor from Section 5.2 for the 0.2% proof strength of steel at the maximum temperature in the

compression flange $\theta_{a,com}$ reached at time t . Conservatively $\theta_{a,com}$ may be assumed to be equal to the uniform temperature θ_a .

The value of $\chi_{LT,fi}$ should be determined according to the following equations:

$$\chi_{LT,fi} = \frac{1}{\phi_{LT,\theta,com} + \sqrt{[\phi_{LT,\theta,com}]^2 - [\lambda_{LT,\theta,com}]^2}} \quad (5.77)$$

with

$$\phi_{LT,\theta,com} = \frac{1}{2} \left[1 + \alpha \bar{\lambda}_{LT,\theta,com} + (\bar{\lambda}_{LT,\theta,com})^2 \right] \quad (5.78)$$

and the imperfection factor, α , which was proposed by the authors, Vila Real *et al* (2001) and later improved Vila Real *et al* (2007) is given by

$$\alpha = 0.65 \sqrt{235/f_y} \quad (5.79)$$

and, for Class 1, 2 and 3

$$\bar{\lambda}_{LT,\theta,com} = \bar{\lambda}_{LT} \sqrt{k_{y,\theta,com} / k_{E,\theta,com}} \quad (5.80a)$$

and for Class 4 cross sections

$$\bar{\lambda}_{LT,\theta,com} = \bar{\lambda}_{LT} \sqrt{k_{0.2p,\theta,com} / k_{E,\theta,com}} \quad (5.80b)$$

where

$k_{E,\theta,com}$ is the reduction factor for the Young's modulus at the maximum steel temperature in the compression flange $\theta_{a,com}$ reached at time t given in Table 5.2.

The non-dimensional slenderness at normal temperature is given by

$$\bar{\lambda}_{LT} = \sqrt{\frac{W_{pl,y} f_y}{M_{cr}}} \quad \text{for Class 1 and 2 cross sections} \quad (5.81a)$$

or

$$\bar{\lambda}_{LT} = \sqrt{\frac{W_{el,y} f_y}{M_{cr}}} \quad \text{for Class 3 cross sections} \quad (5.81b)$$

or

$$\bar{\lambda}_{LT} = \sqrt{\frac{W_{eff,y,min} f_y}{M_{cr}}} \quad \text{for Class 4 cross sections} \quad (5.81c)$$

and

M_{cr} is the elastic critical moment for lateral-torsional buckling, given by Eq. (5.74), based on gross cross sectional properties and takes into account the loading conditions, the real moment distribution and the lateral restraints.

EN 1993-1-2 only considers the influence of the moment distribution between lateral restraints in the calculation for the critical moment. However Vila Real *et al* (2003b and 2007) and Lopes *et al* (2004) have shown that the shape of the moment diagram also affects the value of the lateral torsional buckling resistance moment. There is, in fact, a beneficial effect resulting from reduced plastic zones connected by variable bending along the beam that can be considered at elevated temperature, as shown in Fig. 5.37. This effect is recognised in normal temperature design and EN 1993-1-1 introduces a factor f , which is a function of the shape of the bending moment diagram and its effect is to increase the moment of resistance. It is the opinion of the authors that a similar factor f should be introduced in the next revision of the EN 1993-1-2, Vila Real *et al* (2007).

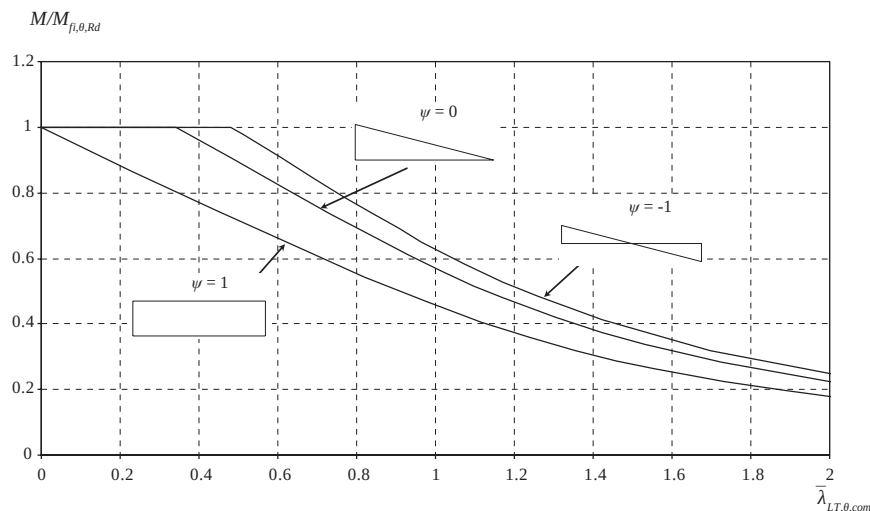


Figure 5.37 – Influence of the shape of the bending moment diagram on the lateral torsional buckling resistance moment

5.5.8. Members subjected to combined bending and axial compression

The design buckling resistance $R_{fi,t,d}$ at time t for a member with a Class 1, Class 2 or Class 3 doubly symmetric cross section subject to combined bending and axial compression should be verified by satisfying expressions (5.82a) and (5.82b).

$$\frac{N_{fi,Ed}}{\chi_{\min,fi} A k_{y,\theta} \frac{f_y}{\gamma_{M,fi}}} + \frac{k_y M_{y,fi,Ed}}{W_y k_{y,\theta} \frac{f_y}{\gamma_{M,fi}}} + \frac{k_z M_{z,fi,Ed}}{W_z k_{y,\theta} \frac{f_y}{\gamma_{M,fi}}} \leq 1 \quad (5.82a)$$

$$\frac{N_{fi,Ed}}{\chi_{z,fi} A k_{y,\theta} \frac{f_y}{\gamma_{M,fi}}} + \frac{k_{LT} M_{y,fi,Ed}}{\chi_{LT,fi} W_y k_{y,\theta} \frac{f_y}{\gamma_{M,fi}}} + \frac{k_z M_{z,fi,Ed}}{W_z k_{y,\theta} \frac{f_y}{\gamma_{M,fi}}} \leq 1 \quad (5.82b)$$

and for doubly symmetric Class 4 cross sections

$$\frac{N_{fi,Ed}}{\chi_{\min,fi} A_{eff} k_{0.2p,\theta} \frac{f_y}{\gamma_{M,fi}}} + \frac{k_y M_{y,fi,Ed}}{W_{eff,y} k_{0.2p,\theta} \frac{f_y}{\gamma_{M,fi}}} + \frac{k_z M_{z,fi,Ed}}{W_{eff,z} k_{0.2p,\theta} \frac{f_y}{\gamma_{M,fi}}} \leq 1 \quad (5.82c)$$

$$\frac{N_{fi,Ed}}{\chi_{z,fi} A_{eff} k_{0.2p,\theta} \frac{f_y}{\gamma_{M,fi}}} + \frac{k_{LT} M_{y,fi,Ed}}{\chi_{LT,fi} W_{eff,y} k_{0.2p,\theta} \frac{f_y}{\gamma_{M,fi}}} + \frac{k_z M_{z,fi,Ed}}{W_{eff,z} k_{0.2p,\theta} \frac{f_y}{\gamma_{M,fi}}} \leq 1 \quad (5.82d)$$

159

where

- A is the area of the gross cross section;
- A_{eff} is the effective area of the cross section when subjected only to uniform compression;
- W_y, W_z are the plastic section modulus, $W_{pl,y}$ or $W_{pl,z}$ for Class 1 and Class 2 sections or the elastic section modulus $W_{el,y}$ or $W_{el,z}$ for Class 3 sections;
- $W_{eff,y}, W_{eff,z}$ are the effective section modulus of the cross section when subjected only to moment about the relevant axis;
- $\chi_{\min,fi}$ should be taken as the lower of the values of $\chi_{y,fi}$ and $\chi_{z,fi}$ determined according to Eq. (5.45);
- $\chi_{LT,fi}$ is as defined in Eq. (5.77);

and for Class 1, Class 2 or Class 3 cross section

$$k_y = 1 - \frac{\mu_y N_{fi,Ed}}{\chi_{y,fi} A k_{y,\theta} \frac{f_y}{\gamma_{M,fi}}} \leq 3 \quad (5.83a)$$

or for Class 4 cross sections

$$k_y = 1 - \frac{\mu_y N_{fi,Ed}}{\chi_{y,fi} A_{eff} k_{0.2p,\theta} \frac{f_y}{\gamma_{M,fi}}} \leq 3 \quad (5.83b)$$

with

$$\mu_y = (2\beta_{M,y} - 5)\bar{\lambda}_{y,\theta} + 0.44\beta_{M,y} + 0.29 \leq 0.8 \quad \text{with } \bar{\lambda}_{y,20^\circ\text{C}} \leq 1.1 \quad (5.84)$$

and for Class 1, Class 2 or Class 3 cross section

$$k_z = 1 - \frac{\mu_z N_{fi,Ed}}{\chi_{z,fi} A k_{y,\theta} \frac{f_y}{\gamma_{M,fi}}} \leq 3 \quad (5.85a)$$

or for Class 4 cross sections

$$k_z = 1 - \frac{\mu_z N_{fi,Ed}}{\chi_{z,fi} A_{eff} k_{0.2p,\theta} \frac{f_y}{\gamma_{M,fi}}} \leq 3 \quad (5.85b)$$

160

with

$$\mu_z = (1.2\beta_{M,z} - 3)\bar{\lambda}_{z,\theta} + 0.71\beta_{M,z} - 0.29 \leq 0.8 \quad (5.86)$$

and for Class 1, Class 2 or Class 3 cross section

$$k_{LT} = 1 - \frac{\mu_{LT} N_{fi,Ed}}{\chi_{z,fi} A k_{y,\theta} \frac{f_y}{\gamma_{M,fi}}} \leq 1 \quad (5.87a)$$

or for Class 4 cross sections

$$k_{LT} = 1 - \frac{\mu_{LT} N_{fi,Ed}}{\chi_{z,fi} A_{eff} k_{0.2p,\theta} \frac{f_y}{\gamma_{M,fi}}} \leq 1 \quad (5.87b)$$

with

$$\mu_{LT} = 0.15 \bar{\lambda}_{z,\theta} \beta_{M,LT} - 0.15 \leq 0.9 \quad (5.88)$$

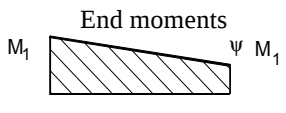
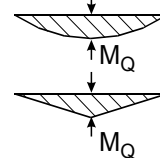
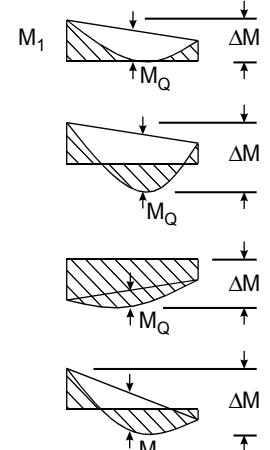
For the equivalent uniform moment factors $\beta_{M,y}$, $\beta_{M,z}$ and $\beta_{M,LT}$ (this last one evaluated using the bending diagram of $M_{y,fi,Ed}$) see Table 5.6.

It should be noted that, although these interaction formulae have been derived based on numerical simulations, the simple model given by Eq. (5.82), does not cover all cases. In some cases the cross sectional capacity can be more critical than the overall stability of section given by Eq. (5.82). This can be the case especially for members subjected to end moments M and ψM when $\psi = -1$ (double curvature), because the point of maximum moment is at the end of the element where it does not influence stability. This usually occurs where the axial load is small and/or the slenderness is low so that secondary bending effects are relatively small. In such cases, design will be controlled by the need to ensure adequate cross sectional resistance at this end of the member. In cases where a uniform moment ($\psi = 1.0$) is applied to the member, the overall buckling check given by Eq. (5.82) will always be more severe than (or in the limit equal to) the cross sectional check, and therefore this latter check need not be performed.

Cross section verification is not specifically mentioned in the fire part of Eurocode 3. As a consequence of clause 1.1.2 (1) of EN 1993-1-2, the formulae from the cold part of the Eurocode should be used, being adapted for elevated temperature (see Section 5.5.9).

The interaction factors in the design formulae (5.82) were developed by Talamona *et al* (1997). The fire part of Eurocode 3 did not adopt the new Method 1 and Method 2 approaches that were introduced into EN 1993-1-1 due to the lack of validation for fire design situation at the time the prEN 1993-1-2 was converted into EN 1993-1-2. Nevertheless, for consistency it is desirable to adopt the $M-N$ interaction formulae used for cold design for design at elevated temperature. Recent published work by Vila Real *et al* (2003c), Lopes *et al* (2004) and Knobloch *et al* (2008) seem to indicate that it is possible to restore the similarity by adapting the interaction formulae that are now presented in the cold part of Eurocode 3 for fire situation. However, they recognise that further development of the interaction factors is needed.

Table 5.6 – Equivalent uniform moment factors

Moment diagram	Equivalent uniform moment factor β_M
<p>End moments</p>  <p>$-1 \leq \psi \leq 1$</p>	$\beta_{M,\psi} = 1.8 - 0.7\psi$
<p>Moments due to in-plane lateral loads</p> 	$\beta_{M,Q} = 1.3$ $\beta_{M,Q} = 1.4$
<p>Moments due to in-plane lateral loads plus end moments</p> 	$\beta_M = \beta_{M,\psi} + \frac{M_Q}{\Delta M} (\beta_{M,Q} - \beta_{M,\psi})$ $M_Q = \max M \text{ due to lateral load only}$ $\Delta M \left\{ \begin{array}{l} \max M \text{ for moment diagram without change of sign} \\ \max M + \min M \text{ for moment diagram with change of sign} \end{array} \right.$

The equivalent uniform moment factors $\beta_{M,y}$, $\beta_{M,z}$ and $\beta_{M,LT}$ should be obtained according to the bending moment diagram between the relevant braced points as follows:

moment factor	bending axis	points braced in direction
$\beta_{M,y}$	y-y	z-z
$\beta_{M,z}$	z-z	y-y
$\beta_{M,LT}$	y-y	y-y

5.5.9. Some verifications of the fire resistance not covered by EN 1993-1-2

Clause 1.1.2 (Scope of Part 1.2 of Eurocode 3) of EN 1993-1-2 states “*This Part 1-2 of EN 1993 deals with the design of steel structures for the accidental situation of fire exposure and is intended to be used in conjunction with EN 1993-1-1 and EN 1991-1-2. This part 1.2 only identifies differences from or supplements to normal temperature design*”.

There are indeed some cases that are not explicitly covered by the fire part of Eurocode 3 and some examples of these are:

- Shear buckling of web without intermediate stiffeners;
- Bending and axial force (for cross section verification);
- Bi-axial bending (for cross section verification);
- Bending, shear and axial force (for cross section verification);
- Torsion;
- Combined shear force and torsional moment.

The next sections present the procedures for verifying some of these cases. In all cases the principle is to modify the formulae from the cold part of Eurocode 3 for use at elevated temperature.

5.5.9.1. Shear buckling resistance for web without intermediate stiffeners

163

The shear buckling resistance for a web without intermediate stiffeners should be verified according to Section 5 of EN 1993-1-5, if

$$\frac{h_w}{t_w} > 72 \frac{\varepsilon}{\eta} \quad (5.89)$$

where

η may be conservatively taken equal to 1.0.

Equation (5.89) can be used at elevated temperature provided that equation (5.33) is used to calculate the value of ε .

Fig. 5.38 shows a composite bridge plate girder after a fire in Rio de Janeiro, Brazil. Shear buckling occurred at elevated temperature although it was not a critical mode of failure at normal temperature.



Figure 5.38 – Shear buckling in a plate girder in fire situation

5.5.9.2. *Cross section verification of a member subjected to combined bending and axial force (compression or tension)*

The fire resistance of a cross section subjected to bending and axial force may be obtained from its plastic resistance, for Class 1 and 2 cross sections, or from its elastic resistance for Class 3 and 4 cross sections.

i) Class 1 and 2 cross sections:

According to EN 1993-1-1, if an axial force is present, allowance should be made for its effect on the plastic moment resistance. For Class 1 and 2 cross sections, the following criterion should be satisfied:

164

$$M_{fi,Ed} \leq M_{N,fi,Rd} \quad (5.90)$$

where $M_{N,fi,Rd}$ is the design plastic moment resistance reduced due to the axial force $N_{fi,Ed}$. The expression for $M_{N,fi,Rd}$ is given by Eq. (5.94) for rectangular solid sections and by Eq. (5.97) for doubly symmetric I- and H-sections or other flanged sections.

ii) Class 3 and 4 cross sections:

For Class 3 and 4 cross sections the maximum longitudinal stress $\sigma_{x,fi,Ed}$ calculated using an elastic analysis and based on the gross cross sectional area for Class 3 cross sections or on the effective cross section for Class 4 cross sections, should satisfy the following criterion:

$$\sigma_{x,fi,Ed} = \frac{N_{fi,Ed}}{A} + \frac{M_{y,fi,Ed}}{W_{el,y}} + \frac{M_{z,fi,Ed}}{W_{el,z}} \leq \frac{k_{y,\theta} f_y}{\gamma_{M,fi}} \quad (5.91)$$

Eq. (5.91) can be written, for Class 3 cross sections, as:

$$\frac{N_{fi,Ed}}{A \frac{k_{y,\theta} f_y}{\gamma_{M,fi}}} + \frac{M_{y,fi,Ed}}{W_{el,y} \frac{k_{y,\theta} f_y}{\gamma_{M,fi}}} + \frac{M_{z,fi,Ed}}{W_{el,z} \frac{k_{y,\theta} f_y}{\gamma_{M,fi}}} \leq 1.0 \quad (5.92)$$

or

$$\frac{N_{fi,Ed}}{N_{fi,pl}} + \frac{M_{y,fi,Ed}}{M_{el,y,fi}} + \frac{M_{z,fi,Ed}}{M_{el,z,fi}} \leq 1.0 \quad (5.93)$$

5.5.9.2.1. Class 1 and 2 rectangular solid sections

For a rectangular solid section, $M_{N,fi,Rd}$ should be taken as

$$M_{N,fi,Rd} = M_{pl,fi,Rd} \left[1 - \left(\frac{N_{fi,Ed}}{N_{pl,fi,Rd}} \right)^2 \right] \quad (5.94)$$

This equation can be deduced using the decomposition of the normal stress diagram for combined bending and axial force shown in Fig. 5.39, Hirt *et al* (2006).

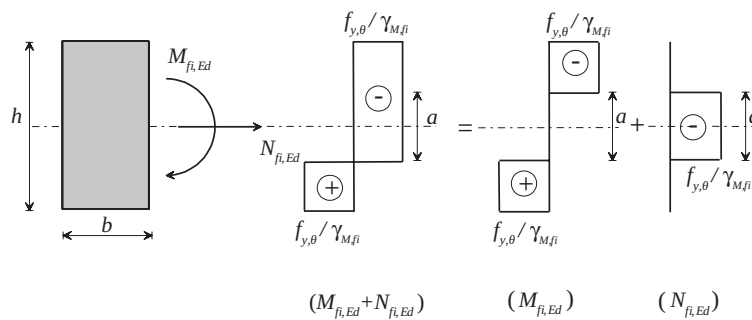


Figure 5.39 – Bending and axial force interaction

The interaction curve for Eq. (5.94) is shown in Fig. 5.40. The interaction curve for Class 3 cross sections, which is based on Eq. (5.93) is also shown in Fig. 5.40.

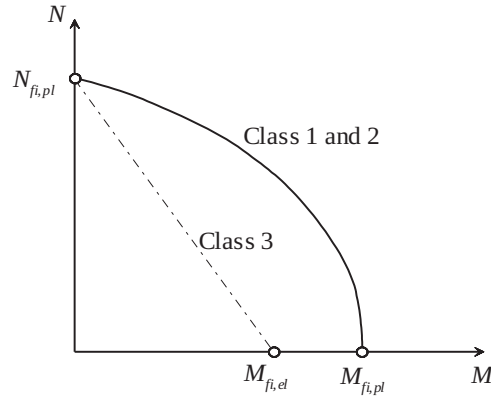


Figure 5.40 – Bending and axial force interaction for rectangular solid sections

5.5.9.2.2. *Class 1 and 2 doubly symmetric I- and H-sections*

For doubly symmetric I- and H-sections or other flanged sections, allowance need not be made for the effect of the axial force on the plastic resistance moment about the y-y axis when both of the following criteria are satisfied:

$$N_{fi,Ed} \leq 0.25N_{pl,fi,Rd} \quad \text{and} \quad N_{fi,Ed} \leq 0.5h_w t_w k_{y,\theta} f_y / \gamma_{M,fi} \quad (5.95)$$

where

166

$$N_{pl,fi,Rd} = Ak_{y,\theta} f_y / \gamma_{M,fi}$$

h_w is the depth of the web;

t_w is the web thickness.

For doubly symmetric I- and H-sections, allowance need not be made for the effect of the axial force on the plastic resistance moment about the z-z axis when:

$$N_{fi,Ed} \leq h_w t_w k_{y,\theta} f_y / \gamma_{M,fi} \quad (5.96)$$

For cross sections where fastener holes are not to be accounted for, the following approximations may be used for standard rolled I- or H-sections and for welded I- or H-sections with equal flanges:

$$M_{N,y,fi,Rd} = M_{pl,y,fi,Rd} (1-n) / (1-0.5a) \quad \text{but} \quad M_{N,y,fi,Rd} \leq M_{pl,y,fi,Rd} \quad (5.97a)$$

$$M_{N,z,\bar{f}i,Rd} = M_{pl,z,\bar{f}i,Rd} \quad \text{if } n \leq a \quad (5.97b)$$

$$M_{N,z,\bar{f}i,Rd} = M_{pl,z,\bar{f}i,Rd} \left[1 - \left(\frac{n-a}{1-a} \right)^2 \right] \quad \text{if } n > a \quad (5.97c)$$

where $n = N_{\bar{f}i,Ed} / N_{\bar{f}i,pl,Rd}$ and $a = (A - 2bt_f) / A$ but $a \leq 0.5$

For cross sections where fastener holes are not to be accounted for, the following approximations may be used for rectangular structural hollow sections of uniform thickness and for welded box sections with equal flanges and equal webs:

$$M_{N,y,\bar{f}i,Rd} = M_{pl,y,\bar{f}i,Rd} (1 - n) / (1 - 0.5a_w), \quad \text{but } M_{N,y,\bar{f}i,Rd} \leq M_{pl,y,\bar{f}i,Rd} \quad (5.98a)$$

$$M_{N,z,\bar{f}i,Rd} = M_{pl,z,\bar{f}i,Rd} (1 - n) / (1 - 0.5a_f), \quad \text{but } M_{N,z,\bar{f}i,Rd} \leq M_{pl,z,\bar{f}i,Rd} \quad (5.98b)$$

where

$$a_w = (A - 2bt) / A \quad \text{but } a_w \leq 0.5 \quad \text{for hollow sections}$$

$$a_w = (A - 2bt_f) / A \quad \text{but } a_w \leq 0.5 \quad \text{for welded box sections}$$

$$a_f = (A - 2ht) / A \quad \text{but } a_f \leq 0.5 \quad \text{for hollow sections}$$

$$a_f = (A - 2ht_w) / A \quad \text{but } a_f \leq 0.5 \quad \text{for welded box sections}$$

According to EN 1993-1-1 for bi-axial bending the following criterion may be used:

$$\left[\frac{M_{y,\bar{f}i,Ed}}{M_{N,y,\bar{f}i,Rd}} \right]^\alpha + \left[\frac{M_{z,\bar{f}i,Ed}}{M_{N,z,\bar{f}i,Rd}} \right]^\beta \leq 1.0 \quad (5.99)$$

in which α and β are constants, which may conservatively be taken as unity. Otherwise the values may be calculated using the following expressions which are based on the results of experimental investigations:

– for I- and H-sections:

$$\alpha = 2; \quad \beta = 5n \quad \text{but } \beta \geq 1$$

5. MECHANICAL ANALYSIS

– for circular hollow sections:

$$\alpha = 2; \beta = 2; \text{ and } M_{N,y,fi,Rd} = M_{N,z,fi,Rd} = M_{pl,fi,Rd} (1 - n^{1.7})$$

– for rectangular hollow sections:

$$\alpha = \beta = \frac{1.66}{1 - 1.13n^2} \text{ but } \alpha = \beta \leq 6$$

where $n = N_{fi,Ed} / N_{fi,pl,Rd}$.

It should be kept in mind that the formulae presented in this section are only for local section capacity check and overall member buckling is ignored. For overall buckling the interaction formulae from Section 5.5.7 should be used for combined bending and compression. For the case of combined bending and tension the lateral buckling effects are much less pronounced, but, depending on the level of axial tension compared to its axial capacity, this effect may be severe if the applied tension loads are small. Eurocode 3 does not require the effect of lateral-torsional buckling when a member is under axial tension and bending to be checked, but designers should use their own judgement when dealing with slender members with low axial tension and high bending moments. According to Ray (1998) the lateral-torsional buckling effects of members with axial tension should be checked with moments alone, ignoring the axial tension which has a beneficial effect. Cross section verification should always be made but in general it doesn't limit the design.

168

5.5.9.2.3. Class 3 doubly symmetric I- and H-sections

For Class 3 cross sections the maximum longitudinal stress should satisfy the criterion, in the absence of shear force:

$$\sigma_{x,fi,Ed} \leq \frac{k_{y,\theta} f_y}{\gamma_{M,fi}} \quad (5.100)$$

where $\sigma_{x,fi,Ed}$ is the design value of the local longitudinal stress due to moment and axial force. Eq. (5.100) can be written as:

$$\frac{N_{fi,Ed}}{A k_{y,\theta} f_y / \gamma_{M,fi}} + \frac{M_{y,fi,Ed}}{W_{el,y} k_{y,\theta} f_y / \gamma_{M,fi}} + \frac{M_{z,fi,Ed}}{W_{el,z} k_{y,\theta} f_y / \gamma_{M,fi}} \leq 1 \quad (5.101)$$

5.5.9.2.4. Class 4 cross sections

In the absence of shear force, for Class 4 cross sections the maximum longitudinal stress $\sigma_{x,fi,Ed}$ calculated using the effective cross should satisfy the criterion:

$$\sigma_{x,fi,Ed} \leq \frac{k_{0.2p,\theta} f_y}{\gamma_{M,fi}} \quad (5.102)$$

where $\sigma_{x,fi,Ed}$ is the design value of the local longitudinal stress due to moment and axial force.

As an alternative to the previous criterion the following simplified criterion may be used:

$$\frac{N_{fi,Ed}}{A_{eff} k_{0.2p,\theta} f_y / \gamma_{M,fi}} + \frac{M_{y,fi,Ed} + N_{Ed} e_{Ny}}{W_{eff,y,min} k_{0.2p,\theta} f_y / \gamma_{M,fi}} + \frac{M_{z,fi,Ed} + N_{fi,Ed} e_{Nz}}{W_{eff,z,min} k_{0.2p,\theta} f_y / \gamma_{M,fi}} \leq 1 \quad (5.103)$$

where

- A_{eff} is the effective area of the cross section when subjected to uniform compression
- $W_{eff,min}$ is the effective section modulus (corresponding to the fibre with the maximum elastic stress) of the cross section when subjected only to moment about the relevant axis
- e_N is the shift of the relevant centroidal axis when the cross section is subjected to compression only (see Fig. 5.26 a)).
For a doubly symmetric cross section $e_N = 0$.

The signs of N_{Ed} , $M_{y,Ed}$, $M_{z,Ed}$ and $\Delta M_i = N_{Ed} e_{Ni}$ depend on the combination of the respective direct stresses.

5.5.9.3. Bending, shear and axial force

Where shear and axial force are presented, allowance should be made for the effect of both shear force and axial force on the resistance moment, as stated in EN 1993-1-1.

Provided that the design value of the shear force $V_{fi,Ed}$ does not exceed 50% of the design plastic shear resistance $V_{fi,pl,Rd}$, no reduction in the resistance for bending and axial force given in Section 5.5.9.2 need be made. However, if $V_{fi,Ed}$ exceeds 50% of $V_{fi,pl,Rd}$, the design resistance of the cross section to combinations of moment and axial force should be calculated using a reduced yield strength as defined in Section 5.5.5.1.

5.6. DESIGN IN THE TEMPERATURE DOMAIN. CRITICAL TEMPERATURE

The critical temperature or collapse temperature of a structural element with a uniform temperature distribution is presented in this section. Collapse occurs when the design value of the relevant effects of actions in the fire situation equals the design value of the resistance of the member in the fire situation at time t . Considering the simplest case of a tension member, collapse occurs when:

$$N_{fi,Ed} = N_{fi,\theta,Rd} \quad (5.104)$$

Substituting the design resistance $N_{fi,\theta,Rd}$ of a tension member with a uniform temperature θ_a , given by Eq. (5.41), gives

$$N_{fi,Ed} = Ak_{y,\theta} f_y / \gamma_{M,fi} \quad (5.105)$$

which means that collapse occurs when the yield strength equals the following expression:

$$f_{y,\theta} = k_{y,\theta} f_y = \frac{N_{fi,Ed}}{A / \gamma_{M,fi}} \quad (5.106)$$

or when the reduction factor for the effective yield strength takes the value

170

$$k_{y,\theta} = \frac{N_{fi,Ed}}{A f_y / \gamma_{M,fi}} \quad (5.107)$$

This equation can be written in the following general form:

$$k_{y,\theta} = \frac{N_{fi,Ed}}{A f_y / \gamma_{M,fi}} = \frac{E_{fi,d}}{R_{fi,d,0}} \quad (5.108)$$

where:

- $E_{fi,d}$ is the design effect of actions in the case of fire;
- $R_{fi,d,0}$ is the value of $R_{fi,d,t}$ for time $t = 0$, i.e., for 20 °C, from Eq. (5.3) with $k_{y,20\text{ °C}} = 1$.

When the value of $k_{y,\theta}$ has been determined from Eq. (5.108), the collapse temperature or critical temperature can be obtained by interpolation from Table 5.2 or by inverting Eq. (5.7), which leads to the following expression for the critical temperature

$$\theta_{a,cr} = 39.19 \ln \left[\frac{1}{0.9674 k_{y,\theta}^{3.833}} - 1 \right] + 482 \quad (5.109)$$

Eurocode 3 adopts this equation, but, instead of the reduction factor, the degree of utilization μ_0 is used:

$$\theta_{a,cr} = 39.19 \ln \left[\frac{1}{0.9674 \mu_0^{3.833}} - 1 \right] + 482 \quad (5.110)$$

where, μ_0 must not be taken less than 0.013. For members with Class 1, Class 2 or Class 3 cross sections and for all tension members, Eurocode 3 defines the degree of utilisation μ_0 at time $t = 0$, i.e., for a temperature of 20 °C, as:

$$\mu_0 = \frac{E_{fi,d}}{R_{fi,d,0}} \quad (5.111)$$

This procedure can only be used for the cases where the load bearing capacity in a fire situation is directly proportional to the effective yield strength, which is the case for tension members and beams where lateral-torsional buckling is not a potential failure mode. For the cases where instability plays a role in the evaluation of $R_{fi,d,t}$ it is not possible to apply Eq. (5.110) directly. This is the case for the flexural buckling of columns, lateral-torsional buckling of beams and members under combined bending and compression. Determination of the critical temperature, in such cases, can be made only by an iterative procedure, as will be shown in Section 5.7. Alternatively an incremental procedure by successive verification in the load domain may be used. This last procedure is convenient for computer implementation whereas the iterative procedure is more suitable for hand calculations.

Eq. (5.111) cannot be used for all types of load. If it is applied, for instance, to a member in compression it leads to

$$\mu_0 = \frac{E_{fi,d}}{R_{fi,d,0}} = \frac{N_{fi,Ed}}{N_{b,fi,0,Rd}} = \frac{N_{fi,Ed}}{\chi_{20^\circ\text{C}} A f_y / \gamma_{M,fi}} \quad (5.112)$$

This expression is wrong because the reduction factor for flexural buckling should in fact not be evaluated at 20 °C but at the collapse temperature, as shown below.

Using Eq. (5.37) the collapse of an axially loaded column is given by

$$N_{\bar{f},Ed} = N_{b,\bar{f},t,Rd} \quad (5.113)$$

Substituting Eq. (5.44) in Eq. (5.113), gives

$$N_{\bar{f},Ed} = \chi_{\bar{f}} A k_{y,\theta} f_y / \gamma_{M,\bar{f}} \quad (5.114)$$

and

$$k_{y,\theta} = \frac{N_{\bar{f},Ed}}{\chi_{\bar{f}} A f_y / \gamma_{M,\bar{f}}} \quad (5.115)$$

which shows that $k_{y,\theta}$ at collapse, is different from the degree of utilisation, μ_0 , at time $t = 0$, as it is defined in Eq. (5.112).

The reduction factor for flexural buckling should be evaluated at the collapse temperature and an iterative procedure is needed, starting with an initial value of the non-dimensional slenderness given, for example, by Eq. (5.51).

Eurocode 3 states that “*The national annex may give default values for critical temperatures*”, but the standard does not recommend a default values. The only default critical temperature given in Eurocode 3 is 350 °C for members with Class 4 cross sections. The option of fixing critical temperatures is quite convenient for the designer. Using this approach a structural analysis in the fire situation can be avoided provided sufficient thermal insulation is applied to maintain the steel temperature below the defined critical temperature during the required fire resistance time.

The definition of a default temperature is quite easy for cases where the load bearing capacity in a fire situation is directly proportional to the effective yield strength. This is the case for tension members and beams where lateral-torsional buckling is not a potential failure mode. In fact assuming that the member is fully loaded at room temperature

$$E_d = R_d \quad (5.116)$$

the effect of the actions in a fire situation can be given by:

$$E_{\bar{f},d} = \eta_{\bar{f}} E_d = \eta_{\bar{f}} R_d \quad (5.117)$$

The degree of utilisation can thus be written, according to Eq. (5.111), as

$$\mu_0 = \frac{E_{\bar{f},d}}{R_{\bar{f},d,0}} = \frac{\eta_{\bar{f}} R_d}{R_d (\gamma_{M0} / \gamma_{M,\bar{f}})} = \eta_{\bar{f}} (\gamma_{M,\bar{f}} / \gamma_{M0}) \quad (5.118)$$

which is the equation given in clause 4.2.4 (4) of EN 1993-1-2 and is valid for tension members and beams where lateral-torsional buckling is not a potential failure mode.

As mentioned in Section 2.1.4 of this book, Eurocode 3 recommends, for simplicity, that a value of $\eta_{\bar{f}} = 0.65$ may be used for most situation. However, for those cases where the imposed load is defined as load category E as given in EN 1991-1-1 (areas susceptible to accumulation of goods, including access areas) Eurocode 3 recommends a value of 0.7.

Tension members:

Using Eq. (5.119) for tension members, with $\gamma_{M0} = \gamma_{M,\bar{f}} = 1.0$, yields

$$\mu_0 = \frac{E_{\bar{f},d}}{R_{\bar{f},d,0}} = \frac{\eta_{\bar{f}} A f_y / \gamma_{M0}}{A f_y / \gamma_{M,\bar{f}}} = \eta_{\bar{f}} (\gamma_{M,\bar{f}} / \gamma_{M0}) = \eta_{\bar{f}} \quad (5.119)$$

which gives a critical temperature according to Eq. (5.110) of 540 °C for all load cases except those where the imposed load is defined as load category E as given in EN 1991-1-1, in which case the critical temperature is 525 °C.

173

Beams where lateral-torsional buckling is not a potential failure mode:

Eq. (5.111) gives for $\gamma_{M0} = \gamma_{M,\bar{f}} = 1.0$

$$\mu_0 = \frac{E_{\bar{f},d}}{R_{\bar{f},d,0}} = \frac{\eta_{\bar{f}} W_y f_y / \gamma_{M0}}{W_y f_y / (k_1 k_2 \gamma_{M,\bar{f}})} = \eta_{\bar{f}} k_1 k_2 \frac{\gamma_{M,\bar{f}}}{\gamma_{M0}} = \eta_{\bar{f}} k_1 k_2 \quad (5.120)$$

which leads to the following critical temperatures according to Eq. (5.110):

– Isostatic beams:

- Isostatic beams heated on four sides ($k_1 = 1.0$; $k_2 = 1.0$):

$$\theta_{a,cr} = 540 \text{ °C};$$

- Unprotected isostatic beams heated on three sides
($k_1 = 0.7$; $k_2 = 1.0$):
 $\theta_{a,cr} = 600$ °C;
- Protected isostatic beams heated on three sides
($k_1 = 0.85$; $k_2 = 1.0$):
 $\theta_{a,cr} = 570$ °C;
- **Hyperstatic beams:**
 - Hyperstatic beams heated on four sides ($k_1 = 1.0$; $k_2 = 0.85$):
 $\theta_{a,cr} = 570$ °C;
 - Unprotected hyperstatic beams heated on three sides
($k_1 = 0.7$; $k_2 = 0.85$):
 $\theta_{a,cr} = 625$ °C;
 - Protected hyperstatic beams heated on four sides
($k_1 = 0.85$; $k_2 = 0.85$):
 $\theta_{a,cr} = 595$ °C.

The following default temperatures can be found in the French and Belgian ENV versions of Part 1-2 of Eurocode 3:

- For tension members:
 - 540 °C;
- For beams where lateral-torsional buckling is not a potential failure mode:
 - 540 °C for isostatic beams;
 - 570 °C for hyperstatic beams;
- For columns, beams with lateral-torsional buckling and beam-columns:
 - 500 °C

For columns, beams with lateral-torsional buckling and beam-columns a critical temperature of 500 °C is usually recommended, but this is an empirical value not based on any analytical procedure.

Although the use of default temperatures is convenient for the designer, this procedure usually leads to conservative but uneconomical design, because it does not take into account the beneficial effect of a lower degree of utilization. In most cases the degree of utilisation is lower than the assumed value of 0.65 or 0.7.

Fig. 5.41 shows the critical temperature of a member, related to the degree of utilisation.

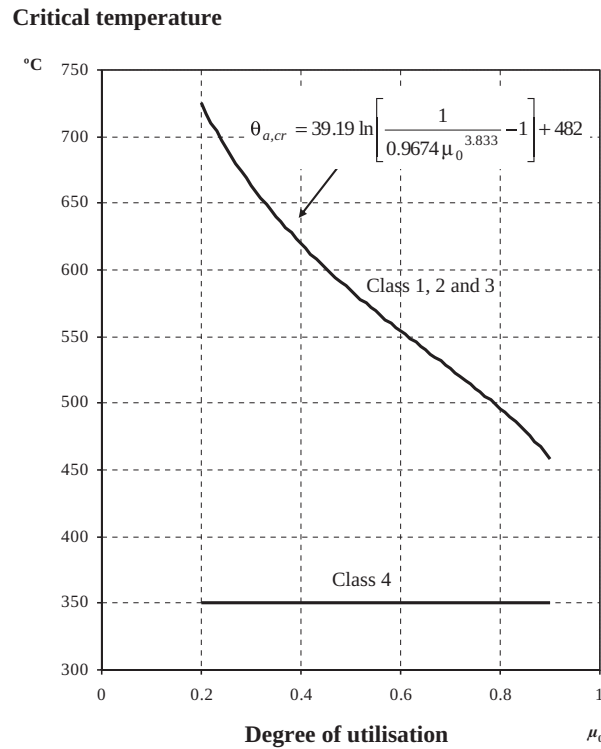


Figure 5.41 – Critical temperature, related to degree of utilisation

The evaluation of the degree of utilisation is trivial for tension members, beams and columns but it is not for beam-columns. For members subjected to combined bending and axial compression failure occurs when:

$$\frac{N_{fi,Ed}}{\chi_{min,fi} A k_{y,\theta} \frac{f_y}{\gamma_{M,fi}}} + \frac{k_y M_{y,fi,Ed}}{W_y k_{y,\theta} \frac{f_y}{\gamma_{M,fi}}} + \frac{k_z M_{z,fi,Ed}}{W_z k_{y,\theta} \frac{f_y}{\gamma_{M,fi}}} = 1 \quad (5.121)$$

$$\frac{N_{\bar{f}i,Ed}}{\chi_{z,\bar{f}i} A k_{y,\theta} \frac{f_y}{\gamma_{M,\bar{f}i}}} + \frac{k_{LT} M_{y,\bar{f}i,Ed}}{\chi_{LT,\bar{f}i} W_y k_{y,\theta} \frac{f_y}{\gamma_{M,\bar{f}i}}} + \frac{k_z M_{z,\bar{f}i,Ed}}{W_z k_{y,\theta} \frac{f_y}{\gamma_{M,\bar{f}i}}} = 1 \quad (5.122)$$

From these equations it is possible to take the value of the reduction factor for the yield strength of steel, $k_{y,\theta} = \mu_0$ as follows

$$k_{y,\theta} = \frac{N_{\bar{f}i,Ed}}{\chi_{\min,\bar{f}i} A \frac{f_y}{\gamma_{M,\bar{f}i}}} + \frac{k_y M_{y,\bar{f}i,Ed}}{W_y \frac{f_y}{\gamma_{M,\bar{f}i}}} + \frac{k_z M_{z,\bar{f}i,Ed}}{W_z \frac{f_y}{\gamma_{M,\bar{f}i}}} = \mu_0 \quad (5.123)$$

$$k_{y,\theta} = \frac{N_{\bar{f}i,Ed}}{\chi_{z,\bar{f}i} A \frac{f_y}{\gamma_{M,\bar{f}i}}} + \frac{k_{LT} M_{y,\bar{f}i,Ed}}{\chi_{LT,\bar{f}i} W_y \frac{f_y}{\gamma_{M,\bar{f}i}}} + \frac{k_z M_{z,\bar{f}i,Ed}}{W_z \frac{f_y}{\gamma_{M,\bar{f}i}}} = \mu_0 \quad (5.124)$$

It should be noted that the iterative procedure to be used with columns under buckling, members under lateral-torsional buckling and members under combined bending and compression for evaluating the critical temperature is only possible for temperatures greater than 400 °C. Below this temperature $k_{y,\theta}$ is equal to 1.0 and the reduction factor for the Young's modulus, $k_{E,\theta}$, decreases until 100 °C. For critical temperatures lower than 400 °C an incremental procedure by successive verification in the resistance domain must be adopted.

176

A flowchart for evaluating the critical temperature is given in Fig. 5.42, Dhima (1999), which shows the iterative procedure for use with members where instability may occur.

The case of combined bending and shear requires special attention when the effect of shear is taken into account to reduce the moment resistance, see Section 5.5.5.1. In this case, if the temperature distribution is not uniform, Eq. (5.69) for bending about major axis should be written in the following form which includes the adaption factors (k_1 and k_2) for a non-uniform temperature distribution:

$$M_{y,V,\bar{f}i,Rd} = \frac{\left[W_{pl,y} - \frac{\rho A_w^2}{4t_w} \right] k_{y,\theta} f_y}{k_1 k_2 \gamma_{M,\bar{f}i}} \quad (5.125)$$

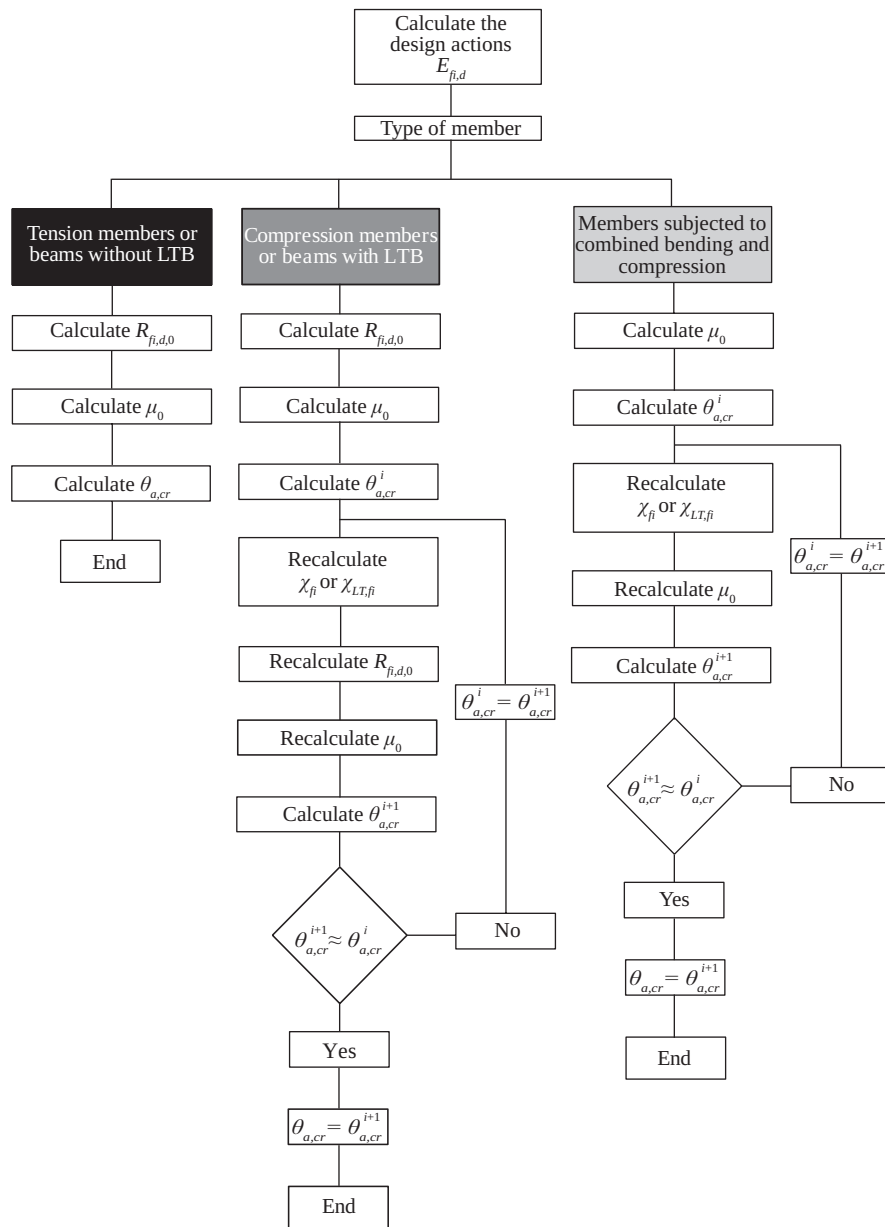


Figure 5.42 – Flowchart for evaluating the critical temperature

Furthermore the following condition must be satisfied

$$M_{y,V,fi,Rd} = \frac{\left[W_{pl,y} - \frac{\left(\frac{2V_{fi,Ed}}{A_v k_{y,\theta} f_y} - 1 \right)^2 \frac{A_w^2}{4t_w}}{\sqrt{3}\gamma_{M,fi}} \right] k_{y,\theta} f_y}{k_1 k_2 \gamma_{M,fi}} \geq M_{fi,Ed} \quad (5.126)$$

where $A_w = h_w t_w$.

For bending about the minor axis the following condition must be satisfied

$$M_{z,V,fi,Rd} = \frac{\left[W_{pl,z} - \frac{\left(\frac{2V_{fi,Ed}}{A_v k_{y,\theta} f_y} - 1 \right)^2 \frac{A_f^2}{8t_f}}{\sqrt{3}\gamma_{M,fi}} \right] k_{y,\theta} f_y}{k_1 k_2 \gamma_{M,fi}} \geq M_{fi,Ed} \quad (5.127)$$

where $A_f = 2bt_f$.

It is not easy to determine the value of $k_{y,\theta}$ from this equation, but it is possible to determine $k_{y,\theta}$ using mathematical manipulation. The program Elefir-EN uses this approach for bending about the major and minor axes.

Although verification of the section under combined bending and axial load is not covered in the fire part of the Eurocode 3, it is presented in this book. It is possible that the stability of a member is adequate under combined axial load and, for example, a bi-triangular bending moment distribution, whereas the combination of axial force and maximum bending moment that is present at one extremity of the member cannot be supported by the section. If the effect of the axial load is to be taken into account in the design value of the resistance moment, then, according to Section 5.5.9.2, at collapse:

$$M_{fi,Ed} = M_{N,fi,Rd} \quad (5.128)$$

where

$M_{N,fi,Rd}$ is the resisting plastic bending moment reduced by the effect of the axial force. This moment can be found by a plastic stress distribution that is in equilibrium with the axial force and the bending moment, as shown in Fig. 5.39, for the case of rectangular solid sections.

For doubly symmetric I- and H-sections with bending about the major axis, Eq. (5.97a) can be developed as:

$$M_{N,y,\bar{f}_i,Rd} = \frac{(1-n)}{(1-0.5a)} M_{pl,y,\bar{f}_i,Rd} \quad (5.129)$$

where

$$a = \frac{(A - 2bt_f)}{A} \text{ but } a \leq 0.5 \quad (5.130)$$

and

$$n = \frac{N_{\bar{f}_i,Ed}}{N_{pl,\bar{f}_i,Rd}} \quad (5.131)$$

For a Class 1 or 2 cross section

$$M_{pl,y,\bar{f}_i,Rd} = W_{pl,y} k_{y,\theta} f_y / \gamma_{M,\bar{f}_i} \quad (5.132)$$

and

$$N_{pl,\bar{f}_i,Rd} = Ak_{y,\theta} f_y / \gamma_{M,\bar{f}_i} \quad (5.133)$$

Thus, Eq. (5.128) becomes:

$$\begin{aligned} M_{\bar{f}_i,Ed} &= M_{N,\bar{f}_i,Rd} = \frac{(1-n)}{(1-0.5a)} M_{pl,y,\bar{f}_i,Rd} \\ &= \left(\frac{1 - \frac{N_{\bar{f}_i,Ed}}{N_{pl,\bar{f}_i,Rd}}}{(1-0.5a)} \right) M_{pl,y,\bar{f}_i,Rd} = \left(\frac{1 - \frac{N_{\bar{f}_i,Ed}}{Ak_{y,\theta} f_y / \gamma_{M,\bar{f}_i}}}{(1-0.5a)} \right) W_{pl,y} k_{y,\theta} f_y / \gamma_{M,\bar{f}_i} \end{aligned} \quad (5.134)$$

 179

from where the reduction factor for the yield strength can be taken as

$$k_{y,\theta} = \frac{N_{\bar{f}_i,Ed}}{Af_y / \gamma_{M,\bar{f}_i}} + (1-0.5a) \frac{M_{\bar{f}_i,Ed}}{W_{pl,y} f_y / \gamma_{M,\bar{f}_i}} = \mu_{0,N} + (1-0.5a) \mu_{0,M} \quad (5.134)$$

where $\mu_{0,N}$ and $\mu_{0,M}$ are the degrees of utilization for axial load and bending moment, respectively.

The critical temperature can be found from either interpolation of the values in Table 5.2 or using Eq. (5.109).

5.7. DESIGN OF CONTINUOUS BEAMS

5.7.1. General

Continuous beams are one of the most popular structural systems used in building construction and particular attention is given to the design of this form of construction in this section.

As many books or chapters have been written on the plastic design of continuous structures, Neal (1977), Wong (2009), Marshal *et al* (1978), only the main principles and those topics relevant to fire design will be addressed here.

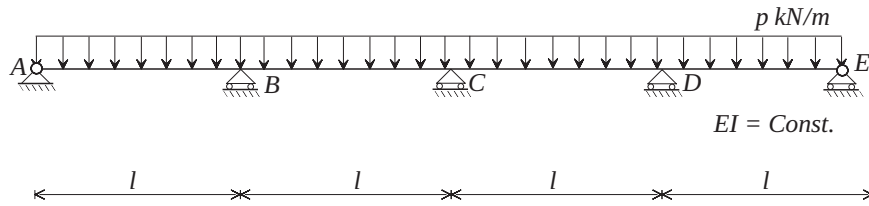
The following principles are assumed, Marshal *et al* (1978):

- i) A perfectly elastic-plastic structural member behaves elastically until a plastic hinge is formed at one section;
- ii) Additional load may be carried if rotation at this hinge allows redistribution of the load to other stable parts of the structure, which is the case for Class 1 cross sections;
- iii) As each plastic hinge is formed, the moment remains constant at the fully-plastic value irrespective of deformation or additional load;
- iv) Collapse occurs when there is no remaining stable element able to carry additional load;
- v) At collapse the structure as a whole, or in part, forms a simple mechanism;
- vi) Looking ahead, it is apparent that, if the location of plastic hinges can be predicted, the collapse load is readily calculated by simple statics.

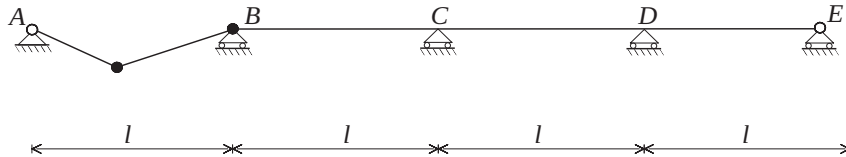
The addition of a hinge into a statically-indeterminate frame reduces the number of indeterminate moments by one, so that, if the number of indeterminates is n , the addition of n hinges produces a simple statically-determinate structure. The addition of one more hinge will allow the structure to move with one degree of freedom, i.e., a mechanism is formed. The number of hinges to form a mechanism is thus $(n+1)$. The criterion, must, of course, be applied to each element of a structure as well as to the structure as a whole, because collapse of one part certainly represents practical failure. Typical collapse mechanisms are shown in Fig. 5.43, for a

four-span continuous beam. The problem is then to determine the lowest load to cause collapse or, conversely, the maximum resistance required for the section.

a) Structural scheme.



b) End span mechanism.



c) Intermediate span mechanism

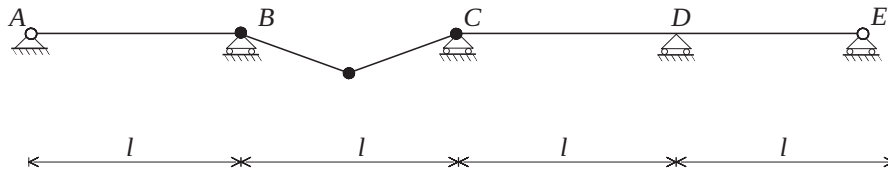


Figure 5.43 – Typical collapse mechanisms for a continuous beam

5.7.2. Continuous beams at room temperature

Consider the four-span continuous beam shown in Fig. 5.43, the load-value to cause collapse, assuming constant strength along all of the spans, is:

i. End span

The collapse occurs when the two plastic hinges shown in Fig. 5.44 are formed.

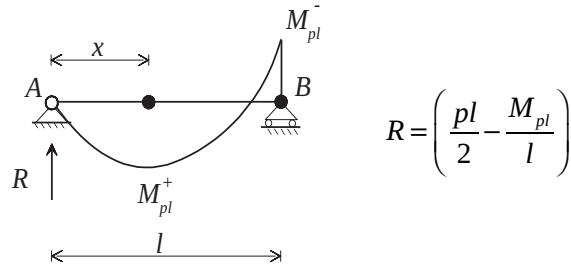


Figure 5.44 – End beam mechanism

It is assumed that the positive and negative plastic moments are equal:

$$M_{pl}^+ = M_{pl}^- = M_{pl}$$

At the hinge section in the span the shear force must be zero:

$$V(x) = \frac{pl}{2} - \frac{M_{pl}}{l} - px = 0 \quad (5.135)$$

which leads to

$$x = \frac{l}{2} - \frac{M_{pl}}{pl} \quad (5.136)$$

From this equation M_{pl} is given as

$$M_{pl} = \frac{pl^2}{2} - pxl \quad (5.137)$$

The maximum load is then obtained by assuming that at the hinge, the moment is equal to the plastic moment:

$$M(x) = \left(\frac{pl}{2} - \frac{M_{pl}}{l} \right) x - \frac{px^2}{2} = M_{pl} \quad (5.138)$$

Substituting Eq. (5.137) into Eq. (5.138), leads to

$$\frac{1}{2}x^2 + lx - \frac{l^2}{2} = 0 \quad (5.139)$$

Solving this second-order equation for x , the position of the

hinge is given by

$$x = (\sqrt{2} - 1)l \approx 0.414l \quad (5.140)$$

Substituting this value into Eq. (5.137), the required plastic resistance moment is given by

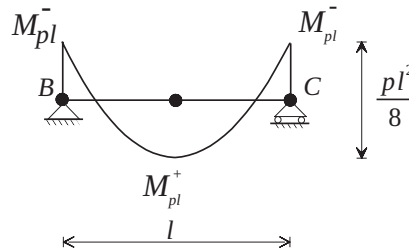
$$M_{pl} = (1.5 - \sqrt{2})pl^2 \quad (5.141)$$

From where the collapse load may be taken as:

$$p = \frac{M_{pl}}{(1.5 - \sqrt{2})l^2} \approx 11.657 \frac{M_{pl}}{l^2} \quad (5.142)$$

ii. Intermediate span

For the collapse of the intermediate span three hinges must be formed, as shown in Fig. 5.45



183

Figure 5.45 – Intermediate beam mechanism

As the plastic hinge is formed at the mid span, the following equation may be written

$$M_{pl}^+ + M_{pl}^- = 2M_{pl} = \frac{pl^2}{8} \quad (5.143)$$

or

$$M_{pl} = \frac{pl^2}{16} \quad (5.144)$$

and the maximum load for collapse is given by:

$$p = \frac{16M_{pl}}{l^2} \quad (5.145)$$

It should be noted that the shear force at the supports must be checked to see whether it can be neglected or not. If not the plastic moment at the supports must be reduced according to Section 5.5.5.3 and an iterative procedure must be used.

5.7.3. Continuous beams under fire conditions

Under fire conditions the plastic resistance moments in the span and at the supports are different. According to Eq. (5.64) these two moments can be written as follows:

$$M_{fi,Rd}^+ = \frac{W_{pl,y} k_y f_y}{k_1 k_2 \gamma_{M,fi}} = \frac{W_{pl,y} k_y f_y}{k_1 \gamma_{M,fi}} \quad (k_2 = 1.0) \quad (5.146)$$

$$M_{fi,Rd}^- = \frac{W_{pl,y} k_y f_y}{k_1 k_2 \gamma_{M,fi}} = \frac{W_{pl,y} k_y f_y}{k_1 k_2 \gamma_{M,fi}} \quad (k_2 = 0.85) \quad (5.147)$$

There exists the following relationship between the plastic moments at the span and at the supports:

184

$$M_{fi,Rd}^+ = k_2 M_{fi,Rd}^- \quad (5.148)$$

Assuming this relation and taking $q_{fi,Ed}$ as the design load under fire conditions for the four-span continuous beam shown in Fig. 5.43, the value of the load to cause collapse is obtained in a similar way to that for normal temperature:

i) End span

The collapse occurs when the two plastic hinges shown in Fig. 5.44 are formed. Now the position of the hinge in the span of the beam takes the value:

$$x = \left(-k_2 + \sqrt{k_2^2 + k_2} \right) l \quad (5.149)$$

and the plastic resistance moment at the support is:

$$\begin{aligned}
 M_{\bar{f},Rd}^- &= \frac{W_{pl,y} k_{y,\theta} f_y}{k_1 k_2 \gamma_{M,\bar{f}}} = \\
 &= \left[\frac{l^2}{2} - \left(-k_2 + \sqrt{k_2^2 + k_2} \right) l^2 \right] q_{\bar{f},Ed}
 \end{aligned} \tag{5.150}$$

From this equation the reduction factor for the yield strength can be taken as

$$k_{y,\theta} = \left[\frac{l^2}{2} - \left(-k_2 + \sqrt{k_2^2 + k_2} \right) l^2 \right] q_{\bar{f},Ed} \frac{k_1 k_2 \gamma_{M,\bar{f}}}{W_{pl,y} f_y} \tag{5.151}$$

which allows the critical temperature to be evaluated by either using Eq. (5.108) or interpolating the values given in Table 5.2.

From Eq. (5.150) it is also possible to evaluate the maximum design load for collapse for a given temperature. When the steel temperature is known, the reduction factor for the yield strength $k_{y,\theta}$ can be obtained from Table 5.2, and the maximum load for collapse given as

$$q_{\bar{f},Rd} = \frac{W_{pl,y} k_{y,\theta} f_y}{k_1 k_2 \gamma_{M,\bar{f}}} \frac{1}{\left[\frac{l^2}{2} - \left(-k_2 + \sqrt{k_2^2 + k_2} \right) l^2 \right]} \tag{5.152}$$

ii) Intermediate span

185

For the intermediate span, Eq. (5.143) can be written as

$$M_{\bar{f},Rd}^+ + M_{\bar{f},Rd}^- = \frac{q_{\bar{f},Rd} l^2}{8} \tag{5.153}$$

which leads to the reduction factor for the yield strength

$$k_{y,\theta} = \frac{q_{\bar{f},Rd} l^2}{8} \frac{k_1 k_2 \gamma_{M,\bar{f}}}{(1+k_2) W_{pl,y} f_y} \tag{5.154}$$

and the maximum design load for collapse for a given temperature is:

$$q_{\bar{f},Rd} = \frac{8 k_{y,\theta} (1+k_2) W_{pl,y} f_y}{l^2 k_1 k_2 \gamma_{M,\bar{f}}} \tag{5.155}$$

If the shear force at the supports is more than half the plastic shear resistance its effect on the moment resistance must be taken into account (see Section 5.5.5.3) and an iterative procedure must be used. Utilization of computer tools is highly recommended. An iterative procedure is used in the program Elefir-EN presented in Chapter 8.

In a fire design situation the factors k_1 and k_2 increase the value of the maximum design load at collapse (see Eq. (5.152) and Eq. (5.155)) and consequently increase the shear force at the supports. In the end spans, the resistance negative moment increases due to these two factors (see Eq. (5.137)) and the shear force at the intermediate supports also increases as can be seen in the following expression

$$V_{fi, support} = q_{fi, Rd} \cdot l/2 + M_{fi, Rd}^- / l.$$

The fact that the shear resistance remains unchanged also contributes to that situation. What happens in the fire design situation is that the yield strength increases for the evaluation of the design value of the resistance moment because it is divided by $k_1 k_2$, but not for the evaluation of shear resistance.

5.8. FIRE RESISTANCE OF STRUCTURAL STAINLESS STEEL MEMBERS

186

Stainless steels can be subdivided in to the following five basic groups, according to their metallurgical structure (Euro Inox, 2006):

- austenitic,
- ferritic,
- martensitic,
- duplex austenitic-ferritic and
- precipitation-hardening groups.

The austenitic stainless steels have good combination of corrosion resistance, forming and fabrication properties. The duplex stainless steels have high strength and wear resistance with very good resistance to stress corrosion cracking. The most commonly used grades, for structural applications, are the austenitic steels 1.4301 (widely known as 304) and 1.4401 (widely known as 316) mainly due to their good weldability. The

existing data on the behaviour of structural stainless steel at high temperatures suggest that they perform very well due to the good strength and stiffness retention characteristics at elevated temperatures.

Stainless steels are known to have non-linear stress-strain relationships with a low proportional stress and an extensive hardening phase (see Fig. 5.46).

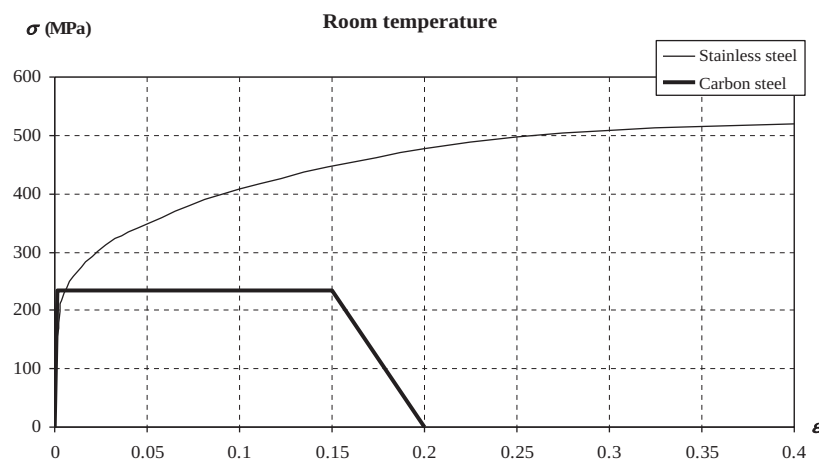


Figure 5.46 – Stress-strain relationships of carbon steel S 235 and stainless steel 1.4301 in fire situation at 20 °C (from EN 1993-1-2)

Unlike carbon steel, stainless steel does not have a well defined yield strength. For stainless steel the ‘effective’ yield strength is taken as the proof strength at 0.2% plastic strain, $f_y = f_{0.2\text{proof}}$.

Fig. 5.47 shows the stress-strain relationships of carbon steel S235 and stainless steel 1.4301 at 600 °C.

Table 5.7 and Table 5.8 compare the mechanical properties of carbon steel S235 and stainless steel 1.4301, at room temperature and at 600 °C respectively.

EN 1993-1-4 “Supplementary rules for stainless steels” (2006) gives design rules for stainless steel structural elements at room temperature, and only makes mention to its fire resistance by referring to the fire part of Eurocode 3, EN 1993-1-2 (2005). Although carbon steel and stainless steel have different constitutive laws, Eurocode 3 states that the structural elements made of these two materials must be checked for their fire

5. MECHANICAL ANALYSIS

resistance with the same formulae. Recent scientific research on the behaviour of structural stainless steel elements under fire conditions have been done (N and Gardner (2007); Lopes *et al* (2008), Lopes *et al* (2009), Uppfeldt *et al* (2008); Vila Real *et al* (2008)), but the results of this work ¹ have not yet been incorporated in the Eurocode.

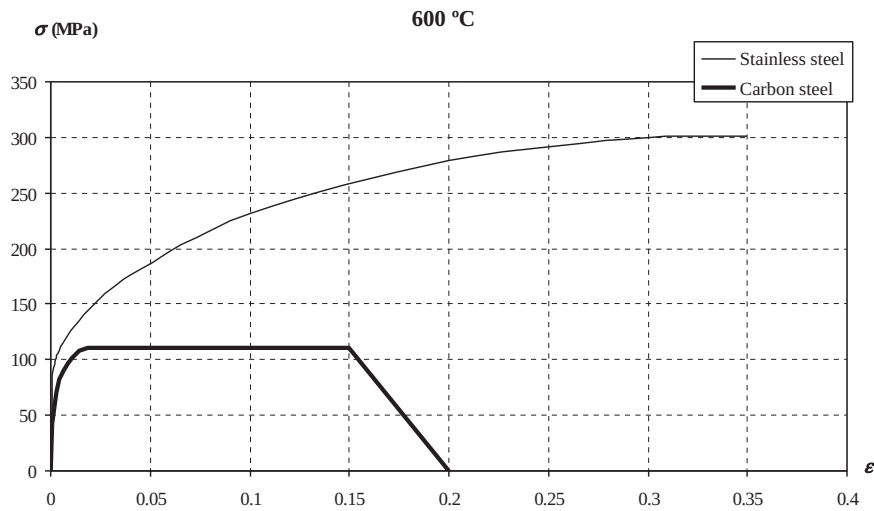


Figure 5.47 – Stress-strain relationships of carbon steel S 235 and stainless steel 1.4301 at 600 °C

188

Table 5.7 – Mechanical properties at room temperature

	Carbon steel S235	Stainless steel 1.4301
Ultimate tensile strength, f_u [Mpa]	360	520
Yield strength, $f_y = f_{0.2\text{proof}}$ [Mpa]	235	210
Ultimate strain, ϵ_u	> 15%	40%

In the fire situation, higher strains than at room temperature are acceptable. Part 1.2 of Eurocode 3 recommends the use of the stress at 2% total strain as the yield strength at elevated temperature θ , $f_{y,\theta} = f_{2,\theta}$, for Class 1, 2 and 3 cross sections and $f_{y,\theta} = f_{0.2\text{proof},\theta}$, for Class 4.

¹ In term of new design equations for stainless steel members.

5.8. FIRE RESISTANCE OF STRUCTURAL STAINLESS STEEL MEMBERS

Table 5.8 – Mechanical properties at 600 °C, Class 1, 2, 3 and 4 cross section

	Carbon steel S235	Stainless steel 1.4301
Yield strength, $f_{y,\theta} = f_{2,\theta}$ (MPa) Class 1, 2 and 3	110.5	146.6
Yield strength, $f_{y,\theta} = f_{0.2\text{proof},\theta}$ (MPa) Class 4	70.5	102.9
Ultimate strain, ϵ_u	15%	35%

Fig. 5.48 and Fig. 5.49 show stress-strain relationships of carbon steel S235 and stainless steel 1.4301 at 20 °C and 600 °C, respectively, for $0 \leq \epsilon \leq 0.02$.

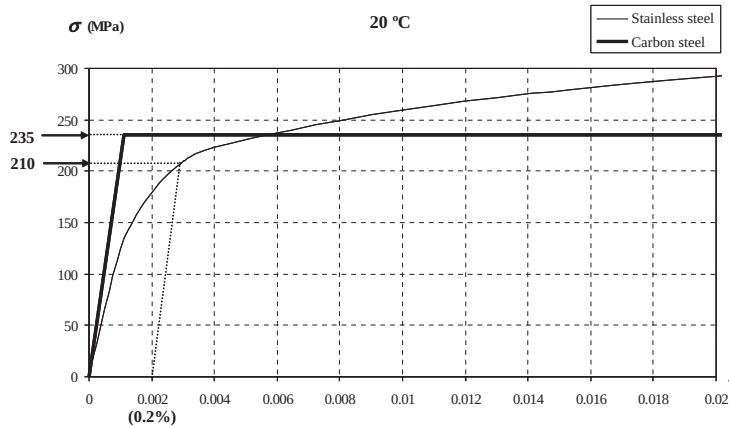


Figure 5.48 – Stress-strain relationships of carbon steel S 235 and stainless steel 1.4301 at 20 °C for $0 \leq \epsilon \leq 0.02$

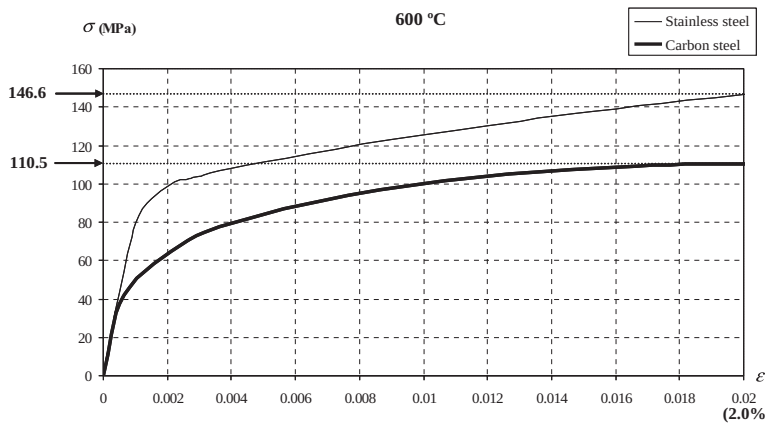


Figure 5.49 – Stress-strain relationships of carbon steel S 235 and stainless steel 1.4301 at 600 °C for $0 \leq \epsilon \leq 0.02$

5. MECHANICAL ANALYSIS

Comparison of the reduction of strength and elastic stiffness of structural carbon steel and stainless steel at elevated temperature for several grades of stainless steels (as defined in EN 1993-1-2) is shown in Fig. 5.50, where $k_{y,\theta} = f_{y,\theta}/f_y$ and $k_{E,\theta} = E_\theta/E$.

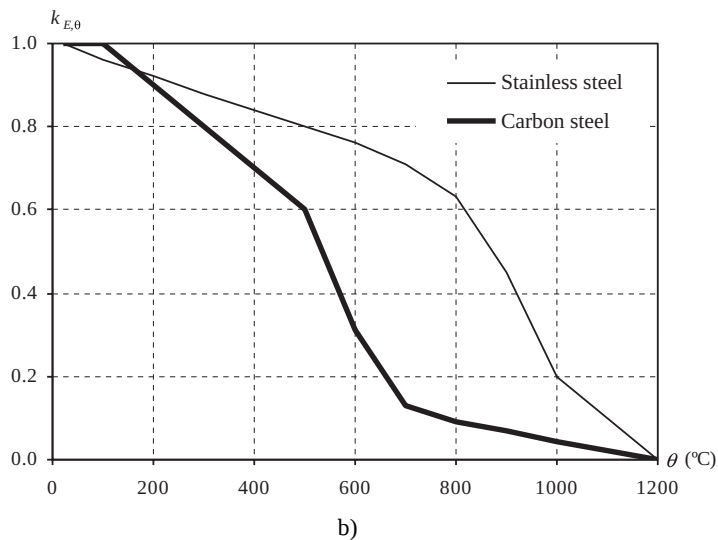
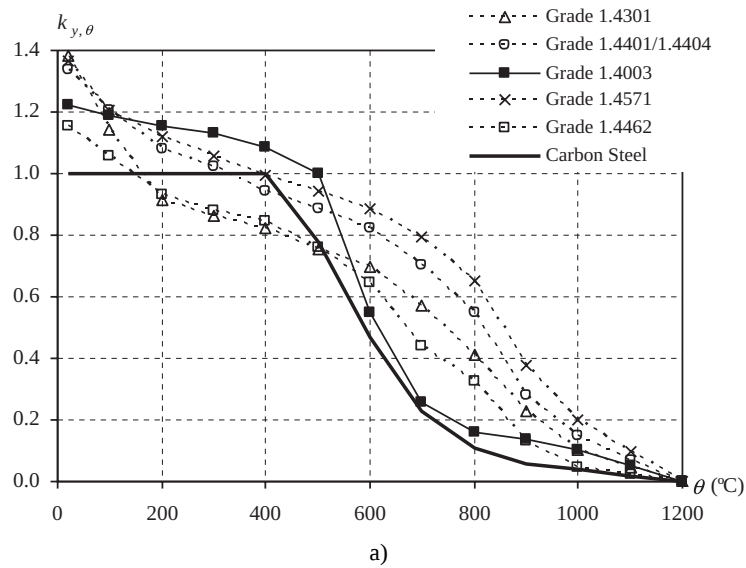


Figure 5.50 – Reduction factors: a) strength reduction factor; b) reduction factor for the Young's modulus

Annex C of EN 1993-1-2 gives a correction factor for the yield strength $k_{2\%,\theta}$ for the use of simple calculation methods which allows for the evaluation of the “effective” yield strength to be used in simple calculation methods according to Eq. (5.156).

$$k_{y,\theta} = \frac{f_{y,\theta}}{f_y} = \left[f_{0.2p,\theta} + k_{2\%,\theta} (f_{u,\theta} - f_{0.2p,\theta}) \right] \frac{1}{f_y} \quad (5.156)$$

where $f_{0.2p,\theta}$ is the proof strength at 0.2% plastic strain, at temperature θ , $k_{2\%,\theta}$ is the correction factor for determination of the “effective” yield strength $f_{y,\theta}$ and $f_{u,\theta}$ is the ultimate tensile strength, at temperature θ . This “effective” yield strength is the stress at 2% total strain.

Table 5.9 presents the variation of the above-mentioned reduction factors for Grade 1.4301 stainless steel. The value of $k_{y,\theta}$ is not given in the Eurocode and in this book it is evaluated for hot rolled plate ($f_y = 210$ MPa; $f_u = 520$ MPa) (see Table 2.1 of EN 1993-1-4) using Eq. (5.156). Annex C of EN 1993-1-2 and Table C.11 of Annex C of this book provide values for other grades of stainless steels.

It is the opinion of the authors that, for the purpose of the simplified rules, the cross sections may be classified as for normal temperature design with a reduced value for ε , as given in Eq. (5.157) instead of Eq. (5.33) as proposed in EN 1993-1-2 for carbon steel.

$$\varepsilon = 0.85 \sqrt{\frac{235}{f_y} \frac{E}{210000}} \quad (5.157)$$

191

which means that at elevated temperature $\varepsilon_\theta = 0.85\varepsilon$, where the parameter ε at normal temperature is given as in EN 1993-1-4 by

$$\varepsilon = \sqrt{\frac{235}{f_y} \frac{E}{210000}} \quad (5.158)$$

If $\sqrt{k_{E,\theta}/k_{y,\theta}}$ is plotted as a function of the temperature, as in Fig. 5.51 for carbon steel and stainless steels, it can be seen that the development of this parameter depends on the steel grade and is quite different for the two types of steel. This figure also shows that considering a value of 0.85 for stainless is on the safe side.

5. MECHANICAL ANALYSIS

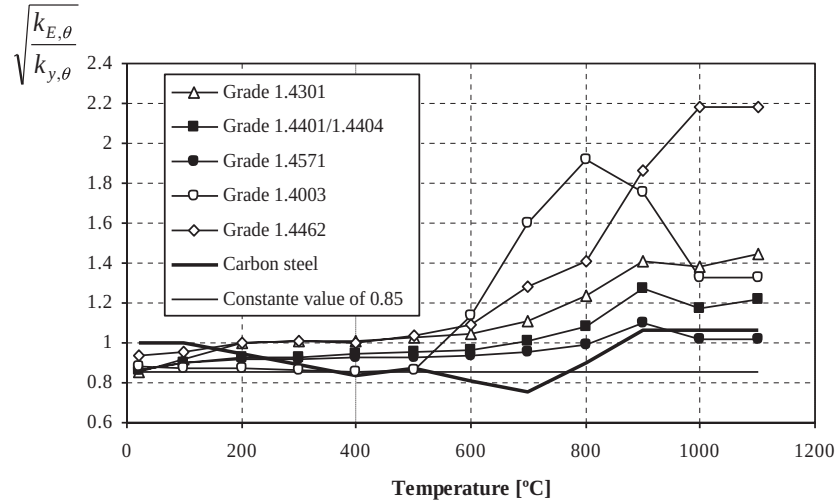


Figure 5.51 – $\sqrt{k_{E,\theta}/k_{y,\theta}}$ as a function of the temperature

Cross sections of compression elements should be classified according to the limits given in Table 5.2 of EN 1993-1-4.

Example 5.13 illustrates the procedure to be adopted to determine the critical temperature of an unprotected stainless steel beam.

Table 5.9 – Factors for determination of strain and stiffness of stainless steel at elevated temperatures for Stainless Steel 1.4301

Steel Temperature θ_a [°C]	$k_{E,\theta} = E_{a,\theta}/E_a$	$k_{0.2p,\theta} = f_{0.2p,\theta}/f_y$	$k_{u,\theta} = f_{u,\theta}/f_u$	$k_{2\%,\theta}$	$k_{y,\theta}$
20	1.00	1.00	1.00	0.26	1.3838
100	0.96	0.82	0.87	0.24	1.1402
200	0.92	0.68	0.77	0.19	0.9131
300	0.88	0.64	0.73	0.19	0.8618
400	0.84	0.60	0.72	0.19	0.8247
500	0.80	0.54	0.67	0.19	0.7526
600	0.76	0.49	0.58	0.22	0.6982
700	0.71	0.40	0.43	0.26	0.5728
800	0.63	0.27	0.27	0.35	0.4095
900	0.45	0.14	0.15	0.38	0.2279
1000	0.20	0.06	0.07	0.40	0.1053
1100	0.10	0.03	0.03	0.40	0.0477
1200	0.00	0.00	0.00	0.40	0.0000

In Table 5.9 the meaning of the symbols are as follows:

$k_{E,\theta}$	Reduction factor (relative to E_a) for the slope of the linear elastic range
$k_{0.2p,\theta}$	Reduction factor (relative to f_y) for proof strength
$k_{u,\theta}$	Reduction factor (relative to f_u) for tensile strength
$k_{2\%,\theta}$	Factor for determination of the yield strength $f_{y,\theta}$
$k_{y,\theta}$	Reduction factor (relative to f_y) for “effective” yield strength

5.9. DESIGN EXAMPLES

In this section, several design examples, covering most of the possible load cases, are presented, with full details. The default value of 1.0 proposed in Eurocode has been adopted for the partial safety factors γ_{M0} and $\gamma_{M,fi}$.

Example 5.1: Member in tension

Consider a HE 200 A profile in S275 grade steel that was designed at normal temperature for an axial tension load $N_{Ed} = 1200$ kN. The unprotected member is heated on all four sides and is part of an office building with a required fire resistance time to the standard fire of $t_{requ} = 30$ minutes (R30).

- a) Evaluate the critical temperature of the profile;
- b) Verify the fire resistance of the member:
 - b1) in the temperature domain;
 - b2) in the time domain;
 - b3) in the resistance domain.

Solution:

- a) Assuming a reduction factor for the load in a fire situation of, $\eta_{fi} = 0.65$, the axial load in fire situation is given by

$$N_{fi,Ed} = \eta_{fi} N_{Ed} = 0.65 \times 1200 = 780 \text{ kN.}$$

The cross sectional area of an HE 200 A is $A = 5380 \text{ mm}^2$. The degree of utilisation takes the value:

$$\mu_0 = \frac{E_{fi,d}}{R_{fi,d,0}} = \frac{N_{fi,Ed}}{Af_y / \gamma_{M,fi}} = \frac{780000}{5380 \cdot 275 / 1.0} = 0.527$$

Using Eq. (5.110), the value of the critical temperature is:

$$\theta_{a,cr} = 39.19 \ln \left[\frac{1}{0.9674 \mu_0^{3.833}} - 1 \right] + 482 = 576.1 \text{ } ^\circ\text{C}$$

Note: another way to obtain the critical temperature is to consider that the collapse occurs when:

$$N_{fi,Ed} = N_{fi,Rd}$$

so

$$N_{fi,Ed} = Ak_{y,\theta} f_y / \gamma_{M,fi}$$

from where $k_{y,\theta}$ can be taken:

$$k_{y,\theta} = \frac{N_{fi,Ed}}{Af_y / \gamma_{M,fi}} = \frac{780000}{5380 \cdot 275 / 1.0} = 0.527$$

Knowing $k_{y,\theta}$ the value of the critical temperature can be obtained using Eq. (5.109):

$$\theta_{a,cr} = 39.19 \ln \left[\frac{1}{0.9674 k_{y,\theta}^{3.833}} - 1 \right] + 482 = 576.1 \text{ } ^\circ\text{C}$$

194

or interpolating in Table 5.2, which gives

$$\theta_{a,cr} = 581.6 \text{ } ^\circ\text{C}$$

This value is close to the one obtained by the Eq. (5.109) or Eq. (5.110)

b1) Verification in the temperature domain

The temperature in the section exposed on 4 sides after 30 min of standard fire ISO 834 exposure is 802 °C (see example 4.3). As this temperature is greater than the critical temperature, the member doesn't fulfil the condition given in Eq. (5.1c), because:

$$\theta_d > \theta_{cr,d}, \text{ at time } t_{fi,requ}$$

and cannot be classified as R30.

b2) Verification in the time domain

The time needed to reach the critical temperature can be obtained by double interpolation of the values given in table of the Annex A.4 for a modified section factor

$$k_{sh} [A_m/V] = 0.618 \cdot 211 = 130.4 \text{ m}^{-1}$$

It is found that the critical temperature is reached at

$$t_{fi,d} = 14.08 \text{ min}$$

leading to the conclusion that the member is not safe because:

$$t_{fi,d} < t_{fi,requ}$$

does not respecting the condition of Eq. (5.1a). The member does not fulfil the fire resistance criterion R30.

b3) Verification in the resistance domain

After 30 minutes of standard fire exposure, the temperature is $\theta_d = 802 \text{ }^\circ\text{C}$. Interpolating for this temperature in Table 5.2 leads to the reduction factor for the yield strength of

$$k_{y,\theta} = 0.109$$

and the resistance of the member after 30 minutes is

$$N_{fi,Rd} = A k_{y,\theta} f_y / \gamma_{M,fi} = 5380 \cdot 0.109 \cdot 275 \times 10^{-3} / 1.0 = 161.3 \text{ kN}$$

which is less than the applied load in fire situation, $N_{fi,Ed} = 780 \text{ kN}$, i. e.,

$$N_{fi,Ed} > N_{fi,Rd}$$

and the condition of Eq. (5.1b) is not satisfied. The member does not fulfil the fire resistance criterion R30.

The procedures for verifying the fire resistance of a tension member were shown in all three domains. To achieve the required fire resistance of R30 the member must be protected.

Example 5.2: Laterally restrained beam

Consider a simply supported restrained beam 4.0 long, constructed from an IPE 300 section, in steel grade S235, supporting a concrete slab. Assuming the steel beam does not act compositely with the concrete slab and that the design load in the fire situation is $q_{fi,Ed} = 33.8$ kN/m, verify if it is necessary to protect the beam for a fire resistance period of R90. If fire protection is needed, use fibre-cement boards.

Solution:

The relevant geometrical characteristics of the profile for the cross section classification are

$$h = 300 \text{ mm}$$

$$b = 150 \text{ mm}$$

$$t_w = 7.1 \text{ mm}$$

$$t_f = 10.7 \text{ mm}$$

$$r = 15 \text{ mm}$$

$$c = b/2 - t_w/2 - r = 56.45 \text{ mm (flange)}$$

$$c = h - 2t_f - 2r = 248.6 \text{ mm (web)}$$

As the steel grade is S235

$$\varepsilon = 0.85\sqrt{235/f_y} = 0.85$$

The class of the flange in compression is

$$c/t_f = 56.45/10.7 = 5.3 < 9\varepsilon = 6.8 \Rightarrow \text{Class 1}$$

For the web in bending the class is

$$d/t_w = 248.6/7.1 = 35 < 72\varepsilon = 61.2 \Rightarrow \text{Class 1}$$

The cross section of the IPE 300 in bending and in fire situation is Class 1. This classification could be directly obtained using the table for cross sectional classification of Annex F, Vila Real *et al* (2009b).

At mid span:

The next step is to calculate the fire resistance of the unprotected beam. The design value of the resistance moment at time $t = 0$, $M_{fi,0,Rd}$, according to Eq. (5.64), is

$$M_{fi,0,Rd} = W_{pl,y} f_y / (k_1 k_2 \gamma_{M,fi})$$

where:

$k_1 = 0.7$ for an unprotected beam exposed on three sides, with a concrete slab on the fourth side;

$k_2 = 1.0$ for sections not at the supports.

The plastic section modulus $W_{pl,y}$ of the IPE 300 profile is

$$W_{pl,y} = 628 \times 10^{-6} \text{ m}^3$$

and

$$M_{fi,0,Rd} = 211 \text{ kNm}$$

The degree of utilisation takes the value

$$\mu_0 = \frac{M_{fi,Ed}}{M_{fi,0,Rd}} = \frac{67.6}{211} = 0.32$$

and from Eq. (5.110) the critical temperature is

$$\theta_{a,cr} = 654 \text{ }^\circ\text{C}$$

Considering that the section factor for the IPE 300 is $A_m/V = 187 \text{ m}^{-1}$, and that

$$h = 300 \text{ mm}$$

$$b = 150 \text{ mm}$$

$$A = 53.8 \text{ cm}^2$$

the box value of the section factor $[A_m/V]_b$, is, according to the Table 4.5

$$[A_m/V]_b = \frac{2h+b}{A} = \frac{2 \cdot 0.3 + 0.15}{53.8 \times 10^{-4}} = 139.4 \text{ m}^{-1}$$

This value could have been taken from the table of Annex E, Vila Real *et al* (2009a), as well as the value of A_m/V , which is

$$A_m/V = 187.7 \text{ m}^{-1}$$

The correction factor for the shadow effect is

$$k_{sh} = 0.9[A_m/V]_b/[A_m/V] = 0.9 \cdot 139.4/187.7 = 0.6684$$

and the modified section factor thus takes the value

$$k_{sh}[A_m/V] = 0.6684 \cdot 187.7 = 125.5 \text{ m}^{-1}$$

This value could be directly obtaining from the table of Annex E, Vila Real *et al* (2009a).

Interpolation of the values given in table of the Annex A.4 yields a time of 18 min to reach the critical temperature, $\theta_{a,cr} = 654 \text{ }^\circ\text{C}$. This is less than the required 90 min and therefore fire protection is necessary to achieve the required fire resistance.

As the value of k_1 depends on whether or not the profile is protected, a new critical temperature must be obtained for the protected section. Considering $k_1 = 0.85$, the design value of the resistance moment at time $t = 0$, $M_{fi,0,Rd}$ is

$$M_{fi,0,Rd} = W_{pl,y} f_y / k_1 k_2 = W_{pl,y} f_y / (0.85 \cdot 1.0) = 174 \text{ kNm}$$

The degree of utilisation takes the value

$$\mu_0 = \frac{M_{fi,Ed}}{M_{fi,0,Rd}} = \frac{67.6}{174} = 0.389$$

and from Eq. (5.110) the critical temperature is

$$\theta_{a,cr} = 624 \text{ }^\circ\text{C}$$

The thickness of a contour encasement protection with fibre-cement boards necessary to prevent the steel temperature exceeding the critical temperature before the required time of 90 minutes is 15 mm (see example 4.4).

At the supports:

Verification of the design shear resistance

$$V_{fi,Ed} = \frac{q_{fi,Ed} \cdot l}{2} = 67.6 \text{ kN}$$

The shear area is

$$A_v = A - 2bt_f + (t_w + 2r)t_f$$

$$= 5380 - 2 \cdot 150 \cdot 10.7 + (7.1 + 2 \cdot 15)10.7 = 2567 \text{ mm}^2$$

Considering that the reduction factor for the yield strength for 624 °C is equal to the degree of utilisation

$$k_{y,\theta} = \mu_0 = 0.389$$

and the design value of the shear force at that temperature is

$$V_{\bar{f}_i,t,Rd} = \frac{A_v k_{y,\theta} f_y}{\sqrt{3} \gamma_{M,\bar{f}_i}} = \frac{2567 \cdot 0.389 \cdot 235}{\sqrt{3} \cdot 1.0} \times 10^{-3} = 135.5 \text{ kN} > V_{\bar{f}_i,Ed} \quad \text{OK!}$$

If interpolation in Table 5.2 was made for 624 °C, $k_{y,\theta} = 0.412$ and

$$V_{\bar{f}_i,t,Rd} = \frac{A_v k_{y,\theta} f_y}{\sqrt{3} \gamma_{M,\bar{f}_i}} = \frac{2567 \cdot 0.412 \cdot 235}{\sqrt{3} \cdot 1.0} \times 10^{-3} = 144 \text{ kN}$$

Example 5.3: Critical temperature of a cross section submitted to combined bending and axial compression

Consider a profile IPE 400 in S355 grade steel, submitted to an axial compression force of $N_{\bar{f}_i,Ed} = 300 \text{ kN}$ and a bending moment about the strong axis of $M_{y,\bar{f}_i,Ed} = 300 \text{ kNm}$. Considering the resistance of the cross section, evaluate the critical temperature of the profile using a) the first and b) the second methodologies presented in section 5.3 for the classification of the cross sections under combined bending and axial compression.

Solution:

The following geometrical characteristics of the IPE 450 are relevant for the classification of the cross section:

$h = 400 \text{ mm}$	$b = 180 \text{ mm}$
$t_w = 8.6 \text{ mm}$	$t_f = 13.5 \text{ mm}$
$r = 21 \text{ mm}$	$h_w = h - 2t_f = 373 \text{ mm}$
$c = b/2 - t_w/2 - r = 64.7 \text{ mm}$ (flange)	$W_{el,y} = 1160000 \text{ mm}^3$
$c = h - 2t_f - 2r = 331 \text{ mm}$ (web)	$W_{pl,y} = 1307000 \text{ mm}^3$
$A = 8450 \text{ mm}^2$	

As the steel grade is S355:

$$\varepsilon = 0.85\sqrt{235/f_y} = 0.69$$

The class of the flange in compression is

$$c/t_f = 64.7/13.5 = 4.79 < 9\varepsilon = 6.2 \Rightarrow \text{Class 1}$$

The classification of the web will be made using the two methodologies presented in section 5.3.

a) Using the first methodology and considering that the web is Class 1 or Class 2, the position of the plastic neutral axis is given by Eq. (5.17):

$$\alpha = \frac{y}{c} = \frac{1}{2} + \frac{N_{fi,Ed}}{2ct_w f_y} = \frac{1}{2} + \frac{300000}{2 \cdot 331 \cdot 8.6 \cdot 355} = 0.65$$

and

$$c/t_w = 331/8.6 = 38.5 < \frac{456\varepsilon}{13\alpha - 1} = 42.3 \Rightarrow \text{Class 2}$$

Thus the cross section is Class 2. Assuming that the axial load needs to be taken into account in the design value of the resistance moment, the reduction factor (relative to f_y) for effective yield strength is given by (see Eq. (5.134)):

200

$$k_{y,\theta} = \frac{N_{fi,Ed}}{A f_y / \gamma_{M,fi}} + (1 - 0.5a) \frac{M_{y,fi,Ed}}{W_{pl,y} f_y / \gamma_{M,fi}} = 0.61$$

Knowing $k_{y,\theta}$ the critical temperature can be evaluated interpolating in Table 3.1 from EN 1993-1-2 or in the Table 5.2 of this book:

$$\theta_{a,cr} = 555 \text{ }^\circ\text{C}$$

It is necessary, now, to check if the effect of the axial load needs to be taken into account in the design value of the resistance moment.

The plastic resistance to axial load at 555 °C is

$$N_{fi,pl} = A k_{y,\theta} f_y / \gamma_{M,fi} = 8450 \cdot 0.61 \cdot 355 \times 10^{-3} / 1.0 = 1830 \text{ kN}$$

According to the Eq. (5.95), as

$$N_{fi,Ed} < 0.25 N_{fi,pl} = 457.5 \text{ kN}$$

and

$$N_{fi,Ed} < 0.5h_w t_w k_{y,\theta} f_y / \gamma_{M,fi} = 347 \text{ kN}$$

the effect of the axial force on the plastic moment resistance does not need to be taken into account. So, the critical temperature is given by

$$M_{y,fi,Ed} = M_{y,fi,Rd} \Rightarrow M_{y,fi,Ed} = W_{pl,y} k_{y,\theta} f_y / \gamma_{M,fi}$$

and

$$k_{y,\theta} = \frac{M_{y,fi,Ed}}{W_{pl,y} f_y / \gamma_{M,fi}} = 0.647$$

Knowing $k_{y,\theta}$ the critical temperature can be evaluated interpolating in Table 3.1 from EN 1993-1-2 or in the Table 5.2 of this book:

$$\theta_{a,cr} = 543 \text{ }^\circ\text{C}$$

At a temperature of 543 °C the yield strength takes the value

$$f_{y,\theta} = k_{y,\theta} f_y = 229.7 \text{ MPa}$$

At this temperature the position of the plastic neutral axis is defined by (see Eq. (5.17)):

$$\alpha = \frac{y}{c} = \frac{1}{2} + \frac{N_{fi,Ed}}{2ct_w f_y} = \frac{1}{2} + \frac{300000}{2 \cdot 331 \cdot 8.6 \cdot 229.7} = 0.729$$

201

and

$$c/t_w = 331/8.6 = 38.5 > \frac{456\varepsilon}{13\alpha - 1} = \frac{456 \cdot 0.69}{13 \cdot 0.729 - 1} = 37.1$$

The web is not Class 2 at a temperature of 543 °C. Let's see if it is Class 3. Eq. (5.30) gives the position of the elastic neutral axis:

$$\psi = 2 \frac{N_{fi,Ed}}{A f_y} - 1 = 2 \frac{300000}{8450 \cdot 229.7} - 1 = -0.691$$

and

$$c/t_w = 331/8.6 = 38.5 < \frac{42\varepsilon}{0.67 + 0.33\psi} = \frac{42 \cdot 0.69}{0.67 + 0.33(-0.691)} = 65.6$$

The web is Class 3. As Class 3 the collapse of the cross section occurs when (see Eq. (5.14)):

$$\frac{N_{\bar{f},Ed}}{N_{\bar{f},pl}} + \frac{M_{y,\bar{f},Ed}}{M_{y,\bar{f},el}} = \frac{N_{\bar{f},Ed}}{Ak_{y,\theta}f_y/\gamma_{M,\bar{f}}} + \frac{M_{y,\bar{f},Ed}}{W_{el,y}k_{y,\theta}f_y/\gamma_{M,\bar{f}}} = 1$$

This equation gives the reduction factor (relative to f_y) for effective yield strength $k_{y,\theta}$:

$$k_{y,\theta} = \frac{N_{\bar{f},Ed}}{Af_y/\gamma_{M,\bar{f}}} + \frac{M_{y,\bar{f},Ed}}{W_{el,y}f_y/\gamma_{M,\bar{f}}} = 0.829$$

Knowing $k_{y,\theta}$ the critical temperature can be evaluated interpolating in Table 3.1 from EN 1993-1-2 or the Table 5.2 of this book:

$$\theta_{a,cr} = 478 \text{ }^\circ\text{C}$$

At this temperature the yield strength takes the value $f_{y,\theta} = k_{y,\theta}f_y = 0.829 \cdot 355 = 294.3$ MPa and according to Eq. (5.17) the cross section is again Class 2, concluding that it is impossible to evaluate the critical temperature of the IPE400 for the given axial compression force and bending moment if the cross sectional classification has to be updated with temperature.

b) Using the second methodology the amplification factor is given from Eq. (5.19)

$$\mu_{ult} = \frac{1}{\frac{N_{\bar{f},Ed}}{N_{pl,\bar{f}}} + (1-0.5a)\frac{M_{y,\bar{f},Ed}}{M_{y,\bar{f},pl}}} = 1.642$$

As $\mu_{ult}M_{y,\bar{f},Ed} > M_{y,\bar{f},pl}$, it is not necessary to take into account the effect of the axial load in the resistance moment and then Eq. (5.20) gives:

$$\mu_{ult} = \frac{M_{y,\bar{f},pl}}{M_{y,\bar{f},Ed}} = \frac{464}{300} = 1.547$$

(using theory of plasticity, Eq. (5.27) gives $\mu_{ult} = 1.492$)

Once the amplification factor is obtained the position of the plastic neutral axis is given by Eq. (5.21):

$$\alpha = \frac{y}{c} = \frac{1}{2} + \frac{N_{ult}}{2ct_w f_y} = \frac{1}{2} + \frac{\mu_{ult} N_{Ed}}{2ct_w f_y} = 0.73$$

(using theory of plasticity, Eq. (5.28) gives $\alpha = 0.72$)

The class of the web is then:

$$c/t_w = 331/8.6 = 38.5 > \frac{456\varepsilon}{13\alpha - 1} = \frac{456 \cdot 0.69}{13 \cdot 0.73 - 1} = 37.1 \Rightarrow \text{the web is not Class 2}$$

Let's check if it is Class 3. Eq. (5.31) gives the position of the elastic neutral axis:

$$\psi = \frac{\sigma_t}{\sigma_c} = -0.759$$

and

$$c/t_w = 331/8.6 = 38.5 < \frac{42\varepsilon}{0.67 + 0.33\psi} = \frac{42 \cdot 0.69}{0.67 + 0.33(-0.76)} = 69.1 \Rightarrow \text{the web}$$

is Class 3

The cross section is Class 3 and does not change with the temperature. So, considering that the profile has a Class 3 cross section the obtained critical temperature is 478 °C, as it was shown.

Conclusions:

Using the first methodology, the cross section of the IPE 400 is classified at 20 °C as Class 2. As a Class 2 cross section its critical temperature is 543 °C, but at this temperature the cross section is Class 3. Considering the cross section as Class 3 the critical temperature becomes 478 °C but at this temperature the cross section is again Class 2. By using the first methodology and updating the class as function of the temperature it is not possible to obtain the critical temperature of this profile.

Using the second methodology the cross section is classified as Class 3 and does not change with the temperature. Thus, considering that the profile has a Class 3 cross section its critical temperature is 478 °C. The other possibility is to use the first methodology classifying the cross section at 20 °C without updating the classification with the temperature. In this case the cross section is Class 2 and the critical temperature is 543 °C. This illustrates that, as mentioned previously, the second methodology is always more conservative.

It is suggested that in fire situation one of the two procedures should be used: i) the first methodology without updating the cross sectional classification with the temperature (the authors believe that this is the procedure suggested in the EN 1993-1-2 if the first methodology is used) or ii) the second methodology that does not depend on the temperature.

Example 5.4: Unprotected column under axial compression

Consider a 3.5 m long HE 180 B column in S275 grade steel, located in an intermediate storey of a braced frame and subject to a compression load of $N_{fi,Ed} = 495$ kN in the fire situation. Assuming that the column doesn't have any fire protection and that the required fire resistance is R30, verify the fire resistance in each of the following domains:

- a) Temperature;
- b) Time;
- c) Resistance.

Solution:

Classification of the cross section:

The relevant geometrical characteristics of the profile for the cross section classification are

$$\begin{aligned} h &= 180 \text{ mm} \\ b &= 180 \text{ mm} \\ t_w &= 8.5 \text{ mm} \\ t_f &= 14 \text{ mm} \\ r &= 15 \text{ mm} \\ c &= b/2 - t_w/2 - r = 70.75 \text{ mm (flange)} \\ c &= h - 2t_f - 2r = 122 \text{ mm (web)} \end{aligned}$$

As the steel grade is S275

$$\varepsilon = 0.85 \sqrt{235 / f_y} = 0.786$$

The class of the flange in compression is

$$c/t_f = 70.75/14 = 5.1 < 9\varepsilon = 7.07 \Rightarrow \text{Class 1}$$

The class of the web in compression is

$$d/t_w = 122/8.5 = 14.4 < 33\varepsilon = 25.9 \Rightarrow \text{Class 1}$$

The cross section of the HE 180 B in fire situation is Class 1. This classification could be directly obtained using the table for cross sectional classification of Annex F, Vila Real *et al* (2009b).

Evaluation of the critical temperature:

For the HE 180 B:

$$\text{Area, } A = 6525 \text{ mm}^2$$

$$\text{Second moment of area, } I_z = 13630000 \text{ mm}^4$$

The design value of the compression load in fire situation: $N_{fi,Ed} = 495 \text{ kN}$

The buckling length for intermediate storey is: $l_{fi} = 0.5L = 0.5 \times 3.5 = 1.75 \text{ m}$.

The Euler critical load takes the value:

$$N_{cr} = \frac{\pi^2 EI}{l_{fi}^2} = 9224414 \text{ N}$$

The non-dimensional slenderness at elevated temperature is given by Eq. (5.48)

$$\bar{\lambda}_\theta = \bar{\lambda} \cdot \sqrt{\frac{k_{y,\theta}}{k_{E,\theta}}}$$

205

This is temperature dependent and an iterative procedure is needed to calculate the critical temperature. Starting with a temperature of 20 °C at which $k_{y,\theta} = k_{E,\theta} = 1.0$, equations (5.48), and (5.49) give:

$$\bar{\lambda}_\theta = \bar{\lambda} \sqrt{\frac{k_{y,\theta}}{k_{E,\theta}}} = \bar{\lambda} = \sqrt{\frac{Af_y}{N_{cr}}} = \sqrt{\frac{6525 \cdot 275}{9224414}} = 0.441$$

The reduction factor for flexural buckling χ is evaluated using Eq. (5.45):

$$\alpha = 0.65 \sqrt{235/f_y} = 0.65 \sqrt{235/275} = 0.601$$

and

$$\phi = \frac{1}{2} (1 + 0.601 \cdot 0.4361 + 0.436^2) = 0.730$$

Therefore the reduction factor for flexural buckling is:

$$\chi_{fi} = \frac{1}{0.730 + \sqrt{0.730^2 - 0.441^2}} = 0.763$$

The design value of the buckling resistance $N_{b,fi,t,Rd}$ at time $t = 0$, is obtained from Eq. (5.44):

$$N_{b,fi,0,Rd} = \chi_{fi} A f_y / \gamma_{M,fi} = 1368 \text{ kN}$$

and the degree of utilisation takes the value:

$$\mu_0 = \frac{N_{fi,Ed}}{N_{fi,0,Rd}} = \frac{495}{1368} = 0.362$$

For this degree of utilisation Eq. (5.104) gives a critical temperature, $\theta_{a,cr} = 635^\circ\text{C}$. Using this temperature, the non-dimensional slenderness $\bar{\lambda}_\theta$ can be corrected, which leads to another critical temperature. The iterative procedure should continue until convergence is reached, as illustrated in the next table:

θ [°C]	$\sqrt{\frac{k_{y,\theta}}{k_{E,\theta}}}$	$\bar{\lambda}_\theta = \frac{\bar{\lambda}}{\sqrt{\frac{k_{y,\theta}}{k_{E,\theta}}}}$	χ_{fi}	$N_{fi,0,Rd} = \chi_{fi} A f_y$ [kN]	$\mu_0 = \frac{N_{fi,Ed}}{N_{fi,0,Rd}}$	$\theta_{a,cr}$ [°C]
20	1.00	0.441	0.763	1368	0.362	635
635	1.25	0.552	0.703	1262	0.392	623
623	1.24	0.548	0.705	1265	0.391	623

After three iterations a critical temperature of $\theta_{a,cr} = 623^\circ\text{C}$ is obtained.

If at the first iteration the non-dimensional slenderness was approximated by Eq. (5.51), then

$$\bar{\lambda}_\theta = 1.2 \bar{\lambda} = 1.2 \times 0.441 = 0.529$$

and the iteration sequence should be:

θ [°C]	$\sqrt{\frac{k_{y,\theta}}{k_{E,\theta}}}$	$\bar{\lambda}_\theta = \frac{\bar{\lambda}}{\sqrt{k_{E,\theta}}}$	χ_{fi}	$N_{fi,0,Rd} = \chi_{fi} A f_y$ [kN]	$\mu_0 = \frac{N_{fi,Ed}}{N_{fi,0,Rd}}$	$\theta_{a,cr}$ [°C]
θ (?)	1.20	0.529	0.715	1283	0.385	625
625	1.24	0.549	0.705	1265	0.391	623
623	1.24	0.548	0.705	1265	0.391	623

Using the approximated value of the non-dimensional slenderness to start the iterative procedure, the value of the critical temperature at the second iteration differs by only 2 °C from the value obtained at the first iteration, and the iterative process could be stopped.

The verification of the fire resistance of the column may be now made.

a) The section factor of the HE 180 B is $A_m/V = 159 \text{ m}^{-1}$.

The box value for the section factor $[A_m/V]_b$ takes the value

$$[A_m/V]_b = \frac{2 \times (b+h)}{A} = \frac{2 \times (0.18+0.18)}{65.25 \times 10^{-4}} = 110.3 \text{ m}^{-1}$$

and the shadow factor k_{sh}

$$k_{sh} = 0.9 [A_m/V]_{box} / [A_m/V] = 0.9 \cdot 110.3 / 159 = 0.624$$

The modified section factor is:

$$k_{sh} [A_m/V] = 0.624 \cdot 159 = 99.2 \text{ m}^{-1}$$

This value could be directly obtaining from the table of Annex E, Vila Real *et al* (2009a).

Interpolating, from table of the Annex A.4 yields the following temperature after 30 minutes:

$$\theta_d = 766 \text{ °C}$$

and

$$\theta_d > \theta_{a,cr} \Rightarrow \text{not satisfactory.}$$

b) By double interpolation of table of the Annex A.4 the time needed to reach a temperature of 623 °C is

$$t_{fi,d} = 17.4 \text{ min}$$

and

$$t_{fi,d} < t_{fi,requ} \Rightarrow \text{not satisfactory.}$$

c) The reduction factors for the yield strength and the Young's modulus after 30 minutes of fire exposure are, interpolating in Table 5.2 for a temperature of 766 °C:

$$k_{y,\theta} = 0.1508 \text{ and } k_{E,\theta} = 0.1036$$

The design value of the buckling resistance is obtained from

$$N_{b,fi,t,Rd} = \chi_{fi} A k_{y,\theta} f_y / \gamma_{M,fi}$$

The non-dimensional slenderness at 766 °C, is

$$\bar{\lambda}_{\theta} = \bar{\lambda} \cdot \sqrt{\frac{k_{y,\theta}}{k_{E,\theta}}} = 0.441 \sqrt{\frac{0.1508}{0.1036}} = 0.532$$

and using

$$\phi_{\theta} = \frac{1}{2} [1 + \alpha \bar{\lambda}_{\theta} + \bar{\lambda}_{\theta}^2]$$

with

$$\alpha = 0.65 \sqrt{235/f_y}$$

gives

$$\phi_{\theta} = 0.8014$$

and the reduction factor for the flexural buckling is:

$$\chi_{fi} = \frac{1}{\phi_{\theta} + \sqrt{\phi_{\theta}^2 - \bar{\lambda}_{\theta}^2}} = 0.714$$

The design value of the buckling resistance after 30 minutes of fire exposure, takes the value:

$$N_{b,fi,t,Rd} = \chi_{fi} A k_{y,\theta} f_y / \gamma_{M,fi} = 0.714 \cdot 6525 \cdot 0.1508 \cdot 275 \times 10^{-3} / 1.0 = 193 \text{ kN}$$

and

$$N_{b,fi,t,Rd} < N_{fi,d} \Rightarrow \text{not satisfactory.}$$

The column does not fulfil the required fire resistance R30.

Example 5.5: Protected Column under axial compression

Consider a 2.8 m long HE 220 B column in S235 grade steel located in an intermediate storey of an office building subject to a permanent load of $G = 730 \text{ kN}$ and a variable load of $Q = 500 \text{ kN}$. If the column is fire protected by 20 mm thick gypsum boards evaluate the fire resistance time of the columns assuming it is heated on all four sides.

Solution:

The design value of the compression load under fire condition, assuming $\psi_1 = 0.5$ from Table 2.1 is

$$N_{fi,Ed} = G + \psi_1 Q = 730 + 0.5 \cdot 500 = 980 \text{ kN}$$

The relevant geometrical characteristics of the profile for the cross section classification are

$$c = 87.25 \text{ mm (flange)}$$

$$c = 152 \text{ mm (web)}$$

$$t_f = 16 \text{ mm}$$

$$t_w = 9.5 \text{ mm}$$

$$r = 18 \text{ mm}$$

As the steel grade is S235

$$\varepsilon = 0.85 \sqrt{235/f_y} = 0.85$$

The class of the flange in compression is

$$c/t_f = 87.25/16 = 5.4 < 9\varepsilon = 7.65 \Rightarrow \text{Class 1}$$

The class of the web in compression is

$$c/t_w = 152/9.5 = 16 < 33\varepsilon = 28 \Rightarrow \text{Class 1}$$

The cross section of the HE 220 B in fire situation is Class 1. This classification could be directly obtained using the table for cross sectional classification of Annex F, Vila Real *et al* (2009b).

The section factor of the HE 220 B has the value, $A_p / V = 96 \text{ m}^{-1}$.

From a table of commercial profiles:

Area, $A = 9100 \text{ mm}^2$

Second moment of area, $I_z = 28430000 \text{ mm}^4$

The buckling length for intermediate storey is: $l_{fi} = 0.5L = 0.5 \times 2.8 = 1.4 \text{ m}$.

The Euler critical load takes the value:

$$N_{cr} = \frac{\pi^2 EI}{l_{fi}^2} = 30063.5 \text{ kN}$$

210

The non-dimensional slenderness in fire situation is, according to Eq. (5.48), given by

$$\bar{\lambda}_\theta = \bar{\lambda} \cdot \sqrt{\frac{k_{y,\theta}}{k_{E,\theta}}}$$

and is temperature dependent. An iterative procedure will be needed, starting from 20 °C. At room temperature $k_{y,\theta} = k_{E,\theta} = 1.0$ and:

$$\bar{\lambda}_\theta = \bar{\lambda} = \sqrt{\frac{Af_y}{N_{cr}}} = 0.267$$

The reduction factor for flexural buckling is obtained as follows:

$$\alpha = 0.65 \sqrt{235/f_y} = 0.65$$

and

$$\phi = \frac{1}{2} \left(1 + 0.65 \cdot 0.267 + 0.267^2 \right) = 0.622$$

Giving

$$\chi_{fi} = \frac{1}{0.622 + \sqrt{0.622^2 - 0.267^2}} = 0.944$$

The design value of the compression force in the fire situation, $N_{b,fi,t,Rd}$ at time $t = 0$ is given by Eq. (5.44) as:

$$N_{fi,0,Rd} = \chi_{fi} A f_y = 1805 \text{ kN}$$

and the degree of utilisation takes the value

$$\mu_0 = \frac{N_{fi,Ed}}{N_{fi,0,Rd}} = \frac{980}{1805} = 0.543$$

which, using Eq. (5.110) gives a critical temperature of $\theta_{a,cr} = 571$ °C. With this temperature the value of the non-dimensional slenderness, $\bar{\lambda}_\theta$, must be updated. The procedure must be repeated until convergence is reached, as shown in the next table.

θ [°C]	$\sqrt{\frac{k_{y,\theta}}{k_{E,\theta}}}$	$\bar{\lambda}_\theta = \frac{\bar{\lambda}}{\sqrt{\frac{k_{y,\theta}}{k_{E,\theta}}}}$	χ_{fi}	$N_{fi,0,Rd} = \chi_{fi} A f_y$ [kN]	$\mu_0 = \frac{N_{fi,Ed}}{N_{fi,0,Rd}}$	$\theta_{a,cr}$ [°C]
20	1.00	0.267	0.844	1805	0.543	571
571	1.19	0.318	0.816	1745	0.562	565
565	1.19	0.318	0.816	1745	0.562	565

Convergence was reached at the third iteration and gives a critical temperature of

$$\theta_{a,cr} = 565 \text{ °C}$$

The next step is to evaluate how long the column takes to reach the critical temperature assuming the column is fire protected by 20 mm thick gypsum boards. Table of the Annex A.6 gives the following properties for the gypsum board material: $\lambda_p = 0.2 \text{ W/(m}\cdot\text{K)}$, $c_p = 1700 \text{ J/(kg}\cdot\text{K)}$, $\rho_p = 800 \text{ kg/m}^3$

and $p = 20\%$. As the thickness of the gypsum boards d_p is 20 mm, the ratio of heat stored in the protection takes the value

$$\phi = \frac{c_p d_p \rho_p}{c_a \rho_a} \cdot \frac{A_p}{V} = \frac{1700 \cdot 0.02 \cdot 800}{600 \cdot 7850} \cdot 96 = 0.554$$

and the corrected modified section factor is given by:

$$\frac{A_p}{V} \cdot \frac{\lambda_p}{d_p} \cdot \frac{1}{1 + \phi/2} = 96 \cdot \frac{0.2}{0.02} \cdot \frac{1}{1 + 0.554/2} = 752 \text{ W}/(\text{m}^3 \cdot \text{K})$$

Based on this value and for a temperature of 565 °C, a double interpolation in table of the Annex A.5 gives a time of 99 minutes.

The delay time due to the moisture content of the fire protection is, according to Eq. (4.21):

$$t_v = \frac{p \rho_p d_p^2}{5 \lambda_p} = \frac{20 \cdot 800 \cdot 0.02^2}{5 \cdot 0.2} = 6 \text{ min}$$

Therefore the time to reach a temperature of 565 °C is:

$$t = 99 + 6 = 105 \text{ min.}$$

Therefore the columns can be classified as R90.

Example 5.6: Restrained beam. Non-uniform temperature distribution

Consider a restrained beam, constructed from an S235, HE 400 B steel section, supporting a concrete slab. Assuming that the beam does not act compositely with the concrete slab, evaluate the resistance bending moment of the steel beam after 30 minutes of standard fire exposure for the following conditions:

- Using the adaptation factor k_1 to take into account the non-uniform temperature distribution across the cross section due to the concrete slab.
- Evaluating the temperatures of the flanges and the web using the shadow effect as defined in Eurocode 4.

Solution:

The relevant geometrical characteristics of the profile for the classification of the cross section are:

$$\begin{aligned} h &= 400 \text{ mm} \\ b &= 300 \text{ mm} \\ t_w &= 13.5 \text{ mm} \\ t_f &= 24 \text{ mm} \\ r &= 27 \text{ mm} \\ c &= b/2 - t_w/2 - r = 116.25 \text{ mm (flange)} \\ c &= h - 2t_f - 2r = 298 \text{ mm (web)} \end{aligned}$$

As the steel grade is S235:

$$\varepsilon = 0.85\sqrt{235/f_y} = 0.85$$

The class of the flange in compression is:

$$c/t_f = 116.25/24 = 4.84 < 9\varepsilon = 7.65 \Rightarrow \text{Class 1}$$

The class of the web in bending is:

$$d/t_w = 298/13.5 = 22.1 < 72\varepsilon = 61.2 \Rightarrow \text{Class 1}$$

The cross section of the HE 400 B in bending and in fire situation is Class 1. This classification could be directly obtained using the table for cross sectional classification of Annex F, Vila Real *et al* (2009b).

213

a) The section factor of an HE 400 B is:

$$A_m/V = 82 \text{ m}^{-1}$$

The box value of the section factor $[A_m/V]_b$ is:

$$[A_m/V]_b = \frac{2h+b}{A} = \frac{2 \cdot 0.4 + 0.3}{197.8 \times 10^{-4}} = 55.6 \text{ m}^{-1}$$

The modified section factor taking into account the shadow effect is:

$$k_{sh} = 0.9 \frac{[A_m/V]_b}{[A_m/V]} = 0.9 \cdot \frac{55.6}{82} = 0.61$$

and

$$k_{sh} [A_m/V] = 0.61 \cdot 82 = 50 \text{ m}^{-1}$$

Interpolating the values in table of the Annex A.5 yields a temperature of 678.5 °C.

At this temperature the reduction factor for the yield strength, according to Table 5.2, is

$$k_{y,\theta} = 0.2816$$

The design value of the resistance moment for non-uniform temperature distribution, according Eq. (5.64) is:

$$M_{\bar{f},t,Rd} = W_{pl,y} k_{y,\theta} f_y / (\gamma_{M,\bar{f}} k_1 k_2)$$

The plastic section modulus for the HE 400 B is

$$W_{pl,y} = 3232 \times 10^{-6} \text{ m}^3$$

Assuming that the adaptation factors for non-uniform temperature for this case are

$$k_1 = 0.7 \text{ and } k_2 = 1.0$$

The resistance moment after 30 minutes of standard fire exposure is

$$\begin{aligned} M_{\bar{f},t,Rd} &= W_{pl,y} k_{y,\theta} f_y / (\gamma_{M,\bar{f}} k_1 k_2) \\ &= 3232000 \cdot 0.2816 \cdot 235 \times 10^{-6} / (1.0 \cdot 0.7 \cdot 1.0) = 306 \text{ kNm} \end{aligned}$$

b) According to Part 1.2 of the Eurocode 4 the shadow factor is defined as

$$k_{shadow} = [0.9] \cdot \frac{e_1 + e_2 + 1/2 \cdot b_1 + \sqrt{h_w^2 + 1/4 \cdot (b_1 - b_2)^2}}{h_w + b_1 + 1/2 \cdot b_2 + e_1 + e_2 - e_w} = 0.592$$

where the symbols are defined in Fig. 5.52. It should be mentioned that this apparently complicated expression is only necessary for mono-symmetric cross section. For doubly symmetric cross sections the expression from EN 1993-1-2 can be used. This value of 0.592 is close to 0.61 previously obtained using the expression given in EN 1993-1-2.

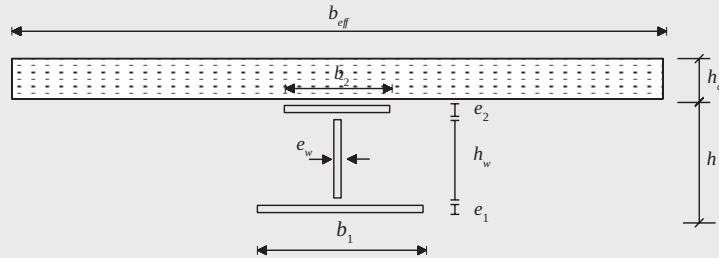


Figure 5.52 – Elements of a cross section

For the HE 400 B:

$$\begin{aligned}
 h &= 400 \text{ mm} \\
 b &= b_1 = b_2 = 300 \text{ mm} \\
 A &= 197.8 \text{ cm}^2 \\
 e_1 &= e_2 = 24 \text{ mm} \\
 e_w &= 13.5 \text{ mm} \\
 h_w &= 352 \text{ mm}
 \end{aligned}$$

The modified section factors for the elements of the profile are:

– Lower flange

$$k_{shadow} \frac{A_1}{V_1} = k_{shadow} \frac{2(b_1 + e_1)}{b_1 e_1} = 53.28 \text{ m}^{-1}$$

– Upper flange

$$k_{shadow} \frac{A_2}{V_2} = k_{shadow} \frac{b_2 + 2e_2}{b_2 e_2} = 28.6 \text{ m}^{-1}$$

– Web

$$k_{shadow} \frac{A_3}{V_3} = k_{shadow} \frac{2}{e_w} = 87.7 \text{ m}^{-1}$$

Interpolating in table of the Annex A.5 yields the following temperatures for the upper and lower flanges and the web:

$$\theta_{\text{lower flange}} = 692 \text{ }^\circ\text{C}$$

$$\theta_{\text{upper flange}} = 538 \text{ }^\circ\text{C}$$

$$\theta_{\text{web}} = 753 \text{ }^\circ\text{C}$$

These temperatures are shown in Fig. 5.53.

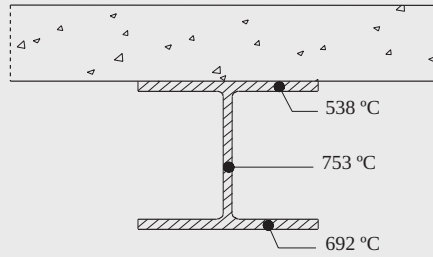


Figure 5.53 – Steel temperatures after 30 min of standard fire exposure

Fig. 5.54 compares the development of the temperatures obtained from Eurocode 3, considering the section factor of the whole cross section, with those from Eurocode 4.

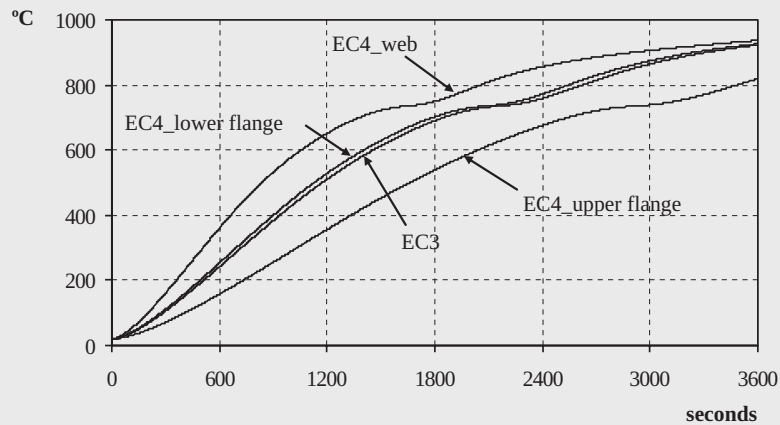


Figure 5.54 – Comparison of the temperatures obtained from EC3 and EC4

To evaluate the resistance moment it is necessary to find the position of the plastic neutral axis. The reduction factors for the yield strength according Table 5.2 are

$$k_{y,538^{\circ}\text{C}} = 0.6622$$

$$k_{y,753^{\circ}\text{C}} = 0.1664$$

$$k_{y,692^{\circ}\text{C}} = 0.2492$$

and the corresponding yield strengths are

$$f_{y,538^{\circ}\text{C}} = 0.6622 \cdot 235 = 155.6 \text{ MPa}$$

$$f_{y,753^{\circ}\text{C}} = 0.1664 \cdot 235 = 39.1 \text{ MPa}$$

$$f_{y,692^{\circ}\text{C}} = 0.2492 \cdot 235 = 58.6 \text{ MPa}$$

Assuming that the plastic neutral axis passes through the upper flange the stress distribution shown in Fig. 5.55, is obtained.

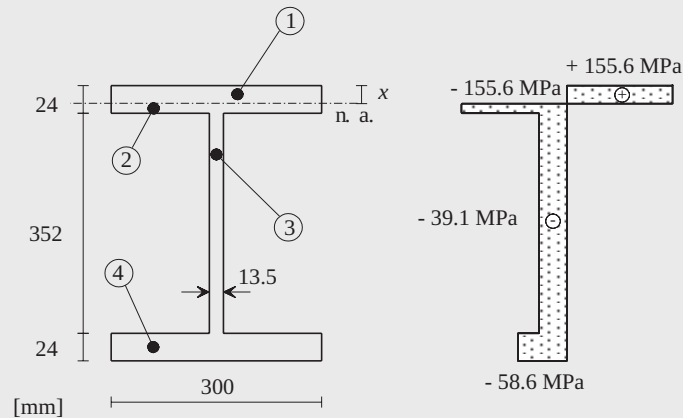


Figure 5.55 – Plastic stress distribution after 30 min of standard fire exposure and location of the plastic neutral axis (n. a.)

The position of the plastic neutral axis is given by Eq. (5.60a) as:

$$\sum_{i=1}^n A_i k_{y,\theta,i} f_{y,i} = 0$$

Substituting the above values in to this expression gives:

$$300x \cdot 155.6 - 300 \cdot (24 - x) \cdot 155.6 - 352 \cdot 13.5 \cdot 39.1 - 300 \cdot 24 \cdot 58.6 = 0$$

Solving this equation gives the following value for x : $x = 18.51 \text{ mm}$

This means the choice of the location of the neutral axis in the upper flange was correct.

The distances from the plastic neutral axis to the centroid of the elemental areas A_i , are

$$z_1 = 9.255 \text{ mm}$$

$$z_2 = 2.745 \text{ mm}$$

$$z_3 = 181.490 \text{ mm}$$

$$z_4 = 369.490 \text{ mm}$$

The design value of the resistance moment is given by Eq. (5.59), as follows

$$\begin{aligned} M_{f_i,t,Rd} &= \sum_{i=1}^4 A_i z_i k_{y,\theta,i} f_{y,i} / \gamma_{M,i} \\ &= (300 \cdot 18.51 \cdot 9.255 \cdot 0.6622 \cdot 235 \\ &\quad + 300 \cdot 5.49 \cdot 2.745 \cdot 0.6622 \cdot 235 \\ &\quad + 352 \cdot 13.5 \cdot 181.49 \cdot 0.1664 \cdot 235 \\ &\quad + 300 \cdot 24 \cdot 369.49 \cdot 0.2492 \cdot 235) \cdot 10^{-6} / 1.0 \\ &= 198 \text{ kNm} \end{aligned}$$

Although this procedure is more accurate than the one presented in item a) it gives a lower resistance moment. This is not the usual situation. Normally the simpler the procedure the more conservative is the solution. However, this is not the case here.

Example 5.7: Restrained and unrestrained beam

Consider a simply supported IPE 300, S235 grade steel beam from an office building, with fork supports. The member is 5.0 m long and is subjected to a transverse uniform load at normal temperature $q_{Ed} = 19.2 \text{ kN/m}$. The transverse loading is assumed to act at the shear centre of the beam. Evaluate the critical temperature for the following conditions:

- a) The beam is lateral restrained.
- b) The beam is unrestrained. Lateral-torsional buckling is not prevented and may therefore occur.

Solution:

In example 5.2 it was concluded that an IPE 300 in bending is Class 1.

For an office building a reduction factor for the loads in a fire situation can be taken as $\eta_{fi} = 0.65$, leading to

$$q_{fi,Ed} = \eta_{fi} q_{Ed} = 0.65 \cdot 19.2 = 12.48 \text{ kN/m}$$

Thus the design value of the moment in a fire situation is

$$M_{fi,Ed} = \frac{q_{fi,Ed} L^2}{8} = \frac{12.48 \cdot 5^2}{8} = 39.0 \text{ kNm}$$

The following data is relevant for solving the problem:

- Young's modulus $E = 210\,000 \text{ N/mm}^2$
- Shear modulus $G = E / [2(1 + \nu)] \text{ N/mm}^2$
- Poisson's ratio $\nu = 0.3$
- Length $L = 5000 \text{ mm}$
- Cross section classification Class 1
- Plastic section modulus $W_{pl,y} = 628400 \text{ mm}^3$
- Second moment of area about the minor axis $I_z = 603.8 \times 10^4 \text{ mm}^4$
- Warping constant $I_w = 125.9 \times 10^9 \text{ mm}^6$
- Torsion constant $I_t = 20.12 \times 10^4 \text{ mm}^4$

a) Determination of the critical temperature based on the design value of the applied moment at mid span

Assuming that the temperature distribution is uniform the resistance moment at time $t = 0$, is

$$M_{fi,0,Rd} = W_{pl,y} f_y / \gamma_{M,fi} = 628400 \cdot 235 \times 10^{-6} / 1.0 = 147.7 \text{ kNm}$$

and the degree of utilisation

$$\mu_0 = \frac{M_{fi,d}}{M_{fi,0,Rd}} = \frac{39.0}{147.7} = 0.264$$

The critical temperature is:

$$\theta_{a,cr} = 39.19 \ln \left(\frac{1}{0.9674 \cdot 0.264^{3.833}} - 1 \right) + 482 = 683 \text{ } ^\circ\text{C}$$

– Verification of shear resistance at the supports

The design value of the shear force in a fire situation at the supports is:

$$V_{fi,Ed} = \frac{q_{fi,Ed} \cdot L}{2} = \frac{12.48 \cdot 5}{2} = 31.2 \text{ kN}$$

The shear area of the IPE 300 is

$$\begin{aligned} A_v &= A - 2bt_f + (t_w + 2r)t_f = \\ &= 5380 - 2 \cdot 150 \cdot 10.7 + (7.1 + 2 \cdot 15) \cdot 10.7 = 2567 \text{ mm}^2 \end{aligned}$$

Assuming that at 683 °C the reduction factor for the yield strength, is

$$k_{y,\theta} = \mu_0 = 0.264$$

the resistance shear force at this temperature, is

$$V_{pl,y,fi,Rd} = \frac{A_v k_{y,\theta} f_y}{\sqrt{3} \gamma_{M,fi}} = \frac{2567 \cdot 0.264 \cdot 235}{\sqrt{3} \cdot 1.0} \times 10^{-3} = 91.9 \text{ kN}$$

$$V_{fi,Ed} = 31.2 < 91.9 \text{ kN} \quad \text{OK.}$$

b) The design lateral-torsional buckling resistance moment $M_{b,fi,0,Rd}$ at time $t = 0$ of a laterally unrestrained beam is given by:

$$M_{b,fi,0,Rd} = \chi_{LT,fi} W_{pl,y} f_y / \gamma_{M,fi}$$

As the reduction factor for the lateral-torsional buckling moment, $\chi_{LT,fi}$, depends on the temperature, an iterative procedure must be used.

This reduction factor in a fire situation is given by:

$$\chi_{LT,fi} = \frac{1}{\phi_{LT,\theta} + \sqrt{[\phi_{LT,\theta}]^2 - [\bar{\lambda}_{LT,\theta}]^2}}$$

with

$$\phi_{LT,\theta} = \frac{1}{2} \left[1 + \alpha \bar{\lambda}_{LT,\theta} + (\bar{\lambda}_{LT,\theta})^2 \right]$$

where the imperfection factor is:

$$\alpha = 0.65 \sqrt{235/f_y}$$

and

$$\bar{\lambda}_{LT,\theta} = \bar{\lambda}_{LT} \sqrt{k_{y,\theta}/k_{E,\theta}}$$

The non-dimensional slenderness at normal temperature is given by:

$$\bar{\lambda}_{LT} = \sqrt{\frac{W_{pl,y} f_y}{M_{cr}}}$$

The elastic critical moment for lateral-torsional buckling, according Eq. (5.74), is given by:

$$M_{cr} = 1.12 \frac{\pi^2 E I_z}{L^2} \sqrt{\frac{I_w}{I_z} + \frac{L^2 G I_t}{\pi^2 E I_z}} \times 10^{-6} = 129.4 \text{ kNm}$$

and

$$\bar{\lambda}_{LT} = \sqrt{\frac{W_{pl,y} f_y}{M_{cr}}} = 1.068$$

At normal temperature

$$\bar{\lambda}_{LT,20^\circ\text{C}} = \bar{\lambda}_{LT} \sqrt{k_{y,20^\circ\text{C}}/k_{E,20^\circ\text{C}}} = 1.068 \sqrt{1.0/1.0} = 1.068$$

and

$$\phi_{LT,20^\circ\text{C}} = \frac{1}{2} (1 + 0.65 \cdot 1.068 + 1.068^2) = 1.42$$

and

$$\chi_{LT,fi} = \frac{1}{1.42 + \sqrt{1.42^2 - 1.068^2}} = 0.424$$

Giving the design lateral-torsional buckling resistance moment $M_{b,fi,0,Rd}$ at time $t = 0$:

$$M_{b,fi,0,Rd} = 0.424 \cdot 628400 \cdot 235 \times 10^{-6} = 62.6 \text{ kNm}$$

5. MECHANICAL ANALYSIS

The degree of utilisation at time $t = 0$, is

$$\mu_0 = \frac{M_{fi,Ed}}{M_{b,fi,0,Rd}} = \frac{39.0}{62.6} = 0.623$$

And the critical temperature

$$\theta_{a,cr} = 39.19 \ln \left(\frac{1}{0.9674 \cdot 0.623^{3.833}} - 1 \right) + 482 = 548 \text{ } ^\circ\text{C}$$

Using this temperature, the non-dimensional slenderness $\bar{\lambda}_{LT,\theta}$ may be corrected. The procedure must be repeated until convergence is reached, as shown in the next table:

θ [$^\circ\text{C}$]	$\sqrt{\frac{k_{y,\theta}}{k_{E,\theta}}}$	$\bar{\lambda}_{LT,\theta} =$ $\bar{\lambda}_{LT} \cdot \sqrt{\frac{k_{y,\theta}}{k_{E,\theta}}}$	$\chi_{LT,fi}$	$M_{b,fi,0,Rd} =$ $\chi_{LT,fi} W_{pl,y} f_y$ [kNm]	$\mu_0 =$ $\frac{M_{fi,Ed}}{M_{b,fi,0,Rd}}$	$\theta_{a,cr}$ [$^\circ\text{C}$]
20	1.00	1.068	0.424	62.6	0.623	548
548	1.16	1.239	0.358	52.9	0.740	515
515	1.15	1.229	0.364	53.8	0.725	519
519	1.15	1.222	0.364	53.8	0.725	519

222

Convergence was reached at a critical temperature of $\theta_{a,cr} = 519 \text{ } ^\circ\text{C}$.

Example 5.8: Beam-column

A 6.0 m long, simply supported beam-column constructed from an IPE 450 section is subjected to a uniform load in a fire situation of $q_{fi,Ed} = 15.89 \text{ kN/m}$ and to an axial compression load of $N_{fi,Ed} = 136.5 \text{ kN}$. Assuming that the steel grade is S235 and that the load is applied at the shear centre of the beam, evaluate the critical temperature in the following conditions:

- When lateral-torsional buckling is prevented.
- When the beam-column is unrestrained. Lateral-torsional buckling is not prevent and may therefore occur.

Solution:

Evaluate the class of the cross section assuming only axial compression. The following geometrical characteristics of the IPE 450 are relevant for the classification of the cross section:

$$\begin{aligned} h &= 450 \text{ mm} \\ b &= 190 \text{ mm} \\ t_w &= 9.4 \text{ mm} \\ t_f &= 14.6 \text{ mm} \\ r &= 21 \text{ mm} \\ c &= b/2 - t_w/2 - r = 69.3 \text{ mm (flange)} \\ c &= h - 2t_f - 2r = 378.8 \text{ mm (web)} \end{aligned}$$

As the steel grade is S235:

$$\varepsilon = 0.85\sqrt{235/f_y} = 0.85$$

The class of the flange in compression is

$$c/t_f = 69.3/14.6 = 4.75 < 9\varepsilon = 7.65 \Rightarrow \text{Class 1}$$

The class of the web in compression is

$$c/t_w = 378.8/9.4 = 40.3 > 42\varepsilon = 35.7 \Rightarrow \text{Class 4}$$

The cross section of the IPE 450 is Class 4 in pure compression. If the classification had been Class 1 or 2 it would not have been necessary to classify the cross section for combined bending and compression because this is a more favourable situation than pure compression.

Considering now the actual pattern of stresses resulting from combined bending and compression, according to Eq. (5.17)

$$\alpha = \frac{y}{c} = \frac{1}{2} + \frac{N}{2ct_w f_y} = \frac{1}{2} + \frac{136500}{2 \cdot 378.8 \cdot 9.4 \cdot 235} = 0.582$$

and

$$c/t_w = 378.8/9.4 = 40.3 < \frac{396\varepsilon}{13\alpha - 1} = 51.3 \Rightarrow \text{Class 1}$$

The Cross section is Class 1. This classification could be directly obtained using the table for cross sectional classification of Annex F, Vila Real *et al* (2009b),

where it can be seen that for a compression force less than 367 kN the profile IPE 450 subjected to combined bending and compression is Class 1.

The following data is relevant for solving the problem:

- Young's modulus $E = 210\,000 \text{ N/mm}^2$
- Shear modulus $G = E / [2(1 + \nu)] \text{ N/mm}^2$
- Poisson's ratio $\nu = 0.3$
- Length $L = 6000 \text{ mm}$
- Buckling length $l_{\bar{n}} = 6000 \text{ mm}$
- Area $A = 9882 \text{ mm}^2$
- Plastic section modulus $W_{pl,y} = 1702 \times 10^3 \text{ mm}^3$
- Second moment of area about major axis $I_y = 33540 \times 10^4 \text{ mm}^4$
- Second moment of area about the minor axis $I_z = 1676 \times 10^4 \text{ mm}^4$
- Warping constant $I_w = 791 \times 10^9 \text{ mm}^6$
- Torsion constant $I_t = 66.87 \times 10^4 \text{ mm}^4$

a) The slenderness at normal temperature:

- Elastic critical load about the weak axis:

$$N_{cr,z} = \frac{\pi^2 EI_z}{l_{\bar{n}}^2} = 964.92 \text{ kN}$$

- Elastic critical load about the strong axis:

$$N_{cr,y} = \frac{\pi^2 EI_y}{l_{\bar{n}}^2} = 19425 \text{ kN}$$

and the non-dimensional slenderness:

- About the weak axis: $\bar{\lambda}_z = \sqrt{\frac{Af_z}{N_{cr,z}}} = 1.551$

- About the strong axis: $\bar{\lambda}_y = \sqrt{\frac{Af_y}{N_{cr,y}}} = 0.346$

thus

$$\bar{\lambda}_{z,20^{\circ}\text{C}} = \bar{\lambda}_z \sqrt{k_{y,20^{\circ}\text{C}}/k_{E,20^{\circ}\text{C}}} = \bar{\lambda}_z = 1.551$$

and

$$\bar{\lambda}_{y,20^{\circ}\text{C}} = \bar{\lambda}_y \sqrt{k_{y,20^{\circ}\text{C}}/k_{E,20^{\circ}\text{C}}} = \bar{\lambda}_y = 0.346$$

The reduction factors for flexural buckling χ_{fi} at normal temperature are:

– About the weak axis:

$$\phi_{z,20^{\circ}\text{C}} = \frac{1}{2} \left(1 + 0.65 \cdot 1.551 + 1.551^2 \right) = 2.207$$

and

$$\chi_{z,fi} = \frac{1}{2.207 + \sqrt{2.207^2 - 1.551^2}} = 0.265$$

– About the strong axis:

$$\phi_{y,20^{\circ}\text{C}} = \frac{1}{2} \left(1 + 0.65 \cdot 0.346 + 0.346^2 \right) = 0.672$$

and

$$\chi_{y,fi} = \frac{1}{0.672 + \sqrt{0.672^2 - 0.346^2}} = 0.801$$

225

As $M_{z,fi,Ed} = 0$, the degree of utilization given by Eq. (5.123), is:

$$\mu_0 = \frac{N_{fi,Ed}}{\chi_{\min,fi} A f_y} + \frac{k_y M_{y,fi,Ed}}{W_{pl,y} f_y}$$

where

$$k_y = 1 - \frac{\mu_y N_{fi,Ed}}{\chi_{y,fi} A k_{y,\theta} \frac{f_y}{\gamma_{M,fi}}} \leq 3$$

with

$$\mu_y = \left(2\beta_{M,y} - 5 \right) \bar{\lambda}_{y,\theta} + 0.44\beta_{M,y} + 0.29 \leq 0.8 \quad \text{with} \quad \bar{\lambda}_{y,20^{\circ}\text{C}} \leq 1.1$$

For a parabolic bending diagram $\beta_{M,y}$ takes the value

$$\beta_{M,y} = 1.3$$

and so

$$\mu_y = (2 \cdot 1.3 - 5) \cdot 0.346 + 0.44 \cdot 1.3 + 0.29 = 0.032$$

and

$$k_y = 1 - \frac{0.032 \cdot 136.5 \times 10^3}{0.801 \cdot 9882 \cdot 235} = 0.998$$

The moment at the mid span is

$$M_{fi,Ed} = \frac{q_{fi,Ed} \cdot L^2}{8} = \frac{15.89 \cdot 6^2}{8} = 71.5 \text{ kNm}$$

From which the degree of utilization is:

$$\mu_0 = \frac{136.5 \times 10^3}{0.265 \cdot 9882 \cdot 235} + \frac{0.998 \cdot 71.5 \times 10^6}{1702 \times 10^3 \cdot 235} = 0.400$$

By interpolation in Table 5.2, the critical temperature is $\theta_{a,cr} = 629^\circ\text{C}$.

The non-dimensional slenderness at elevated temperature is a function of the temperature and the following iterative procedure is needed:

– **First iteration:**

For $\theta_{a,cr} = 629^\circ\text{C}$, the reduction factors for the yield strength and the Young's modulus are

$$k_{y,629^\circ\text{C}} = 0.400$$

and

$$k_{E,629^\circ\text{C}} = 0.258$$

and the corrected non-dimensional slenderness is:

$$\bar{\lambda}_{z,629^\circ\text{C}} = 1.551 \sqrt{0.400/0.258} = 1.933$$

and

$$\bar{\lambda}_{y,629^\circ\text{C}} = 0.346 \sqrt{0.400/0.258} = 0.431$$

The reduction factors for the flexural buckling χ_{fi} at temperature of 629 °C are:

– About the weak axis:

$$\phi_{z,629^{\circ}\text{C}} = \frac{1}{2} \left(1 + 0.65 \cdot 1.933 + 1.933^2 \right) = 2.997$$

and

$$\chi_{z,fi} = \frac{1}{2.997 + \sqrt{2.997^2 - 1.933^2}} = 0.189$$

– About the strong axis:

$$\phi_{y,629^{\circ}\text{C}} = \frac{1}{2} \left(1 + 0.65 \cdot 0.431 + 0.431^2 \right) = 0.733$$

and

$$\chi_{y,fi} = \frac{1}{0.733 + \sqrt{0.733^2 - 0.431^2}} = 0.754$$

The updated μ_y is:

$$\mu_y = (2 \cdot 1.3 - 5) \cdot 0.431 + 0.44 \cdot 1.3 + 0.29 = -0.172$$

and

$$k_y = 1 - \frac{-0.172 \cdot 136.5 \times 10^3}{0.754 \cdot 9882 \cdot 0.400 \cdot 235} = 1.034$$

227

and the degree of utilization is:

$$\mu_0 = \frac{136.5 \times 10^3}{0.189 \cdot 9882 \cdot 235} + \frac{1.034 \cdot 71.5 \times 10^6}{1702 \times 10^3 \cdot 235} = 0.496$$

By interpolation in Table 5.2, the critical temperature is $\theta_{a,cr} = 592$ °C.

– **Second iteration:**

For $\theta_{a,cr} = 592$ °C, the reduction factors for the yield strength and the Young's modulus are

$$k_{y,592^{\circ}\text{C}} = 0.496$$

and

$$k_{E,592^{\circ}\text{C}} = 0.334$$

and the corrected non-dimensional slenderness

$$\bar{\lambda}_{z,592^\circ} = 1.551\sqrt{0.496/0.334} = 1.890$$

and

$$\bar{\lambda}_{y,592^\circ\text{C}} = 0.346\sqrt{0.496/0.334} = 0.421$$

The reduction factors for the flexural buckling χ_{fi} at a temperature of 592 °C are:

– About the weak axis:

$$\phi_{z,592^\circ\text{C}} = \frac{1}{2}\left(1 + 0.65 \cdot 1.890 + 1.890^2\right) = 2.900$$

and

$$\chi_{z,fi} = \frac{1}{2.900 + \sqrt{2.900^2 - 1.890^2}} = 0.196$$

– About the strong axis:

$$\phi_{y,592^\circ\text{C}} = \frac{1}{2}\left(1 + 0.65 \cdot 0.421 + 0.421^2\right) = 0.726$$

and

$$\chi_{z,fi} = \frac{1}{0.726 + \sqrt{0.726^2 - 0.419^2}} = 0.760$$

The value of the corrected μ_y is:

$$\mu_y = (2 \cdot 1.3 - 5) \cdot 0.421 + 0.44 \cdot 1.3 + 0.29 = -0.149$$

and

$$k_y = 1 - \frac{-0.149 \cdot 136.5 \times 10^3}{0.760 \cdot 9882 \cdot 0.496 \cdot 235} = 1.023$$

The degree of utilization takes the value

$$\mu_0 = \frac{136.5 \times 10^3}{0.196 \cdot 9882 \cdot 235} + \frac{1.023 \cdot 71.5 \times 10^6}{1702 \times 10^3 \cdot 235} = 0.483$$

By interpolation in Table 5.2, the critical temperature is:

$$\theta_{a,cr} = 596 \text{ }^{\circ}\text{C}$$

After one more iteration the critical temperature converges to the value:

$$\theta_{a,cr} = 595 \text{ }^{\circ}\text{C}$$

– Cross section verification

The design value of the shear force in the fire situation at the supports is:

$$V_{fi,Ed} = \frac{q_{fi,Ed} \cdot L}{2} = 47.67 \text{ kN}$$

The shear area of the IPE 450 is

$$\begin{aligned} A_v &= A - 2bt_f + (t_w + 2r)t_f = \\ &= 9880 - 2 \cdot 190 \cdot 14.6 + (9.4 + 2 \cdot 21) \cdot 14.6 = 5082 \text{ mm}^2 \end{aligned}$$

At 595 °C the reduction factor for the yield strength, interpolating in Table 5.2, is

$$k_{y,\theta} = 0.4855$$

and the resistance shear force at that temperature, is

$$V_{fi,Rd} = \frac{A_v k_{y,\theta} f_y}{\sqrt{3} \gamma_{M,fi}} = \frac{5082 \cdot 0.4855 \cdot 235}{\sqrt{3} \cdot 1.0} \times 10^{-3} = 334.8 \text{ kN}$$

$$V_{fi,Ed} = 47.67 < V_{fi,Rd} = 334.8 \text{ kN} \quad \text{OK.}$$

Check if the effect of the axial load needs to be taken into account in the design value of the resistance moment:

The plastic resistance to axial load at 595 °C is

$$N_{fi,pl} = A k_{y,\theta} f_y / \gamma_{M,fi} = 9880 \cdot 0.486 \cdot 235 \times 10^{-3} / 1.0 = 1128.4 \text{ kN}$$

As

$$N_{fi,Ed} < 0.25 N_{fi,pl} = 281.8 \text{ kN}$$

and

$$\begin{aligned} N_{fi,Ed} &< 0.5h_w t_w k_{y,\theta} f_y / \gamma_{M,fi} = \\ &= 0.5 \cdot (450 - 2 \cdot 14.6) \cdot 9.4 \cdot 0.486 \cdot 235 \times 10^{-3} / 1.0 = 225.9 \text{ kN} \end{aligned}$$

the effect of the axial force on the plastic moment resistance does not need to be taken into account (see Section 5.5.9.2).

b) Lateral-torsional buckling is a potential mode of failure. The degree of utilization of the beam is evaluated according to Eq. (5.123) taking $M_{z,fi,Ed} = 0$:

$$\mu_0 = \frac{N_{fi,Ed}}{\chi_{z,fi} A f_y} + \frac{k_{LT} M_{y,fi,Ed}}{\chi_{LT,fi} W_{pl,y} f_y}$$

The elastic critical moment for lateral-torsional buckling is

$$M_{cr} = 1.12 \frac{\pi^2 E I_z}{L^2} \sqrt{\frac{I_w}{I_z} + \frac{L^2 G I_t}{\pi^2 E I_z}} \times 10^{-6} = 347.2 \text{ kNm}$$

And the non-dimensional slenderness for lateral-torsional buckling

$$\bar{\lambda}_{LT} = \sqrt{\frac{W_{pl,y} f_y}{M_{cr}}} = 1.073$$

230

And at normal temperature

$$\bar{\lambda}_{LT,20^\circ\text{C}} = \bar{\lambda}_{LT} \sqrt{k_{y,20^\circ\text{C}} / k_{E,20^\circ\text{C}}} = 1.073 \sqrt{1.0 / 1.0} = 1.073$$

and

$$\phi_{LT,20^\circ\text{C}} = \frac{1}{2} \left(1 + 0.65 \cdot 1.073 + 1.073^2 \right) = 1.425$$

and

$$\chi_{LT,fi} = \frac{1}{1.425 + \sqrt{1.425^2 - 1.073^2}} = 0.423$$

and

$$\mu_{LT} = 0.15 \bar{\lambda}_{z,20^\circ\text{C}} \beta_{M,LT} - 0.15 \leq 0.9$$

$\lambda_{z,20^\circ\text{C}}$ was calculated in the previous section and has the value:

$$\lambda_{z,20^{\circ}\text{C}} = 1.551$$

and

$$\beta_{M,LT} = 1.3$$

giving

$$\mu_{LT} = 0.15 \cdot 1.551 \cdot 1.3 - 0.15 = 0.152$$

and

$$k_{LT} = 1 - \frac{\mu_{LT} N_{fi,Ed}}{\chi_{z,fi} A k_{y,\theta} \frac{f_y}{\gamma_{M,fi}}} \leq 1$$

At 20 °C $\chi_{z,fi}$ was calculated in the previous section and has the value:

$$\chi_{z,fi} = 0.265$$

giving

$$k_{LT} = 1 - \frac{0.152 \cdot 136.5 \times 10^3}{0.265 \cdot 9882 \cdot 1.0 \cdot \frac{235}{1.0}} = 0.966$$

The degree of utilization is:

$$\mu_0 = \frac{136.5 \times 10^3}{0.265 \cdot 9882 \cdot 235} + \frac{0.966 \cdot 71.5 \times 10^6}{0.423 \cdot 1702 \times 10^3 \cdot 235} = 0.630$$

231

By interpolation in Table 5.2, the critical temperature is:

$$\theta_{a,cr} = 548^{\circ}\text{C}$$

An iterative procedure is needed.

– First iteration:

For $\theta_{a,cr} = 548^{\circ}\text{C}$, the reduction factors for the yield strength and the Young's modulus are

$$k_{y,548^{\circ}\text{C}} = 0.630$$

and

$$k_{E,548^{\circ}\text{C}} = 0.460$$

the updated non-dimensional slenderness are:

$$\bar{\lambda}_{z,548^{\circ}\text{C}} = 1.551\sqrt{0.630/0.460} = 1.816$$

and

$$\phi_{z,548^{\circ}\text{C}} = \frac{1}{2}\left(1 + 0.65 \cdot 1.816 + 1.816^2\right) = 2.739$$

and the reduction factor for the lateral-torsional buckling is:

$$\chi_{z,\text{fi}} = \frac{1}{2.739 + \sqrt{2.739^2 - 1.816^2}} = 0.209$$

and the non-dimensional slenderness for lateral-torsional buckling is:

$$\bar{\lambda}_{LT,548^{\circ}\text{C}} = 1.073\sqrt{0.630/0.460} = 1.257$$

and

$$\phi_{LT,548^{\circ}\text{C}} = \frac{1}{2}\left(1 + 0.65 \cdot 1.257 + 1.257^2\right) = 1.698$$

and the reduction factor for the lateral-torsional buckling is

$$\chi_{LT,\text{fi}} = \frac{1}{1.698 + \sqrt{1.698^2 - 1.257^2}} = 0.352$$

and

$$\begin{aligned} \mu_{LT} &= 0.15\bar{\lambda}_{z,547^{\circ}\text{C}}\beta_{M,LT} - 0.15 \\ &= 0.15 \cdot 1.816 \cdot 1.3 - 0.15 \\ &= 0.204 \end{aligned}$$

and

$$\begin{aligned} k_{LT} &= 1 - \frac{\mu_{LT} N_{\text{fi},Ed}}{\chi_{z,\text{fi}} A k_{y,547^{\circ}\text{C}} \frac{f_y}{\gamma_{M,\text{fi}}}} \\ &= 1 - \frac{0.204 \cdot 136.5 \times 10^3}{0.209 \cdot 9882 \cdot 0.630 \cdot \frac{235}{1.0}} = 0.909 \end{aligned}$$

The degree of utilization is:

$$\mu_0 = \frac{136.5 \times 10^3}{0.209 \cdot 9882 \cdot 235} + \frac{0.909 \cdot 71.5 \times 10^6}{0.352 \cdot 1702 \times 10^3 \cdot 235} = 0.743$$

By interpolation in Table 5.2, the critical temperature is:

$$\theta_{a,cr} = 512 \text{ }^{\circ}\text{C}$$

– **Second iteration:**

For $\theta_{a,cr} = 512 \text{ }^{\circ}\text{C}$

$$k_{y,512^{\circ}\text{C}} = 0.743$$

and

$$k_{E,512^{\circ}\text{C}} = 0.565$$

The updated non-dimensional slenderness is:

$$\bar{\lambda}_{z,512^{\circ}\text{C}} = 1.551\sqrt{0.743/0.565} = 1.778$$

and

$$\phi_{z,512^{\circ}\text{C}} = \frac{1}{2}\left(1 + 0.65 \cdot 1.778 + 1.778^2\right) = 2.659$$

And the reduction factor for the flexural buckling about the minor axis is:

$$\chi_{z,\text{fi}} = \frac{1}{2.659 + \sqrt{2.659^2 - 1.778^2}} = 0.216$$

The non-dimensional slenderness is:

$$\bar{\lambda}_{LT,512^{\circ}\text{C}} = 1.073\sqrt{0.743/0.565} = 1.230$$

and

$$\phi_{LT,512^{\circ}\text{C}} = \frac{1}{2}\left(1 + 0.65 \cdot 1.230 + 1.230^2\right) = 1.657$$

and the reduction factor for the lateral-torsional buckling is:

$$\chi_{LT,\text{fi}} = \frac{1}{1.657 + \sqrt{1.657^2 - 1.230^2}} = 0.361$$

and

$$\begin{aligned}\mu_{LT} &= 0.15\bar{\lambda}_{z,512^{\circ}\text{C}}\beta_{M,LT} - 0.15 \\ &= 0.15 \cdot 1.778 \cdot 1.3 - 0.15 \\ &= 0.197\end{aligned}$$

and

$$k_{LT} = 1 - \frac{\mu_{LT} N_{fi,Ed}}{\chi_{z,fi} A k_{y,515^\circ\text{C}} \frac{f_y}{\gamma_{M,fi}}}$$

$$= 1 - \frac{0.197 \cdot 136.5 \times 10^3}{0.216 \cdot 9882 \cdot 0.743 \cdot \frac{235}{1.0}} = 0.928$$

The degree of utilization is:

$$\mu_0 = \frac{136.5 \times 10^3}{0.216 \cdot 9882 \cdot 235} + \frac{0.928 \cdot 71.5 \times 10^6}{0.361 \cdot 1702 \times 10^3 \cdot 235} = 0.731$$

By interpolation in Table 5.2, the critical temperature is:

$$\theta_{a,cr} = 516^\circ\text{C}$$

After two more iterations the critical temperature converges to the following value:

$$\theta_{a,cr} = 515^\circ\text{C}$$

Example 5.9: Beam-column with restrained lateral displacements

Consider a 3.0 m high, HE 200 B column in an intermediate storey of a braced frame, subjected to a bi-triangular bending moment diagram with moments at the ends in fire situation of $M_{y,fi,Ed} = \pm 50$ kNm about major axis and to an axial compression load in fire situation of $N_{fi,Ed} = 800$ kN. Assuming that the steel grade is S235, and that lateral-torsional buckling is not allowed, evaluate the critical temperature of the column.

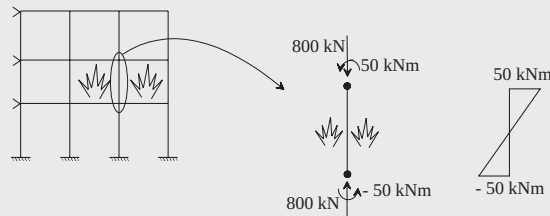


Figure 5.56 – Beam-column in a braced frame

Solution:

Evaluate the class of the cross section assuming only axial compression. The following geometrical characteristics of the HE 200 B are relevant for the classification of the cross section:

$$h = 200 \text{ mm}$$

$$b = 200 \text{ mm}$$

$$t_w = 9 \text{ mm}$$

$$t_f = 15 \text{ mm}$$

$$r = 18 \text{ mm}$$

$$c = b/2 - t_w/2 - r = 77.5 \text{ mm (flange)}$$

$$c = h - 2t_f - 2r = 134 \text{ mm (web)}$$

As the steel grade is S235:

$$\varepsilon = 0.85 \sqrt{235/f_y} = 0.85$$

The class of the flanges in compression is:

$$c/t_f = 77.5/15 = 5.17 < 9\varepsilon = 7.65 \Rightarrow \text{Class 1}$$

The class of the web in compression is:

$$c/t_w = 134/9 = 14.9 < 33\varepsilon = 28.5 \Rightarrow \text{Class 1}$$

The cross section of the HE 200 B is Class 1 in pure compression. As this is the most severe situation, nothing is to be gained by conducting additional calculations with the actual pattern of stresses resulting from combined bending and compression. The cross section is Class 1.

The following data is relevant for solving the problem:

- | | |
|--|---|
| – Young's modulus | $E = 210000 \text{ N/mm}^2$ |
| – Shear modulus | $G = E/[2(1+\nu)] \text{ N/mm}^2$ |
| – Poisson's ratio | $\nu = 0.3$ |
| – Length | $L = 3000 \text{ mm}$ |
| – Area | $A = 7808 \text{ mm}^2$ |
| – Plastic section modulus | $W_{pl,y} = 642.5 \times 10^3 \text{ mm}^3$ |
| – Second moment of area about major axis | $I_y = 5696 \times 10^4 \text{ mm}^4$ |

The buckling length in fire situation is (intermediate storey):

$$l_{fi} = 0.5L = 0.5 \cdot 3000 = 1500 \text{ mm}$$

The Euler critical load takes the value:

$$N_{cr} = \frac{\pi^2 EI}{l_{fi}^2} = 52469.45 \text{ kN}$$

The non-dimensional slenderness:

$$\bar{\lambda}_y = \sqrt{\frac{Af_y}{N_{cr}}} = 0.187$$

and

$$\bar{\lambda}_{y,20^\circ\text{C}} = \bar{\lambda}_y \sqrt{k_{y,20^\circ\text{C}}/k_{E,20^\circ\text{C}}} = \bar{\lambda}_y = 0.187$$

The imperfection factor is

$$\alpha = 0.65 \sqrt{235/f_y} = 0.65$$

and reduction factor for the flexural buckling, χ_{fi} , is:

$$\phi_{y,20^\circ\text{C}} = \frac{1}{2} \left(1 + 0.65 \cdot 0.187 + 0.187^2 \right) = 0.578$$

and

$$\chi_{y,fi} = \frac{1}{0.578 + \sqrt{0.578^2 - 0.187^2}} = 0.889$$

Considering that $M_{z,fi,Ed} = 0$, the reduction factor for the yield strength given by Eq. (5.123), is:

$$k_{y,\theta} = \frac{N_{fi,Ed}}{\chi_{fi} A f_y} + \frac{k_y M_{y,fi,Ed}}{W_{pl,y} f_y}$$

where

$$k_y = 1 - \frac{\mu_y N_{fi,Ed}}{\chi_{y,fi} A k_{y,\theta} \frac{f_y}{\gamma_{M,fi}}} \leq 3$$

with

$$\mu_y = (2\beta_{M,y} - 5)\bar{\lambda}_{y,\theta} + 0.44\beta_{M,y} + 0.29 \leq 0.8 \quad \text{with} \quad \bar{\lambda}_{y,20^\circ\text{C}} \leq 1.1$$

For a bi-triangular bending diagram, $\beta_{M,y}$ takes the value

$$\beta_{M,y} = 2.5$$

and thus

$$\mu_y = (2 \cdot 2.5 - 5)0.187 + 0.44 \cdot 2.5 + 0.29 = 1.39 > 0.8 \Rightarrow \mu_0 = 0.8$$

The interaction factor k_y , is

$$k_y = 1 - \frac{0.8 \cdot 800 \times 10^3}{0.889 \cdot 7808 \cdot 235} = 0.607$$

and the reduction factor for the yield strength is:

$$k_{y,\theta} = \frac{800 \times 10^3}{0.889 \cdot 7808 \cdot 235} + \frac{0.607 \cdot 50 \times 10^6}{642.5 \times 10^3 \cdot 235} = 0.692$$

By interpolation in Table 5.2, the critical temperature is

$$\theta_{a,cr} = 528.4^\circ\text{C}$$

The non-dimensional slenderness at elevated temperature is a function of the temperature and the following iterative procedure is needed:

237

– **First iteration:**

For $\theta_{a,cr} = 528.4^\circ\text{C}$, the reduction factors for the yield strength and the Young's modulus are:

$$k_{y,528.4^\circ\text{C}} = 0.692$$

and

$$k_{E,528.4^\circ\text{C}} = 0.518$$

and the corrected non-dimensional slenderness is:

$$\bar{\lambda}_{y,528.4^\circ\text{C}} = 0.187 \sqrt{0.692/0.517} = 0.216$$

The reduction factor χ_{fi} at the temperature of 528.4 °C is:

$$\phi_{y,528.4^{\circ}\text{C}} = \frac{1}{2} \left(1 + 0.65 \cdot 0.216 + 0.216^2 \right) = 0.594$$

and

$$\chi_{y,fi} = \frac{1}{0.594 + \sqrt{0.594^2 - 0.216^2}} = 0.872$$

and the corrected μ_y is:

$$\mu_y = 0.8$$

The interaction factor k_y , is:

$$k_y = 0.422$$

and the reduction factor for the yield strength is:

$$k_{y,\theta} = \frac{N_{fi,Ed}}{\chi_{y,fi} A f_y} + \frac{k_y M_{y,fi,Ed}}{W_{pl,y} f_y} = 0.640$$

By interpolation in Table 5.2, the critical temperature is:

$$\theta_{a,cr} = 545.3 \text{ }^{\circ}\text{C}$$

238

– **Second iteration:**

For $\theta_{a,cr} = 545.3 \text{ }^{\circ}\text{C}$, the reduction factors for the yield strength and the Young's modulus are:

$$k_{y,545.3^{\circ}\text{C}} = 0.640$$

and

$$k_{E,545.3^{\circ}\text{C}} = 0.469$$

and the corrected non-dimensional slenderness is:

$$\bar{\lambda}_{y,545.3^{\circ}\text{C}} = 0.187 \sqrt{0.640/0.469} = 0.218$$

The reduction factor χ_{fi} at the temperature of 545.3 °C is:

$$\phi_{y,545.3^{\circ}\text{C}} = 0.595$$

and

$$\chi_{y,\bar{f}_i} = 0.871$$

and the corrected μ_y is:

$$\mu_y = 0.8$$

and

$$k_y = 0.374$$

By interpolation in Table 5.2, the critical temperature is:

$$\theta_{a,cr} = 550.2 \text{ }^\circ\text{C}$$

After four iterations the critical temperature is

$$\theta_{a,cr} = 552 \text{ }^\circ\text{C}$$

– Cross section verification

Because the interaction formulae rely on the concept of the equivalent moment factor, it is necessary to check the cross section at the ends of the member, ECCS (2006).

$$V_{y,fi,Ed} = \frac{M_{y,fi,Ed,top} - M_{y,fi,Ed,bottom}}{L} = \frac{50 - (-50)}{3} = 33.33 \text{ kN}$$

$$A_v = A - 2bt_f + (t_w + 2r)t_f = 2483 \text{ mm}^2$$

239

At 552 °C the reduction factor for the yield strength by interpolation in Table 5.2 is

$$k_{y,\theta} = 0.618$$

and the resistance shear force at this temperature is

$$V_{pl,y,fi,Rd} = \frac{A_v k_{y,\theta} f_y}{\sqrt{3} \gamma_{M,fi}} = \frac{2483 \cdot 0.618 \cdot 235}{\sqrt{3}} \times 10^{-3} = 208.2 \text{ kN}$$

$$V_{y,fi,Ed} = 33.33 < 0.5 V_{pl,y,fi,Rd} = 0.5 \cdot 208.2 = 104.1 \text{ kN}$$

The effect of shear on the plastic moment resistance does not need to be taken into account.

The plastic resistance to axial load at 552 °C is

$$N_{\bar{f}_i,pl} = Ak_{y,\theta} f_y / \gamma_{M,\bar{f}_i} = 7808 \cdot 0.618 \cdot 235 \times 10^{-3} / 1.0 = 1134 \text{ kN}$$

as

$$N_{\bar{f}_i,Ed} > 0.25 N_{\bar{f}_i,pl} = 283.5 \text{ kN}$$

and

$$\begin{aligned} N_{\bar{f}_i,Ed} &> 0.5 h_w t_w k_{y,\theta} f_y / \gamma_{M,\bar{f}_i} = \\ &= 0.5 \cdot (200 - 2 \cdot 15) \cdot 9 \cdot 0.618 \cdot 235 \times 10^{-3} / 1.0 = 111.0 \text{ kN} \end{aligned}$$

the effect of the axial force on the plastic moment resistance needs to be taken into account (see Section 5.5.9.2).

The plastic moment resistance at 552 °C, is

$$\begin{aligned} M_{pl,y,\bar{f}_i,Rd} &= W_{pl,y} k_{y,\theta} f_y / \gamma_{M,\bar{f}_i} = \\ &= 642.5 \times 10^3 \cdot 0.618 \times 235 \times 10^{-6} / 1.0 = 93.3 \text{ kNm} \end{aligned}$$

$$a = \frac{(A - 2bt_f)}{A} = \frac{7808 - 2 \cdot 200 \cdot 15}{7808} = 0.232 \leq 0.5$$

$$n = \frac{N_{\bar{f}_i,Ed}}{N_{pl,\bar{f}_i,Rd}} = \frac{800}{1134} = 0.706$$

and the design plastic moment resistance reduced due to the axial force $N_{\bar{f}_i,Ed}$ is

$$\begin{aligned} M_{N,y,\bar{f}_i,Rd} &= \frac{(1-n)}{(1-0.5a)} M_{pl,y,\bar{f}_i,Rd} = \frac{(1-0.706)}{(1-0.5 \cdot 0.232)} M_{pl,y,\bar{f}_i,Rd} = \\ &= 0.334 M_{pl,y,\bar{f}_i,Rd} = 0.334 \cdot 93.3 = 31.2 \text{ kNm} \end{aligned}$$

The axial force yields a reduction in the bending resistance of 67%.

The design value of the applied moment is greater than the design plastic moment resistance reduced due to the axial force:

$$M_{\bar{f}_i,Ed} = 50 \text{ kNm} > 31.2 \text{ kNm} \Rightarrow \text{not satisfactory}$$

The critical temperature should be calculated from the cross section verification instead of the member verification. From Eq. (5.128):

$$\begin{aligned}
 k_{y,\theta} &= \frac{N_{\bar{f}i,Ed}}{Af_y/\gamma_{M,\bar{f}i}} + (1-0.5a) \frac{M_{\bar{f}i,Ed}}{W_{pl,y}f_y/\gamma_{M,\bar{f}i}} = \\
 &= \frac{800 \times 10^3}{7808 \cdot 235/1.0} + (1-0.5 \cdot 0.232) \frac{50 \times 10^6}{642.5 \times 10^3 \cdot 235} / 1.0 = 0.729
 \end{aligned}$$

By interpolation in Table 5.2, the following critical temperature is obtained:

$$\theta_{a,cr} = 516.5 \text{ }^\circ\text{C}$$

Check if the applied axial load at this temperature still needs to be taken into account.

The axial plastic resistance load at 516.5 °C is

$$N_{\bar{f}i,pl} = Ak_{y,\theta}f_y/\gamma_{M,\bar{f}i} = 7808 \cdot 0.729 \cdot 235 \times 10^{-3}/1.0 = 1338 \text{ kN}$$

as

$$N_{\bar{f}i,Ed} > 0.25N_{\bar{f}i,pl} = 334.5 \text{ kN}$$

and

$$\begin{aligned}
 N_{\bar{f}i,Ed} &> 0.5h_w t_w k_{y,\theta} f_y / \gamma_{M,\bar{f}i} = \\
 &= 0.5 \cdot (200 - 2 \cdot 15) \cdot 9 \cdot 0.729 \cdot 235 \times 10^{-3} / 1.0 = 131.0 \text{ kN}
 \end{aligned}$$

The temperature of 516.5 °C was calculated in the previous section and the critical temperature to be considered for the beam-column is

$$\theta_{a,cr} = \min(552 \text{ }^\circ\text{C}; 516.5 \text{ }^\circ\text{C}) = 516.5 \text{ }^\circ\text{C}$$

Example 5.10: Class 4 column subjected to axial compression

Consider a 3.2 m high, HE 500 A column in steel grade S460 in an intermediate storey of a braced frame, subjected to an axial compression load. Evaluate the critical temperature of the column for the following axial loads in a fire situation:

a) $N_{\bar{f}i,Ed} = 5460 \text{ kN}$.

b) $N_{\bar{f}i,Ed} = 3520 \text{ kN}$.

Solution

The following geometrical characteristics of the HE 500 A are relevant for the classification of the cross section:

$$h = 490 \text{ mm}$$

$$b = 300 \text{ mm}$$

$$t_w = 12 \text{ mm}$$

$$t_f = 23 \text{ mm}$$

$$r = 27 \text{ mm}$$

$$c = b/2 - t_w/2 - r = 117 \text{ mm (flange)}$$

$$c = h - 2t_f - 2r = 390 \text{ mm (web)}$$

As the steel grade is S460

$$\varepsilon = 0.85\sqrt{235/f_y} = 0.608$$

The class of the flanges in compression is

$$c/t_f = 117/23 = 5.09 < 9\varepsilon = 5.47 \Rightarrow \text{Class 1}$$

The class of the web in compression is

$$c/t_w = 390/12 = 32.5 > 42\varepsilon = 25.5 \Rightarrow \text{Class 4}$$

The cross section of the HE 500 A is Class 4 in pure compression.

242

Part 1.2 of Eurocode 3 suggests a default critical temperature for Class 4 cross section of 350 °C. However the standard allows the critical temperature to be calculated using the conventional proof strength at 0.2% plastic strain rather than the stress at 2% total strain as the yield strength.

Evaluation of the effective cross section:

The effective area of the web in compression is obtained using EN 1993-1-5. At normal temperature the web is Class 4. The web slenderness is given by

$$\bar{\lambda}_p = \sqrt{\frac{f_y}{\sigma_{cr}}} = \frac{\bar{b}/t}{28.4\varepsilon\sqrt{k_\sigma}}$$

where for the case under consideration:

$$\bar{b} = b_w = 390 \text{ mm}$$

$$t = t_w = 12 \text{ mm}$$

$$\varepsilon = \sqrt{235/f_y} = 0.7148 \quad (\text{note this factor is evaluated at normal temperature})$$

$$k_\sigma = 4$$

The diagram of stresses is uniform and so $\psi = 1.0$. Eq. (5.35) for internal compression elements gives:

$$\bar{\lambda}_p = \frac{390/12}{28.4 \cdot 0.7148 \cdot \sqrt{4}} = 0.800 > 0.673$$

and

$$\rho = \frac{\bar{\lambda}_p - 0.055(3 + \psi)}{\bar{\lambda}_p^2}$$

giving

$$\rho = \frac{0.8 - 0.055(3 + 1)}{0.8^2} = 0.906$$

and the effective width of the web, b_{eff} , is

$$b_{eff} = \rho \bar{b} = 0.906 \cdot 390 = 353.3 \text{ mm}$$

The non-effective area of the web is represented in Fig. 5.57:

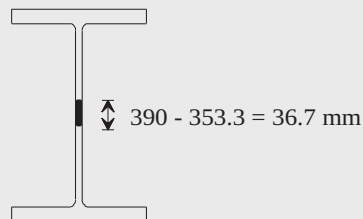


Figure 5.57 – Effective cross section

The effective area is:

$$A_{eff} = A - 36.7 \cdot t_w = 19750 - 36.7 \cdot t_w = 19309.6 \text{ mm}^2$$

The buckling length for an intermediate storey is:

$$l_{fi} = 0.5L = 0.5 \times 3.2 = 1.6 \text{ m.}$$

The second moments of area are:

$$I_y = 86970 \times 10^4 \text{ mm}^4$$

$$I_z = 10370 \times 10^4 \text{ mm}^4$$

and the elastic critical loads about both the major and minor axes are:

$$N_{cr,y} = \frac{\pi^2 EI_y}{l_{fi}^2} = 704123.02 \text{ kN}$$

$$N_{cr,z} = \frac{\pi^2 EI_z}{l_{fi}^2} = 83957.18 \text{ kN}$$

Flexural buckling will occur about the minor axis.

Evaluation of the critical temperature:

The non-dimensional slenderness at elevated temperature is given by Eq. (5.48b)

$$\bar{\lambda}_\theta = \bar{\lambda} \cdot \sqrt{\frac{k_{0.2p,\theta}}{k_{E,\theta}}}$$

where, the non-dimensional slenderness at normal temperature is given by Eq. (5.49b):

$$\bar{\lambda} = \sqrt{\frac{A_{eff} f_y}{N_{cr}}}$$

An iterative procedure is needed to calculate the critical temperature. Starting with a temperature of 20 °C at which $k_{0.2p,\theta} = k_{E,\theta} = 1.0$, equations (5.48b), and (5.49b) give:

$$\bar{\lambda}_\theta = \bar{\lambda} \sqrt{\frac{k_{0.2p,\theta}}{k_{E,\theta}}} = \bar{\lambda} = \sqrt{\frac{A_{eff} f_y}{N_{cr}}} = \sqrt{\frac{19309.6 \cdot 460}{83957180}} = 0.325$$

The reduction factor for the flexural buckling χ_{fi} is evaluated using Eq. (5.45):

$$\alpha = 0.65\sqrt{235/f_y} = 0.65\sqrt{235/460} = 0.4646$$

and

$$\phi = \frac{1}{2}\left(1 + 0.4646 \cdot 0.325 + 0.325^2\right) = 0.628$$

giving the reduction factor for the flexural buckling

$$\chi_{fi} = \frac{1}{0.628 + \sqrt{0.628^2 - 0.325^2}} = 0.857$$

The design value of the buckling resistance $N_{b,fi,0,Rd}$ at time $t = 0$, is obtained from Eq. (5.44):

$$N_{b,fi,0,Rd} = \chi_{fi} A_{eff} k_{0.2p,\theta} f_y / \gamma_{M,fi} = \chi_{fi} A_{eff} f_y / \gamma_{M,fi} = 7612 \text{ kN}$$

and the degree of utilisation takes the value:

$$\mu_0 = \frac{N_{fi,d}}{N_{fi,0,Rd}} = \frac{5460}{7612} = 0.7172$$

By interpolation on the right column of Table 5.2 for the proof strength at 0.2% plastic strain, the following intermediate critical temperature is obtained

$$\theta_{a,cr} = 349 \text{ }^\circ\text{C}.$$

Using this temperature the non-dimensional slenderness $\bar{\lambda}_\theta$ can be corrected, which leads to another critical temperature. The iterative procedure should continue until convergence is reached, as illustrated in the next table:

θ [°C]	$\sqrt{\frac{k_{0.2p,\theta}}{k_{E,\theta}}}$	$\bar{\lambda}_\theta = \frac{\bar{\lambda}}{\sqrt{\frac{k_{0.2p,\theta}}{k_{E,\theta}}}}$	χ_{fi}	$N_{fi,0,Rd} = \chi_{fi} A_{eff} f_y$ [kN]	$\mu_0 = \frac{N_{fi,Ed}}{N_{fi,0,Rd}}$	$\theta_{a,cr}$ [°C]
20	1.00	0.325	0.857	7612	0.7172	349
349	0.977	0.318	0.861	7648	0.7139	351
351	0.976	0.317	0.861	7648	0.7139	351

5. MECHANICAL ANALYSIS

After three iterations a critical temperature of $\theta_{a,cr} = 351 \text{ }^\circ\text{C}$ is obtained.

It should be noted that the critical temperature obtained by calculation is close to the default temperature given in the Eurocode 3. This is because the degree of utilization is high. In most cases the degree of utilization is less than 0.7. If the degree of utilization is less than 0.7 the default critical temperature of $350 \text{ }^\circ\text{C}$ will be conservative, as shown in the next section.

b) For an axial load of $N_{fi,Ed} = 3520 \text{ kN}$, and making similar calculations to the previous section, a critical temperature of $531 \text{ }^\circ\text{C}$ (see iteration sequence below) is obtained.

$\theta \text{ [}^\circ\text{C]}$	$\sqrt{\frac{k_{0.2p,\theta}}{k_{E,\theta}}}$	$\bar{\lambda}_\theta = \frac{\bar{\lambda}}{\sqrt{\frac{k_{0.2p,\theta}}{k_{E,\theta}}}}$	χ_{fi}	$N_{fi,0,Rd} = \chi_{fi} A_{eff} f_y$ [kN]	$\mu_0 = \frac{N_{fi,Ed}}{N_{fi,0,Rd}}$	$\theta_{a,cr} \text{ [}^\circ\text{C]}$
20	1.00	0.325	0.857	7612	0.462	529
529	0.948	0.308	0.865	7700	0.458	531
531	0.948	0.308	0.865	7700	0.458	531

This temperature is much higher than the default temperature of $350 \text{ }^\circ\text{C}$.

Example 5.11: Class 4 beam-column

Consider a $L = 2.7 \text{ m}$ high welded beam-column in steel grade S355, as shown in Fig. 5.58. Assuming that the beam-column is subjected to a uniform bending moment diagram which design value in fire situation is $M_{y,fi,Ed} = 20 \text{ kNm}$ about major axis and to an axial compression force in fire situation of $N_{fi,Ed} = 20 \text{ kN}$ and that the buckling length about the major and minor axis in is $l_{fi} = L = 2700 \text{ mm}$, evaluate:

- the critical temperature of the beam-column;
- the fire resistance of the beam-column at a temperature of $600 \text{ }^\circ\text{C}$.

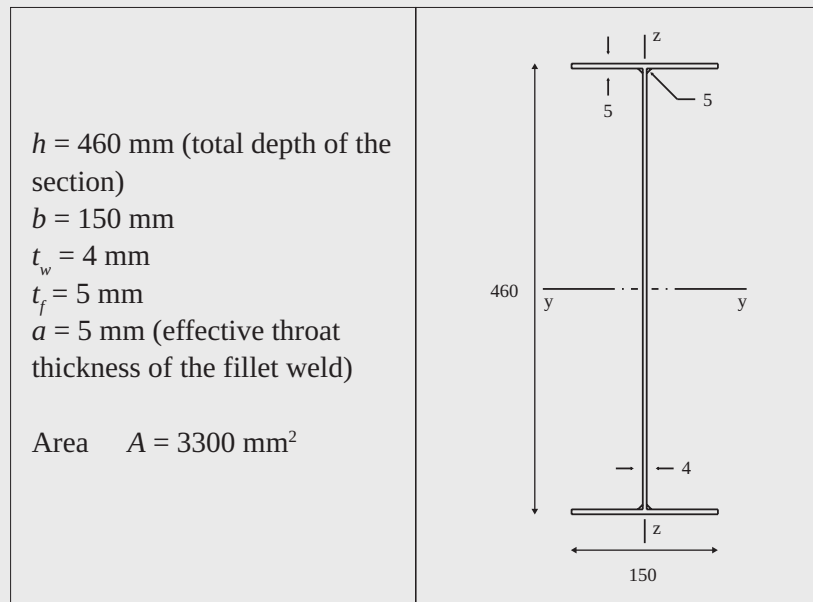


Figure 5.58 – Dimensions of the built up cross section

Solution

To solve this example the following formulae will be used:

- For the fire resistance of the cross section, Eq. (6.44) from EN 1993-1-1 adapted to fire, i. e., Eq. (5.103) from this book:

$$\frac{N_{fi,Ed}}{A_{eff} k_{0.2p,\theta} \frac{f_y}{\gamma_{M,fi}}} + \frac{M_{y,fi,Ed}}{W_{eff,y,min} k_{0.2p,\theta} \frac{f_y}{\gamma_{M,fi}}} \leq 1$$

- For the fire resistance of the beam-column, Eq. (4.21c) and Eq. (4.21d) from EN 1993-1-2, adapted to profiles with class 4 cross sections, i. e., Eq. (5.82c) and Eq. (5.82d) from this book:

$$\frac{N_{fi,Ed}}{\chi_{min,fi} A_{eff} k_{0.2p,\theta} \frac{f_y}{\gamma_{M,fi}}} + \frac{k_y M_{y,fi,Ed}}{W_{eff,y} k_{0.2p,\theta} \frac{f_y}{\gamma_{M,fi}}} \leq 1$$

$$\frac{N_{fi,Ed}}{\chi_{z,fi} A_{eff} k_{0.2p,\theta} \frac{f_y}{\gamma_{M,fi}}} + \frac{k_{LT} M_{y,fi,Ed}}{\chi_{LT,fi} W_{eff,y} k_{0.2p,\theta} \frac{f_y}{\gamma_{M,fi}}} \leq 1$$

a) Fig. 5.59 shows the geometry of a fillet weld.

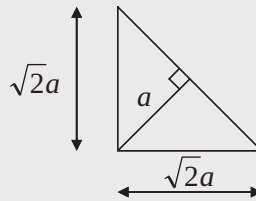


Figure 5.59 – Effective throat thickness of the fillet weld

$$c_f = b/2 - t_w/2 - \sqrt{2} \cdot 5 = 65.93 \text{ mm (flange)}$$

$$c_w = h - 2t_f - 2\sqrt{2} \cdot 5 = 435.86 \text{ mm (web)}$$

As the steel grade is S355

$$\varepsilon = 0.85 \sqrt{235/f_y} = 0.692$$

Classification of cross section

Combined bending about y-y (major axis) and compression:

– The class of the flange in compression is:

$$c_f/t_f = 65.93/5 = 13.16 \text{ mm} > 14\varepsilon = 9.7 \Rightarrow \text{Class 4}$$

– The class of the web in combined bending about y-y (major axis) and compression is:

Class 1 or 2:

$$\alpha = \frac{1}{2} + \frac{N_{Ed}}{2ct_w f_y} = \frac{1}{2} + \frac{20 \times 10^3}{2 \cdot 435.86 \cdot 4 \cdot 355} = 0.516$$

As $\alpha > 0.5$, and

$$c_w/t_w = 435.86/4 = 108.96 > \frac{496\varepsilon}{13\alpha - 1} = 60.13$$

The web is not Class 1 or 2

Class 3:

$$\psi = \frac{2N_{Ed}}{Af_y} - 1 = \frac{2 \cdot 20 \times 10^3}{3300 \cdot 355} - 1 = -0.966$$

$$c_w/t_w = 435.86/4 = 108.96 > 42\varepsilon / (0.67 + 0.33\psi) = 82.8 \Rightarrow \text{Class 4}$$

The cross section of the welded profile is Class 4 in combined bending about y-y (major axis) and compression.

Evaluation of the effective area and effective section modulus:

Effective area:

The effective area of the cross section in pure compression is obtained using EN 1993-1-5.

The normalised slenderness is given by

$$\bar{\lambda}_p = \sqrt{\frac{f_y}{\sigma_{cr}}} = \frac{\bar{b}/t}{28.4\varepsilon\sqrt{k_\sigma}}$$

For the flanges under compression:

$$\bar{b} = c_f = 65.93 \text{ mm}$$

$$t = t_f = 5 \text{ mm}$$

$$\varepsilon = \sqrt{235/f_y} = 0.814 \text{ (note: this factor is evaluated at normal temperature)}$$

$$k_\sigma = 0.43$$

giving

$$\bar{\lambda}_p = \frac{65.93/5}{28.4 \cdot 0.814 \sqrt{0.43}} = 0.87 > 0.748$$

and

$$\rho = \frac{\bar{\lambda}_p - 0.188}{\bar{\lambda}_p^2} = \frac{0.87 - 0.188}{0.87^2} = 0.901$$

5. MECHANICAL ANALYSIS

and the effective width of the flange, b_{eff} , is (see Fig. 5.60 with $\sigma_1 = \sigma_2$):

$$b_{eff} = \bar{\rho} \bar{b} = 0.901 \cdot 65.93 = 59.39 \text{ mm}$$

$$b = 2b_{eff} + t_w + 2\sqrt{2} \cdot 5 = 2 \cdot 59.39 + 4 + 2\sqrt{2} \cdot 5 = 136.93 \text{ mm}$$

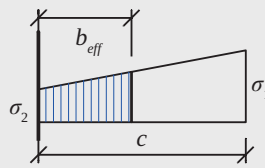


Figure 5.60 – Effective^p width b_{eff} of outstand compression elements (EN 1993-1-5)

For the web under uniform compression ($\psi = 1.0$):

$$\bar{b} = c_w = 435.86 \text{ mm}$$

$$t = t_w = 4 \text{ mm}$$

$$\varepsilon = \sqrt{235/f_y} = 0.814 \text{ (note: this factor is evaluated at normal temperature)}$$

$$k_\sigma = 4$$

250

giving

$$\bar{\lambda}_p = \frac{435.86/4}{28.4 \cdot 0.814 \sqrt{4}} = 2.358 > 0.5 + \sqrt{0.085 - 0.055\psi} = 0.673$$

and

$$\rho = \frac{\bar{\lambda}_p - 0.055(3 + \psi)}{\bar{\lambda}_p^2} = \frac{2.358 - 0.055(3 + 1)}{2.358^2} = 0.385 \leq 1.0$$

and the effective width of the web, b_{eff} , is (see Fig. 5.61):

$$b_{eff} = \bar{\rho} \bar{b} = 0.385 \cdot 435.86 = 167.61 \text{ mm}$$

$$b_{e1} = 0.5b_{eff} = 0.5 \cdot 167.61 = 83.80 \text{ mm}$$

$$b_{e2} = 0.5b_{eff} = 0.5 \cdot 167.61 = 83.80 \text{ mm}$$

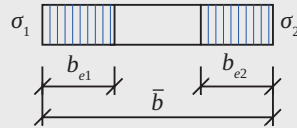


Figure 5.61 – Effective^p width $b_{eff} = b_{e1} + b_{e2}$ of internal compression elements (EN 1993-1-5)

The effective area of the cross section is shown in Fig. 5.62, obtained with the program SteelClass, Couto *et al* (2014).

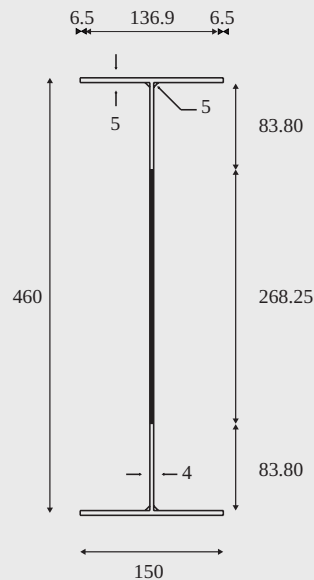


Figure 5.62 – Effective cross section when subjected to uniform compression

$$A_{eff} = A - (268.25 \cdot 4 + 4 \cdot 6.5 \cdot 5) = 2096.28 \text{ mm}^2$$

Effective section modulus y-y (major axis):

The effective section modulus of the cross section in bending about y-y (major axis) is obtained using clause 4.4(3) of EN 1993-1-5: “For flange elements of I-sections and box girders the stress ratio ψ used in Table 4.1 and Table 4.2 should be based on the properties of the gross cross sectional area, due allowance being made for shear lag in the flanges if relevant. For web elements the stress ratio ψ used in Table 4.1 should be obtained using a stress

distribution based on the effective area of the compression flange and the gross area of the web”.

As the flange is under uniform compression, its effective area is the same as the one already obtained when the effective area of the cross section under axial compression was evaluated, i. e.:

$$b_{eff} = \bar{\rho}b = 0.901 \times 65.93 = 59.39 \text{ mm}$$

$$b = 2b_{eff} + t_w + 2\sqrt{2} \cdot 5 = 2 \cdot 59.39 + 4 + 2\sqrt{2} \cdot 5 = 136.93 \text{ mm}$$

Evaluation of the new position of the centre of gravity, considering the effective area of the compression flange and the gross area of the web:

$$A' = A - [(150 - 136.93) \cdot 5] = 3234.646 \text{ mm}^2$$

$$z'_G = \frac{\left(A \cdot \frac{460}{2} \right) - \left[((150 - 136.93) \cdot 5) \cdot \left(460 - \frac{5}{2} \right) \right]}{A'} = 225.40 \text{ mm}$$

where z'_G is the distance from the centre of gravity to the bottom of lower flange.

Evaluation of the stress ratio ψ :

252

$$\psi = \frac{\sigma_2}{\sigma_1} = -\frac{b_t}{b_c}$$

where b_c and b_t are defined in Fig. 5.63 and take the values:

$$b_t = z'_G - t_f - a\sqrt{2} = 225.40 - 5 - 5\sqrt{2} = 213.33 \text{ mm}$$

$$b_c = h - z'_G - t_f - a\sqrt{2} = 460 - 225.40 - 5 - 5\sqrt{2} = 222.53 \text{ mm}$$

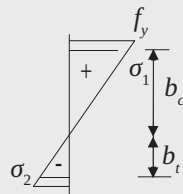


Figure 5.63 – Compression and tension parts of the web

$$\psi = -\frac{b_t}{b_c} = -\frac{213.33}{222.53} = -0.9587$$

$$k_\sigma = 7.81 - 6.29\psi + 9.78\psi^2 = 22.83$$

The normalised slenderness is given by

$$\bar{\lambda}_p = \sqrt{\frac{f_y}{\sigma_{cr}}} = \frac{\bar{b}/t}{28.4\varepsilon\sqrt{k_\sigma}}$$

and

$$\bar{\lambda}_p = \frac{435.86/4}{28.4 \cdot 0.814 \sqrt{22.83}} = 0.987 > 0.5 + \sqrt{0.085 - 0.055\psi} = 0.871$$

and

$$\rho = \frac{\bar{\lambda}_p - 0.055(3 + \psi)}{\bar{\lambda}_p^2} = \frac{0.987 - 0.055(3 + (-0.9587))}{0.987^2} = 0.898 \leq 1.0$$

and the effective width of the web, b_{eff} , is (see Fig. 5.64):

$$b_{eff} = \rho b_c = \rho c_w / (1 - \psi) = 0.898 \cdot 435.86 / (1 - (-0.9587)) = 199.82 \text{ mm}$$

$$b_{e1} = 0.4b_{eff} = 0.4 \cdot 199.82 = 79.93 \text{ mm}$$

$$b_{e2} = 0.6b_{eff} = 0.6 \cdot 199.82 = 119.89 \text{ mm}$$

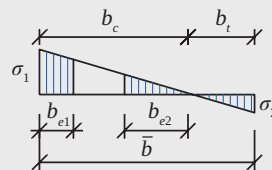


Figure 5.64 – Effective^p width $b_{eff} = b_{e1} + b_{e2}$ of internal compression elements (EN 1993-1-5)

The length of the non-effective area of the web is:

$$b = b_c - b_{e1} - b_{e2} = 222.53 - 79.93 - 119.89 = 22.71 \text{ mm}$$

The new position of the centre of gravity should be evaluated:

$$A'' = A - (150 - 136.93) \cdot 5 - 22.71 \cdot 4 = 3143.846 \text{ mm}^2$$

$$z''_G = \frac{\left(A \cdot \frac{460}{2} \right) - \left[(150 - 136.93) \cdot 5 \cdot \left(460 - \frac{5}{2} \right) \right]}{A''} - \frac{\left[22.71 \cdot 4 \cdot \left(460 - 5 - \sqrt{2} \cdot 5 - 79.93 - \frac{22.71}{2} \right) \right]}{A''}$$

$$= 221.6 \text{ mm}$$

The effective area of the cross section under bending about the major axis is depicted in Fig. 5.65, obtained with the program SteelClass, Couto *et al* (2014), where $209.5 = 221.6 - t_f - \sqrt{2}a$.

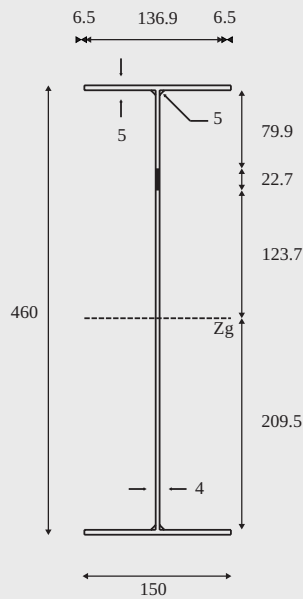


Figure 5.65 – Effective cross section when subjected only to moment about the major axis

The second moment of area of the effective cross section when subjected only to moment, takes the value:

$$I_{eff,y} = 102947672 \text{ mm}^4$$

and the effective section modulus is

$$W_{eff,y,\min} = \min\left(\frac{I_{eff,y}}{z''_G}; \frac{I_{eff,y}}{h - z''_G}\right) = 431848 \text{ mm}^3$$

Evaluation of the critical temperature

As the bending moment diagram along the member is uniform the cross sectional capacity is not more critical than the overall stability of the member. Although it is not necessary, in this case, to check the resistance of the cross section, this verification will be done here as an example.

Cross sectional verification

The collapse occurs, when

$$\frac{N_{fi,Ed}}{A_{eff} k_{0.2p,\theta} \frac{f_y}{\gamma_{M,fi}}} + \frac{M_{y,fi,Ed}}{W_{eff,y,\min} k_{0.2p,\theta} \frac{f_y}{\gamma_{M,fi}}} = 1$$

from where it is possible to obtain the value of the reduction factor for the 0.2% proof strength of steel, $k_{0.2p,\theta}$ at collapse.

$$k_{0.2p,\theta} = \frac{N_{fi,Ed}}{A_{eff} \frac{f_y}{\gamma_{M,fi}}} + \frac{M_{y,fi,Ed}}{W_{eff,y,\min} \frac{f_y}{\gamma_{M,fi}}}$$

Substituting values in this equation, comes

$$k_{0.2p,\theta} = \frac{N_{fi,Ed}}{A_{eff} \frac{f_y}{\gamma_{M,fi}}} + \frac{M_{y,fi,Ed}}{W_{eff,y,\min} \frac{f_y}{\gamma_{M,fi}}} = \frac{20}{744.18} + \frac{20}{153.31} = 0.157$$

By interpolation on Table 5.2 of this book or in Table E.1 of EN1993-1-2 for the proof strength at 0.2% plastic strain, the following critical temperature is obtained

$$\theta_{a,cr} = 684 \text{ }^\circ\text{C}$$

Buckling resistance of the beam-column

The buckling length is:

$$l_{\bar{f}} = L = 2700 \text{ mm}$$

The non-dimensional slenderness at elevated temperature is given by:

$$\bar{\lambda}_{\theta} = \bar{\lambda} \cdot \sqrt{\frac{k_{0.2p,\theta}}{k_{E,\theta}}}$$

This non-dimensional slenderness depends on the temperature and an iterative procedure is needed to calculate the critical temperature. Starting with a temperature of 20 °C at which $k_{0.2p,\theta} = k_{E,\theta} = 1.0$, the non-dimensional slenderness for flexural buckling and for lateral-torsional buckling:

$$\bar{\lambda}_{20^{\circ}\text{C}} = \bar{\lambda} = \sqrt{\frac{A_{eff} f_y}{N_{cr}}}$$

$$\bar{\lambda}_{LT,20^{\circ}\text{C}} = \bar{\lambda}_{LT} = \sqrt{\frac{W_{eff} f_y}{M_{cr}}}$$

where the Euler critical load

256

$$\text{– about the major axis: } N_{cr,y} = \frac{\pi^2 EI_y}{l_{\bar{f}}^2} = \frac{\pi^2 \cdot 210 \cdot 108012500}{2700^2} = 30709 \text{ kN}$$

$$\text{– about the minor axis: } N_{cr,z} = \frac{\pi^2 EI_z}{l_{\bar{f}}^2} = \frac{\pi^2 \cdot 210 \cdot 2814900}{2700^2} = 800 \text{ kN}$$

and the elastic critical moment assuming is given by Eq. (5.73) with $C_1 = 1.0$

$$\text{– } M_{cr} = C_1 \frac{\pi^2 EI_z}{L^2} \sqrt{\frac{I_w}{I_z} + \frac{L^2 GI_t}{\pi^2 EI_z}} = 185.875 \text{ kNm}$$

coming

$$\text{– } \bar{\lambda}_{y,20^{\circ}\text{C}} = \bar{\lambda}_y = \sqrt{\frac{A_{eff} f_y}{N_{cr,y}}} = 0.156$$

$$- \bar{\lambda}_{z,20^{\circ}\text{C}} = \bar{\lambda}_z = \sqrt{\frac{A_{\text{eff}} f_y}{N_{\text{cr},z}}} = 0.964$$

$$- \bar{\lambda}_{LT,20^{\circ}\text{C}} = \bar{\lambda}_{LT} = \sqrt{\frac{W_{\text{eff},y} f_y}{M_{\text{cr}}}} = 0.908$$

The reduction factor for the flexural buckling χ_{fi} and lateral-torsional buckling $\chi_{LT,fi}$ are evaluated using:

$$\alpha = 0.65 \cdot \sqrt{235/f_y} = 0.65 \cdot \sqrt{235/355} = 0.529$$

The reduction factors for flexural buckling χ_{fi} at normal temperature are:

– about the major axis:

$$\phi_{y,20^{\circ}\text{C}} = \frac{1}{2} \left[1 + \alpha \bar{\lambda}_{y,20^{\circ}\text{C}} + \bar{\lambda}_{y,20^{\circ}\text{C}}^2 \right] = 0.553$$

and

$$\chi_{y,20^{\circ}\text{C}} = \frac{1}{\phi_{y,20^{\circ}\text{C}} + \sqrt{\phi_{y,20^{\circ}\text{C}}^2 - \bar{\lambda}_{y,20^{\circ}\text{C}}^2}} = 0.922$$

– about the minor axis:

$$\phi_{z,20^{\circ}\text{C}} = \frac{1}{2} \left[1 + \alpha \bar{\lambda}_{z,20^{\circ}\text{C}} + \bar{\lambda}_{z,20^{\circ}\text{C}}^2 \right] = 1.220$$

and

$$\chi_{z,20^{\circ}\text{C}} = \frac{1}{\phi_{z,20^{\circ}\text{C}} + \sqrt{\phi_{z,20^{\circ}\text{C}}^2 - \bar{\lambda}_{z,20^{\circ}\text{C}}^2}} = 0.508$$

The reduction factor for lateral-torsional buckling $\chi_{LT,fi}$ at normal temperature is:

$$\phi_{LT,20^{\circ}\text{C}} = \frac{1}{2} \left[1 + \alpha \bar{\lambda}_{LT,20^{\circ}\text{C}} + \bar{\lambda}_{LT,20^{\circ}\text{C}}^2 \right] = 1.153$$

and

$$\chi_{LT,20^{\circ}\text{C}} = \frac{1}{\phi_{LT,20^{\circ}\text{C}} + \sqrt{\phi_{LT,20^{\circ}\text{C}}^2 - \bar{\lambda}_{LT,20^{\circ}\text{C}}^2}} = 0.537$$

Considering Eq. (5.82c) the collapse occurs when the reduction factor for the 0.2% proof strength of steel, $k_{0.2p,\theta}$ takes the value:

$$k_{0.2p,\theta} = \frac{N_{fi,Ed}}{\chi_{\min,fi} A_{eff} \frac{f_y}{\gamma_{M,fi}}} + \frac{k_y M_{y,fi,Ed}}{W_{eff,y} \frac{f_y}{\gamma_{M,fi}}}$$

where

$$k_y = 1 - \frac{\mu_y N_{fi,Ed}}{\chi_{y,fi} A_{eff} k_{0.2p,\theta} \frac{f_y}{\gamma_{M,fi}}} \leq 3$$

with

$$\mu_y = (2\beta_{M,y} - 5)\bar{\lambda}_{y,\theta} + 0.44\beta_{M,y} + 0.29 \leq 0.8 \quad \text{with} \quad \bar{\lambda}_{y,20^\circ\text{C}} \leq 1.1$$

For a uniform bending diagram $\beta_{M,y}$ takes the value, with $\psi = 1$

$$\beta_{M,y} = 1.8 - 0.7\psi = 1.8 - 0.7 \times 1.0 = 1.1$$

and so

$$\mu_y = (2 \cdot 1.1 - 5) \cdot 0.156 + 0.44 \cdot 1.1 + 0.29 = 0.338$$

258

and

$$k_y = 1 - \frac{\mu_y N_{fi,Ed}}{\chi_{y,fi} A_{eff} k_{0.2p,\theta} \frac{f_y}{\gamma_{M,fi}}} = 0.990$$

From which the degree of utilization is:

$$k_{0.2p,\theta} = \frac{N_{fi,Ed}}{\chi_{\min,fi} A_{eff} \frac{f_y}{\gamma_{M,fi}}} + \frac{k_y M_{y,fi,Ed}}{W_{eff,y} \frac{f_y}{\gamma_{M,fi}}} = 0.182$$

By interpolation on the Table 5.2 for the proof strength at 0.2% plastic strain, the following intermediate critical temperature is obtained

$$\theta_{a,cr} = 669 \text{ } ^\circ\text{C}$$

The non-dimensional slenderness at elevated temperature is a function of the temperature and the following iterative procedure is needed:

θ [°C]	$\bar{\lambda}_{y,\theta}$	$\bar{\lambda}_{z,\theta}$	$\chi_{\min,fi}$	k_y	$k_{0.2p,\theta}$	$\theta_{a,cr}$ [°C]
20	0.156	0.964	0.508	0.990	0.182	669
669	0.155	0.956	0.512	0.943	0.176	673
673	0.155	0.956	0.512	0.943	0.176	673

After two iterations a critical temperature of $\theta_{a,cr} = 673$ °C is obtained.

Considering now Eq. (5.82d) the collapse occurs when the reduction factor for the 0.2% proof strength of steel, $k_{0.2p,\theta}$ takes the value:

$$k_{0.2p,\theta} = \frac{N_{fi,Ed}}{\chi_{z,fi} A_{eff} \frac{f_y}{\gamma_{M,fi}}} + \frac{k_{LT} M_{y,fi,Ed}}{\chi_{LT,fi} W_{eff,y} \frac{f_y}{\gamma_{M,fi}}}$$

where

$$k_{LT} = 1 - \frac{\mu_{LT} N_{fi,Ed}}{\chi_{z,fi} A_{eff} k_{0.2p,\theta} \frac{f_y}{\gamma_{M,fi}}} \leq 1$$

with

$$\mu_{LT} = 0.15 \bar{\lambda}_{z,\theta} \beta_{M,LT} - 0.15 \leq 0.9$$

For a uniform bending diagram $\beta_{M,LT}$ takes the value, with $\psi = 1$

$$\beta_{M,LT} = 1.8 - 1.7\psi = 1.8 - 1.7 \times 1.0 = 1.1$$

and so

$$\mu_y = 0.15 \cdot 0.964 \cdot 1.1 - 0.15 = 0.0096$$

and

$$k_{LT} = 1 - \frac{\mu_{LT} N_{fi,Ed}}{\chi_{z,fi} A_{eff} k_{0.2p,\theta} \frac{f_y}{\gamma_{M,fi}}} = 0.9995$$

coming

$$k_{0.2p,\theta} = \frac{N_{fi,Ed}}{\chi_{z,fi} A_{eff} \frac{f_y}{\gamma_{M,fi}}} + \frac{k_{LT} M_{y,fi,Ed}}{W_{eff,y} \frac{f_y}{\gamma_{M,fi}}} = 0.2957$$

By interpolation on the Table 5.2 for the proof strength at 0.2% plastic strain, the following intermediate critical temperature is obtained

$$\theta_{a,cr} = 603 \text{ }^{\circ}\text{C}$$

The non-dimensional slenderness at elevated temperature is a function of the temperature and the following iterative procedure is needed:

θ [°C]	$\bar{\lambda}_{z,\theta}$	$\bar{\lambda}_{LT,\theta}$	$\chi_{z,fi}$	$\chi_{LT,fi}$	μ_{LT}	k_{LT}	$k_{0.2p,\theta}$	$\theta_{a,cr}$ [°C]
20	0.964	0.908	0.508	0.573	0.0096	1.000	0.296	603
602	0.948	0.893	0.517	0.545	0.0064	0.999	0.291	605
605	0.949	0.895	0.516	0.544	0.0067	0.999	0.292	605

After two iterations a critical temperature of $\theta_{a,cr} = 605 \text{ }^{\circ}\text{C}$ is obtained.

The critical temperature of the beam-column should be

$$\theta_{a,cr} = \min(684 \text{ }^{\circ}\text{C}; 673 \text{ }^{\circ}\text{C}; 605 \text{ }^{\circ}\text{C}) = 605 \text{ }^{\circ}\text{C}$$

b) At 600 °C the reduction factor for the 0.2% proof strength of steel, $k_{0.2p,\theta}$ takes the value:

$$k_{0.2p,\theta} = 0.30$$

– Cross section verification

Substituting the value of $k_{0.2p,\theta}$ in the equation

$$\frac{N_{fi,Ed}}{A_{eff} k_{0.2p,\theta} \frac{f_y}{\gamma_{M,fi}}} + \frac{M_{y,fi,Ed}}{W_{eff,y,\min} k_{0.2p,\theta} \frac{f_y}{\gamma_{M,fi}}} \leq 1$$

it comes:

$$0.524 < 1$$

which means that the cross section of the beam-column resists to a temperature of 600 °C.

– Buckling verification of the beam-column

Substituting the value of $k_{0.2p,\theta}$ in the equation

$$\frac{N_{fi,Ed}}{\chi_{\min,fi} A_{eff} k_{0.2p,\theta} \frac{f_y}{\gamma_{M,fi}}} + \frac{k_y M_{y,fi,Ed}}{W_{eff,y} k_{0.2p,\theta} \frac{f_y}{\gamma_{M,fi}}} \leq 1$$

it comes:

$$0.594 < 1$$

Substituting the value of $k_{0.2p,\theta}$ in the equation

$$\frac{N_{fi,Ed}}{\chi_{z,fi} A_{eff} k_{0.2p,\theta} \frac{f_y}{\gamma_{M,fi}}} + \frac{k_{LT} M_{y,fi,Ed}}{\chi_{LT} W_{eff,y} k_{0.2p,\theta} \frac{f_y}{\gamma_{M,fi}}} \leq 1$$

it comes:

$$0.971 < 1$$

which means that the buckling resistance of the beam-column is verified at a temperature of 600 °C.

Example 5.12: Three-span continuous beam

Consider a three-span continuous beam in an office building, with equal spans of 6.0 m, constructed from an IPE 300 section in S235 grade steel, as shown in the Fig. 5.66. The beam is subjected to a permanent uniform load of $G_k = 20$ kN/m (including the weight of the profile) and a live load of $Q_k = 8$ kN/m.

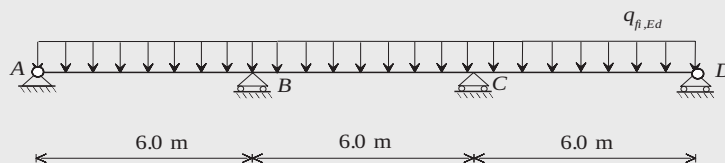


Figure 5.66 – Continuous beam

Assuming that the out of plane displacements are restrained and that the beam is unprotected and supports a concrete slab, evaluate the critical temperature using the following procedure:

- The forces are obtained using elastic analysis.
- The forces are obtained using global plastic analysis.

Solution

According to Section 2.1.1, the load in the fire situation, taking $\psi_{fi} = \psi_2$, is

$$q_{fi,Ed} = G_k + \psi_2 Q_k = 20 + 0.3 \cdot 8 = 22.4 \text{ kN/m}$$

This value could be obtained by multiplying the load at normal temperature, q_{Ed} , by the reduction factor for the design load in fire situation, η_{fi} , evaluated as

$$\eta_{fi} = \frac{G_k + \psi_{fi} Q_k}{\gamma_g G_k + \gamma_Q Q_k} = \frac{20 + 0.3 \cdot 8}{1.35 \cdot 20 + 1.5 \cdot 8} = 0.574$$

The load at normal temperature is

$$q_{Ed} = \gamma_G G_k + \gamma_Q Q_k = 1.35 \cdot 20 + 1.5 \cdot 8 = 39 \text{ kN/m}$$

and so

$$q_{fi,Ed} = \eta_{fi} q_{Ed} = 0.574 \cdot 39 = 22.4 \text{ kN/m}$$

It should be noted that the reduction factor for the design load in the fire situation is lower than the value of 0.65 recommended by the Eurocode, which leads to more economical results.

The relevant geometric characteristics of the profile are

$$h = 300 \text{ mm}$$

$$b = 150 \text{ mm}$$

$$t_w = 7.1 \text{ mm}$$

$$t_f = 10.7 \text{ mm}$$

$$r = 15 \text{ mm}$$

$$A = 5381 \text{ mm}^2$$

$$W_{pl,y} = 628400 \text{ mm}^3$$

The cross section of the IPE 300 in bending is Class 1 (see example 5.2).

a) Elastic design

The elastic bending diagram and the shear forces at the supports are shown in Fig. 5.67.

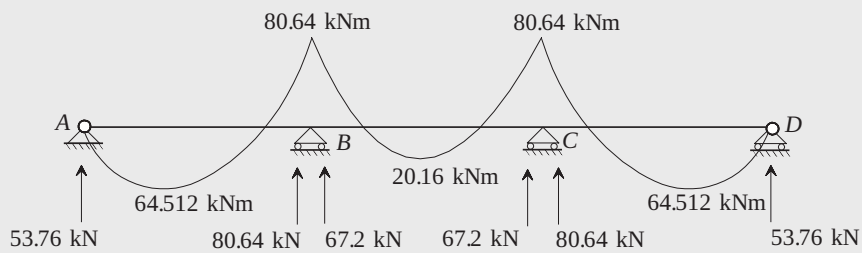


Figure 5.67 – Bending diagram and shear forces

Critical temperature only considering the moment at the intermediate support:

The design value of the resistance moment at time $t = 0$, $M_{fi,0,Rd}$, according to Eq. (5.64), is

$$M_{fi,0,Rd} = W_{pl,y} f_y / (k_1 k_2) \gamma_{M,fi}$$

where:

$k_1 = 0.7$ for unprotected beam exposed on three sides, with a concrete slab on the side four ;

$k_2 = 0.85$ for a section at the supports.

and so

$$M_{fi,0,Rd} = \frac{W_{pl,y} f_y}{k_1 k_2 \gamma_{M,fi}} = \frac{628400 \cdot 235}{0.7 \cdot 0.85 \cdot 1.0} \times 10^{-6} = 248.2 \text{ kNm}$$

The degree of utilisation takes the value

$$\mu_0 = \frac{M_{fi,Ed}}{M_{fi,0,Rd}} = \frac{80.64}{248.2} = 0.325$$

By interpolation in Table 5.2 the critical temperature is

$$\theta_{a,cr} = 661^\circ \text{C}$$

Critical temperature only considering the shear force at the support:

The design value of the resistance shear force at time $t = 0$, $V_{fi,0,Rd}$, according to Eq. (5.55), is

$$V_{fi,0,Rd} = \frac{A_v f_y}{\sqrt{3} \gamma_{M,fi}}$$

The shear area of the IPE 300 is

$$\begin{aligned} A_v &= A - 2bt_f + (t_w + 2r)t_f \\ &= 5381 - 2 \cdot 150 \cdot 10.7 + (7.1 + 2 \cdot 15)10.7 = 2567 \text{ mm}^2 \end{aligned}$$

and so

$$V_{fi,0,Rd} = \frac{A_v f_y}{\sqrt{3} \gamma_{M,fi}} = \frac{2567 \cdot 235}{\sqrt{3} \cdot 1.0} \times 10^{-3} = 348.28 \text{ kN}$$

The degree of utilisation takes the value

$$\mu_0 = \frac{V_{fi,Ed}}{V_{fi,0,Rd}} = \frac{80.64}{348.28} = 0.232$$

By interpolation in Table 5.2 the critical temperature is

$$\theta_{a,cr} = 699.4 \text{ }^\circ\text{C}$$

264

Critical temperature due to combined bending and shear:

Assuming that the effect of the shear force must be taken into account in the design value of the resistance moment, i.e., that $V_{fi,Ed} > 0.5 V_{fi,t,Rd}$, at collapse according to Eq. (5.126)

$$M_{fi,Ed} = M_{y,v,fi,Rd} = \frac{\left[W_{pl,y} - \left(\frac{2V_{fi,Ed}}{\frac{A_v k_{y,\theta} f_y}{\sqrt{3} \gamma_{M,fi}}} - 1 \right) \frac{A_w^2}{4t_w} \right] k_{y,\theta} f_y}{k_1 k_2 \gamma_{M,fi}}$$

The unknown in this equation is the reduction factor for the yield strength, $k_{y,\theta}$. By mathematical manipulation it is

$$k_{y,\theta} = 0.336$$

By interpolation in Table 5.2, the critical temperature is

$$\theta_{a,cr} = 656 \text{ }^\circ\text{C}$$

At this temperature the shear resistance is

$$V_{pl,fi,Rd} = \frac{A_v k_{y,\theta} f_y}{\sqrt{3} \gamma_{M,fi}} = \frac{2567 \cdot 0.336 \cdot 235}{\sqrt{3} \cdot 1.0} \times 10^{-3} = 117.0 \text{ kN}$$

and

$$V_{pl,fi,Rd} > V_{fi,Ed} \text{ OK.}$$

and

$$V_{fi,Ed} > 0.5V_{pl,fi,Rd}$$

and the assumption that the effect of the shear force should be taken into account was correct.

The critical temperature is the smallest of the three calculated temperatures:

$$\theta_{a,cr} = \min(660.5 \text{ }^\circ\text{C}; 699.4 \text{ }^\circ\text{C}; 656 \text{ }^\circ\text{C}) = 656 \text{ }^\circ\text{C}$$

It can be concluded that the critical temperature is due to the interaction between bending moment and shear.

Verification in the span

As the ratio between the maximum positive moment in the span (see Fig. 5.67) and the negative moment at the intermediate support is less than 0.85, there is no need to verify the fire resistance in the span.

b) Plastic design

i) End span

According to Eq. (5.151) the reduction factor for the yield strength is

$$k_{y,\theta} = \left[\frac{l^2}{2} - \left(-0.85 + \sqrt{0.85^2 + 0.85} \right) l^2 \right] q_{fi,Ed} \frac{0.85 k_1 \gamma_{M,fi}}{W_{pl,y} f_y} = 0.312$$

With this reduction factor interpolating in Table 5.2 leads to the critical temperature

$$\theta_{a,cr} = 665.8 \text{ }^{\circ}\text{C}$$

At this temperature, the resistance moment at the intermediate support and the resistance shear force are

$$M_{fi,Rd} = \frac{W_{pl,y} k_y \theta f_y}{k_1 k_2 \gamma_{M,fi}} = \frac{628400 \cdot 0.312 \cdot 235}{0.7 \cdot 0.85 \cdot 1.0} \times 10^{-6} = 77.4 \text{ kNm}$$

and

$$V_{pl,fi,Rd} = \frac{A_v k_y \theta f_y}{\sqrt{3} \gamma_{M,fi}} = \frac{2567 \cdot 0.312 \cdot 235}{\sqrt{3} \cdot 1.0} \times 10^{-3} = 108.7 \text{ kN}$$

The reaction at the right support is

$$V_{fi,Ed} = \frac{q_{fi,Ed} \cdot l}{2} + \frac{M_{left} - M_{right}}{l} = \frac{22.4 \cdot 6}{2} + \frac{0 - (-77.4)}{6} = 80.1 \text{ kN}$$

This reaction is more than half of the resistance shear force at 665.8 °C, $0.5V_{pl,fi,Rd} = 0.5 \cdot 108.7 = 54.4 \text{ kN}$. The resistance moment at the intermediate support must be reduced due to the effect of the shear force. An iterative procedure, not easily done by hand calculation, must be carried out. This iterative procedure, implemented in the program Elefir-EN, presented in Chapter 8, gives a critical temperature of

$$\theta_{a,cr} = 664 \text{ }^{\circ}\text{C}$$

ii) Intermediate span

According to Eq. (5.154) with $k_2 = 0.85$, the reduction factor for the yield strength is

$$k_{y,\theta} = \frac{q_{fi,Ed} l^2}{8} \frac{0.85 k_1 \gamma_{M,fi}}{1.85 W_{pl,y} f_y} = 0.2197$$

With this reduction factor, interpolating in Table 5.2 leads to the critical temperature

$$\theta_{a,cr} = 708.6 \text{ }^{\circ}\text{C}$$

At this temperature, the resistance moment at the intermediate support and the resistance shear force are

$$M_{fi,Rd} = \frac{W_{pl,y} k_y f_y}{k_1 k_2 \gamma_{M,fi}} = \frac{628400 \cdot 0.2197 \cdot 235}{0.7 \cdot 0.85 \cdot 1.0} \times 10^{-6} = 54.53 \text{ kNm}$$

and

$$V_{pl,fi,Rd} = \frac{A_v k_y f_y}{\sqrt{3} \gamma_{M,fi}} = \frac{2567 \cdot 0.2197 \cdot 235}{\sqrt{3} \cdot 1.0} \times 10^{-3} = 76.52 \text{ kN}$$

The reaction at the intermediate supports is

$$V_{fi,Ed} = \frac{q_{fi,Ed} \cdot l}{2} + \frac{M_{right} - M_{left}}{l} = \frac{22.4 \cdot 6}{2} + \frac{-54.53 - (-54.53)}{6} = 67.2 \text{ kN}$$

This reaction is more than half of the resistance shear force at 708.6 °C, $0.5V_{pl,fi,Rd} = 0.5 \cdot 76.52 = 38.26 \text{ kN}$. The resistance moment at the intermediate support must be reduced due to the effect of the shear force. Again an iterative procedure must be performed. This iterative procedure, implemented in the program Elefir-EN, presented in Chapter 8, gives a critical temperature of

$$\theta_{a,cr} = 699.3 \text{ °C}$$

The critical temperature of the continuous beam is the lowest from the temperature of the two analysed spans:

$$\theta_{a,cr} = \min(664 \text{ °C}; 699.3 \text{ °C}) = 664 \text{ °C}$$

Final note:

The following table compares the critical temperatures obtained by elastic and plastic analyse.

Critical temperature, $\theta_{a,cr}$ [°C]		
Elastic analysis	Plastic analysis	%
656	664	+ 1.2

% - Gain with plastic design.

Contrary to what usually happens at normal temperature, in fire situation, plastic design is not as beneficial.

The first reason is the factor k_2 that leads to a multiplication of the bending resistance on the intermediate supports by $1/0.85 = 1.18$. This leads to the fact that the ratio between bending strength at the support and in the span is very close to the ratio between elastic bending moment at the first support and in the first span ($=1.25$, see Fig. 5.67). The plastic hinges thus develop nearly simultaneously and there is very limited possibility for load redistribution. It can be noted that, for the same continuous beam at normal temperature, the increase of the resistance to a uniform load is 16.57% and, as usually at normal temperature, the interaction with shear does not need be considered.

The second reason is the fact that, if the temperature is slightly increased by a plastic redistribution, this is accompanied by a reduction of the shear capacity and the interaction between shear and bending moment can become more critical at the intermediate supports.

The benefit of plastic load redistribution can be greater for other configurations of span and/or loading.

Example 5.13: Member subjected to combined bending and tension

Consider an HE 200 A section in S355 grade steel subjected to tension and major axis end moments as shown in Fig. 5.68.

- Evaluate the critical temperature.
- Verify the fire resistance of the member after 30 minutes of standard fire exposure on four sides.

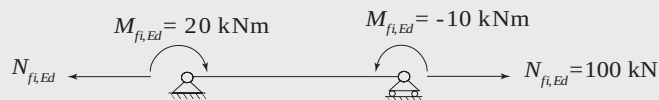


Figure 5.68 – Combined bending and tension

Solution:

The evaluation of the resistance of a member subject to combined bending and tension should be made at the level of the cross section. If the tension force is too small, it is sometimes advisable to check the effect of the lateral-torsional buckling if it is not prevented. Neglecting the tension force and checking bending for lateral-torsional buckling, is safe and good practice.

Part 1.2 of Eurocode 3 doesn't make reference to the case when members are subjected to combined bending and tension. However, based on Clause 1.1.2, the method in Part 1.1 of Eurocode 3 is adapted for use at elevated temperature.

The relevant geometric characteristics of the profile are

$$\begin{aligned}
 h &= 190 \text{ mm} \\
 b &= 200 \text{ mm} \\
 t_w &= 6.5 \text{ mm} \\
 t_f &= 10 \text{ mm} \\
 h_w &= 200 - 2 \cdot 10 = 180 \text{ mm} \\
 r &= 18 \text{ mm} \\
 A &= 5380 \text{ mm}^2 \\
 W_{el,y} &= 388600 \text{ mm}^3 \\
 W_{pl,y} &= 429500 \text{ mm}^3 \\
 c &= b/2 - t_w/2 - r = 78.75 \text{ mm (flange)} \\
 c &= h - 2t_f - 2r = 134 \text{ mm (web)}
 \end{aligned}$$

269

As the steel grade is S355

$$\varepsilon = 0.85 \sqrt{355/f_y} = 0.6916$$

Evaluation of the elastic stresses at the extreme fibre of the cross section on the left hand-side support shows that the section is in compression (+) and in tension (-):

$$\sigma_{x,fi,Ed} = \frac{N_{fi,Ed}}{A} \pm \frac{M_{fi,Ed}}{W_{el,y}} = \begin{cases} -70.05 \text{ MPa} \\ +32.88 \text{ MPa} \end{cases}$$

The class of the flange in compression is

$$c/t_f = 78.75/10 = 7.875 < 14\varepsilon = 9.68 \Rightarrow \text{Class 3}$$

The class of the web in combined bending and tension, according Eq. (5.17) is:

$$\alpha = \frac{1}{2} + \frac{N_{fi,Ed}}{2ct_w f_y} = 0.5 + \frac{-100000}{2 \cdot 134 \cdot 6.5 \cdot 355} = 0.3383$$

$$c/t_w = 134/6.5 = 20.6 < \frac{36\epsilon}{\alpha} = 36.0 \Rightarrow \text{Class 1}$$

The cross section of the HE 200 A in combined bending and tension in fire situation is Class 3.

a) Base on Eq. (5.91), the highest elastic stress at the extreme fibre must verify the following equation, at the collapse:

$$\sigma_{x,fi,Ed} = \frac{N_{fi,Ed}}{A} + \frac{M_{y,fi,Ed}}{W_{y,el}} = \frac{k_{y,\theta} f_y}{\gamma_{M,fi}}$$

From this equation the reduction factor for the yield strength is

$$k_{y,\theta} = \frac{N_{fi,Ed}}{A f_y / \gamma_{M,fi}} + \frac{M_{fi,Ed}}{W_{el,y} f_y / \gamma_{M,fi}}$$

$$k_{y,\theta} = \frac{100000}{5380 \cdot 355 / 1.0} + \frac{20 \times 10^6}{388600 \cdot 355 / 1.0} = 0.19734$$

Interpolating in Table 5.2, gives a critical temperature of:

$$\theta_{a,cr} = 727.2 \text{ } ^\circ\text{C}$$

b) The uniform temperature of the profile after 30 minutes of standard fire exposure was evaluated in Example 4.3 of Chapter 4 as:

$$\theta_a = 802 \text{ } ^\circ\text{C}$$

Because the temperature in the member is higher than the critical temperature calculated above, it can be concluded that the fire resistance of 30 minutes is not achieved. The example will nevertheless be continued, assuming that the critical temperature has not been calculated.

For this temperature the reduction factor for the yield strength is, from Table 5.2:

$$k_{y,\theta} = 0.11$$

As the section is Class 3 Eq. (5.91) must be verified:

$$\sigma_{x,fi,Ed} = \frac{N_{fi,Ed}}{A} + \frac{M_{y,fi,Ed}}{W_{y,el}} \leq \frac{k_{y,\theta} f_y}{\gamma_{M,fi}}$$

or

$$\frac{N_{fi,Ed}}{A k_{y,\theta} f_y / \gamma_{M,fi}} + \frac{M_{y,fi,Ed}}{W_{y,el} k_{y,\theta} f_y / \gamma_{M,fi}} \leq 1.0$$

Since

$$\frac{100000}{5380 \cdot 0.11 \cdot 355 / 1.0} + \frac{20 \times 10^6}{388600 \cdot 0.11 \cdot 355 / 1.0} = 1.79 > 1.0$$

the member has no fire resistance after 30 minutes of standard fire exposure. The profile should be changed or fire protection should be used.

Example 5.14: Laterally restrained stainless steel beam

Suppose that a welded section equivalent to the IPE 300 of the Example 5.2 is made of Grade 1.4301 stainless steel. What is the critical temperature if it is subjected to the same bending moment of $M_{fi,Ed} = 67.6$ kNm and what is the time needed to reach the critical temperature if the profile is unprotected and exposed to the ISO 834 fire curve as in Example 5.2?

Solution:

For the Grade 1.4301 stainless steel:

$$f_y = 210 \text{ N/mm}^2$$

$$E = 200\,000 \text{ N/mm}^2$$

The relevant geometric characteristics of the profile are as follow:

$$h = 300 \text{ mm}$$

$$b = 150 \text{ mm}$$

$$t_w = 7.1 \text{ mm}$$

$$t_f = 10.7 \text{ mm}$$

$$r = 15 \text{ mm}$$

$$c = b/2 - t_w/2 - r = 56.45 \text{ mm (flange)}$$

$$c = h - 2t_f - 2r = 248.6 \text{ mm (web)}$$

$$W_{pl,y} = 628 \times 10^{-6} \text{ m}^3$$

Classification of the cross section

$$\varepsilon = 0.85 \sqrt{\frac{235}{f_y} \frac{E}{210000}} = 0.85 \cdot 1.032 = 0.877$$

The class of the flange in compression is (see Table 5.2 from EN 1993-1-4):

$$c/t_f = 56.45/10.7 = 5.3 < 9\varepsilon = 7.9 \Rightarrow \text{Class 1 (the throat thickness of the fillet weld was neglected)}$$

On the other hand for the web in bending the class is (see Table 5.2 from EN 1993-1-4):

$$d/t_w = 248.6/7.1 = 35 < 56.0\varepsilon = 49.1 \Rightarrow \text{Class 1 (the throat thickness of the fillet weld was neglected)}$$

The cross section of the stainless steel IPE 300 in bending and in fire situation is of Class 1.

The collapse occurs when

$$M_{fi,Ed} = M_{fi,\theta,Rd} = W_{pl,y} k_{y,\theta} f_y / (k_1 k_2 \gamma_{M,fi})$$

i.e.

$$k_{y,\theta} = \frac{M_{fi,Ed}}{W_{pl,y} f_y / (k_1 k_2 \gamma_{M,fi})} = \frac{67.6}{628000 \cdot 210 / (1.0 \cdot 0.7 \cdot 1.0)} \times 10^6 = 0.359$$

Interpolation in Table 5.9 or in Table C.11 leads to the critical temperature:

$$\theta_{a,cr} = 828 \text{ }^\circ\text{C}$$

which is higher than the critical temperature of 654 °C if the beam is in carbon steel (see example 5.2). This result confirms the good behaviour of the stainless steel at elevated temperature.

The modified section factor has the value

$$k_{sh} [A_m / V] = 0.669 \cdot 187 = 125 \text{ m}^{-1}$$

Double interpolation in table of the Annex A.8 yields a time of 33.6 min to reach the critical temperature, $\theta_{a,cr} = 828 \text{ }^\circ\text{C}$, which allows for the classification of the beam as R30, whereas the fire resistance is R15 if the beam is made of carbon steel grade S235 (see Example 5.2).

Chapter 6

ADVANCED CALCULATION MODELS

6.1. GENERAL

Simple calculation models based on equilibrium between the energy transferred to the section and the energy required to heat up the section have been presented in Chapter 4. The mechanical models presented in Chapter 5 are based on modified room temperature models for structural stability which allow for variations of yield strength with temperature.

These simple thermal and mechanical models are based on certain simplifying assumptions. In the case of the simple thermal models the temperature is assumed to be uniform throughout the section or within prescribed zones of the section. For the mechanical models the stability of the whole structure is based on the behaviour of individual members and indirect fire actions are not taken into account.

The limitations of these simple methods can be removed by advanced calculation models which are based on fundamental physical behaviour.

Advanced calculation models normally comprise separate models¹, one for the determination of the temperatures in the members (thermal response model) and one for the mechanical response of the structure (mechanical response model). In the terminology of the Eurocodes, *advanced calculation models* are thus related to the calculation of the behaviour of the structure. Models for the determination of the behaviour of the fire in a compartment are called in Eurocode 1 *advanced fire models*.

¹ The Eurocode says *should include separate models*. A single fully coupled model would as well be based on the fundamental physical behaviour and would, in fact, be more advanced than two separate uncoupled models.

These have been discussed in Chapter 3, with more information provided in Annex B. This chapter is dedicated to advanced calculation models for the behaviour of the structure.

A large number of computer programs are available in which different features of the advanced calculation model have been implemented. A few were specifically developed to analyse a particular problem within the frame of a research project or a Ph.D. thesis. These are usually available and used only by the Ph. D. candidate or the project partners and they are typically not used anymore when the project is finished. Other programs are the result of continuous development from a research group. Such programs are dedicated to the behaviour of structures subjected to fire, but they have a much wider field of application than the Ph.D. software. In Europe, some of the most popular programs are; *Adaptic*, developed at the Imperial College London (Song *et al*, 2000), *Vulcan*, developed at the University of Sheffield (Huang *et al*, 2003) and *SAFIR*¹, developed at the University of Liege (Franssen, 2005). The last two programs are used outside their university of origin for research projects and practical applications. Finally, some research groups or design offices use commercial, general purpose software that can be adapted to cover the fire situation. For example, *Ansys* is used by CTICM in France, while *ABAQUS* is the favourite tool at the University of Edinburgh. In this later University, efforts are being undertaken to adapt *OpenSees*, an open source software primarily developed for the behaviour of buildings subjected to seismic action, in order to have it used for buildings subjected to the fire action (Jiang & Usmani, 2013).

274

The international fire model survey (Olenick and Carpenter, 2003) is a good introduction to the various structural fire models, but, although this survey has been updated, things are moving fast in the field of structural fire behaviour and the information provided is unavoidably out-of-date.

No software can claim to be *100% Eurocode compliant* because this is the utilisation of a tool that makes an application Eurocode compliant, not the lines of source code that have been written. However, it is essential that data such as the material thermal or mechanical properties of steel given in the Eurocodes are implemented accurately in the software or, alternatively, allowance is made for the data to be input by the user in a clear and simple way. Like most tools, the expertise and competence of the user is paramount to achieving an accurate model of the true behaviour of the structure.

¹ This software has been used for the examples of this chapter.

It is not the aim of this chapter to discuss all the features of the existing software. Rather, the aim is to present the essential features that characterise the advanced calculation model, in order to give the reader some information that will help him either to choose a program that suits the application that he wants to treat or to be in a position to give a judgement on the accuracy of the results presented to him.

6.2. THERMAL RESPONSE MODEL

Thermal response model has been developed to predict the development of temperatures in structural elements and, when present, in the insulating materials that protect the structure.

The transfer of heat in solids is governed by Fourier's equation (see Chapter 4). The transient form of this equation must be considered in order to represent the continuous variation of temperatures within the structure during a fire.

For structures with complex geometries, temperature dependent material properties and non-linear boundary conditions, it is not possible to get an exact solution to Fourier's equation. An approximate solution is therefore sought by subdividing the structure into a large number of small elements.

The finite element method is the most widely used technique for calculating temperatures in structures subjected to the fire although the method of finite differences has also been used in the past¹. The boundary elements method could also be used, but no application of this technique in fire problems is known to the authors. These methods are nowadays quite easy to use, in the sense that user-friendly computer programs have been developed. The specific knowledge required for developing such software is not needed for utilising one of these, but it is preferable that the user has some basic knowledge of the theory of heat transfer.

In advanced thermal models, some approximations have also to be made. In the finite element method, the geometry of the structure is approximated, for example, by a series of linear or second order polynomial curves. A temperature distribution is also assumed in each finite element. The temperature is calculated only at specific points in the section, namely the nodes where the elements are

¹ This method is essentially suitable for regular geometries.

joined, and at discrete time intervals. Contact between adjacent materials (for example, an insulating material and a steel member) is usually assumed as perfect. Simple heat transfer by conduction is often assumed in insulating materials whereas, in fact, the heat transfer at the local level may involve a lot of complex phenomena. Typical examples are mineral wool mats and intumescent paintings. Evaporation, migration, condensation of moisture in some insulating materials are treated in a simplified manner or even conservatively neglected, as allowed by the Eurocode.

Nevertheless, the finite element method, when applied in an appropriate manner, provides a good representation of the temperatures measured in steel elements during fire tests. It is essential that the *effective* thermal properties of insulating materials are derived from recalculation of tests made in the same conditions, without extrapolation. For example, the thermal conductivity of mineral wool that is given at room temperature for normal temperature applications cannot be used in the fire situation. Effective properties of intumescent paints determined for certain film thicknesses and certain fire durations cannot be used for longer durations or higher thicknesses.

Advanced thermal calculation models can be used with any heating curve, providing that the material properties are known in the relevant temperature range. Particular attention should for example be paid to the cooling phase of natural fires, a phase during which the thermal properties of most insulating materials have not been investigated.

276

It is mentioned in Eurocode 3 that advanced calculation methods may be used with any type of section. A program written for a specific type of section, e.g. for circular hollow steel sections, may still qualify as an advanced model provided that it is used for the relevant applications.

When the temperatures are calculated in a steel section by the advanced calculation model, the temperatures through the section are not uniform. For example, Fig. 6.1 shows the temperature distribution in a HE300A hot rolled section calculated after 30 minutes of exposition to the standard fire. Whereas the simple calculation model, see for example Elefir-EN in Chapter 8, yields a uniform temperature of 760 °C, the temperature calculated by the advanced calculation model varies between 737 and 804 °C.

These temperature differences are small and have little influence on the mechanical behaviour, at least for the cases where the temperature distribution is symmetrical in the section.

The flux at the boundary of the section, see Eq. (3.4), was calculated with a configuration factor ϕ equal to 1.0, and the flux has been multiplied by a shadow factor k_{sh} equal to 0.617, see Chapter 3. This shadow factor was considered with a unique value on the whole boundary, for simplicity reasons. If, on the contrary, the web, the inner parts of the flanges and the outer parts of the flanges are treated separately, different shadow factors can be calculated based on the view factors between each of these surfaces and the environment. In that case, the thin web would receive less heat and the relatively thick flanges would receive more heat than with a unique shadow factor, and the differences between the simple calculation model and the advanced model would be smaller. A more detailed discussion about the application of shadow factors in the general calculation model may be found in Section 6.4. If the temperature is calculated in a protected steel section, the results between the numerical model and the simple model are even closer. This is because the section heats up less quickly, leaving time for the temperature within the section to equalize.

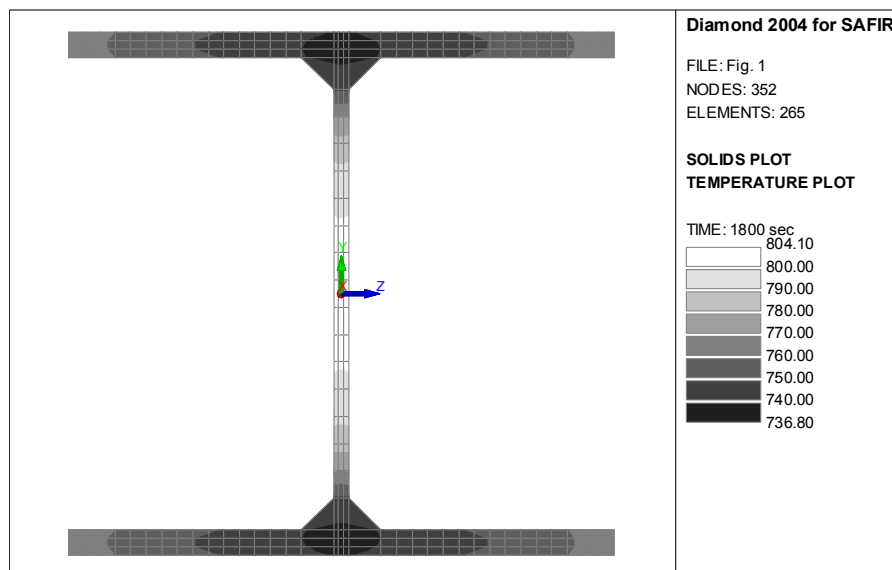


Figure 6.1 – Temperature in a HE300A heated on 4 sides after 30 minutes of standard fire

Higher differences are observed when the boundary conditions are not symmetrical. Figure 6.2, for example, shows the temperature distribution in the same section that is heated only on 3 sides. The upper side of this section is not subjected to the fire and, to model this, an adiabatic boundary condition has been

6. ADVANCED CALCULATION MODELS

imposed on this side. The boundary conditions are thus similar to those that are considered in the simple calculation model¹. The temperatures calculated by the advanced model range from 663 to 788 °C, whereas the simple calculation model yields a uniform temperature of 735 °C. Because the boundary conditions are the same, the average value of the non-uniform temperatures calculated by the advanced model is very close to the uniform temperature calculated by the simple model. The differences observed locally in the section are significantly higher than those given in Fig. 6.1 and, more importantly, the gradients are not symmetrically distributed within the section. The upper flange is colder by about 89 °C than the lower flange. If the section is used as a column, where the material that protects the upper flange² is the façade wall, the thermal gradient will induce additional lateral displacements, the influence of which will have a crucial effect on the buckling strength of the column. Only a model that considers these thermal gradients across the depth of the section is able to predict these large displacement effects.

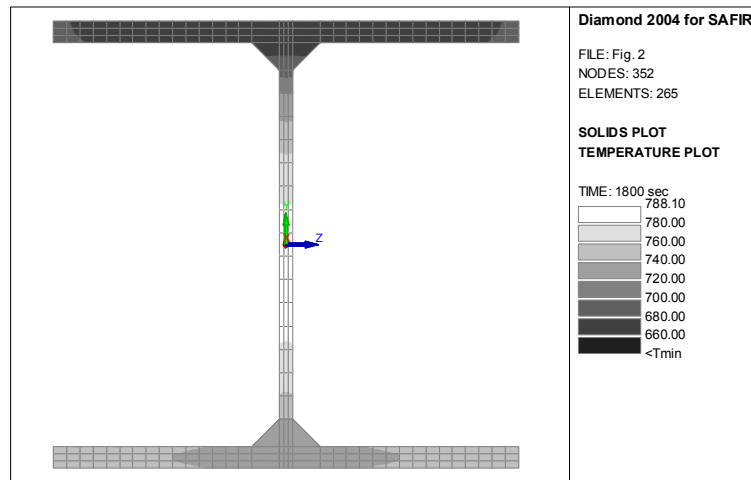


Figure 6.2 – Temperature in a HE300A heated on 3 sides after 30 minutes of standard fire

The effect of the thermal gradient across the depth of the section may not be as significant on the ultimate bending capacity, for example, in a beam. This is because large displacements do not induce additional effects of action in beams, at least when there is no axial restraint.

¹ Shaddow factor $k_{sh} = 0.559$.

² In fact, now, the outer flange.

In beams, however, the material that is present on the upper flange and protects the section from the fire is often concrete of the slab. This concrete not only protects the upper side of the section from direct exposure by the fire but also acts as a heat sink. Some heat is transferred from the upper flange to the concrete slab.

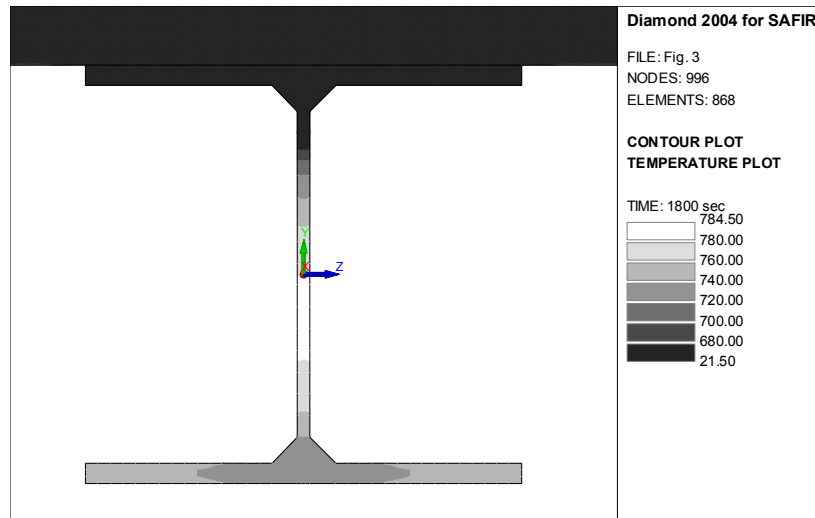


Figure 6.3 – Temperature in a HE300A with a concrete slab on the upper flange

Figure 6.3 shows the temperature distribution that has been calculated by the advanced calculation model for the same HE300A steel section with a siliceous concrete slab on its upper flange. Perfect contact is assumed between steel and concrete. The upper limit has been chosen for the thermal conductivity of concrete, see EN 1994-1-2. The temperature in the upper flange is significantly reduced, from 680 in Fig. 6.2 to around 480 °C in Fig. 6.3. Because the effect of the heat sink cannot be taken into account exactly in the simple thermal calculation model, an adaptation factor κ_1 is introduced in the simple mechanical calculation model, see Section 5.4.5.2. For an unprotected steel beam protected by a concrete slab on the upper flange, this factor has a value of 0.70, which increases the bending moment capacity from 1.0 to $1 / 0.70$, i.e., to 1.43. When the advanced model is used, the heat sink effect of the concrete slab is directly considered in the thermal model and there is no need to introduce an adaptation factor in the mechanical model. However, in the mechanical advanced model, this beneficial effect has little influence on the overall bending resistance of the section. This is because the presence of the concrete slab has a

6. ADVANCED CALCULATION MODELS

small effect on the temperatures in the lower flange (a reduction of 4 °C is seen in this example). Consequently, the increase in capacity in the upper flange is not seen in the lower flange. For example, if the temperatures are evaluated by the general calculation model in the steel section of example 5.6 subjected to the standard fire, first with an adiabatic boundary condition on the upper side of the upper flange and then with due consideration for a concrete slab on the upper flange, and if the ultimate bending resistance is evaluated after 30 minutes, a value of 193 kNm is obtained with the adiabatic boundary condition and a value of 197 kNm is obtained when the presence of the concrete slab is taken into account explicitly. The ratio of $197/193 = 1.02$ is very different from the ratio of 1.43 allowed in the simple calculation model. A more detailed discussion about this effect may be found in Section 6.4.

There are some situations where the hypothesis of a uniform temperature distribution in the section is totally unrealistic and where the real temperature cannot be approached, even in term of average value, by the simple calculation model. This is the case, for example, when a steel profile is used as a column and a separating concrete wall is located between the flanges, see Figure 6.4

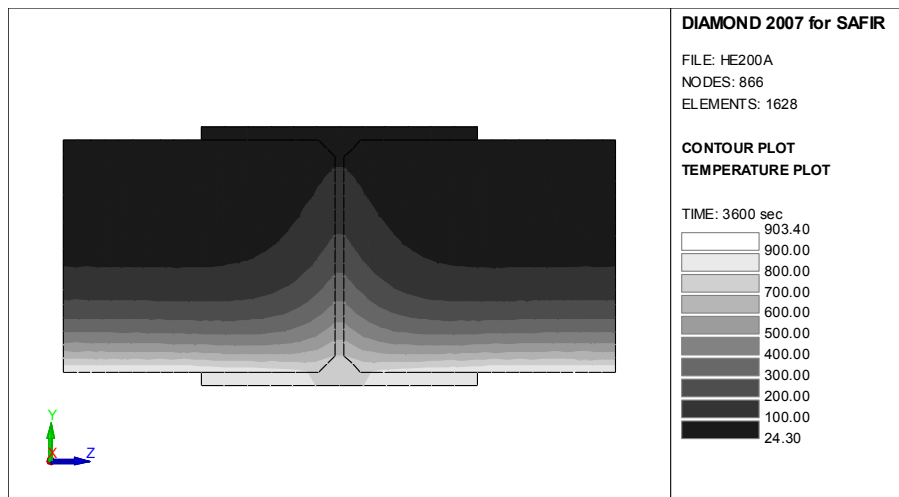


Figure 6.4 – Temperature in a HE200A inserted in a concrete wall after 60 minutes of standard fire

In this case, it is impossible to obtain a satisfactory approximation for the average temperature of the profile as well as for the average temperature of each part of the section, (exposed flange, web and unexposed flange), by using the simple concept of thermal massivity that is fundamental to the

simple calculation model. The advanced calculation model is required to get an accurate representation of the temperature distribution. If the profile is a column, it is essential to get a realistic representation of the temperature distribution because the thermal gradients may have a detrimental influence on its load bearing capacity or fire resistance duration.

The advanced calculation model is also appropriate for calculating the temperature development in elements or substructure that present a three dimensional character. Typical application is in the joints between linear elements or between linear elements and floors. The presence of concrete, in the floor and possibly also in composite steel concrete beams and columns, plus the presence of a large number of parts with different thicknesses (which implies different thermal massivity) make it very difficult to give an accurate description of the real temperature distribution based on the concept of thermal massivity. Fig. 6.5 shows a 3D model of a joint between a column made of a concrete filled steel section and a composite beam made of a steel hot rolled profile and a composite slab.

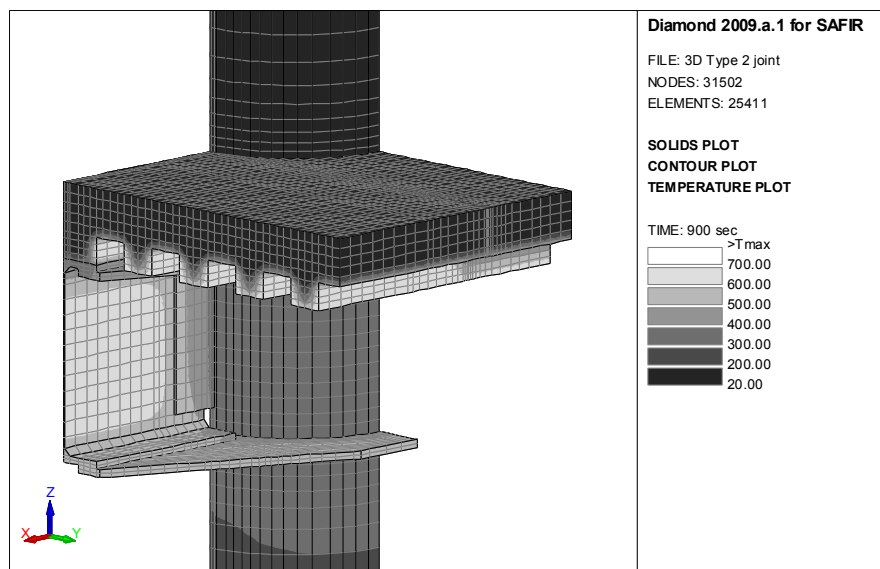


Figure 6.5 – Temperature in a composite joint
(courtesy of Elisabetta Alderighi, Univ. of Pisa)

All examples presented in this Section are based on the hypothesis that the thermal attack from the fire is uniform on the complete boundary of the

section. More elaborate techniques, involving the calculation of view factors, may be required in cases where the fire source is localised, or involving the computation of impinging radiative intensities from different directions when the fire environment is calculated by a Computational Fluid Dynamic (CFD) model (Tondini *et al*, 2012).

6.3. MECHANICAL RESPONSE MODEL

Different types of finite element can be used to model the structure, depending on the type of structure and type of behaviour that has to be considered. It is important to understand what type of element is required in which situation and, above all, what types of failure mode are not covered by the analysis. According to the Eurocode, these failure modes not covered by the analysis should be eliminated by appropriate means. Because the Eurocode gives no guidance about what the appropriate means are, and because these means vary with each failure mode, engineering judgement is required.

Two dimensional Bernoulli type beam finite elements have been the workhorse of structural fire modelling for many years, for steel, concrete and composite members. Typical failure modes not covered by such elements for the analysis of steel elements are shear failure, local buckling and out-of-plane lateral-torsional buckling.

Three dimensional Bernoulli type beam elements have been introduced to represent the situations when the structure deflects in three directions. These can also be used for plane structures that are loaded in their plane, but can fail out of plane, for example by lateral-torsional buckling.

At the fire limit state, the deformations in a steel structure can be very large. This is due to a number of reasons. Firstly, the stiffness of steel decreases with increases in temperature and, secondly, thermal elongation and thermal gradients may induce additional displacements. The analysis must be able to model these large displacements and this must be taken into account in the formulation of the elements. Fig. 6.6, for example, shows the deformed shape calculated at failure of a steel industrial building. A fire wall is present in the centre of the building in such a way that only two bays are subjected to the fire.

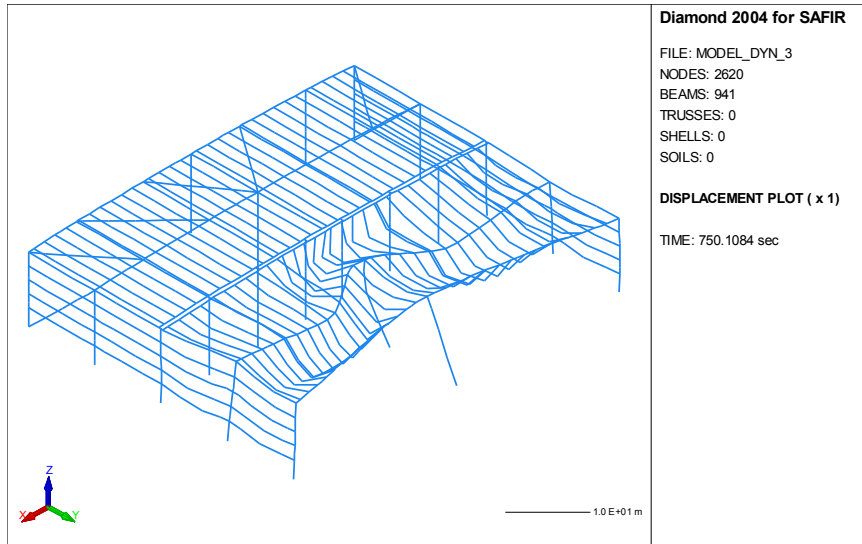


Figure 6.6 – Large displacements in a steel frame partially subjected to the fire (Courtesy of COPERFIL *Construccion*)

The indirect effects of action, i.e. the variation of effects of actions induced by restrained thermal expansion, must be taken into account in an advanced mechanical model. Fig. 6.7, for example, shows the bending moment distribution in a 3D frame subjected to a fire on the ground floor. On the left-hand side is the distribution under design loads in the fire situation at time $t = 0$. On the right-hand side is the significantly different distribution calculated after 3129 seconds, just before failure. Between these two extreme situations, the effects of actions vary continuously during the course of the fire.

283

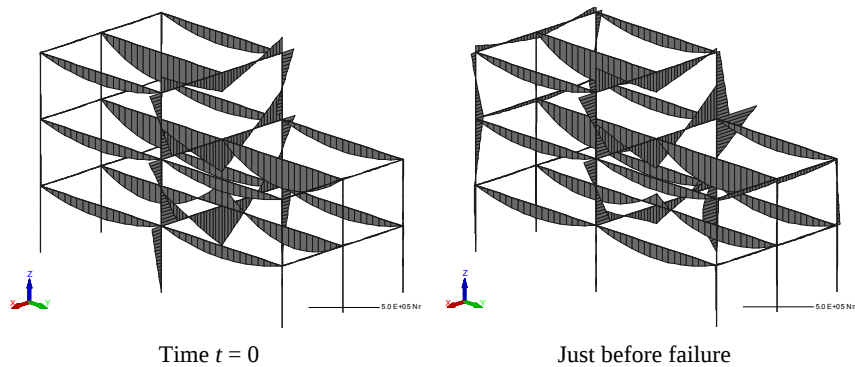


Figure 6.7 – Bending moment distribution in a 3D frame

The most dangerous aspect of Bernoulli beam elements, either 2D or 3D, is that such elements see and treat any section as a Class 1 section, in the sense of the Eurocode. This means that the section will be able to develop the full plastic moment capacity and to maintain the bending moment for very large curvatures, at least with a steel material that has a horizontal plateau in the stress-strain relationship up to a strain of 15%. The minimum requirement is that the users should verify the class of the sections and adopt an alternative strategy where Class 2, 3 or 4 sections are present in the structure. Because of this, the assertion of Eurocode 3 that advanced calculation methods may be used with any type of section must be given some nuance. In fact, not any tool, in other words not any element type, can be used with any type of section.

Shell finite elements that capture the membrane as well as the bending behaviour of thin steel plates can be used to represent the webs and flanges that make up steel sections. When these elements are used, the problem of determining the class of the sections and of adopting a strategy for Class 2, 3 and 4 sections is no longer present because such elements are able to model local buckling. Fig. 6.8 shows the web post-buckling that occurs in a steel cellular beam modelled by shell elements. If the presence of a collaborating concrete slab on the steel beam creates a composite member, different finite elements can be combined to model the member. For example, shell elements can be used to model the steel beam, while beam elements can be used to model the concrete slab.

284

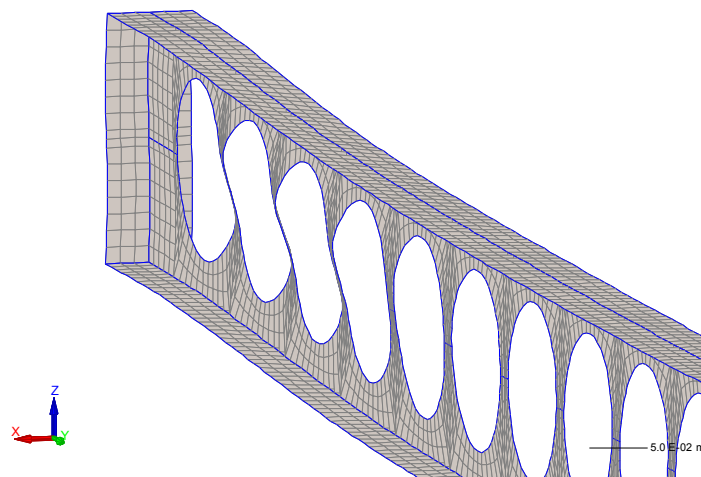
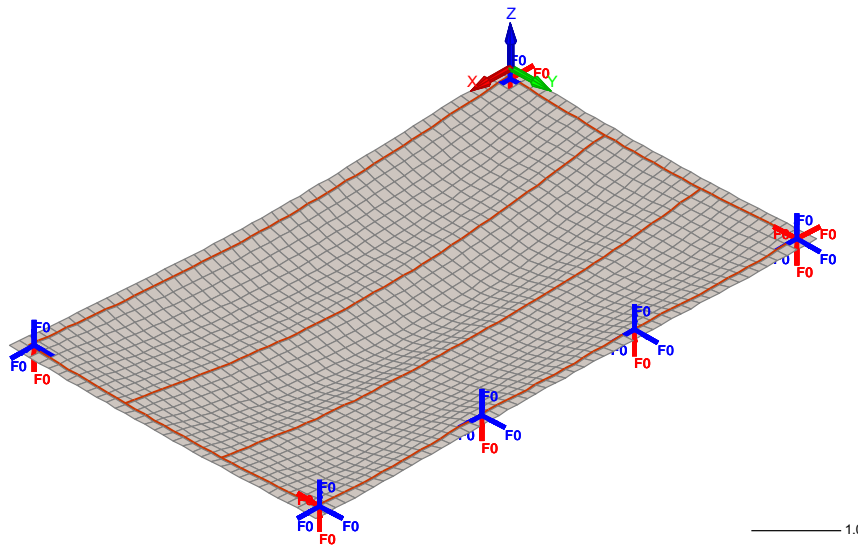


Figure 6.8 – Deformed shape of a cellular beam modelled by shell elements

These shell elements are computationally much more expensive and can be used at the present¹ only for the analysis of single elements or, at most, substructures of limited size. The analysis of a complete steel building with shell elements is still out of practical reach.

Shell elements can also be used to represent concrete slabs. Concrete shell elements are nowadays utilised more and more to simulate the membrane action that may develop in concrete or composite slabs as a result of the large displacements induced during a fire by thermal gradients. The membrane action may allow significant savings on the thermal insulation of the supporting steel profiles, because a certain number of these profiles can be left unprotected. Fig. 6.9 shows, first, the deformed shape of a $15 \times 9 \text{ m}^2$ floor made of a composite slab supported on steel beams, after one hour of standard fire. The four edge beams are thermally protected while the two internal secondary beams are not. The lower part of the figure shows the compression ring that develops in the concrete slab and supports the central part of the slab that is in tension.

This membrane behaviour is thus particularly favourable for the competitiveness of steel solutions, but this technique is a matter of analysis of concrete or composite steel concrete slabs and will thus not be treated in detail here.



¹ This means in 2014.

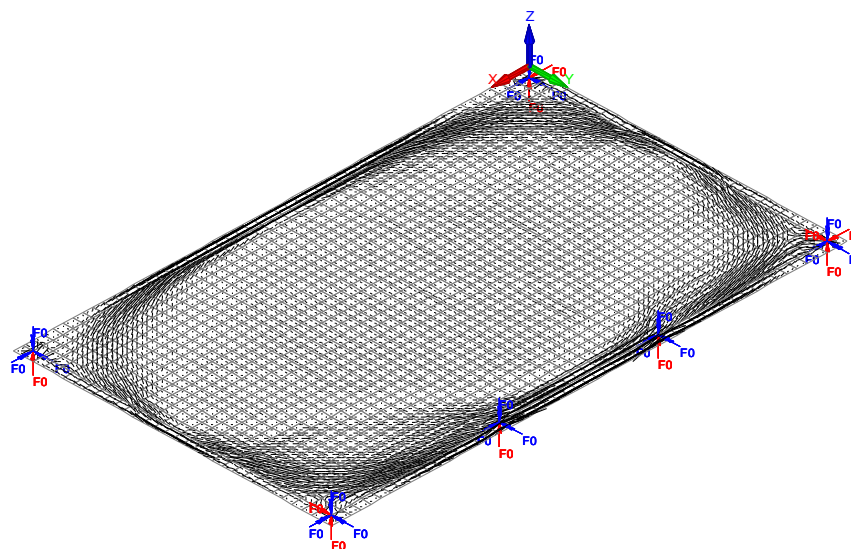


Figure 6.9 – Deformed shape and compression forces in a composite floor

Solid elements can be used for the analysis of connections, but are not suitable for the analysis of entire structures. Such elements can be used to represent in detail the behaviour not only of each plate or stiffener, but also of the bolts and nuts that may be present in the joint. It is often necessary to combine these solid elements with contact elements to represent changes in contact between some elements of the joint during the fire. These contact elements introduce a high level of non-linearity in the problem. Being even more expensive than shell elements, solid elements are used mainly in research projects and not yet for practical applications.

The non-linear material model recommended in the Eurocode should ideally be taken into account in the program, including the effects of loading and unloading on the stiffness of the structure, which means that a damage model or a plasticity model has to be used. Damage or plasticity models, or a combination of both, can be used for concrete, whereas a plasticity model is generally used for steel. The fact that plasticity from 2% to 15% strain is without strain hardening¹ and the fact that a descending branch is present for higher values of the strain may jeopardise convergence when one or several points of integration of the structure enter in these regimes. If it is tempting to introduce a slight level of strain hardening or an infinitely long plateau in

¹ At least for temperatures higher than 400 °C.

the constitutive model to improve convergence, doing so does not comply with the Eurocode recommendations.

Due to the high level of non-linearity that occurs in a structure when it is subjected to fire, it is appropriate to perform a transient analysis. This means that the external loads are first applied on the structure at room temperature and the temperatures are then progressively increased until collapse. This is different to an evaluation of the load bearing capacity at a certain required fire resistance time that can be performed using a steady state analysis. The most straightforward and simple way to perform a transient analysis is to perform a series of subsequent static analyses at successive time steps. From each time step to the next one, the fact that the temperatures have changed is considered in the modifications of the material properties and thermal elongation and a new static position of equilibrium is searched for. The procedure continues until the time, in fact until the temperature distribution, for which it is impossible to reach a state of equilibrium.

This procedure was found to be adequate as long as simple structures and simple behaviours were modelled. It was yet quickly discovered that premature numerical failures were detected when localised and/or temporary failures occurred in some parts of more complex structures. A typical example is the buckling of a bar in a statically indeterminate structure. Even when there is no localised failure, the quasi-static analysis may stop at a moment when the failure of the heated structure is very near, maybe only a few seconds away, but the displacements reached when the program stops are not large enough to judge about the development or not of a possible progressive collapse or, in other words, about the fact that the remaining part of the structure that is not affected by the fire will be entailed to collapse. It is nowadays more and more frequent to perform the mechanical analysis in a dynamic way, which means that the terms of inertia (mass \times acceleration) are taken into account. Reasonable computational times may still be achieved owing to the fact that, as long as no element is approaching failure, the time steps can remain as long as in a quasi-static analysis. The time steps are reduced, maybe drastically, to simulate the very short period of time during which the local failure develops, but may be increased again, ideally automatically by the programme, thereafter when the collapsed element has seen a nearly total unloading.

Advanced calculation models can be very ductile especially when a dynamic procedure is used, in the sense that they can simulate the behaviour of the load bearing structure until very large displacements are obtained. It is the responsibility of the user not to take automatically the last time when convergence of the numerical process was possible as the fire resistance time. The evolution of the displacements of the structure has to be observed and the decision may have to be taken that the fire resistance time is reached before the end of the simulation. The Eurocode, for example, explicitly recommends that the deformation at the ultimate limit state should be limited to ensure that compatibility is maintained between all parts of the structure. Compatibility is not maintained if one of the members loses adequate support. Another state of deformation that is obviously unacceptable is when a beam deflects below ground level. Less obvious situations may arise.

If, on the contrary, the displacements are limited at the last converged time step, it is advised to search for a degree of freedom¹ representing the global situation of the structure for which the curve showing the evolution as a function of time shows a vertical asymptote at the end. This is a good indication that the structure is indeed suffering from a global collapse. This behaviour is often called a *runaway failure*. If no vertical asymptote can be found, this may be due to a numerical failure, a lack of convergence caused by numerical problems before physical failure of the structure. When one or several points of integration of the model see the stress-related strain exceed 15%, the material enters in the descending branch with its associated negative stiffness. In that case, the rather fragile failure may not be associated with a runaway failure, even if no numerical failure is to be blamed.

288

6.4 SOME COMPARISONS BETWEEN THE SIMPLE AND THE ADVANCED CALCULATION MODELS

In this section, it is discussed whether simple calculation methods are systematically on the safe side compared to advanced calculation models, as implied by the definition of simple calculation model given in the Eurocode. It will be shown that, in fact, there are several aspects for which this is not automatically the case.

¹ A displacement or a rotation

6.4.1 Shadow factor

The flux at the surface of an unprotected steel element is given by Eq. (3.4) which has been repeated here for clarity reasons.

$$\dot{h}_{net} = \alpha_c (\theta_g - \theta_m) + \Phi \varepsilon_m \varepsilon_f \sigma \left[(\theta_r + 273)^4 - (\theta_m + 273)^4 \right] \quad (3.4)$$

In this equation, Φ is the configuration factor, normally taken as 1.0 although it is mentioned that a lower value could be chosen to take account of the shadow effect.

In convex sections, Φ is indeed taken as 1,0 and Eq. (3.4) is applied as such in Eq. (4.16) for calculating the temperature in unprotected sections with the simple calculation model.

$$\Delta\theta_{a,t} = k_{sh} \frac{A_m / V}{c_a \rho_a} \dot{h}_{net,d} \Delta t \quad [^{\circ}\text{C}] \quad (4.16)$$

Eq. (3.4) is also used in advanced calculation models and, because k_{sh} is taken equal to 1 for convex sections in the simple model, the uniform temperature calculated with a simple calculation model is very close to the average value of the temperatures calculated with the advanced calculation model.

For concave sections, it can be shown that, physically, the amount of radiative energy that crosses the so called “box section”, i.e. the smallest convex section that can encompass the real section, cannot have increased when it meets the surface of the steel element. For convection, on the other hand, and except in very closed cavities (e.g. in Hollerith composite profiles), mass transfer provided by air circulating in the concave re-entrant parts of the section can bring in energy and, finally, the convective heat transfer in these cavities is of the same order of magnitude as the one that occurs on the convex parts of the section. A modification of Eq. (3.4) to consider the concave character of the section should thus happen essentially on the radiative part of the net heat flux.

Yet, it has been decided in Eurocode 3 not to use the possibility to choose values of Φ lower than 1 in Eq. (3.4) when using the simple calculation model; A correction factor k_{sh} calculated by Eq. (6.1)¹ in most

¹ See Eq. (4.17b)

cases is applied on both terms of the net heat flux given by Eq. (3.4), the convective term as well as the radiative term.

$$k_{sh} = A_{m,b}/A_m \quad (6.1)$$

This approximation has been introduced because it allows keeping one single geometrical parameter to represent each section (namely, the ratio $A_{m,b}/V$) instead of two parameters (namely A_m/V and Φ) if the correction is applied only on the radiative part of the flux. This approximation is not on the safe side, but it is justified because the convective heat flux is smaller than the radiative flux in Eq. (3.4). Typical values for sections heated by the ISO curve show that the radiative flux is quickly equal to 5 or more times the convective flux.

Another factor 0.9 is even applied in the calculation of k_{sh} for I-sections under nominal fire actions. The origin of this factor and why it is limited to I-sections under nominal fire actions are unknown to the authors of this book.

If, applying the advanced calculation model in a numerical analysis, the fire curve is applied on the whole perimeter of the section in a way that the heat flux is calculated according to Eq. (3.4) on the whole perimeter, the protection to radiation provided by the concave nature of the section is not considered and the advanced model will yield temperatures that are higher than the simple calculation model.

290

In order to illustrate the discussion, some calculations have been performed under ISO fire with a section that has the properties of HE200B, namely $A_m/V = 147.2$ and $A_{m,b}/V = 102.4$. The results are presented in Fig. 6.10.

If the simple model is applied with the flux calculated with the assumption that the concave shape has an influence only on the radiative flux, then Eq. (3.4) is used with $\Phi = A_{m,b}/A_m = 102.4 / 147.2 = 0.696$ and k_{sh} is taken as 1 in Eq. (4.16). The result is supposed to be the most physically correct that could be obtained with the simple model. It is presented as a thick line under caption “SM – phi” in Fig. 6.10. The temperature after 30 minutes is 780 °C.

If now the approximation is made that the influence of the concave shape is applied on both terms of Eq. (3.4), convective as well as radiative, then Φ is taken as 1 in Eq. (3.4) but $k_{sh} = 0.696$ is used in Eq. (4.16). The result is shown as a dotted line under caption “SM – Am,b” on Fig. 6.10.

The temperature after 30 minutes is 771 °C (the difference is indeed very small: -1.1%).

If, in addition, the factor 0.9 is introduced as in the Eurocode, k_{sh} in Eq. (4.16) will be taken as 0.626 and the result is shown by the thin line under caption “SM – EC3” in Fig. 6.10. The temperature after 30 minutes is 756 °C (-3,1%).

If the calculation is made with Eq (3.4) applied on the whole perimeter and $\Phi = 1$, which are the hypotheses of the advanced calculation model, the highest dotted line under caption “AM” of Fig. 6.10 is obtained. The temperature after 30 minutes is 813 °C (+4,2% compared to the most physically correct value but +7.6 % compared to the Eurocode value).

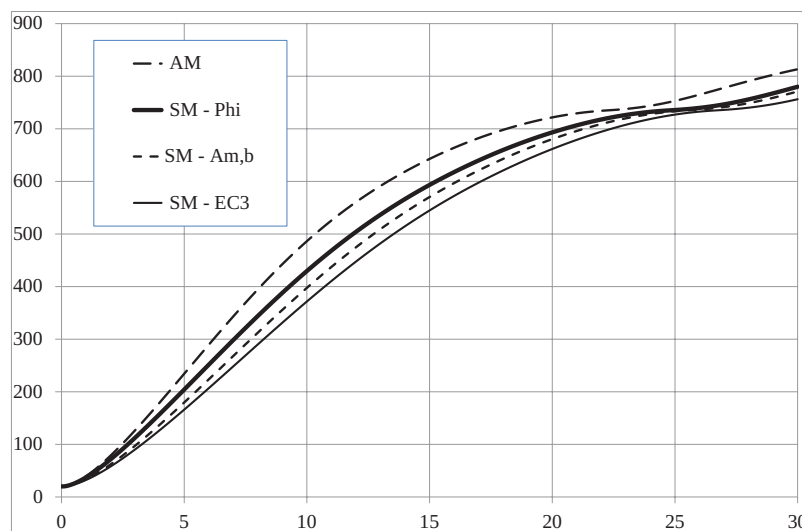


Figure 6.10 – Temperature evolution with different models

Other values will be obtained with different situations. The differences between the results obtained with different hypotheses are higher for massive sections, short fire resistance times and highly concave shapes. They are reduced for thin sections, long fire resistance times and less concave shapes.

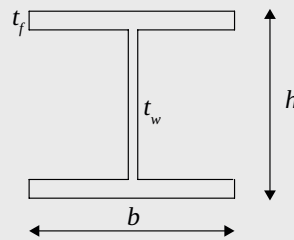
Different techniques exist that allow considering the concave nature of the section in advanced calculation models. The most simple ones rely on a modification of the boundary properties of the material that appear in Eq. (3.4): coefficient of convection and/or emissivity. The modification can be made with average values for the whole section but it is also possible to differentiate for

6. ADVANCED CALCULATION MODELS

different boundaries of the section, for example convex part of the section on one hand (with no modification on this part) and concave part of the section on the other hand. Also the concave part can be differentiated, e.g. between the web and the interior sides of the flanges for an H section (see Fig. 4.25).

Example 6.1: Calculate the factors to be used for modifying the boundary properties of the section HE200B with the three techniques mentioned in the previous paragraph. The influence of the root-fillet will be neglected for simplicity reasons.

Depth of the section:	$h = 200 \text{ mm}$
Width of the section:	$b = 200 \text{ mm}$
Thickness of the web:	$t_w = 9 \text{ mm}$
Thickness of the flanges:	$t_f = 15 \text{ mm}$



292

Global correction factor:

$$\text{Boxed contour of the section: } A_{m,b} = 2 \times (200 + 200) = 800 \text{ mm}$$

$$\text{True contour of the section: } A_m = 800 + 2 \times (200 - 9) = 1182 \text{ mm}$$

$$\text{Correction factor: } 800/1182 = 0.677$$

Two correction factors:

Convex parts of the section (external side and lateral sides of the flanges):
Correction factor = 1.

Concave parts of the section (internal side of the flanges plus web)

True contour of this part:

$$(200 - 2 \times 15) + 2 \times 191/2 = 361 \text{ mm (2 times)}$$

Box contour of this part (opening through which the fire is “seen”):

$$200 - 2 \times 15 = 170 \text{ mm (2 times)}$$

$$\text{Correction factor: } 170/361 = 0.471$$

Three correction factors:

Convex parts of the section (external side and lateral sides of the flanges):

Correction factor = 1.

Web

The rule of Hottel is being used

$$\text{Diagonal of the chamber: } (170^2 + 95.5^2)^{0.5} = 195 \text{ mm}$$

$$\text{Correction factor: } (2 \times 195 - 2 \times 95.5) / (2 \times 170) = 0.585$$

Internal side of the flanges

The rule of Hottel is being used

$$\text{Correction factor: } (95.5 + 170 - 195 - 0) / (2 \times 95.5) = 0.369$$

In order to get a result that is as close as possible to the simple calculation model, these correction factors should be applied to the convection factor as well as to the emissivity of the material and, if the nominal fire is being used, again by a factor 0.9.

It is conceptually possible to program in a software the computation of the view factor between each individual finite element at the boundary of the section and the opening through which the fire is “seen”. It is also possible to take into account the mutual radiative interaction between different parts of the concave boundary which “see” each other. Compared to the previously mentioned technique, these two refined would slightly influence the temperature distribution in the section but would hardly modify the average value of the calculated temperatures.

6.4.2 Buckling curves

A buckling curve is presented in Eurocode 3 to be used in the simple model for the fire resistance of steel columns.

The shape of this curve, the equation that would represent it as well as the parameters that would be considered in the equation have been obtained from an extensive campaign of some 200 000 numerical simulations made with the advanced model (Talamona *et al*, 1997). When the equation obtained from the simulations was compared with a data base of experimental test results, it was observed that the numerical results and the experimental results showed the same response as a function of the relevant parameters but the numerical results were, generally, slightly lower than the experimental results (Franssen *et al*, 1998). This was attributed to the fact that both the geometrical imperfections as well as the residual stresses had been considered with their characteristic values in the simulations whereas the probability of the simultaneous occurrence of the characteristic for both factors is very low. As a consequence, the buckling curve was calibrated to better represent the experimental results; the imperfection factor used in the buckling curve was set to 0,65, see Eq. (4.6) of Eurocode 3.

Now, if a steel column is modelled in an advanced calculation model, it is not known which level of imperfections have to be modelled to obtain the same results as the simple calculation model (these supposed to correspond to the experimental results). It would be interesting if only a geometric imperfection of given amplitude could yield this result because the introduction of a residual stresses pattern in a model is more complex than the introduction of an initial imperfection. Whether this is possible and, if so, what is the amplitude of the required imperfection is not known to the authors.

294

The buckling curve for steel members in compression has been exclusively determined from numerical analyses and experimental results made on hot rolled H or I sections. Yet, they are applied as such for all sections types, welded sections, hollow steel sections, angles, U or C sections.

Numerical analyses performed recently on hot rolled C sections and welded I sections (Nauar, 2014), considering appropriate residual stress distributions have shown that the buckling curve proposed in EN 1993-1-2 can also be used for these types of sections. Yet, in the team of the first author and, approximately at the same time, in the team of Professor Schaumann from Leibniz University of Hannover (private communication), some results obtained numerically on columns with non-conventional sections types, essentially welded box sections with very thick flanges, have been found to be significantly different from those provided by the buckling curve of the

Eurocode. This question has not been investigated thoroughly but users of advanced calculation models may be well advised to calculate the entire buckling curve if they eventually obtain some results of axially loaded columns with non-conventional cross sections that differ from those predicted by the simple calculation model. They will then be able to judge whether the difference comes from a numerical failure that appeared for particular length being investigated or whether it comes from a difference in buckling curve.

6.4.3 Factor κ_2

According to clauses (3) and (8) of section 4.2.3.3 of Part 1-2 of Eurocode 3, the plastic bending resistance of class 1 and class 2 members can be divided by a factor $\kappa_2 = 0.85$ at the supports of statically indeterminate beams. The plastic bending resistance is thus 1.18 times higher on the supports than the value calculated on the base of a temperature distribution that is not disturbed by the supports. This effect is not represented as such in an analysis performed with an advanced model, namely with a numerical model based on beam finite elements.

It can easily be calculated in the load domain that, at a given requested fire resistance time, the load bearing capacity of a central span in a continuous beam supporting a uniformly distributed load is given by Eq. (6.2) if there is no favourable effect on the supports (see Eq. (5.145) of this book).

$$P_{cr} = 16 \frac{M_{pl}}{L^2} \quad (6.2)$$

295

If the factor κ_2 is taken into account on the supports, the load bearing capacity at the same time is given by Eq. (6.3), with M_{pl} the plastic resistance of the section in the span (see Eq. (5.155) of this book with $\kappa_1 = 1.0$).

$$P_{cr} = 8 \times (1 + 1.18) \frac{M_{pl}}{L^2} = 17.4 \frac{M_{pl}}{L^2} \quad (6.3)$$

The first result is likely to be provided by the advanced model and the second one by the simple calculation model. There is thus an additional safety margin provided by the advanced model compared to the simple model.

It can easily be calculated that the effect of increasing the bending resistance on the supports by 18% is equivalent to a reduction of the span to

$(16/17.4)^{0.5} = 96\%$ of the theoretical distance between the supports. This means that the advanced model would yield the same answer as the simple model if a length of 2% of the span is left unheated from each support (slightly different figures would be calculated for the end spans of a continuous beam).

The discussion above is based on the hypothesis that the advanced model analysis will detect plasticity exactly on the supports which means, for the beam finite element, that yielding is evaluated at the ends of the element and if yielding of a single section along the length of the beam finite element completely annihilate the bending stiffness of the element. This is not the case for typical displacement based beam finite elements. If, for example, integration is performed by a Gauss integration scheme in a conventional displacement based finite element, the first point where yielding is evaluated is close to the supports, but not exactly on the supports. For example, with two points of integrations on the length of the element, the first point is approximately at a distance of $0.21 L_{el}$ from the end of the element, with L_{el} being the length of the finite element. If 10 beam finite elements are used on the length of the beam, then $L_{el} = L/10$ and yielding will be evaluated at a distance of $0.02 L$ from the support, which is exactly the value giving the increase of capacity provided by the favourable effect from non-uniform temperature on the supports.

6.4.4 Factor κ_1

According to clauses (3) and (7) of section 4.2.3.3 of EN 1993-1-2, the plastic bending resistance of Class 1 and Class 2 members can be divided by a factor $\kappa_1 = 0.70$ for unprotected beams exposed on 3 sides with a concrete slab on side four, which means on the upper side of the upper flange¹. This factor is applied to the reference bending resistance that is calculated on the base of the temperature distribution that does not take the slab into account.

In fact, the slab is taken into account in the temperature distribution for the reference bending resistance by considering the fact that the upper side of the steel section is not affected by the fire; an adiabatic boundary condition is assumed to exist on this surface and, as a consequence, the section factor A_m/V of the section is reduced compared to that of a section heated on 4 sides.

¹ The factor is 0.85 for protected beams.

The factor κ_1 stems from the fact that the slab has another effect on the temperature distribution. Not only does it protect the upper flange from the application of the fire, but it also absorbs heat from the flange for its own heating. Heat is transferred from the flange to the concrete slab that acts as a heat sink.

This thermal effect can easily be reproduced in thermal analyses performed with an advanced thermal model; instead of just representing the steel section with an adiabatic boundary, the concrete slab is introduced in the model. When this is done, it is indeed observed that the temperature in the upper flange is lower compared to the situation when the slab is not modelled. For example, Fig. 6.11 presents the temperature distribution calculated after 30 minutes of ISO fire in an unprotected IPE300 section, on the left with the upper slab in the model and on the right with an adiabatic boundary condition. The temperature in the upper flange is reduced from 780 to 690° when the slab is taken into account.

Yet, dividing the bending strength by 0.70 amounts to multiply the strength by 1.43 and such an increase cannot be observed in the mechanical analyses performed with advanced models. The reason is that the increase of compression capacity provided to the upper flange does not add much to the bending capacity of the section if the tensile capacity of the lower flange is kept the same (the temperature in the lower flange is, in Fig. 6.11, around 825 °C in both cases). It is equivalent to increase the compression capacity of a reinforced concrete beam that has been designed to fail at the same time by tension in the steel bars and by compression in the concrete; failure will occur for a very similar bending moment, by tension in the bars. In the steel beams, there is a slight effect because the cooling extends somehow in the web, but by no way can this lead to an increase of bending capacity of more than 40%. For example, if the sections of Fig. 6.11 are used in a 5 meters simply supported beam, the load bearing capacity after 30 minutes of fire calculated by a non-linear finite element analysis is increased from 7.97 kN/m when the slab is replaced by an adiabatic boundary condition to 8.56 kN/m when the slab is considered in the thermal model (the slab is not acting in a composite action with the steel beam). The increase is for this example of 7.4%, equivalent to a value of the coefficient κ_1 equal to 0.93. Other values would be obtained with other geometries.

6. ADVANCED CALCULATION MODELS

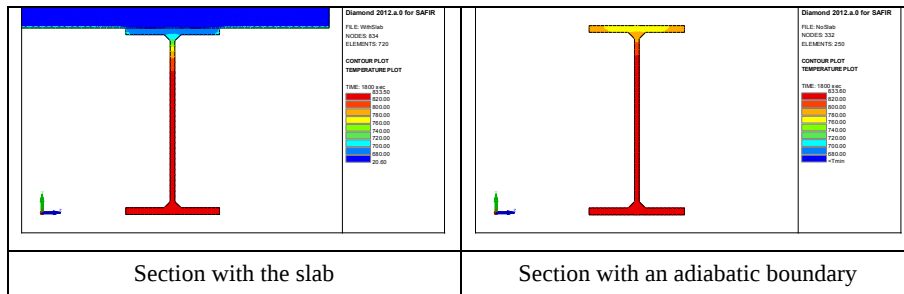


Figure 6.11 – Temperature distribution with two different models

To the knowledge of the authors, there is no way that the advanced model can yield the strength increase allowed for by the simple model.

The aim here is to highlight the possible difference between advanced and simple calculation models. Another question is which model better describes the behaviour of steel sections in experimental tests or in real structures under fire. It is possible that a concrete slab supported on a steel section will develop some level of composite action that, perhaps, can be activated in accidental actions and can explain lower values of κ_1 factors used in the simple model.

Chapter 7

JOINTS

7.1. GENERAL

This chapter addresses the fire design of bolted and welded joints. Tests and observations from real fires have shown that joints perform well in fires and in many cases may be left unprotected. For the case of bolted joints, Eurocode 3 states that net-section failure at fastener holes does not need be considered, provided that there is a fastener in each hole. This is because the steel temperature in the joint is lower due to the presence of the additional joint material.

The recommendations presented in the *Model Code on Fire Engineering* (ECCS, 2001) do not go this far but instead suggest that a lower level of fire protection may be used for joints. It is well known that joints are not heated to the same degree as other parts of the structure because they are shielded by the incoming beams and columns. Furthermore, the mass of steel around the joint increases locally, possibly reducing the section factor A_m/V . This effect is recognized and taken into account in Eurocode 3 by the use of the adaptation factor k_2 that is used at the supports of statically indeterminate beams, see 5.5.6.2.

Eurocode 3 states that the fire resistance of bolted and welded joints may be assumed to be sufficient, provided that the following conditions are satisfied:

1. The thermal resistance $(d_f/\lambda_f)_c$ of the joint's fire protection is equal to or greater than the minimum value of the thermal resistance $(d_f/\lambda_f)_m$ of fire protection applied to any of the connected members, where:
 d_f is the thickness of the fire protection material. ($d_f = 0$ for unprotected members.)

- λ_f is the effective thermal conductivity of the fire protection material.
2. The utilisation of the joint is equal to or less than the maximum utilisation of any of the connected members. As a simplification, the utilisation of the joint and its connected members may be calculated at ambient temperature.
 3. The resistance of the joint at ambient temperature is calculated in accordance with the recommendations given in EN 1993-1-8.

A careful interpretation of the above conditions reveals that if the connected members are unprotected, the joint can also be left unprotected.

Furthermore, if a member is oversized in order to reach a satisfactory fire resistance time, instead of applying thermal protection for example, then the joints must also be oversized.

As an alternative to the above method, the fire resistance of a joint may be determined using the method given in Annex D of Part 1.2 of Eurocode 3. This method is presented and discussed in the following sections. Significant research has been conducted on the behaviour of steel joints in the fire situation. This includes research on the temperature distribution within a joint and the mechanical behaviour of a steel joint at elevated temperature (Block *et al* (2004 and 2007); Franssen and Brauwes (2002); Santiago *et al* (2007 and 2008a,b,c); Simões da Silva *et al* (2001 and 2005); Spyrou *et al* (2004a,b,c) Wald *et al* (2004)). The results from this ongoing research have not been taken into account in the Eurocode.

7.2. STRENGTH OF BOLTS AND WELDS AT ELEVATED TEMPERATURE

Table 7.1 gives the strength reduction factors for bolts and welds at elevated temperatures and Fig. 7.1 is a graphical representation of these data.

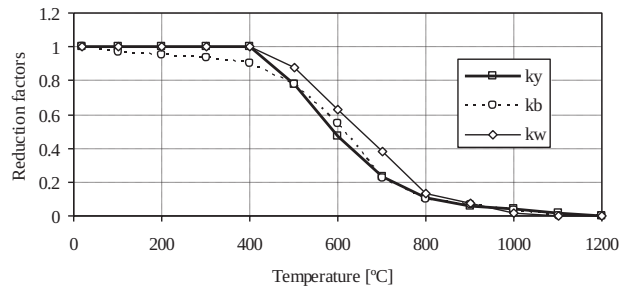
Table 7.1 – Strength Reduction Factors for Bolts and Welds

Temperature, θ_a [°C]	Reduction factor for bolts, $k_{b,\theta}$ (Tension and shear)	Reduction factor for welds, $k_{w,\theta}$
20	1.000	1.000
100	0.968	1.000
150	0.952	1.000

Table 7.1 – Strength Reduction Factors for Bolts and Welds

Temperature, θ_a [°C]	Reduction factor for bolts, $k_{b,\theta}$ (Tension and shear)	Reduction factor for welds, $k_{w,\theta}$
200	0.935	1.000
300	0.903	1.000
400	0.775	0.876
500	0.550	0.627
600	0.220	0.378
700	0.100	0.130
800	0.067	0.074
900	0.033	0.018
1000	0.000	0.000

Fig. 7.1 compares the reduction factors for structural steel (k_y), bolts (k_b) and welds (k_w) It can be seen that bolts start losing their strength at lower temperatures than either structural steel or welds.

Figure 7.1 – Reduction factors for structural steel (k_y), bolts (k_b) and welds (k_w)

7.3. TEMPERATURE OF JOINTS IN FIRE

When verifying the fire resistance of a joint, the temperature distribution of the joint components should be evaluated. These temperatures may be assessed using the local A/V value of the parts forming the joint. As a simplification, a uniform temperature distribution may be assumed within the joint. This temperature may be calculated using the maximum value of the A/V ratios of the connected steel members adjacent to the joint. For beam-to-column and beam-to-beam joints, where the beams are supporting a concrete floor, the temperature

distribution, θ_h , of the joint may be determined from the temperature of the bottom flange of the connected beam at mid span using the following method.

- i) If the depth of the beam is less than or equal to 400 mm

$$\theta_h = 0.88\theta_0 \left[1 - 0.3(h/D) \right] \quad (7.1)$$

where

- θ_h is the temperature at height h (mm) of the steel beam (Fig. 7.2);
 θ_0 is the bottom flange temperature of the steel beam remote from the connection, evaluated with Eqs. (4.16) or (4.19);
 h is the height of the component being considered above the bottom of the beam in (mm) (Fig. 7.2);
 D is the depth of the beam in (mm).

- ii) If the depth of the beam is greater than 400 mm

- For $h \leq D/2$

$$\theta_h = 0.88\theta_0 \quad (7.2)$$

- For $h > D/2$

$$\theta_h = 0.88\theta_0 \left[1 + 0.2(1 - 2h/D) \right] \quad (7.3)$$

where the meaning of the symbols is the same as for Eq. (7.1).

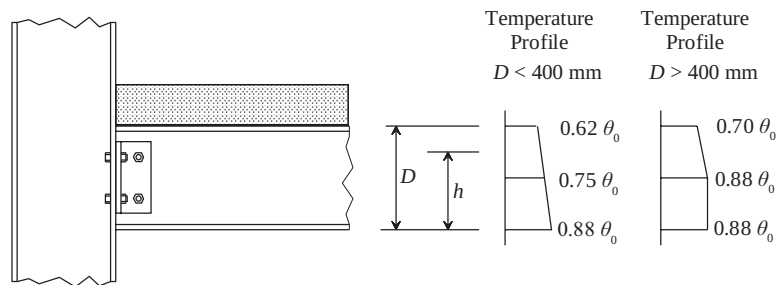


Figure 7.2 – Temperature profile within the depth of a joint in which the connected beam supports a concrete slab

7.4. BOLTED CONNECTIONS

The design fire resistance of bolts loaded in shear and tension should be determined using the methods described in Sections 7.4.1 and 7.4.2 respectively.

7.4.1. Design Fire Resistance of Bolts in Shear

7.4.1.1. Category A: Bearing Type

The design fire resistance of bolts loaded in shear should be determined from:

$$F_{v,t,Rd} = F_{v,Rd} k_{b,\theta} \frac{\gamma_{M2}}{\gamma_{M,fi}} \quad (7.4)$$

where

$F_{v,Rd}$ is the design shear resistance of the bolt per shear plane calculated assuming that the shear plane passes through the threads of the bolt (Table 3.4 of EN 1993-1-8);

$k_{b,\theta}$ is the reduction factor determined for the appropriate bolt temperature from Table 7.1;

γ_{M2} is the partial safety factor at normal temperature [= 1.25¹];

$\gamma_{M,fi}$ is the partial safety factor for fire conditions [= 1.0¹].

The design bearing resistance of bolts in fire should be determined from:

$$F_{b,t,Rd} = F_{b,Rd} k_{b,\theta} \frac{\gamma_{M2}}{\gamma_{M,fi}} \quad (7.5)$$

where

$F_{b,Rd}$ is the design bearing resistance of bolts at normal temperature determined from Table 3.4 of EN 1993-1-8.

303

7.4.1.2. Category B (slip resistance at serviceability) and Category C (slip resistance at ultimate state)

Slip restraint connections should be considered as having slipped in fire and the resistance of a single bolt should be calculated according to 7.4.1.1. for bearing type bolts.

7.4.2. Design Fire Resistance of Bolts in Tension

7.4.2.1. Category D and E: Non-preloaded and preloaded bolts

The design tension resistance of a single bolt in fire should be determined from:

¹ A different value can be given in the National Annexes

$$F_{ten,t,Rd} = F_{t,Rd} k_{b,\theta} \frac{\gamma_{M2}}{\gamma_{M,fi}} \quad (7.6)$$

where

$F_{t,Rd}$ is the tension resistance at normal temperature, determined from Table 3.4 of EN 1993-1-8.

7.5. DESIGN FIRE RESISTANCE OF WELDS

7.5.1. Butt Welds

According to the Eurocode 3 the design strength of a full penetration butt weld, for temperatures up to 700 °C, should be taken as equal to the strength of the weaker connected part using the appropriate reduction factors for structural steel given in Table 5.2 of Chapter 5. For temperatures above 700 °C the reduction factors for fillet welds given in Table 7.1 can also be used for butt welds.

7.5.2. Fillet Welds

The design resistance per unit length of a fillet weld in fire should be determined from:

304

$$F_{w,t,Rd} = F_{w,Rd} k_{w,\theta} \frac{\gamma_{M2}}{\gamma_{M,fi}} \quad (7.7)$$

where

$F_{w,Rd}$ is the design weld resistance per unit length at normal temperature determined from Clause 4.5.3. EN 1993-1-8;

$k_{w,\theta}$ is the strength reduction factors for welds determined from Table 7.1.

7.6. DESIGN EXAMPLES

In this section, several design examples, are presented, with full details. The default value of 1.0 and 1.25 proposed in Eurocode have been adopted for the partial safety factors $\gamma_{M,fi}$ and γ_{M2} , respectively.

Example 7.1: Consider the S355 bolted tension joint in an office building shown in Fig. 7.3. Assuming that the design value of tension force at normal temperature is $N_{Ed} = 300$ kN, that the bolts are Grade 4.6, M20 and that the shear plane passes through the unthreaded portion of the bolt, verify that the unprotected joint has fire resistance criterion R30.

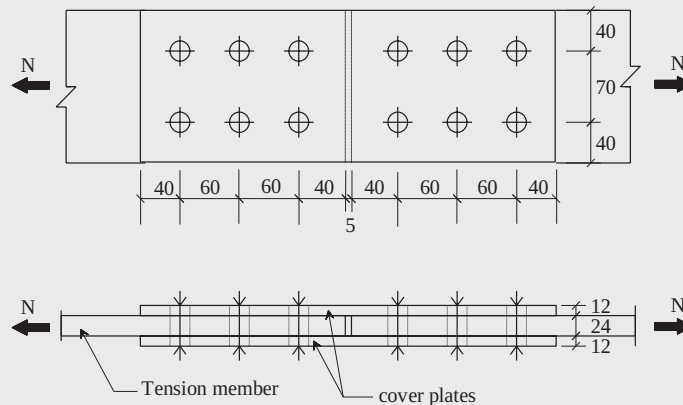


Figure 7.3 – Bolted joint of a member subject to tension

Solution:

As the member belongs to an office building, the design value of the tension force in a fire situation can be obtained from the value at normal temperature using the reduction factor for fire situation given in the Eurocode 3, $\eta_{fi} = 0.65$:

$$N_{fi,Ed} = \eta_{fi} \cdot N_{Ed} = 0.65 \cdot 300 = 195 \text{ kN}$$

The section factors of the tension member and the joint are respectively:

$$\left[\frac{A_m}{V} \right]_{member} = \frac{2(0.024 + 0.15)}{0.024 \cdot 0.15} = 96.7 \text{ m}^{-1}$$

and

$$\left[\frac{A_m}{V} \right]_{joint} = \frac{2(0.048 + 0.15)}{0.048 \cdot 0.15} = 55 \text{ m}^{-1}$$

After 30 minutes of standard fire exposure the member and the joint have the following temperatures obtained from table of the Annex A.4 using $k_{sh} = 1.0$

$$\theta_{a,member} = 763 \text{ }^{\circ}\text{C}$$

and

$$\theta_{a,joint} = 700 \text{ }^{\circ}\text{C}$$

Verification of the fire resistance of the gross cross section

For a temperature of 763 °C, the reduction factor for the effective yield strength from Table 5.2, has the value

$$k_{y,763^{\circ}\text{C}} = 0.1544$$

As net-section failure at fastener holes need not be considered (provided that there is a fastener in each hole) the gross cross section design resistance $N_{fi,\theta,Rd}$ of the tension member with a uniform temperature $\theta_a = 763 \text{ }^{\circ}\text{C}$ is:

$$\begin{aligned} N_{fi,\theta,Rd} &= Ak_{y,763^{\circ}\text{C}}f_y/\gamma_{M,fi} = \\ &= 24 \cdot 150 \cdot 0.1544 \cdot 355/1.0 = 197 \times 10^3 \text{ N} = 197 \text{ kN} \end{aligned}$$

After 30 minutes of standard fire exposure, the design resistance in tension exceeds the design load and therefore the joint is satisfactory:

$$N_{fi,Ed} < N_{fi,t,Rd}$$

According to Eurocode 3, net-section failure at fastener holes need not be considered, provided that there is a fastener in each hole. This is because the steel temperature is lower at joints due to the presence of additional joint material. In fact, in this example, the temperature at the joint is lower than that of the member. This assumption can be confirmed if the resistance of the tension member is evaluated using the net area of its cross section:

$$A_{net} = A - 2d_0 = 24 \cdot 150 - 2 \cdot 22 = 3556 \text{ mm}^2$$

At 700 °C the reduction factor for the effective yield strength from Table 5.2, has the value

$$k_{y,700^{\circ}\text{C}} = 0.23$$

and the design resistance $N_{fi,\theta,Rd}$ of the tension member with a uniform temperature $\theta_a = 700 \text{ }^{\circ}\text{C}$ is:

$$\begin{aligned} N_{fi,\theta,Rd} &= A_{net}k_{y,700^{\circ}\text{C}}f_y/\gamma_{M,fi} = \\ &= 3556 \cdot 0.23 \cdot 355/1.0 \times 10^{-3} = 290.3 \text{ kN} \end{aligned}$$

This value is bigger than then resistance of 197 kN of the gross cross section
 There is also no need to check the fire resistance of the cover plates in this example, because their thickness is equal to half of the thickness of the connected members and should resist to half of the applied tension force. On the other hand their temperature is lower than the temperature of the members.

Verification of the shear resistance of the bolts in fire situation

As the joint has six bolts with two shear planes, the shear force per bolt is:

$$F_{fi,Ed} = \frac{N_{fi,d}}{6 \cdot 2} = \frac{195}{12} = 16.25 \text{ kN}$$

The design shear resistance of the bolt per shear plane calculated assuming that the shear plane passes through the threaded part of the bolt (see definition of $F_{v,Rd}$ given in Eq. (7.4)) as given in Eurocode 3 Part 1-8. For an M20 Grade 4.6 bolt at room temperature, Part 1-8 of Eurocode 3 gives the following expression:

$$F_{v,Rd} = \frac{0.6f_{ub}A_s}{\gamma_{M2}} = \frac{0.6 \cdot 400 \cdot 245}{1.25} = 47 \times 10^3 \text{ N} = 47 \text{ kN}$$

The strength reduction factor for bolts at 700 °C is determined from Table 7.1:

$$k_{b,700^\circ} = 0.1$$

and the design value of the shear resistance of a bolt after 30 minutes of standard fire exposure is

$$F_{v,t,Rd} = F_{v,Rd} k_{b,700^\circ} \frac{\gamma_{M2}}{\gamma_{M,fi}} = 47 \cdot 0.1 \cdot \frac{1.25}{1.0} = 5.9 \text{ kN}$$

This value is lower than the design value of the shear load applied on the bolt

$$F_{fi,Ed} > F_{v,t,Rd}$$

To satisfy the fire resistance criterion R30 the joint should be protected with a fire protection material. Alternatively the fire resistance of the bolt group can be improved by using larger diameter bolts, higher grade bolts or by using a larger number of bolts. Another option is to carry out a more accurate evaluation of the load level in the joint as this may result in a value lower than the value of 0.65 used in this example.

Verification of the bearing resistance

According to Part 1-8 of Eurocode 3 the bearing resistance at room temperature is given by:

$$F_{b,Rd} = \frac{k_1 \alpha_b f_u d t}{\gamma_{M2}}$$

where

– for end bolts in the direction of load transfer (see Fig. 7.4)

$$\alpha_b = \min \left(\frac{e_1}{3d_0}; \frac{f_{ub}}{f_u}; 1.0 \right)$$

– for inner bolts in the direction of load transfer (see Fig. 7.4)

$$\alpha_b = \min \left(\frac{p_1}{3d_0} - \frac{1}{4}; \frac{f_{ub}}{f_u}; 1.0 \right)$$

In the safe side it can be considered that all the bolts have the minimum bearing resistance:

$$\alpha_b = \min \left(\frac{e_1}{3d_0}; \frac{p_1}{3d_0} - \frac{1}{4}; \frac{f_{ub}}{f_u}; 1.0 \right)$$

308

There are only edge bolts in the direction perpendicular to the direction of load transfer, thus (see Fig. 7.4)

$$k_1 = \min \left(2.8 \frac{e_2}{d_0} - 1.7; 1.4 \frac{p_2}{d_0} - 1.7; 2.5 \right)$$

for all the bolts of the connection.

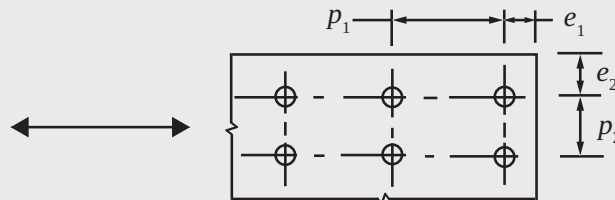


Figure 7.4 – Symbols for spacing of fasteners (EN 1993-1-1)

In this case

$$e_1 = 40 \text{ mm}; p_1 = 60 \text{ mm}; t = 24 \text{ mm}$$

$$e_2 = 40 \text{ mm}; p_2 = 70 \text{ mm};$$

$$d = 20 \text{ mm}; d_0 = 22 \text{ mm};$$

$$f_{ub} = 400 \text{ N/mm}^2; f_u = 490 \text{ N/mm}^2$$

leading to

$$\alpha_b = \min\left(\frac{40}{3 \cdot 22}; \frac{60}{3 \cdot 22} - \frac{1}{4}; \frac{400}{490}; 1.0\right) = \min(0.61; 0.66; 0.82; 1.0) = 0.61$$

and

$$k_1 = \min\left(2.8 \frac{40}{22} - 1.7; 1.4 \frac{70}{22} - 1.7; 2.5\right) = \min(3.39; 2.75; 2.5) = 2.5$$

and so

$$F_{b,Rd} = \frac{2.5 \cdot 0.61 \cdot 490 \cdot 20 \cdot 24}{1.25} = 287 \times 10^3 \text{ N} = 287 \text{ kN}$$

At 700 °C the bearing resistance is:

$$F_{b,t,Rd} = F_{b,Rd} k_{b,700^\circ} \frac{\gamma_{M2}}{\gamma_{M,fi}} = 287 \cdot 0.1 \cdot \frac{1.25}{1.0} = 35.9 \text{ kN}$$

309

The total bearing resistance for all six bolts is

$$F_{b,t,Rd,TOTAL} = 6 \cdot 35.9 = 215.3 \text{ kN}$$

It can be concluded that six Grade 4.6, M20 bolts are sufficient to transmit the tension force of 195 kN, considering the bearing resistance:

$$N_{fi,Ed} = 195 \text{ kN} < F_{b,t,Rd,TOTAL} = 215.3 \text{ kN}$$

This example has shown that, although the resistance of the joint at normal temperature is satisfactory and that no fire protection is needed for the member in tension, the shear resistance of the bolt group in the fire situation is lower than the applied load.

Example 7.2: Consider a welded tension joint in S355 steel, as shown in Fig. 7.5. Assuming that the design value of the tension force in the fire situation is $N_{fi,Ed} = 190$ kN and that the throat thickness of the fillet welds is 6 mm, verify if the unprotected joint has a fire resistance of R30.

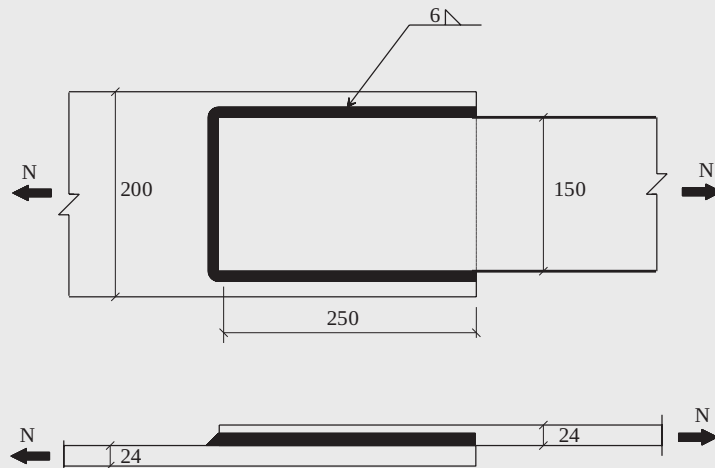


Figure 7.5 – Welded tension joint

Solution:

Verification of the fire resistance of the gross cross section

The gross cross section of the connected members is $150 \times 24 \text{ mm}^2$. This is the same as the previous example, where it was found that the design tension resistance after 30 minutes of standard fire exposure is:

$$N_{fi,t,Rd} = 197 \text{ kN}$$

This is higher than the applied tension load in fire situation $N_{fi,Ed} = 190$ kN.

Verification of the fire resistance of the fillet weld

The section factor, A_m/V , of the joint can be determined by considering a cross section perpendicular to the main direction of the joint.

$$\frac{A_m}{V} = \frac{0.2 + 4 \cdot 0.024 + 2 \cdot 0.025 + 0.15}{0.2 \cdot 0.024 + 0.15 \cdot 0.024} = 59 \text{ m}^{-1}$$

Assuming $k_{sh} = 1.0$, the temperature of the joint can be determined from table of the Annex A.4 by interpolating between the values of 40 and 60 m^{-1} .

$$\theta = 717 \text{ }^\circ\text{C}$$

According to the simplified method for design resistance of fillet weld presented in EN 1993-1-8, the design resistance of the fillet weld may be assumed to be adequate if, at every point along its length, the resultant of all the forces per unit length transmitted by the weld satisfy the following criterion:

$$F_{w,Ed} \leq F_{w,Rd}$$

$$F_{w,Rd} = \frac{f_u / \sqrt{3}}{\beta_w \gamma_{M2}} a$$

where

$$f_u = 490 \text{ N/mm}^2, \text{ for the steel grade S355}$$

$$\beta_w = 0.9, \text{ for the steel grade S355}$$

$$a = 6 \text{ mm (effective throat thickness of the fillet weld)}$$

$$\gamma_{M2} = 1.25$$

leading to

$$F_{w,Rd} = \frac{f_u / \sqrt{3}}{\beta_w \gamma_{M2}} a = \frac{490 / \sqrt{3}}{0.9 \cdot 1.25} \cdot 6 = 1509 \text{ N/mm} = 1.51 \text{ kN/mm}$$

The design resistance per unit length of the fillet weld in fire should be determined from Eq. (7.7), here rewritten:

$$F_{w,t,Rd} = F_{w,Rd} k_{w,\theta} \frac{\gamma_{M2}}{\gamma_{M,\bar{f}}}$$

311

The reduction factor for welds can be determined from Table 7.1 by interpolating between 700 and 800 °C:

$$k_{w,717^\circ\text{C}} = 0.12$$

leading to

$$F_{w,t,Rd} = 1.51 \cdot 0.12 \cdot \frac{1.25}{1.0} = 0.2265 \text{ kN/mm}$$

Multiplying this value by the total length of the fillet weld ($l = 650 \text{ mm}$) the design value of the fire resistance of the fillet weld is:

$$F_{w,t,Rd,TOTAL} = 0.2265 \cdot 650 = 147.2 \text{ kN}$$

This value is lower than the applied axial load in the fire situation, $N_{fi,Ed} = 190$ kN. The required fire resistance of R30 is not achieved and fire protection should be used or the thickness of the fillet weld should be increased (a thickness of 8 mm would be enough).

Example 7.3: Consider a beam-to-column joint between an IPE 270 beam and a HE 160 B column in steel grade S235 connected by a double angle cleat L120×80×8, welded to the web of the beam and bolted with Grade 4.6 M16 to the flange of the column, as shown in Fig. 7.6. Assuming that the design value of the shear force at the connection in fire situation is $V_{fi,Ed} = 30$ kN, verify the shear resistance of the bolts in fire situation, if the shear plane passes through the unthreaded portion of the bolt and the required fire resistance is R30.

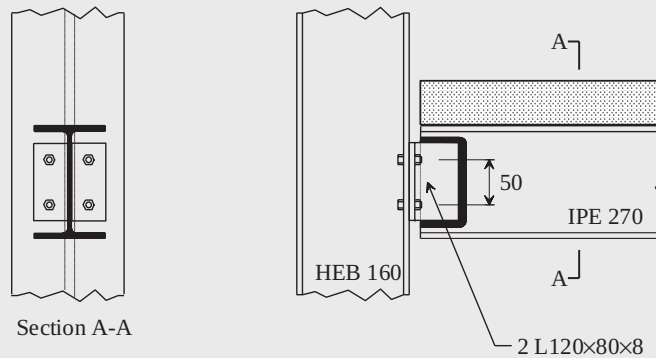


Figure 7.6 – Double angle cleat. Beam-to-column connection

Solution:

The relevant characteristics of the IPE 270 to solve this design example are:

$$b = 135 \text{ mm}$$

$$t_f = 6.6 \text{ mm}$$

The section factor of the bottom flange of the beam is:

$$\frac{A_m}{V} = \frac{2(b+t_f)}{bt_f} = \frac{2 \cdot (0.135 + 0.0066)}{0.135 \cdot 0.0066} = 318 \text{ m}^{-1}$$

Making a conservative assumption of $k_{sh} = 1.0$, the temperature of the bottom flange of the beam can be determined from table of the Annex A.4 by interpolating between 300 and 400 m⁻¹. This gives a temperature after 30 minutes of:

$$\theta_0 = 835.4 \text{ }^\circ\text{C}$$

The height of the first row of bolts above the bottom of the beam is $h = 110 \text{ mm}$, and accordingly to Eq. (7.3), its temperature takes the value:

$$\theta_h = 0.88 \cdot 835.4 \cdot [1 - 0.3 \cdot (110/270)] = 645 \text{ }^\circ\text{C}$$

At this temperature, Table 7.1, gives the following strength reduction factor for bolts:

$$k_{b,645^\circ\text{C}} = 0.166$$

The design shear resistance of the bolt per shear plane calculated assuming that the shear plane passes through the threads portion of the bolt, as EN 1993-1-2 imposes, is, for a M16 bolts of Class 4.6 at normal temperature, given in Part 1-8 of Eurocode 3:

$$F_{v,Rd} = \frac{0.6 f_{ub} A_s}{\gamma_{M2}} = \frac{0.6 \cdot 400 \cdot 157}{1.25} = 30.1 \times 10^3 \text{ N} = 30.1 \text{ kN}$$

The design value of the shear resistance of a bolt after 30 minutes of standard fire exposure is

$$F_{v,t,Rd} = F_{v,Rd} k_{b,645^\circ\text{C}} \frac{\gamma_{M2}}{\gamma_{M,fi}} = 30.1 \cdot 0.166 \cdot \frac{1.25}{1.0} = 6.25 \text{ kN}$$

This value is lower than the applied shear load on the bolts, i.e., $30/4 = 7.5 \text{ kN}$ (4 bolts and only one shear plane) and thus the bolts do not satisfy the fire resistance criterion R30.

Example 7.4: Evaluate the critical temperature of the beam-to-column joint of the previous example, only considering the shear fire resistance of the bolts. What is the time needed for the bolts to reach this temperature?

Solution:

The failure of a bolt under shear force occurs when the following equation is verified:

$$V_{fi,Ed} = F_{v,t,Rd}$$

The design value of shear in fire situation for each bolt is

$$V_{fi,Ed} = 30/4 = 7.5 \text{ kN}$$

The shear resistance of the bolts per shear plane is given by

$$F_{v,t,Rd} = F_{v,Rd} k_{b,\theta} \frac{\gamma_{M2}}{\gamma_{M,fi}} = \frac{0.6 \cdot f_{ub} A_s}{\gamma_{M2}} k_{b,\theta} \frac{\gamma_{M2}}{\gamma_{M,fi}}$$

so

$$7500 = \frac{0.6 \cdot 400 \cdot 157}{1.25} k_{b,\theta} \frac{1.25}{1.0}$$

from where

$$k_{b,\theta} = 0.199$$

Interpolation in the Table 7.1 gives the critical temperature

$$\theta_{b,cr} = 617.5 \text{ } ^\circ\text{C}$$

The time needed for the first row of bolts reach this temperature can now be evaluated.

Knowing that the distance from the first row of bolts to the bottom flange of the beam is $h = 110\text{mm}$, Eq. (7.3) leads to:

$$617.5 = 0.88 \cdot \theta_0 \left[1 - 0.3 \left(\frac{110}{270} \right) \right]$$

From this equation, the temperature θ_0 of the bottom flange needed for the first row of bolts to reach a temperature of $617.5 \text{ } ^\circ\text{C}$, is:

$$\theta_0 = 799 \text{ } ^\circ\text{C}$$

The time needed for the bottom flange of the beam with a section factor of $A_m/V = 318 \text{ m}^{-1}$, to reach this temperature, can be obtained by interpolation in table of the Annex A.4:

$$t_{fi,d} = 24.7 \text{ minutes}$$

Chapter 8

THE COMPUTER PROGRAM "ELEFIR-EN"

8.1. GENERAL

This chapter describes the computer program Elefir-EN which has been developed for the fire design of structural members in accordance with the simple calculation model given in the Eurocodes.

Guidance paper L (concerning the Construction Products Directive - 89/106/EEC) gives information on the “Application and use of Eurocodes” (European Commission, 2007), and states that one of the aims and benefits of the Eurocode programme is that it allows common design aids and software to be developed for use in all Member States. In the late 1990’s the University of Liege, Belgium, created the computer program, Elefir, which is based on the simplified fire design rules given in the ENV versions of the Eurocode 1 and Eurocode 3. More recently, the University of Aveiro, Portugal, has updated this software so that it aligns with the new versions of the Eurocodes, (EN 1991-1-2 and EN 1993-1-2). A number of new capabilities have been introduced. This updated version of the computer program is called Elefir-EN to reflect its origin and to highlight the fact that it is now based on the EN versions of the Eurocodes, Vila Real and Franssen (2010). The program was developed using Visual Basic and is fully compatible with Windows standards. As most of the rules presented in the previous chapters are covered in the software, only particular aspects of the software will be presented in this chapter.

The software is an essential tool for structural engineers in the design office, enabling quick and accurate calculations to be produced, reducing

8. THE COMPUTER PROGRAM "ELEFIR-EN"

design time and the probability of errors in the application of the equations. It can also be used by academics and students.

8.2. BRIEF DESCRIPTION OF THE PROGRAM

Elefir-EN allows the user to calculate the fire resistance of simple steel members, made of carbon steel or stainless steel, loaded about the strong axis or about the weak axis. Calculations can be performed in the time domain, resistance domain and temperature domain, as defined in Chapter 5. Fig. 8.1 shows the first screen of the program.



Figure 8.1 – First screen of the software Elefir-EN

8.2.1. Available thermal calculations

The program allows the user to choose the section type, the fire exposure, type of fire protection and the heating curve. All of these options are explained below.

- Typical cross sectional shapes include: HD, HE, HL, HP, IPE, UB, UC, W, L, RHS and CHS from a database or user-defined dimensions can be included (see Fig. 8.2);

8.2. BRIEF DESCRIPTION OF THE PROGRAM

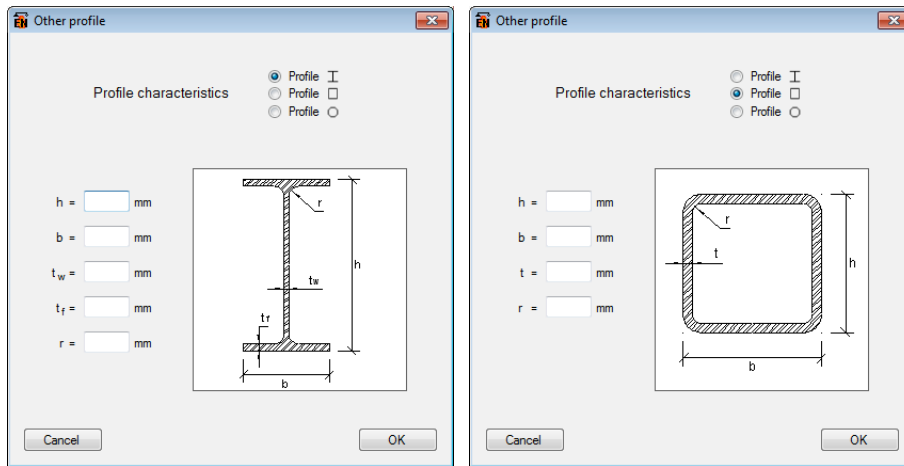
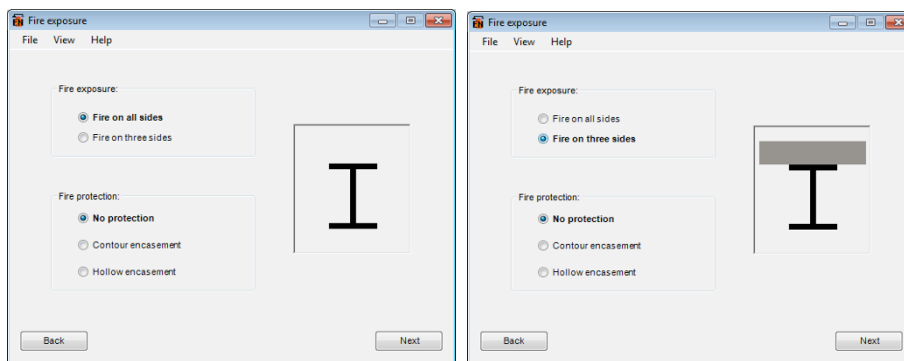


Figure 8.2 – Dialog box for user-defined sections

- There are two options for fire exposure: the section can be exposed to fire on either three or four sides (see Fig. 8.3). Alternatively, the value of the section factor can be introduced directly;



a)

b)

Figure 8.3 – Options for fire exposure. a) four sides; b) three sides

- Options for fire protection include: no protection, contour encasement and hollow encasement (see Fig. 8.4);

8. THE COMPUTER PROGRAM "ELEFIR-EN"

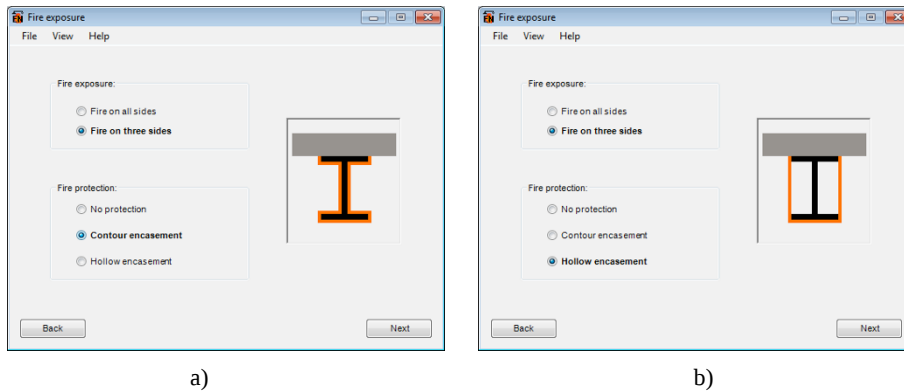


Figure 8.4 – Options for fire protection. a) contour encasement; b) hollow encasement

- The properties of several fire protection materials are available, according to ECCS (1995) (see Annex A.6) and new insulating material can also be added to the database by the user. The properties of the introduced material can also be temperature dependent;
- Several heating curves are available, and these include (see Fig. 8.5): the ISO 834 curve, the hydrocarbon curve, the parametric fire curves, user-defined curves and localized fires impacting or not impacting the ceiling (see Fig. 8.6);

318

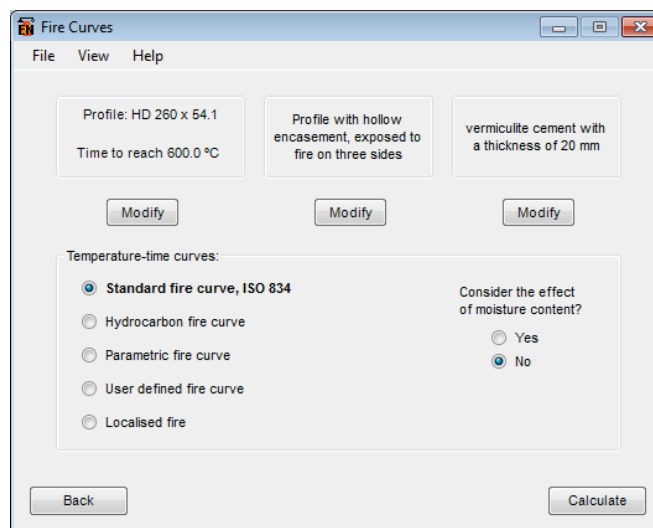
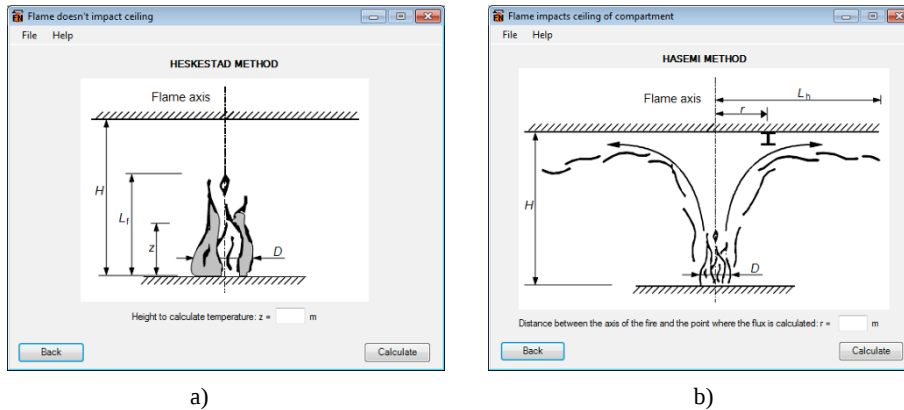
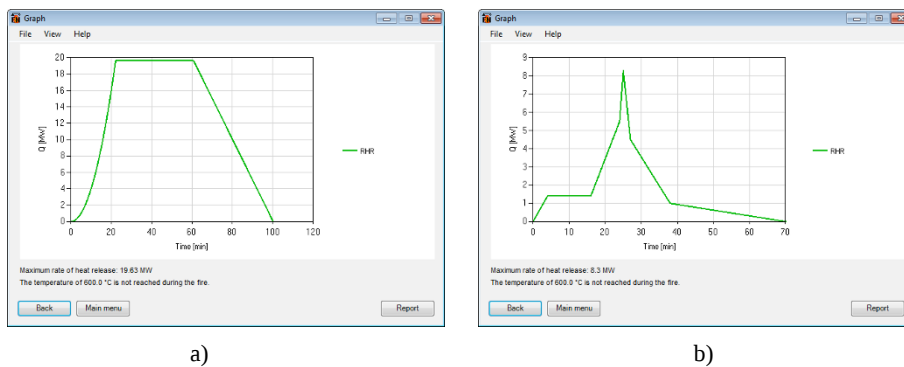


Figure 8.5 – Heating curves and option for the effect of moisture content



a) b)
Figure 8.6 – Localised fires. a) Hesquestad method; b) Hasemi method

- The Rate of Heat Release (*RHR*) necessary for the definition of the localised fires can be defined as a t^2 curve for the growing phase according to Eq. (E.5) of Eurocode 1 (see also Eq. (B.2) from Annex B of this book) or can be introduced as a user-defined curve. Fig. 8.7 shows an example of a *RHR* curve proposed by Eurocode 1 and a curve defined by the user representing the *RHR* of a single burning car fire (Joyeux *et al*, 2001);



a) b)
Figure 8.7 – RHR – Rate of Heat Release. a) According Eurocode 1; b) User-defined curve

- For parametric fire curves the dialog box allows the compartment dimensions and the location and size of the openings to be defined (see Fig. 8.8);

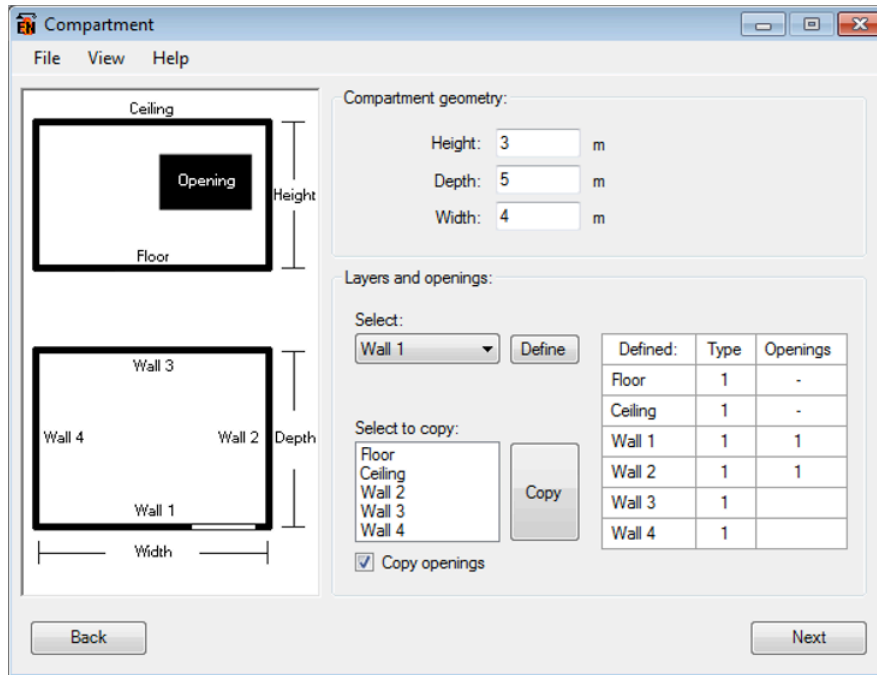


Figure 8.8 – Dialog box for defining the compartment dimensions

- For parametric fires or localised fires the type of occupancy, the fire growth rate, the fire load density as well as the type of active fire fighting measures (sprinkler, detection, automatic alarm transmission, firemen ...) as defined in Annex E of EN 1991-1-2, can be selected from the dialog box shown in Fig. 8.9 and Fig. 8.10. It should be noted that the choice for openings in the dialog box of localised fires (see Fig. 8.10) has been introduced to take into account if the fire is ventilation controlled or not, so that the plateau level is reduced according to Eq. (E.6) from Annex E of EN 1991-1-2 (see also Section B.4 of Annex B of this book). The option “no” openings must be chosen if the user does not want to take into account the effect of oxygen content, or in case of a fire in open air;

8.2. BRIEF DESCRIPTION OF THE PROGRAM

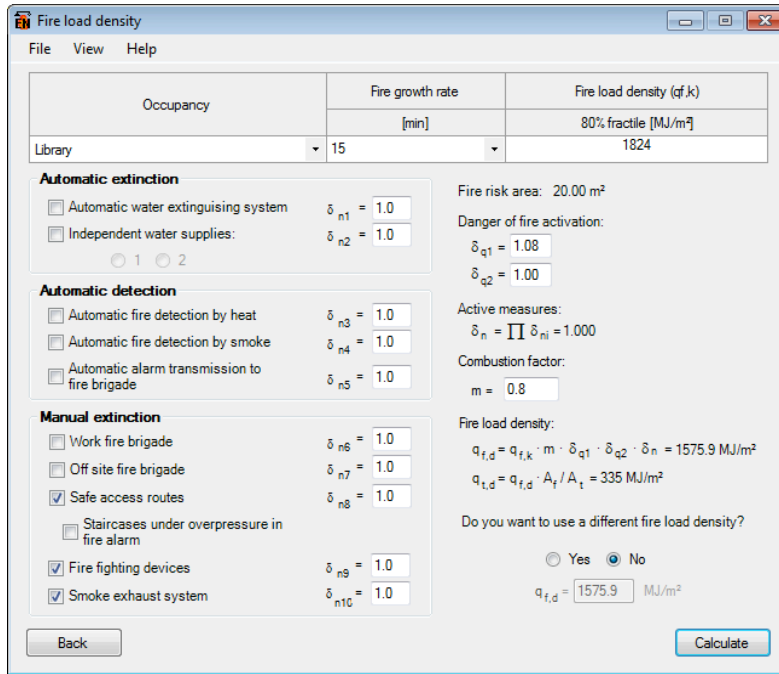


Figure 8.9 – Dialog box for defining parametric fires

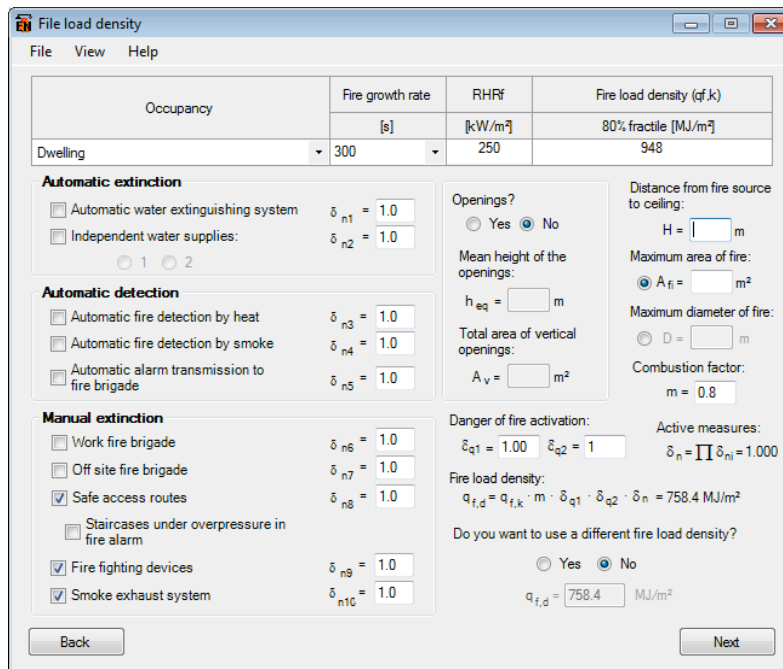


Figure 8.10 – Dialog box for defining localised fires

8.2.2. Available mechanical calculations

The following calculations and choices can be done:

- The critical temperature and the critical time of a member subjected to tension, compression, shear, bending, bending and tension, bending and compression, bending and shear can be calculated (see Fig. 8.11). The option "Element submitted to bending and axial force (cross sectional verification)" allows for the cross section verification of fire resistance of an element submitted to combined moment and tension or compression;
- From the screen of Fig. 8.11, the safety factors can be chosen. Clicking on the button "Safety factors" the screen of Fig. 8.12 appears;
- From the menu item "Tools" (see Fig. 8.13) it is possible to add new materials to the data base of wall lining materials and of insulating materials, shown in Fig. 8.14 and Fig. 8.15 respectively;

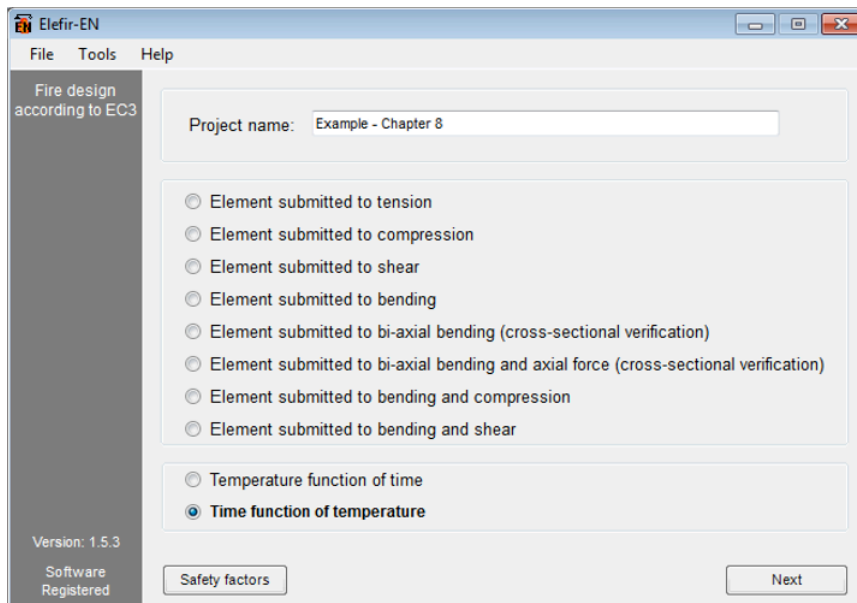


Figure 8.11 – Main menu

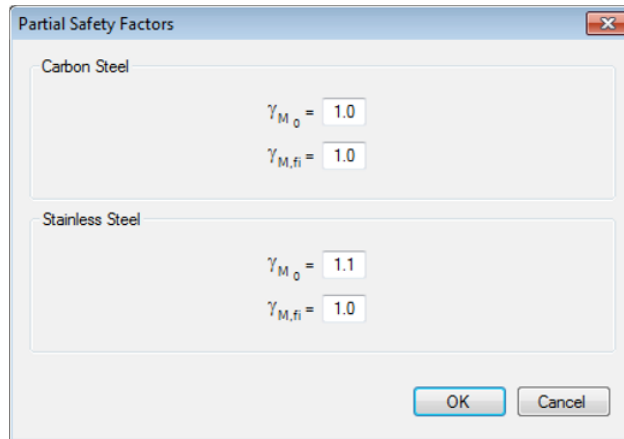


Figure 8.12 – Safety factors

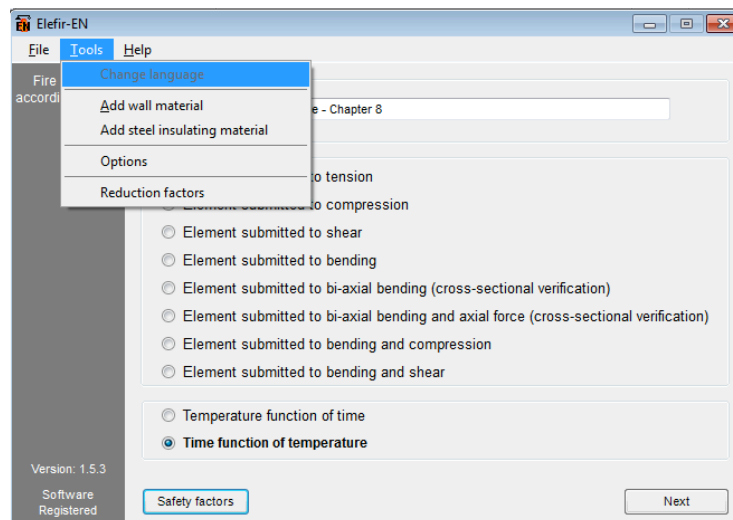


Figure 8.13 – Menu tools

- The “Options” in the menu item “Tools” are related with the possibility of choosing the way of calculating the critical temperature of carbon steel members either by using expression (4.22) from EN 1993-1-2 or by interpolation on the table 3.1 from EN 1993-1-2 and also with the possibility of using shadow effect or not, as shown in Fig. 8.16.

8. THE COMPUTER PROGRAM "ELEFIR-EN"

Material	Unit mass [kg/m ³]	Thermal conductivity [W/mK]	Specific heat [J/kgK]
Gas-concrete bricks	550	0.14	840
Heavy bricks	2000	1.2	1000
Light perforated bricks	700	0.15	840
Normal bricks	1600	0.7	840
Light weight concrete	1600	0.8	840
Middle weight concrete	1800	1.15	1000
Normal weight concrete	2300	1.6	1000
Gypsum board	900	0.25	1000
Gypsum finery	1150	0.485	1000
Steel	7850	45	600
Granite stone	2600	2.8	1000
Glass wool	60	0.037	1030
Rock wool	60	0.037	1030
Heavy wood	720	0.2	1880
Normal wood	450	0.1	1112

Figure 8.14 – Wall lining materials

Material	Unit mass [kg/m ³]	Thermal conductivity [W/mK]	Specific heat [J/kgK]	Moisture content [%]
vermiculite cement	350	0.12	1200	15
perlite	350	0.12	1200	15
vermiculite and cement	550	0.12	1100	15
perlite and cement	550	0.12	1100	15
vermiculite and gypsum	650	0.12	1100	15
perlite and gypsum	650	0.12	1100	15
vermiculite and cement boards	800	0.20	1200	15
perlite and cement boards	800	0.20	1200	15
fibre-silicate boards	600	0.15	1200	3
fibre-calcium-silicate boards	600	0.15	1200	3
fibre-cement boards	800	0.15	1200	5
gypsum boards	800	0.20	1700	20
compressed fibre silicate boards	150	0.20	1200	2
compressed mineral-wool boards	150	0.20	1200	2
compressed stone-wool boards	150	0.20	1200	2

Figure 8.15 – Fire protection materials

324

- From the menu item “Tools”, it is also possible to choose “Reduction factors” for evaluating these factors as function of the temperature or the temperature function of the value of these factors (see Fig. 8.17);

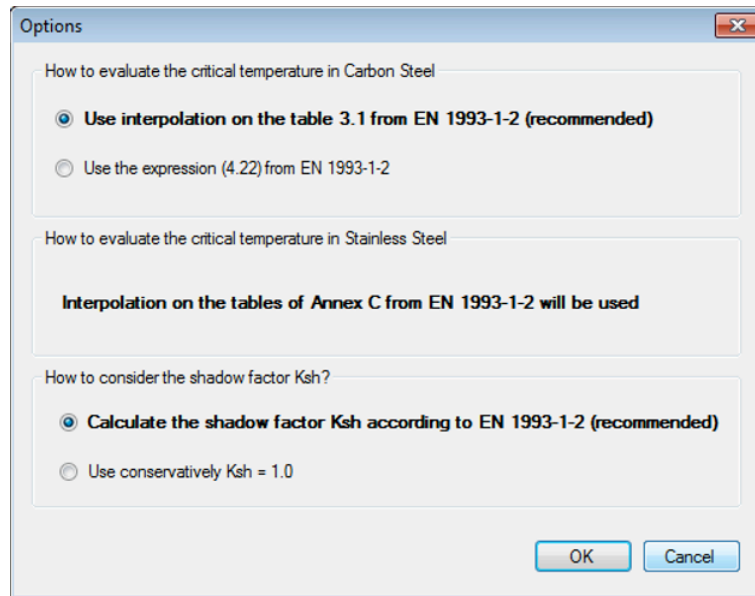
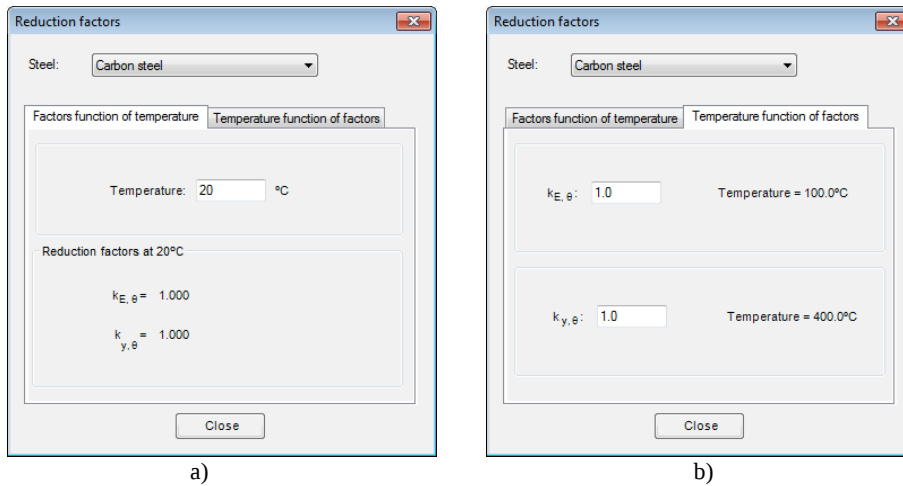


Figure 8.16 – Options menu



a) Reduction factors function of the temperature;
 b) Temperature function of the reduction factors

- For combined bending and compression, several load cases are possible in both y and z directions: end moments (see Fig. 8.18 a), in-plane lateral loads (see Fig. 8.18b) or in-plane lateral loads (uniform or point loads) with end moments (see Fig. 8.18c);

8. THE COMPUTER PROGRAM "ELEFIR-EN"

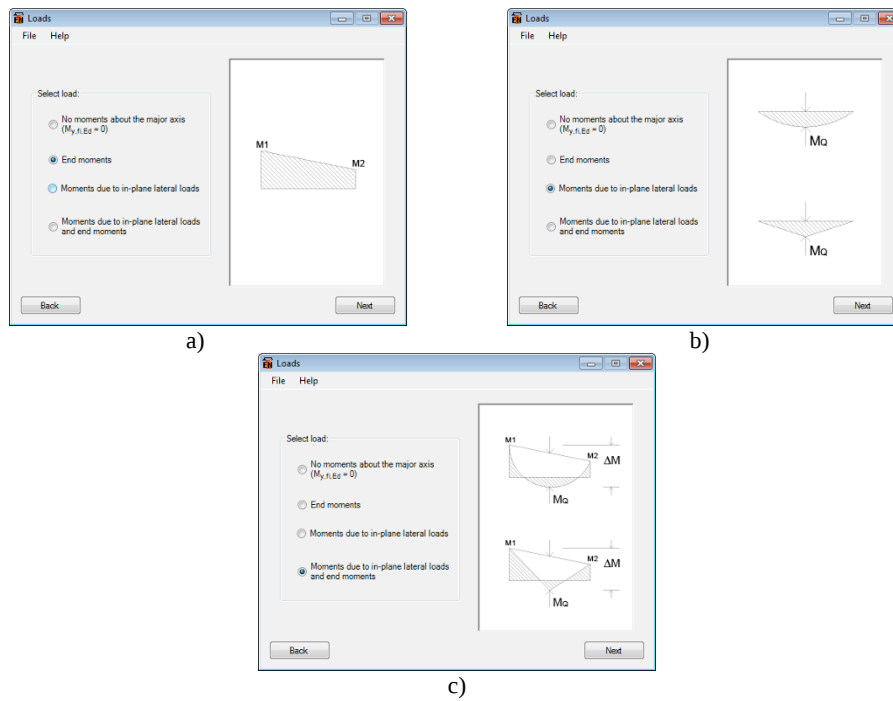


Figure 8.18 – Possible load cases for bending

- The time to reach the critical temperature of the element. For the case of critical temperature due to the shear force, the program allows for the choice between the section factor of the full cross section and the section factor of the web;
- The steel temperature after a certain period of time;
- The thickness of the fire protection material needed to ensure a certain fire resistance. Fig. 8.19 shows the charts for the development of the temperature in the compartment and in a steel member subjected to a parametric fire. Fig. 8.19a) shows the development of the steel temperature for an unprotected steel member. Fig. 8.19b) shows the development of the steel temperature after the program automatically evaluated the thickness of insulating material so that the maximum temperature of the steel is lower than the critical temperature during the complete duration of the fire including the decay phase, and Fig. 8.19c) depicts the development of the steel temperature after the program automatically defined the thickness of the fire protection material so that the critical temperature is not reached until 30 minutes of fire exposure.
- Global plastic analysis of continuous beams (see Fig. 8.20);

8.2. BRIEF DESCRIPTION OF THE PROGRAM

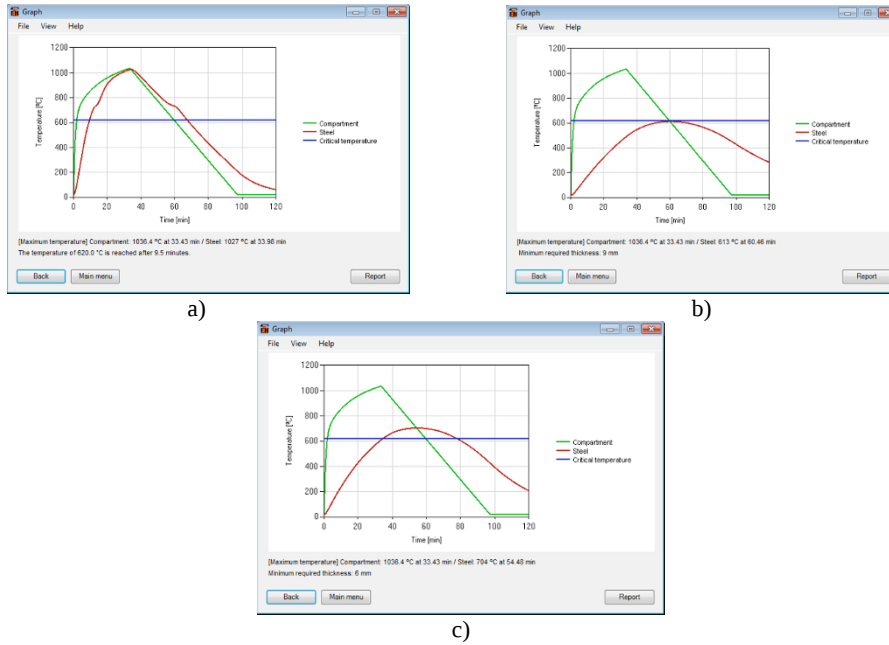


Figure 8.19 – Development of the compartment and steel temperature for a parametric fire. a) Unprotected member; b) and c) Protected member

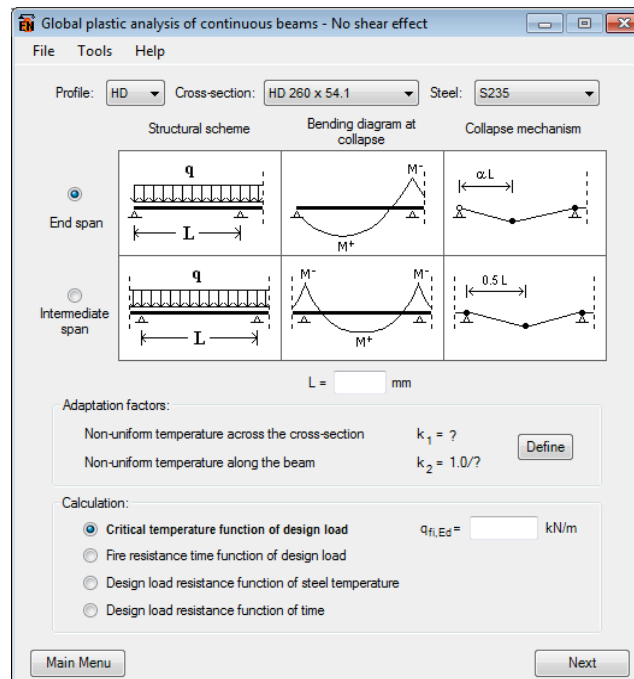


Figure 8.20 – Dialog box for the global plastic analysis of continuous beams

8. THE COMPUTER PROGRAM "ELEFIR-EN"

- The design moment resistance can be evaluated considering or not lateral-torsional buckling (see Fig. 8.21). Several load cases are possible: end moments, transverse load with several end conditions (see Fig. 8.22). The elastic critical moment is calculated based on the work done by Galéa (2002) which is also presented in ECCS (2006).

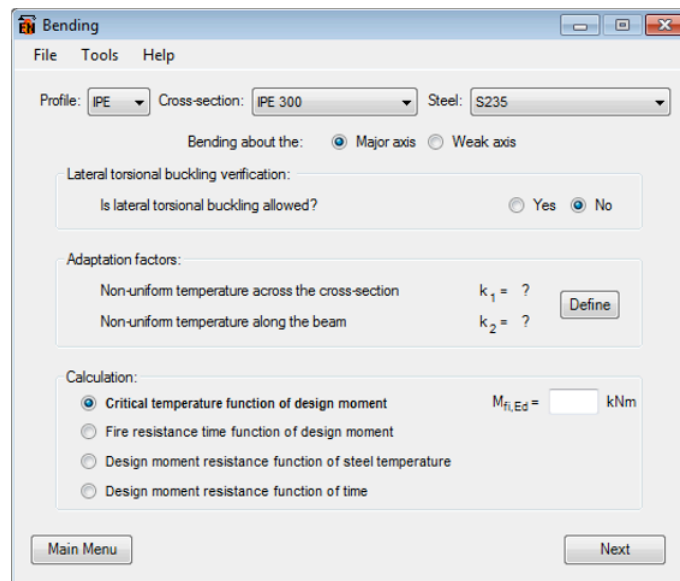


Figure 8.21 – Dialog box for bending

328

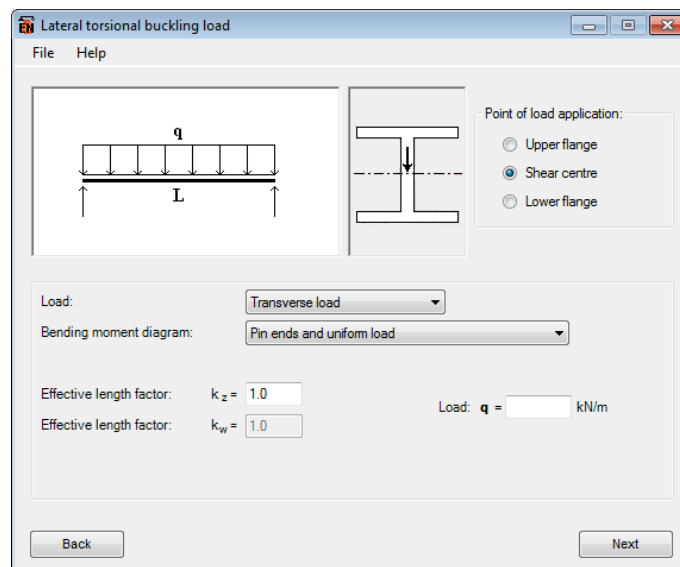


Figure 8.22 – Dialog box for bending with lateral-torsional buckling

8.3. DEFAULT CONSTANTS USED IN THE PROGRAM

The following coefficients and factors are used in the program:

α_c the coefficient of heat transfer by convection given in Eq.(3.4) is taken as:

	α_c [W/m ² K]
Standard fire curve ISO 834	25
Hydrocarbon curve	50
Parametric fire, localised fires or user-defined fire curves	35

- ϕ the configuration factor (see Chapter 3 and Section 4.9) is taken as $\phi = 1$;
- ε_m the surface emissivity of the member (see Eq. (3.4)) is taken as $\varepsilon_m = 0.7$ for carbon steel and $\varepsilon_m = 0.4$ for stainless steel;
- ε_f the emissivity of the fire (see Eq.(3.4)) is taken as $\varepsilon_f = 1.0$;
- ρ_a the unit mass of steel, is taken as $\rho_a = 7850$ [kg/m³];
- k_2 the adaptation factor for non-uniform temperature along the beam in the global plastic analysis of continuous beams is taken as $k_2 = 1$ for the positive moment resistance in the span and $k_2 = 0.85$ for the negative moment resistance at the supports (see Section 5.6.3);
- Δt the time interval used for solving Eq. (4.16) and Eq. (4.19) is taken as $\Delta t = 1$ second;
- A_m/V the section factor internally used for evaluating the fictitious gas temperature in the case of a localised fire impinging the ceiling, is taken as $A_m/V = 10000$ m⁻¹ with a time interval $\Delta t = 1$ second in Eq. (4.16) (see Section 4.10.2).

8.4. DESIGN EXAMPLE

A simply supported HE 220 B column which forms part of an office building is subject to the axial compression load and uniform transverse load shown in Fig. 8.23. The design values of the axial and uniform load at room temperature are $N_{Ed} = 200$ kN and $q_{Ed} = 20$ kN/m respectively. The column is exposed to a standard fire on all four sides. The steel grade is S235. Assuming that the member can buckle about both the y - y or z - z axes, that the column is not supported against lateral-torsional buckling and that the uniform load is applied on the upper flange, evaluate the following:

8. THE COMPUTER PROGRAM "ELEFIR-EN"

- The critical temperature.
- The fire resistance.
- The thickness of mineral fibre required for the column to be classified as R60.

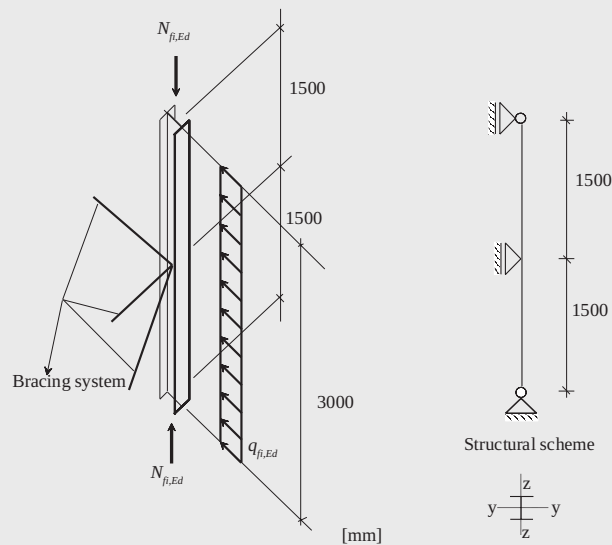


Figure 8.23 – HE 220 B under major axis load and bracing system

Solution:

Total length:

$$L_y = 3000 \text{ mm}; L_z = 1500 \text{ mm}$$

Buckling length:

$$l_{y,fi} = k_{y,fi} L_y = 1.0 \times 3000 = 3000 \text{ mm}; l_{z,fi} = k_{z,fi} L_z = 1.0 \times 1500 = 1500 \text{ mm}$$

Load in fire situation:

$$N_{fi,Ed} = \eta_{fi} N_{Ed} = 0.65 N_{Ed} = 130 \text{ kN}$$

$$q_{fi,Ed} = \eta_{fi} q_{Ed} = 0.65 q_{Ed} = 13 \text{ kN/m}$$

The maximum moment in the span is

$$M_{y,fi,Ed} = \frac{q_{fi,Ed} \times L^2}{8} = \frac{13 \times 3^2}{8} = 14.625 \text{ kNm}$$

Fig.8.24 depicts the $M_{y,fi,Ed}$ bending diagram and Fig. 8.25 shows the corresponding bending diagram for LTB.

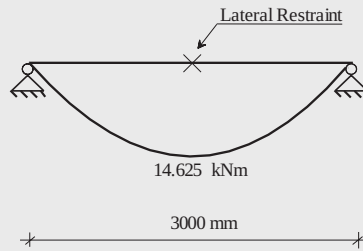


Figure 8.24 – $M_{y,fi,Ed}$ bending diagram

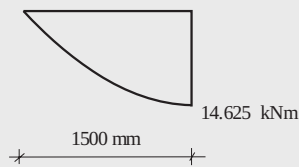
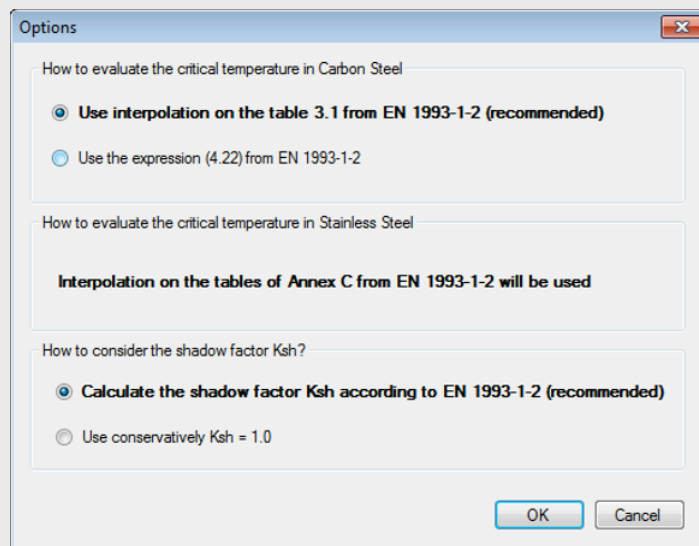


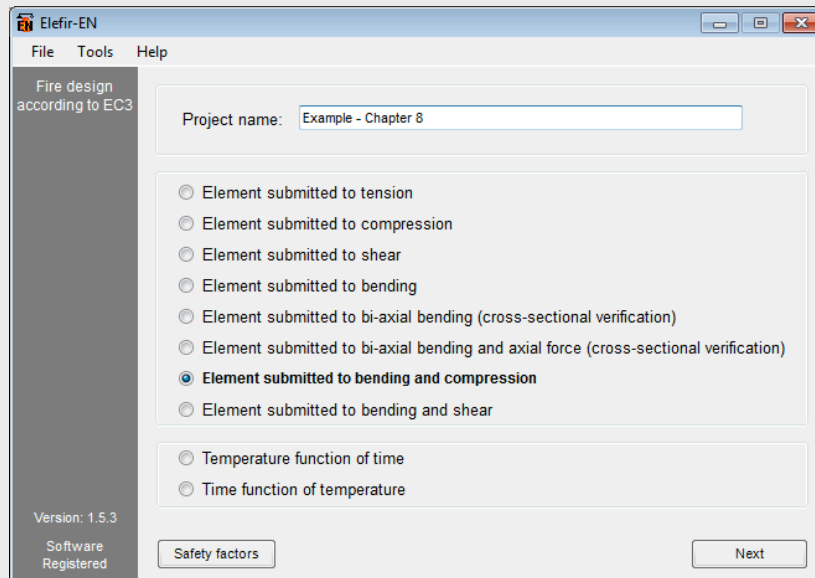
Figure 8.25 – $M_{y,fi,Ed}$ bending diagram for LTB

The following figure shows the options chosen for solving this example, which can be achieved clicking on the menu item “Tools” and after in “Options” (see Fig. 8.13).

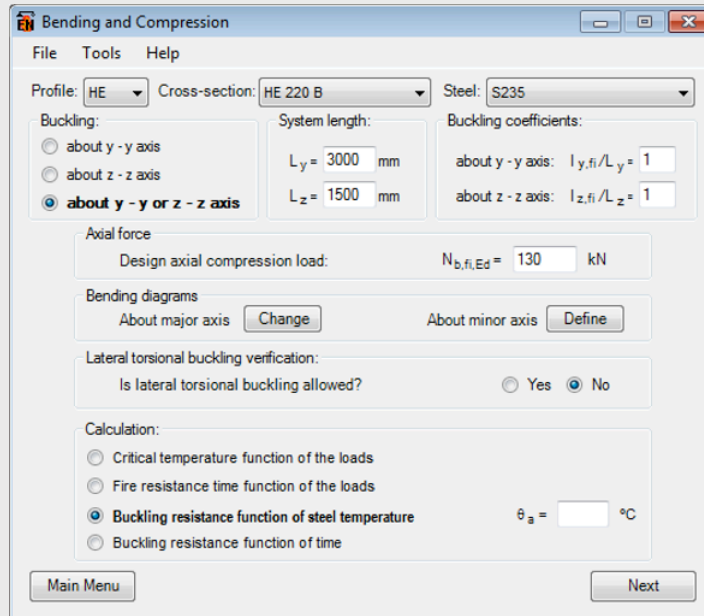


8. THE COMPUTER PROGRAM "ELEFIR-EN"

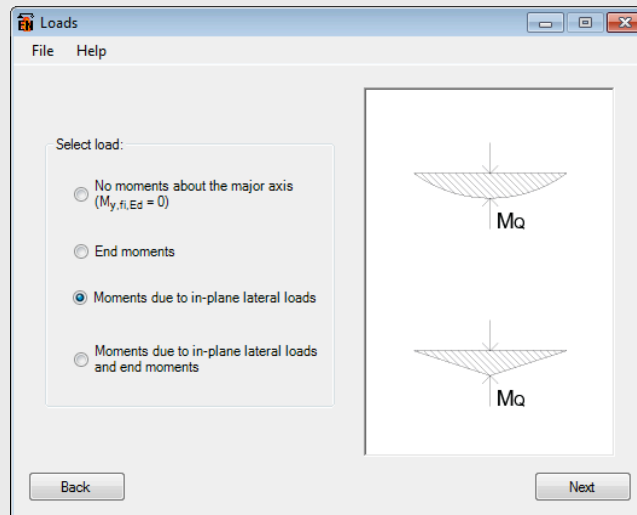
The following figures illustrate the choices to be made in the Elefir-EN for this example:



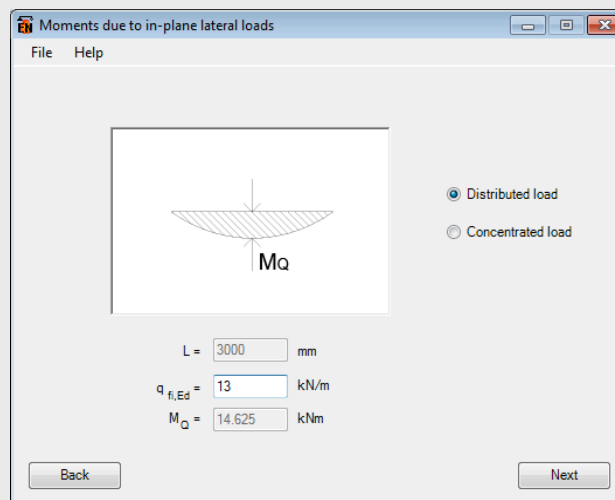
Clicking on the button "Element submitted to bending and compression", opens the following dialog box.



Clicking on the button "define" on the line "About major axis" opens the following dialogue box.



Clicking on the button "Moments due to in-plane lateral loads", opens the following dialogue box.



The length L cannot be changed because it was already defined as 3000 mm as the length for flexural buckling about y-y. Choosing Lateral torsional buckling verification the length between lateral restraints also cannot be changed because it is the same as the buckling length for flexural buckling about z-z that was already introduced as 1500 mm.

8. THE COMPUTER PROGRAM "ELEFIR-EN"

Clicking on the button "define" on the line "loads" of the lateral-torsional buckling option, opens the following dialogue box

It should be mentioned that the boxes that cannot be changed in this screen, is because, according the data already introduced, these options cannot be

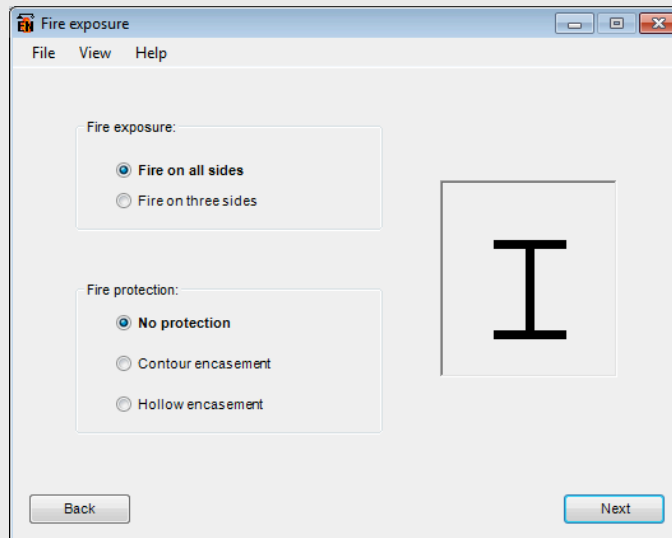
modified, or, which is the case for the effective length factors, the program only has the constants C_1 and C_2 for evaluating the elastic critical moment (see Eq. (5.74) defined for $k_z = k_w = 1.0$. For other values the user should evaluate the critical moment and introduce it in the next screen.

Clicking on the button "Next", the following screen is shown, with the value of the calculated critical temperature. The program chooses the lower critical temperature for buckling resistance and cross sectional resistance.

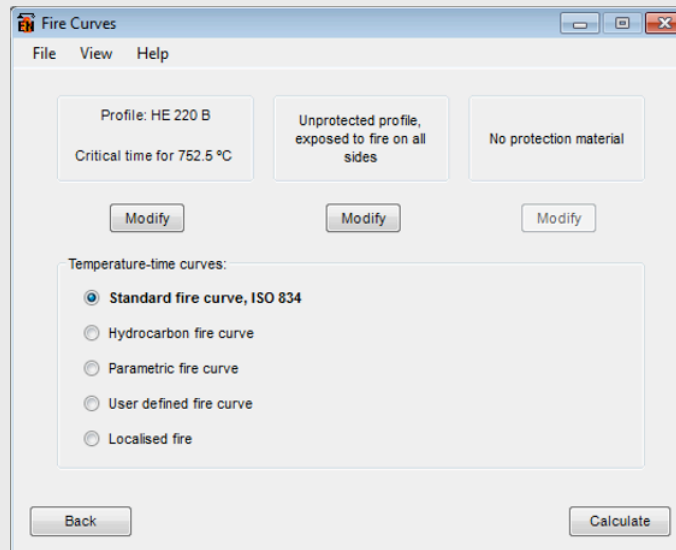
335

8. THE COMPUTER PROGRAM "ELEFIR-EN"

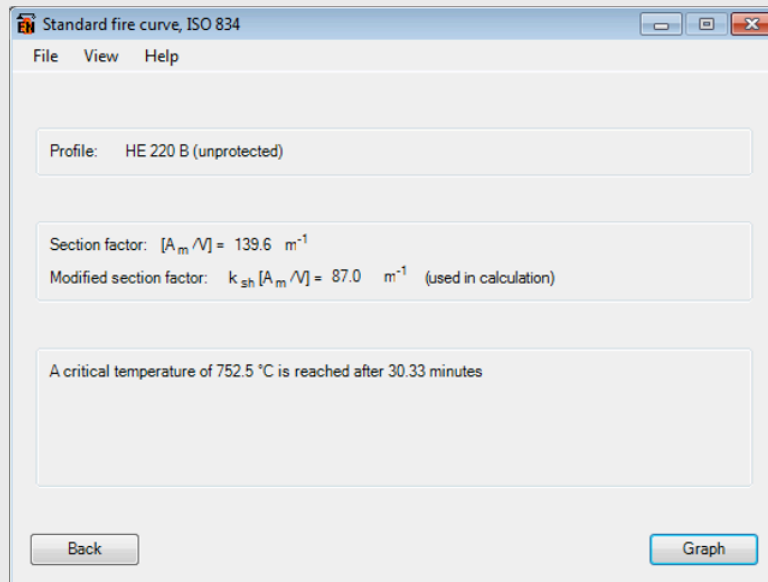
Clicking on the button "Critical time", opens the following dialogue box for choosing the fire protection applied to the profile.



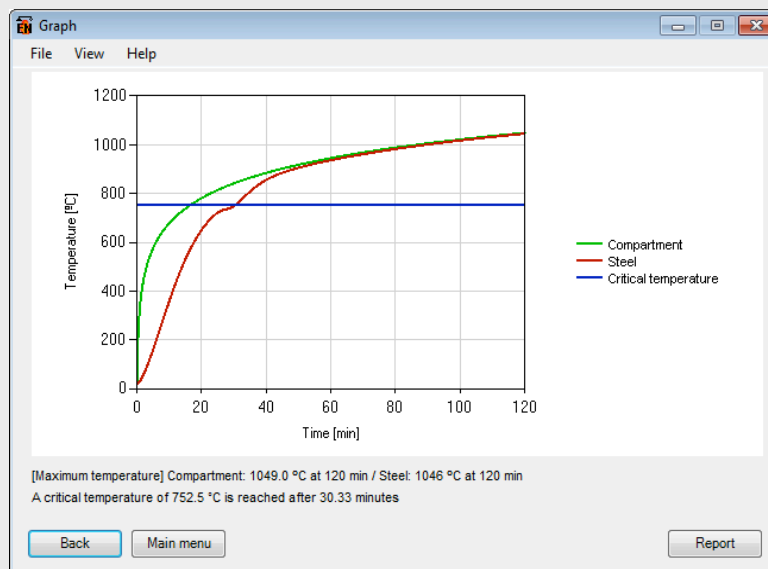
Clicking on the button "Next", opens the following dialogue box for choosing the fire exposure curve.



Clicking on the button "Calculate", the following screen is shown, with the time needed to reach the critical temperature.

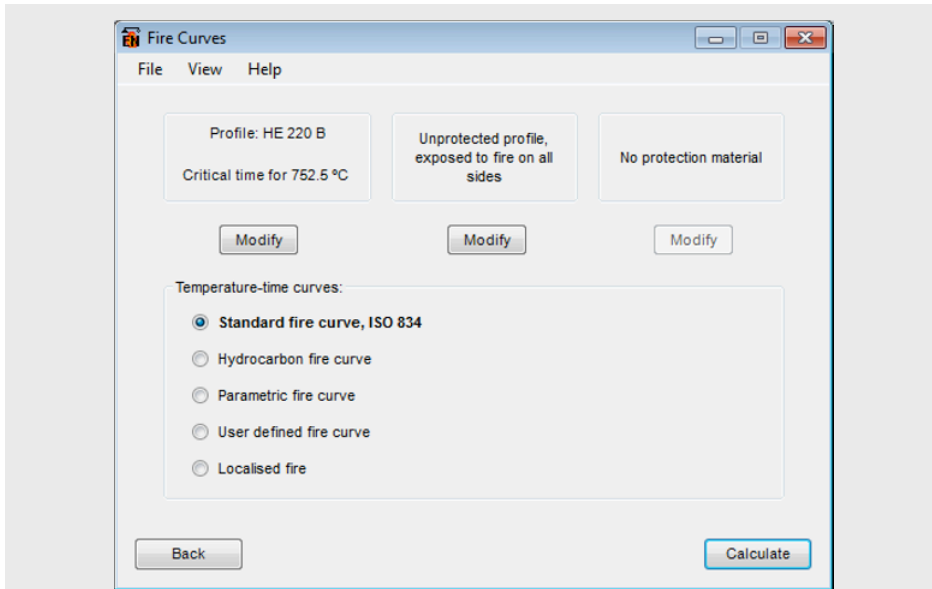


Clicking on the button "Graph", the following screen is shown.

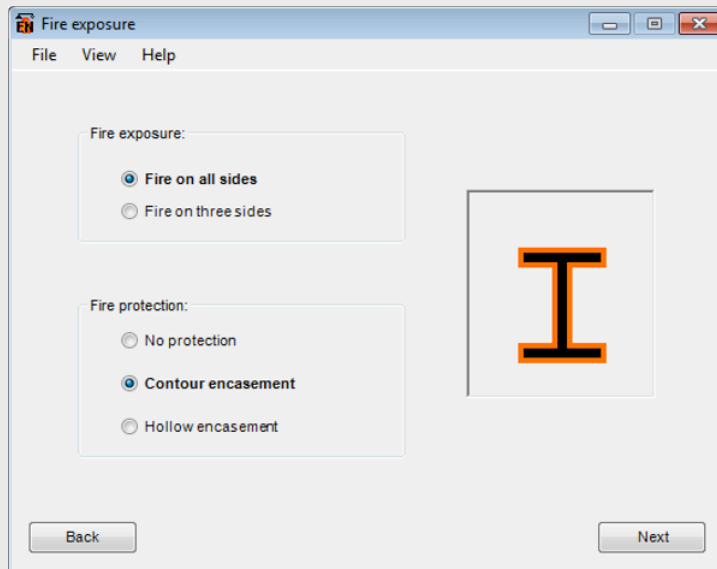


As the fire resistance of the analysed beam-column is less than the required 60 minutes, clicking on the button "Back", the following screen is shown, where the fire protection material can be selected to improve the fire resistance of the member.

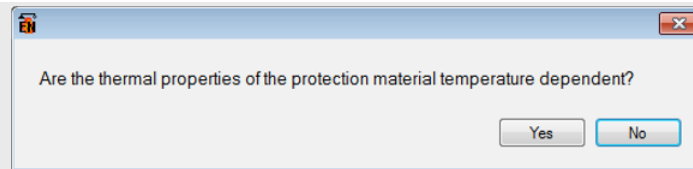
8. THE COMPUTER PROGRAM "ELEFIR-EN"



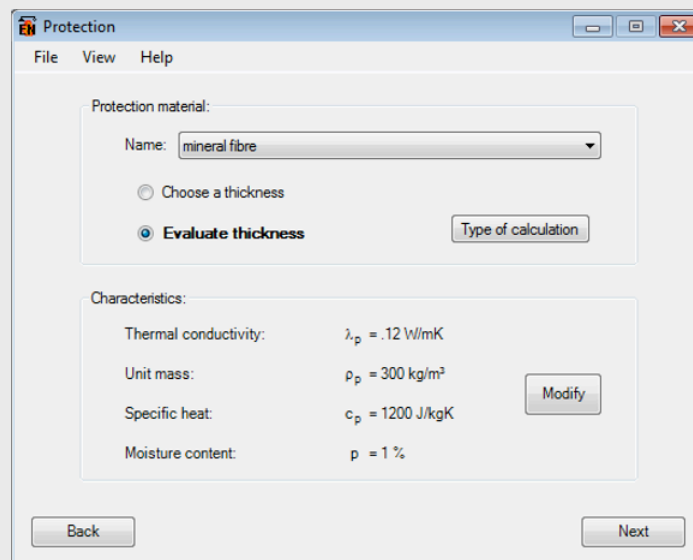
Clicking on the button "Modify" below "Unprotected profile, exposed to fire on all sides", the following screen is shown for choosing the type of encasement.



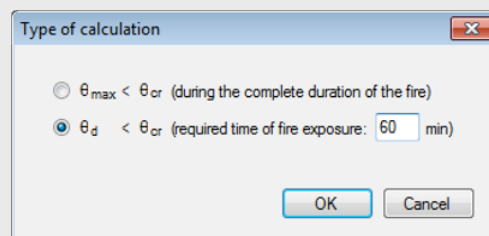
Clicking on the button "Next", the following screen appears for choosing the case where the thermal properties of the protection material are temperature dependent or not.



Considering that the protection material is not temperature dependent, clicking on the button “No”, opens the following dialogue box for choosing the fire protection material and its thickness or the type of calculation for evaluating the thickness.

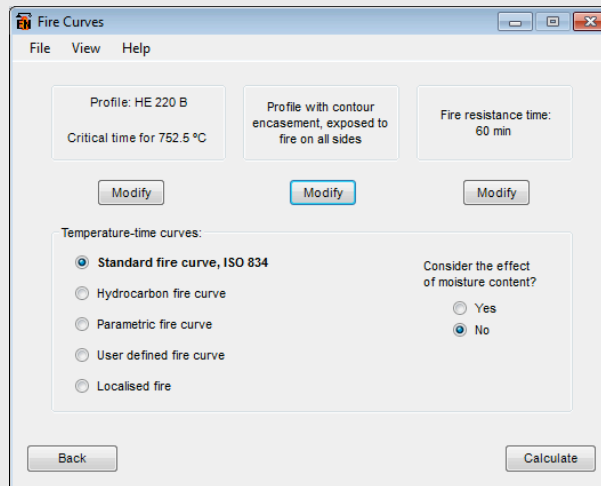


Clicking on the button "Type of calculation", the following dialogue box is opened for choosing the required thickness of the fire protection material so that the maximum temperature doesn't reach the critical temperature during the complete duration of the fire or the design temperature for the required time of fire exposure is lower than the critical temperature.

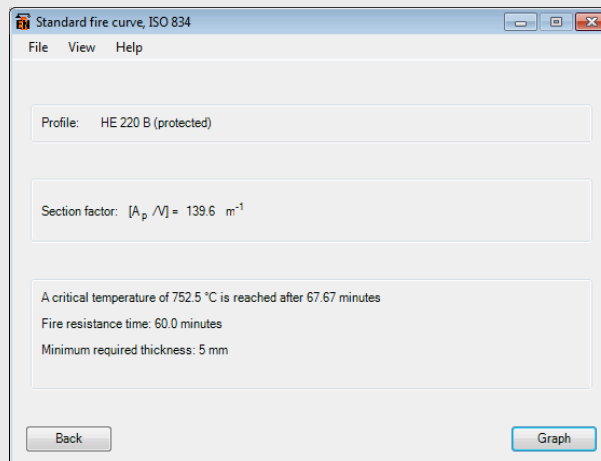


8. THE COMPUTER PROGRAM "ELEFIR-EN"

Clicking on the button "OK" and on the button "Next" of the next screen, the following screen is shown for choosing the fire curve and if the effect of moisture content must be taken into account or not.



Clicking on the button "Calculate", the following screen is shown with the value of the needed thickness.



340

In conclusion:

- Critical temperature: 752.5 °C;
- Fire resistance: 30.35 minutes. The member can be classified as R30;
- With 5 mm of mineral fibre, the fire resistance is improved to 67.7 minutes and the member can be classified as R60.

The next bordered text is the report generated by Elefir-EN for the present example, which can be obtained clicking on the button “View” in the last screen.

ELEFIR-EN REPORT
Project name: Example - Chapter 8
Date: 24/08/2014
$\gamma_{M0} = 1.00$
$\gamma_{M,fi} = 1.00$
Temperature evaluated using interpolation on the table 3.1 from EN 1993-1-2.
PROFILE
HE 220 B (Class 1)
$h = 220 \text{ mm}$
$b = 220 \text{ mm}$
$t_w = 9.5 \text{ mm}$
$t_f = 16 \text{ mm}$
$r = 18 \text{ mm}$
$A = 9100 \text{ mm}^2$
$P = 1.27 \text{ m}^2/\text{m}$
$i_y = 94.3 \text{ mm}$
$i_z = 55.9 \text{ mm}$
$W_{el,y} = 735500 \text{ mm}^3$
$W_{pl,y} = 827000 \text{ mm}^3$
$I_y = 80910000 \text{ mm}^4$
$W_{el,z} = 258480 \text{ mm}^3$
$W_{pl,z} = 393900 \text{ mm}^3$
$I_z = 28430000 \text{ mm}^4$
$I_t = 765700 \text{ mm}^4$
$I_w = 295400000000 \text{ mm}^6$
STEEL
Carbon steel, S235
Young modulus: 210 GPa
ELEMENT SUBMITTED TO BENDING AND COMPRESSION
Critical temperature function of the loads
System length: $L_y = 3000 \text{ mm}$; $L_z = 1500 \text{ mm}$
Buckling coefficients: $i_{y,fi}/L_y = 1$; $i_{z,fi}/L_z = 1$
Design axial compression load: $N_{b,fi,Ed} = 130 \text{ kN}$
About major axis - Moments due to in-plane lateral loads
$M_Q = 14.625 \text{ kNm}$
Distributed load: $q = 13 \text{ kN/m}$
Lateral torsional buckling is allowed.

8. THE COMPUTER PROGRAM "ELEFIR-EN"

LATERAL TORSIONAL BUCKLING

Point of load application: Upper flange

Load: Transverse load

Bending moment diagram: End moments and uniform load

Bending moment ratio: $\psi = 0$

Effective length factor: $k_z = 1.0$; $k_w = 1.0$

Load: $q = 13$ kN/m

Moment: $M_{fi,Ed} = 14.625$ kNm

Length between lateral restraints: 1500 mm

$C_1 = 1.320$

$C_2 = 0.125$

$M_{Cr} = 3457.562$ kNm

EXPOSURE

Fire exposure: Fire on all sides

Fire protection: Contour encasement

PROTECTION

Protection material: mineral fibre

Thermal conductivity: $\lambda = .12$ W/mK

Unit mass: $\rho = 300$ kg/m³

Specific heat: $c = 1200$ J/kgK

Moisture content: $p = 1$ %

RESULTS

Consider the effect of moisture content? No

Standard fire curve, ISO 834

Section factor: $[A_p/V] = 139.6$ m⁻¹

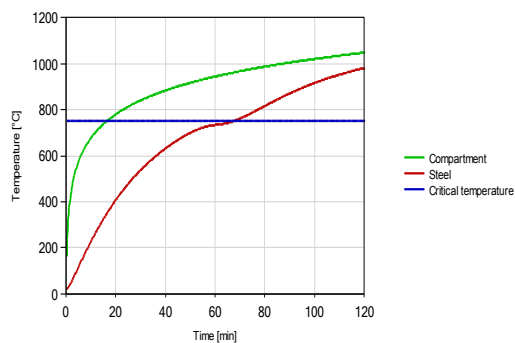
A critical temperature of 752.5 °C is reached after 67.67 minutes

Fire resistance time: 60.0 minutes

Minimum required thickness: 5 mm

GRAPH

FIRE COMPARTMENT AND STEEL TEMPERATURE



[Maximum temperature] Compartment: 1049.0 °C at 120.00 min / Steel: 982.0 °C at 120.00 min

Chapter 9

CASE STUDY

9.1. DESCRIPTION OF THE CASE STUDY

This chapter presents a case study that looks at the issues that a designer may be faced with when assessing the fire resistance and/or structural fire performance of a complete building. Although it is applied to a hypothetical building, this approach allows most of the recommendations and concepts presented in the previous chapters to be applied. Not all the details of the calculations are presented because all the models applied here have been presented and detailed examples have been given in previous chapters.

The case study is a single storey hall used primarily for indoor sport activities such as tennis and basketball, but it is occasionally used for concerts and exhibitions organised by local clubs.

The hall is 84 m long and 66 m wide and is constructed from a series of portal frames spaced at 6 m centres. The height of the building is 10 m at the eaves and 12 m at the crest. The portal frames are made from IPE 500 hot rolled steel columns supporting a lattice truss girder which spans 66 m. The lattice truss is made from hot rolled HEA280 members which form the upper and lower cords and the internal members are formed from square hollow sections (SHS) with sections varying from 140×5.6 at the ends to 100×4 and 80×4 at the centre. The columns are simply supported. The internal members of the truss girders are rigidly fixed to the cords, while the connections between the truss girder and the columns are hinged.

The roof is made of corrugated steel sheets spanning between the frames.

The in-plane stability of each frame is ensured by the frame itself. Stability in the longitudinal direction of the building is ensured by two bracing systems located one at each end of the building. Diagonals of the

9. CASE STUDY

bracing systems in the vertical planes are made of 90×90×9 angles. Square tubes form the horizontal bracing systems and other tubes link all the frames to the bracing systems. Square tubes also link the columns at mid-level. These tubes are constructed from 100×4, except for the tubes at the eaves of the building which are made of 120×5 sections.

All sections are made of S355 steel grade.

The building has sufficient means of safe escape routes on all four façades. The requirement is thus that the building either presents a fire resistance of 15 minutes to the standard fire, or there must be no progressive collapse within 30 minutes of a real (natural) fire and the collapse must be toward the inside of the building.

9.2. FIRE RESISTANCE UNDER STANDARD FIRE

9.2.1. Thermal calculations

The section factor, or massivity, of all structural members must be evaluated. For square hollow sections, the section factor is a simple ratio of the perimeter and the area of the cross section. For H and I sections and for angles, the modified section factor is used which takes account of the shadow effect. It has to be taken into account that, in the columns, the presence of concrete panels that form the façade leaves only 3 sides exposed.

The temperature of the steel sections after 15 minutes of standard fire can be calculated using Elefir-EN. The results are summarised in columns 2 and 3 of Table 9.1.

Table 9.1 – Steel section temperatures

Section	Section factor [m^{-1}]	θ after 15 min. [$^{\circ}C$]
(1)	(2)	(3)
IPE500	93.5	550
HE280A	101.8	570
SHS 140×5.6	183.2	674
SHS 120×5	205.7	685
SHS 100×4	256.6	701
SHS 80×4	258.3	702
90×90×9	198.0	682

9.2.2. Structural calculation

9.2.2.1. Loading

The dead weight comes from the steel members (78.5 kN/m^3), the roof panels (0.25 kN/m^2) plus the weight of the electrical and lighting equipment suspended from the roof and estimated to be 0.10 kN/m^2 .

The basic wind pressure¹ is 0.63 kN/m^2 with external pressure coefficients $C_{pe} = +0.8$ or -0.5 and internal pressure coefficients $C_{pi} = \pm 0.3$. It is assumed that the worst wind loading condition occurs when the inside of the building is subject to a lower pressure as this situation minimises the external wind uplift on the structure. It should normally be verified that the maximum uplift, with overpressure in the building, is not sufficient to change the sign of the axial forces in the members of the truss. This check is not made here. In this case study a single load combination is considered for the wind effect because of the limitations on space. This load combination corresponds to the wind blowing in the plane of the frames and is schematically represented on Figure 9.1. The uplift on the roof and the outward pressure on the right hand façade is equal to $(0.5-0.3) \times 0.63 = 0.126 \text{ kN/m}^2$. The pressure of the left hand façade is equal to $(0.8+0.3) \times 0.63 = 0.693 \text{ kN/m}^2$.

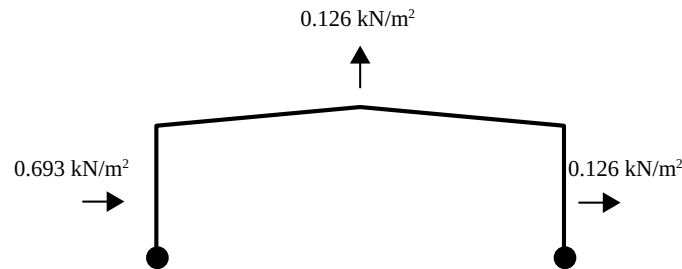


Figure 9.1 – Schematic representation of the characteristic wind load

Eq. (2.1a) will be used for the design load combination in the fire situation. The design value of the constant load is thus equal to the dead load of the steel members plus, assuming that the steel sheets are simply

¹ A precise and detailed evaluation of the wind pressure according to the Eurocode has not been performed here because of space limitation. The values presented here are arbitrary. In a real case, the wind loads would have been determined as part of the room temperature design.

9. CASE STUDY

supported on the roof, a distributed load of $0.25 \times 6 = 1.5$ kN/m on the upper chord of the truss and a distributed load of $0.10 \times 6 = 0.60$ kN/m on the lower chord¹. According to Table 2.1, the wind load applied to the left hand column of the frames is equal to $0.2 \times 6 \times 0.693 = 0.832$ kN/m and the wind uplift on the roof and wind pressure on the right hand façade are equal to $0.2 \times 6 \times 0.126 = 0.151$ kN/m.

According to Eq. (5.5) of EN 1993-1-1, an initial global sway imperfection of $H/200 = 50$ mm has been given to the frame, in the same direction as the wind.

The forces in the structure are calculated by applying the design loads in the fire situation to the structure at room temperature. Any simple analytical method can be used even those based on elastic behaviour that do not include the effects of large displacements. Such methods are allowed because the loading in the fire situation is always less than that at ambient temperature and the displacements are normally small and plasticity does not normally occur at ambient temperature. For this case study the software SAFIR is used.

The analysis is performed for a 2D frame, first loaded only by the dead weight, then in the situation when the wind is parallel to the frames. The analysis of the structure subject to the wind acting perpendicular to the frames can be performed without a computer program because only statically determinate elements are involved in the analysis.

346

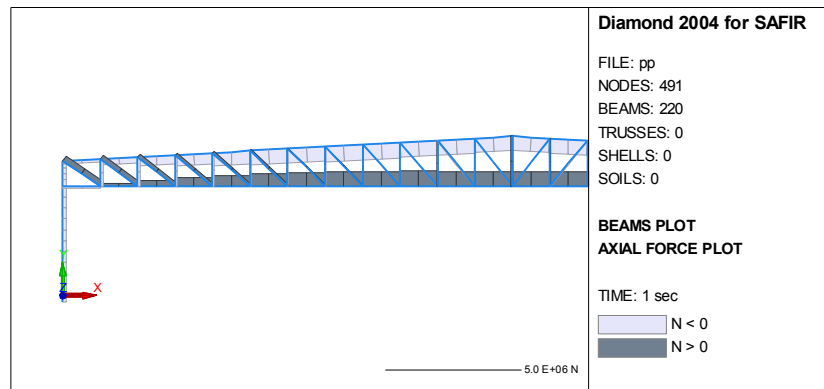


Figure 9.2 – Axial forces under dead load

Figure 9.2 shows the distribution of axial forces in the elements of the frame under dead load, while Figure 9.3 shows the distribution of bending moments under combined dead load and wind load.

¹ The concrete wall panels are self-supported.

9.2. FIRE RESISTANCE UNDER STANDARD FIRE

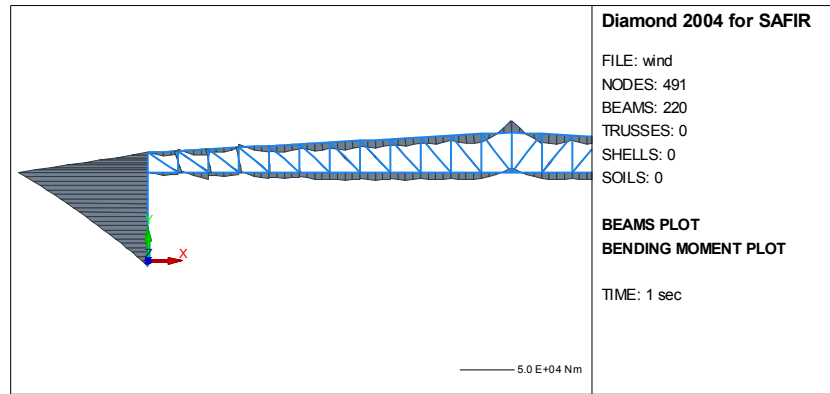


Figure 9.3 – Bending moments under dead load and wind load

Table 9.2 gives the maximum effects of actions in each type of member.

Table 9.2 – Effects of actions (compression is negative)

Section	N	M_1	M_2	q	$l_{fi,y}$	$l_{fi,z}$
-	[kN]	[kNm]	[kNm]	[kN/m]	[m]	[m]
IPE 500	-139.4	0	135.9	0	16.300	-
	-139.4	0	0	0	-	4.075
	-135.9	0	170.9	0.69	16.300	-
	-135.9	0	0	0	-	4.075
HEA280A	-567.3	5.5	7.7	2.26	2.750	-
	-567.3	0	0	0	-	5.500
	550.8	5.8	7.0	1.36	-	-
140×5.6	-111.1	3.8	-3.8	0	1.003	-
	-111.1	0	0	0	-	2.005
	211.9	0	0	0	-	-
100×4	-60.5	0.9	-0.8	0	1.235	-
	-60.5	0	0	0	-	2.470
	96.0	-0.2	0.3	0	-	-
80×4	-48.9	0.3	-0.3	0	1.313	-
	-48.9	0	0	0	-	2.625
	56.1	0.1	-0.1	0	-	-
120×5	-25.2	0	0	0	6.000	6.000
90×90×9	31.3	0	0	0	-	-
100×4	-23.1	0	0	0	6.000	6.000

9. CASE STUDY

The maximum effects of actions in most of the members occur under the dead load only loading condition. An exception is in the IPE 500 columns, where the maximum bending moment occurs under the combined dead and wind load loading condition. For these columns, the buckling length in the plane of the frame $l_{fi,y}$ is estimated as 2 times the length from the base of the column to the bottom chord of the lattice girder, see Figure 9.4. The displacement is fixed at the bottom of the column with rotation allowed while, at the top of the column, the displacement is free while the rotation is restrained by the lattice girder. The buckling length out of the plane of the frame $l_{fi,z}$ is taken as 0.5 times the length from the base of the column to the bottom chord of the lattice girder because of the presence of horizontal elements stabilizing the column at mid-height.

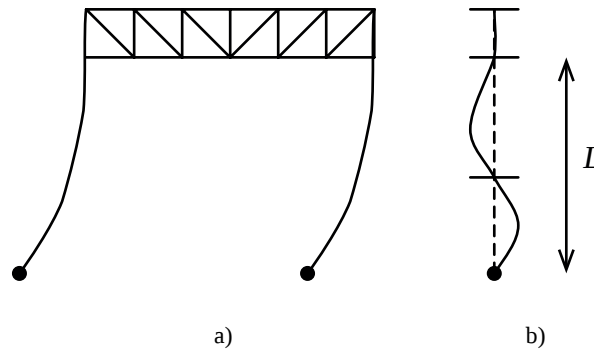


Figure 9.4 – Buckling length in the columns
a) in the plane of the frame; b) out of the plane of the frame

For the upper and lower cords of the lattice girder (HEA280), the buckling length in the plane of the truss is taken as the node-to-node distance whereas the buckling length out of the plane is taken as 2 times the node-to-node distance because of the presence of horizontal stabilising elements at every other node.

For the internal elements of the truss, the buckling length is taken as half the node-to-node distance in the plane of the frame because the cords are stiff elements in bending and the connections between the internal elements and the cords are considered as rigid. The out-of-plane buckling length of the internal elements is taken as the node to node distance as the torsional stiffness of the cords is neglected. The node-to-node distance is longer for the thinner elements that are closer to the centre of the girder,

because of the slope of the roof. These internal tubular elements are subjected not only to axial forces but also to bending moments because of the rigid connection to the cord. However, these bending moments are small because the truss is made of triangular cells, which favours axial forces.

The horizontal stabilising elements located at the eaves of the building (120×5) are loaded by the wind pressure from the façade, see Figure 9.5. Each node of the bracing truss is loaded by a force equal to $0.2 \times 0.693 \text{ kN/m}^2 \times 5.5 \text{ m} \times 11 \text{ m} / 2 = 4.20 \text{ kN}$.

The maximum force in the eave member 120×5, noted as A on Figure 9.5, is calculated as: $(11 \times 4.2 \text{ kN} + 2 \times 2.1 \text{ kN}) / 2 = 25.2 \text{ kN}$.

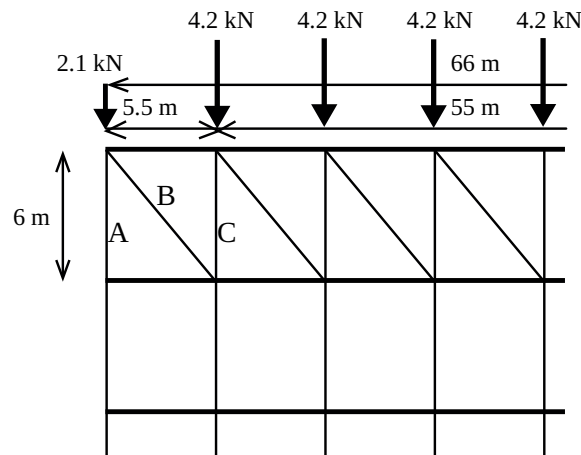


Figure 9.5 – Plan view of an horizontal bracing system

The tensile force in the most external diagonal of the horizontal bracing noted B on the Figure is calculated as:

$$(25.2 \text{ kN} - 2.1 \text{ kN}) \times 8.14 \text{ m} / 6 \text{ m} = 31.3 \text{ kN}$$

The compression force in the most external 100×4 tube noted C on the Figure is $11 \times 4.2 \text{ kN} / 2 = 23.1 \text{ kN}$

9.2.2.2. Fire resistance by the simple calculation model

If the calculations are made "by hand", with the help of only a pocket calculator, it is far easier to operate in the load domain. The temperature being determined at the required fire duration of 15 minutes, see Table 9.1, the material properties, f_y and E , at the relevant temperature can be determined

9. CASE STUDY

directly and the load bearing capacity of the members is determined directly without any iteration being required, even for members in compression.

Here, the calculation will be made in the time domain with the help of the software Elefir-EN. Examples have been presented in the previous chapters for detailed application of all the equations.

Table 9.3 – Results of the mechanical analyses

Section	$N^{(*)}$	Load ratio	Critical temperature	R_f
-	[kN]	[-]	[°C]	[min.]
IPE 500	-139.4	0.34	656	18.1
	-135.9	0.38	638	17.2
HEA280A	-567.3	0.47	602	16.3
	550.8	0.18	746	27.7
140×5.6	-111.1	0.18	739	21.7
	211.9	0.20	725	18.9
100×4	-60.5	0.27	683	13.8
	96.0	0.19	734	18.7
80×4	-48.9	0.37	644	11.8
	56.1	0.14	777	23.4
120×5	-25.2	0.18	739	21.1
90×90×9	31.3	0.06	916	50.8
100×4	-23.1	0.34	653	12.2

(*) Compression is negative.

The columns have sufficient fire resistance for the combined dead load and wind load loading case.

In the truss girders, the cords as well as the heaviest internal members of the truss girders achieve the required 15 minutes fire resistance. The lightest internal members subjected to compression have a fire resistance of 14 and 12 minutes and should be strengthened to increase their fire resistance. A more detailed analysis of all the internal members would indicate which members need to be strengthened. It is possible that, in the truss girders, the most internal members made of 100×4 or 80×4 square hollow sections could be maintained and only the most external members need to be increased. In conclusion, a few of the 100×4 members should be replaced by 140×5.6 sections and a few of the 80×4 members should be replaced by 100×4 sections.

In the horizontal bracings, the most external 100×4 sections in compression should also be replaced by 120×5 sections in order to increase their fire resistance that is only equal to 12 minutes.

9.2.2.3. Fire resistance by the general calculation model

The horizontal bracing systems are made from statically determinate members. Therefore it is likely that an analysis using the general calculation model would not yield a result different from an analysis using the simple calculation model.

The main frames, on the other hand, have a level of redundancy and an analysis of a frame, considered as a substructure, using the general calculation model could yield a higher fire resistance than an analysis based on the behaviour of each member taken in isolation (11.8 minutes in this case).

The frame has first been analysed as a 2D substructure at room temperature. The design loads in the fire situation have been applied and increased proportionally until failure. The load multiplier at failure is equal to 5.76 for dead loads only and 5.79 for combined dead and wind loads. The global load level for the frames at the beginning of the fire is thus equal to $1 / 5.76 = 0.17$.

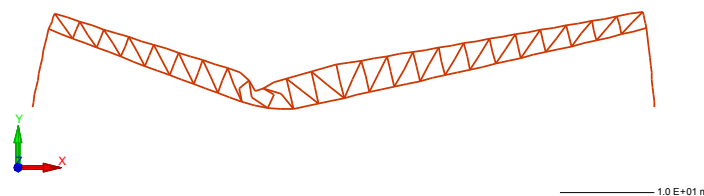


Figure 9.6 – Deformed shape at room temperature under dead loads

Fig. 9.6 shows the deformed shape of the frame at failure subject to dead loads only (no amplification of the displacements). A detailed examination of the results indicates that failure is initiated by buckling of the upper cord, immediately followed by failure in the adjacent internal members.

The frame was then analysed in the fire situation. The fire resistance time was calculated as 19 min. 20 sec. for the combined dead and wind load loading case and 18 min. 32 sec. under dead loads only. Fig. 9.7 shows the

9. CASE STUDY

deformed shape of the structure for the latter case. Failure in the fire situation is initiated by the buckling of the most external 100×4 SHS vertical member, immediately followed by failure of the other internal members with similar sections. The failure mode in the fire situation is different from the failure mode at room temperature because of the faster temperature increase of the thinner members.

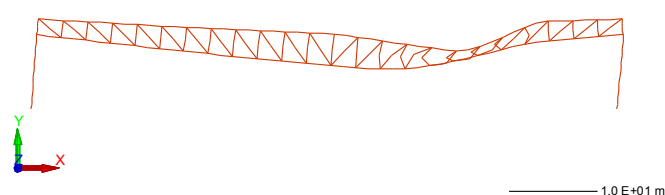


Figure 9.7 – Deformed shape under dead loads at elevated temperature

These results indicate that the structure may have a fire resistance of 15 minutes, but some additional verification must be performed. The possibility of a failure by out of plane buckling of the columns has, for example, not been checked with this 2D model. Furthermore, out of plane failure of the truss girder between points of lateral fixity and the out of plane buckling of the internal members have not been checked. To investigate these modes of failure, a 3D model was built and analysed for the dead load only load combination¹. An initial out of plane imperfection of the columns equal to 1/250 of the length between points of lateral supports was introduced into the model.

352

Fig. 9.8 shows the 3D model with the supports that have been considered in the out of plane direction. The fire resistance of the 3D model is 16 minutes and 9 seconds. This shows that, when the frame is analysed as a substructure, it is not necessary to increase the size of the elements that were found as too weak in an analysis made element by element.

Fig. 9.9 shows the deformed shape of the frame at failure. The failure mode shows that the out of plane displacements of the columns are limited and that out of plane buckling of the column is not the main mode of failure. Failure is triggered by loss of strength in the truss girder with only the lower cord of the truss girder showing increasing out of plane displacements during collapse. When compared to Fig. 9.7, Fig. 9.9 shows that the 3D model is

¹ From now on, only this load combination will be considered.

numerically more "ductile" and allows a better view inside a failure mode that develops toward the inside of the building, whereas this was not as clear in the 2D model.

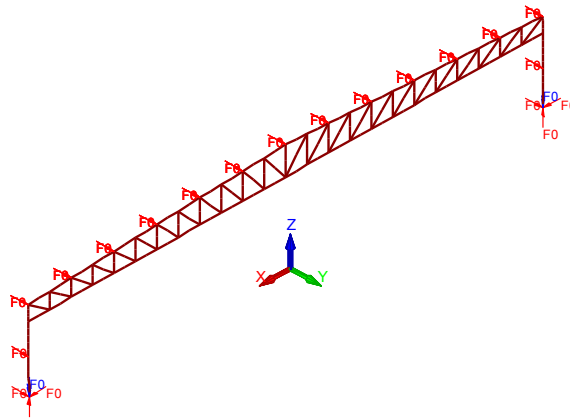


Figure 9.8 – 3D model with the supports

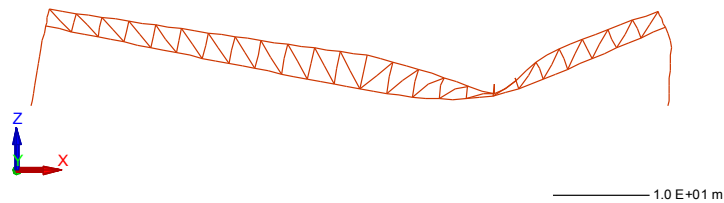


Figure 9.9 – Deformation of the 3D model at collapse

9.3. FIRE RESISTANCE UNDER NATURAL FIRE

9.3.1. Temperature development in the compartment

Although the building is classified as a sports hall there is a possibility that it could be used as a theatre. Therefore the sports hall will be re-analysed under a natural fire that could occur in a theatre. Some choices have to be made and some hypotheses have to be taken for evaluating the development of temperatures in the compartment. Although Eurocode 1, to be supplemented by the relevant National Annex, gives some guidance and

9. CASE STUDY

recommendation for some important parameters, it is wise in a real project to have approval of the Authority Having Jurisdiction on the main hypotheses before the calculations are started.

The following data are used in this example:

Floor:

Normal weight concrete

Ceiling:

Insulated sandwich panels with steel sheets (0.7-150-0.7 mm in depth)

Walls:

Insulated concrete sandwich panels (40-150-40 mm in depth)

Fire characteristics:

Characteristic fire load density: $q_{f,k} = 365 \text{ MJ/m}^2$ (see Table E.4, Theatre)

Fire growth rate: Fast (See table E.5, Theatre)

RHR density: $RHR_f = 500 \text{ kW/m}^2$ (See Table E.5, Theatre)

Floor area: $A_f = 5544 \text{ m}^2 \Rightarrow$ Danger of fire activation $\delta_{q1} = 2.03$ (See Table E.1)

Danger of fire activation: $\delta_{q2} = 1.0$ (see Table E.1)

Automatic fire detection by smoke: $\delta_{n4} = 0.73$ (See Table E.2)

Off-site fire brigade: $\delta_{n7} = 0.78$ (See Table E.2)

Combustion efficiency factor: $m = 0.8$

Design fire load density: $q_{f,d} = 0.8 \times 2.03 \times 0.73 \times 0.78 \times 365 = 337.5 \text{ MJ/m}^2$

Openings:

Porosity of the walls: 0.1 %

Doors: 2.6 m in height and 20 m in cumulated width, open from the start of the fire.

Openings in the roof: 18 units of 2 m diameter (= 1% of the floor area), open when the temperature in the hot zone is equal to 80 °C.

The development of the temperature in the compartment has been calculated using the two zone model OZone (OZone V2.2; Cadorin *et al*, 2003). Fig. 9.10 shows the development of the temperature in the hot zone (continuous line) and in the cold zone (dotted line). Flash-over occurs at 28 minutes because the temperature of the hot zone has reached 300 °C and the hot zone is deep enough to encompass combustible material that is present in the compartment. From this time on the situation turns into a one zone situation.

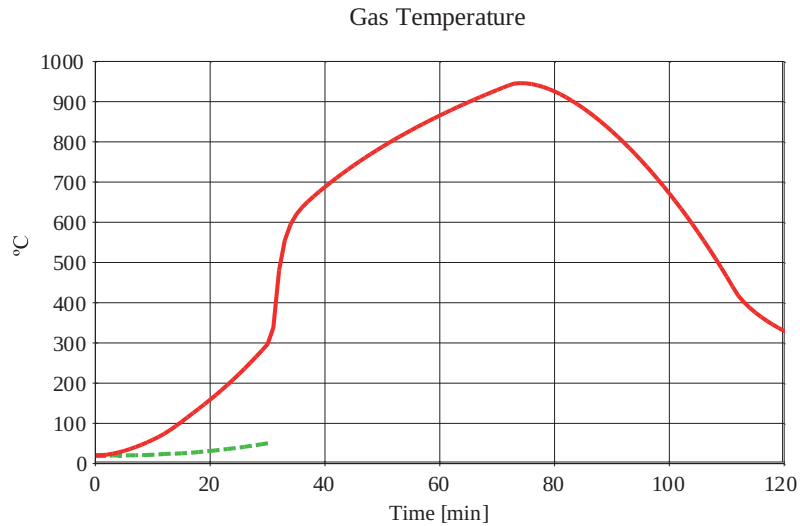


Figure 9.10 – Development of the gas temperature

This figure shows that, for the frames that are sufficiently far away from the initial localised fire source, and are heated only by the hot zone gases, the temperatures during the first 30 minutes are too low to challenge the structure. It has been verified that the frames subjected to the hot zone temperature described in Fig. 9.10 collapse after 39 minutes and 10 seconds. Collapse of the structure that occurs 11 minutes after flash-over is no more a threat for the occupants who would not have yet evacuated the building, because they cannot possibly have survived to the high temperatures that developed in the compartment after the flash-over. Because failure is clearly toward the inside¹, it does not pose a threat either to the fire brigade who could be attacking the fire from the outside and could be located close to the façades.

The behaviour of a frame that is located just above the fire source must also be analysed because this frame is subjected to a much more severe thermal attack than the other frames. The localised fire model given by Eq. (C.2) of Eurocode 1 (see also Eq. 3.24 from this book) will be used here because the flame length calculated from Eq. (C.1) (see also Eq. 3.23 from this book) does not reach the ceiling.

¹ The failure mode is similar to the one depicted on Fig. 9.9.

9. CASE STUDY

Table 9.4 gives the main characteristics of the localised fire up to flash-over. According to Clause (11) of Annex C, the model is valid only for *RHR* up to 50 MW and a fire diameter up to 10 m which means, in this case, up to 15 minutes of fire. These limits do not mean that the model is wrong for larger and more powerful fires, only that there is no experimental evidence of the applicability of the model beyond these limits. The designer is nevertheless left with no other option but to extrapolate the model. Alternatively the engineer could perform a CFD calculation, assuming that such models are more reliable than the simple model for fire sources of more than 100 MW in a fire compartment.

The fire source is positioned on the ground at the location where the analysis under uniform temperature distribution shows failure of the truss girder (at approximately 1/3 of the length of the frame), see Fig. 9.9. The temperatures given by Eq. (C.2) of Eurocode 1 for the centreline of the fire have been applied on a width of 16.5 m, which is approximately equal to the diameter of the localised fire at time of maximum extension before flash-over. This is on the safe side because the temperature is expected to decrease away from the centre line.

Fig. 9.11 shows (in bold lines) the elements that have been subjected to the effects of the localised fire. The other elements are subjected to the temperature of the hot zone. For this fire scenario, collapse is calculated at 38 minutes and 39 seconds. This time is very similar to the time of collapse under the effects of the hot zone only model. This means that, for this fire scenario, the effects of the localised fire on the structure are negligible compared to the effects of flash-over.

Another scenario that could be more critical for the frame is the scenario corresponding to a localised fire that occurs near or around one of the frame columns. One of the columns has been divided into thermal zones 1 meter high and each zone has been subjected to the fire curves taken from the relevant column of Table 9.4. The rest of the frame is subjected to the hot zone curve of Fig. 9.10. Under this fire scenario, failure is observed after some 19 minutes and 30 seconds by out of plane buckling of the inferior part of the column that is heated by the local fire. This situation is not satisfactory because it occurs before flash-over, that means at a time when some occupants might not have left the building or, more likely, when the fire brigade has entered the building to fight the fire from the inside.

9.3. FIRE RESISTANCE UNDER NATURAL FIRE

Table 9.4 – Characteristics of the localised fire

<i>t</i> min.	<i>RHR</i> MW	<i>A</i> m ²	<i>D</i> m	<i>Lf</i> m	<i>z</i>	<i>z</i>	<i>z</i>	<i>z</i>	<i>z</i>	<i>z</i>	<i>z</i>
					0.5 m	1.5 m	2.5 m	3.5 m	10.0 m	11.0 m	12.0 m
					θ °C	θ °C	θ °C	θ °C	θ °C	θ °C	θ °C
0	0.0	0.00	0.00	0.00	20	20	20	20	20	20	20
1	0.2	0.32	0.64	1.14	900	336	156	98	34	32	30
2	0.6	1.28	1.28	1.81	900	680	325	201	53	49	45
3	1.4	2.88	1.91	2.35	900	900	478	301	75	67	61
4	2.6	5.12	2.55	2.81	900	900	604	391	98	87	78
5	4.0	8.00	3.19	3.22	900	900	705	469	120	107	96
6	5.8	11.52	3.83	3.58	900	900	783	535	142	126	113
7	7.8	15.68	4.47	3.91	900	900	844	590	164	145	130
8	10.2	20.48	5.11	4.22	900	900	889	637	184	164	147
9	13.0	25.92	5.74	4.50	900	900	900	675	204	181	163
10	16.0	32.00	6.38	4.76	900	900	900	707	223	198	178
11	19.4	38.72	7.02	5.00	900	900	900	732	240	214	193
12	23.0	46.08	7.66	5.23	900	900	900	753	257	230	207
13	27.0	54.08	8.30	5.44	900	900	900	770	272	244	221
14	31.4	62.72	8.94	5.64	900	900	900	784	287	258	233
15	36.0	72.00	9.57	5.82	900	900	900	794	301	271	245
16	41.0	81.92	10.21	6.00	900	900	900	803	313	283	257
17	46.2	92.48	10.85	6.16	900	900	900	809	325	294	268
18	51.8	103.68	11.49	6.32	900	900	900	813	336	305	278
19	57.8	115.52	12.13	6.46	900	900	900	817	347	315	288
20	64.0	128.00	12.77	6.60	900	900	900	818	357	324	297
21	70.6	141.12	13.40	6.73	900	900	900	819	366	333	306
22	77.4	154.88	14.04	6.85	900	900	900	819	374	342	314
23	84.6	169.28	14.68	6.97	900	900	900	819	382	350	322
24	92.2	184.32	15.32	7.08	900	900	900	819	390	357	329
25	100.0	200.00	15.96	7.18	900	900	900	819	396	364	336
26	108.2	216.32	16.60	7.28	900	900	900	819	403	370	342
27	116.6	233.28	17.23	7.37	900	900	900	819	409	377	348

357

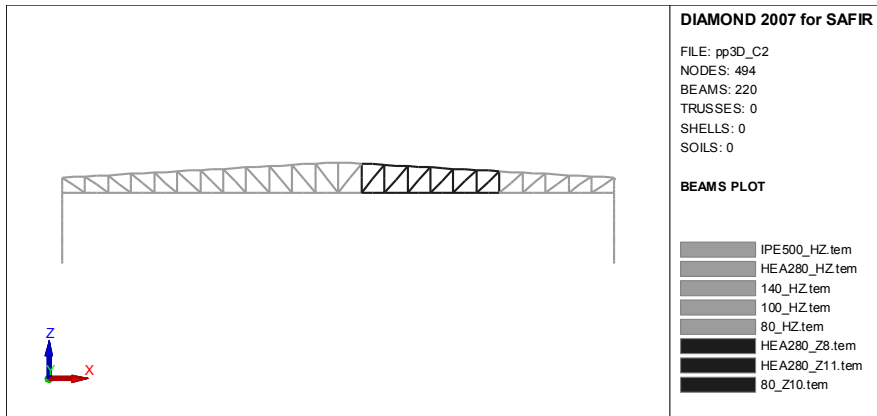


Figure 9.11 – Zone subjected to the localised fire

9. CASE STUDY

The designer has several options to prevent this situation from developing. Each of the following situations must be verified by a new numerical calculation:

- a) The columns can be built in a higher steel grade, S460 for example. In this case, the time of collapse is increased to 22 minutes and 10 seconds.
- b) Out of plane rotation at the base of the column can be restrained. For the example shown in this section, the time of collapse is increased to 26 minutes and 50 seconds.
- c) The out of plane displacements of the columns can be prevented by adding additional bracing at $\frac{1}{4}$ of the height of the columns. Collapse is then observed after 31 minutes and 50 seconds. This result should be confirmed with a new refined model because the actual model has only 3 beam finite elements on the first $\frac{1}{4}$ of the column height and this may be too crude to track the buckling mode in this first quarter of the column height.
- d) The columns can be thermally protected from the base to a level that has to be determined. With this model collapse is observed just a few seconds before 30 minutes if two meters of the columns are protected in such a way that the steel temperature remains at 20°C. In a real application, it might be wise to extend the protection for 1 or 2 additional meters because the steel temperature will increase slightly even in the protected sections and to cover some uncertainty about the vertical position of the fire source. Protecting the columns up to, say, 4 meters might be appropriate. The question of the protection of the bracing members in the lower parts of the façades should also be examined.
- e) An alternative is to check whether the collapse of the column that is close to the localised fire leads to a global collapse of the building or whether the collapse is limited to one frame. It is indeed possible that the loads carried by the truss girder can be transferred to the adjacent frames by tension forces developing in the horizontal bracing members. This solution requires extensive numerical modelling and, also, verification that the tensile forces can be transferred through the joints. This solution has not been addressed because of space limitations.

Solutions a) and b) have to be applied before the building is constructed, whereas solution e) can be tried on an existing building and solutions c) and d) can be used as a retrofit if solution e) cannot be examined or proved.

REFERENCES

Allen HC, Bulson PS (1980). *Background to buckling*, McGraw– Hill Book Company Limited, United Kingdom.

Anderberg Y, Oredsson O (1995). *Steel columns under partial fire exposure – An introductory study*, First European IAFSS symposium, ETH Höndergger, Zürich.

Block F, Burgess I, Davison B (2004). *Numerical and analytical studies of joint component behaviour in fire*, *Proceedings of Third International Workshop "Structures in Fire"*, Ottawa.

Block F, Burgess I, Davison B, Plank RJ (2007). *The development of a component-based connection element for end-plate connections in fire*. *Fire Safety Journal*, 42(6-7), pp.498-506.

Buchanan A (2001). *Structural design for fire safety*, John Wiley & Sons.

Bureau A (2005). *Classification des sections selon l’Eurocode 3 tableaux de classement des profiles laminés en I*, CTICM, *Revue Construction Métallique*, pp. 59-73, n° 4.

Cadorin J-F, Franssen J-M (2003). *A tool to design steel elements submitted to compartment fires – OZone V2. Part 1: pre- and post-flashover compartment fire model*, *Fire Safety Journal*, Elsevier, 38, 395-427.

Cadorin J-F, Pintea D, Dotreppe J-C, Franssen J-M (2003). *A tool to design steel elements submitted to compartment fires – Ozone V2. Part 2: Methodology and application*, *Fire Safety Journal*, Elsevier, 38, 429-451.

Couto C, Vila Real P, Lopes N, Amaral C (2014). *SteelClass – a software for Cross-sectional Classification*, University of Aveiro.

Dhima D (1999). *Calcul Simplifié de la Temperature Critique Selon la Norme XP ENV 1993-1-2*, *Revue Construction Métallique*, n° 3, pp. 89-105.

Drysdale D (1999). *An Introduction to Fire Dynamics*, 2nd edition, John Wiley & Sons.

ECCS (1983). *European Recommendations for the Fire Safety of Steel Structures*. European Convention for Constructional Steelwork. ECCS, Elsevier.

REFERENCES

ECCS TC3 (1995). *Fire Resistance of Steel Structures. Fire Safety of Steel Structures*. European Convention for Constructional Steelwork. ECCS Technical Note No. 89, Brussels, Belgium.

ECCS TC3 (2001). *Model Code on Fire Engineering*. ECCS publication No. 111, Brussels, Belgium.

ECCS (2006). *Rules for Member Stability in EN 1993-1-1: Background documentation and Design Guidelines*. European Convention for Constructional Steelwork. ECCS publication no. 119, Brussels, Belgium.

Elefir-EN V1.1 (version 1.1.1), (2010). University of Aveiro & University of Liege, <http://elefiren.web.ua.pt>.

EN 1990 (2002). *Eurocode: Basis of Structural Design*. CEN, European Committee for Standardization, Brussels, Belgium.

EN 1991-1-1 (2002). *Eurocode 1: Actions on structures - Part 1-1: General actions - Densities, self-weight, imposed loads for buildings*. CEN, European Committee for Standardization, Brussels, Belgium.

EN 1991-1-2 (2002). *Eurocode 1: Actions on structures - Part 1-2: General actions - Actions on structures exposed to fire*. CEN, European Committee for Standardization, Brussels, Belgium.

EN 1991-1-3 (2003). *Eurocode 1 - Actions on structures – Part 1–3: General actions – Snow loads*. CEN, European Committee for Standardization, Brussels, Belgium.

EN 1991-1-4 (2005). *Eurocode 1: Actions on structures – Part 1–4: General actions – Wind actions*. CEN, European Committee for Standardization, Brussels, Belgium.

EN 1993-1-1 (2005). *Eurocode 3: Design of steel Structures. Part 1.1: General Rules and Rules for Buildings*. CEN, European Committee for Standardization, Brussels, Belgium.

EN 1993-1-2 (2005). *Eurocode 3: Design of steel Structures. Part 1.2: Structural fire design*. CEN, European Committee for Standardization, Brussels, Belgium.

EN 1993-1-4 (2006). *Eurocode 3: Design of steel Structures. Part 1.4: Supplementary Rules for Stainless Steels*. CEN, European Committee for Standardization, Brussels, Belgium.

EN 1993-1-5 (2006). *Eurocode 3: Design of steel Structures. Part 1.5: Eurocode 3 - Design of steel structures - Part 1-5: Plated structural elements*. CEN, European Committee for Standardization, Brussels, Belgium.

EN 1993-1-8 (2005). *Eurocode 3: Design of steel structures – Part 1–8: Design of Joints*. CEN, European Committee for Standardization, Brussels, Belgium.

EN 1994-1-1 (2004). *Eurocode 4: Design of composite steel and concrete structures – Part 1–1: General rules and rules for buildings*. CEN, European Committee for Standardization, Brussels, Belgium.

EN 1994-1-2 (2005). *Eurocode 4: Design of composite steel and concrete structures- Part 1-2: General rules - Structural fire design*. CEN (Comité Européen de Normalisation), Brussels, Belgium.

EN 1363-2 (1999). *Fire resistance tests. Part 2 – Alternative and additional procedures*. CEN, European Committee for Standardization, Brussels, Belgium.

EN 10025-2 (2004). *Hot rolled products of structural steels – Part 2: Technical delivery conditions for non-alloy structural steels*. CEN, European Committee for Standardization, Brussels, Belgium.

EN 10210-1 (2006). *Hot finished structural hollow sections of non-alloy and fine grain steels. Part 1: Technical delivery requirements*. CEN, European Committee for Standardization, Brussels, Belgium.

EN 10210-2 (2006). *Hot finished structural hollow sections of non-alloy and fine grain steels. Part 2: Tolerances, dimensions and sectional properties*. CEN, European Committee for Standardization, Brussels, Belgium.

EN 10219-1 (2006). *Cold formed welded structural hollow sections of non-alloy and fine grain steels. Part 1: Technical delivery requirements*. CEN, European Committee for Standardization, Brussels, Belgium.

EN 10219-2 (2006). *Cold formed welded structural hollow sections of non-alloy and fine grain steels. Part 2: Tolerances, dimensions and sectional properties*. CEN, European Committee for Standardization, Brussels, Belgium.

EN 13381-1 (2009). *Test methods for determining the contribution to the fire resistance of structural members. Part 1. Horizontal protective membranes*. CEN, European Committee for Standardization, Brussels, Belgium.

EN 13381-2 (2008). *Test methods for determining the contribution to the fire resistance of structural members. Part 2. Vertical protective membranes*. CEN, European Committee for Standardization, Brussels, Belgium.

EN 13381-4 (2013). *Test method for determining the contribution to the fire resistance of structural members. Part 4: Applied protection to steel members*. CEN TC 127, European Committee for Standardization, Brussels, Belgium.

REFERENCES

EN 13501-2 (2003). *Fire classification of construction products and building elements. Part 2: Classification using data from fire resistance tests, excluding ventilation services*. CEN, European Committee for Standardization, Brussels, Belgium.

ENV 1993-1-1 (1992). *Eurocode 3: Design of steel Structures – Part 1–1: General Rules and Rules for Buildings*. CEN, European Committee for Standardization, Brussels, Belgium.

ENV 1993-1-2 (1995). *Eurocode 3, Design of Steel Structures – Part 1–2: General rules – Structural fire design*. CEN, European Committee for Standardization, Brussels, Belgium.

ESDEP (1995). *European Steel Design Education Programme*, ESDEP Society.

EUROPEAN COMMISSION (2001). “*Demonstration of real fire tests in car parks and high buildings*”, Contract n° 7215 PP 025.

EUROPEAN COMMISSION (27 November 2007). *Guidance paper L (concerning the Construction Products Directive - 89/106/EEC) - Application and use of Eurocodes*, Brussels, Belgium.

Euro Inox and Steel Construction Institute (2006). *Design Manual for Structural Stainless Steel*, 3rd edition.

Ferreira J, Vila Real P, Couto C (2014). *GeM – a software for applying the General Method of Eurocode 3*, University of Aveiro.

362

Franssen J-M, Schleich J-B, Cajot, L-G (1995). *A simple model for fire resistance of axially-loaded members according to Eurocode 3*; Journal of Constructional Steel Research, Vol. 35; pp. 49-69.

Franssen J-M, Talamona D, Kruppa J, Cajot L-G (1998). *Stability of Steel Columns in Case of Fire : Experimental evaluation*. Journal of Structural Engineering, 124(2), pp. 158-163.

Franssen J-M, Brauwiers (2002). *Numerical determination of 3D temperature fields in steel joints*, Second International Workshop "Structures in Fire", Christchurch, New Zealand.

Franssen J-M (2005). *SAFIR: A Thermal/Structural Program Modeling Structures under Fire*, Engineering Journal, A.I.S.C., Vol 42, No. 3, 143-158.

Franssen J-M (2006). *Calculation of temperature in fire-exposed bare steel structures: Comparison between ENV 1993-1-2 and EN 1993-1-2*. Fire Safety Journal, 41, pp.139-143.

Franssen J-M, Kodur V, Zaharia R (2009). *Designing steel structures for fire safety*, Taylor and Francis, The Netherlands.

Galéa Y (2002). *Déversement Élastique d'une poutre à Section Bi-symétrique soumise à des Moments d'extrémité et une charge répartie ou concentrée*, CTICM, Construction Métallique, No. 2, pp. 59-83.

Gardner L, Nethercot DA (2011). *Designer's Guide to Eurocode 3: Design of Steel Buildings, EN 1993-1-1, -1-3 and -1-8*, Second Edition, Thomas Telford.

Hirt MA, Bez R, Nussbaumer A (2006). *Construction métallique, notions fondamentales et methods de dimensionnement*, Traité de Génie Civil de l'École polytechnique fédérale de Lausanne, Press Polytechniques et Universitaires Romandes.

Huang Z, Burgess IW, Plank RJ (2003). *Modelling Membrane Action of Concrete Slabs in Composite Buildings in Fire. Part I: Theoretical Development*, Journal of Structural Engineering, ASCE, 129 (8), pp. 1093-1102.

Incropera FP, De Witt DP (1990). *Fundamentals of Heat and Mass Transfer*, third edition, Wiley.

ISO, International Organization for Standardization (1975). ISO 834. *Fire-Resistance Tests - Elements of Building Construction*.

Jiang J, Usmani A (2013), *Modeling of steel frame structures in fire using OpenSees*, Computers & Structures, Vol. 118, No. Special Issue, 03.2013, pp. 90-99

Joyeux D, Kruppa J, Cajot L-G, Schleich J-B (2001). *Demonstration of real fire tests in car parks and high buildings*, Final report, ECSC Contract N0. 7215 PP 025.

Knobloch M, Fontana M, Frangi A, (2008). *Steel beam-columns subjected to fire*, Ernst & Sohn, Steel Construction, Issue 1.

Lopes N, Simões da Silva L, Vila Real P, Piloto P (2004). *New Proposals for the Design of Steel Beam-Columns under Fire Conditions, Including a New Approach for the Lateral-Torsional Buckling of Beams*, Computer & Structures, Elsevier, 82/17-19, pp. 1463-1472.

Lopes N, Vila Real P, Simões da Silva L, Franssen J-M (2008). *Duplex stainless steel columns and beam-columns in case of fire*, proceedings of the 5th International Conference on Structures in Fire SiF'08, pp. 90-100, Singapore.

Lopes N (2009). *Behaviour of stainless steel structures in case of fire*, PhD thesis, University of Aveiro, Portugal

Ng KT, Gardner L (2007). *Buckling of stainless steel columns and beams in fire*, Engineering Structures, Elsevier, Vol. 29, pp. 717-730.

REFERENCES

- Marshall WT, Nelson HM (1978). *Structures*, PITMAN, 2nd edition.
- Nauar K, (2014). *Buckling curves of steel profiles at elevated temperature*, Master's Thesis, ArGenCo Dpt, Univ. of Liege.
- Neal BG, (1977). *The Plastic Methods of Structural Analysis*, CHAPMAN and HALL, 3rd edition.
- Olenick SM, Carpenter DJ, (2003). *An Updated International Survey of Computer Models for Fire and Smoke*, SFPE, Journal of Fire Protection Engineering, 12-2, pp. 87-110.
- Ozone V2.2.6 (2009). University of Liege, ARCELORMITTAL, <http://www.arcelormittal.com/sections/>.
- Purkiss JA (2007). *Fire safety Engineering - Design of structures*, 2nd edition, Butterworth-Heinemann, Elsevier.
- Ray SS (1998). *Structural steelwork – Analysis and design*, Blackwell Science.
- Santiago A, Simões da Silva L, Vila Real P (2007). *Experimental investigation of the behaviour of a steel sub-frame under a natural fire*, Proceedings of the 3rd International Conference of Steel and Composite Structures (Eds.: Y.W. Wang, C.K. Choi), pp.681-686, Manchester, UK.
- Santiago A, Simões da Silva L, Vila Real P (2008a). *Effect of Joint Typologies on the 3D Behaviour of a Steel Frame under a Natural Fire*. Proceedings of Fifth International Workshop “Structures in Fire”, Singapore.
- Santiago A, Simões da Silva L, Vila Real P (2008b). *Recommendations for the design of end-plate beam-to-column steel joints subjected to a natural fire*. Proceedings of EUROSTEEL'08, Graz, Austria.
- Santiago A, Simões da Silva L, Vila Real P, Veljkovic M (2008c). *Numerical study of a steel sub-frame in fire*, Computers and Structures Volume 86, Issue 15-16, pp. 1619-1632.
- Sarraj M, Burgess I, Davison B, Plank RJ (2006). *Finite element modelling on fin plate steel connections in fire*. Proceedings of Fourth International Workshop “Structures in Fire”, Aveiro, Portugal, pp.315-26.
- SCI (2005). *Steel Designer's Manual – Sixth Edition*. The Steel Construction Institute.
- SEMI-COMP+, Valorisation Project (2012). “Valorisation action of plastic member capacity of semi-compact steel sections – a more economic design”, RFS2-CT-2010-00023.

Simões da Silva L, Santiago A, Vila Real P (2001). *A component model for the behaviour of steel joint at high temperatures*, Journal of Constructional Steel Research, 57(11), pp.1169-1195.

Simões da Silva L, Santiago A, Vila Real P, Moore D (2005). *Behaviour of steel joints and fire loading*, International Journal of Steel and Composite Structures 5(6), pp.485-513.

Simões da Silva L, Simões R, Gervásio H (2010). *Design of Steel Structures*, ECCS Press and Ernst & Sohn a Wiley Company.

Song L, Izzuddin BA, Elnashai AS, Dowling PJ (2000). *An integrated adaptive environment for fire and explosion analysis of steel frames – Part I: Analytical models*, Journal of Constructional Steel Research, Elsevier, Vol. 53, pp. 63-85.

Spyrou S, Davidson JB, Burgess I, Plank R (2004). *Experimental and analytical studies of steel joint components at high temperature*, Fire and Materials, 28, pp.83-94.

Spyrou S, Davidson JB, Burgess I, Plank R (2004). *Experimental and analytical investigation of the ‘compression zone’ components within a steel joint at high temperature*, Journal of Constructional Steel Research, 60, pp.841-865.

Spyrou S, Davidson JB, Burgess I, Plank R (2004). *Experimental and analytical investigation of the ‘tension zone’ components within a steel joint at high temperature*, Journal of Constructional Steel Research, 60, pp.867-896.

SSEDTA (2001). *Structural Steelwork Eurocodes, a trans-national approach*, ESDEP – European Steel Design Education Programme, ESDEP Society.

Talamona D, Franssen J-M, Schleich J-B, Kruppa J (1997). *Stability of steel columns in case of fire: Numerical modelling*, Journal of Structural Engineering 123, 6, pp. 713-720.

Tondini N, Vassart N, Franssen J-M (2012). *Development of an interface between CFD and FE software*, proceedings of the 7th International Conference on Structures in Fire SiF'12, Fontana, Frangi & Knobbloch ed., ETH Zürich, pp. 459 - 468

Trahair NS (1993). *Flexural–torsional buckling of structures*, E&FN SPON.

Trahair NS, Bradford MA (1998). *The behaviour and design of steel structures to AS 4100*, Third edition – Australian, E & FN SPON.

Trahair NS, Bradford, MA Nethercot, DA (2001). *The behaviour and design of steel structures to BS5950*, Spon Press.

REFERENCES

Twilt L; Leur PHE; Both C (2001). *Characteristics of the heat transfer for calculating the temperature development in structural steel work exposed to standard fire condition under plate thermocouple control*, Proceedings of the first international workshop “Structures in Fire”, Copenhagen, J-M Franssen ed..

Uppfeldt B, Outinen T, Veljkovic M (2008). *A design model for stainless steel box columns in fire*, Journal of Constructional Steel Research, Elsevier, Vol. 64 (11), pp. 1294–1301.

Vila Real P, Franssen J-M, (2001). *Numerical Modeling of Lateral Buckling of Steel I Beams Under Fire Conditions – Comparison with Eurocode 3*, Vol. 11, No. 2, pp. 112-128, Journal of Fire Protection Engineering, USA.

Vila Real P (2003a). *Fire design of steel structures according Eurocode 3*, (in Portuguese), Ed. ORION.

Vila Real P, Lopes N, Simões da Silva L, Franssen J-M (2003b). *Lateral-Torsional Buckling of Unrestrained Steel Beams Under Fire Conditions: Improvement of EC3 Proposal*, Computers & Structures, Elsevier, Vol. 82, pp. 1737-1744.

Vila Real P, Lopes N, Simões da Silva L, Piloto P, Franssen J-M (2003c). *Towards a consistent safety format of steel beam-columns: application of the new interaction formulae at ambient temperature to elevated temperatures*. Steel & Composite Structures, an International Journal, Techno-Press, Vol. 3, No. 6, 383-401.

Vila Real P, Lopes N, Simões da Silva L, Franssen J-M (2007). *Parametric analysis of the Lateral-torsional buckling resistance of Steel beams in case of fire*, Fire Safety Journal, Elsevier, Volume 42, Issues 6-7, pp. 416-424.

Vila Real P, Lopes N, Simões da Silva L, Franssen J-M (2008). *Lateral-torsional buckling of Stainless steel I-beams in case of fire*, Journal of Constructional Steel Research, Elsevier, Vol. 64 (11), pp. 1302–1309.

Vila Real P, Couto C, Lopes N (2009a). *Tables for section factors of unprotected and protected steel profiles*, LERF, University of Aveiro, internal report T09027.

Vila Real P, Couto C, Lopes N (2009b). *Tables for cross-sectional classification under normal and fire temperature*, LERF, University of Aveiro, internal report T09028.

Vila Real P, Franssen J-M – Elefir-EN V1.2.3 (2010). *Software for fire design of steel structural members according the Eurocode 3*. <http://elefiren.web.ua.pt>.

Vila Real P, Couto C, Lopes N (2011). *Modelling of multiple localised fires and steel structural members response using the software Elefir-EN*, proceedings of the Application of Structural Fire Engineering, Prague, Czech Republic, pp. 73-78, ISBN – 978-80-01-04798-9.

Vila Real P (2014). *On the classification of cross-sections under bending and axial compression at elevated temperature*, Commemorative publication on the occasion of Prof. Peter Schaumann's 60th birthday, Leibniz Universität Hannover, pp. 221-230.

Wald F, Simões da Silva L, Moore D, Santiago A (2004). *Experimental Behaviour of Steel Joints under Natural Fire*, Proceedings of the Fifth Workshop on Connections in Steel Structures V: Innovated Steel Connections, Amsterdam, The Netherlands.

Wang YC (2002). *Steel and Composite Structures - Behaviour and design for fire safety*, Spon Press.

Wang Z (2004). *Heat Transfer Analysis of Insulated Steel Members Exposed to Fire*. Master Thesis, School of Civil Engineering and Env. Engng., NTU, Singapore.

Wong MB (2009). *Plastic Analysis and Design of Steel Structures*. Elsevier, Butterworth-Heinemann, 1st ed.

Annex A

THERMAL DATA FOR CARBON STEEL AND STAINLESS STEEL SECTIONS

This annex gives the basic data necessary to calculate the temperature of protected and unprotected steel sections. Tables and graphs are presented that give the temperature development of steel sections subjected to the standard fire curve ISO 834. Thermal properties of some fire protection and fire compartment lining materials are also presents in this annex.

A.1. THERMAL PROPERTIES OF CARBON STEEL

369

To evaluate the thermal response of steel members the thermal properties should be known. This section describes the thermal properties of carbon steel according Part 1-2 of Eurocode 3.

A.1.1. Specific heat

The specific heat of steel c_a should be determined from the following expressions:

- for $20\text{ °C} \leq \theta_a < 600\text{ °C}$

$$c_a = 425 + 7.73 \times 10^{-1} \theta_a - 1.69 \times 10^{-3} \theta_a^2 + 2.22 \times 10^{-6} \theta_a^3 \quad [\text{J/kgK}]$$

- for $600\text{ °C} \leq \theta_a < 735\text{ °C}$

$$c_a = 666 + 13002 / (738 - \theta_a) \quad [\text{J/kgK}]$$

A. THERMAL DATA FOR CARBON STEEL AND STAINLESS STEEL SECTIONS

- for $735\text{ °C} \leq \theta_a < 900\text{ °C}$

$$c_a = 545 + 17820 / (\theta_a - 731) \quad [\text{J/kgK}]$$

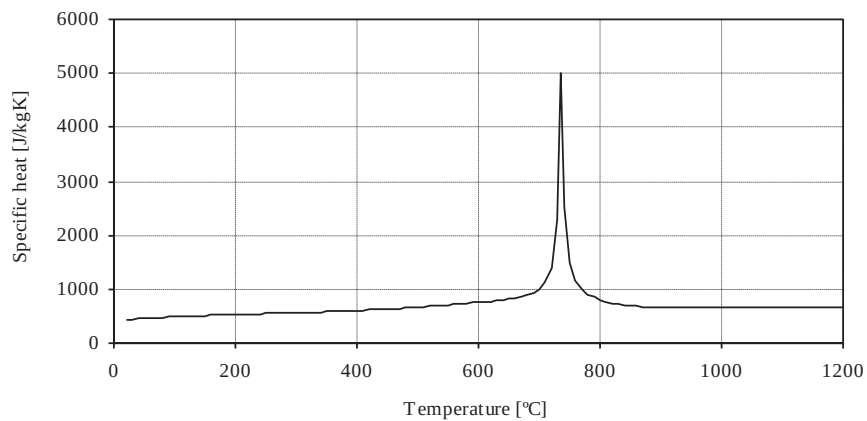
- for $900\text{ °C} \leq \theta_a \leq 1200\text{ °C}$

$$c_a = 650 \quad [\text{J/kgK}]$$

where

θ_a is the steel temperature [$^{\circ}\text{C}$].

The variation of the specific heat with temperature is illustrated in Fig. A.1.



370

Figure A.1 – Specific heat of carbon steel

A.1.2. Thermal conductivity

The thermal conductivity of steel λ_a should be determined from the following expressions:

- for $20\text{ °C} \leq \theta_a < 800\text{ °C}$

$$\lambda_a = 54 - 3.33 \times 10^{-2} \theta_a \quad [\text{W/mK}]$$

- for $800\text{ °C} \leq \theta_a \leq 1200\text{ °C}$

$$\lambda_a = 27.3 \quad [\text{W/mK}]$$

where

θ_a is the steel temperature [°C].

The variation of the thermal conductivity with temperature is illustrated in Fig. A.2

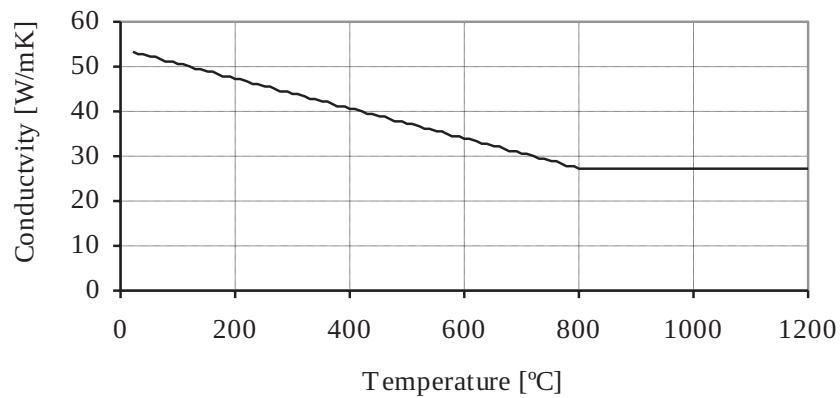


Figure A.2 – Conductivity of carbon steel

A.1.3. Thermal elongation

The thermal elongation of steel $\Delta l/l$ should be determined from the following expressions:

371

$$\Delta l/l = \begin{cases} 1.2 \times 10^{-5} \theta_a + 0.4 \times 10^{-8} \theta_a^2 - 2.416 \times 10^{-4} & 20 \text{ °C} \leq \theta_a < 750 \text{ °C} \\ 1.1 \times 10^{-2} & 750 \text{ °C} \leq \theta_a \leq 860 \text{ °C} \\ 2 \times 10^{-5} \theta_a - 6.2 \times 10^{-3} & 860 \text{ °C} < \theta_a \leq 1200 \text{ °C} \end{cases}$$

where

- l is the length at 20 °C;
- Δl is the temperature induced expansion;
- θ_a is the steel temperature [°C].

The variation of the thermal elongation with temperature is illustrated in Fig. A.3.

A. THERMAL DATA FOR CARBON STEEL AND STAINLESS STEEL SECTIONS

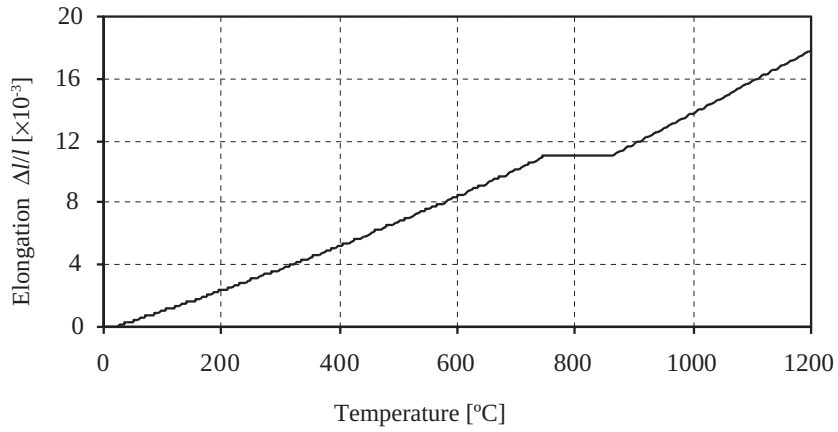
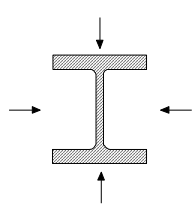
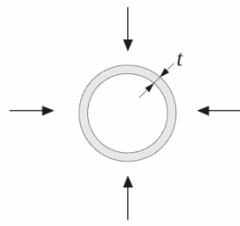
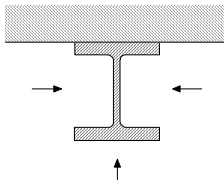
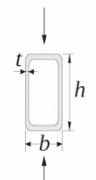
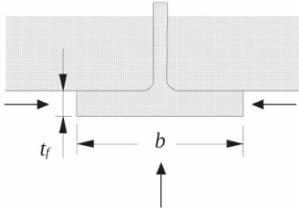
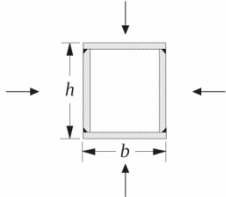
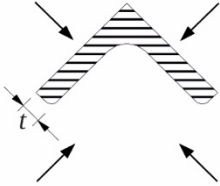
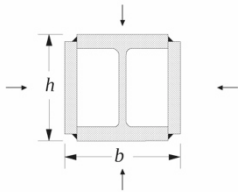
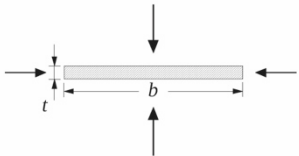
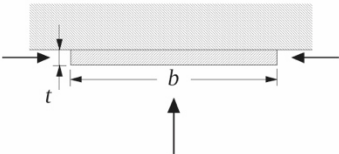


Figure A.3 – Thermal elongation of carbon steel

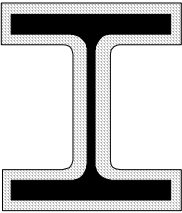
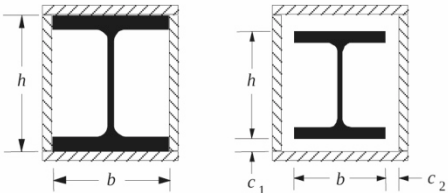
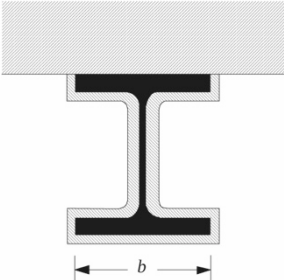
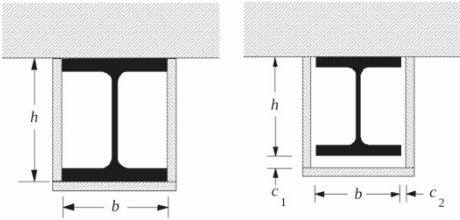
A.2. SECTION FACTOR A_m/V [m⁻¹] FOR UNPROTECTED STEEL MEMBERS

<p>Open section exposed to fire on all sides:</p> $\frac{A_m}{V} = \frac{\text{perimeter}}{\text{cross section area}}$ 	<p>Tube exposed to fire on all sides:</p> $A_m/V \approx 1/t$ 
<p>Open section exposed to fire on three sides:</p> $\frac{A_m}{V} = \frac{\text{surface exposed to fire}}{\text{cross section area}}$ 	<p>Hollow section (or welded box section of uniform thickness) exposed to fire on all sides:</p> <p>If $t \ll b$: $A_m/V \approx 1/t$</p> 

A.2. SECTION FACTOR A_m/V [M^{-1}] FOR UNPROTECTED STEEL MEMBERS

<p>I-section flange exposed to fire on three sides:</p> $A_m/V = (b + 2t_f)/(bt_f)$ <p>If $t_f \ll b$: $A_m/V \approx 1/t_f$</p> 	<p>Welded box section exposed to fire on all sides:</p> $\frac{A_m}{V} = \frac{2(b+h)}{\text{cross section area}}$ <p>If $t \ll b$: $A_m/V \approx 1/t$</p> 
<p>Angle exposed to fire on all sides:</p> $A_m/V \approx 2/t$ 	<p>I-section with box reinforcement, exposed to fire on all sides:</p> $\frac{A_m}{V} = \frac{2(b+h)}{\text{cross section area}}$ 
<p>Flat bar exposed to fire on all sides:</p> $A_m/V = 2(b+t)/(bt)$ <p>If $t \ll b$: $A_m/V \approx 2/t$</p> 	<p>Flat bar exposed to fire on three sides:</p> $A_m/V = (b + 2t)/(bt)$ <p>If $t \ll b$: $A_m/V \approx 1/t$</p> 

A.3. SECTION FACTOR A_p / V [m⁻¹] FOR PROTECTED STEEL MEMBERS

Sketch	Description	Section factor (A_p/V)
	Contour encasement of uniform thickness	$\frac{\text{steel perimeter}}{A}$
	Hollow encasement of uniform thickness*	$\frac{2(b+h)}{\text{steel cross section area}}$
	Contour encasement of uniform thickness, exposed to fire on three sides	$\frac{\text{steel perimeter} - b}{\text{steel cross section area}}$
	Hollow encasement of uniform thickness, exposed to fire on three sides *	$\frac{2h + b}{\text{steel cross section area}}$
* The clearance dimensions c_1 and c_2 should not normally exceed $h/4$		

A.4. TABLES AND NOMOGRAMS FOR EVALUATING THE TEMP. IN UNPROTECTED STEEL
MEMBERS SUBJECTED TO THE STANDARD FIRE CURVE ISO 834

**A.4. TABLES AND NOMOGRAMS FOR EVALUATING THE
TEMPERATURE IN UNPROTECTED STEEL MEMBERS
SUBJECTED TO THE STANDARD FIRE CURVE ISO 834**

Temperature of unprotected steel in °C, exposed to the ISO 834 fire curve

for different values of $k_{sh} \frac{A_m}{V}$, [m⁻¹]

Time [min.]	10 m ⁻¹	15 m ⁻¹	20 m ⁻¹	25 m ⁻¹	30 m ⁻¹	40 m ⁻¹	60 m ⁻¹	100 m ⁻¹	200 m ⁻¹	300 m ⁻¹	400 m ⁻¹
0	20	20	20	20	20	20	20	20	20	20	20
1	21	22	23	24	24	26	29	34	48	61	73
2	25	27	29	31	33	38	46	62	100	133	162
3	29	33	37	41	45	53	68	97	161	214	259
4	33	40	46	52	59	71	94	136	226	296	351
5	39	48	57	65	74	90	122	178	291	373	430
6	45	57	68	79	90	111	151	221	354	441	494
7	51	66	80	94	108	133	181	265	413	498	545
8	58	76	93	110	126	156	213	308	466	545	584
9	65	86	106	126	144	180	245	351	512	583	615
10	73	97	120	142	164	204	277	392	552	614	640
11	80	108	134	159	183	229	309	432	587	640	660
12	88	119	149	177	204	253	340	469	616	662	678
13	97	131	164	195	224	278	372	503	641	680	693
14	105	143	179	213	244	303	402	535	663	695	705
15	114	155	194	231	265	328	432	565	682	708	716
16	122	167	210	249	286	353	460	591	697	718	725
17	131	180	225	268	307	377	487	615	710	727	732
18	140	193	241	286	328	401	513	638	721	733	736
19	150	206	257	305	348	425	538	658	729	737	743
20	159	218	273	323	369	448	561	676	734	743	754
21	168	232	289	342	389	470	583	692	738	754	767
22	178	245	305	360	409	491	604	706	744	767	780
23	188	258	321	378	429	512	623	717	754	780	790
24	197	271	337	396	448	532	641	726	767	791	799
25	207	284	353	414	467	552	658	732	780	801	807
26	217	298	369	432	485	570	674	735	792	809	813
27	227	311	385	449	503	588	688	739	803	816	820

A. THERMAL DATA FOR CARBON STEEL AND STAINLESS STEEL SECTIONS

Temperature of unprotected steel in °C, exposed to the ISO 834 fire curve
for different values of $k_{sh} \frac{A_m}{V}$, [m⁻¹]

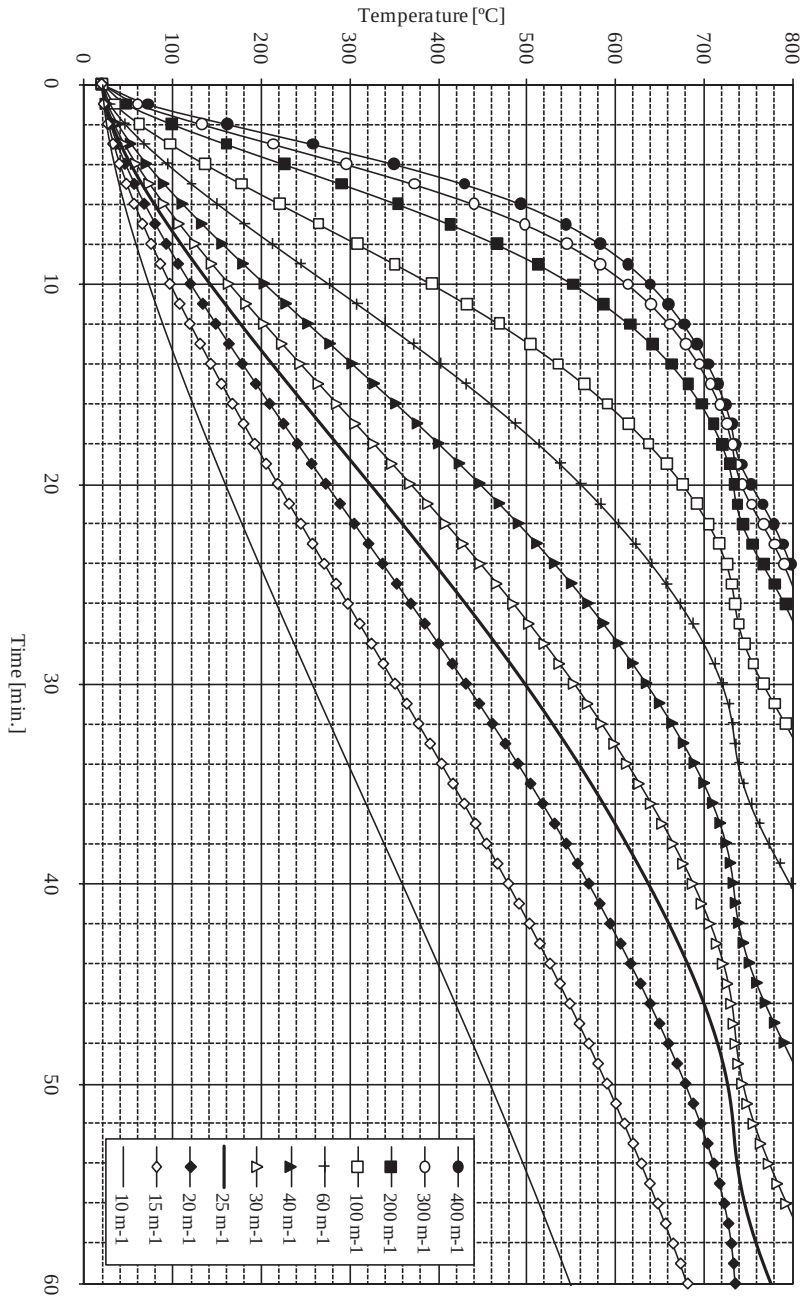
Time [min.]	10 m ⁻¹	15 m ⁻¹	20 m ⁻¹	25 m ⁻¹	30 m ⁻¹	40 m ⁻¹	60 m ⁻¹	100 m ⁻¹	200 m ⁻¹	300 m ⁻¹	400 m ⁻¹
28	237	324	401	466	521	604	701	746	813	823	826
29	247	338	416	482	538	621	712	756	821	829	831
30	257	351	431	498	554	636	721	767	828	835	837
31	267	364	446	514	570	651	728	780	835	840	842
32	277	377	461	530	585	665	733	793	841	845	847
33	288	391	476	545	600	678	736	805	846	850	852
34	298	404	490	559	614	690	740	816	851	855	856
35	308	416	504	574	628	701	745	827	856	860	861
36	318	429	518	587	641	711	753	836	861	864	865
37	329	442	532	601	654	719	763	844	866	868	870
38	339	454	545	614	666	726	774	852	870	873	874
39	349	467	558	626	677	731	786	859	874	877	878
40	359	479	570	638	688	734	798	865	878	881	882
41	369	491	582	650	698	737	810	871	882	884	885
42	379	503	594	661	707	740	822	876	886	888	889
43	389	514	606	672	716	746	832	881	890	892	893
44	399	526	617	683	722	752	842	885	893	895	896
45	409	537	628	692	728	761	852	889	897	899	900
46	419	548	639	701	732	771	860	894	900	902	903
47	429	559	650	709	735	781	868	897	904	906	906
48	439	570	660	717	737	792	875	901	907	909	910
49	449	580	670	723	740	803	882	905	910	912	913
50	458	590	679	728	744	814	888	908	914	915	916
51	468	600	688	732	750	825	894	911	917	918	919
52	477	610	697	734	757	835	899	915	920	921	922
53	487	620	704	736	765	845	904	918	923	924	925
54	496	629	711	739	774	854	908	921	926	927	928
55	505	638	718	743	784	863	913	924	928	930	930
56	514	648	723	747	794	872	917	927	931	932	933
57	523	656	728	753	804	880	920	930	934	935	936
58	532	665	731	760	814	887	924	933	937	938	938
59	541	673	734	768	825	894	927	935	939	940	941
60	549	681	736	777	834	901	931	938	942	943	944

A.4. TABLES AND NOMOGRAMS FOR EVALUATING THE TEMP. IN UNPROTECTED STEEL
MEMBERS SUBJECTED TO THE STANDARD FIRE CURVE ISO 834

Temperature of unprotected steel in °C, exposed to the ISO 834 fire curve
for different values of $k_{sh} \frac{A_m}{V}$, [m⁻¹]

Time [min.]	10 m ⁻¹	15 m ⁻¹	20 m ⁻¹	25 m ⁻¹	30 m ⁻¹	40 m ⁻¹	60 m ⁻¹	100 m ⁻¹	200 m ⁻¹	300 m ⁻¹	400 m ⁻¹
61	558	689	738	786	844	907	934	941	944	946	946
62	566	696	741	796	853	912	937	943	947	948	949
63	574	703	744	805	862	917	940	946	949	950	951
64	583	709	749	815	871	922	942	948	952	953	953
65	591	715	755	824	879	927	945	951	954	955	956
66	598	720	761	834	887	931	948	953	957	958	958
67	606	725	769	843	894	935	950	956	959	960	960
68	614	728	776	852	901	939	953	958	961	962	963
69	622	731	785	861	907	943	955	960	963	964	965
70	629	734	793	869	914	946	958	963	966	967	967
71	636	735	802	877	919	949	960	965	968	969	969
72	644	737	811	885	925	953	963	967	970	971	971
73	651	739	820	893	930	956	965	969	972	973	973
74	658	742	829	900	935	958	967	971	974	975	975
75	665	745	837	906	939	961	969	973	976	977	977
76	671	750	846	913	944	964	972	975	978	979	979
77	678	755	855	919	948	966	974	978	980	981	981
78	684	760	863	925	952	969	976	980	982	983	983
79	690	767	871	930	955	971	978	982	984	985	985
80	696	773	879	935	959	974	980	984	986	987	987
81	702	780	886	940	962	976	982	985	988	989	989
82	707	788	893	945	966	978	984	987	990	991	991
83	712	795	900	949	969	980	986	989	992	992	993
84	716	803	907	954	972	983	988	991	993	994	995
85	720	811	914	958	974	985	990	993	995	996	996
86	724	819	920	961	977	987	992	995	997	998	998
87	727	827	926	965	980	989	993	997	999	1000	1000
88	730	835	931	969	982	991	995	998	1001	1001	1002
89	732	843	937	972	985	993	997	1000	1002	1003	1003
90	734	851	942	975	987	995	999	1002	1004	1005	1005

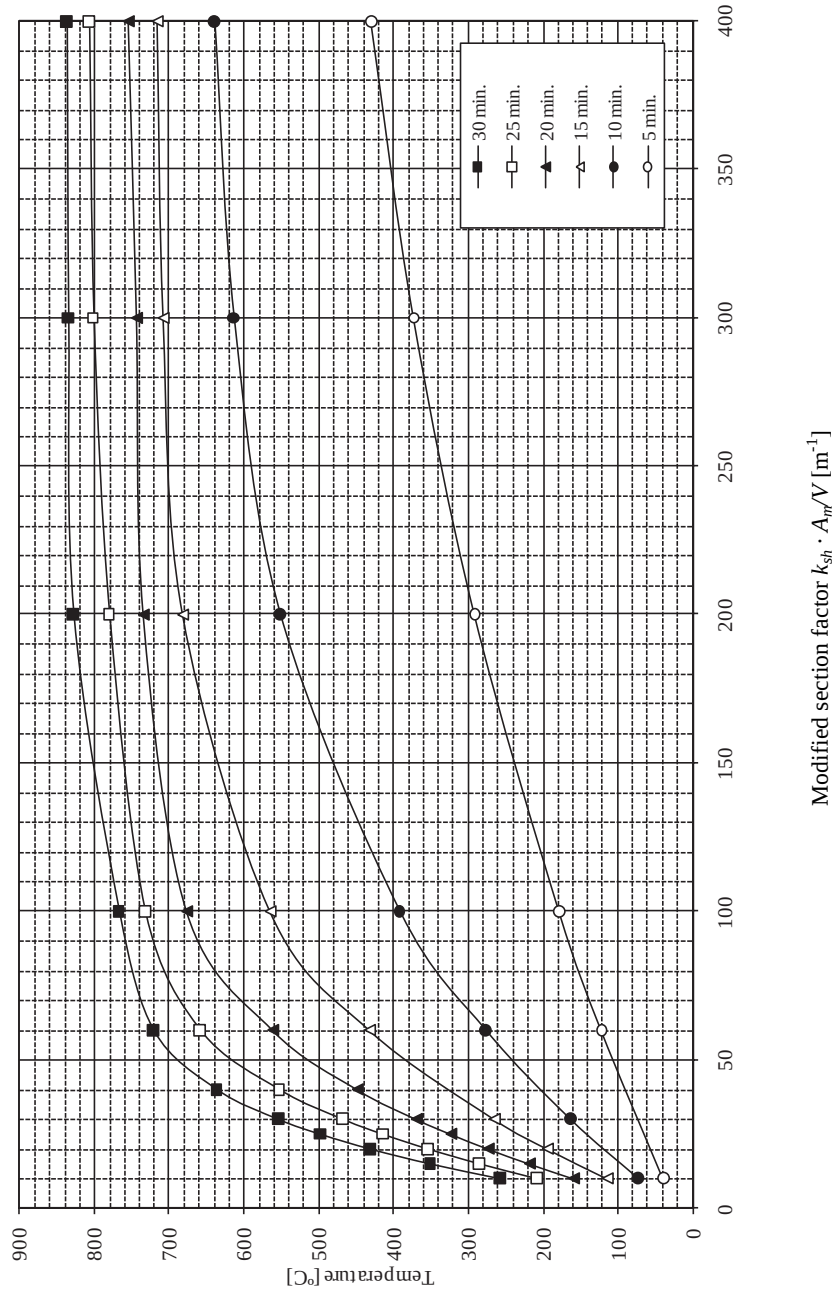
A. THERMAL DATA FOR CARBON STEEL AND STAINLESS STEEL SECTIONS



A.4. TABLES AND NOMOGRAMS FOR EVALUATING THE TEMP. IN UNPROTECTED STEEL

MEMBERS SUBJECTED TO THE STANDARD FIRE CURVE ISO 834

Nomogram for unprotected steel members subjected to the ISO 834 fire curve, for different time duration



A. THERMAL DATA FOR CARBON STEEL AND STAINLESS STEEL SECTIONS

A.5. TABLES AND NOMOGRAMS FOR EVALUATING THE TEMPERATURE IN PROTECTED STEEL MEMBERS SUBJECTED TO THE STANDARD FIRE CURVE ISO 834

Temperature of protected steel in °C, exposed to the ISO 834 fire curve

for different values of $\frac{A_p \lambda_p}{V d_p}$, [W/m³K]

Time [min.]	100 W/m ³ K	200 W/m ³ K	300 W/m ³ K	400 W/m ³ K	600 W/m ³ K	800 W/m ³ K	1000 W/m ³ K	1500 W/m ³ K	2000 W/m ³ K
0	20	20	20	20	20	20	20	20	20
5	24	27	31	35	41	48	55	71	86
10	29	38	46	54	70	85	100	133	164
15	35	49	62	75	100	123	145	194	237
20	41	61	79	97	130	160	189	251	305
25	47	72	96	118	159	197	231	305	366
30	54	84	113	140	188	232	271	354	421
35	60	97	130	161	216	266	309	400	470
40	67	109	147	181	244	298	346	442	514
45	74	121	163	202	270	329	380	481	554
50	80	133	179	222	296	359	413	516	589
55	87	145	196	241	321	387	443	549	621
60	94	156	211	261	345	414	472	578	650
65	100	168	227	279	368	440	499	606	676
70	107	180	242	298	391	465	525	631	699
75	114	191	258	316	412	488	549	655	717
80	120	202	273	333	433	510	571	676	729
85	127	214	287	350	453	531	592	695	735
90	134	225	302	367	472	552	612	712	742
95	140	236	316	383	491	571	631	724	755
100	147	247	330	399	509	589	649	732	773
105	153	258	343	415	526	606	666	736	793
110	160	268	357	430	542	623	682	742	815
115	166	279	370	445	558	638	696	753	838

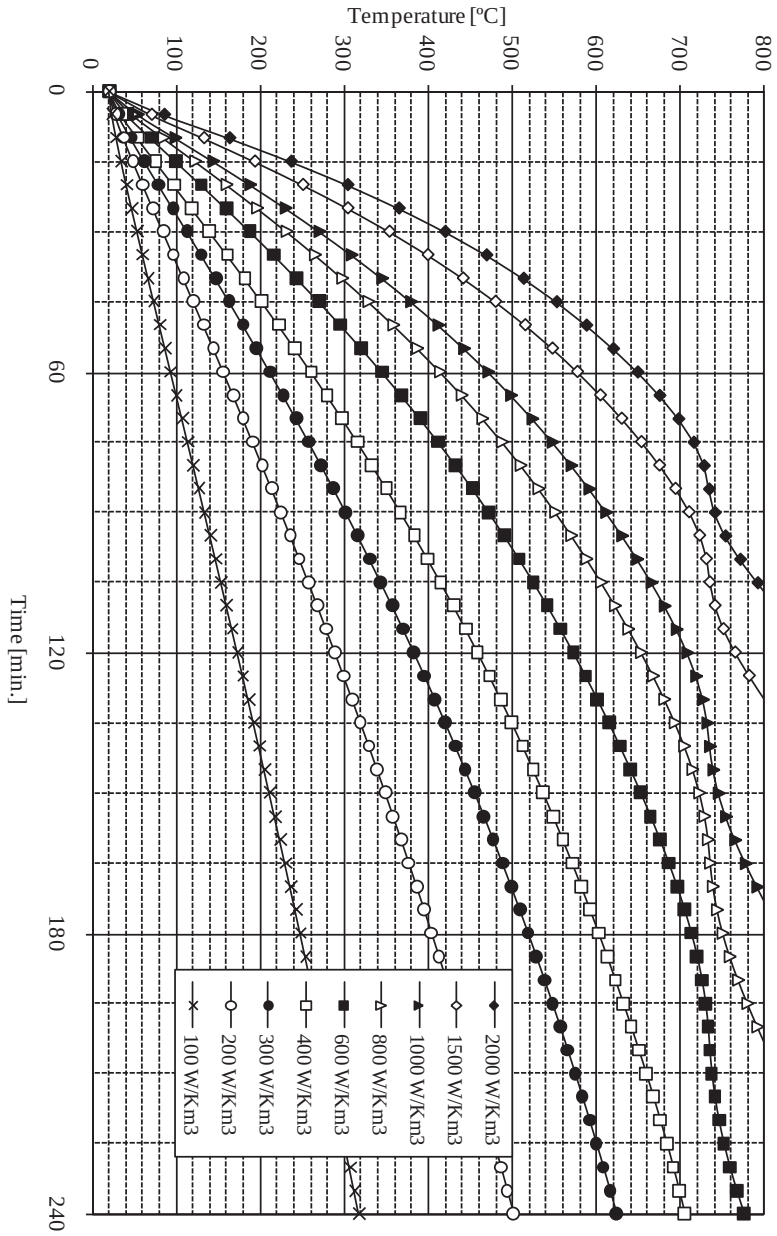
A.5. TABLES AND NOMOGRAMS FOR EVALUATING THE TEMP. IN PROTECTED STEEL
MEMBERS SUBJECTED TO THE STANDARD FIRE CURVE ISO 834

Temperature of protected steel in °C, exposed to the ISO 834 fire curve
for different values of $\frac{A_p \lambda_p}{V d_p}$, [W/m³K]

Time [min.]	100 W/m ³ K	200 W/m ³ K	300 W/m ³ K	400 W/m ³ K	600 W/m ³ K	800 W/m ³ K	1000 W/m ³ K	1500 W/m ³ K	2000 W/m ³ K
120	173	289	383	459	573	654	709	767	859
120	173	289	383	459	573	654	709	767	859
125	179	299	395	473	588	668	719	783	880
130	186	310	408	486	602	681	727	801	899
135	192	320	420	500	616	694	733	820	918
140	198	330	432	512	629	705	736	839	935
145	205	339	444	525	642	715	740	858	950
150	211	349	455	537	654	723	746	876	964
155	217	359	466	549	665	729	755	893	978
160	223	368	477	560	677	733	766	910	990
165	230	377	488	572	687	736	778	925	1002
170	236	387	498	582	697	739	792	940	1013
175	242	396	509	593	706	744	807	954	1023
180	248	404	519	603	714	751	821	967	1032
185	254	413	528	613	721	759	836	979	1041
190	260	422	538	623	727	769	851	991	1049
195	266	431	548	633	731	780	866	1001	1057
200	272	439	557	642	734	792	880	1012	1064
205	277	447	566	651	736	804	894	1021	1071
210	283	455	575	660	738	817	907	1031	1078
215	289	464	583	668	742	830	920	1039	1084
220	295	472	592	677	747	843	933	1048	1090
225	301	479	600	685	753	856	945	1056	1096
230	306	487	608	692	760	869	956	1063	1101
235	312	495	616	699	768	881	967	1070	1107
240	318	502	624	706	777	893	978	1077	1111

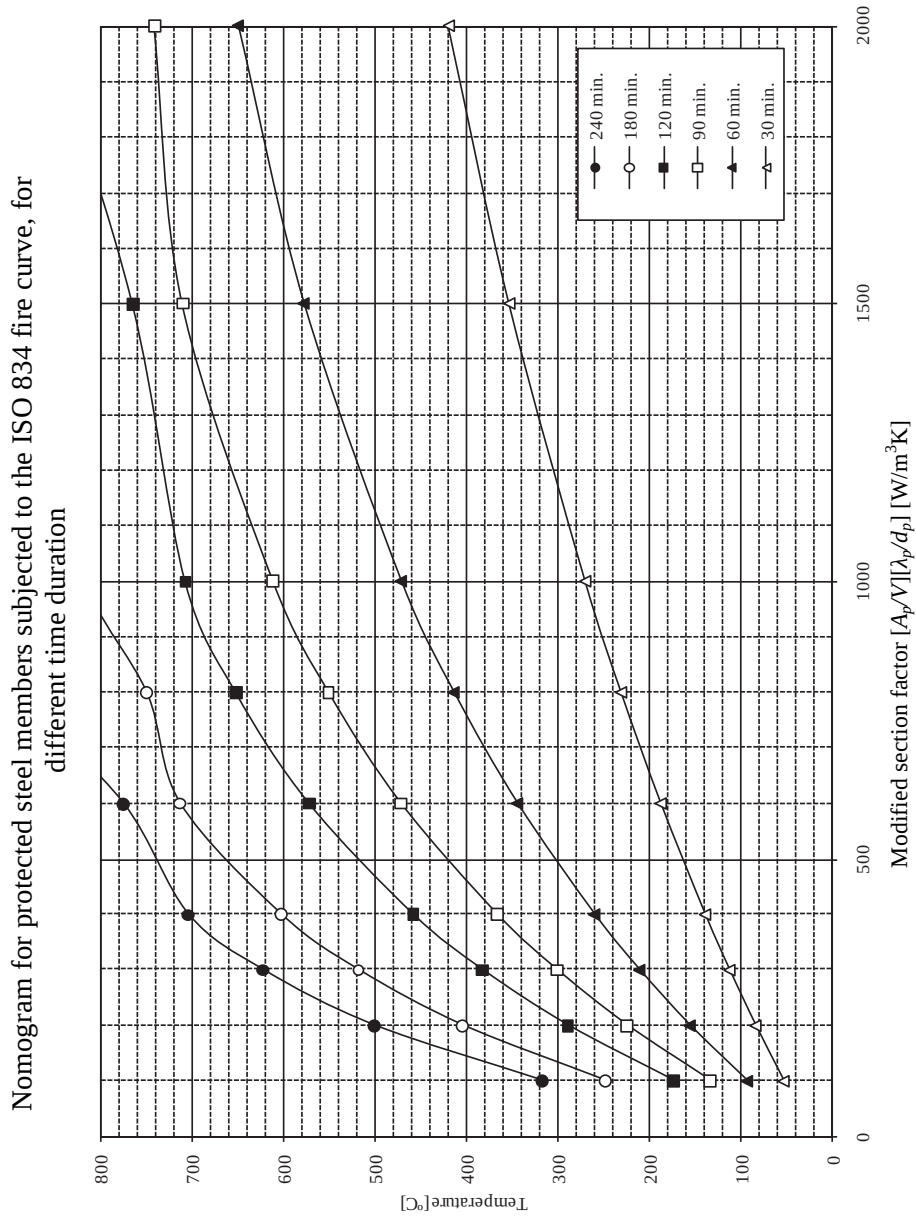
A. THERMAL DATA FOR CARBON STEEL AND STAINLESS STEEL SECTIONS

Nomogram for protected steel members subjected to the ISO 834 fire curve, for different values of $[A_p V] [\lambda_p / d_p]$ [$\text{W}/\text{K}\cdot\text{m}^3$]



A.5. TABLES AND NOMOGRAMS FOR EVALUATING THE TEMP. IN PROTECTED STEEL

MEMBERS SUBJECTED TO THE STANDARD FIRE CURVE ISO 834



A.6. THERMAL PROPERTIES OF SOME FIRE PROTECTION MATERIALS

Properties of fire protection materials (ECCS, 1995)

Material	Unit mass, ρ_p [kg / m ³]	Moisture content, p %	Thermal conductivity, λ_p [W / (mK)]	Specific heat, c_p [J/(kgK)]
Sprays				
– mineral fibre	300	1	0.12	1200
– vermiculite cement	350	15	0.12	1200
– perlite	350	15	0.12	1200
High density sprays				
– vermiculite (or perlite) and cement	550	15	0.12	1100
– vermiculite (or perlite) and gypsum	650	15	0.12	1100
Boards				
– vermiculite (or perlite) and cement	800	15	0.20	1200
– fibre-silicate or fibre-calcium -silicate	600	3	0.15	1200
– fibre-cement	800	5	0.15	1200
– gypsum boards	800	20	0.20	1700
Compressed fibre boards				
– fibre silicate, mineral- wool, stone-wool	150	2	0.20	1200
Concrete	2300	4	1.60	1000
Light weight concrete	1600	5	0.80	840
Concrete bricks	2200	8	1.00	1200
Brick with holes	1000	-	0.40	1200
Solid bricks	2000	-	1.20	1200

A.7. THERMAL PROPERTIES OF STAINLESS STEEL

A.7.1. Specific heat

The specific heat of stainless steel c_a may be determined from the following expression:

$$c_a = 450 + 0.280 \times \theta_a - 2.91 \times 10^{-4} \theta_a^2 + 1.34 \times 10^{-7} \theta_a^3 \quad [\text{J/kgK}]$$

where

θ_a is the steel temperature [°C].

The variation of the specific heat with temperature is illustrated in Fig. A.4.

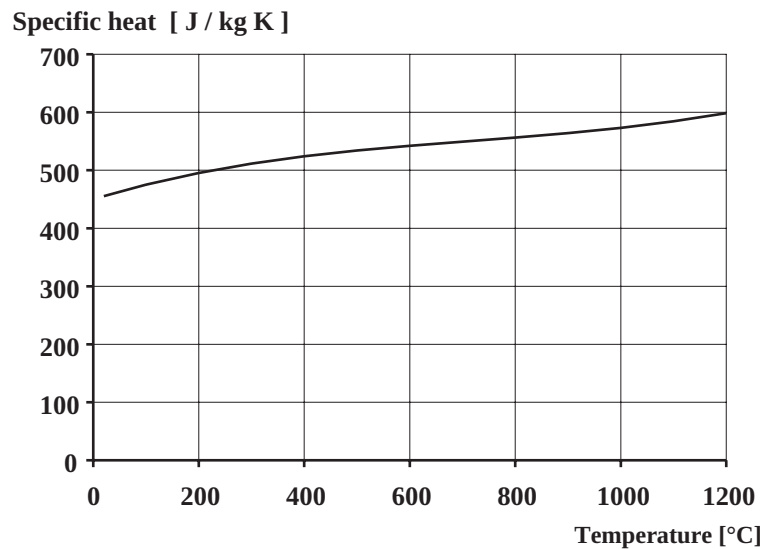


Figure A.4 – Specific heat of stainless steel as a function of the temperature

A.7.2. Thermal conductivity

The thermal conductivity of stainless steel λ_a may be determined from the following expression:

$$\lambda_a = 14.6 + 1.27 \times 10^{-2} \theta_a \quad [\text{W/mK}]$$

where

θ_a is the steel temperature [°C].

The variation of the thermal conductivity with temperature is illustrated in Fig. A.5.

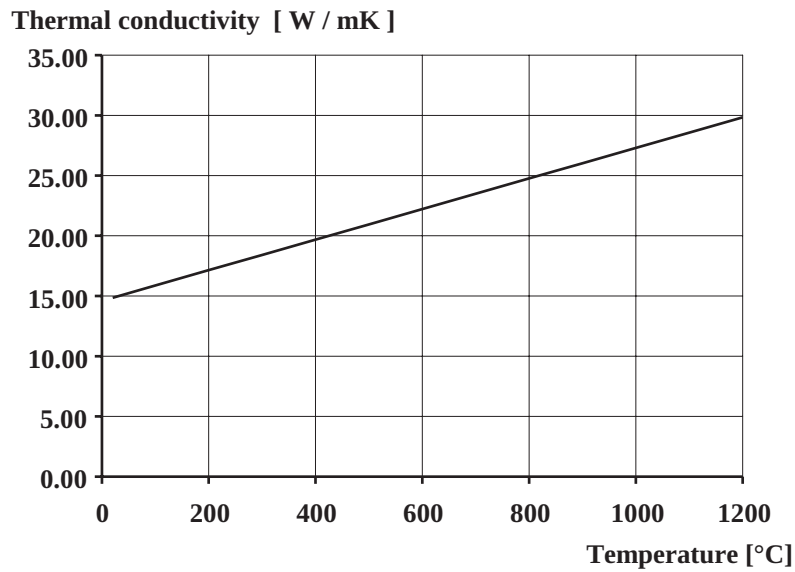


Figure A.5 – Thermal conductivity of stainless steel as a function of the temperature

386

A.7.3. Thermal elongation

The thermal elongation of austenitic stainless steel $\Delta l/l$ may be determined from the following expression:

$$\Delta l/l = (16 + 4.79 \times 10^{-3} \theta_a - 1.243 \times 10^{-6} \theta_a^2) \times (\theta_a - 20) 10^{-6}$$

where

l is the length at 20 °C;

Δl is the temperature induced expansion;

θ_a is the steel temperature [°C].

The variation of the thermal elongation with temperature is illustrated in Fig. A.6.

**A.8. TABLES AND NOMOGRAMS FOR EVALUATING THE TEMP. IN UNPROTECTED STAINLESS
STEEL MEMBERS SUBJECTED TO THE STANDARD FIRE CURVE ISO 834**

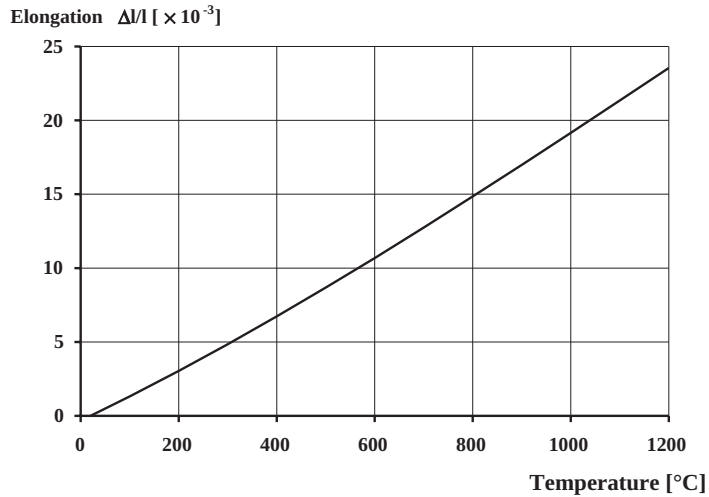


Figure A.6 – Thermal elongation of stainless steel as a function of the temperature

A.8. TABLES AND NOMOGRAMS FOR EVALUATING THE TEMPERATURE IN UNPROTECTED STAINLESS STEEL MEMBERS SUBJECTED TO THE STANDARD FIRE CURVE ISO 834

Temperature of unprotected stainless steel in °C, exposed to the ISO 834

387

fire curve for different values of $k_{sh} \frac{A_m}{V}$, [m^{-1}]

Time [min.]	10 m^{-1}	15 m^{-1}	20 m^{-1}	25 m^{-1}	30 m^{-1}	40 m^{-1}	60 m^{-1}	100 m^{-1}	200 m^{-1}	300 m^{-1}	400 m^{-1}
0	20	20	20	20	20	20	20	20	20	20	20
1	21	22	22	23	24	25	27	32	43	54	65
2	24	25	27	29	31	34	41	54	86	114	141
3	27	30	33	36	40	46	58	82	136	183	224
4	30	35	40	45	50	60	78	113	191	254	307
5	34	41	48	55	62	75	100	147	246	324	384
6	39	48	57	65	74	91	123	182	302	389	451

A. THERMAL DATA FOR CARBON STEEL AND STAINLESS STEEL SECTIONS

Temperature of unprotected stainless steel in °C, exposed to the ISO 834
fire curve for different values of $k_{sh} \frac{A_m}{V}$, [m⁻¹]

Time [min.]	10 m ⁻¹	15 m ⁻¹	20 m ⁻¹	25 m ⁻¹	30 m ⁻¹	40 m ⁻¹	60 m ⁻¹	100 m ⁻¹	200 m ⁻¹	300 m ⁻¹	400 m ⁻¹
7	43	55	66	76	87	108	147	218	356	449	509
8	48	62	75	88	101	126	172	254	408	502	557
9	53	70	85	100	115	144	198	291	456	548	596
10	59	77	96	113	130	163	224	327	501	587	627
11	65	86	106	126	146	183	250	363	541	620	652
12	70	94	117	140	161	202	277	399	578	647	673
13	76	103	129	153	177	222	303	433	610	670	691
14	83	112	140	167	193	242	330	466	638	690	706
15	89	121	152	181	210	263	356	498	663	706	719
16	95	130	164	196	226	283	382	528	684	721	731
17	102	140	176	210	243	304	408	557	703	733	742
18	109	149	188	225	260	324	434	584	719	745	752
19	116	159	201	240	277	345	459	610	734	755	761
20	122	169	213	255	294	365	483	634	747	764	770
21	130	179	226	270	311	386	507	656	758	773	778
22	137	189	238	285	328	406	530	676	768	781	785
23	144	199	251	300	345	426	553	695	778	789	793
24	151	210	264	315	362	446	575	713	786	796	800
25	159	220	277	330	379	465	595	729	794	803	806
26	166	231	290	345	396	484	616	743	802	810	813
27	174	241	303	360	413	503	635	757	809	816	819
28	181	252	316	375	429	522	653	769	815	822	824
29	189	262	329	390	446	540	671	780	822	827	830

A.8. TABLES AND NOMOGRAMS FOR EVALUATING THE TEMP. IN UNPROTECTED STAINLESS
STEEL MEMBERS SUBJECTED TO THE STANDARD FIRE CURVE ISO 834

Temperature of unprotected stainless steel in °C, exposed to the ISO 834

fire curve for different values of $k_{sh} \frac{A_m}{V}$, [m⁻¹]

Time [min.]	10 m ⁻¹	15 m ⁻¹	20 m ⁻¹	25 m ⁻¹	30 m ⁻¹	40 m ⁻¹	60 m ⁻¹	100 m ⁻¹	200 m ⁻¹	300 m ⁻¹	400 m ⁻¹
30	197	273	342	405	462	558	688	791	828	833	835
31	204	284	355	420	479	576	704	800	833	838	841
32	212	294	368	435	495	593	719	809	839	843	846
33	220	305	382	450	511	610	733	817	844	848	850
34	228	316	395	465	526	626	747	825	849	853	855
35	236	327	408	479	542	642	759	832	854	858	860
36	244	337	421	494	557	657	771	839	858	862	864
37	252	348	433	508	572	672	783	845	863	867	868
38	260	359	446	522	587	686	793	851	867	871	872
39	268	370	459	536	601	700	803	856	872	875	876
40	276	381	472	550	616	713	812	862	876	879	880
41	284	391	484	564	630	726	821	867	880	883	884
42	292	402	497	577	643	738	830	871	884	887	888
43	300	413	509	590	656	750	837	876	887	890	892
44	309	424	522	603	669	762	845	880	891	894	895
45	317	435	534	616	682	773	852	884	895	897	899
46	325	445	546	629	694	783	858	888	898	901	902
47	333	456	558	641	706	793	865	892	902	904	905
48	341	466	570	653	718	803	870	896	905	907	909
49	350	477	582	665	730	812	876	900	908	911	912
50	358	488	594	677	741	821	881	903	911	914	915
51	366	498	605	689	751	829	886	907	915	917	918

A. THERMAL DATA FOR CARBON STEEL AND STAINLESS STEEL SECTIONS

Temperature of unprotected stainless steel in °C, exposed to the ISO 834
fire curve for different values of $k_{sh} \frac{A_m}{V}$, [m⁻¹]

Time [min.]	10 m ⁻¹	15 m ⁻¹	20 m ⁻¹	25 m ⁻¹	30 m ⁻¹	40 m ⁻¹	60 m ⁻¹	100 m ⁻¹	200 m ⁻¹	300 m ⁻¹	400 m ⁻¹
52	374	508	616	700	762	837	891	910	918	920	921
53	383	519	628	711	772	845	896	913	921	923	924
54	391	529	639	721	781	852	900	917	924	926	927
55	399	539	649	732	791	859	904	920	927	929	930
56	408	550	660	742	800	866	908	923	929	931	932
57	416	560	671	752	809	872	912	926	932	934	935
58	424	570	681	762	817	878	916	929	935	937	938
59	432	580	691	771	825	884	919	932	938	939	940
60	440	589	701	780	833	889	923	934	940	942	943
61	449	599	711	789	841	895	926	937	943	945	945
62	457	609	721	798	848	900	929	940	945	947	948
63	465	618	730	806	855	905	932	942	948	949	950
64	473	628	739	814	862	909	935	945	950	952	953
65	481	637	749	822	868	914	938	948	953	954	955
66	489	647	757	830	875	918	941	950	955	957	957
67	497	656	766	837	881	922	944	953	957	959	960
68	505	665	775	844	887	926	947	955	960	961	962
69	514	674	783	851	892	930	949	957	962	963	964
70	522	683	791	858	898	933	952	960	964	966	966
71	529	691	799	865	903	937	955	962	966	968	969
72	537	700	807	871	908	940	957	964	969	970	971
73	545	709	814	877	913	944	960	966	971	972	973
74	553	717	822	883	917	947	962	969	973	974	975

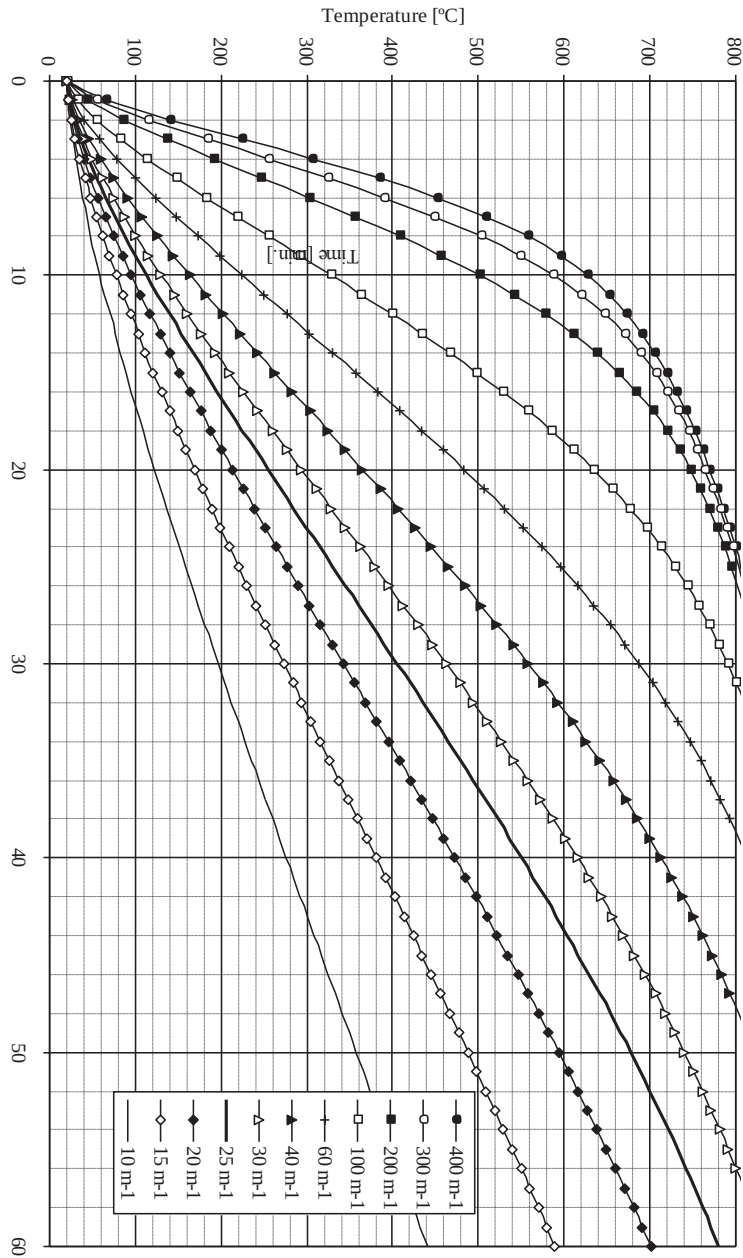
A.8. TABLES AND NOMOGRAMS FOR EVALUATING THE TEMP. IN UNPROTECTED STAINLESS
STEEL MEMBERS SUBJECTED TO THE STANDARD FIRE CURVE ISO 834

Temperature of unprotected stainless steel in °C, exposed to the ISO 834
fire curve for different values of $k_{sh} \frac{A_m}{V}$, [m⁻¹]

Time [min.]	10 m ⁻¹	15 m ⁻¹	20 m ⁻¹	25 m ⁻¹	30 m ⁻¹	40 m ⁻¹	60 m ⁻¹	100 m ⁻¹	200 m ⁻¹	300 m ⁻¹	400 m ⁻¹
75	561	725	829	889	922	950	964	971	975	976	977
76	569	733	836	894	926	953	967	973	977	978	979
77	577	741	843	900	930	956	969	975	979	980	981
78	584	749	849	905	934	959	971	977	981	982	983
79	592	757	856	910	938	961	973	979	983	984	985
80	600	765	862	915	942	964	975	981	985	986	987
81	607	772	868	919	946	967	977	983	987	988	989
82	615	780	874	924	949	969	980	985	989	990	990
83	622	787	880	928	953	972	982	987	991	992	992
84	630	794	886	933	956	974	984	989	992	994	994
85	637	801	891	937	959	976	986	991	994	995	996
86	644	808	897	941	962	979	988	993	996	997	998
87	652	815	902	945	965	981	990	994	998	999	999
88	659	821	907	948	968	983	991	996	1000	1001	1001
89	666	828	912	952	971	985	993	998	1001	1002	1003
90	673	834	917	955	974	987	995	1000	1003	1004	1005

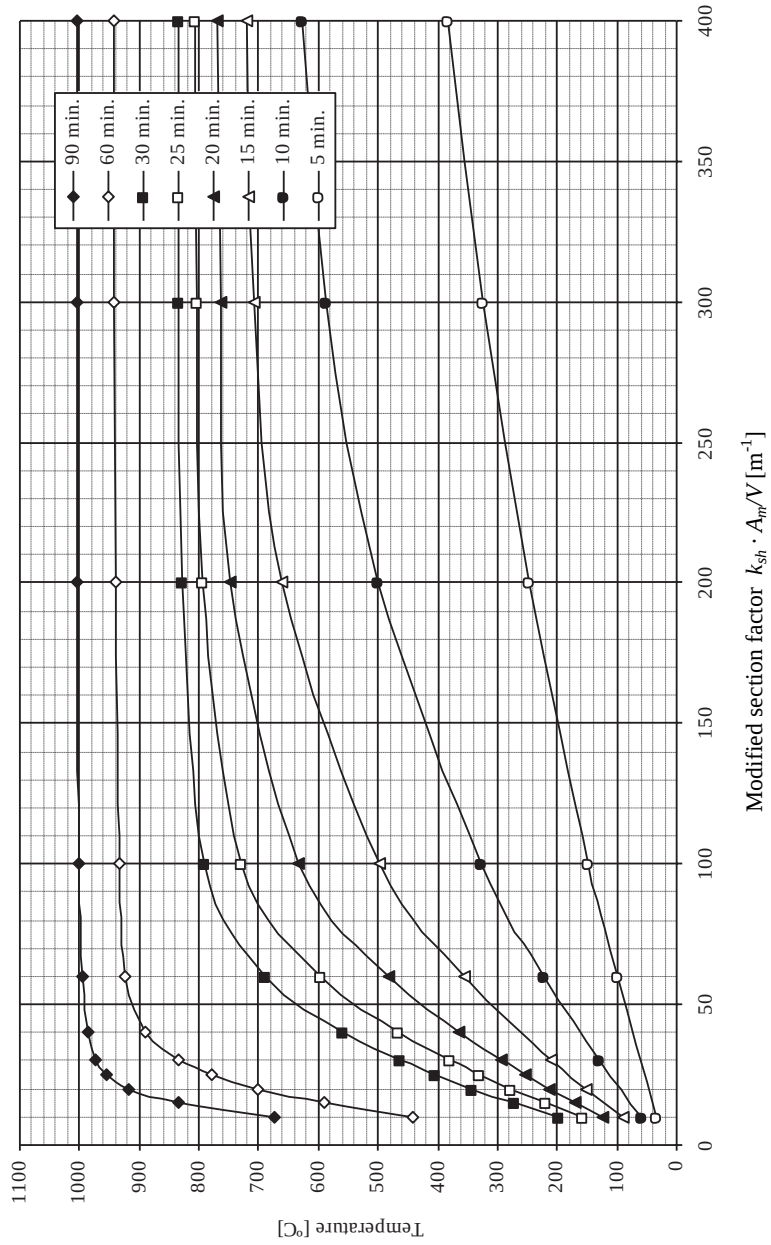
A. THERMAL DATA FOR CARBON STEEL AND STAINLESS STEEL SECTIONS

Nomogram for unprotected stainless steel members subjected to the ISO 834 fire curve, for different values of $k_{sh} \cdot A_m^2/V [m^{-1}]$



A.8. TABLES AND NOMOGRAMS FOR EVALUATING THE TEMP. IN UNPROTECTED STAINLESS
 STEEL MEMBERS SUBJECTED TO THE STANDARD FIRE CURVE ISO 834

Nomogram for unprotected stainless steel members subjected to the ISO 834 fire
 curve, for different time duration



A.9. THERMAL PROPERTIES OF SOME FIRE COMPARTMENT LINING MATERIALS

Properties of the enclosure surface materials

Material	Unit mass, ρ [kg/m ³]	Thermal conductivity, λ_p [W / (mK)]	Specific heat, c_p [J/(kgK)]
Bricks			
– gas-concrete bricks	550	0.14	840
– heavy bricks	2000	1.2	1000
– light perforated bricks	700	0.15	840
– normal bricks	1600	0.7	840
Concrete			
– light weight concrete	1600	0.8	840
– middle weight concrete	1800	1.15	1000
– normal weight concrete	2300	1.6	1000
Gypsum			
– gypsum board	900	0.25	1000
– gypsum finery	1150	0.485	1000
Steel			
– carbon Steel	7850	45	600
Stone			
– granite stone	2600	2.8	1000
Wool			
– glass wool	60	0.037	1030
– rock wool	60	0.037	1030
Wood			
– heavy wood	720	0.2	1880
– normal wood	450	0.1	1113

Note: The properties in this table may be used for evaluating the b factor, as defined by Annex A of EN 1991-1-2, when calculating parametric fire curves (also see Eq. (3.5)). The values given in this table should not be used to evaluate the temperature of fire protected structural members. For the properties of fire protection materials see table of the Annex A.6.

Annex B

INPUT DATA FOR NATURAL FIRE MODELS

B.1. INTRODUCTION

Application of nominal time-temperature fire curves does not require any data to be input. The temperature is directly obtained as a function of time by a mathematical expression.

This is not the case when natural fire models are used.

Some information is directly related to the geometry of the compartment: dimensions, nature of the boundaries such as walls, floor and ceiling, size of the windows and doors, etc. This information is specific to each project, but it is usually available to the designer, particularly if he is responsible for the design of the building at room temperature. More effort may be required to gather this information when an engineer specialised in fire problems is involved at a later stage of the design.

Other information is related to the nature of the fire, its development and its severity. Some information is presented in Eurocode 1 and is discussed in this annex.

B.2. FIRE LOAD DENSITY

The fire load density can be determined for a specific project by performing a fire load survey. In this case, the content as well as the combustible parts of the construction (e.g. construction elements that may

B. INPUT DATA FOR NATURAL FIRE MODELS

char, linings and finishings) should be taken into account. Net calorific values of the combustible materials have to be considered and modified by the effect of moisture if relevant.

Most often, the characteristic fire load density is determined from a classification of occupancy of the compartment. Such classification may be proposed on a national level. Informative annex E of Eurocode 1 gives a table that lists characteristic fire load densities for a selection of occupancies, see Table B.1 taken from the Eurocode.

Table B.1 – Characteristic fire load densities $q_{f,k}$ [MJ/m²] for different occupancies

Occupancy	Average	$q_{f,k}$ 80% Fractile
Dwelling	780	948
Hospital (room)	230	280
Hotel (room)	310	377
Library	1500	1824
Office	420	511
Classroom of a school	285	347
Shopping centre	600	730
Theatre (cinema)	300	365
Transport (public space)	100	122
NOTE Gumbel distribution is assumed for the 80% fractile.		

396

The 80% fractile from this table is taken as the *characteristic* value of the fire load density for the content. Fire loads from the construction material of the building should be added to these values if relevant.

A *design* value of the fire load $q_{f,d}$ is then calculated based on the characteristic value $q_{f,k}$ using Eq. (B.1).

$$q_{f,d} = \delta_{q1} \delta_{q2} \delta_n m q_{f,k} \quad (\text{B.1})$$

The factor m is a combustion factor, the value of which is between 0 and 1. For mainly cellulosic materials, a value of 0.8 may be taken.

The factor δ_{q1} takes into account the risk of fire activation, i.e., the risk that a severe fire occurs. The risk of a fire occurring is higher in compartments with larger area. Table B.2 gives the value of this factor for different compartment floor areas. For other values of the floor area, logarithmic interpolation should be performed between the values given, see example B.1.

Table B.2 – Factor δ_{q1} for different floor areas

Compartment floor area A_f [m ²]	Factor δ_{q1}
25	1.10
250	1.50
2 500	1.90
5 000	2.00
10 000	2.13

The factor δ_{q2} takes into account the risk of fire activation due to the type of occupancy. The nature of some occupancy is more likely to lead to a severe fire than others. Table B.3 gives the value of this factor for different types of occupancy.

Table B.3 – Factor δ_{q2} for different types of occupancy

Examples of occupancy	Factor δ_{q2}
Art gallery, museum, swimming pool	0.78
Offices, residence, hotel, paper industry	1.00
Manufactory for machinery and engines	1.22
Chemical laboratory, painting workshop	1.44
Manufactory of fireworks or paints	1.66

The factor δ_n takes into account the effect of active fire fighting measures. It is calculated as the product of different factors δ_{ni} , each one representing the effect of a different measure.

- δ_{n1} is equal to 0.61 if there is an automatic water extinguishing system, equal to 1.0 otherwise.
- δ_{n2} is equal to 1.00 if there is one single water supply to the water extinguishing system, equal to 0.87 if there is an additional independent water supply, equal to 0.70 if there are two additional independent water supplies.
- δ_{n3} is equal to 0.87 if there is an automatic fire detection and alarm by heat, equal to 1.0 otherwise.
- δ_{n4} is equal to 0.73 if there is an automatic fire detection and alarm by smoke, equal to 1.0 otherwise. If both detection systems are present, by heat and by smoke, only $\delta_{n4} = 0.73$ is considered; δ_{n3} is taken as 1.00.

B. INPUT DATA FOR NATURAL FIRE MODELS

- δ_{n5} is equal to 0.87 if there is an automatic transmission of alarm to the fire brigade.
- δ_{n6} is equal to 0.61 if there is a work fire brigade, i.e., a fire brigade that is permanently on site. In that case δ_{n7} is equal to 1.00.
- δ_{n7} is equal to 0.78 if there is an off site fire brigade, but no work fire brigade.
- δ_{n8} is equal to 1.00 if the normal rules about safe access routes, which are almost always prescribed, have been complied with. If not, this factor is equal to 1.50. If, in addition to safe access routes, the staircases are put under overpressure in case of fire alarm, this factor can be taken as 0.90.
- δ_{n9} is equal to 1.00 if normal fire fighting devices for first intervention by the occupants are present, equal to 1.50 if not.
- δ_{n10} is equal to 1.00 if there is a smoke exhaust system in the staircases, equal to 1.50 if not.

Because Annex E is informative, the values of the different factors that are present in Eq. (B.1) can be modified in the National Annex of each member state. The whole Annex E can also be rejected in the National Annex.

With the slow, medium, fast or ultra-fast character of the fire that has been presented in Section 3.3, the fire load density is sufficient to apply the parametric fire model of Eurocode 1. More parameters are required for advanced models and will be discussed in the next section.

B.3. RATE OF HEAT RELEASE DENSITY

In this section are discussed the parameters which, in addition to the fire load density, are required to apply localised fire models. The rate of heat release density is the most important one.

Depending on the type of occupancy of the fire compartment, a table allows determining whether the growth of the fire is slow, medium or fast, see Table B.4. This table is only valid for occupancies that lead to a factor δ_{q2} equal to 1.0. In that sense, Table B.4 gives some additional types of occupancies that could be added in the third line of Table B.3. In some cases, e.g. some storage warehouses, the growth rate can be even more rapid, either

ultra-fast or even faster. This has to be assessed individually based on the type of good and type of storage (pallets on racks, for example).

Table B.4 – Fire growth rate and *RHR* density for different types of occupancy

Occupancy	Fire growth rate	<i>RHR_f</i> [kW/m ²]
Transport (public space)	Slow	250
Dwelling, hospital room, hotel room, office, classroom of a school	Medium	250
Shopping centre	Fast	250
Library, theatre (cinema)	Fast	500

The power released by the fire *Q*, often called the rate of heat release *RHR*, can be calculated as a function of time according to Eq. (B.2).

$$Q(t) = 10^6 \left(t/t_\alpha \right)^2 \leq A_{fi} RHR_f \quad (B.2)$$

where *t_α* the time to reach 1 MW, is equal to 600 seconds for slow fire, 300 seconds for medium fires, 150 seconds for fast fires and 75 seconds for ultra-fast fires. The *RHR* is equal to 4 MW after 2 *t_α* and equal to 9 MW after 3 *t_α*. The sense of the limitation to a certain value is explained hereafter.

Table B.4 also gives the rate of heat release density, called in the Eurocode the maximum rate of heat release per square meter¹. The area of the fire *A(t)* is directly obtained from this value and from Eq. (B.2), see Eq. (B.3) in which *A_{fi}* is the maximum area that the fire can reach. In a compartment with a uniformly distributed fire load, this maximum area may be taken as the area of the compartment. For a localised fire load, e.g., a ticket counter in a railways hall, this area is the one on which the fire load is present.

$$A(t) = Q(t) / RHR_f \leq A_{fi} \quad (B.3)$$

The limitation of *A* in Eq. (B.3) means that, as a consequence, *Q* as given by Eq. (B.2) is also limited to *A_{fi}* × *RHR_f*.

The diameter of the fire is given by Eq. (B.4), assuming a circular fire source.

$$D(t) = \sqrt{4A(t) / \pi} \quad (B.4)$$

¹ Significantly higher values can be obtained in storage racks, for example.

B. INPUT DATA FOR NATURAL FIRE MODELS

The quantity of combustible energy E_d , i.e., the total fire load, present in the compartment or in the localised fire source, is directly given by Eq. (B.5).

$$E_d = q_{fd} A_{fi} \quad (\text{B.5})$$

The decay phase starts when 70% of the total fire load has been consumed. During this cooling down phase, the rate of heat release Q is assumed to decrease linearly whereas it is reasonable to assume that the area of the fire remains constant.

Example B.1: Calculate the evolution of the rate of heat release and flame length of a localised fire in a ticket counter that has an area of 36 m². It is assumed that the flame does not touch the ceiling.

If the ticket counter is considered as a library, Table B.4 recommends a *fast* fire, with a time constant t_α of 150 seconds.

$RHR_f = 500 \text{ kW/m}^2$, see Table B.4

$q_{f,k} = 1824 \text{ MJ/m}^2$, see Table B.1

$m = 0.8$ (paper is mainly cellulosic)

$\delta_{q1} = (\log(36) - \log(25)) / ((\log(250) - \log(25)) \times 0.40 + 1.10) = 1.163$, Table B.2

$\delta_{q2} = 1.0$ by analogy with occupancies from Table B.3

- $\delta_{n1} = 1.0$, no automatic water extinguishing system.
- $\delta_{n2} = 1.0$, no water system.
- $\delta_{n3} = 1.0$.
- $\delta_{n4} = 0.73$, automatic fire detection and alarm by smoke.
- $\delta_{n5} = 1.0$, no automatic transmission of alarm to the fire brigade.
- $\delta_{n6} = 1.0$, no work fire brigade.
- $\delta_{n7} = 0.78$, off site fire brigade but no work fire brigade.
- $\delta_{n8} = 1.0$, safe access routes.
- $\delta_{n9} = 1.0$, normal fire fighting devices.
- $\delta_{n10} = 1.0$, no staircases and, thus, no requirement of an air exhaust system.

$\Rightarrow \delta_n = 0.73 \times 0.78 = 0.569$

$q_{f,d} = 1824 \times 0.8 \times 1.163 \times 1.0 \times 0.569 = 966 \text{ MJ/m}^2$

B.3. RATE OF HEAT RELEASE DENSITY

Details of the calculations are given in the table below. Values presented in bold characters mark the transition from one regime to another.

At $t = 636$ seconds, the area of the fire has reached A_{fi} .

At $t = 1777$ seconds, 70% of the fire load has been consumed.

At $t = 2633$ seconds, the flame length is equal to 0.

At $t = 2936$ seconds, all fire load has been consumed.

t	t	Q(t)	E(t)	A	D	Lf
seconds	min.	W	J	m ²	m	m
		Eq. (B.2)	Int. (Q(t) dt)	Eq. (B.3)	Eq. (B.4)	Eq. (3.23)
0	0.00	0	0	0.00	0.00	0.00
60	1.00	160 000	3 200 000	0.32	0.64	1.14
120	2.00	640 000	25 600 000	1.28	1.28	1.81
180	3.00	1 440 000	86 400 000	2.88	1.91	2.35
240	4.00	2 560 000	204 800 000	5.12	2.55	2.81
300	5.00	4 000 000	400 000 000	8.00	3.19	3.22
360	6.00	5 760 000	691 200 000	11.52	3.83	3.58
420	7.00	7 840 000	1 097 600 000	15.68	4.47	3.91
480	8.00	10 240 000	1 638 400 000	20.48	5.11	4.22
540	9.00	12 960 000	2 332 800 000	25.92	5.74	4.50
600	10.00	16 000 000	3 200 000 000	32.00	6.38	4.76
636	10.61	18 000 000	3 818 385 356	36.00	6.77	4.91
900	15.00	18 000 000	8 563 246 763	36.00	6.77	4.91
1200	20.00	18 000 000	13 963 246 763	36.00	6.77	4.91
1500	25.00	18 000 000	19 363 246 763	36.00	6.77	4.91
1777	29.61	18 000 000	24 343 200 000	36.00	6.77	4.91
2000	33.33	14 532 051	27 975 987 926	36.00	6.77	3.94
2250	37.50	10 650 063	31 123 752 168	36.00	6.77	2.67
2500	41.67	6 768 076	33 301 019 516	36.00	6.77	1.08
2633	43.88	4 703 405	34 063 671 106	36.00	6.77	0.00
2936	48.93	0	34 776 000 000	36.00	6.77	0.00

Fig. B.1 shows the evolution of the rate of heat release, whereas Fig. B.2 shows the evolution of the flame length.

B. INPUT DATA FOR NATURAL FIRE MODELS

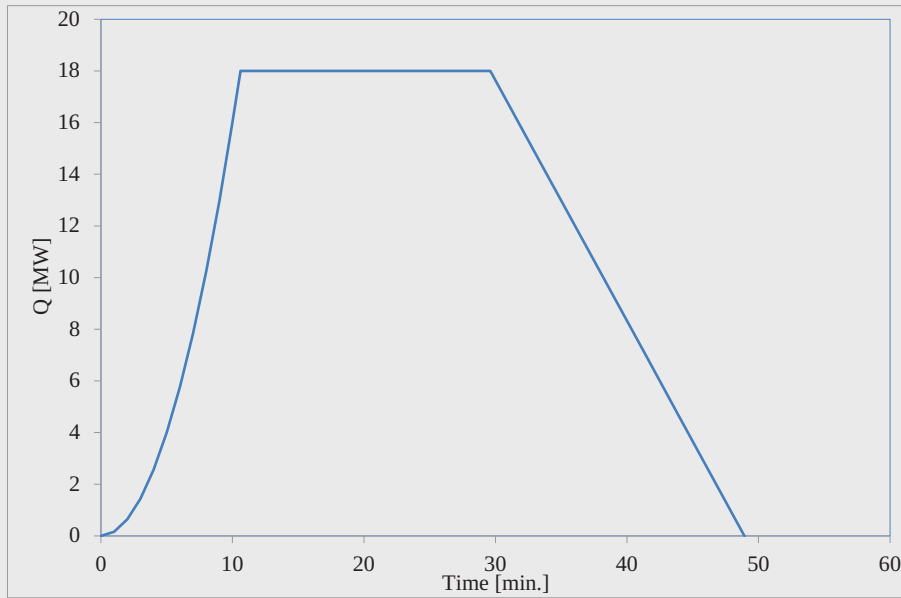


Figure B.1 – Evolution of the *RHR* as a function of time

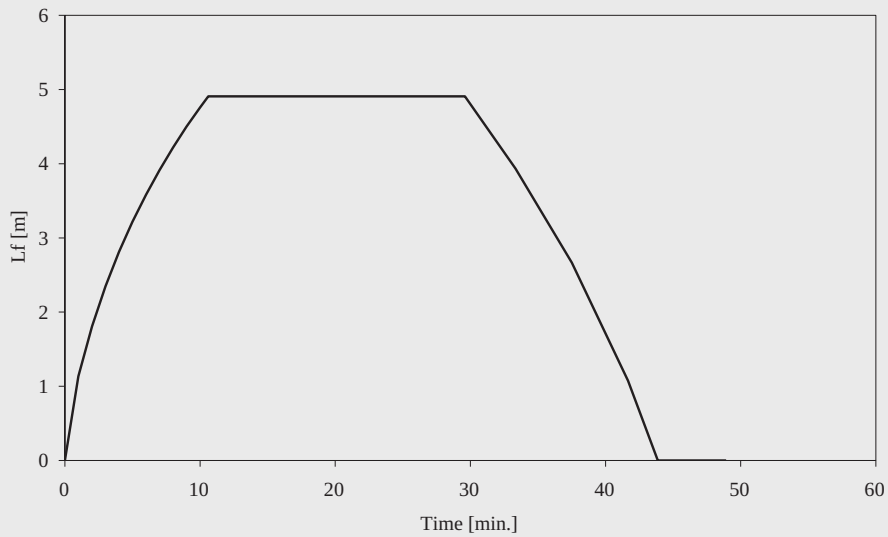


Figure B.2: – Evolution of the flame length as a function of time

B.4. VENTILATION CONTROL

The *RHR* curve that can be defined according to Section B.2 and B.3 assumes that enough air is available to sustain the combustion, see dotted line on Figure B.3. If the fire develops in a building, the oxygen that is present in the compartment is quickly consumed and the combustion needs additional oxygen supply to continue. This supply is provided by the current of fresh air that enters in the compartment through the lower part of the openings. If the openings are not sufficiently large, the development of the fire is limited.

As mentioned in Section 3.3, the capacity of the openings to supply fresh air to the fire in a compartment is proportional to the size of the opening multiplied by the square root of the height of the opening. The Rate of Heat Release in the compartment can not exceed the maximum value given by Eq. (B.6) where dimensions are in meters and Q_{\max} is in MW.

$$Q_{\max} = 1.4 A_v \sqrt{h_{eq}} \quad (\text{B.6})$$

where A_v is the area of vertical openings and h_{eq} is the mean height of the openings, see Eq. (3.9).

When the *RHR* is limited by Eq. (B.6), the curve that describes the evolution of Q as a function of time must be extended in such a way that the total amount of combustible material present in the compartment is consumed in the compartment, see solid line on Figure B.3. In other words, the surface under the *RHR* curve is maintained and the duration of the fire is extended.

403

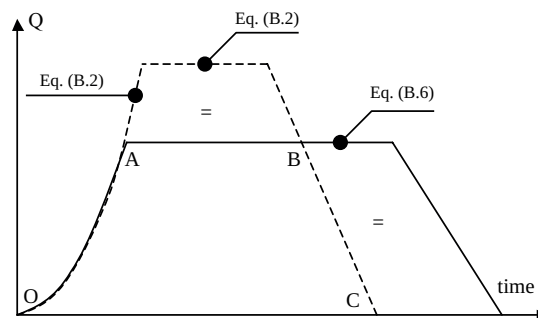


Figure B.3 – Modification of the *RHR* curve in case of ventilation control - Principle

B. INPUT DATA FOR NATURAL FIRE MODELS

This hypothesis is on the safe side for the evaluation of the fire performance of the structure in the compartment. Another possibility would be to assume that the difference between the curve of the fuel control situation and the curve of the ventilation control situation is lost for the compartment in the form of external flaming¹. The duration of the fire is not extended. In that case, the *RHR* curve follows the path O-A-B-C of Figure B.3. The energy above the line A-B is release by combustion that occurs outside the compartment.

In zone models and in CFD models, it is possible that the limitation of combustion by ventilation control is automatically taken into account by the program if the amount of air present in the compartment and the amount of air coming in through the openings is computed during the calculation. If this is the case, the user can enter the fuel controlled *RHR* curve and the transition to the ventilation controlled situation will be automatically activated during the calculation.

It has to be noted that, in some cases, especially if the fire load is localised, it is possible that the maximum value of the *RHR* in the ventilation control situation is higher than the fuel controlled *RHR*. In that case, the maximum value of the *RHR* is still governed by the fire area, see Eq. (B.2).

Example B.2: Modify the *RHR* curve of Figure B.1 if the fire described in Example B.1 occurs in a compartment with five windows of 2 meters wide and 1 meter high.

$$A_v = 5 \times 2 \times 1 = 10 \text{ m}^2$$

$$\sqrt{h} = 1 \text{ m}^{1/2}$$

$Q_{\max} = 1.4 \times 10 \times 1 = 14 \text{ MW} < 18 \text{ MW}$, see Eq. (B.6). The fire is controlled by the ventilation.

The *RHR* curve is modified as shown by the dotted line on Figure B.4. The table below shows how the values used to build this curve have been calculated.

¹ This hypothesis may be more critical for other aspects of fire safety engineering, namely the fire extension to upper floors.

t,alpha	150	seconds	
RHR,f	500 000	W/m ²	
A,fi	36	m ²	
q,fd	966 000 000	J/m ²	
E,d	34 776 000 000	J	
E cooling	24 343 200 000	J	
t	t	Q(t)	E(t)
seconds	min.	W	J
		Eq. (B.2), (B.6)	Int. (Q(t) dt)
0	0.00	0	0
60	1.00	160 000	4 800 000
120	2.00	640 000	28 800 000
180	3.00	1 440 000	91 200 000
240	4.00	2 560 000	211 200 000
300	5.00	4 000 000	408 000 000
360	6.00	5 760 000	700 800 000
420	7.00	7 840 000	1 108 800 000
480	8.00	10 240 000	1 651 200 000
540	9.00	12 960 000	2 347 200 000
561	9.35	14 000 000	2 633 631 236
600	10.00	14 000 000	3 176 150 724
900	15.00	14 000 000	7 376 150 724
1200	20.00	14 000 000	11 576 150 724
1500	25.00	14 000 000	15 776 150 724
1800	30.00	14 000 000	19 976 150 724
2112	35.20	14 000 000	24 343 200 000
2485	41.41	10 500 000	28 907 550 000
2857	47.62	7 000 000	32 167 800 000
3230	53.83	3 500 000	34 123 950 000
3602	60.04	0	34 776 000 000

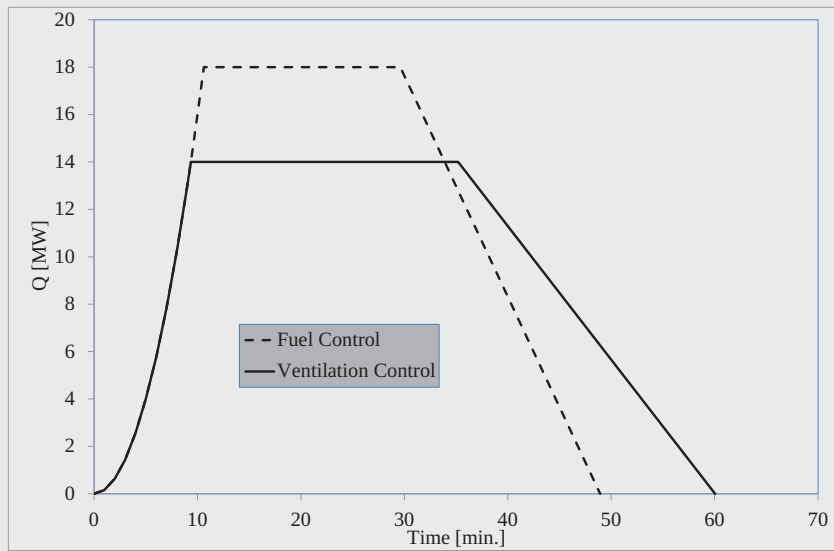


Figure B.4 – Modification of the *RHR* curve in case of ventilation control - Example

B.5. FLASH-OVER

If the fire develops in a building, the temperature in the compartment usually increases as long as the decay phase in the *RHR* curve has not started. The increase of temperature is fast in the t^2 phase of the *RHR* curve and much slower in the plateau of the *RHR* curve. Under certain conditions linked to the temperature in the compartment¹, the flash-over can occur in the compartment. If this is the case, the model, either zone model or CFD model, should consider that all combustible material present in the compartment is involved and the *RHR* curve moves instantaneously to one of the plateaus calculated by Eq. (B.2) or (B.6) depending on the ventilation in the compartment, see the full line on Figure B.5.

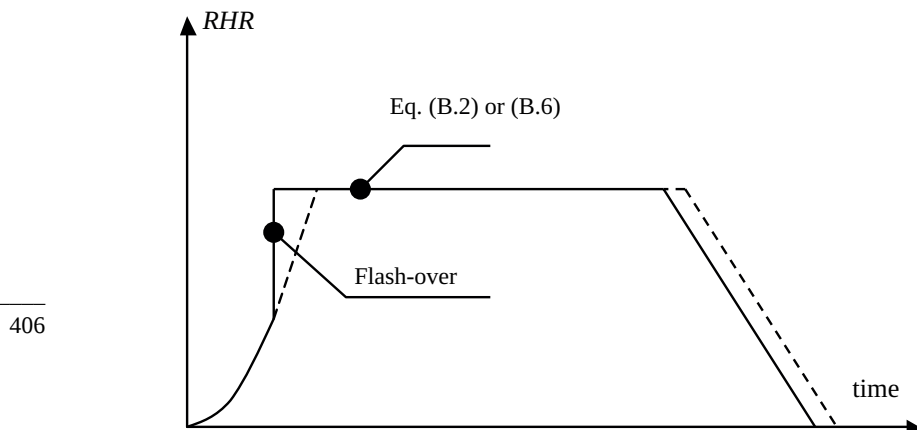


Figure B.5 – Modification of the *RHR* curve in case of flash-over

¹ A value of 500 °C is typically considered.

Annex C

MECHANICAL PROPERTIES OF CARBON STEEL AND STAINLESS STEEL

C.1. MECHANICAL PROPERTIES OF CARBON STEEL

C.1.1. Mechanical properties of carbon steel at room temperature (20 °C)

Before presenting the mechanical properties of carbon steel at elevated temperature, the properties at room temperature will be given. The elastic constants used at room temperature, for the design of steel structures, are:

- modulus of elasticity $E = 2100000 \text{ N/mm}^2$ 407
- shear modulus $G = \frac{E}{2(1+\nu)} = 81000 \text{ N/mm}^2$
- Poisson's ratio $\nu = 0.3$
- unit mass $\rho_a = 7850 \text{ kg/m}^3$

The yield strength, f_y , and the ultimate tensile strength, f_u , for hot rolled structural steel and structural hollow sections at room temperature are given in the product standards EN 10025, EN 10210 and EN 10219 respectively. Simplifications are given in Tables C.1 and C.2, which are taken from EN 1993-1-1.

C. MECHANICAL PROPERTIES OF CARBON STEEL AND STAINLESS STEEL

Table C.1 – Nominal values of yield strength f_y and ultimate tensile strength f_u for hot rolled structural steel

Standard and steel grade	Nominal thickness of the element t [mm]			
	$t \leq 40$ mm		$40 \text{ mm} < t \leq 80$ mm	
	f_y [N/mm ²]	f_u [N/mm ²]	f_y [N/mm ²]	f_u [N/mm ²]
EN 10025-2				
S235	235	360	215	360
S275	275	430	255	410
S355	355	490	335	470
S450	440	550	410	550
EN 10025-3				
S275 N/NL	275	390	255	370
S355 N/NL	355	490	335	470
S420 N/NL	420	520	390	520
S460 N/NL	460	540	430	540
EN 10025-4				
S275 M/ML	275	370	255	360
S355 M/ML	355	470	335	450
S420 M/ML	420	520	390	500
S460 M/ML	460	540	430	530
EN 10025-5				
S 235 W	235	360	215	340
S355 W	355	490	335	490
EN 10025-6				
S460 Q/QL/QL1	460	570	440	550

Table C.2 – Nominal values of yield strength f_y and ultimate tensile strength f_u for structural hollow sections

Standard and steel grade	Nominal thickness of the element t [mm]			
	$t \leq 40$ mm		$40 \text{ mm} < t \leq 80$ mm	
	f_y [N/mm ²]	f_u [N/mm ²]	f_y [N/mm ²]	f_u [N/mm ²]
EN 10025-2				
S235 H	235	360	215	340
S275 H	275	430	255	410
S355 H	355	510	335	490
S275 NH/NLH	275	390	255	370
S355 NH/NLH	355	490	335	470
S420 NH/NLH	420	540	390	520
S460 NH/NLH	460	560	430	550
EN 10025-3				
S235 H	235	360		
S275 H	275	430		
S355 H	355	510		
S275 NH/NLH	275	370		
S355 NH/NLH	355	470		
S460 NH/NLH	460	550		
S275 MH/MLH	275	360		
S355 MH/MLH	355	470		
S420 MH/MLH	420	500		
S460 MH/MLH	460	350		

C.1.2. Stress-strain relationship for carbon steel at elevated temperatures (without strain-hardening)

According to Part 1.2 of Eurocode 3 the strength and stiffness properties of steel at elevated temperatures shall be obtained from the constitutive law described in Table C.3 and depicted in Fig. C.1. This figure shows that the stress-strain relationship for carbon steel at elevated temperatures, split into four zones: a linear branch until the proportional limit $f_{p,\theta}$ is reached; an elliptic transition which ends at the effective yield strength f_y ; a yield plateau; and finally a linear descending branch which occurs at large strains and can be used in advanced calculation models.

In Table C.3 and Fig. C.1 the meaning of the symbols is:

- $f_{y,\theta}$ effective yield strength;
- $f_{p,\theta}$ proportional limit;
- $E_{a,\theta}$ slope of the linear elastic range;
- $e_{p,\theta}$ strain at the proportional limit;
- $e_{y,\theta}$ yield strain;
- $e_{t,\theta}$ limiting strain for yield strength;
- $e_{u,\theta}$ ultimate strain.

Table C.3 – Steel constitutive law at elevated temperatures

Strain range	Stress σ	Tangent modulus
$\varepsilon \leq \varepsilon_{p,\theta}$	$\varepsilon E_{a,\theta}$	$E_{a,\theta}$
$\varepsilon_{p,\theta} < \varepsilon < \varepsilon_{y,\theta}$	$f_{p,\theta} - c + (b/a) \left[a^2 - (\varepsilon_{y,\theta} - \varepsilon)^2 \right]^{0.5}$	$\frac{b(\varepsilon_{y,\theta} - \varepsilon)}{a \left[a^2 - (\varepsilon_{y,\theta} - \varepsilon)^2 \right]^{0.5}}$
$\varepsilon_{y,\theta} \leq \varepsilon \leq \varepsilon_{t,\theta}$	$f_{y,\theta}$	0
$\varepsilon_{t,\theta} < \varepsilon < \varepsilon_{u,\theta}$	$f_{y,\theta} \left(1 - (\varepsilon - \varepsilon_{t,\theta}) / (\varepsilon_{u,\theta} - \varepsilon_{t,\theta}) \right)$	-
$\varepsilon = \varepsilon_{u,\theta}$	0.00	-
Parameters	$\varepsilon_{p,\theta} = f_{p,\theta} / E_{a,\theta}$ $\varepsilon_{y,\theta} = 0.02$	$\varepsilon_{t,\theta} = 0.15$ $\varepsilon_{u,\theta} = 0.20$
Functions	$a^2 = (\varepsilon_{y,\theta} - \varepsilon_{p,\theta})(\varepsilon_{y,\theta} - \varepsilon_{p,\theta} + c / E_{a,\theta})$ $b^2 = c(\varepsilon_{y,\theta} - \varepsilon_{p,\theta})E_{a,\theta} + c^2$ $c = \frac{(f_{y,\theta} - f_{p,\theta})^2}{(\varepsilon_{y,\theta} - \varepsilon_{p,\theta})E_{a,\theta} - 2(f_{y,\theta} - f_{p,\theta})}$	

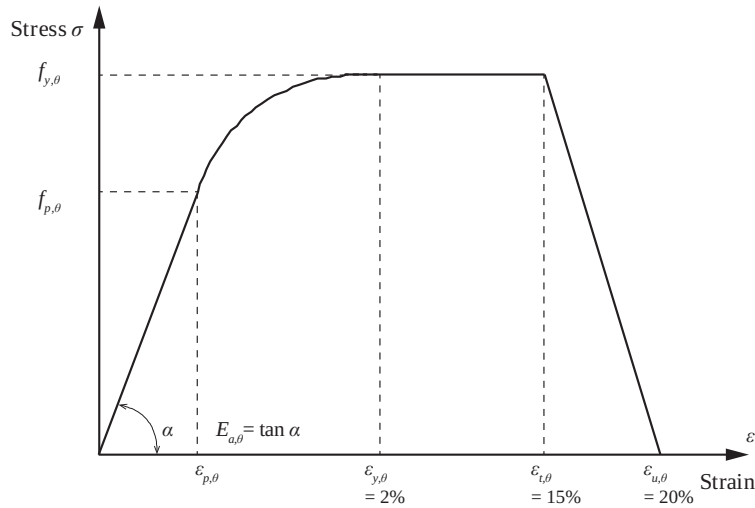


Figure C.1 – Stress-strain relationship for carbon steel at elevated temperatures

The stress-strain relationship for carbon steel at elevated temperatures presented in Table C.1 is quantified in Tables C.4 to C.7 for the steel grades S235, S275, S355 and S460 respectively. Graphical representation of the data given in Tables C.4 to C.7 is given in Figs C.2 to C.5, respectively.

Table C.4 – Stress-strain relationship for S235 carbon steel at elevated temperatures

Strain	Effective yield strength $f_{y,\theta}$							
	Steel temperature θ_a [°C]							
	100	200	300	400	500	600	700	800
0.0000	0.000	0.000	0.000	0.000	0.000	0.000	0.000	0.000
0.0005	105.045	94.470	83.895	73.555	62.980	32.665	13.630	9.400
0.0010	210.090	188.940	153.220	118.675	99.640	52.405	22.795	14.100
0.0015	235.000	199.515	165.675	133.715	110.450	59.690	26.555	15.510
0.0020	235.000	203.745	173.430	144.290	117.970	64.860	29.375	16.685
0.0025	235.000	206.800	179.305	152.750	124.080	69.325	31.725	17.390
0.0030	235.000	209.620	184.475	160.035	129.485	72.850	33.605	18.330
0.0035	235.000	211.735	188.940	166.380	133.950	76.140	35.485	18.800

C. MECHANICAL PROPERTIES OF CARBON STEEL AND STAINLESS STEEL

Table C.4 – Stress-strain relationship for S235 carbon steel at elevated temperatures

Strain	Effective yield strength $f_{y,\theta}$							
	Steel temperature θ_a [°C]							
	100	200	300	400	500	600	700	800
0.0040	235.000	213.850	192.935	172.255	138.180	78.960	36.895	19.505
0.0045	235.000	215.495	196.460	177.425	141.940	81.545	38.305	19.975
0.0050	235.000	217.140	199.515	182.125	145.230	83.895	39.715	20.445
0.0055	235.000	218.785	202.570	186.590	148.520	86.245	40.890	20.915
0.0060	235.000	220.195	205.155	190.585	151.340	88.125	42.065	21.385
0.0065	235.000	221.370	207.740	194.345	154.160	90.005	43.005	21.620
0.0070	235.000	222.545	210.090	197.870	156.510	91.885	43.945	22.090
0.0075	235.000	223.720	212.205	201.160	158.860	93.295	44.885	22.325
0.0080	235.000	224.660	214.320	203.980	160.975	94.940	45.590	22.795
0.0085	235.000	225.600	216.200	206.800	163.090	96.350	46.295	23.030
0.0090	235.000	226.540	218.080	209.620	164.970	97.760	47.235	23.265
0.0095	235.000	227.245	219.725	211.970	166.850	98.935	47.705	23.500
0.0100	235.000	228.185	221.135	214.320	168.495	100.110	48.410	23.735
0.0110	235.000	229.595	223.955	218.550	171.550	102.225	49.585	24.205
0.0120	235.000	230.770	226.540	222.075	174.135	104.105	50.525	24.440
0.0130	235.000	231.710	228.420	225.365	176.250	105.515	51.465	24.910
0.0140	235.000	232.650	230.300	227.950	178.130	106.925	52.170	25.145
0.0150	235.000	233.355	231.710	230.065	179.775	108.100	52.640	25.380
0.0160	235.000	234.060	232.885	231.945	181.185	108.805	53.110	25.615
0.0170	235.000	234.530	233.825	233.355	182.125	109.510	53.580	25.615
0.0180	235.000	234.765	234.295	234.295	182.830	109.980	53.815	25.850
0.0190	235.000	235.000	234.765	234.765	183.065	110.450	54.050	25.850
0.0200	235.000	235.000	235.000	235.000	183.300	110.450	54.050	25.850

C.1. MECHANICAL PROPERTIES OF CARBON STEEL

Table C.5 – Stress-strain relationship for S275 carbon steel at elevated temperatures

Strain	Effective yield strength $f_{y,\theta}$							
	Steel temperature θ_a [°C]							
	100	200	300	400	500	600	700	800
0.0000	0.000	0.000	0.000	0.000	0.000	0.000	0.000	0.000
0.0005	105.050	94.600	83.875	73.425	62.975	32.450	13.750	9.350
0.0010	210.100	188.925	168.025	132.550	111.925	58.300	25.025	15.950
0.0015	275.000	231.000	190.025	152.075	126.225	67.925	29.975	17.875
0.0020	275.000	236.775	200.200	165.550	135.850	74.250	33.550	19.250
0.0025	275.000	240.900	207.900	176.000	143.550	79.750	36.300	20.350
0.0030	275.000	244.200	214.225	184.800	149.875	84.150	38.775	21.175
0.0035	275.000	246.950	219.450	192.775	155.375	88.000	40.700	22.000
0.0040	275.000	249.425	224.400	199.650	160.325	91.575	42.625	22.550
0.0045	275.000	251.625	228.525	205.975	165.000	94.600	44.275	23.375
0.0050	275.000	253.550	232.375	211.750	169.125	97.350	45.925	23.925
0.0055	275.000	255.475	235.950	216.975	172.700	100.100	47.300	24.475
0.0060	275.000	257.125	239.250	221.650	176.275	102.575	48.675	24.750
0.0065	275.000	258.775	242.275	226.325	179.575	104.775	50.050	25.300
0.0070	275.000	260.150	245.300	230.450	182.600	106.975	51.150	25.850
0.0075	275.000	261.250	247.775	234.300	185.350	108.900	52.250	26.125
0.0080	275.000	262.625	250.250	237.875	187.825	110.550	53.075	26.400
0.0085	275.000	263.725	252.450	241.450	190.300	112.475	54.175	26.950
0.0090	275.000	264.825	254.650	244.475	192.775	113.850	55.000	27.225
0.0095	275.000	265.925	256.575	247.500	194.700	115.500	55.825	28.050
0.0100	275.000	266.750	258.500	250.250	196.900	116.875	56.375	28.050
0.0110	275.000	268.400	261.800	255.200	200.475	119.350	57.750	28.600
0.0120	275.000	269.775	264.825	259.600	203.500	121.550	59.125	28.875
0.0130	275.000	271.150	267.300	263.450	206.250	123.475	59.950	29.425
0.0140	275.000	272.250	269.500	266.475	208.450	125.125	61.050	29.700
0.0150	275.000	273.075	271.150	269.225	210.375	126.225	61.600	29.700
0.0160	275.000	273.900	272.525	270.875	211.475	127.050	62.150	29.975
0.0170	275.000	274.175	273.625	272.800	213.125	128.150	62.700	30.250
0.0180	275.000	274.725	274.450	274.175	213.950	128.700	62.975	30.250
0.0190	275.000	275.000	274.725	274.725	214.225	129.250	63.250	30.250
0.0200	275.000	275.000	275.000	275.000	214.500	129.250	63.250	30.250

C. MECHANICAL PROPERTIES OF CARBON STEEL AND STAINLESS STEEL

Table C.6 – Stress-strain relationship for S355 carbon steel at elevated temperatures

Strain	Effective yield strength $f_{y,\theta}$							
	Steel temperature θ_a [°C]							
	100	200	300	400	500	600	700	800
0.0000	0.000	0.000	0.000	0.000	0.000	0.000	0.000	0.000
0.0005	105.080	80.230	84.135	73.485	62.835	32.660	13.490	9.585
0.0010	210.160	188.860	167.915	146.970	126.025	64.965	27.335	18.460
0.0015	314.885	283.645	233.235	184.600	154.425	81.650	35.500	22.010
0.0020	355.000	301.040	250.630	204.480	168.980	91.590	40.470	23.785
0.0025	355.000	307.430	262.345	219.745	179.985	99.045	44.730	25.560
0.0030	355.000	312.400	271.575	232.170	188.860	105.080	47.925	26.625
0.0035	355.000	316.660	279.030	243.175	196.670	110.760	51.120	27.690
0.0040	355.000	320.210	285.775	252.760	203.770	115.375	53.605	28.755
0.0045	355.000	323.050	291.810	261.280	209.805	119.635	56.090	29.465
0.0050	355.000	325.890	297.135	269.090	215.485	123.540	58.220	30.530
0.0055	355.000	328.375	302.105	276.190	220.455	127.445	59.995	31.240
0.0060	355.000	330.860	306.720	282.935	225.425	130.640	61.770	31.950
0.0065	355.000	332.990	310.980	288.970	229.685	133.835	63.545	32.305
0.0070	355.000	334.765	314.530	294.650	233.945	136.675	64.965	33.015
0.0075	355.000	336.540	318.080	299.975	237.495	141.645	66.385	33.370
0.0080	355.000	338.315	321.630	304.945	241.045	144.130	67.805	34.080
0.0085	355.000	339.735	324.825	309.560	244.595	146.260	69.225	34.435
0.0090	355.000	341.155	327.665	313.820	247.435	148.035	70.290	34.790
0.0095	355.000	342.575	330.150	318.080	250.275	150.165	71.355	35.465
0.0100	355.000	343.995	332.635	321.630	253.115	151.940	72.420	35.855
0.0110	355.000	346.125	337.250	328.375	257.730	155.135	74.195	36.210
0.0120	355.000	348.255	341.155	334.410	261.990	156.555	75.970	36.920
0.0130	355.000	349.675	344.705	339.380	265.540	159.040	77.390	37.630
0.0140	355.000	351.095	347.545	343.640	268.735	161.170	78.455	37.985
0.0150	355.000	352.515	349.675	347.190	271.220	162.945	79.520	38.340
0.0160	355.000	353.225	351.805	350.030	273.350	164.365	80.230	38.695
0.0170	355.000	353.935	353.225	352.160	274.770	165.430	80.940	38.695
0.0180	355.000	354.645	354.290	353.935	276.190	166.140	81.295	39.050
0.0190	355.000	355.000	354.645	354.645	276.545	166.850	81.650	39.050
0.0200	355.000	355.000	355.000	355.000	276.900	166.850	81.650	39.050

C.1. MECHANICAL PROPERTIES OF CARBON STEEL

Table C.7 – Stress-strain relationship for S460 carbon steel at elevated temperatures

Strain	Effective yield strength $f_{y,\theta}$							
	Steel temperature θ_a [°C]							
	100	200	300	400	500	600	700	800
0.0000	0.000	0.000	0.000	0.000	0.000	0.000	0.000	0.000
0.0005	104.880	94.300	84.180	73.600	63.020	32.660	13.800	9.660
0.0010	210.220	189.060	167.900	147.200	126.040	65.320	27.140	18.860
0.0015	315.100	283.360	252.080	213.900	181.700	94.300	40.020	26.220
0.0020	419.980	374.900	307.740	247.020	206.540	109.940	47.840	29.440
0.0025	460.000	391.000	327.520	270.020	223.100	120.980	53.820	31.740
0.0030	460.000	399.280	341.780	288.420	236.440	130.180	58.420	33.580
0.0035	460.000	405.720	353.740	304.060	247.480	138.000	63.020	34.960
0.0040	460.000	410.780	363.400	317.860	257.600	144.900	66.700	36.340
0.0045	460.000	415.380	372.140	330.280	266.340	150.880	69.920	37.720
0.0050	460.000	419.520	379.500	341.320	274.160	156.400	72.680	38.640
0.0055	460.000	423.200	386.860	351.440	281.060	161.460	75.440	39.560
0.0060	460.000	426.420	392.840	360.640	287.960	166.060	78.200	40.480
0.0065	460.000	429.180	398.820	368.920	293.940	170.200	80.500	41.400
0.0070	460.000	431.940	404.340	376.740	299.460	174.340	82.800	42.320
0.0075	460.000	434.700	409.400	384.100	304.980	178.020	84.640	43.240
0.0080	460.000	437.000	414.000	391.000	309.580	181.700	86.480	43.700
0.0085	460.000	438.840	418.140	397.440	314.180	184.920	88.320	44.160
0.0090	460.000	441.140	422.280	403.420	318.320	187.680	90.160	45.080
0.0095	460.000	442.980	425.960	408.940	322.460	190.440	91.540	45.540
0.0100	460.000	444.820	429.180	414.000	326.140	193.200	92.920	46.000
0.0110	460.000	448.040	435.620	423.660	332.580	197.800	95.680	46.920
0.0120	460.000	450.340	441.140	431.480	338.560	201.940	97.980	47.840
0.0130	460.000	452.640	445.740	438.380	343.620	205.160	99.820	48.300
0.0140	460.000	454.940	449.420	444.360	347.760	208.380	101.660	49.220
0.0150	460.000	456.320	452.640	449.420	350.980	210.680	102.580	49.680
0.0160	460.000	457.700	455.400	453.100	353.740	212.520	103.960	50.140
0.0170	460.000	458.620	457.240	456.320	356.040	214.360	104.880	50.140
0.0180	460.000	459.540	459.080	458.160	357.420	215.280	105.340	50.600
0.0190	460.000	459.540	459.540	460.000	358.340	216.200	105.800	50.600
0.0200	460.000	460.000	460.000	460.000	358.800	216.200	105.800	50.600

C. MECHANICAL PROPERTIES OF CARBON STEEL AND STAINLESS STEEL

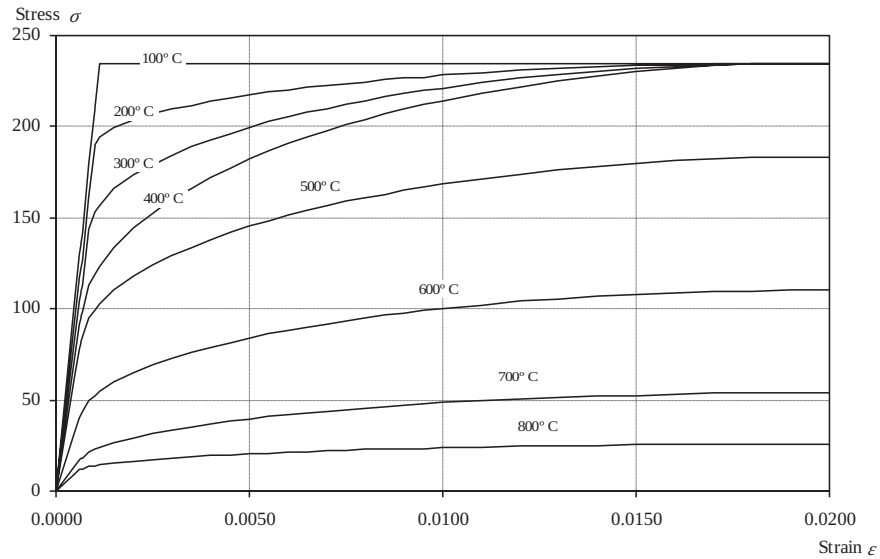


Figure C.2 – Stress-strain relationship for S235 carbon steel at elevated temperatures

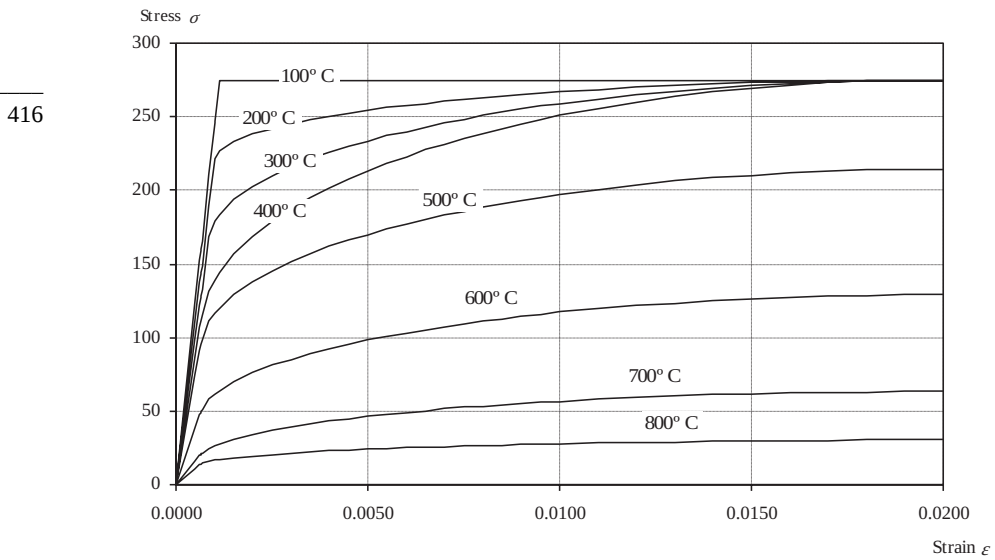


Figure C.3 – Stress-strain relationship for S275 carbon steel at elevated temperatures

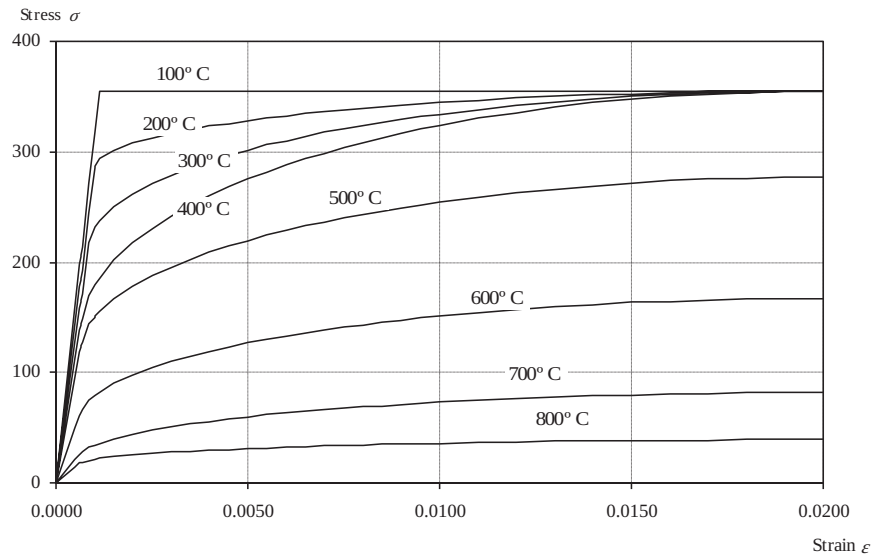


Figure C.4 – Stress-strain relationship for S355 carbon steel at elevated temperatures

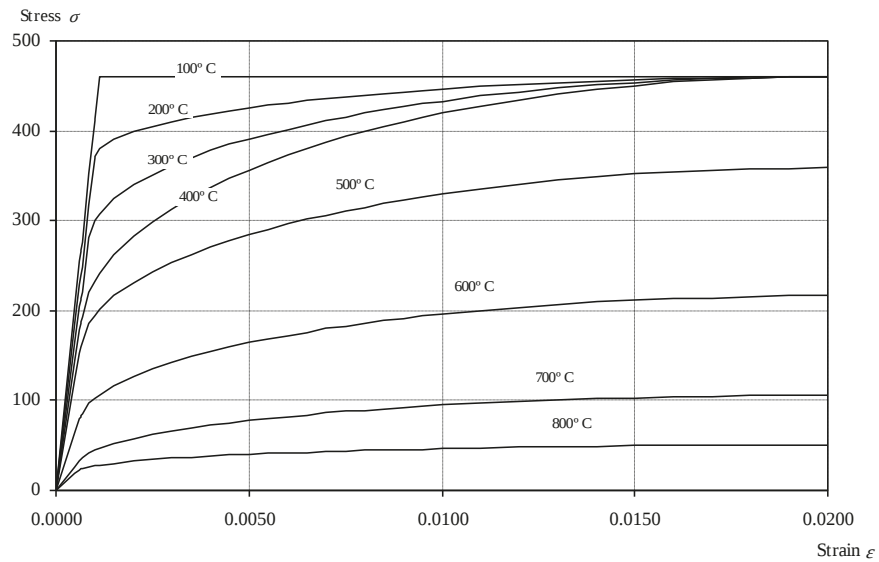


Figure C.5 – Stress-strain relationship for S460 carbon steel at elevated temperatures

C.1.3. Stress-strain relationship for carbon steel at elevated temperatures (with strain-hardening)

For temperatures below 400 °C, the stress-strain relationship specified in C.1.2 may be extended by adding the strain-hardening option given below, providing local or overall buckling does not lead to premature collapse.

$$0.02 < \varepsilon < 0.04 \Rightarrow \sigma_a = 50(f_{u,\theta} - f_{y,\theta})\varepsilon + 2f_{y,\theta} - f_{u,\theta} \quad (C.1a)$$

$$0.04 < \varepsilon < 0.15 \Rightarrow \sigma_a = f_{u,\theta} \quad (C.1b)$$

$$0.15 < \varepsilon < 0.20 \Rightarrow \sigma_a = f_{u,\theta} [1 - 20(\varepsilon - 0.15)] \quad (C.1c)$$

$$0.20 < \varepsilon \Rightarrow \sigma_a = 0.00 \quad (C.1d)$$

where

$f_{u,\theta}$ is the ultimate strength at elevated temperature, allowing for strain-hardening.

This alternative stress-strain relationship for steel, allowing for strain hardening, is illustrated in Figure C.6.

The ultimate strength at elevated temperature, allowing for strain hardening, should be determined as follows:

$$\theta_a < 300^\circ\text{C} \Rightarrow f_{u,\theta} = 1.25f_{y,\theta} \quad (C.2a)$$

$$300^\circ\text{C} < \theta_a < 400^\circ\text{C} \Rightarrow f_{u,\theta} = f_{y,\theta} (2 - 0.0025\theta_a) \quad (C.2b)$$

$$400^\circ\text{C} < \theta_a \Rightarrow f_{u,\theta} = f_{y,\theta} \quad (C.2c)$$

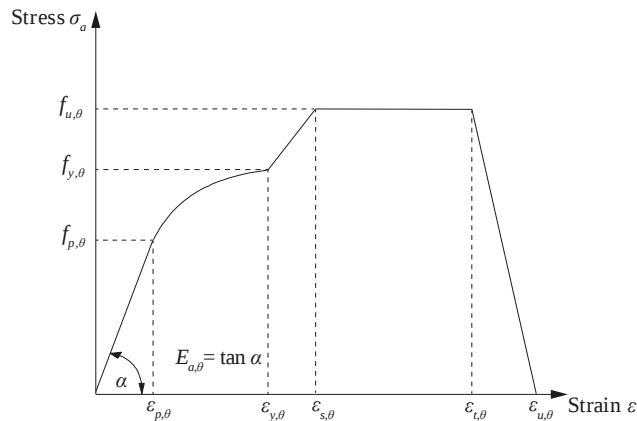


Figure C.6 – Alternative stress-strain relationship for steel allowing for strain-hardening

The variation of the alternative stress-strain relationship with temperature is illustrated in figure C.7.

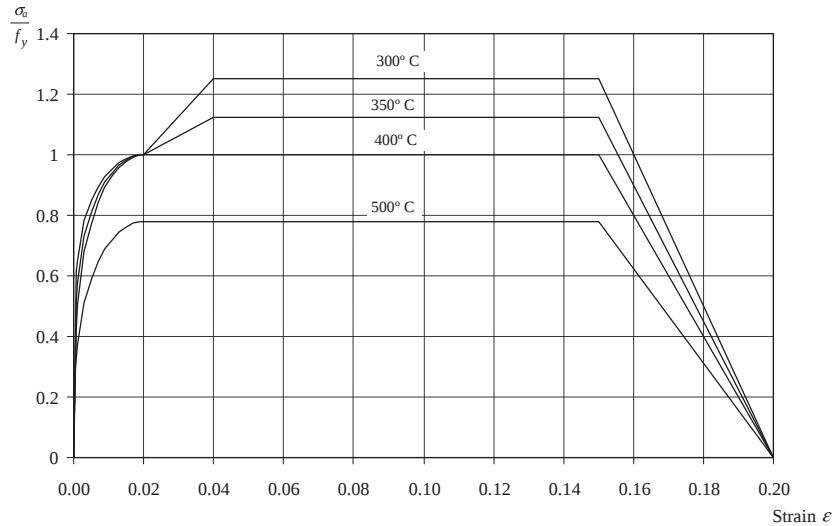


Figure C.7 – Alternative stress-strain relationship for steel allowing for strain-hardening for different temperatures

C.1.4. Mechanical properties to be used with class 4 cross sections and simple calculation models

According to the Eurocode 3 advanced calculation models may be used for the design of Class 4 sections when all stability effects are taken into account. This means that, if the numerical calculation is carried out using the finite element method, shell elements should be used to capture local buckling. The mechanical properties to be used with advanced calculation models are the ones defined in the previous sections of this annex.

With simple calculation models, the resistance of members with a Class 4 cross section should be verified with the equations given in Chapter 5, in which the area is replaced by the effective area and the section modulus is replaced by the effective section modulus. The design strength of steel should be taken as the 0.2 percent proof strength and the effective cross sectional area and the effective section modulus should be determined in accordance with EN 1993-1-3 and EN 1993-1-5, i.e., based on the material properties at 20 °C.

C. MECHANICAL PROPERTIES OF CARBON STEEL AND STAINLESS STEEL

The reduction factors for the design strength of carbon steels relative to the yield strength at 20 °C, illustrated in Figure C.8 may be taken from Table C.8:

- design strength , relative to yield strength at 20 °C: $k_{0.2p,\theta} = f_{0.2p,\theta} / f_y$
- slope of linear elastic range, relative to slope at 20 °C: $k_{E,\theta} = E_{a,\theta} / E_a$

Reduction factors for the design proof strength of stainless steels relative to the proof strength at 20 °C may be taken from Table C.9 of next Section C.2.

Table C.8 – Reduction factors for carbon steel for the design of class 4 sections at elevated temperatures

Steel Temperature θ_a	Reduction factor (relative to f_y) for the design strength of hot rolled and welded thin walled sections $k_{0.2p,\theta} = f_{0.2p,\theta} / f_y$	Reduction factor (relative to f_{yb}) for the design strength of cold formed thin walled sections $k_{0.2p,\theta} = f_{0.2p,\theta} / f_{yb}$
20 °C		1.00
100 °C		1.00
200 °C		0.89
300 °C		0.78
400 °C		0.65
500 °C		0.53
600 °C		0.30
700 °C		0.13
800 °C		0.07
900 °C		0.05
1000 °C		0.03
1100 °C		0.02
1200 °C		0.00
<p>NOTE 1: For intermediate values of the steel temperature, linear interpolation may be used.</p> <p>NOTE 2: The definition for f_{yb} should be taken from EN 1993-1-3.</p>		

C.2. MECHANICAL PROPERTIES OF STAINLESS STEEL

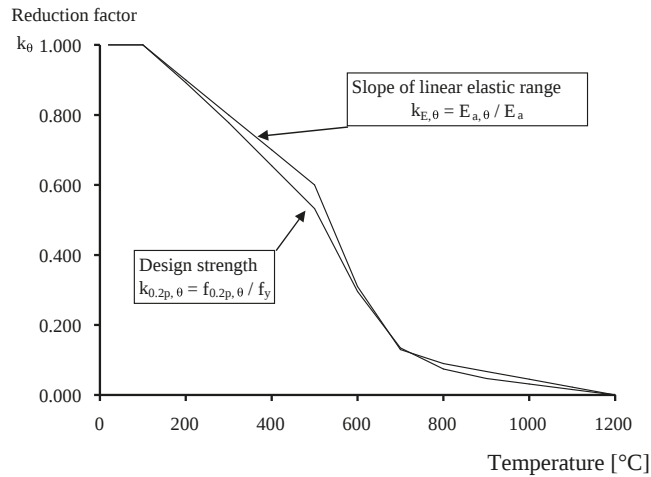


Figure C.8 – Reduction factors for the stress-strain relationship of cold formed and hot rolled thin walled steel at elevated temperatures

C.2. MECHANICAL PROPERTIES OF STAINLESS STEEL

The mechanical properties of stainless steels are given in Annex C of EN 1993-1-2 for steel grades 1.4003, 1.4301, 1.4401, 1.4571, 1.4003 and 1.4462. Table 2.1 from EN 1993-1-4 is reproduced here as Table C.9 for the above five Grades of structural stainless steel and gives the nominal values of the yield strength f_y , the ultimate tensile strength f_u and the modulus of elasticity.

421

Table C.9 – Nominal values of the yield strength f_y , the ultimate tensile strength f_u and Young's modulus E for structural stainless steels according to EN 10088

Type of stainless steel	Grade	Product form								Modulus of elasticity E
		Cold rolled strip		Hot rolled strip		Hot rolled plate		Bars, rods and sections		
		Nominal thickness t								
		$t \leq 6$ mm		$t \leq 12$ mm		$t \leq 75$ mm		$t \leq 250$ mm		
f_y	f_u	f_y	f_u	f_y	f_u	f_y	f_u	E		
MPa	MPa	MPa	MPa	MPa	MPa	MPa	MPa			
Ferritic steel	1.4003	280	450	280	450	250 ¹⁾	450 ¹⁾	260 ²⁾	450 ²⁾	220
Austenitic steels	1.4301	230	540	210	520	210	520	190	500	200
	1.4401	240	530	220	530	220	520	200	500	
	1.4404									
	1.4571									
Austenitic - ferritic steel	1.4462	480	660	460	660	460	640	450	650	200

¹⁾ $t \leq 125$ mm.

²⁾ $t \leq 100$ mm.

C. MECHANICAL PROPERTIES OF CARBON STEEL AND STAINLESS STEEL

Table C.1 from Annex C of EN 1993-1-2 provides reduction factors, relative to the appropriate value at 20 °C, for the stress-strain relationship of several stainless steels at elevated temperatures as follows:

- Slope of linear elastic range, relative to slope at 20 °C: $k_{E,\theta} = E_{a,\theta} / E_a$
- Proof strength, relative to yield strength at 20 °C: $k_{0.2p,\theta} = f_{0.2p,\theta} / f_y$
- Tensile strength, relative to tensile strength at 20 °C: $k_{u,\theta} = f_{u,\theta} / f_u$

For the use of simple calculation methods, table C.1 from EN 1993-1-2 gives the correction factor $k_{2\%,\theta}$ for the determination of the yield strength using:

$$f_{y,\theta} = f_{0.2p,\theta} + k_{2\%,\theta} (f_{u,\theta} - f_{0.2p,\theta}) \quad (C.3)$$

This procedure leads to an “effective” yield strength, $f_{y,\theta} = k_{y,\theta} f_y$, which is the stress at 2% total strain.

For the use of advanced calculation methods Table C.2 from EN 1993-1-2 gives additional values for the stress-strain relationship (see Fig. C.9) of several stainless steels at elevated temperatures as follows:

- slope at proof strength, relative to slope at 20 °C: $k_{E_{ct},\theta} = E_{ct,\theta} / E_a$
- ultimate strain: $e_{u,\theta}$

422

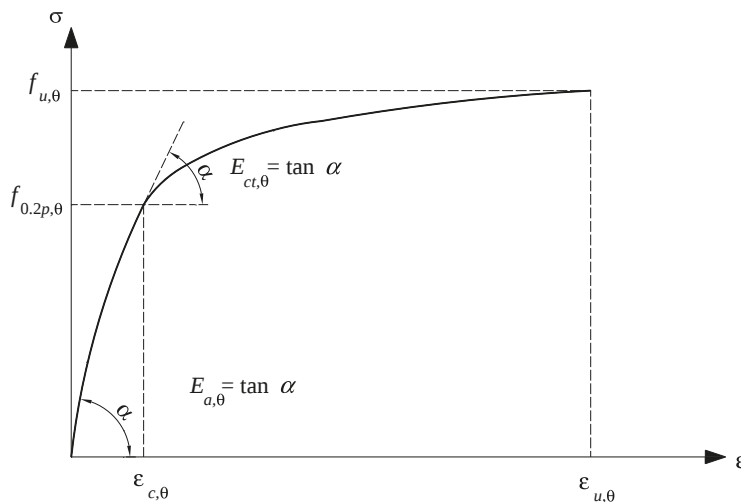


Figure C.9 – Stress-strain relationship for stainless steel at elevated temperatures

Table. C.10 – Parameters for defining stress-strain relationship for stainless steel at elevated temperatures

Strain range	Stress σ	Tangent modulus E_t
$\varepsilon \leq \varepsilon_{c,\theta}$	$\frac{E \cdot \varepsilon}{1 + a \cdot \varepsilon^b}$	$\frac{E(1 + a \cdot \varepsilon^b - a \cdot b \cdot \varepsilon^b)}{(1 + a \cdot \varepsilon^b)^2}$
$\varepsilon_{c,\theta} < \varepsilon \leq \varepsilon_{u,\theta}$	$f_{0.2p,\theta} - e + (d/c)\sqrt{c^2 - (\varepsilon_{u,\theta} - \varepsilon)^2}$	$\frac{d \cdot (\varepsilon_{u,\theta} - \varepsilon)}{c\sqrt{c^2 - (\varepsilon_{u,\theta} - \varepsilon)^2}}$
Parameters	$\varepsilon_{c,\theta} = f_{0.2p,\theta} / E_{a,\theta} + 0.002$	
Functions	$a = \frac{E_{a,\theta} \varepsilon_{c,\theta} - f_{0.2p,\theta}}{f_{0.2p,\theta} \varepsilon_{c,\theta}^b} \quad b = \frac{(1 - \varepsilon_{c,\theta} E_{ct,\theta} / f_{0.2p,\theta}) E_{a,\theta} \varepsilon_{c,\theta}}{(E_{a,\theta} \varepsilon_{c,\theta} / f_{0.2p,\theta} - 1) f_{0.2p,\theta}}$ $c^2 = (\varepsilon_{u,\theta} - \varepsilon_{c,\theta}) \left(\varepsilon_{u,\theta} - \varepsilon_{c,\theta} + \frac{e}{E_{ct,\theta}} \right) \quad d^2 = e (\varepsilon_{u,\theta} - \varepsilon_{c,\theta}) E_{ct,\theta} + e^2$ $e = \frac{(f_{u,\theta} - f_{0.2p,\theta})^2}{(\varepsilon_{u,\theta} - \varepsilon_{c,\theta}) E_{ct,\theta} - 2(f_{u,\theta} - f_{0.2p,\theta})}$	

where

- $f_{u,\theta}$ is the tensile strength;
- $f_{0.2p,\theta}$ is the proof strength at 0.2% plastic strain;
- $E_{a,\theta}$ is the slope of the linear elastic range;
- $E_{ct,\theta}$ is the slope at proof strength;
- $\varepsilon_{c,\theta}$ is the total strain at proof strength;
- $\varepsilon_{u,\theta}$ is the ultimate strain.

Eq. (C.3) leads to

$$\begin{aligned}
 k_{y,\theta} &= \frac{f_{y,\theta}}{f_y} = \left[f_{0.2p,\theta} + k_{2\%,\theta} (f_{u,\theta} - f_{0.2p,\theta}) \right] \frac{1}{f_y} \\
 &= k_{0.2p,\theta} + k_{2\%,\theta} \left(k_{u,\theta} \frac{f_u}{f_y} - k_{0.2p,\theta} \right)
 \end{aligned}
 \tag{C.4}$$

This equation was used to evaluate the value of the reduction factor for the yield strength given in the right four columns in Table C.11.

C. MECHANICAL PROPERTIES OF CARBON STEEL AND STAINLESS STEEL

Table C.11 – Reduction factors of stainless steel at elevated temperatures

θ_a [°C]	$k_{0,2p,\theta}$	$k_{u,\theta}$	$k_{2\%,\theta}$	Cold rolled	Hot rolled	Hot rolled	Bars, rods and sections
				strip	Strip	plate	
$k_{y,\theta}$							
Grade 1.4301							
20	1	1	0.26	1.3504	1.3838	1.3838	1.4242
100	0.82	0.87	0.24	1.1134	1.1402	1.1402	1.1727
200	0.68	0.77	0.19	0.8943	0.9131	0.9131	0.9358
300	0.64	0.73	0.19	0.8440	0.8618	0.8618	0.8834
400	0.6	0.72	0.19	0.8072	0.8247	0.8247	0.8460
500	0.54	0.67	0.19	0.7363	0.7526	0.7526	0.7724
600	0.49	0.58	0.22	0.6818	0.6982	0.6982	0.7180
700	0.4	0.43	0.26	0.5585	0.5728	0.5728	0.5902
800	0.27	0.27	0.35	0.3974	0.4095	0.4095	0.4242
900	0.14	0.15	0.38	0.2206	0.2279	0.2279	0.2368
1000	0.06	0.07	0.4	0.1017	0.1053	0.1053	0.1097
1100	0.03	0.03	0.4	0.0462	0.0477	0.0477	0.0496
1200	0	0	0.4	0.0000	0.0000	0.0000	0.0000
Grade 1.4401 / 1.4404							
20	1	1	0.24	1.2900	1.3382	1.3273	1.3600
100	0.88	0.93	0.24	1.1617	1.2065	1.1964	1.2268
200	0.76	0.87	0.24	1.0387	1.0806	1.0711	1.0996
300	0.71	0.84	0.24	0.9848	1.0253	1.0161	1.0436
400	0.66	0.83	0.21	0.9063	0.9413	0.9334	0.9572
500	0.63	0.79	0.2	0.8529	0.8846	0.8775	0.8990
600	0.61	0.72	0.19	0.7962	0.8237	0.8174	0.8361
700	0.51	0.55	0.24	0.6791	0.7056	0.6996	0.7176
800	0.4	0.34	0.35	0.5228	0.5467	0.5413	0.5575
900	0.19	0.18	0.38	0.2689	0.2826	0.2795	0.2888
1000	0.1	0.09	0.4	0.1395	0.1467	0.1451	0.1500
1100	0.05	0.04	0.4	0.0653	0.0685	0.0678	0.0700
1200	0	0	0.4	0.0000	0.0000	0.0000	0.0000

C.2. MECHANICAL PROPERTIES OF STAINLESS STEEL

Table C.11 – Reduction factors of stainless steel at elevated temperatures

θ_a [°C]	$k_{0,2p,\theta}$	$k_{u,\theta}$	$k_{2\%,\theta}$	Cold rolled	Hot rolled	Hot rolled	Bars, rods and sections
				strip	Strip	plate	
$k_{y,\theta}$							
Grade 1.4571							
20	1	1	0.25	1.3125	1.3636	1.3409	1.3750
100	0.89	0.88	0.25	1.1625	1.2075	1.1875	1.2175
200	0.83	0.81	0.25	1.0781	1.1195	1.1011	1.1288
300	0.77	0.8	0.24	1.0172	1.0565	1.0390	1.0652
400	0.72	0.8	0.22	0.9576	0.9936	0.9776	1.0016
500	0.69	0.77	0.21	0.9089	0.9420	0.9273	0.9494
600	0.66	0.71	0.21	0.8569	0.8874	0.8738	0.8942
700	0.59	0.57	0.25	0.7631	0.7923	0.7793	0.7988
800	0.5	0.38	0.35	0.6243	0.6515	0.6394	0.6575
900	0.28	0.22	0.38	0.3617	0.3788	0.3712	0.3826
1000	0.15	0.11	0.4	0.1890	0.1980	0.1940	0.2000
1100	0.075	0.055	0.4	0.0945	0.0990	0.0970	0.1000
1200	0	0	0.4	0.0000	0.0000	0.0000	0.0000
Grade 1.4003							
20	1	1	0.37	1.2246	1.2246	1.2960	1.2704
100	1	0.94	0.37	1.1890	1.1890	1.2560	1.2320
200	1	0.88	0.37	1.1533	1.1533	1.2161	1.1935
300	0.98	0.86	0.37	1.1288	1.1288	1.1902	1.1681
400	0.91	0.83	0.42	1.0881	1.0881	1.1553	1.1311
500	0.8	0.81	0.4	1.0007	1.0007	1.0632	1.0408
600	0.45	0.42	0.45	0.5513	0.5513	0.5877	0.5746
700	0.19	0.21	0.46	0.2579	0.2579	0.2765	0.2698
800	0.13	0.12	0.47	0.1595	0.1595	0.1704	0.1665
900	0.1	0.11	0.47	0.1361	0.1361	0.1461	0.1425
1000	0.07	0.09	0.47	0.1051	0.1051	0.1132	0.1103
1100	0.035	0.045	0.47	0.0525	0.0525	0.0566	0.0552
1200	0	0	0.47	0.0000	0.0000	0.0000	0.0000

C. MECHANICAL PROPERTIES OF CARBON STEEL AND STAINLESS STEEL

Table C.11 – Reduction factors of stainless steel at elevated temperatures

θ_a [°C]	$k_{0.2p,\theta}$	$k_{u,\theta}$	$k_{2\%,\theta}$	Cold rolled	Hot rolled	Hot rolled	Bars, rods and sections
				strip	Strip	plate	
$k_{y,\theta}$							
Grade 1.4462							
20	1	1	0.35	1.1313	1.1522	1.1370	1.1556
100	0.91	0.93	0.35	1.0391	1.0585	1.0444	1.0617
200	0.8	0.85	0.32	0.9180	0.9343	0.9224	0.9369
300	0.75	0.83	0.3	0.8674	0.8823	0.8714	0.8847
400	0.72	0.82	0.28	0.8341	0.8478	0.8378	0.8500
500	0.65	0.71	0.3	0.7479	0.7606	0.7513	0.7627
600	0.56	0.57	0.33	0.6338	0.6451	0.6369	0.6469
700	0.37	0.38	0.4	0.4310	0.4401	0.4335	0.4416
800	0.26	0.29	0.41	0.3169	0.3240	0.3188	0.3251
900	0.1	0.12	0.45	0.1293	0.1325	0.1301	0.1330
1000	0.03	0.04	0.47	0.0418	0.0429	0.0421	0.0431
1100	0.015	0.02	0.47	0.0209	0.0214	0.0210	0.0215
1200	0	0	0.47	0.0000	0.0000	0.0000	0.0000

When the parameters of Table C.11 are used in the equations of Table C.10, this can lead to a stress-strain relationship with positive curvature; the stiffness increases for positive strains. This occurs at very high temperatures (see Fig. C.10) and thus it is not generally an issue in practical problems, but can lead to unexpected results in some numerical simulations. This problem was treated by Lopes (2009) who has proposed different reduction factors for the Young's modulus in the temperature range of 1000 °C to 1200 °C.

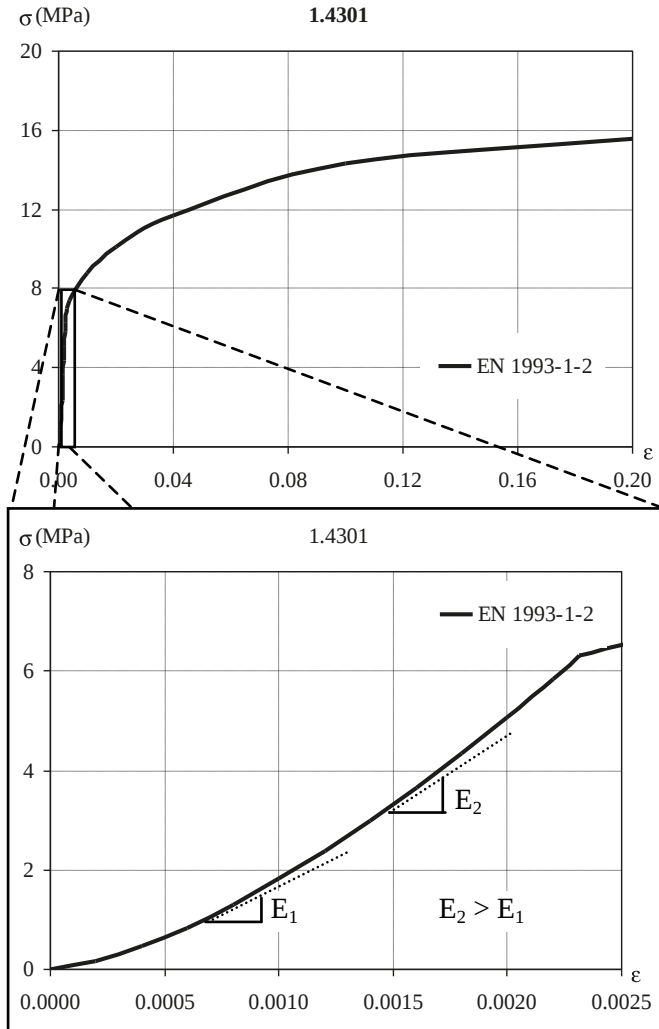


Figure C.10 – Stress-strain relationship of the stainless steel 1.4301 at 1100 °C

Annex D

TABLES FOR SECTION CLASSIFICATION AND EFFECTIVE WIDTH EVALUATION

In this Annex the maximum width-to-thickness ratios for compression elements needed for the classification of the cross section of hot rolled and welded profiles subject to compression, bending or a combination of compression and bending are presented. The effective widths of internal and outstand compression elements are also given. Tables D.1, D.2, and D.3 are taken from EN 1993-1-1 and tables D.4 and D.5 are from EN 1993-1-5. For stainless steel cross sections Table 5.2 from EN 1993-1-4 should be used.

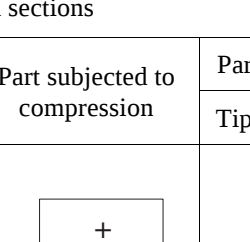
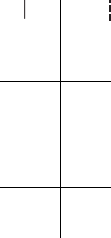
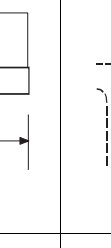
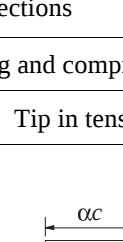
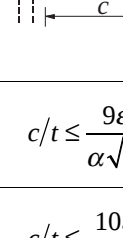
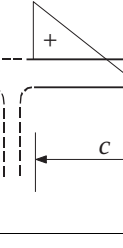
D. TABLES FOR SECTION CLASSIFICATION AND EFFECTIVE WIDTH EVALUATION

Table D.1 – Maximum with-to-thickness ratios for compression parts

Internal compression parts			
Class	Part subjected to bending	Part subjected to compression	Part subjected to bending and compression
1	$c/t \leq 72\epsilon$	$c/t \leq 33\epsilon$	$\alpha > 0.5: c/t \leq \frac{396\epsilon}{13\alpha - 1}$ $\alpha \leq 0.5: c/t \leq \frac{36\epsilon}{\alpha}$
2	$c/t \leq 83\epsilon$	$c/t \leq 38\epsilon$	$\alpha > 0.5: c/t \leq \frac{456\epsilon}{13\alpha - 1}$ $\alpha \leq 0.5: c/t \leq \frac{41.5\epsilon}{\alpha}$
3	$c/t \leq 124\epsilon$	$c/t \leq 42\epsilon$	$\psi > -1: c/t \leq \frac{42\epsilon}{0.67 + 0.33\psi}$ $\psi \leq -1^*): c/t \leq 62\epsilon(1 - \psi)\sqrt{-\psi}$

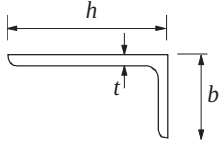
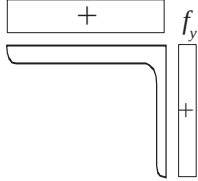
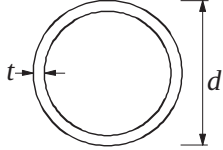
*) $\psi \leq -1$ applies where either the compression stress $\sigma \leq f_y$ or the tensile strain $\epsilon_y > f_y/E$

Table D.2 – Maximum with-to-thickness ratios for compression parts

Outstand compression flanges			
		Rolled sections	Welded sections
Class	Part subjected to compression	Part subjected to bending and compression	
		Tip in compression	Tip in tension
Stress distribution in parts (compression positive)			
1	$c/t \leq 9\epsilon$	$c/t \leq \frac{9\epsilon}{\alpha}$	$c/t \leq \frac{9\epsilon}{\alpha\sqrt{\alpha}}$
2	$c/t \leq 10\epsilon$	$c/t \leq \frac{10\epsilon}{\alpha}$	$c/t \leq \frac{10\epsilon}{\alpha\sqrt{\alpha}}$
Stress distribution in parts (compression positive)			
3	$c/t \leq 14\epsilon$	$c/t \leq 21\epsilon\sqrt{k_\sigma}$ For k_σ see EN 1993-1-5	

D. TABLES FOR SECTION CLASSIFICATION AND EFFECTIVE WIDTH EVALUATION

Table D.3 – Maximum with-to-thickness ratios for compression parts

<p>Refer also to “Outstand flanges” (see Table D.1.2)</p> <p style="text-align: center;">Angles</p>  <p style="text-align: right;">Does not apply to angles in continuous contact with other components</p>	
Class	Section in compression
Stress distribution in parts (compression positive)	
3	$h/t \leq 15\epsilon$; $\frac{b+h}{2t} \leq 11.5\epsilon$
<p>Tubular sections</p> 	
Class	Section in compression and/or compression
1	$d/t \leq 50\epsilon^2$
2	$d/t \leq 70\epsilon^2$
3	$d/t \leq 90\epsilon^2$ NOTE For $d/t > 90\epsilon^2$ see EN 1993-1-6.

D. TABLES FOR SECTION CLASSIFICATION AND EFFECTIVE WIDTH EVALUATION

Table D.4 – Internal compression elements

Stress distribution (compression positive)				Effective ^p width b_{eff}		
				$\underline{\psi = 1:}$ $b_{eff} = \rho \bar{b}$ $b_{e1} = 0.5b_{eff}$ $b_{e2} = 0.5b_{eff}$		
				$\underline{1 > \psi \geq 0:}$ $b_{eff} = \rho \bar{b}$ $b_{e1} = \frac{2}{5 - \psi} b_{eff}$ $b_{e2} = b_{eff} - b_{e1}$		
				$\underline{\psi < 0:}$ $b_{eff} = \rho b_c = \rho \bar{b} / (1 - \psi)$ $b_{e1} = 0.4b_{eff}$ $b_{e2} = 0.6b_{eff}$		
$\psi = \sigma_2 / \sigma_1$	1	$1 > \psi > 0$	0	$0 > \psi > -1$	-1	$-1 > \psi > -3$
Buckling factor k_σ	4.0	$8.2 / (1.05 + \psi)$	7.81	$7.81 - 6.29\psi + 9.78\psi^2$	23.9	$5.98(1 - \psi)^2$

D. TABLES FOR SECTION CLASSIFICATION AND EFFECTIVE WIDTH EVALUATION

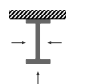
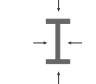
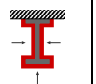
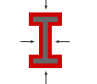
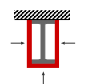
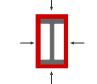
Table D.5 – Outstand compression elements

Stress distribution (compression positive)		Effective ^p width b_{eff}			
		$\frac{1 > \psi \geq 0:}{b_{eff} = \rho c}$			
		$\frac{\psi < 0:}{b_{eff} = \rho b_c = \rho c / (1 - \psi)}$			
$\psi = \sigma_2 / \sigma_1$	1	0	-1	$1 \geq \psi \geq -3$	
Buckling factor k_σ	0.43	0.57	0.85	$0.57 - 0.21\psi + 0.07\psi^2$	
		$\frac{1 > \psi \geq 0:}{b_{eff} = \rho c}$			
		$\frac{\psi < 0:}{b_{eff} = \rho b_c = \rho c / (1 - \psi)}$			
$\psi = \sigma_2 / \sigma_1$	1	$1 > \psi > 0$	0	$0 > \psi > -1$	-1
Buckling factor k_σ	0.43	$0.578 / (\psi + 0.34)$	1.70	$1.7 - 5\psi + 17.1\psi^2$	23.8

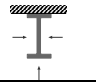
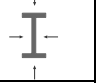
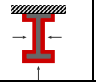
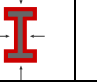
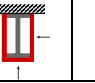
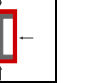
Annex E

SECTION FACTORS OF EUROPEAN HOT ROLLED IPE AND HE PROFILES

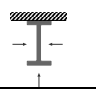
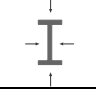
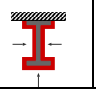
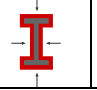
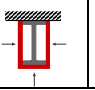
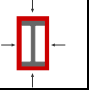
This annex presents tables with values of the section factor for unprotected (A_m/V) and protected (A_p/V), I and H European hot rolled steel profiles as well as values of the modified section factor $k_{sh}A_m/V$ in accordance with EN 1993-1-2.

Designation IPE	Unprotected sections		Protected sections			
						
	$k_{sh}A_m/V$		A_p/V			
	3 sides	4 sides	contour 3 sides	contour 4 sides	hollow 3 sides	hollow 4 sides
IPE AA 80	288.1	353.7	442.2	515.1	320.1	393.0
IPE A 80	285.0	349.8	437.3	509.4	316.6	388.7
IPE 80	242.7	296.9	369.1	429.3	269.6	329.8
IPE AA 100	263.1	320.9	398.3	462.6	292.3	356.5
IPE A 100	257.3	313.7	389.5	452.2	285.9	348.5
IPE 100	222.8	270.9	335.0	388.3	247.6	301.0
IPE AA 120	251.8	305.9	381.6	441.7	279.8	339.9
IPE A 120	244.8	297.2	370.9	429.1	272.0	330.2
IPE 120	207.3	250.9	311.4	359.8	230.3	278.8
IPE AA 140	243.2	294.5	368.9	425.9	270.3	327.2

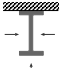
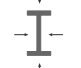
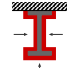
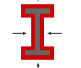
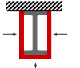
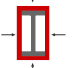
E. SECTION FACTORS OF EUROPEAN HOT ROLLED IPE AND HE PROFILES

Designation IPE	Unprotected sections		Protected sections			
						
	$k_{sh} A_m/V$		A_p/V			
	3 sides	4 sides	contour 3 sides	contour 4 sides	hollow 3 sides	hollow 4 sides
IPE A 140	233.6	282.6	353.7	408.2	259.6	314.0
IPE 140	193.7	233.8	291.5	336.0	215.2	259.8
IPE AA 160	230.7	278.6	349.9	403.1	256.4	309.6
IPE A 160	220.0	265.6	331.5	382.1	244.4	295.1
IPE 160	180.0	216.7	269.2	310.0	200.0	240.8
IPE AA 180	209.9	252.9	316.2	364.0	233.2	281.0
IPE A 180	204.3	246.1	307.7	354.1	227.0	273.5
IPE 180	169.8	204.1	254.0	292.1	188.7	226.8
IPE O 180	151.4	182.0	226.2	260.1	168.3	202.2
IPE AA 200	193.9	233.3	290.0	333.7	215.5	259.2
IPE A 200	189.2	227.5	282.6	325.1	210.2	252.8
IPE 200	157.9	189.5	234.4	269.5	175.4	210.5
IPE O 200	142.3	171.0	211.6	243.4	158.1	190.0
IPE AA 220	181.0	217.7	271.5	312.3	201.1	241.9
IPE A 220	173.0	208.0	259.0	297.9	192.2	231.1
IPE 220	148.2	177.8	221.0	253.9	164.7	197.6
IPE O 220	133.8	160.7	199.5	229.4	148.7	178.6
IPE AA 240	168.2	202.3	251.5	289.3	186.9	224.8
IPE A 240	160.5	193.0	239.6	275.7	178.4	214.4
IPE 240	138.1	165.7	205.1	235.8	153.5	184.1
IPE O 240	124.8	149.9	185.4	213.3	138.7	166.6
IPE A 270	153.6	184.6	230.1	264.5	170.7	205.1
IPE 270	132.4	158.8	197.4	226.8	147.1	176.5
IPE O 270	114.4	137.2	170.1	195.4	127.1	152.4
IPE A 300	144.0	173.0	216.3	248.6	160.0	192.3
IPE 300	125.5	150.6	187.7	215.6	139.4	167.3

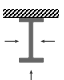
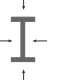
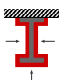
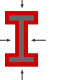
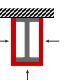
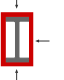
E. SECTION FACTORS OF EUROPEAN HOT ROLLED IPE AND HE PROFILES

Designation IPE	Unprotected sections		Protected sections			
						
	$k_{sh} A_m/V$		A_p/V			
	3 sides	4 sides	contour 3 sides	contour 4 sides	hollow 3 sides	hollow 4 sides
IPE O 300	108.9	130.7	162.7	186.9	121.0	145.2
IPE A 330	133.9	160.3	199.3	228.5	148.8	178.1
IPE 330	117.9	140.9	174.8	200.3	131.0	156.5
IPE O 330	102.9	123.0	152.3	174.7	114.3	136.6
IPE A 360	124.5	148.4	184.5	211.1	138.3	164.9
IPE 360	110.2	131.2	162.7	186.1	122.4	145.8
IPE O 360	96.3	114.7	142.1	162.5	107.0	127.5
IPE A 400	119.9	142.1	175.6	200.3	133.2	157.9
IPE 400	104.4	123.6	152.3	173.6	116.0	137.3
IPE O 400	92.4	109.4	134.8	153.6	102.7	121.6
IPE A 450	114.0	133.9	165.1	187.3	126.6	148.8
IPE 450	99.3	116.6	143.2	162.4	110.3	129.6
IPE O 450	84.2	98.8	121.2	137.5	93.6	109.8
IPE A 500	106.4	124.2	152.6	172.4	118.2	138.0
IPE 500	93.1	108.6	133.1	150.3	103.4	120.7
IPE O 500	79.8	93.0	113.7	128.5	88.6	103.4
IPE A 550	100.3	116.5	142.3	160.3	111.5	129.4
IPE 550	88.0	102.1	124.4	140.1	97.8	113.4
IPE O 550	76.4	88.6	107.8	121.3	84.9	98.5
IPE A 600	92.9	107.3	130.9	146.9	103.2	119.3
IPE 600	81.9	94.6	115.1	129.2	91.0	105.1
IPE O 600	66.0	76.2	92.4	103.8	73.3	84.7
IPE 750 x 137	91.0	104.5	128.2	143.2	101.1	116.1
IPE 750 x 147	84.8	97.5	119.4	133.5	94.2	108.3
IPE 750 x 173	72.9	83.8	102.6	114.7	81.0	93.1
IPE 750 x 196	64.8	74.4	91.0	101.7	72.0	82.7

E. SECTION FACTORS OF EUROPEAN HOT ROLLED IPE AND HE PROFILES

Designation HE	Unprotected sections		Protected sections			
						
	$k_{sh} A_m/V$		A_p/V			
	3 sides	4 sides	contour 3 sides	contour 4 sides	hollow 3 sides	hollow 4 sides
HE 100 AA	162.7	220.4	290.4	354.5	180.8	244.9
HE 100 A	124.0	166.4	217.5	264.6	137.7	184.9
HE 100 B	103.8	138.5	179.6	218.1	115.4	153.8
HE 100 C	74.0	97.6	124.8	151.0	82.2	108.4
HE 100 M	58.5	76.5	96.4	116.4	65.0	85.0
HE 120 AA	163.5	221.6	295.2	359.7	181.7	246.2
HE 120 A	123.8	166.5	220.2	267.6	137.5	185.0
HE 120 B	95.3	127.1	166.5	201.8	105.9	141.2
HE 120 C	69.1	91.3	118.1	142.8	76.8	101.4
HE 120 M	55.0	72.1	92.2	111.1	61.1	80.1
HE 140 AA	155.0	209.7	281.3	342.2	172.2	233.0
HE 140 A	116.4	156.5	208.3	252.9	129.3	173.9
HE 140 B	87.9	117.2	154.7	187.2	97.7	130.2
HE 140 C	64.8	85.8	111.9	135.2	72.0	95.3
HE 140 M	52.0	68.3	88.2	106.3	57.8	75.9
HE 160 AA	135.0	182.4	243.8	296.4	150.0	202.6
HE 160 A	107.6	144.7	192.3	233.5	119.6	160.8
HE 160 B	79.6	106.1	139.6	169.1	88.4	117.9
HE 160 C	60.0	79.5	103.6	125.2	66.7	88.3
HE 160 M	48.8	64.1	82.8	99.9	54.2	71.3
HE 180 AA	126.7	171.1	229.6	278.9	140.8	190.1
HE 180 A	103.7	139.5	186.3	226.0	115.2	155.0
HE 180 B	74.4	99.2	131.2	158.8	82.7	110.3
HE 180 C	56.9	75.4	98.9	119.5	63.3	83.8
HE 180 M	46.5	61.3	79.7	96.1	51.7	68.1
HE 200 AA	116.7	157.6	210.9	256.2	129.7	175.1

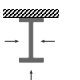
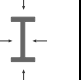
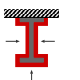
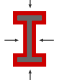
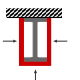
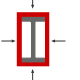
E. SECTION FACTORS OF EUROPEAN HOT ROLLED IPE AND HE PROFILES

Designation HE	Unprotected sections		Protected sections			
						
	$k_{sh} A_m/V$		A_p/V			
	3 sides	4 sides	contour 3 sides	contour 4 sides	hollow 3 sides	hollow 4 sides
HE 200 A	97.0	130.5	174.0	211.2	107.8	145.0
HE 200 B	69.1	92.2	121.8	147.4	76.8	102.4
HE 200 C	53.7	71.2	93.3	112.7	59.7	79.1
HE 200 M	44.3	58.4	75.9	91.6	49.2	64.9
HE 220 AA	110.1	148.5	199.4	242.1	122.3	165.0
HE 220 A	89.6	120.4	161.0	195.2	99.5	133.7
HE 220 B	65.3	87.0	115.4	139.6	72.5	96.7
HE 220 C	51.3	68.0	89.5	108.1	57.0	75.6
HE 220 M	42.5	56.1	73.4	88.5	47.3	62.4
HE 240 AA	102.5	138.3	185.3	225.0	113.9	153.6
HE 240 A	82.0	110.2	147.0	178.3	91.1	122.4
HE 240 B	61.1	81.5	107.9	130.6	67.9	90.6
HE 240 C	44.6	59.0	77.4	93.4	49.5	65.6
HE 240 M	35.5	46.7	60.7	73.1	39.5	51.9
HE 260 AA	97.6	131.5	175.9	213.6	108.4	146.1
HE 260 A	78.8	105.8	141.0	171.0	87.6	117.5
HE 260 B	59.3	79.1	104.6	126.6	65.9	87.8
HE 260 C	43.5	57.6	75.6	91.3	48.3	64.0
HE 260 M	34.8	45.7	59.5	71.7	38.6	50.8
HE 280 AA	93.2	125.5	168.3	204.2	103.6	139.5
HE 280 A	75.8	101.7	136.0	164.7	84.3	113.1
HE 280 B	57.5	76.7	101.8	123.1	63.9	85.2
HE 280 C	42.5	56.3	74.1	89.4	47.2	62.5
HE 280 M	34.0	44.8	58.5	70.5	37.8	49.8
HE 300 AA	87.7	118.0	158.0	191.8	97.4	131.2
HE 300 A	70.4	94.4	126.0	152.6	78.2	104.9

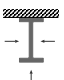
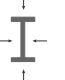
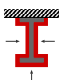

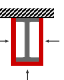

E. SECTION FACTORS OF EUROPEAN HOT ROLLED IPE AND HE PROFILES

Designation HE	Unprotected sections		Protected sections			
	$k_{sh} A_m/V$		A_p/V			
	3 sides	4 sides	contour 3 sides	contour 4 sides	hollow 3 sides	hollow 4 sides
HE 300 B	54.3	72.4	96.0	116.2	60.4	80.5
HE 300 C	37.8	50.0	65.6	79.1	42.0	55.5
HE 300 M	29.4	38.6	50.2	60.4	32.7	42.9
HE 320 AA	85.8	114.4	152.2	183.9	95.3	127.1
HE 320 A	66.6	88.3	117.0	141.2	74.0	98.1
HE 320 B	52.4	69.2	91.2	109.8	58.3	76.9
HE 320 C	37.4	49.0	64.0	76.9	41.6	54.5
HE 320 M	29.6	38.5	49.9	59.8	32.9	42.8
HE 340 AA	84.2	111.0	147.0	176.8	93.5	123.4
HE 340 A	64.7	84.9	112.0	134.5	71.9	94.4
HE 340 B	51.6	67.4	88.4	105.9	57.3	74.9
HE 340 M	30.3	39.1	50.4	60.2	33.7	43.4
HE 360 AA	82.6	107.9	142.0	170.2	91.7	119.9
HE 360 A	63.0	81.9	107.4	128.4	70.0	91.0
HE 360 B	50.8	65.8	85.8	102.4	56.5	73.1
HE 360 M	31.0	39.7	51.0	60.7	34.4	44.1
HE 400 AA	80.7	103.7	135.2	160.7	89.7	115.2
HE 400 A	61.1	78.1	101.4	120.3	67.9	86.8
HE 400 B	50.1	63.7	82.3	97.4	55.6	70.8
HE 400 M	32.3	40.8	52.1	61.5	35.9	45.4
HE 450 AA	81.4	102.7	132.5	156.1	90.5	114.1
HE 450 A	59.7	74.8	96.1	113.0	66.3	83.1
HE 450 B	49.5	61.9	79.2	92.9	55.0	68.8
HE 450 M	33.9	42.1	53.3	62.5	37.7	46.8
HE 500 AA	81.8	101.5	129.8	151.7	90.9	112.8
HE 500 A	58.3	72.0	91.6	106.8	64.8	80.0

E. SECTION FACTORS OF EUROPEAN HOT ROLLED IPE AND HE PROFILES

Designation HE	Unprotected sections		Protected sections			
						
	$k_{sh} A_m/V$		A_p/V			
	3 sides	4 sides	contour 3 sides	contour 4 sides	hollow 3 sides	hollow 4 sides
HE 500 B	49.0	60.4	76.5	89.1	54.5	67.1
HE 500 M	35.4	43.4	54.5	63.4	39.3	48.2
HE 550 AA	79.2	96.8	122.7	142.3	88.0	107.6
HE 550 A	58.6	71.4	90.1	104.3	65.2	79.3
HE 550 B	49.6	60.2	75.7	87.5	55.1	66.9
HE 550 M	36.8	44.6	55.7	64.3	40.9	49.5
HE 600 AA	79.1	95.5	120.2	138.5	87.9	106.2
HE 600 A	58.8	70.7	88.7	101.9	65.3	78.6
HE 600 B	50.0	60.0	74.9	86.0	55.6	66.7
HE 600 M	38.2	45.8	56.8	65.2	42.5	50.9
HE 600 x 337	33.0	39.5	48.9	56.1	36.7	43.9
HE 600 x 399	28.5	34.1	42.0	48.2	31.7	37.9
HE 650 AA	78.8	94.2	117.7	134.8	87.6	104.7
HE 650 A	58.9	70.0	87.2	99.6	65.4	77.8
HE 650 B	50.3	59.7	74.1	84.6	55.9	66.4
HE 650 M	39.5	46.9	57.9	66.0	43.9	52.1
HE 650 x 343	34.3	40.7	50.1	57.1	38.1	45.2
HE 650 x 407	29.6	35.0	43.0	49.0	32.9	38.9
HE 700 AA	77.3	91.5	113.6	129.3	85.9	101.6
HE 700 A	58.0	68.4	84.6	96.2	64.5	76.0
HE 700 B	49.9	58.7	72.5	82.2	55.5	65.3
HE 700 M	40.8	47.9	58.9	66.8	45.3	53.3
HE 700 x 352	35.4	41.6	50.9	57.8	39.3	46.2
HE 700 x 418	30.5	35.8	43.7	49.5	33.9	39.7
HE 800 AA	75.8	88.1	108.0	121.7	84.2	97.9
HE 800 A	59.2	68.6	83.9	94.4	65.8	76.3

E. SECTION FACTORS OF EUROPEAN HOT ROLLED IPE AND HE PROFILES

Designation HE	Unprotected sections		Protected sections			
						
	$k_{sh} A_m/V$		A_p/V			
	3 sides	4 sides	contour 3 sides	contour 4 sides	hollow 3 sides	hollow 4 sides
HE 800 B	51.2	59.2	72.2	81.2	56.9	65.8
HE 800 M	43.0	49.7	60.4	67.9	47.8	55.3
HE 800 x 373	37.2	43.0	52.1	58.6	41.3	47.8
HE 800 x 444	31.8	36.7	44.4	49.9	35.3	40.8
HE 900 AA	72.8	83.5	101.4	113.3	80.9	92.8
HE 900 A	58.4	66.8	81.0	90.4	64.9	74.3
HE 900 B	50.9	58.2	70.3	78.4	56.6	64.6
HE 900 M	45.1	51.5	62.1	69.3	50.1	57.2
HE 900 x 391	38.9	44.4	53.5	59.7	43.2	49.4
HE 900 x 466	33.2	37.9	45.5	50.7	36.9	42.1
HE 1000 AA	71.4	81.0	97.7	108.3	79.4	90.0
HE 1000 x 249	64.2	72.7	87.8	97.2	71.3	80.8
HE 1000 A	59.2	67.0	80.6	89.2	65.7	74.4
HE 1000 B	51.8	58.5	70.3	77.8	57.5	65.0
HE 1000 M	47.0	53.1	63.7	70.5	52.2	59.0
HE 1000 x 393	42.0	47.5	56.7	62.8	46.7	52.7
HE 1000 x 415	39.9	45.1	53.8	59.6	44.3	50.1
HE 1000 x 438	38.2	43.1	51.5	57.0	42.4	47.9
HE 1000 x 494	34.1	38.5	45.8	50.7	37.8	42.8
HE 1000 x 584	29.4	33.2	39.3	43.6	32.6	36.8

Annex F

CROSS SECTIONAL CLASSIFICATION OF EUROPEAN HOT ROLLED IPE AND HE PROFILES

This annex gives tables with the cross sectional classification of European hot rolled IPE and HE profiles subjected to pure compression, pure bending about strong axis (M_y), pure bending about weak axis (M_z) and combined compression and bending moment, on steel grades S235, S275, S355 and S460 under normal and high temperatures, according to EN 1993-1-1 and EN 1993-1-2.

F.1. CROSS SECTIONAL CLASSIFICATION FOR PURE COMPRESSION AND PURE BENDING

443

Designation IPE	Pure Bending y-y				Pure Bending z-z				Compression							
	Normal Temperature		High Temperatures		Normal Temperature		High Temperatures		Normal Temperature		High Temperatures					
	S 235	S 275	S 355	S 460	S 235	S 275	S 355	S 460	S 235	S 275	S 355	S 460				
IPE AA 80	1	1	1	1	1	1	1	1	1	1	1	1	1	1	1	1
IPE A 80	1	1	1	1	1	1	1	1	1	1	1	1	1	1	1	1
IPE 80	1	1	1	1	1	1	1	1	1	1	1	1	1	1	1	1
IPE AA 100	1	1	1	1	1	1	1	1	1	1	1	1	1	1	1	2
IPE A 100	1	1	1	1	1	1	1	1	1	1	1	1	1	1	1	2

F. CROSS SECTIONAL CLASSIFICAT. OF EU HOT ROLLED IPE AND HE PROFILES

Designation IPE	Pure Bending y-y				Pure Bending z-z				Compression			
	Normal Temperature		High Temperatures		Normal Temperature		High Temperatures		Normal Temperature		High Temperatures	
	S 235	S 275	S 355	S 460	S 235	S 275	S 355	S 460	S 235	S 275	S 355	S 460
IPE 100	1	1	1	1	1	1	1	1	1	1	1	1
IPE AA 120	1	1	1	1	1	1	1	1	1	1	2	3
IPE A 120	1	1	1	1	1	1	1	1	1	1	2	3
IPE 120	1	1	1	1	1	1	1	1	1	1	1	2
IPE AA 140	1	1	1	1	1	1	1	1	1	1	2	3
IPE A 140	1	1	1	1	1	1	1	1	1	1	2	3
IPE 140	1	1	1	1	1	1	1	1	1	1	1	2
IPE AA 160	1	1	1	1	1	1	1	2	1	2	3	4
IPE A 160	1	1	1	1	1	1	1	1	1	1	2	3
IPE 160	1	1	1	1	1	1	1	1	1	1	1	2
IPE AA 180	1	1	1	1	1	1	1	2	2	2	3	4
IPE A 180	1	1	1	1	1	1	1	1	2	2	3	4
IPE 180	1	1	1	1	1	1	1	1	1	1	2	3
IPE O 180	1	1	1	1	1	1	1	1	1	1	1	2
IPE AA 200	1	1	1	1	1	1	1	1	2	3	4	4
IPE A 200	1	1	1	1	1	1	1	1	2	3	4	4
IPE 200	1	1	1	1	1	1	1	1	1	1	2	3
IPE O 200	1	1	1	1	1	1	1	1	1	1	1	2
IPE AA 220	1	1	1	1	1	1	1	2	2	3	4	4
IPE A 220	1	1	1	1	1	1	1	1	2	3	4	4
IPE 220	1	1	1	1	1	1	1	1	1	1	2	4
IPE O 220	1	1	1	1	1	1	1	1	1	1	2	2
IPE AA 240	1	1	1	1	1	1	1	1	3	4	4	4
IPE A 240	1	1	1	1	1	1	1	1	2	3	4	4
IPE 240	1	1	1	1	1	1	1	1	1	2	2	4
IPE O 240	1	1	1	1	1	1	1	1	1	1	2	3
IPE A 270	1	1	1	1	1	1	1	2	3	4	4	4
IPE 270	1	1	1	1	1	1	1	1	2	2	3	4
IPE O 270	1	1	1	1	1	1	1	1	1	1	2	3

F.1. CROSS SECTIONAL CLASSIFICATION FOR PURE COMPRESSION AND PURE BENDING

Designation IPE	Pure Bending y-y				Pure Bending z-z				Compression													
	Normal Temperature		High Temperatures		Normal Temperature		High Temperatures		Normal Temperature		High Temperatures											
	S 235	S 275	S 355	S 460	S 235	S 275	S 355	S 460	S 235	S 275	S 355	S 460										
IPE A 300	1	1	1	1	1	1	1	1	1	1	1	1	3	3	4	4	4	4	4	4	4	4
IPE 300	1	1	1	1	1	1	1	1	1	1	1	1	1	1	2	2	4	4	3	4	4	4
IPE O 300	1	1	1	1	1	1	1	1	1	1	1	1	1	1	1	2	3	4	2	3	4	4
IPE A 330	1	1	1	1	1	1	1	1	2	1	1	1	1	1	1	1	1	2	3	4	4	4
IPE 330	1	1	1	1	1	1	1	1	1	1	1	1	1	1	2	3	4	4	4	4	4	4
IPE O 330	1	1	1	1	1	1	1	1	1	1	1	1	1	1	1	2	3	4	2	3	4	4
IPE A 360	1	1	1	1	1	1	1	1	2	1	1	1	1	1	1	1	1	2	4	4	4	4
IPE 360	1	1	1	1	1	1	1	1	1	1	1	1	1	1	2	3	4	4	4	4	4	4
IPE O 360	1	1	1	1	1	1	1	1	1	1	1	1	1	1	1	2	3	4	3	3	4	4
IPE A 400	1	1	1	1	1	1	1	1	2	1	1	1	1	1	1	1	1	1	4	4	4	4
IPE 400	1	1	1	1	1	1	1	1	1	1	1	1	1	1	3	3	4	4	4	4	4	4
IPE O 400	1	1	1	1	1	1	1	1	1	1	1	1	1	1	2	2	3	4	3	4	4	4
IPE A 450	1	1	1	1	1	1	2	2	1	1	1	1	1	1	1	1	1	1	4	4	4	4
IPE 450	1	1	1	1	1	1	1	1	1	1	1	1	1	1	3	4	4	4	4	4	4	4
IPE O 450	1	1	1	1	1	1	1	1	1	1	1	1	1	1	2	2	4	4	3	4	4	4
IPE A 500	1	1	1	1	1	1	2	3	1	1	1	1	1	1	1	1	1	1	4	4	4	4
IPE 500	1	1	1	1	1	1	1	1	1	1	1	1	1	1	3	4	4	4	4	4	4	4
IPE O 500	1	1	1	1	1	1	1	1	1	1	1	1	1	1	2	3	4	4	3	4	4	4
IPE A 550	1	1	1	2	1	1	2	3	1	1	1	1	1	1	1	1	1	1	4	4	4	4
IPE 550	1	1	1	1	1	1	1	1	1	1	1	1	1	1	4	4	4	4	4	4	4	4
IPE O 550	1	1	1	1	1	1	1	1	1	1	1	1	1	1	2	3	4	4	4	4	4	4
IPE A 600	1	1	1	2	1	1	2	3	1	1	1	1	1	1	1	1	1	1	4	4	4	4
IPE 600	1	1	1	1	1	1	1	1	1	1	1	1	1	1	4	4	4	4	4	4	4	4
IPE O 600	1	1	1	1	1	1	1	1	1	1	1	1	1	1	2	2	4	4	3	4	4	4
IPE 750 × 137	1	1	2	3	1	2	3	3	1	1	1	1	1	1	1	1	2	3	4	4	4	4
IPE 750 × 147	1	1	1	2	1	1	2	3	1	1	1	1	1	1	1	1	2	3	4	4	4	4
IPE 750 × 173	1	1	1	1	1	1	1	1	2	1	1	1	1	1	1	1	1	1	4	4	4	4
IPE 750 × 196	1	1	1	1	1	1	1	1	2	1	1	1	1	1	1	1	1	1	4	4	4	4

F. CROSS SECTIONAL CLASSIFICAT. OF EU HOT ROLLED IPE AND HE PROFILES

Designation HE	Pure Bending y-y				Pure Bending z-z				Compression							
	Normal Temperature		High Temperatures		Normal Temperature		High Temperatures		Normal Temperature		High Temperatures					
	S 235	S 275	S 355	S 460	S 235	S 275	S 355	S 460	S 235	S 275	S 355	S 460				
HE 100 AA	1	1	1	2	1	1	2	3	1	1	1	2	1	1	2	3
HE 100 A	1	1	1	1	1	1	1	1	1	1	1	1	1	1	1	1
HE 100 B	1	1	1	1	1	1	1	1	1	1	1	1	1	1	1	1
HE 100 C	1	1	1	1	1	1	1	1	1	1	1	1	1	1	1	1
HE 100 M	1	1	1	1	1	1	1	1	1	1	1	1	1	1	1	1
HE 120 AA	1	2	3	3	2	3	3	3	1	2	3	3	2	3	3	3
HE 120 A	1	1	1	1	1	1	1	2	1	1	1	1	1	1	1	2
HE 120 B	1	1	1	1	1	1	1	1	1	1	1	1	1	1	1	1
HE 120 C	1	1	1	1	1	1	1	1	1	1	1	1	1	1	1	1
HE 120 M	1	1	1	1	1	1	1	1	1	1	1	1	1	1	1	1
HE 140 AA	2	3	3	3	3	3	3	4	2	3	3	3	3	3	3	4
HE 140 A	1	1	1	2	1	1	2	3	1	1	1	2	1	1	2	3
HE 140 B	1	1	1	1	1	1	1	1	1	1	1	1	1	1	1	1
HE 140 C	1	1	1	1	1	1	1	1	1	1	1	1	1	1	1	1
HE 140 M	1	1	1	1	1	1	1	1	1	1	1	1	1	1	1	1
HE 160 AA	1	2	3	3	3	3	3	4	1	2	3	3	3	3	3	4
HE 160 A	1	1	1	2	1	1	2	3	1	1	1	2	1	1	2	3
HE 160 B	1	1	1	1	1	1	1	1	1	1	1	1	1	1	1	1
HE 160 C	1	1	1	1	1	1	1	1	1	1	1	1	1	1	1	1
HE 160 M	1	1	1	1	1	1	1	1	1	1	1	1	1	1	1	1
HE 180 AA	2	3	3	3	3	3	3	4	2	3	3	3	3	3	3	4
HE 180 A	1	1	2	3	1	2	3	3	1	2	3	3	1	2	3	3
HE 180 B	1	1	1	1	1	1	1	1	1	1	1	1	1	1	1	1
HE 180 C	1	1	1	1	1	1	1	1	1	1	1	1	1	1	1	1
HE 180 M	1	1	1	1	1	1	1	1	1	1	1	1	1	1	1	1
HE 200 AA	2	3	3	3	3	3	4	4	2	3	3	3	3	3	4	4
HE 200 A	1	1	2	3	2	3	3	3	1	1	2	3	2	3	3	3
HE 200 B	1	1	1	1	1	1	1	1	1	1	1	1	1	1	1	1
HE 200 C	1	1	1	1	1	1	1	1	1	1	1	1	1	1	1	1

F.1. CROSS SECTIONAL CLASSIFICATION FOR PURE COMPRESSION AND PURE BENDING

Designation HE	Pure Bending y-y				Pure Bending z-z				Compression			
	Normal Temperature		High Temperatures		Normal Temperature		High Temperatures		Normal Temperature		High Temperatures	
	S 235	S 275	S 355	S 460	S 235	S 275	S 355	S 460	S 235	S 275	S 355	S 460
HE 200 M	1	1	1	1	1	1	1	1	1	1	1	1
HE 220 AA	3	3	3	4	3	3	4	4	3	3	3	4
HE 220 A	1	1	2	3	2	3	3	3	1	1	2	3
HE 220 B	1	1	1	1	1	1	1	1	1	1	1	1
HE 220 C	1	1	1	1	1	1	1	1	1	1	1	1
HE 220 M	1	1	1	1	1	1	1	1	1	1	1	1
HE 240 AA	3	3	3	4	3	3	4	4	3	3	3	4
HE 240 A	1	1	2	3	2	3	3	3	1	1	2	3
HE 240 B	1	1	1	1	1	1	1	2	1	1	1	1
HE 240 C	1	1	1	1	1	1	1	1	1	1	1	1
HE 240 M	1	1	1	1	1	1	1	1	1	1	1	1
HE 260 AA	3	3	3	4	3	3	4	4	3	3	3	4
HE 260 A	1	1	3	3	2	3	3	3	1	1	3	3
HE 260 B	1	1	1	1	1	1	1	2	1	1	1	1
HE 260 C	1	1	1	1	1	1	1	1	1	1	1	1
HE 260 M	1	1	1	1	1	1	1	1	1	1	1	1
HE 280 AA	3	3	3	4	3	4	4	4	3	3	3	4
HE 280 A	1	2	3	3	3	3	3	4	1	2	3	3
HE 280 B	1	1	1	1	1	1	1	3	1	1	1	1
HE 280 C	1	1	1	1	1	1	1	1	1	1	1	1
HE 280 M	1	1	1	1	1	1	1	1	1	1	1	1
HE 300 AA	3	3	3	4	3	4	4	4	3	3	3	4
HE 300 A	1	2	3	3	2	3	3	3	1	2	3	3
HE 300 B	1	1	1	1	1	1	1	3	1	1	1	1
HE 300 C	1	1	1	1	1	1	1	1	1	1	1	1
HE 300 M	1	1	1	1	1	1	1	1	1	1	1	1
HE 320 AA	3	3	3	4	3	3	4	4	3	3	3	4
HE 320 A	1	1	2	3	1	2	3	3	1	1	2	3
HE 320 B	1	1	1	1	1	1	1	2	1	1	1	1

F. CROSS SECTIONAL CLASSIFICAT. OF EU HOT ROLLED IPE AND HE PROFILES

Designation HE	Pure Bending y-y				Pure Bending z-z				Compression			
	Normal Temperature		High Temperatures		Normal Temperature		High Temperatures		Normal Temperature		High Temperatures	
	S 235	S 275	S 355	S 460	S 235	S 275	S 355	S 460	S 235	S 275	S 355	S 460
HE 320 C	1	1	1	1	1	1	1	1	1	1	1	1
HE 320 M	1	1	1	1	1	1	1	1	1	1	1	1
HE 340 AA	3	3	3	4	3	3	3	4	3	3	3	4
HE 340 A	1	1	1	3	1	2	3	3	1	1	1	3
HE 340 B	1	1	1	1	1	1	1	1	1	1	1	1
HE 340 M	1	1	1	1	1	1	1	1	1	1	1	1
HE 360 AA	2	3	3	3	3	3	4	4	2	3	3	3
HE 360 A	1	1	1	2	1	1	2	3	1	1	1	2
HE 360 B	1	1	1	1	1	1	1	1	1	1	1	1
HE 360 M	1	1	1	1	1	1	1	1	1	1	1	1
HE 400 AA	2	2	3	3	3	3	3	4	2	2	3	4
HE 400 A	1	1	1	1	1	1	1	3	1	1	2	2
HE 400 B	1	1	1	1	1	1	1	1	1	1	1	1
HE 400 M	1	1	1	1	1	1	1	1	1	1	1	1
HE 450 AA	1	2	3	3	3	3	3	4	1	2	3	3
HE 450 A	1	1	1	1	1	1	1	2	1	1	2	3
HE 450 B	1	1	1	1	1	1	1	1	1	1	1	2
HE 450 M	1	1	1	1	1	1	1	1	1	1	1	1
HE 500 AA	1	2	3	3	2	3	3	3	2	3	4	4
HE 500 A	1	1	1	1	1	1	1	1	1	2	3	4
HE 500 B	1	1	1	1	1	1	1	1	1	1	2	2
HE 500 M	1	1	1	1	1	1	1	1	1	1	1	1
HE 550 AA	1	1	2	3	2	2	3	3	3	3	4	4
HE 550 A	1	1	1	1	1	1	1	1	2	2	4	4
HE 550 B	1	1	1	1	1	1	1	1	1	1	2	3
HE 550 M	1	1	1	1	1	1	1	1	1	1	1	1
HE 600 AA	1	1	2	3	1	2	3	3	1	2	3	3
HE 600 A	1	1	1	1	1	1	1	1	2	3	4	4
HE 600 B	1	1	1	1	1	1	1	1	1	2	3	4

F.1. CROSS SECTIONAL CLASSIFICATION FOR PURE COMPRESSION AND PURE BENDING

Designation HE	Pure Bending y-y				Pure Bending z-z				Compression														
	Normal Temperature		High Temperatures		Normal Temperature		High Temperatures		Normal Temperature		High Temperatures												
	S 235	S 275	S 355	S 460	S 235	S 275	S 355	S 460	S 235	S 275	S 355	S 460											
HE 600 M	1	1	1	1	1	1	1	1	1	1	1	1	1	2	3								
HE 600 × 337	1	1	1	1	1	1	1	1	1	1	1	1	1	1	1								
HE 600 × 399	1	1	1	1	1	1	1	1	1	1	1	1	1	1	1								
HE 650 AA	1	1	1	3	1	2	3	3	1	1	1	3	1	2	3	3	4	4	4	4			
HE 650 A	1	1	1	1	1	1	1	1	1	1	1	1	1	1	1	3	4	4	4	4			
HE 650 B	1	1	1	1	1	1	1	1	1	1	1	1	1	1	2	2	3	4	3	4	4	4	
HE 650 M	1	1	1	1	1	1	1	1	1	1	1	1	1	1	1	1	1	2	1	1	2	3	
HE 650 × 343	1	1	1	1	1	1	1	1	1	1	1	1	1	1	1	1	1	1	1	1	1	2	
HE 650 × 407	1	1	1	1	1	1	1	1	1	1	1	1	1	1	1	1	1	1	1	1	1	1	
HE 700 AA	1	1	1	2	1	1	2	3	1	1	1	2	1	1	2	3	4	4	4	4	4	4	
HE 700 A	1	1	1	1	1	1	1	1	1	1	1	1	1	1	1	3	4	4	4	4	4	4	
HE 700 B	1	1	1	1	1	1	1	1	1	1	1	1	1	1	2	2	4	4	3	4	4	4	
HE 700 M	1	1	1	1	1	1	1	1	1	1	1	1	1	1	1	1	2	3	1	2	3	4	
HE 700 × 352	1	1	1	1	1	1	1	1	1	1	1	1	1	1	1	1	1	1	1	1	1	2	3
HE 700 × 418	1	1	1	1	1	1	1	1	1	1	1	1	1	1	1	1	1	1	1	1	1	1	
HE 800 AA	1	1	1	1	1	1	2	3	1	1	1	1	1	1	2	3	4	4	4	4	4	4	
HE 800 A	1	1	1	1	1	1	1	2	1	1	1	1	1	1	1	4	4	4	4	4	4	4	
HE 800 B	1	1	1	1	1	1	1	1	1	1	1	1	1	1	3	3	4	4	4	4	4	4	
HE 800 M	1	1	1	1	1	1	1	1	1	1	1	1	1	1	1	2	3	4	2	3	4	4	
HE 800 × 373	1	1	1	1	1	1	1	1	1	1	1	1	1	1	1	1	2	2	1	2	3	4	
HE 800 × 444	1	1	1	1	1	1	1	1	1	1	1	1	1	1	1	1	1	1	1	1	1	2	
HE 900 AA	1	1	1	1	1	1	2	3	1	1	1	1	1	1	2	4	4	4	4	4	4	4	
HE 900 A	1	1	1	1	1	1	1	2	1	1	1	1	1	1	1	4	4	4	4	4	4	4	
HE 900 B	1	1	1	1	1	1	1	1	1	1	1	1	1	1	3	4	4	4	4	4	4	4	
HE 900 M	1	1	1	1	1	1	1	1	1	1	1	1	1	1	2	3	4	4	4	4	4	4	
HE 900 × 391	1	1	1	1	1	1	1	1	1	1	1	1	1	1	1	2	2	4	2	3	4	4	
HE 900 × 466	1	1	1	1	1	1	1	1	1	1	1	1	1	1	1	1	1	2	1	1	2	4	
HE 1000 AA	1	1	1	2	1	1	2	3	1	1	1	1	1	1	1	4	4	4	4	4	4	4	
HE 1000 × 249	1	1	1	2	1	1	2	3	1	1	1	1	1	1	1	4	4	4	4	4	4	4	

F. CROSS SECTIONAL CLASSIFICAT. OF EU HOT ROLLED IPE AND HE PROFILES

Designation HE	Pure Bending y-y				Pure Bending z-z				Compression															
	Normal Temperature		High Temperatures		Normal Temperature		High Temperatures		Normal Temperature		High Temperatures													
	S 235	S 275	S 355	S 460	S 235	S 275	S 355	S 460	S 235	S 275	S 355	S 460												
HE 1000 A	1	1	1	2	1	1	2	3	1	1	1	1	1	1	1	1	4	4	4	4	4	4	4	4
HE 1000 B	1	1	1	1	1	1	1	2	1	1	1	1	1	1	1	1	4	4	4	4	4	4	4	4
HE 1000 M	1	1	1	1	1	1	1	1	1	1	1	1	1	1	1	1	3	4	4	4	4	4	4	4
HE 1000 × 393	1	1	1	1	1	1	1	1	1	1	1	1	1	1	1	1	2	3	4	4	3	4	4	4
HE 1000 × 415	1	1	1	1	1	1	1	1	1	1	1	1	1	1	1	1	2	2	3	4	3	4	4	4
HE 1000 × 438	1	1	1	1	1	1	1	1	1	1	1	1	1	1	1	1	1	2	3	4	2	3	4	4
HE 1000 × 494	1	1	1	1	1	1	1	1	1	1	1	1	1	1	1	1	1	1	2	3	1	2	3	4
HE 1000 × 584	1	1	1	1	1	1	1	1	1	1	1	1	1	1	1	1	1	1	1	2	1	1	2	3

F.2. CROSS SECTIONAL CLASSIFICATION FOR COMBINED COMPRESSION AND BENDING MOMENT

This annex gives tables for the cross sectional classification of European hot rolled profiles (IPE and HE sections) for the case of combined compression and bending moment about the strong axis (M_y) (using Eq. (5.17) and Eq. (5.30)) and the weak axis (M_z) for normal and high temperature. Although for the case of combined compression and bending about the weak axis the classification is the same as for pure compression whatever the magnitude of the compression force, it was decided nevertheless to consider it in these tables. For each column the given value, N_{Ed} or $N_{fi,Ed}$, is the maximum compression force for which the profile remains in the specified class of that column. Cases where the section is always Class 1, 2 or 3 whatever the value of the compression force, are denoted by an asterisk (*). A profile with all the cells empty is Class 4. Also denoted by an asterisk are the cases where the compression force exceeds the value shown on the left cell, but the section class does not change for bigger values of that force.

The following examples illustrate the use of the tables:

1. Consider a profile IPE 360 in steel grade S355 under fire condition.

F.2. CROSS SECTIONAL CLASSIFICATION FOR COMBINED COMPR. AND BENDING MOMENT

a) For combined compression and bending about the strong axis:

If $N_{\bar{f}_i,Ed} \leq 240$ kN \Rightarrow Class 1

If $240 < N_{\bar{f}_i,Ed} \leq 385$ kN \Rightarrow Class 2

If $385 < N_{\bar{f}_i,Ed} \leq 1714$ kN \Rightarrow Class 3

If $N_{\bar{f}_i,Ed} > 1714$ kN \Rightarrow Class 4

b) For combined compression and bending about the weak axis:

Class 4 whatever the magnitude of the compression force.

2. Consider a profile IPE 180 in steel grade S275 under fire condition.

a) For combined compression and bending about the strong axis:

If $N_{\bar{f}_i,Ed} \leq 190$ kN \Rightarrow Class 1

If $N_{\bar{f}_i,Ed} > 190$ kN \Rightarrow Class 2

b) For combined compression and bending about the weak axis:

Class 2 whatever the magnitude of the compression force.

S235												
Maximum compression force N_{Ed} or $N_{\bar{f}_i,Ed}$ (kN)												
Designation IPE	Bending about y-y						Bending about z-z					
	Normal Temperature Section class			High Temperature Section class			Normal Temperature Section class			High Temperature Section class		
	Class 1	Class 2	Class 3	Class 1	Class 2	Class 3	Class 1	Class 2	Class 3	Class 1	Class 2	Class 3
IPE AA 80	*			*			*			*		
IPE A 80	*			*			*			*		
IPE 80	*			*			*			*		
IPE AA 100	*			*			*			*		
IPE A 100	*			*			*			*		
IPE 100	*			*			*			*		
IPE AA 120	*			*			*			*		
IPE A 120	*			*			*			*		
IPE 120	*			*			*			*		
IPE AA 140	*			91	*		*				*	
IPE A 140	*			91	*		*				*	
IPE 140	*			*			*			*		

F. CROSS SECTIONAL CLASSIFICAT. OF EU HOT ROLLED IPE AND HE PROFILES

S235												
Maximum compression force N_{Ed} or $N_{fi,Ed}$ (kN)												
Bending about y-y						Bending about z-z						
Designation IPE	Normal Temperature Section class			High Temperature Section class			Normal Temperature Section class			High Temperature Section class		
	Class 1	Class 2	Class 3	Class 1	Class 2	Class 3	Class 1	Class 2	Class 3	Class 1	Class 2	Class 3
IPE AA 160	*			90	120	*	*					*
IPE A 160	*			94	*		*				*	
IPE 160	*			*			*			*		
IPE AA 180	140	*		100	134	*		*				*
IPE A 180	140	*		100	134	*		*				*
IPE 180	*			*			*			*		
IPE O 180	*			*			*			*		
IPE AA 200	148	*		104	141	*		*				*
IPE A 200	148	*		104	141	*		*				*
IPE 200	*			205	*		*				*	
IPE O 200	*			*			*			*		
IPE AA 220	150	*		103	144	581		*				
IPE A 220	181	*		128	174	*		*				*
IPE 220	*			215	*		*				*	
IPE O 220	*			*			*			*		
IPE AA 240	148	198	*	99	141	632			*			
IPE A 240	190	*		132	182	753		*				
IPE 240	*			233	*		*				*	
IPE O 240	*			*			*			*		
IPE A 270	193	259	*	128	184	773			*			
IPE 270	335	*		242	322	*		*				*
IPE O 270	*			357	*		*				*	
IPE A 300	231	312	*	151	220	887			*			
IPE 300	371	*		262	355	*		*				*
IPE O 300	*			383	*		*				*	

F.2. CROSS SECTIONAL CLASSIFICATION FOR COMBINED COMPR. AND BENDING MOMENT

S235												
Maximum compression force N_{Ed} or $N_{fi,Ed}$ (kN)												
Bending about y-y						Bending about z-z						
Designation IPE	Normal Temperature Section class			High Temperature Section class			Normal Temperature Section class			High Temperature Section class		
	Class 1	Class 2	Class 3	Class 1	Class 2	Class 3	Class 1	Class 2	Class 3	Class 1	Class 2	Class 3
IPE A 330	255	346	*	164	242	1006			*			
IPE 330	401	*		280	384	1444		*				
IPE O 330	*			421	*		*				*	
IPE A 360	232	326	1341	138	219	1023						
IPE 360	441	*		304	422	1596		*				
IPE O 360	*			484	640	*	*					*
IPE A 400	241	347	1427	136	226	1080						
IPE 400	493	653	*	334	470	1768			*			
IPE O 400	709	*		507	680	*		*				*
IPE A 450	254	380	1532	130	237	1147						
IPE 450	557	749	*	367	530	1920			*			
IPE O 450	904	*		644	867	*		*				*
IPE A 500	299	452	1756	147	277	1309						
IPE 500	626	851	*	402	594	2126			*			
IPE O 500	1045	*		736	1001	*		*				*
IPE A 550	323	499	1951	149	298	1446						
IPE 550	732	999	3135	467	694	2421						
IPE O 550	1128	*		782	1079	3497		*				
IPE A 600	373	582	2248	167	344	1662						
IPE 600	835	1148	3558	526	791	2741						
IPE O 600	1688	*		1205	1620	*		*				*
IPE 750 ×137	327	614	2275	43	287	1616						
IPE 750 ×147	697	1075	3142	322	644	2329						
IPE 750 ×173	1008	1458	4274	563	945	3232						
IPE 750 ×196	1359	1887	5507	836	1285	4225						

F. CROSS SECTIONAL CLASSIFICAT. OF EU HOT ROLLED IPE AND HE PROFILES

Designation IPE	S275											
	Maximum compression force N_{Ed} or $N_{fi,Ed}$ (kN)											
	Bending about y-y						Bending about z-z					
	Normal Temperature Section class			High Temperature Section class			Normal Temperature Section class			High Temperature Section class		
Class 1	Class 2	Class 3	Class 1	Class 2	Class 3	Class 1	Class 2	Class 3	Class 1	Class 2	Class 3	
IPE AA 80	*			*			*			*		
IPE A 80	*			*			*			*		
IPE 80	*			*			*			*		
IPE AA 100	*			*			*			*		
IPE A 100	*			*			*			*		
IPE 100	*			*			*			*		
IPE AA 120	*			*			*			*		
IPE A 120	*			*			*			*		
IPE 120	*			*			*			*		
IPE AA 140	*			91	*		*				*	
IPE A 140	*			91	*		*				*	
IPE 140	*			*			*			*		
IPE AA 160	126	*		89	120	*		*				*
IPE A 160	129	*		92	124	*		*				*
IPE 160	*			*			*			*		
IPE AA 180	140	*		97	134	501		*				
IPE A 180	140	*		97	134	516		*				
IPE 180	*			190	*		*				*	
IPE O 180	*			*			*			*		
IPE AA 200	147	195	*	100	140	566			*			
IPE A 200	147	195	*	100	140	582			*			
IPE 200	*			206	*		*				*	
IPE O 200	*			*			*			*		
IPE AA 220	148	200	*	97	141	600			*			
IPE A 220	181	239	*	122	172	695			*			
IPE 220	*			214	284	*	*					*
IPE O 220	*			301	*		*				*	
IPE AA 240	144	198	844	91	137	650						
IPE A 240	188	252	*	126	180	779			*			
IPE 240	321	*		231	308	*		*				*
IPE O 240	*			335	*		*				*	

F.2. CROSS SECTIONAL CLASSIFICATION FOR COMBINED COMPR. AND BENDING MOMENT

Designation IPE	S275											
	Maximum compression force N_{Ed} or $N_{fi,Ed}$ (kN)											
	Bending about y-y						Bending about z-z					
	Normal Temperature Section class			High Temperature Section class			Normal Temperature Section class			High Temperature Section class		
Class 1	Class 2	Class 3	Class 1	Class 2	Class 3	Class 1	Class 2	Class 3	Class 1	Class 2	Class 3	
IPE A 270	187	258	1033	117	178	795						
IPE 270	337	*		236	323	1247		*				
IPE O 270	*			357	*		*			*		
IPE A 300	223	311	1187	137	211	910						
IPE 300	370	*		253	353	1351		*				
IPE O 300	528	*		380	507	*		*				*
IPE A 330	244	344	1348	146	231	1029						
IPE 330	398	530	*	268	380	1495			*			
IPE O 330	583	*		415	559	*		*				*
IPE A 360	216	318	1382	115	202	1039						
IPE 360	435	586	*	287	414	1648			*			
IPE O 360	672	*		475	644	*		*				*
IPE A 400	220	335	1465	106	204	1090						
IPE 400	483	657	*	311	459	1822			*			
IPE O 400	710	*		492	679	2519		*				
IPE A 450	225	360	1566	90	206	1149						
IPE 450	540	747	2567	335	511	1972						
IPE O 450	904	*		623	865	3040		*				
IPE A 500	260	426	1791	96	237	1308						
IPE 500	600	844	2850	359	566	2176						
IPE O 500	1041	1379	*	706	993	3366			*			
IPE A 550	275	465	1986	87	249	1439						
IPE 550	700	990	3248	414	660	2476						
IPE O 550	1116	1495	*	741	1063	3616			*			
IPE A 600	315	541	2285	92	284	1651						
IPE 600	795	1133	3682	460	748	2798						
IPE O 600	1691	*		1168	1617	5114		*				
IPE 750 × 137	215	526	2274		172	1561						
IPE 750 × 147	595	1003	3197	190	537	2318						
IPE 750 × 173	917	1403	4387	435	849	3259						
IPE 750 × 196	1282	1853	5689	716	1202	4302						

F. CROSS SECTIONAL CLASSIFICAT. OF EU HOT ROLLED IPE AND HE PROFILES

S355												
Maximum compression force N_{Ed} or $N_{fi,Ed}$ (kN)												
Bending about y-y						Bending about z-z						
Designation IPE	Normal Temperature Section class			High Temperature Section class			Normal Temperature Section class			High Temperature Section class		
	Class 1	Class 2	Class 3	Class 1	Class 2	Class 3	Class 1	Class 2	Class 3	Class 1	Class 2	Class 3
IPE AA 80	*			*			*			*		
IPE A 80	*			*			*			*		
IPE 80	*			*			*			*		
IPE AA 100	*			*			*			*		
IPE A 100	*			*			*			*		
IPE 100	*			*			*			*		
IPE AA 120	*			109	*		*				*	
IPE A 120	*			109	*		*				*	
IPE 120	*			*			*			*		
IPE AA 140	126	*		88	121	444		*				
IPE A 140	126	*		88	121	464		*				
IPE 140	*			172	*		*				*	
IPE AA 160	124	167	*	82	118	452			*			
IPE A 160	129	171	*	86	123	500			*			
IPE 160	*			183	*		*				*	
IPE AA 180	137	186	*	88	130	528			*			
IPE A 180	137	186	*	88	130	543			*			
IPE 180	262	*		188	251	*		*				*
IPE O 180	*			275	*		*				*	
IPE AA 200	141	195	771	88	134	593						
IPE A 200	141	195	793	88	134	609						
IPE 200	284	*		202	273	*		*				*
IPE O 200	*			279	*		*				*	
IPE AA 220	138	197	819	80	130	622						
IPE A 220	173	240	947	107	164	727						
IPE 220	298	*		206	285	1123		*				
IPE O 220	414	*		299	398	*		*				*
IPE AA 240	131	192	889	70	122	669						
IPE A 240	178	251	1063	107	168	812						
IPE 240	322	*		220	307	1274		*				
IPE O 240	462	*		333	444	*		*				*

F.2. CROSS SECTIONAL CLASSIFICATION FOR COMBINED COMPR. AND BENDING MOMENT

S355												
Maximum compression force N_{Ed} or $N_{fi,Ed}$ (kN)												
	Bending about y-y						Bending about z-z					
Designation IPE	Normal Temperature Section class			High Temperature Section class			Normal Temperature Section class			High Temperature Section class		
	Class 1	Class 2	Class 3	Class 1	Class 2	Class 3	Class 1	Class 2	Class 3	Class 1	Class 2	Class 3
IPE A 270	169	250	1088	90	158	817						
IPE 270	331	447	*	216	315	1316			*			
IPE O 270	495	*		347	474	1887		*				
IPE A 300	199	298	1247	101	185	932						
IPE 300	357	491	1840	224	338	1417						
IPE O 300	529	699	*	360	505	2009			*			
IPE A 330	214	327	1411	103	199	1049						
IPE 330	379	529	2040	231	358	1562						
IPE O 330	579	772	*	389	552	2230			*			
IPE A 360	175	291	1430	60	158	1040						
IPE 360	409	579	2251	240	385	1714						
IPE O 360	664	890	*	441	633	2510			*			
IPE A 400	166	297	1505	37	148	1078						
IPE 400	446	644	2490	251	419	1885						
IPE O 400	691	942	*	443	656	2651			*			
IPE A 450	152	306	1591		130	1118						
IPE 450	485	721	2700	252	452	2024						
IPE O 450	878	1200	4140	558	832	3196						
IPE A 500	167	355	1813		140	1264						
IPE 500	526	803	2984	251	487	2218						
IPE O 500	998	1382	4588	618	945	3524						
IPE A 550	161	377	1999		131	1379						
IPE 550	609	937	3396	284	563	2519						
IPE O 550	1054	1484	4935	629	994	3767						
IPE A 600	177	433	2296		141	1575						
IPE 600	681	1065	3841	301	627	2837						
IPE O 600	1643	2243	6964	1049	1559	5379						
IPE 750 × 137		313	2200			1390						
IPE 750 × 147	350	815	3221		285	2222						
IPE 750 × 173	687	1240	4500	139	609	3219						
IPE 750 × 196	1071	1720	5913	429	981	4338						

F. CROSS SECTIONAL CLASSIFICAT. OF EU HOT ROLLED IPE AND HE PROFILES

S460												
Maximum compression force N_{Ed} or $N_{fi,Ed}$ (kN)												
Bending about y-y						Bending about z-z						
Designation IPE	Normal Temperature Section class			High Temperature Section class			Normal Temperature Section class			High Temperature Section class		
	Class 1	Class 2	Class 3	Class 1	Class 2	Class 3	Class 1	Class 2	Class 3	Class 1	Class 2	Class 3
IPE AA 80	*			*			*			*		
IPE A 80	*			*			*			*		
IPE 80	*			*			*			*		
IPE AA 100	*			116	*		*				*	
IPE A 100	*			116	*		*				*	
IPE 100	*			*			*			*		
IPE AA 120	151	*		108	145	*		*				*
IPE A 120	151	*		108	145	*		*				*
IPE 120	*			170	*		*				*	
IPE AA 140	123	167	*	80	117	468			*			
IPE A 140	123	167	*	80	117	490			*			
IPE 140	237	*		171	228	*		*				*
IPE AA 160	116	165	617		109	470						
IPE A 160	122	171	682	74	116	522						
IPE 160	253	*		178	243	*		*				*
IPE AA 180	126	182	722		118	546						
IPE A 180	126	182	743	70	118	562						
IPE 180	261	347	*	177	250	977			*			
IPE O 180	380	*		272	365	*		*				*
IPE AA 200	127	189	812	66	119	609						
IPE A 200	127	189	835	66	119	626						
IPE 200	282	377	*	187	268	1110			*			
IPE O 200	386	*		271	370	1461		*				
IPE AA 220	118	185	855		108	631						
IPE A 220	155	231	996	80	145	746						
IPE 220	289	395	1530	185	275	1182						
IPE O 220	416	*		285	398	1586		*				
IPE AA 240	106	176	921	37	96	670						
IPE A 240	156	238	1114	75	145	828						
IPE 240	310	427	1737	195	294	1338						
IPE O 240	463	611	*	316	442	1822			*			

F.2. CROSS SECTIONAL CLASSIFICATION FOR COMBINED COMPR. AND BENDING MOMENT

S460												
Maximum compression force N_{Ed} or $N_{fi,Ed}$ (kN)												
	Bending about y-y						Bending about z-z					
Designation IPE	Normal Temperature Section class			High Temperature Section class			Normal Temperature Section class			High Temperature Section class		
	Class 1	Class 2	Class 3	Class 1	Class 2	Class 3	Class 1	Class 2	Class 3	Class 1	Class 2	Class 3
IPE A 270	136	228	1125		123	817						
IPE 270	308	441	1799	178	290	1366						
IPE O 270	486	656	*	317	462	1993			*			
IPE A 300	155	268	1285			927						
IPE 300	323	476	1940	171	301	1458						
IPE O 300	508	702	2740	316	481	2106						
IPE A 330	161	289	1449		143	1037						
IPE 330	336	506	2141	167	312	1598						
IPE O 330	551	770	3044	334	520	2329						
IPE A 360	105	238	1443		87	999						
IPE 360	352	546	2352	160	325	1741						
IPE O 360	626	883	3428	372	590	2615						
IPE A 400	80	228	1502		59	1017						
IPE 400	373	598	2591	151	342	1902						
IPE O 400	635	921	3626	352	595	2740						
IPE A 450	36	212	1565		12	1026						
IPE 450	384	652	2788	118	346	2019						
IPE O 450	802	1169	4373	438	750	3298						
IPE A 500	21	235	1773			1148						
IPE 500	393	708	3062	80	348	2191						
IPE O 500	895	1332	4828	462	833	3617						
IPE A 550		230	1939			1232						
IPE 550	448	822	3480	78	395	2482						
IPE O 550	919	1409	5168	435	851	3838						
IPE A 600		255	2219			1399						
IPE 600	484	921	3923	51	422	2780						
IPE O 600	1506	2189	7360	830	1410	5556						
IPE 750 ×137			2000			1078						
IPE 750 ×147		500	3125			1988						
IPE 750 ×173	315	945	4486		227	3028						
IPE 750 ×196	714	1453	6008		611	4215						

F. CROSS SECTIONAL CLASSIFICAT. OF EU HOT ROLLED IPE AND HE PROFILES

S235												
Maximum compression force N_{Ed} or $N_{fi,Ed}$ (kN)												
	Bending about y-y						Bending about z-z					
Designation HE	Normal Temperature Section class			High Temperature Section class			Normal Temperature Section class			High Temperature Section class		
	Class 1	Class 2	Class 3	Class 1	Class 2	Class 3	Class 1	Class 2	Class 3	Class 1	Class 2	Class 3
HE 100 AA	*			*			*			*		
HE 100 A	*			*			*			*		
HE 100 B	*			*			*			*		
HE 100 C	*			*			*			*		
HE 100 M	*			*			*			*		
HE 120 AA	*				*		*				*	
HE 120 A	*			*			*			*		
HE 120 B	*			*			*			*		
HE 120 C	*			*			*			*		
HE 120 M	*			*			*			*		
HE 140 AA		*				*		*				*
HE 140 A	*			*			*			*		
HE 140 B	*			*			*			*		
HE 140 C	*			*			*			*		
HE 140 M	*			*			*			*		
HE 160 AA	*					*	*					*
HE 160 A	*			*			*			*		
HE 160 B	*			*			*			*		
HE 160 C	*			*			*			*		
HE 160 M	*			*			*			*		
HE 180 AA		*				*		*				*
HE 180 A	*			*			*			*		
HE 180 B	*			*			*			*		
HE 180 C	*			*			*			*		
HE 180 M	*			*			*			*		
HE 200 AA		*				*		*				*
HE 200 A	*				*		*				*	
HE 200 B	*			*			*			*		
HE 200 C	*			*			*			*		
HE 200 M	*			*			*			*		
HE 220 AA			*			*			*			*

F.2. CROSS SECTIONAL CLASSIFICATION FOR COMBINED COMPR. AND BENDING MOMENT

S235												
Maximum compression force N_{Ed} or $N_{fi,Ed}$ (kN)												
Designation HE	Bending about y-y						Bending about z-z					
	Normal Temperature Section class			High Temperature Section class			Normal Temperature Section class			High Temperature Section class		
	Class 1	Class 2	Class 3	Class 1	Class 2	Class 3	Class 1	Class 2	Class 3	Class 1	Class 2	Class 3
HE 220 A	*				*		*				*	
HE 220 B	*			*			*			*		
HE 220 C	*			*			*			*		
HE 220 M	*			*			*			*		
HE 240 AA			*			*			*			*
HE 240 A	*				*		*				*	
HE 240 B	*			*			*			*		
HE 240 C	*			*			*			*		
HE 240 M	*			*			*			*		
HE 260 AA			*			*			*			*
HE 260 A	*				*		*				*	
HE 260 B	*			*			*			*		
HE 260 C	*			*			*			*		
HE 260 M	*			*			*			*		
HE 280 AA			*			*			*			*
HE 280 A	*					*		*				*
HE 280 B	*			*			*			*		
HE 280 C	*			*			*			*		
HE 280 M	*			*			*			*		
HE 300 AA			*			*			*			*
HE 300 A	*					*		*			*	
HE 300 B	*			*			*			*		
HE 300 C	*			*			*			*		
HE 300 M	*			*			*			*		
HE 320 AA			*			*			*			*
HE 320 A	*			*			*			*		
HE 320 B	*			*			*			*		
HE 320 C	*			*			*			*		
HE 320 M	*			*			*			*		
HE 340 AA			*			*			*			*
HE 340 A	*			*			*			*		

F. CROSS SECTIONAL CLASSIFICAT. OF EU HOT ROLLED IPE AND HE PROFILES

Designation HE	S235											
	Maximum compression force N_{Ed} or $N_{fi,Ed}$ (kN)											
	Bending about y-y						Bending about z-z					
	Normal Temperature Section class			High Temperature Section class			Normal Temperature Section class			High Temperature Section class		
Class 1	Class 2	Class 3	Class 1	Class 2	Class 3	Class 1	Class 2	Class 3	Class 1	Class 2	Class 3	
HE 340 B	*			*			*			*		
HE 340 M	*			*			*			*		
HE 360 AA		*				*		*				*
HE 360 A	*			*			*			*		
HE 360 B	*			*			*			*		
HE 360 M	*			*			*			*		
HE 400 AA		*				*		*				*
HE 400 A	*			*			*			*		
HE 400 B	*			*			*			*		
HE 400 M	*			*			*			*		
HE 450 AA	748	*				*		*				*
HE 450 A	*			823	*		*				*	
HE 450 B	*			*			*			*		
HE 450 M	*			*			*			*		
HE 500 AA	764	*			731	3028		*				
HE 500 A	*			822	1087	*	*					*
HE 500 B	*			*			*			*		
HE 500 M	*			*			*			*		
HE 550 AA	892	1179	*		852	3250			*			
HE 550 A	1148	*		813	1101	*		*				*
HE 550 B	*			1432	*		*				*	
HE 550 M	*			*			*			*		
HE 600 AA	902	1214	*	593	858	3164			*			
HE 600 A	1163	*		800	1112	4959		*				
HE 600 B	*			1426	*		*				*	
HE 600 M	*			*			*			*		
HE 600 × 337	*			*			*			*		
HE 600 × 399	*			*			*			*		
HE 650 AA	910	1249	4026	574	862	3103						
HE 650 A	1176	1571	*	784	1120	4839			*			
HE 650 B	1966	*		1416	1888	*		*				*

F.2. CROSS SECTIONAL CLASSIFICATION FOR COMBINED COMPR. AND BENDING MOMENT

Designation HE	S235											
	Maximum compression force N_{Ed} or $N_{fi,Ed}$ (kN)											
	Bending about y-y						Bending about z-z					
	Normal Temperature Section class			High Temperature Section class			Normal Temperature Section class			High Temperature Section class		
Class 1	Class 2	Class 3	Class 1	Class 2	Class 3	Class 1	Class 2	Class 3	Class 1	Class 2	Class 3	
HE 650 M	*			*			*			*		
HE 650 × 343	*			*			*			*		
HE 650 × 407	*			*			*			*		
HE 700 AA	915	1282	4066	552	864	3109						
HE 700 A	1332	1788	*	881	1268	5096			*			
HE 700 B	2170	*		1550	2082	*		*				*
HE 700 M	*			*			*			*		
HE 700 × 352	*			*			*			*		
HE 700 × 418	*			*			*			*		
HE 800 AA	930	1355	4142	509	870	3124						
HE 800 A	1211	1699	6052	728	1143	4625						
HE 800 B	2039	2703	*	1381	1946	6984			*			
HE 800 M	*			2552	*		*				*	
HE 800 × 373	*			*			*			*		
HE 800 × 444	*			*			*			*		
HE 900 AA	925	1413	4294	441	856	3192						
HE 900 A	1215	1771	6079	666	1138	4585						
HE 900 B	2067	2810	*	1332	1963	6845			*			
HE 900 M	3098	*		2151	2964	9557		*				
HE 900 × 391	*			3778	*		*				*	
HE 900 × 466	*			*			*			*		
HE 1000 AA	904	1459	4363	354	826	3196						
HE 1000 × 249	1050	1640	5171	465	967	3820						
HE 1000 A	1050	1640	5660	465	967	4181						
HE 1000 B	1889	2672	8251	1114	1779	6287						
HE 1000 M	2689	3646	*	1742	2555	8283			*			
HE 1000 × 393	4312	*		3034	4132	*		*				*
HE 1000 × 415	5191	*		3739	4985	*		*				*
HE 1000 × 438	*			4163	*		*				*	
HE 1000 × 494	*			*			*			*		
HE 1000 × 584	*			*			*			*		

F. CROSS SECTIONAL CLASSIFICAT. OF EU HOT ROLLED IPE AND HE PROFILES

S275												
Maximum compression force N_{Ed} or $N_{fi,Ed}$ (kN)												
Bending about y-y						Bending about z-z						
Designation HE	Normal Temperature Section class			High Temperature Section class			Normal Temperature Section class			High Temperature Section class		
	Class 1	Class 2	Class 3	Class 1	Class 2	Class 3	Class 1	Class 2	Class 3	Class 1	Class 2	Class 3
HE 100 AA	*			*			*			*		
HE 100 A	*			*			*			*		
HE 100 B	*			*			*			*		
HE 100 C	*			*			*			*		
HE 100 M	*			*			*			*		
HE 120 AA		*				*		*				*
HE 120 A	*			*			*			*		
HE 120 B	*			*			*			*		
HE 120 C	*			*			*			*		
HE 120 M	*			*			*			*		
HE 140 AA			*			*			*			*
HE 140 A	*			*			*			*		
HE 140 B	*			*			*			*		
HE 140 C	*			*			*			*		
HE 140 M	*			*			*			*		
HE 160 AA		*				*		*				*
HE 160 A	*			*			*			*		
HE 160 B	*			*			*			*		
HE 160 C	*			*			*			*		
HE 160 M	*			*			*			*		
HE 180 AA			*			*			*			*
HE 180 A	*				*		*				*	
HE 180 B	*			*			*			*		
HE 180 C	*			*			*			*		
HE 180 M	*			*			*			*		
HE 200 AA			*			*			*			*
HE 200 A	*					*	*					*
HE 200 B	*			*			*			*		
HE 200 C	*			*			*			*		
HE 200 M	*			*			*			*		
HE 220 AA			*			*			*			*

F.2. CROSS SECTIONAL CLASSIFICATION FOR COMBINED COMPR. AND BENDING MOMENT

S275												
Maximum compression force N_{Ed} or $N_{fi,Ed}$ (kN)												
Bending about y-y						Bending about z-z						
Designation HE	Normal Temperature Section class			High Temperature Section class			Normal Temperature Section class			High Temperature Section class		
	Class 1	Class 2	Class 3	Class 1	Class 2	Class 3	Class 1	Class 2	Class 3	Class 1	Class 2	Class 3
HE 220 A	*					*	*					*
HE 220 B	*			*			*			*		
HE 220 C	*			*			*			*		
HE 220 M	*			*			*			*		
HE 240 AA			*			*			*			*
HE 240 A	*					*	*					*
HE 240 B	*			*			*			*		
HE 240 C	*			*			*			*		
HE 240 M	*			*			*			*		
HE 260 AA			*			*			*			*
HE 260 A	*					*	*					*
HE 260 B	*			*			*			*		
HE 260 C	*			*			*			*		
HE 260 M	*			*			*			*		
HE 280 AA			*						*			
HE 280 A		*				*		*				*
HE 280 B	*			*			*			*		
HE 280 C	*			*			*			*		
HE 280 M	*			*			*			*		
HE 300 AA			*						*			
HE 300 A		*				*		*				*
HE 300 B	*			*			*			*		
HE 300 C	*			*			*			*		
HE 300 M	*			*			*			*		
HE 320 AA			*			*			*			*
HE 320 A	*				*		*				*	
HE 320 B	*			*			*			*		
HE 320 C	*			*			*			*		
HE 320 M	*			*			*			*		
HE 340 AA			*			*			*			*
HE 340 A	*				*		*				*	

F. CROSS SECTIONAL CLASSIFICAT. OF EU HOT ROLLED IPE AND HE PROFILES

S275												
Maximum compression force N_{Ed} or $N_{fi,Ed}$ (kN)												
Bending about y-y						Bending about z-z						
Designation HE	Normal Temperature Section class			High Temperature Section class			Normal Temperature Section class			High Temperature Section class		
	Class 1	Class 2	Class 3	Class 1	Class 2	Class 3	Class 1	Class 2	Class 3	Class 1	Class 2	Class 3
HE 340 B	*			*			*			*		
HE 340 M	*			*			*			*		
HE 360 AA			*			*			*			*
HE 360 A	*			709	*		*				*	
HE 360 B	*			*			*			*		
HE 360 M	*			*			*			*		
HE 400 AA		*				*		*				*
HE 400 A	*			830	*		*				*	
HE 400 B	*			*			*			*		
HE 400 M	*			*			*			*		
HE 450 AA		*				3280		*				
HE 450 A	*			820	1084	*	*					*
HE 450 B	*			*			*			*		
HE 450 M	*			*			*			*		
HE 500 AA		1013	*			3129			*			
HE 500 A	1141	*		807	1094	*		*				*
HE 500 B	*			1452	*		*				*	
HE 500 M	*			*			*			*		
HE 550 AA	876	1186	*		833	3352			*			
HE 550 A	1146	*		783	1095	5311		*				
HE 550 B	*			1433	*		*				*	
HE 550 M	*			*			*			*		
HE 600 AA	873	1211	4230		826	3247						
HE 600 A	1147	1544	*	755	1092	5122			*			
HE 600 B	1968	*		1410	1889	*		*				*
HE 600 M	*			*			*			*		
HE 600 × 337	*			*			*			*		
HE 600 × 399	*			*			*			*		
HE 650 AA	867	1233	4167		815	3168						
HE 650 A	1145	1573	6458	722	1085	4976						
HE 650 B	1977	*		1382	1893	7740		*				

F.2. CROSS SECTIONAL CLASSIFICATION FOR COMBINED COMPR. AND BENDING MOMENT

S275												
Maximum compression force N_{Ed} or $N_{fi,Ed}$ (kN)												
Bending about y-y						Bending about z-z						
Designation HE	Normal Temperature Section class			High Temperature Section class			Normal Temperature Section class			High Temperature Section class		
	Class 1	Class 2	Class 3	Class 1	Class 2	Class 3	Class 1	Class 2	Class 3	Class 1	Class 2	Class 3
HE 650 M	*			*			*			*		
HE 650 × 343	*			*			*			*		
HE 650 × 407	*			*			*			*		
HE 700 AA	857	1253	4194	464	801	3159						
HE 700 A	1293	1786	6809	804	1223	5234						
HE 700 B	2174	*		1502	2079	7966		*				
HE 700 M	*			2962	*		*				*	
HE 700 × 352	*			*			*			*		
HE 700 × 418	*			*			*			*		
HE 800 AA	840	1300	4247	385	775	3145						
HE 800 A	1132	1660	6241	609	1058	4697						
HE 800 B	1998	2717	*	1287	1898	7197			*			
HE 800 M	3536	*		2512	3392	*		*				*
HE 800 × 373	*			4307	*		*				*	
HE 800 × 444	*			*			*			*		
HE 900 AA	797	1325	4375	274	723	3183						
HE 900 A	1098	1699	6233	503	1014	4617						
HE 900 B	1986	2789	9171	1191	1873	7007						
HE 900 M	3067	4102	*	2043	2922	9885			*			
HE 900 × 391	5200	*		3748	4995	*		*				*
HE 900 × 466	*			*			*			*		
HE 1000 AA	733	1334	4417	138	649	3155						
HE 1000 × 249	884	1523	5254	251	794	3793						
HE 1000 A	884	1523	5752	251	794	4152						
HE 1000 B	1753	2601	8498	915	1635	6373						
HE 1000 M	2588	3623	11093	1564	2444	8485						
HE 1000 × 393	4292	5689	*	2909	4097	12249			*			
HE 1000 × 415	5218	*		3648	4996	14287		*				
HE 1000 × 438	5774	*		4093	5536	*		*				*
HE 1000 × 494	*			6390	*		*				*	
HE 1000 × 584	*			*			*			*		

F. CROSS SECTIONAL CLASSIFICAT. OF EU HOT ROLLED IPE AND HE PROFILES

S355												
Maximum compression force N_{Ed} or $N_{fi,Ed}$ (kN)												
	Bending about y-y						Bending about z-z					
Designation HE	Normal Temperature Section class			High Temperature Section class			Normal Temperature Section class			High Temperature Section class		
	Class 1	Class 2	Class 3	Class 1	Class 2	Class 3	Class 1	Class 2	Class 3	Class 1	Class 2	Class 3
HE 100 AA	*				*		*				*	
HE 100 A	*			*			*			*		
HE 100 B	*			*			*			*		
HE 100 C	*			*			*			*		
HE 100 M	*			*			*			*		
HE 120 AA			*			*			*			*
HE 120 A	*			*			*			*		
HE 120 B	*			*			*			*		
HE 120 C	*			*			*			*		
HE 120 M	*			*			*			*		
HE 140 AA			*			*			*			*
HE 140 A	*				*		*				*	
HE 140 B	*			*			*			*		
HE 140 C	*			*			*			*		
HE 140 M	*			*			*			*		
HE 160 AA			*			*			*			*
HE 160 A	*				*		*				*	
HE 160 B	*			*			*			*		
HE 160 C	*			*			*			*		
HE 160 M	*			*			*			*		
HE 180 AA			*			*			*			*
HE 180 A		*				*		*				*
HE 180 B	*			*			*			*		
HE 180 C	*			*			*			*		
HE 180 M	*			*			*			*		
HE 200 AA			*						*			
HE 200 A		*				*		*				*
HE 200 B	*			*			*			*		
HE 200 C	*			*			*			*		
HE 200 M	*			*			*			*		
HE 220 AA			*						*			

F.2. CROSS SECTIONAL CLASSIFICATION FOR COMBINED COMPR. AND BENDING MOMENT

S355												
Maximum compression force N_{Ed} or $N_{fi,Ed}$ (kN)												
Designation HE	Bending about y-y						Bending about z-z					
	Normal Temperature Section class			High Temperature Section class			Normal Temperature Section class			High Temperature Section class		
	Class 1	Class 2	Class 3	Class 1	Class 2	Class 3	Class 1	Class 2	Class 3	Class 1	Class 2	Class 3
HE 220 A		*				*		*				*
HE 220 B	*			*			*			*		
HE 220 C	*			*			*			*		
HE 220 M	*			*			*			*		
HE 240 AA			*						*			
HE 240 A		*				*		*				*
HE 240 B	*			*			*			*		
HE 240 C	*			*			*			*		
HE 240 M	*			*			*			*		
HE 260 AA			*						*			
HE 260 A			*			*			*			*
HE 260 B	*			*			*			*		
HE 260 C	*			*			*			*		
HE 260 M	*			*			*			*		
HE 280 AA			*						*			
HE 280 A			*			*			*			*
HE 280 B	*			*			*			*		
HE 280 C	*			*			*			*		
HE 280 M	*			*			*			*		
HE 300 AA			*						*			
HE 300 A			*			*			*			*
HE 300 B	*			*			*			*		
HE 300 C	*			*			*			*		
HE 300 M	*			*			*			*		
HE 320 AA			*						*			
HE 320 A		*				*		*				*
HE 320 B	*			*			*			*		
HE 320 C	*			*			*			*		
HE 320 M	*			*			*			*		
HE 340 AA			*						*			
HE 340 A	*					*	*					*

F. CROSS SECTIONAL CLASSIFICAT. OF EU HOT ROLLED IPE AND HE PROFILES

S355												
Maximum compression force N_{Ed} or $N_{fi,Ed}$ (kN)												
Designation HE	Bending about y-y						Bending about z-z					
	Normal Temperature Section class			High Temperature Section class			Normal Temperature Section class			High Temperature Section class		
	Class 1	Class 2	Class 3	Class 1	Class 2	Class 3	Class 1	Class 2	Class 3	Class 1	Class 2	Class 3
HE 340 B	*			*			*			*		
HE 340 M	*			*			*			*		
HE 360 AA			*						*			
HE 360 A	*				*		*				*	
HE 360 B	*			*			*			*		
HE 360 M	*			*			*			*		
HE 400 AA			*			3710			*			
HE 400 A	1145	*		825	1099	*		*				*
HE 400 B	*			*			*			*		
HE 400 M	*			*			*			*		
HE 450 AA			4467			3448						
HE 450 A	1139	*		790	1089	6042		*				
HE 450 B	*			1485	*		*				*	
HE 450 M	*			*			*			*		
HE 500 AA			4271			3255						
HE 500 A	1128	1512	*	748	1074	5882			*			
HE 500 B	2001	*		1446	1923	*		*				*
HE 500 M	*			*			*			*		
HE 550 AA		1167	4580			3473						
HE 550 A	1105	1521	7237	692	1047	5570						
HE 550 B	1986	*		1392	1902	8949		*				
HE 550 M	*			*			*			*		
HE 600 AA		1166	4446			3329						
HE 600 A	1076	1527	6994	630	1013	5323						
HE 600 B	1965	2605	*	1331	1875	8516			*			
HE 600 M	*			3530	*		*				*	
HE 600 × 337	*			*			*			*		
HE 600 × 399	*			*			*			*		
HE 650 AA	744	1161	4349			3214						
HE 650 A	1042	1527	6808	560	973	5124						
HE 650 B	1938	2621	*	1263	1843	8166			*			

F.2. CROSS SECTIONAL CLASSIFICATION FOR COMBINED COMPR. AND BENDING MOMENT

S355												
Maximum compression force N_{Ed} or $N_{fi,Ed}$ (kN)												
Designation HE	Bending about y-y						Bending about z-z					
	Normal Temperature Section class			High Temperature Section class			Normal Temperature Section class			High Temperature Section class		
	Class 1	Class 2	Class 3	Class 1	Class 2	Class 3	Class 1	Class 2	Class 3	Class 1	Class 2	Class 3
HE 650 M	*			3228	*		*				*	
HE 650 × 343	*			*			*			*		
HE 650 × 407	*			*			*			*		
HE 700 AA	701	1152	4346		638	3171						
HE 700 A	1165	1725	7165	610	1086	5376						
HE 700 B	2113	2884	10847	1351	2006	8379						
HE 700 M	4089	*		2925	3924	*		*				*
HE 700 × 352	*			4978	*		*				*	
HE 700 × 418	*			*			*			*		
HE 800 AA	615	1137	4346		541	3095						
HE 800 A	922	1522	6464	328	838	4711						
HE 800 B	1846	2662	9837	1038	1732	7445						
HE 800 M	3508	4684	*	2344	3344	12287			*			
HE 800 × 373	5936	*		4287	5703	*		*				*
HE 800 × 444	*			*			*			*		
HE 900 AA	490	1090	4418		406	3063						
HE 900 A	804	1487	6380	128	708	4543						
HE 900 B	1743	2656	9607	840	1616	7147						
HE 900 M	2903	4079	13488	1739	2738	10302						
HE 900 × 391	5216	*		3566	4982	16144		*				
HE 900 × 466	*			6523	*		*				*	
HE 1000 AA	333	1016	4400		237	2966						
HE 1000 × 249	489	1214	5275		387	3615						
HE 1000 A	489	1214	5775		387	3957						
HE 1000 B	1398	2361	8778	446	1264	6364						
HE 1000 M	2285	3460	11629	1121	2120	8667						
HE 1000 × 393	4114	5702	16697	2543	3892	12820						
HE 1000 × 415	5116	6919	*	3332	4864	15073			*			
HE 1000 × 438	5719	7649	*	3809	5449	16752			*			
HE 1000 × 494	8828	*		6291	8469	*		*				*
HE 1000 × 584	*			9998	*		*				*	

F. CROSS SECTIONAL CLASSIFICAT. OF EU HOT ROLLED IPE AND HE PROFILES

S460												
Maximum compression force N_{Ed} or $N_{fi,Ed}$ (kN)												
	Bending about y-y						Bending about z-z					
Designation HE	Normal Temperature Section class			High Temperature Section class			Normal Temperature Section class			High Temperature Section class		
	Class 1	Class 2	Class 3	Class 1	Class 2	Class 3	Class 1	Class 2	Class 3	Class 1	Class 2	Class 3
HE 100 AA		*				*		*				*
HE 100 A	*			*			*			*		
HE 100 B	*			*			*			*		
HE 100 C	*			*			*			*		
HE 100 M	*			*			*			*		
HE 120 AA			*			*			*			*
HE 120 A	*				*		*				*	
HE 120 B	*			*			*			*		
HE 120 C	*			*			*			*		
HE 120 M	*			*			*			*		
HE 140 AA			*						*			
HE 140 A		*				*		*				*
HE 140 B	*			*			*			*		
HE 140 C	*			*			*			*		
HE 140 M	*			*			*			*		
HE 160 AA			*						*			
HE 160 A		*				*		*				*
HE 160 B	*			*			*			*		
HE 160 C	*			*			*			*		
HE 160 M	*			*			*			*		
HE 180 AA			*						*			
HE 180 A			*			*			*			*
HE 180 B	*			*			*			*		
HE 180 C	*			*			*			*		
HE 180 M	*			*			*			*		
HE 200 AA			*						*			
HE 200 A			*			*			*			*
HE 200 B	*			*			*			*		
HE 200 C	*			*			*			*		
HE 200 M	*			*			*			*		
HE 220 AA												

F.2. CROSS SECTIONAL CLASSIFICATION FOR COMBINED COMPR. AND BENDING MOMENT

S460												
Maximum compression force N_{Ed} or $N_{fi,Ed}$ (kN)												
Bending about y-y						Bending about z-z						
Designation HE	Normal Temperature Section class			High Temperature Section class			Normal Temperature Section class			High Temperature Section class		
	Class 1	Class 2	Class 3	Class 1	Class 2	Class 3	Class 1	Class 2	Class 3	Class 1	Class 2	Class 3
HE 220 A			*			*			*			*
HE 220 B	*			*			*			*		
HE 220 C	*			*			*			*		
HE 220 M	*			*			*			*		
HE 240 AA												
HE 240 A			*			*			*			*
HE 240 B	*				*		*				*	
HE 240 C	*			*			*			*		
HE 240 M	*			*			*			*		
HE 260 AA												
HE 260 A			*			*			*			*
HE 260 B	*				*		*				*	
HE 260 C	*			*			*			*		
HE 260 M	*			*			*			*		
HE 280 AA												
HE 280 A			*						*			
HE 280 B	*					*	*					*
HE 280 C	*			*			*			*		
HE 280 M	*			*			*			*		
HE 300 AA												
HE 300 A			*			*			*			*
HE 300 B	*					*	*					*
HE 300 C	*			*			*			*		
HE 300 M	*			*			*			*		
HE 320 AA												
HE 320 A			*			*			*			*
HE 320 B	*				*		*				*	
HE 320 C	*			*			*			*		
HE 320 M	*			*			*			*		
HE 340 AA												
HE 340 A			*			6118			*			

F. CROSS SECTIONAL CLASSIFICAT. OF EU HOT ROLLED IPE AND HE PROFILES

S460												
Maximum compression force N_{Ed} or $N_{fi,Ed}$ (kN)												
Bending about y-y						Bending about z-z						
Designation HE	Normal Temperature Section class			High Temperature Section class			Normal Temperature Section class			High Temperature Section class		
	Class 1	Class 2	Class 3	Class 1	Class 2	Class 3	Class 1	Class 2	Class 3	Class 1	Class 2	Class 3
HE 340 B	*			1317	*		*				*	
HE 340 M	*			*			*			*		
HE 360 AA			*						*			
HE 360 A		*				6346		*				
HE 360 B	*			1390	*		*				*	
HE 360 M	*			*			*			*		
HE 400 AA			5061									
HE 400 A	1148	*				6670		*				
HE 400 B	*			1537	*		*				*	
HE 400 M	*			*			*			*		
HE 450 AA			4719									
HE 450 A	1109	1511	*		1053	6365			*			
HE 450 B	2051	*		1463	1968	*		*				*
HE 450 M	*			*			*			*		
HE 500 AA			4468			3311						
HE 500 A	1063	1500	8034	630	1002	6127						
HE 500 B	2010	*		1379	1921	10122		*				
HE 500 M	*			*			*			*		
HE 550 AA			4773			3514						
HE 550 A	999	1473	7628	529	932	5731						
HE 550 B	1950	2633	*	1274	1854	9455			*			
HE 550 M	*			3928	*		*				*	
HE 600 AA			4589			3317						
HE 600 A	926	1439	7309	418	854	5408						
HE 600 B	1880	2609	11619	1158	1778	8916						
HE 600 M	*			3536	4674	*	*					*
HE 600 × 337	*			*			*			*		
HE 600 × 399	*			*			*			*		
HE 650 AA			4444			3153						
HE 650 A	845	1398	7054	297	767	5137						
HE 650 B	1802	2579	11164	1033	1693	8471						

F.2. CROSS SECTIONAL CLASSIFICATION FOR COMBINED COMPR. AND BENDING MOMENT

S460												
Maximum compression force N_{Ed} or $N_{fi,Ed}$ (kN)												
Bending about y-y						Bending about z-z						
Designation HE	Normal Temperature Section class			High Temperature Section class			Normal Temperature Section class			High Temperature Section class		
	Class 1	Class 2	Class 3	Class 1	Class 2	Class 3	Class 1	Class 2	Class 3	Class 1	Class 2	Class 3
HE 650 M	4469	*		3144	4281	*		*				*
HE 650 × 343	*			5445	*		*				*	
HE 650 × 407	*			*			*			*		
HE 700 AA		953	4398			3060						
HE 700 A	927	1565	7406	295	837	5369						
HE 700 B	1938	2815	11465	1069	1815	8656						
HE 700 M	4076	5415	*	2751	3889	15501			*			
HE 700 × 352	*			4978	6590	*	*					*
HE 700 × 418	*			*			*			*		
HE 800 AA	253	848	4318			2894						
HE 800 A	572	1255	6535		476	4539						
HE 800 B	1543	2473	10236	623	1413	7512						
HE 800 M	3324	4663	16775	1999	3137	12822						
HE 800 × 373	5961	*		4083	5695	20061		*				
HE 800 × 444	*			7453	*		*				*	
HE 900 AA	11	694	4303			2761						
HE 900 A	333	1109	6339		224	4249						
HE 900 B	1311	2350	9866	283	1165	7066						
HE 900 M	2540	3878	14133	1215	2352	10508						
HE 900 × 391	5026	6923	22015	3149	4761	16944						
HE 900 × 466	9036	*		6332	8654	27068		*				
HE 1000 AA		499	4196			2564						
HE 1000 × 249		705	5093			3203						
HE 1000 A		705	5575			3506						
HE 1000 B	812	1907	8841		658	6093						
HE 1000 M	1739	3077	11959	414	1551	8586						
HE 1000 × 393	3682	5489	17566	1893	3429	13153						
HE 1000 × 415	4757	6808	20606	2725	4469	15636						
HE 1000 × 438	5406	7602	22876	3232	5099	17468						
HE 1000 × 494	8776	11693	*	5889	8368	25050			*			
HE 1000 × 584	13797	*		9903	13246	*		*				*

ELEFIR - EN

FIRE DESIGN OF STEEL STRUCTURAL MEMBERS ACCORDING TO EUROCODE 3

This book includes a **licence of the software Elefir-EN**.

To obtain it, please send an email to publications@steelconstruct.com with the subject “Elefir – EN | Bookcode” with a proof of the payment of the book in attachment, and after that you will receive a code to download the program and make your registration with the bookcode on the website:

www.steelconstruct.com

WILEY END USER LICENSE AGREEMENT

Go to www.wiley.com/go/eula to access Wiley's ebook EULA.



© Michael Meadows

Fire Design of Steel Structures 2nd Edition

This book explains and illustrates the rules that are given in the Eurocodes for designing steel structures subjected to fire. After the first introductory chapter, Chapter 2 explains how to calculate the mechanical actions (loads) in the fire situation based on the information given in EN 1990 and EN 1991. Chapter 3 is dedicated to the models which represent the thermal actions created by the fire. Chapter 4 describes the procedures to be used to calculate the temperature of the steelwork from the temperature of the compartment and Chapter 5 shows how the information given in EN 1993-1-2 is used to determine the load bearing capacity of the steel structure. Chapter 6 presents the essential features that characterise the advanced calculation models, for thermal and mechanical response. The methods used to evaluate the fire resistance of bolted and welded connections are described in Chapter 7. Chapter 8 describes a computer program called 'Elefir-EN' which is based on the simple calculation models given in the Eurocode and allows designers to quickly and accurately calculate the performance of steel components in the fire situation. Chapter 9 looks at the issues that a designer may be faced with when assessing the fire resistance of a complete building. This is done via a case study and addresses most of the concepts presented in the previous chapters.

For this second edition the authors revised and extended the content. The book contains some new sections, e.g. a comparison between the simple and the advanced calculation models, as well as additional examples.

Jean-Marc Franssen is Professor at the Department of Architecture, Geology, Environment and Construction of the University of Liege in Belgium. He is leading the group of fire safety engineering and is the Director of the Fire Resistance Laboratory. He is a member of the Technical Committee TC3 – Fire of ECCS. He founded the Structures in Fire (SiF) movement of which he is the chairman of the Steering Committee. He was a member of the draft team of EN 1993-1-2.

Paulo Vila Real is Professor at the Department of Civil Engineering of the University of Aveiro in Portugal. He is the Head of Department and the Director of the Fire Resistance Laboratory. He is the Chairman of the Technical Committee TC3 – Fire Safety of ECCS, a member of the European Working Groups for Eurocode 3: Part 1-2 and Eurocode 4: Part 1-2 and a member of the Steering Committee of the Structures in Fire (SiF) movement. He was in charge of writing the Portuguese National Annexes to the fire parts of the Eurocodes on actions, concrete, steel, composite and aluminium structures.



ECCS Eurocode Design Manuals

EUROPEAN CONVENTION FOR CONSTRUCTIONAL STEELWORK
CONVENTION EUROPÉENNE DE LA CONSTRUCTION MÉTALLIQUE
EUROPÄISCHE KONVENTION FÜR STAHLBAU

publications@steelconstruct.com
www.steelconstruct.com